ADVANCES IN COLLOID SCIENCE

VOLUME I

CONTRIBUTORS TO VOLUME I

THOMAS F. ANDERSON, *RCA Fellow of the National Research Council, RCA Manufacturing Company, Camden, N. J.*

JOHN T. EDSALL, *Department of Physical Chemistry, Harvard Medical School, Boston, Mass.*

P. H. EMMETT, *School of Engineering, The Johns Hopkins University, Baltimore, Md.*

HENRY EYRING, *Frick Chemical Laboratory, Princeton University, Princeton, N. J.*

ERNST A. HAUSER, *Department of Chemical Engineering, Massachusetts Institute of Technology, Cambridge, Mass.*

K. L. HERTEL, *Department of Physics, The University of Tennessee, Knoxville, Tenn.*

G. M. KRAAY, *Department of Rubber Research, Experimental Station West-Java, Buitenzorg, Java, Netherlands East Indies*

JAMES W. MCBAIN, *Department of Chemistry, Stanford University, California*

KURT H. MEYER, *Chemical Laboratory, University of Geneva, Geneva, Switzerland*

W. O. MILLIGAN, *Department of Chemistry, The Rice Institute, Houston, Texas*

ROBERT J. MYERS, *The Resinous Products and Chemical Company, Inc., Philadelphia, Pa.*

R. E. POWELL, *Frick Chemical Laboratory, Princeton University, Princeton, N. J.*

R. R. SULLIVAN, *Agricultural Experiment Station, The University of Tennessee, Knoxville, Tenn.*

ARNE TISELIUS, *Institute of Physical Chemistry, Upsala University, Upsala, Sweden*

G. E. VAN GILS, *Department of Rubber Research, Experimental Station West-Java, Buitenzorg, Java, Netherlands East Indies*

HARRY B. WEISER, *Department of Chemistry, The Rice Institute, Houston, Texas*

Advances in Colloid Science

Edited by

ELMER O. KRAEMER, Ph.D.
Biochemical Research Foundation of the Franklin Institute, Newark, Delaware

In Collaboration with

FLOYD E. BARTELL, Ph.D.
Professor of Chemistry
University of Michigan
Ann Arbor, Mich.

S. S. KISTLER, Ph.D.
Associate Director of Research
Norton Company
Worcester, Mass.

VOLUME I

With 161 Illustrations

1942
INTERSCIENCE PUBLISHERS, INC.
NEW YORK, N. Y.

First printing, 1942
Second printing (by photo-offset), 1946

Printed in the United States of America

PREFACE

According to the plans of the editors and the publishers, this is the first of a series of volumes intended to provide a medium in which recent significant discoveries or advances in Colloid Science, either experimental or theoretical, may be presented in a more comprehensive and unified fashion than is possible in the regular technical periodicals. Since in each instance the author (or authors) will have been closely identified with the development under discussion, it is to be expected that the contributions should have an individualistic point of view, and should show a definite emphasis upon the author's own part in the development in question. The contributions are thus not intended to be reviews or compilations from the literature in the usual sense, and the editors are willing to share any censure that readers may be inclined sometimes to level at an author because he has apparently failed to do adequate justice to other investigators in the field.

The present is an unfortunate time, in a sense, to launch a project of this sort. It was the natural hope of the editors that "Advances in Colloid Science" could cover world-wide developments. Very much to their regret, they found it impossible to realize their hopes in this first volume, but they shall attempt to maintain an optimistic attitude, and shall look forward to the day when the artificial barriers of nation and race will disappear in the domain of science.

With reference to this first volume, the editors wish to express their appreciation for the cordial and cooperative manner with which the various contributors have accepted the spirit and purposes of this venture. Especial thanks are also due the publishers for the generosity of their efforts in aiding to bring these contributions together. The editors further gratefully acknowledge the granting of permission by the American Chemical Society, American Institute

of Physics, American Society for Testing Materials, Long Island Biological Association, The Williams & Wilkins Company and by the publishers of the *Biological Bulletin* and the *Journal of Biological Chemistry* to reprint illustrations from their publications.

Inasmuch as the editors plan for additional volumes when the conditions warrant them, they would find it very helpful if authors would favor the editors with reprints of important papers in Colloid Science, particularly if published outside the United States.

E. O. K.
December, 1941 F. E. B.
S. S. K.

CONTENTS

THE MEASUREMENT OF THE SURFACE AREAS OF FINELY DIVIDED OR POROUS SOLIDS BY LOW TEMPERATURE ADSORPTION ISOTHERMS

P. H. EMMETT*

School of Engineering, Johns Hopkins University, Baltimore, Maryland

CONTENTS

I. Introduction

The idea of measuring surface areas of solids by means of gas adsorption is not new; both physical and chemical types of adsorption have been so employed in the past.

One of the earliest attempts to use activated (*i. e.*, chemical) adsorption for this purpose was that of Benton (6) on Pt catalysts. More recently de Boer and Dippel (19) estimated the surface of vacuum sublimed CaF_2 from the chemisorption of water on the surface of the tiny CaF_2 crystals. Similarly, Emmett and Brunauer (21) have made use of the chemisorption of CO at $-195°$ C. to measure the surface areas of iron synthetic ammonia catalysts. These examples serve merely to illustrate instances in which surface areas can be estimated by chemisorption or activated adsorption. In general, the use of chemical adsorption for this purpose is not widely applicable because of certain limitations inherent in the method. In the first place, one must find a gas that will be chemically adsorbed

* Present address: Mellon Institute, Pittsburgh, Pa.

by the surface and must find a means of ascertaining the volume of gas corresponding to a complete monolayer. Furthermore, if the solid contains more than one constituent it is very probable that the surface area obtained will be that of only one of the two or more substances of which it is composed.

Physical or van der Waals adsorption of gases has been used hitherto for determining the relative but not the absolute surface areas of certain solids. For example, Russel and Taylor (44) used the adsorption of carbon dioxide at 0° C. and 1 atmosphere pressure to compare the surfaces of promoted and unpromoted nickel catalysts. Without doubt such measurements were useful for rough comparisons but could not yield accurate results in the absence of assurance that the same fraction of the surface was covered with the adsorbed gas on the one adsorbent as on the other, at a given temperature and pressure. Benton and White (7) suggested that "breaks" in one of their adsorption isotherms for nitrogen on iron catalysts at −191.5° C. and pressures of 13 and 48 cm. might indicate the completion of a first and second layer of molecules, respectively, on the adsorbent. Subsequent work (21) has shown that these particular "breaks" disappear as soon as correction is made for the deviation of the adsorbate nitrogen from the perfect gas laws in the dead space surrounding the adsorbent. Nevertheless, the idea of trying to use low temperature isotherms for absolute surface area measurements arose, as far as the author's participation in this work is concerned, largely from the work of Benton.

About seven years ago it became desirable to measure the surface area of porous iron synthetic ammonia catalysts, in order to decide whether the increase in activity resulting from promoter additions could best be attributed to an increase in the total surface area or to an increase in the activity per unit area. A search of the literature revealed that no method for measuring the absolute surface areas of such metallic catalysts without at the same time exposing them to air or to liquids had been described. Accordingly, work was undertaken to investigate further Benton and White's (7) suggestion as to the point corresponding to a monolayer on the adsorption isotherms of an inert gas, such as nitrogen, near its boiling point. The method resulting from the ensuing research will be described in the present chapter. The experimental method, the empirical and theoretical means used to select a point on the isotherms corresponding to a monolayer, the general theory of such adsorptions and the con-

firmatory evidence that has been obtained to substantiate the method by comparing the results that it yields with those obtained by entirely different methods, will all be discussed.

II. Experimental Apparatus and Procedure

The adsorption apparatus used in making the low temperature adsorption measurements is of standard design. A typical set-up is shown in Fig. 1. It includes an adsorption bulb, a calibrated gas

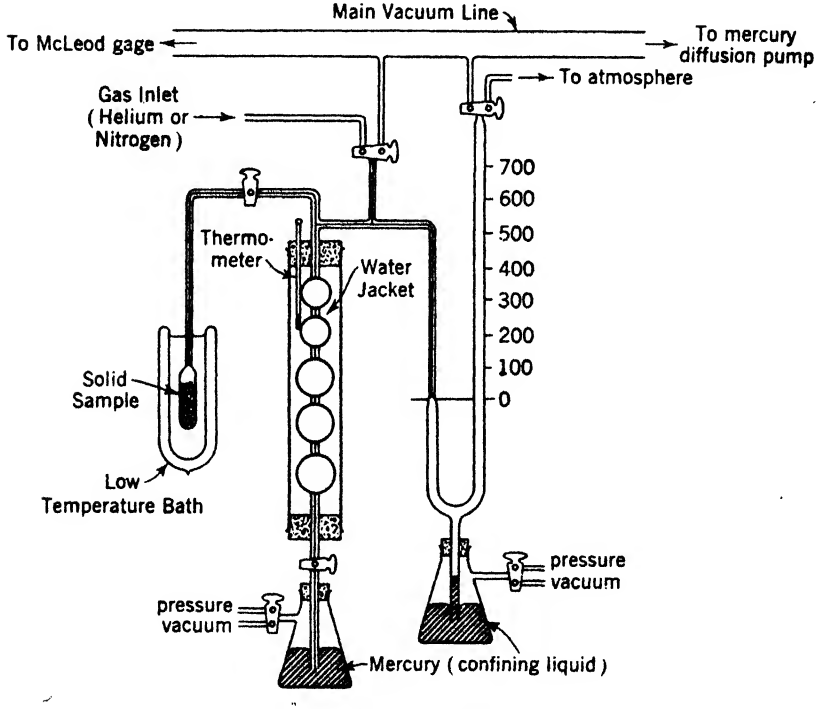

Fig. 1.—Adsorption apparatus.

buret, a manometer, a high-vacuum oil pump and Langmuir diffusion pump, and a McLeod gauge. The method of operation will be clear from the following brief description: The adsorption bulb containing a sufficient sample of adsorbent to furnish a total area of at least 2 square meters is sealed to the rest of the system by 2-mm. capillary tubing as indicated in Fig. 1. At the beginning of an experiment.

the adsorbent is evacuated *in situ* at a temperature sufficient to remove water vapor and physically adsorbed gases (usually 110° C.). The dead space in the adsorption bulb up to the stopcock is then determined with pure helium. To make this dead space determination a volume of purified helium is admitted into the buret, the stopcock to the evacuated adsorbent being closed. The volume of helium is measured in an obvious manner with the calibrated buret and manometer. After placing the desired cold bath around the sample bulb (liquid nitrogen at about 77 78° K. or liquid oxygen at 90° K. are convenient baths) one opens the stopcock between the sample and the buret and determines the volume of helium required to fill the adsorption bulb. Such a calibration assumes, of course, that helium is not adsorbed by the adsorbent but merely fills in the space around it. This assumption is justified because at adsorption temperatures of 77° K. or higher the adsorption of helium will always be very small compared to that of the adsorbate being used. After the dead space is calibrated, one again evacuates the system to remove the helium and then, after closing the stopcock to the adsorbent, admits to the buret the adsorbate to be used (nitrogen for example) and measures the quantity taken. The stopcock to the sample bulb is then opened and the sample let stand long enough to effect equilibration. The volume of gas (S.T.P.) adsorbed is given by the equation

$$V_a = V_t - V_h(1 + \alpha) - V_b \qquad (1)$$

where V_a is the volume of gas adsorbed, V_t is the total volume of adsorbate that has been admitted to the system, V_h is the volume of adsorbate required to fill the dead space to the pressure p of the experiment, α is the correction factor required to take into account the gas imperfection of the adsorbate at the low temperature being used and V_b is the volume of adsorbate remaining in the buret at the time of measurement. By repeatedly adding successive amounts of adsorbate through the buret system one can obtain a series of values for adsorption as a function of pressure at a given bath temperature of the adsorbent and thus obtain the data for an adsorption isotherm.

The corrections (21) for the deviation of various simple gases from the perfect gas laws are as follows: nitrogen at −195.8°, 5% and at −183°, 2.87%; oxygen at −183°, 3.17%; argon at −195.8°, 8.7%, and at −183°, 3.0%; carbon monoxide at −183°, 2.68%; methane at −140°, 5.92%; NO at −140°, 4.0%; N_2O at −78°, 5.84%;

CO_2 at $-78°$, 2.09% and at 25°, 0.58%; ammonia at $-36°$, 2.64% and at 25°, 1.185%; *n*-butane at 0°, 10.8%, and at 25°, 3.2%. All deviations refer to 760 mm. and are assumed to vary linearly with pressure.

The type of isotherm obtained for nitrogen at $-195.8°$ C. on a typical iron synthetic ammonia catalyst (21) is illustrated in Fig. 2. Obviously the use of such an isotherm in measuring the surface area of the catalyst entails (*a*) selecting the point on the curve corresponding to the completion of a monolayer of adsorbed molecules and (*b*)

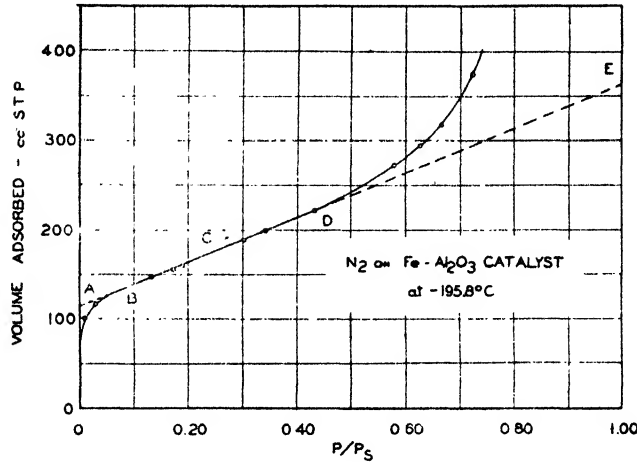

Fig. 2.—Adsorption isotherm for nitrogen on a $Fe\text{-}Al_2O_3$ catalyst at 77.3° K.

assigning a value for the average area covered by each adsorbed molecule. The selecting of the point corresponding to a monolayer on the isotherms is the crux of the entire problem of using adsorption isotherms for measuring surface areas. Both an empirical method arrived at from several converging types of evidence and a theoretical method for accomplishing this have been developed and will be discussed in the next two sections. In assigning a value to the average area occupied by an adsorbed molecule on the surface it has seemed reasonable (21) to calculate the diameter of the adsorbed molecules from the densities of the liquefied or of the solidified adsorbate. If the physically adsorbed molecules are close-packed

on the surface one arrives at the following equation for the average area per molecule:

$$\text{Area per molecule} = 4(0.866)\left[\frac{M}{4\sqrt{2}N\rho}\right]^{2/3} \qquad (2)$$

where M is the molecular weight of the gas, N is Avogadro's number and ρ is the density of the solidified or liquefied gas. This equation is derived on the assumption that the molecules are hexagonally

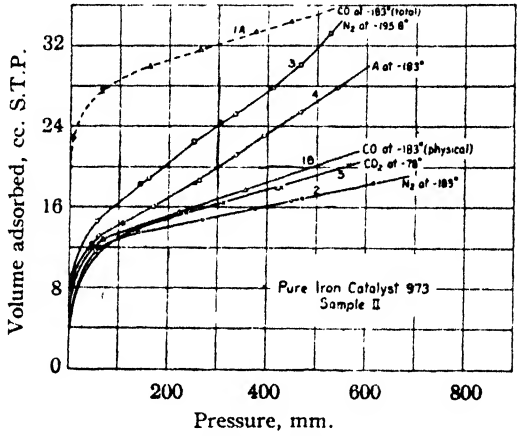

Fig. 3.—Low temperature adsorption isotherms on a sample of pure iron catalyst. Solid circles, squares and triangles are desorption points.

close-packed in the solidified and in the liquefied gas. For solid nitrogen, argon, carbon monoxide and a number of other gases such close packing is known to exist since these gases when solidified have face-centered cubic structures. The assumption is believed to be reasonable for all molecules that are approximately symmetrical. In Table I are listed values for "Area (S)" obtained (21) for the different adsorbates by inserting in the above equation the values for the density of the solidified gas, and "Area (L)" obtained by using the density of the liquefied gas.

III. The Adsorbed Monolayer

Before a theory for the S-shaped adsorption isotherms was developed a conclusion as to which point on the isotherm corresponded

to a monolayer was reached (10, 21) empirically on the basis of a large number of adsorption experiments on iron catalysts. It was decided that point *B* on isotherms such as shown in Fig. 2 corresponded approximately to the completion of a monolayer of adsorbed gas. The evidence for this selection was threefold:

1. The earliest carbon monoxide adsorption experiments on pure iron catalysts (21) gave a valuable clue to the point on the isotherms corresponding to a monolayer of physically adsorbed gas. It was noted that the isotherm for the total adsorption of carbon monoxide corresponded to much larger adsorptions at a given temperature than those for nitrogen (Fig. 3). Further investigation revealed that part of the adsorbed carbon monoxide was readily removable by evacuation at $-78°$, whereas the remainder was tightly bound by the iron catalyst. Repetition of a $-183°$ run after an intervening evacuation at $-78°$ yielded curve 1*B*, Fig. 3, designated as the isotherm for physically adsorbed carbon monoxide. The rapidity of the irreversible adsorption is evidenced by the fact that the desorption point shown at about 80 mm. on curve 1*A* agrees closely with the corresponding adsorption point taken several hours sooner. The volume of this tightly bound or chemisorbed carbon monoxide was considered to be the difference between curves 1*A* and 1*B* and was approximately the same as the volume of gas at point *B*, the beginning of the long linear part of the isotherm for the physical adsorption of nitrogen or carbon monoxide. The formation of what appeared to be a monolayer of tightly bound carbon monoxide over the entire iron surface constituted the first concrete evidence that the volume of gas corresponding to point *B* on the isotherm for physically adsorbed carbon monoxide was approximately a monolayer. Detailed consideration of the possible spacing of the iron atoms on the various crystal faces that might be exposed by the tiny iron crystals of which the catalyst is composed showed that the volume of chemisorbed carbon monoxide required to cover the surface might be 3 per cent less than the physically adsorbed monolayer, or 19 or 68 per cent greater depending on whether the exposed iron faces were 111, 110 or 100 planes. Actually the average observed value for chemisorbed carbon monoxide on pure iron catalysts is 15 to 25 per cent greater than the volume of physically adsorbed carbon monoxide at point *B*.

2. A determination of the adsorption isotherms for a number of gases, such as nitrogen, argon, carbon monoxide, oxygen, carbon dioxide and butane, showed that the calculation of a catalyst area on

the assumption that point B corresponded to a monolayer gave better agreement between surface area values obtained by one gas compared to another than if any of the other possible points A, C, D or E was selected (Fig. 1). The details of this comparison have been presented elsewhere (21) for ten different samples of iron synthetic ammonia catalysts. With point B assumed as the monolayer, the maximum deviation for the surface calculated for one gas from the average of the values calculated from all the gases was about 10 per cent. This evidence not only favors the choice of point B for a monolayer but is

TABLE I

AREA OCCUPIED BY EACH ADSORBED MOLECULE

Gas	Density of solidified gas, g./cc.	Temp., ° C.	Area (S), sq. Å.	Density of liquefied gas, g./cc.	Temp., ° C.	Area (L), sq. Å.
N_2	1.026	−252.5	13.8	0.751	−183	17.0
				0.808	−195.8	16.2
O_2	1.426	−252.5	12.1	1.14	−183	14.1
A	1.65	−233	12.8	1.374	−183	14.4
CO	...	−252.5	13.7	0.763	−183	16.8
CO_2	1.565	− 80	14.1	1.179	− 56.6	17.0
CH_4	...	−253	15.0	0.3916	−140	18.1
C_4H_{10}	...	...	32.0	0.601	0	32.1
NH_3	...	− 80	11.7	0.688	− 36	12.9
NO	...	...	...	1.269	−150	12.5
N_2O	...	...	14.4	1.199	− 80	16.8

in agreement with the assumption that there are no marked differences in the packing of the various adsorbed molecules on the surfaces and that the area values per molecule given in Table I form a suitable basis for calculating the absolute areas of the catalysts.

3. A plot of the difference between the heat of adsorption of the adsorbate and its heat of liquefaction yielded curves of the type shown in Fig. 4. These heats of adsorption were calculated in the usual fashion with the help of the Clausius-Clapeyron equation. For curves 1, 2 and 3 the point B values are 125, 115 and 6.5 cc., respectively. It is evident that the selection of a point corresponding to a volume of adsorbed gas 25 per cent smaller than that at point B yields a heat of adsorption that has the high value characteristic of first layer adsorption whereas the selection of a volume 25 per cent greater than point B corresponds to a heat of adsorption a few

hundred calories greater than the heat of liquefaction of the gas and probably characteristic of adsorption in second and higher layers. This is a further confirmation of the selection of point B as corresponding approximately to the monolayer of adsorbed gas.

On the basis of this empirical evidence the method of measuring surface areas has been extended to a variety of porous or finely divided solids other than iron catalysts (11, 22, 23). The interpre-

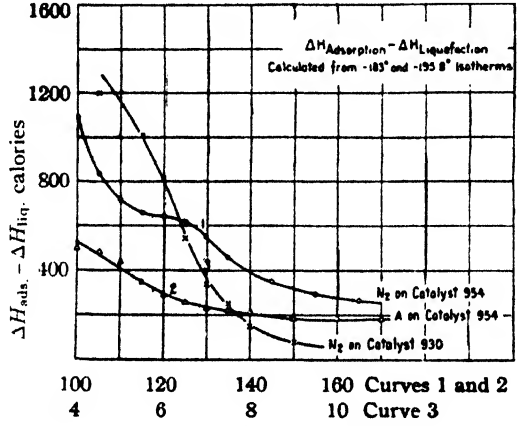

Fig. 4.—Variation of $\Delta H_{ads.} - \Delta H_{liq.}$ with volume of gas adsorbed.

tation of the isotherms is assumed to be the same for these miscellaneous materials as for iron, provided the curves are S-shaped. Before presenting detailed examples of such applications it will be well to review and summarize briefly the development of a theory to explain the S-shaped curves since with the help of the theory it has become possible to plot the adsorption data in such a manner as to obtain directly a value of V_m, the volume of gas necessary to form a monolayer of adsorbed gas on a given adsorbent, and thus to supplement the purely empirical selection of point B as representing the monolayer.

IV. Theory of the Adsorption of Gases in Multimolecular Layers

In a recent paper (12) a theory for the S-shaped adsorption isotherms has been developed, which postulates the building up of multi-

molecular adsorption layers on the catalyst surface. In the introduction to their paper the authors show that the formation of multilayers of gases, such as nitrogen, argon, etc., at low temperatures on solids by virtue of polarizing effects (9, 18) transmitted from the first layer to successively higher layers is not to be expected. Such transmitted polarization effects will be very small. They then carry out a derivation of an isotherm equation for multimolecular layers that is similar to Langmuir's (35) derivation for unimolecular layers. The equations obtained appear to represent the S-shaped adsorption isotherms and at the same time to yield reasonable values for the heat of adsorption in the first layer and for the volume of gas required to form a unimolecular layer on the adsorbents.

In carrying out the derivation, the authors let s_0, s_1, s_2 . . . . s_i represent the area of the adsorbent covered by 0, 1, 2, 3 . . . . and i layers of adsorbate. By considering the detailed balancing between the adsorption and desorption from the various layers they then arrive at a series of equations as follows:

$$a_1 p s_0 = b_1 s_1 e^{-E_1/RT} \tag{3}$$

where a_1 and b_1 are constants, p is the pressure and E_1 is the average heat of adsorption of the gas in the first layer. This equation states that the rate of condensation of molecules on the bare surface at equilibrium is equal to the rate of escape of molecules from the first layer. Similarly,

$$a_2 p s_1 = b_2 s_2 e^{-E_2/RT} \tag{4}$$

$$a_3 p s_2 = b_3 s_3 e^{-E_3/RT} \tag{5}$$

$$a_i p s_{i-1} = b_i s_i e^{-E_i/RT} \tag{6}$$

where E_2, E_3, E_i are the heats of adsorption in the second, third and ith layer. The total surface area of the catalyst is given by

$$A = \sum_{i=0}^{i=\infty} s_i \tag{7}$$

and the total volume adsorbed by

$$V = V_0 \sum_{i=0}^{i=\infty} i s_i \tag{8}$$

where V_0 is the volume of gas adsorbed on one square centimeter of

the adsorbent surface when it is covered with a complete unimolecular layer of adsorbed gas. It follows that

$$\frac{V}{A\,V_0} = \frac{V}{V_m} = \frac{\sum_{i=0}^{i=\infty} i s_i}{\sum_{i=0}^{i=\infty} s_i} \tag{9}$$

where V_m is the volume of gas adsorbed when the entire adsorbent surface is covered with a complete unimolecular layer.

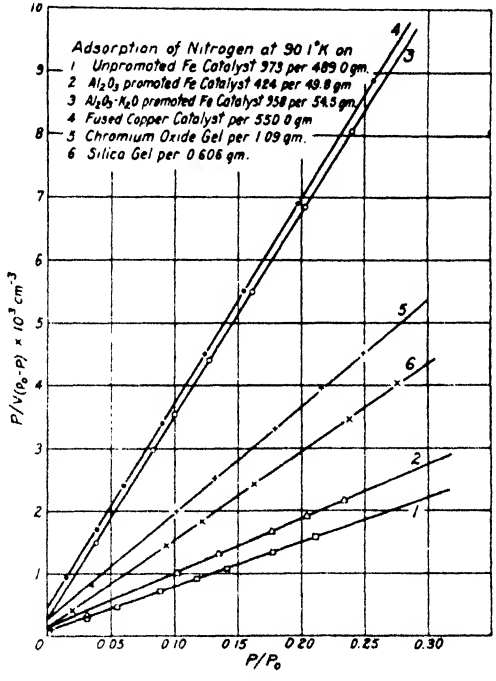

Fig. 5.—Linear plots of adsorption data for nitrogen according to equation (10).

The summation indicated in this last equation can be carried out as indicated in the original paper (12) if one makes the simplifying assumptions that $E_2 = E_3 = \ldots . E_i = E_L$, and that $b_2/a_2 = b_3/a_3 = \ldots . . b_i/a_i$. When terms are appropriately transformed the following equation is obtained:

$$\frac{p}{V(p_0 - p)} = \frac{1}{V_m c} + \frac{(c-1)p}{V_m c p_0} \tag{10}$$

where p_0 is the liquefaction pressure of the adsorbate, and c is approximately $e^{-(E_1-E_L)/RT}$.

The application of this equation to determine V_m for various isotherms is illustrated (12) by the curves in Fig. 5 representing adsorption data for nitrogen on a number of different adsorbents at 90.1° K. As will be noted, the plots of the left side of the above equation against p/p_0 yield straight lines over the relative pressure range 0.05 to about 0.35. From the slope and intercepts of such plots both c and V_m can be evaluated.

TABLE II

VOLUME OF ADSORBED NITROGEN IN A MONOLAYER ON VARIOUS ADSORBENTS[a]

Substance	V_m, cc./g.	Point B, cc./g.
Unpromoted Fe catalyst 973 I	0.13	0.12
Unpromoted Fe catalyst 973 II	0.29	0.27
Fe-Al_2O_3 catalyst 954	2.86	2.78
Fe-Al_2O_3 catalyst 424	2.23	2.09
Fe-Al_2O_3-K_2O catalyst 931	0.81	0.76
Fe-Al_2O_3 catalyst 958	0.56	0.55
Fe-K_2O catalyst 930	0.14	0.12
Fused Cu catalyst	0.05	0.05
Commercial Cu catalyst	0.09	0.10
Cr_2O_3 gel	53.3	50.5
Cr_2O_3 glowed	6.09	6.14
Silica gel	116.2	127.0

[a] The values shown in columns 2 and 3 were obtained from nitrogen adsorption isotherms at about 77° K.

The application of this theory to the data previously obtained and the comparison of the resulting values of V_m with the values for point B on the isotherms previously selected afford a fourth type of evidence that tends to support the use of low temperature isotherms for surface area measurements. A comparison (12) of the volume of gas required to form a monolayer as judged by point B and by V_m are shown in Table II. It is evident that the agreement between the values for the volume of gas required to form a monolayer as obtained in the two different ways is excellent. This linear type of plot has supplanted the empirical method of obtaining the volume of gas required for a monolayer because it is easier to use and is not susceptible

to the uncertainty that is involved in selecting point B, the lower extremity of the long linear part of the S-shaped isotherms.

The linear equation of the type illustrated in Fig. 5 has one distinct advantage over the empirical method of judging the point corresponding to a monolayer. If a material is known to give an S-shaped low temperature nitrogen adsorption isotherm, only a few adsorption points need to be determined in the relative pressure range 0.05 to

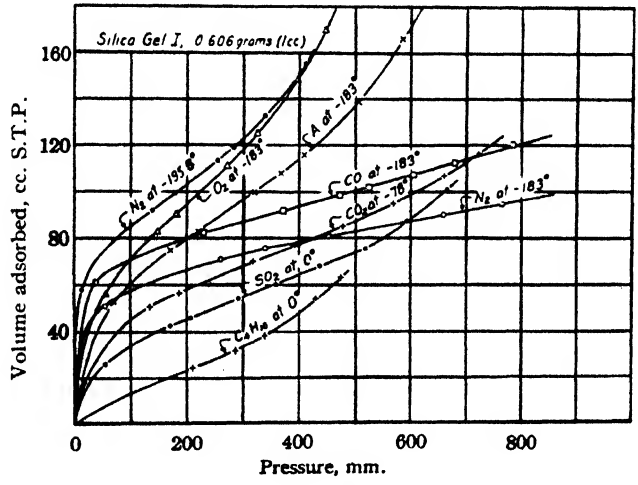

Fig. 6.—Adsorption isotherms for various gases on silica gel (11).

0.3 to fix approximately the slope of the plots of equation (10) and hence to yield a value for V_m. In fact, a single adsorption point taken at about 0.3 relative pressure will, when connected with the origin on such a plot, give a line whose slope will usually differ by less than 5 per cent from that drawn with the help of a number of adsorption points. In practice, therefore, it has proved convenient to fix the slope of the linear plot by determining only 3 or 4 adsorption points and then to calculate the value of V_m and hence the surface area of the adsorbent.

On some solids, the adsorption isotherms for butane at 0° are almost linear from the origin to a fairly high relative pressure. Such a curve is shown (11) in comparison with the isotherms for nitrogen, argon and other gases on silica gel in Fig. 6. On a curve such as that

for butane in this figure it is obviously impossible to select a point B. It has been found, however, that plotting the data for butane according to equation (10) yields a straight line from which a value for V_m can be evaluated that corresponds to an area for the silica gel in satisfactory agreement (12) with that obtained from other gases (Table III). The slightly lower value for the surface area as judged by the butane isotherms is not unreasonable since the larger butane molecule is in all probability excluded from some of the surface accessible to the smaller molecules.

If the summation of the multimolecular layers is limited to layers n molecules thick, one obtains in place of equation (10) the following relationship:

$$V = \frac{V_m c x[1 - (n + 1)x^n + nx^{n+1}]}{(1 - x)[1 + (c - 1)x - cx^{n+1}]} \tag{12}$$

where x is the ratio of the pressure at which the adsorption is V to the saturation pressure p_0, and V_m and c have the same meaning as in equation (10).

TABLE III

VALUE OF CONSTANTS FOR ADSORPTION ISOTHERMS ON SILICA GEL

Gas	Temp., ° C.	V_m, cc./g.	Surface in sq. m /g.		Point B, cc./g.	E_1-E_L, cal. per mole
			Solid packing	Liquid packing		
N_2	−195.8	127.9	477	560	135.3	719
N_2	−183	116.2	434	534	127.0	794
A	−183	119.3	413	464	122.0	594
O_2	−183	125.1	410	477	132.0	586
CO	−183	121.2	449	550	132.0	973
CO_2	− 78	99.0	378	455	102.3	1335
C_4H_{10}	0	44.7	387	387	28.1	930

Equation (12) has two important limiting cases. When $n = 1$, it reduces to the Langmuir equation (35) in the form

$$p/V = p_0/cV_m + p/V_m \tag{13}$$

The usual arbitrary constants of the Langmuir equation are here replaced by p_0, c and V_m. It thus becomes possible to use the Langmuir equation in this form to calculate isotherms at one temperature

from those at another by taking into consideration the manner in which p_0, c and V_m change with temperature. Such an application of the equation is illustrated by the curves of Fig. 7 for some of the data of Goldmann and Polanyi (12, 28) for ethyl chloride on charcoal. By plotting the 0° isotherm according to equation (13), c and V_m are evaluated. Neglecting the slight change that V_m would undergo with temperatures one can calculate the isotherms for −15.3 and 20° as shown by the solid lines in Fig. 7. The agreement with the experimental values in the higher pressure portion of the isotherms

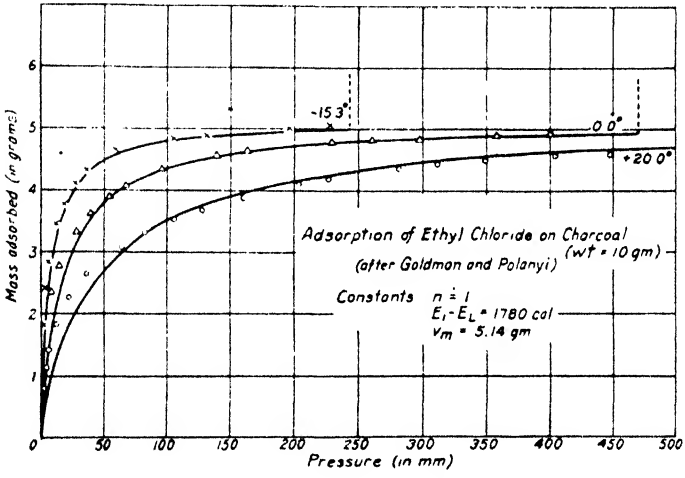

Fig. 7.—Adsorption of ethyl chloride on charcoal. Isotherms for −15.3° and 20.0° are calculated (11) from the 0.0° isotherm.

seems quite satisfactory. In the region below $p/p_0 = 0.1$, deviations from the calculated curve exist that are similar to those below about 0.05 relative pressure in the general S-shaped isotherm plots.

The second limiting case of equation (12) is for $n = \infty$. Equation (12) in this instance becomes the same as equation (10). Furthermore, for values of p/p_0 smaller than about 0.4, equation (12) becomes identical with equation (10) if n is as large as 4 or 5. It has been pointed out in an earlier publication (12) that by evaluating V_m and c for a low temperature isotherm by equation (10) and then determining n by fitting the curve to equation (12), it becomes possible to calculate isotherms at one temperature from those at another.

It should be emphasized at this point that the development of equation (12) makes no assumption as to the physical reason for the thickness of the adsorption being limited to n layers. One likely explanation would be that cracks, crevices and capillaries in the adsorbent are of such a size that no more than n layers can be adsorbed without the two layers from the opposite walls meeting. Such an interpretation, however, would naturally lead one to conclude that in charcoal, for which $n = 1$, the capillaries are only a few Ångström units in diameter—a conclusion that seems at variance with many of

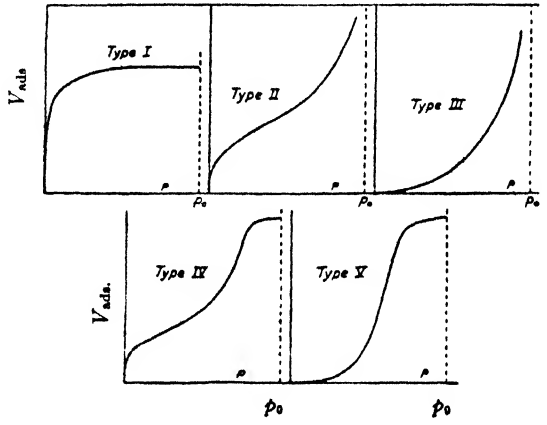

Fig. 8.—Five types of van der Waals adsorption isotherms.

the adsorption data in the literature. Accordingly, for the present it seems best to reserve final judgment as to the reason for the number of layers being restricted to n.

In a second paper on multimolecular adsorption (13), the theory outlined above has recently been extended so as to make it include the region between $p/p_0 = 0.35$ and 1. It should be understood at the outset that this extension in no way affects the validity of the treatment so far presented for the use of equation (10) in the relative pressure range 0.05 to 0.35 for determining V_m. Nevertheless, the picture that this second paper affords leads to some interesting conclusions as to the reason for the shape of some of the S-shaped isotherms in the regions of higher pressure and will be briefly discussed at this point.

All known types of physical adsorption isotherms can be divided into the five classes (13) shown in Fig. 8. Types I and II are, obviously, the Langmuir and the standard S-shaped varieties that are adequately accounted for on the basis of equations (13) and (10), respectively. Type III represents the isotherms such as are obtained for bromine and iodine on silica gel. For bromine it is known that the heat of adsorption is only slightly higher than the heat of liquefaction. By assuming as a first approximation that $E_1 = E_L$ for bromine on silica gel it was shown (13) that, according to equation (10) and the data of Reyerson (42), V_m would be 3.62 millimoles per

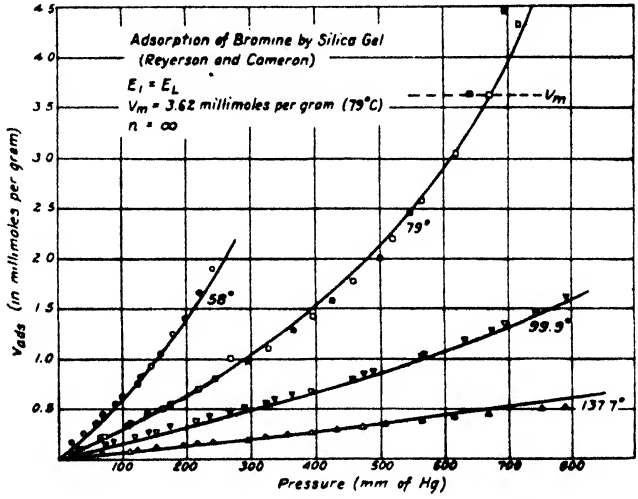

Fig. 9.—Adsorption of bromine by silica gel (Reyerson and Cameron). Isotherms at 58°, 99.9° and 137.7° calculated (13) from 79° isotherm by equation (10) on the assumption that $E_1 = E_L$ and $n = \infty$.

gram at 79°. Using the simple form of the multimolecular adsorption equation (assuming $n = \infty$) the authors (13) obtained the results shown in Fig. 9. The solid curves were all calculated from the 79° isotherm assuming that the area of the monolayer of adsorbed bromine expands according to the two-thirds power of the coefficient of expansion of liquid bromine. For iodine, it is necessary to assume that the heat of adsorption is less than the heat of liquefaction by about 3500 calories. With this assumption the data for iodine (43) also are com-

pletely explained by the multimolecular layer adsorption theory, as shown in Fig. 10, the isotherms at 137.6°, 158.3° and 198.5° being calculated from the 178.4° isotherm.

Type IV isotherm is a very common one that frequently has been found to represent the adsorption of vapors on silica gel (26), titania gel (31), iron oxide gel (34, 41) and similar porous materials. To explain such isotherms for the very special case in which the capillaries are assumed to be bounded by plane parallel walls, the authors (13)

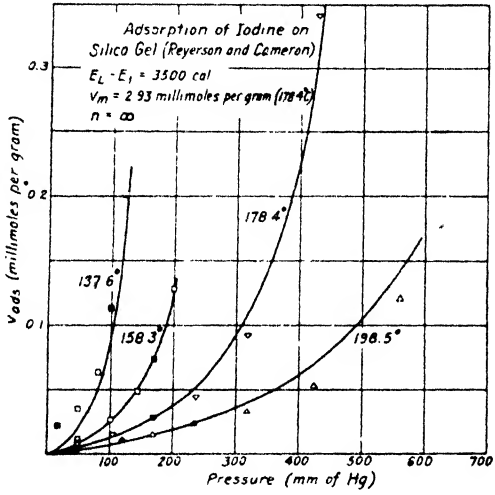

Fig. 10.—Adsorption of iodine by silica gel (Reyerson and Cameron). Isotherms at 137.6°, 158.3° and 198.5° calculated (13) from 178.4° isotherm by equation (10), taking V_m as 2.98 millimoles, $n = \infty$ and $E_L - E_1 = 3500$ cal.

carried out a detailed statistical analysis that takes into account the fact that the last layer of molecules going into a crack will be attracted by the multimolecular layer on both walls and hence will have a heat of adsorption that is Q calories higher than that of the next lower layers. A very complicated equation results that, with considerable labor, can be applied to experimental data. In Fig. 11 is shown the type of fit obtained, for example, when this equation is applied to the data of Lambert and Clark (34) for the adsorption of benzene on

ferric oxide gel. The agreement between the calculated curves and the experimental points is certainly very satisfactory.

It must not be supposed, however, that the above theory constitutes the only or even the most plausible explanation of the

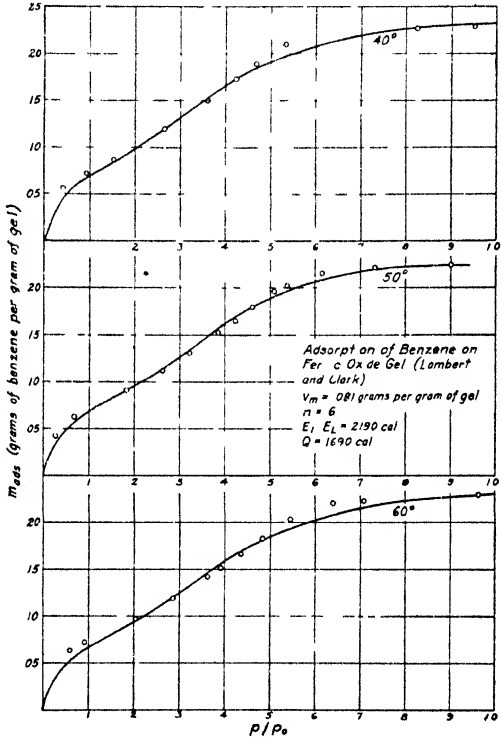

Fig 11 — Adsorption of benzene on ferric oxide gel (Lambert and Clark) The isotherms for 40° and 60° were calculated (13) from the data and constants for the 50° curve.

higher pressure portion of type IV isotherms. Indeed it offers no explanation for the well-known hysteresis that characterizes the desorption of gases and vapors from many porous solids. Other explanations of such type IV isotherms are not lacking in the literature. Foster (26), for example, believes that multilayer adsorption explains satisfactorily the portion of the type IV isotherms in the lower pres-

sure range but that the upper part of the curve is influenced by the existence of capillary condensation. Strictly speaking, there is no very satisfactory basis as yet for comparing the theory of capillary condensation with the above-outlined extension of the multimolecular hypothesis because the theory used in explaining the curves in Fig. 6 assumes plane parallel walls as the boundaries of the adsorption region, an assumption which precludes capillary condensation until the pressure reaches the liquefaction pressure p_0 (16). For cylindrical capillaries to which the capillary condensation theory is usually ap-

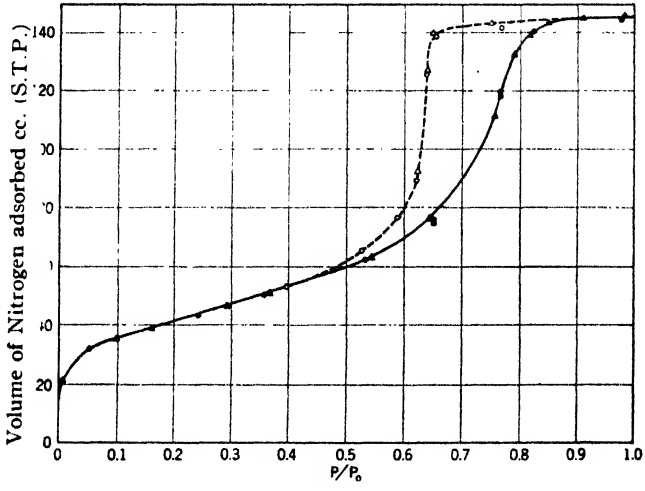

Fig. 12.—The adsorption of nitrogen on porous glass at 79° K.

plied the multilayer hypothesis has not yet been extended to the higher pressure regions.

Cohan (16) has recently pointed out that the well-known hysteresis that usually accompanies type IV isotherms (Fig. 12) gives a definite clue to their possible interpretation. For open-end cylindrical capillaries, he has shown that the relation between the minimum pressure at which capillaries of radius r would fill, in consequence of the deposition of successive layers of the liquid (not by condensation at a meniscus), is given by equation

$$\ln p/p_0 = \frac{-vs}{rRT} \qquad (14)$$

where v represents the molal volume of the condensed adsorbate, s its surface tension and R, T, p and p_0 have their usual significance. On the other hand, in desorption, evaporation must be from a meniscus from which, according to the well-known Kelvin equation, the relation between evaporation and radius r' is

$$\ln p/p_0 = \frac{-2vs}{r'RT} \tag{15}$$

It is evident from equations (14) and (15) that for a given cylindrical capillary the partial pressure of desorption, p_d, should be equal to the

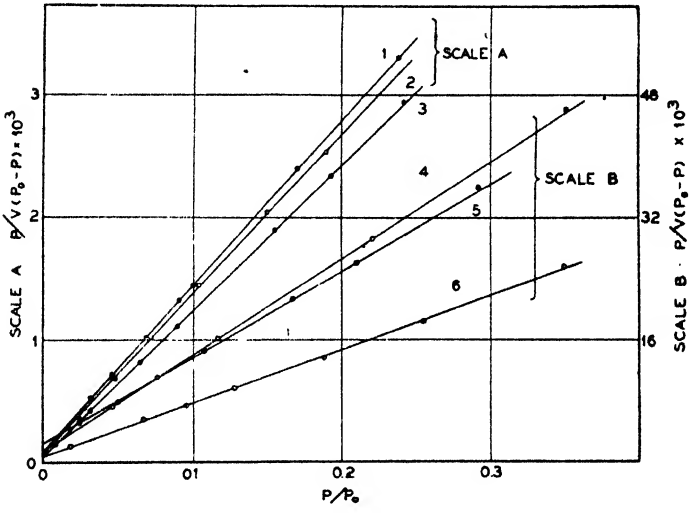

Fig. 13.—Adsorption data for nitrogen on carbon blacks at 79° K. plotted according to equation (10). Curve 1, Wyex; 2, Micronex; 3, Arrow black; 4, Thermax; 5, Thermatomic; and 6, P-33. Weights of samples as in Table IV.

square of the adsorption pressure, p_a. Investigation of some recently obtained isotherms for nitrogen on porous glass* shows that such a relationship between the adsorption and desorption curves exists for adsorption pressures as low as about 0.80 relative pressure. (Fig. 12.)

* To be published.

A reasonable picture of an isotherm (such as shown in Fig. 12) that is consistent with all known phenomena seems to be the following. In the lower part of the curve, multilayer adsorption occurs on all the capillaries that are large enough to permit the adsorption of more than a single layer of molecules. Above a relative pressure which has a definite value for each adsorbate, condensation will occur in open-end cylindrical capillaries of a given radius r according to equation (14) and in various other capillaries according to equation (15). On the larger capillaries multilayers will continue to build up until the point of condensation is reached. The leveling off of the curve at high relative pressures indicates a definite upper limit to the size of the capillaries present. In desorption, the emptying of capillaries can follow equation (15) though Foster suggests that the radius of the

TABLE IV

SURFACE AREA MEASUREMENTS ON CARBON BLACK SAMPLES

Material	Weight, g.	V_m, cc.	Area, sq. m./g.	Diameter of average particle	
				By adsorption, microns	By ultramicroscopic count, microns[a]
Micronex	3.08	75.2	106.7	0.031	0.061
P-33	2.86	14.42	22.12	0.151	0.159
Arrow black	3.29	84.8	112.7	0.029	...
Wyex	2.95	74.2	110.2	0.030	...
Thermax	4.44	7.8	7.69	0.43	...
Thermatomic carbon	5.497	8.54	6.81	0.49	1.12
Acetylene black	0.792	11.68	64.5	0.052	0.130

[a] Gehman and Morris (27).

meniscus must be calculated not from the cross section of the entire capillary but from that portion not occupied by the multimolecular layer expected for the particular relative pressure involved (26). According to the postulates of Cohan (16), hysteresis will be absent and the desorption and adsorption curves will superimpose if the capillaries are wedge-shaped, closed-end cylinders or cylinders having at least one constriction whose diameter is as small as four molecular diameters. It is also possible that incomplete wetting of the capillaries by adsorbate as proposed by Zsigmondy (48) and by Patrick (39) and the existence of conical or bottle-shaped pores as suggested by Kraemer (33) may play a part in hysteresis phenomena.

V. Particle Size Measurements

A fifth type of evidence tending to show the reliability of the low temperature adsorption isotherm method for measuring surface areas is found in some recent studies on carbon black (24), zinc oxide pigments and microscopic glass spheres.* The average particle size, d_3, calculated from the surface area measurements by the equation

$$\text{Area} = \frac{6}{\rho d_3}$$

where ρ is the density of the solid particles, is in excellent agreement with average particle diameters calculated by a variety of other methods. It is, of course, realized that an accurate comparison of particle sizes calculated from the surface area as obtained by adsorption cannot be made with those obtained from microscopic or ultramicroscopic counts until the size distribution curve for the particles in the sample is known (40, 29). For simplicity the influence of shape factors and size distribution curves on the cross-comparisons among the various methods will be neglected.

TABLE V

SURFACE AREA MEASUREMENTS ON ZnO PIGMENTS

	F-1601	K-1602	G-1603	KH-1604
Area by adsorption, sq. m./g.	9.48	8.80	3.88	0.66
Av. particle size, microns				
By direct microscopic count	0.21	0.25	0.49	1.40
By adsorption of methyl stearate	0.19	0.24	0.55	4.50
By ultramicroscopic count	0.135	0.16	0.26	0.82
By permeability	0.12	0.15	0.25	1.25
By adsorption of nitrogen (L)	0.115	0.124	0.28	1.68
By adsorption of nitrogen (S)	0.135	0.145	0.33	1.97

The linear plots for the adsorption isotherms on six standard carbon blacks are shown in Fig. 13. The surface areas and calculated particle sizes of these blacks are summarized in Table IV. In the last column is shown for comparison the average particle size for some of the same commercial black as determined by the ultramicroscopic method (27) about eight years prior to the time at which the samples

* To be published.

were selected for the adsorption runs. The largest deviation is by a factor of about 2.5. Considering that the nitrogen runs and ultramicroscopic measurements were made on samples of the standard blacks purchased at widely separated times, the agreement seems satisfactory.

Two of the six carbon blacks referred to above have been examined by an electron microscope and assigned average particle diameters in remarkable agreement with those deduced from the nitrogen isotherms. The diameter of the average particles of Micronex is 2.8×10^{-6} cm. according to the electron microscope results (40) and 2.8 to 3.1×10^{-6} from the adsorption method, the smaller value being obtained if the carbon density is assumed to be 2.0 and the larger one if it is assumed

TABLE VI

SURFACE AREA MEASUREMENTS ON SIZED GLASS BEADS

Area by adsorption of nitrogen (L)	0.532 sq. m./g.
Av. diameter calculated from adsorption of nitrogen (L)	4.50 microns
Av. diameter calculated from adsorption of nitrogen (S)	5.30 microns
Diam. by microscopic observation	7.00 microns
Area after cleaning the beads with cleaning solution	0.748 sq. m./g.

to be 1.8. Furthermore, in the recent A.S.T.M. symposium on particle size held in Washington, D. C., in March, 1941, it was pointed out that electron microscope values for a commercial acetylene black yield particle diameters of 5.0×10^{-6} cm. compared to the value 5.2×10^{-6} as per Table IV for a density of 1.8. This agreement is certainly very much closer than one would consistently expect, for it must be borne in mind that we have no way of knowing whether the correct value for the area covered by a nitrogen molecule adsorbed on the surface is 16.2 sq. Å., as judged from the density of liquid nitrogen, or 13.8 sq. Å. as judged by the density of solid nitrogen. Even an approximate agreement between the two methods is very reassuring.

Through the courtesy of the New Jersey Zinc Co. it has been possible to compare measurements by several different methods on four standard samples of ZnO pigments. The results of such comparisons are shown in Table V. It will be noted that the average particle sizes as judged by the nitrogen adsorption isotherms are in excellent

agreement with those obtained by permeability measurements (15, 47) and ultramicroscopic counts for samples F-1601, K-1602 and G-1603. The results on sample KH-1604 are really not comparable with each other since the sample is a reheated zinc oxide that was treated differently for the ultramicroscopic tests than for the adsorption runs. The latter runs were made on the sintered oxide; the ultramicroscopic count was made on a sample that has been dispersed in rubber with a resulting breaking up of many of the larger sintered agglomerates. This is discussed in detail in the original paper (24). The particle size values shown in Table VI, as determined by the adsorption of methyl stearate (25) and by direct microscopic count, are a little larger than those obtained by the nitrogen adsorption method. This is not surprising since direct microscopic count will miss some of the smaller particles and adsorption from solution would be expected to give slightly smaller surface areas than adsorption from the gas phase because of the improbability of large organic molecules diffusing into very small cracks or capillaries that might exist.

Still another test of the low temperature adsorption isotherm method for measuring surface areas has been made with the help of a sample of sized glass beads, prepared by Bloomquist and Clark (8). Microscopic examination showed the particles to average about 7 microns in diameter. The surface area of a sample of these beads was determined by the low temperature nitrogen isotherm as 0.532 sq. meters per gram (Table VI). The average particle size, using 2.51 as the density of the beads, calculated to be 4.5 microns if the Area (L) value for the nitrogen molecule is taken and 5.30 if the Area (S) value is taken. In other words, the surface area is a little larger than one would calculate on the basis of the microscopic examination of the beads. This is consistent with the probable etching produced by cleaning the beads with cleaning solution after their preparation. Any roughening or etching of the surface would make the surface area measured by nitrogen adsorption too large and the resulting calculated diameter too small. To show that this was a probable explanation, the beads were given an additional treatment with cleaning solution and were then measured again by nitrogen isotherms. The area was found to be 40 per cent higher after this treatment. Thus, the agreement between the nitrogen adsorption values of Table VI and the microscopic examination becomes excellent if one assumes that the initial treatment with cleaning solution produced about a 40 per cent increase in surface area by slightly etching the glass.

As a final comparison of the adsorption isotherm method with other methods for measuring surface areas, attention is called to the work of Palmer and Clark (38) who determined the adsorption isotherms of acetone, benzene, and other organic vapors on samples of vitreous silica whose total surface area has been measured by comparing the initial rate of solution in hydrofluoric acid with the rate of solution of a known geometric area of the same glass. If one plots the acetone isotherms according to equation (10), one obtains a very good straight line whose slope corresponds to a V_m value of 50.6 micromoles of acetone on a 14.67 g. sample of vitreous silica. The specific surface of this sample was 4690 sq. cm. according to Palmer and Clark's measurements of the rate of solution in HF. If one uses for the area occupied by one acetone molecule on the surface the value 26.9 sq. Å. (which is obtained from the density of liquid acetone at 25°), one obtains from the above V_m value a specific surface of 5640 sq. cm., which is about 20 per cent larger than Palmer and Clark's value. If, on the other hand, one uses for the area occupied by an acetone molecule the value 20.5 sq. Å. obtained by N. K. Adam for close-packed films on water of long chain compounds terminating in the —CO—CH_3 group one obtains for the specific surface 4290 sq. cm., which is about 8 per cent smaller than the value of Palmer and Clark. These data appear therefore to indicate a very good agreement between the two methods, and to confirm further the reliability of the method of measuring surface areas by means of adsorption isotherms of gases taken near their boiling points.

The evidence cited thus far in the present chapter represents the experimental and theoretical basis upon which the method rests. Taken as a whole it appears to leave little doubt as to the wide applicability of the adsorption method to the measuring of surface areas of finely divided and porous materials. It will now be well to summarize briefly some of the applications as well as limitations of the method.

VI. Applications and Limitations of the Method

The applications that have been made of the low temperature isotherm method for measuring the surface areas of iron synthetic ammonia catalysts fall into three groups according to whether they have been related to (*a*) a study of promoter distribution on the catalyst surface, (*b*) a study of the relative activities of the inner

and outer part of the catalyst surface or (*c*) a study of the chemisorption of various gases on iron.

The rapid irreversible chemisorption of carbon monoxide on iron catalysts referred to above has proved very useful. It provided a means of measuring, for the first time, the fraction of an iron catalyst surface covered by promoters (20). In Fig. 14 are reproduced curves showing the total adsorption of carbon monoxide on pure iron, and on iron promoted with potassium oxide and aluminum oxide. The

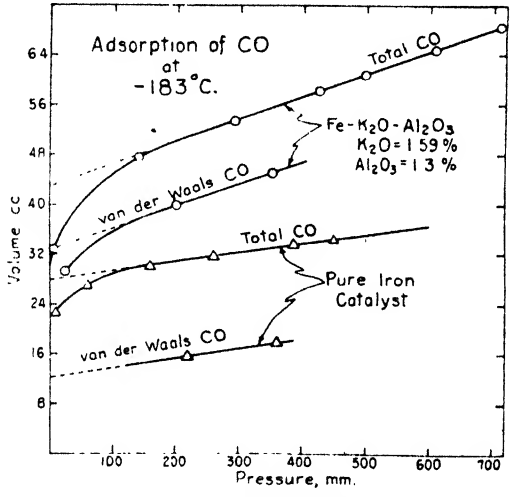

Fig. 14.—Adsorption of carbon monoxide at −183° C. on a doubly promoted and a pure iron catalyst.

difference between the curves marked "total CO" and those marked "van der Waals CO" represents the volume of chemisorbed carbon monoxide in each instance. The small ratio of chemisorbed carbon monoxide to physically adsorbed carbon monoxide in a monolayer on the promoted catalyst in comparison with the approximately 1:1 ratio on pure iron suggests that only about 40 per cent of the surface of the promoted catalyst is made up of iron atoms, about 60 per cent being covered with the one or two per cent of promoter present. This has been discussed in detail elsewhere (14). Experiments on the adsorption of carbon dioxide at −78° on these catalysts confirmed this interpretation relative to the accumulation of promoter in the

surface of the iron catalyst by showing that only the catalysts containing alkali chemisorb appreciable amounts of carbon dioxide (Fig. 15). The volume of this chemisorption is consistent with the interpretation given above relative to the fraction of the surface of a doubly promoted iron catalyst covered with alkali.

A second application (22) of the surface area method to ammonia catalysis has been made in connection with experiments to determine to what extent the "inner" surface is active, compared to the outer or geometric surface. It has been found possible to measure the

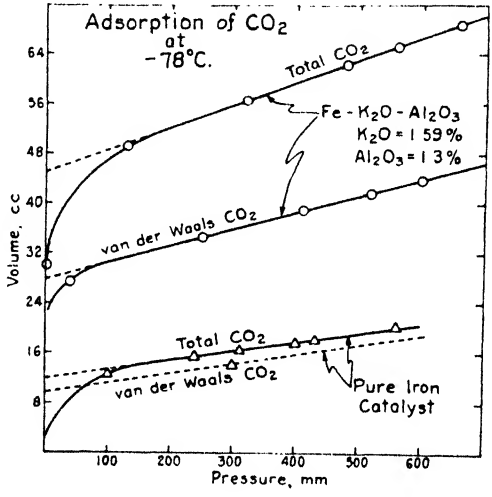

Fig. 15.—Adsorption of carbon dioxide at −78° C. on a doubly promoted and a pure iron catalyst.

activity of an ammonia catalyst of two widely different mesh sizes toward ammonia decomposition and to show that the activity per unit weight of catalyst remains constant, as does the total surface, even though the outer surface changes several-fold. One is led to the conclusion that all of the inner surface or some given fraction of it is able to participate in the ammonia decomposition at a rate substantially the same as that possessed by the outer part of the catalyst.

In a recently published (14) series of experiments on the chemisorption of CO, O_2, N_2, H_2, and CO_2 on iron ammonia catalysts, the measurement of the total surface area and of the fraction of the surface covered by promoter permitted a very intimate picture to be

TABLE VII

SPECIFIC SURFACE OF VARIOUS ADSORBENTS

Adsorbent	Specific surface, sq. m./g.	Adsorbent	Specific surface, sq. m./g.
1. Fe_3O_4 catalyst (unreduced)	0.02	17. NiO catalyst supported on pumice, 89.8% pumice	4.28
2. Fe catalyst 973, sample I (unpromoted). 0.15% Al_2O_3 impurity	0.55	18. Cr_2O_3 gel	228
3. Fe catalyst 973, sample II (unpromoted). 0.15% Al_2O_3 impurity	1.24	19. Cr_2O_3 "glowed"	28.3
4. Fe-Al_2O_3 catalyst 954. 10.2% Al_2O_3	11.03	20. Glaucosil	82
5. Fe-Al_2O_3 catalyst 424. 1.03% Al_2O_3, 0.19% ZrO_2	9.44	21. Silica gel I (non-electrodialyzed)	584
6. Fe-Al_2O_3-K_2O catalyst 931. 1.3% Al_2O_3, 1.59% K_2O	4.78	22. Silica gel II (electrodialyzed)	614
7. Fe-Al_2O_3-K_2O catalyst 958. 0.35% Al_2O_3, 0.08% K_2O	2.50	23. Dried bacteria	0.17
8. Fe-K_2O catalyst 930. 1.07% K_2O	0.56	24. Dried bacteria (pulverized)	3.41
9. Cecil soil, 9418	32.3	25. KCl (finer than 200 mesh)	0.24
10. Cecil soil, colloid, 9418	58.6	26. $CuSO_4.5H_2O$ (40–100 mesh)	0.16
11. Barnes soil, 10,308	44.2	27. $CuSO_4$ anhydrous	6.23
12. Barnes soil, colloid, 10,308	101.2	28. Granular Darco B	576
13. Fused copper catalyst	0.23	29. Granular Darco G	2123
14. Commercial copper catalyst	0.42	30. Cement	1.08
15. Pumice	0.38	31. Cuprene	20.7
16. Ni catalyst supported on pumice, 91.8% pumice	1.27	32. Paper	1.59
		33. $ZrSiO_4$	2.76
		34. Graphite	30.73
		35. TiO_2	9.88
		36. $BaSO_4$	4.30
		37. Lithopone—before calcining and grinding	34.8
		Lithopone — calcined but not ground	1.37
		Lithopone — calcined and ground	3.43
		38. Porous glass	125.2

Examples 1 to 29 are from References (11) and (21); 30 to 37 from Reference (24); and 38 from unpublished work.

obtained of the relative disposition of the various adsorbed gases on the metal surface. Similar experiments on steel sheets recently undertaken by Armbruster and Austin (1) appear to be very promis-

ing and ought to reveal a great deal of information in regard to the adsorption and diffusion of gases through steel. The use of low temperature nitrogen isotherms in studying surface areas has now been extended to a variety of materials. These include paint pigments, inorganic salts, clays, carbon black, soils, soil colloids, cement, cuprene, paper, iron catalysts, copper catalysts, supported nickel catalysts, bacteria, porous glass, glass beads, powdered glass, powdered silver, as well as a number of metals and alloys, including tungsten powder, Fe-Co, Fe-Ni, Co-Ni, Pd and Ag-Pd. A partial list of such determinations is shown in Table VII. The correlations

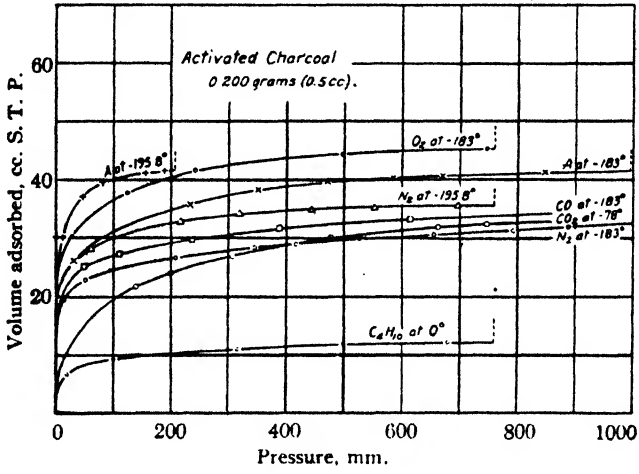

Fig. 16.—Low temperature adsorption isotherms on charcoal.

that have been effected between the surface areas and properties of industrial products are for the most part not as yet published. In the field of carbon blacks, however, a paper by Smith, Thornhill and Bray (46) has shown some very interesting results obtained by measuring the surface area of the carbons by the nitrogen adsorption method. Up to the present time the method has been applied successfully in the author's laboratory to more than five hundred different samples of solids. In addition, it is known that similar measurements are being made by a number of industries.

On only two substances have the low temperature nitrogen adsorption isotherms failed to show the characteristic S-shape illustrated in Figs. 2 and 3. On a sample of coconut shell charcoal (Fig. 16)

a Langmuir type curve has been found (11). The corresponding Langmuir plots are given in Fig. 17. On partially dehydrated chabazite the method has been found inapplicable. In some work as yet unpublished, it has been shown that a sample of chabazite 50 per cent dehydrated by evacuation at about 100° C. will adsorb hydrogen at 77° K. and nitrogen at 195° K., but no nitrogen at 77° K. The capillaries in this instance seem to be so small that nitrogen molecules at liquid nitrogen temperature cannot enter. With chabazite that is 95 to 100 per cent dehydrated, nitrogen iso-

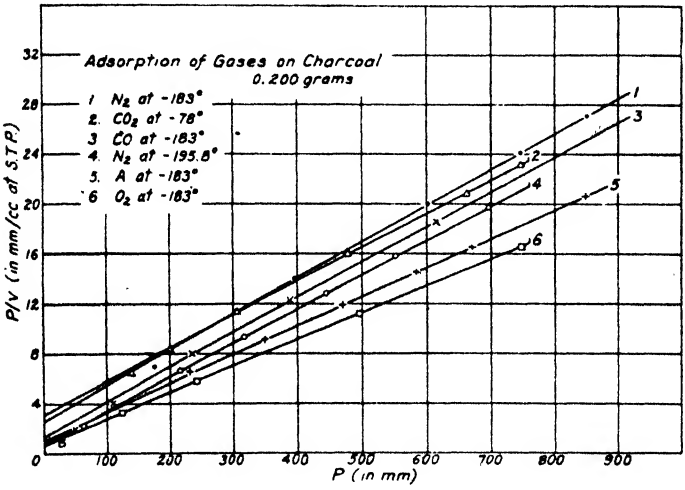

Fig. 17.—Linear plots, according to equation (13), of low temperature adsorption data for gases on charcoal.

therms are obtained that resemble those for charcoal. However, there is one marked difference between the adsorption characteristics of charcoal and chabazite: no butane is adsorbed by a sample of chabazite that is able to adsorb about 200 cc. of nitrogen per gram. This conforms to the experiments of Schmidt (45) who showed that dehydrated chabazite was capable of adsorbing only small molecules. Charcoal, on the other hand, adsorbs about 80 per cent as much butane as one would expect from the size of the butane molecules, compared to N_2, A, O_2 and similar gases.

In conclusion it may be well to bring up to date a recent critical discussion (17) of all isotherms as regards their conforming to the theory of multilayer adsorption. Barrett, Birnie and Cohen (5)

have recently obtained S-shaped curves for the adsorption of water vapor on crushed fused silica. The isotherms of Armbruster and Austin (1) for the adsorption of ethyl iodide by steel are likewise S-shaped, though the upper pressure limit of their runs was only a small fraction of the saturation pressure. Orr (36) has recently made a number of experimental determinations of the adsorption of O_2, A and N_2 on surfaces of alkali halides to test certain theoretical conclusions that he has reached (37) relative to the heats and nature of the adsorption on these materials. His results and calculations appear to give an excellent picture of the low temperature adsorption on alkali halides; the experiments appear to confirm his theoretical conclusions. His experimental isotherms are definitely S-shaped and indicate the formation of multimolecular layers on the non-porous halide crystals. Askey and Feachem (2) point out that argon can be used for measuring the relative surfaces of a given kind of material by comparing the zero pressure extrapolations of the long linear portions of the S-shaped adsorption isotherms, such as illustrated in Fig. 2. In fact, their procedure is equivalent to comparing the point A values on the various isotherms (see Fig. 2). According to them, this method was used by the I.C.I. (Alkali) Limited for about five years before their 1938 publication. Bangham and Mosallam (3) determined the adsorption of benzene vapor on smooth squares of mica of known geometric area. Their isotherms are S-shaped and yield point B values that appear consistent with the expected adsorption of benzene, 0.3 cc. of vapor being adsorbed as a monolayer by about 1.8 sq. meters of surface. In some of their experiments, superimposed upon the general S-shape of the isotherms is a series of breaks similar to those that have been reported by a number of workers. The explanation of such minor breaks is not at present clear. These breaks, together with minor irregularities in the shapes of the S-shaped curves that have been mentioned in the literature from time to time, must, it seems, all eventually be accounted for by suitable refinement of the general theory that explains the over-all shape of the isotherms.

Only a few isotherms have been reported that would definitely not fit into any of the five types of isotherms shown in Fig. 8. A paper by Harbard and King (30) presents a number of isotherms obtained for the adsorption of CCl_4 on chromium oxide that are extremely hard to understand. Some of them seem to show no multilayer formation but break directly at a relative pressure of about 0.5 from

monolayer adsorption into what the authors term capillary condensation. These results are, accordingly, extremely baffling if real. The measurements of Barrer (4) on the adsorption of H_2, N_2 and NH_3 on various zeolites give Type I isotherms similar to those obtained by Dr. Thomas DeWitt and the author on chabazite.* The curves appear to conform to the modification of equation (11) that has been obtained when $n = 1$. Borghs and Itterbeek (32) measured the adsorption of nitrogen, neon and hydrogen at low temperature on sheets of electrolytic copper whose geometric surface areas were known. The measurements were carried up to only a small fraction of the saturation pressure so that it is impossible to judge the true surface area of their samples. However, the curves for neon and nitrogen were clearly for physical adsorption and were not inconsistent with the S-shaped curves. The conclusion that they reach to the effect that, even at the low relative pressure used, 7 and 11 layers, respectively, of nitrogen and neon are formed definitely depends upon the sample being non-porous. The authors are careful to state that these calculations are based on the "apparent macroscopic surface." It would seem that the true surface of the copper samples is larger than the macroscopic surface, by a factor of more than 10, since it seems certain that under the experimental conditions as much as a monolayer of neither nitrogen nor neon was formed.

In conclusion, it may be well to tabulate the possible uses and limitations of the method that have been described in the present chapter for measuring the surface area and particle size of colloids or other porous or finely divided solids. The following characteristics of the method should be kept in mind by those contemplating its use:

1. It can be used for measuring the surface areas of either porous or non-porous solids, but can yield values for the particle size only if the material is non-porous. Furthermore, in order to calculate accurately the particle size from the surface area, one must know the true density of the solid, must make assumptions relative to the influence of shape factors (29) and must know the approximate shape of the size distribution curve (40, 33a).

2. The method as described in the present chapter is limited to solids with a sufficiently large surface area to yield an adsorption value well beyond the experimental errors involved. This means that a sample of 50 cc. of the finely divided solid should have a total

* To be published.

surface area of at least 20,000 sq. cm., corresponding to non-porous particles smaller than about 20 microns. There is no known lower limit to the particle size to which the method can be applied, although up to the present the smallest particles studied by the author have been Micronex carbon black (about 0.031 microns in diameter).

3. Modifications of the method to make it applicable to samples having smaller surface areas have been carried out by using as a measuring gas some substance that at the temperature of the runs has a vapor pressure lower than 1 mm. and by employing high vacuum technique. Such work has already been published recently by Armbruster and Austin (1) who measured the adsorption of ethyl iodide on steel sheets at room temperature.

4. Layers of chemisorbed nitrogen, oxygen, carbon monoxide and similar impurities will not, it has been found, alter appreciably the volume of an inert gas needed to form a monolayer on a finely divided solid. Of course, if a material contains a sufficient number of very small pores, it is conceivable that such chemisorbed gases might effectively block some of the capillaries and thus change the apparent surface area of the sample. It should be kept in mind in this connection that the gas used for the adsorption measurements should be entirely inert toward the solid adsorbent; otherwise a mixture of chemisorption, physical adsorption and possibly chemical reaction will all be involved.

5. One must expect the surface areas of porous materials as measured by gas adsorption to depend somewhat upon the size of the molecules of adsorbate since the smallest capillaries can probably not be entered by larger molecules. For non-porous finely divided solids this factor should be of little importance except in so far as large molecules may, as a rule, be adsorbed in several different orientations and may therefore entail some uncertainty as to the actual area covered by each adsorbed molecule.

6. Due cognizance must be taken of liquid water or other substances that may be clogging the capillaries of porous solids. Evacuation at temperatures sufficiently high to remove such condensates must be employed if the total surface area of the porous solid is desired. Unfortunately it may sometimes be impossible to remove such liquid films without altering the structure of the solids. Evacuation at 110° C. to remove water sometimes produces a larger surface and sometimes a smaller one than if the evacuation had been carried out at 25° C. (23).

7. The method is believed to be applicable to all systems in which the isotherm near the boiling point of the adsorbate is S-shaped. Fortunately on only two substances, charcoal and chabazite, have Langmuir type isotherms been encountered for such physical adsorption up to the present time even though hundreds of samples of various materials have been studied. Even with physical adsorption isotherms of the Langmuir type a value of V_m can be obtained by plotting the data according to equation (13), but up to the present time the selection of V_m in this way seems open to question, especially in those instances in which the pore size does not seem to be small enough to cause the adsorption to be restricted to a single layer.

8. The six or seven independent types of evidence that seem to support the proposed method for measuring surface areas by low temperature adsorption isotherms lend a feeling of security to its employment. However, the author prefers to consider the method as still being in its test period and hopes that all users will be critical of it and will employ it with care.

Bibliography

1. M. H. Armbruster and J. B. Austin, *J. Am. Chem. Soc.*, **61**, 1117 (1939).
2. P. J. Askey and C. G. P. Feachem, *J. Soc. Chem. Ind.*, **57**, 272 (1938).
3. D. H. Bangham and S. Mosallam, *Proc. Roy. Soc. London*, (A)**166**, 558 (1938).
4. R. M. Barrer, *Proc. Roy. Soc. London*, (A)**167**, 393 (1938).
5. H. M. Barrett, A. W. Birnie and M. Cohen, *J. Am. Chem. Soc.*, **62**, 2839 (1940).
6. A. F. Benton, *Ibid.*, **48**, 1850 (1926).
7. A. F. Benton and T. A. White, *Ibid.*, **54**, 1820 (1932).
8. C. R. Bloomquist and A. Clark, *Ind. Eng. Chem., Anal. Ed.*, **12**, 61 (1940).
9. R. S. Bradley, *J. Chem. Soc.*, **1936**, 1799.
10. S. Brunauer and P. H. Emmett, *J. Am. Chem. Soc.*, **57**, 1754 (1935).
11. S. Brunauer and P. H. Emmett, *Ibid.*, **59**, 2682 (1937).
12. S. Brunauer, P. H. Emmett and E. Teller, *Ibid.*, **60**, 309 (1938).
13. S. Brunauer, L. S. Deming, W. E. Deming and E. Teller, *Ibid.*, **62**, 1723 (1940).
14. S. Brunauer and P. H. Emmett, *Ibid.*, **62**, 1732 (1940).
15. P. C. Carman, *Trans. Inst. Chem. Engrs. London*, **15**, 150 (1937); *J. Soc. Chem. Ind.* (Transactions), **57**, 225 (1938); *Ibid.*, **58**, 2 (1939). Permeability measurements on ZnO pigments are from a private communication.
16. L. H. Cohan, *J. Am. Chem. Soc.*, **60**, 433 (1938).
17. Committee on Catalysis, National Research Council, 12th Report, Chap. V, John Wiley and Sons, New York, 1939.
18. J. H. de Boer and C. Zwikker, *Z. physik. Chem.*, (B)**3**, 407 (1929).
19. J. H. de Boer and C. F. Dippel, *Ibid.*, (B)**25**, 399 (1934).

20. P. H. Emmett and S. Brunauer, *J. Am. Chem. Soc.*, **59**, 310 (1937).
21. P. H. Emmett and S. Brunauer, *Ibid.*, **59**, 1553 (1937).
22. P. H. Emmett and S. Brunauer, *Trans. Electrochem. Soc.*, **71**, 383 (1937).
23. P. H. Emmett, S. Brunauer and K. Love, *Soil Sci.*, **45**, 57 (1938).
24. P. H. Emmett and T. DeWitt, *Ind. Eng. Chem., Anal. Ed.*, **13**, 28 (1941).
25. W. W. Ewing, *J. Am. Chem. Soc.*, **61**, 1317 (1939).
26. A. H. Foster, *Proc. Roy. Soc.*, (A)**150**, 77 (1935); *Trans. Faraday Soc.*, **28**, 645 (1932).
27. S. C. Gehman and T. C. Morris, *Ind. Eng. Chem., Anal. Ed.*, **4**, 157 (1932).
28. F. Goldmann and M. Polanyi, *Z. physik Chem.*, **132**, 321 (1928).
29. H. Green, *J. Franklin Inst.*, **204**, 713 (1927).
30. E. H. Harbard and A. King, *J. Chem. Soc.*, **1940**, 19.
31. I. Higuti, *Bull. Inst. Phys. Chem. Research Tokyo*, **19**, 951 (1940).
32. J. Borghs and A. van Itterbeek, *Physica*, **7**, 17 (1940).
33. E. O. Kraemer, *A Treatise on Physical Chemistry.* Edited by H. S. Taylor. D. Van Nostrand Co., New York, 1931, Chap. XX, p. 1661.
33a. E. O. Kraemer, *J. Franklin Inst.*, **231**, 1 (1941).
34. B. Lambert and A. M. Clark, *Proc. Roy. Soc. London*, (A)**122**, 497 (1929).
35. I. Langmuir, *J. Am. Chem. Soc.*, **38**, 2221 (1916).
36. J. C. Orr, *Proc. Roy. Soc. London*, (A)**173**, 349 (1939).
37. J. C. Orr, *Trans. Faraday Soc.*, **35**, 1247 (1939).
38. W. G. Palmer and R. E. D. Clark, *Proc. Roy. Soc. London*, (A)**149**, 360 (1935).
39. W. H. Patrick and J. McGavack, *J. Am. Chem. Soc.*, **42**, 946 (1920).
40. A. Prebus and Columbian Carbon Co., *Columbian Colloidal Carbons*, Vol. II, *The Particle Size and Shape of Colloidal Carbon as Revealed by the Electron Microscope*, 1940; *Ind. Eng. Chem., News Edition*, **18**, 492 (1940).
41. K. S. Rao, *Current Sci.*, **9**, 70 (1940).
42. L. H. Reyerson and A. E. Cameron, *J. Phys. Chem.*, **39**, 181 (1936).
43. L. H. Reyerson and A. W. Wishart, *Ibid.*, **41**, 943 (1937).
44. W. W. Russel and H. S. Taylor, *J. Phys. Chem.*, **29**, 1325 (1925).
45. O. Schmidt, *Z. physik Chem.*, **133**, 265 (1928).
46. W. R. Smith, F. S. Thornhill and R. I. Bray, *Ind. Eng. Chem.*, **33**, 1303 (1941).
47. R. R. Sullivan and K. L. Hertel, this volume, p. 37.
48. R. Zsigmondy, *Z. anorg. Chem.*, **71**, 356 (1911).

THE PERMEABILITY METHOD FOR DETERMINING SPECIFIC SURFACE OF FIBERS AND POWDERS

R. R. SULLIVAN AND K. L. HERTEL

University of Tennessee, Agricultural Experiment Station, Knoxville, Tennessee

CONTENTS

I. Introduction

A knowledge of the amount of surface associated with a given volume of a finely divided material is of first importance in many processes. For instance: rates of solution, rates of chemical activity, coverage of pigments, "finish" of lacquers, "setting" of cement, frictional forces on fibers in yarn, adsorption of dyes, filtering action of a granular bed—these all depend to a considerable extent upon the specific surface of the finely divided phase of the material. The great need for satisfactory methods of measuring particle surface rather than an "equivalent particle size" has become more and more evident in technical literature during the last few years.

During the past decade much progress has been made in the interpretation of results of fluid flow through porous media, particularly with regard to the correlation of the permeability and the specific surface of the media. Permeability measurements now appear to provide a method of specific surface determination which is satisfactory in many respects.

In this chapter certain aspects of the theory underlying the flow of fluids through porous media will be reviewed. Data of various workers will be given to show the validity and range of the equations developed for the determination of the specific surface from permeability measurements. Certain aspects of the experimental technique will be considered and desirable precautions pointed out. An attempt has been made to make the list of references at the end of the chapter fairly complete.

II. Theoretical Considerations

The mathematical difficulties involved in obtaining a rigorous and detailed solution of the hydrodynamical equations for the general case of fluid flow through porous media have remained insurmountable. The equations used for relating the flow to the properties of the media have therefore been obtained either by approximate solutions of the hydrodynamical equations or by the correlating of experimentally determined relationships with theoretical deductions based on qualitative reasoning. An excellent review of the whole field has been given by Carman (24, 25, 26), who has also supplied many data for confirmation of the relationships obtained.

Two different types of flow are recognized for smooth straight channels: (1) *viscous flow*, (2) *turbulent flow*. For viscous flow, sometimes called *laminar flow*, the fluid elements flow along fixed *streamlines* which are parallel to the walls of the channel. For turbulent flow, however, the streamline pattern is broken up, and the fluid elements flow through the channel in an irregular manner. The only forces to be overcome in viscous flow are those of the internal friction of the fluid, whereas, for turbulent flow, inertial forces dominate. Since viscous forces depend upon the first power of the fluid velocity (relative to the channel boundary), and inertial forces depend upon the second power of the velocity, the two types of flow in straight channels may be characterized by this dependence.*

However, when the flow is through a curved channel, a channel of non-uniform cross section or a bed of granular particles, the flow may still follow a fixed streamline pattern (laminar flow) and yet not be purely viscous, since inertial forces are involved in the movement of

* Except for rough channels, turbulent flow in actual pipes where viscous forces are still present usually results in the changing of the pressure gradient approximately with the 1.75 power of the velocity (88).

the fluid along the curved streamlines. For this reason, the drawing of analogies between flow through porous media and flow through straight channels, such as pipes of constant cross section, has been criticized by certain workers (6).

Perhaps the most fundamental law regarding the flow through porous media is the empirical relation deduced by Darcy, in 1856, from measurements of the flow of water through sand and through sandstone (34). His law expressed in equation form is

$$Q = K_1 A \frac{\Delta p}{L} \tag{1}$$

where Q is the volume rate of flow through the bed, Δp is the pressure drop across the bed, A is the area of the bed and L is the depth of the bed. The similarity between Darcy's law for porous media and the Hagen-Poiseuille law for viscous flow through a circular capillary,

$$Q = \frac{r^2 A}{8\mu} \frac{\Delta p}{L} \tag{2}$$

where r is the capillary radius and μ is the coefficient of viscosity, makes it appear profitable to disregard the objections raised in the last paragraph, and to draw further comparisons between flow through porous media and flow through straight channels. As will appear later, these comparisons prove highly valuable where the flow is viscous.

The law of mechanical similarity, or the equivalent method of dimensional analysis introduced by Osborne Reynolds (94), has been useful in representing the character of flow through pipes, both for laminar and for turbulent flow. The law of mechanical similarity states that two different motions taking place in two geometrically similar vessels are mechanically similar when they have the same value for the ratio of inertial force to frictional force at points similarly situated with respect to the two vessels.* The ratio of the inertial to the frictional force becomes $(\rho/\mu)Va$ (see, for instance, Prandtl and Tietjens, "Applied Hydro- and Aero-Mechanics," p. 8), where ρ is the fluid density, μ is the coefficient of viscosity, V is the fluid velocity and a is a characteristic linear dimension associated with the geometry of the vessel. For pipes, a is taken as the radius of the pipe and V the macroscopic velocity of flow. The expression $(\rho/\mu)Va$ is called

* Gravitation and other body forces are neglected in this formulation.

Reynolds' number after Osborne Reynolds, and is denoted by R. Reynolds' number, being the ratio of two forces, is a dimensionless quantity and is therefore independent of the units used. Reynolds' number, therefore, applies equally well to large and to small systems which are geometrically similar. Thus, "if in two different flows around geometrically similar bodies the quantity $(\rho/\mu)Va$ is the same, it is to be expected that the streamlines themselves are also geometrically similar" (92). Hence, for geometrically similar channels or vessels the character of the flow is determined by Reynolds' number, R. For smooth pipes it is found that small initial disturbances are damped out and the flow through pipes becomes laminar for values of R equal to or less than about 1000. The smallest value of R for which turbulence is maintained is called the critical value of Reynolds' number. Where great care is exercised in avoiding the initial disturbances at the entrance and also disturbances at the exit of a pipe critical values of R as high as 20,000 or higher have been observed (92).

The dimensionless character of R and its usefulness in representing types of flow have led to the formation of other dimensionless groups associated with flow (14, 15, 63, 102, 104, 113, 128, 131). A common procedure has been to plot on logarithmic paper the dimensionless group $a\Delta p/2\rho L V^2$, called the *friction factor*, as a function of Reynolds' number, R. Due to the dimensionless character of the quantities plotted, a unique curve is obtained for all channels or vessels of similar geometry. From the Hagen-Poiseuille law for capillaries and the Darcy law for porous media it is observed that, in either case where viscous flow is present, one should have the friction factor inversely proportional to Reynolds' number, and that when the flow is no longer viscous the simple inverse proportionality should no longer hold. Setting the friction factor inversely proportional to R,

$$K''\left(\frac{a\Delta p}{2\rho L V^2}\right) = R^{-1} = \frac{\mu}{\rho}\frac{1}{Va}$$

$$V = \frac{K''a^2}{2\mu}\frac{\Delta p}{L}; \quad \text{also } Q = A'V = \frac{K''a^2A'}{2\mu}\frac{\Delta p}{L} \tag{3}$$

which agrees with either the Hagen-Poiseuille or the Darcy law, although it amplifies the Darcy law somewhat. A' is the cross-sectional area open to flow and is proportional to A for homogeneous porous media. The K'' depends upon the type of geometry of the channel,

but on the basis of the law of mechanical similarity it should be constant for any particular type of geometry. Tests over wide ranges have shown this to be the case. Thus, if the friction factor is plotted against Reynolds' number on logarithmic paper it should yield a straight line of slope -1, for cases of viscous flow. Curves for all

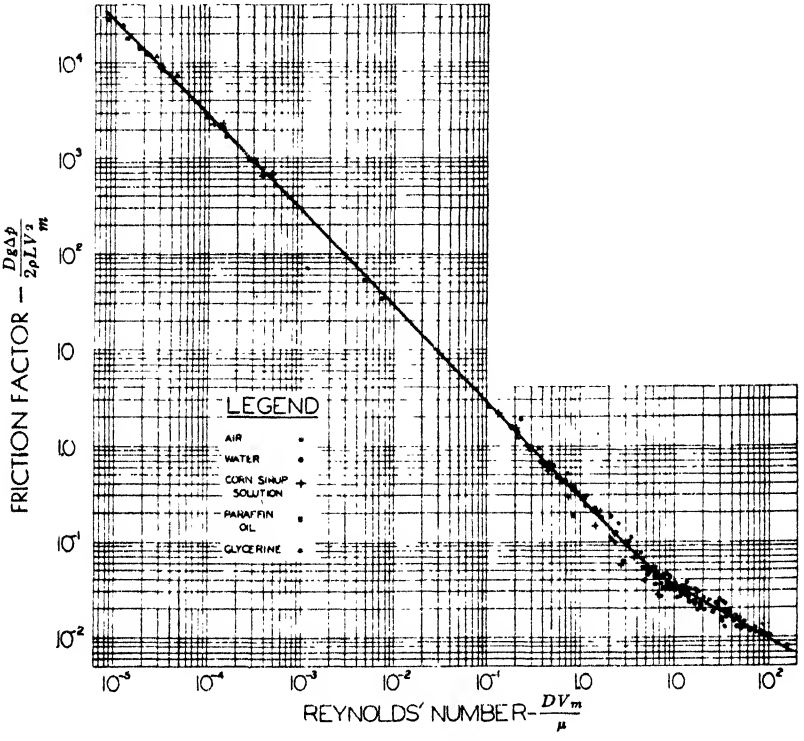

Fig. 1.—Friction factor *vs.* Reynolds' number for porous carbon. D = mean effective pore diameter, ft.; g = acceleration of gravity = 32.2 ft./sec.^{2}; Δp = pressure drop, lb./in.^{2}; ρ = fluid density, lb./ft.^{3}; L = thickness of porous medium, ft.; V_m = mean fluid velocity, ft./sec.; μ = viscosity, lb./ft.-sec.

channels having the same value of K'' will be coincident. Figure 1, reproduced from the work of Hatfield (59), shows such a curve for the flow of various fluids through different samples of porous carbon. A range of fluid density of 1140 fold, a viscosity range of 31,000 fold, a sample thickness of 5 fold, a pore diameter of 40 fold, a pressure difference of 214 fold and a superficial velocity range of 600,000 fold were

covered by the data plotted in Fig. 1. The excellent agreement of the points with the straight-line portion of the curve is at once proof of the relationship expressed by equation (3) for viscous flow, and also is indicative of the essential constancy of K'' for the samples of porous carbon used in the experiment. It appears from this curve that the value of R for which the flow through porous carbon ceases to be viscous is about $R = 4$.

For porous media, equation (3) is frequently written

$$Q = \frac{KA}{\mu} \frac{\Delta p}{L} \tag{4}$$

The K of equation (4) now is defined as the *permeability* of the medium and is equal to the "volume of a fluid of unit viscosity passing through a unit cross section of the medium in unit time under the action of a unit pressure gradient" (88).

When equation (3) is to be applied to straight channels of non-circular cross section, the radius of the channel can no longer be used for the characteristic linear dimension associated with the cross section of the channel. It has become customary in such cases to use the *mean hydraulic radius*, m, as the characteristic linear dimension. The mean hydraulic radius is by definition the cross-sectional area normal to flow divided by the perimeter presented to fluid, or, alternatively, m is the volume of fluid in the channel divided by the surface presented to the fluid. Equation (3) may then be written for the case of flow through a straight channel,

$$V = \frac{m^2}{k_0 \mu} \frac{\Delta p}{L} \tag{5}$$

where V is the macroscopic velocity of flow through the channel and k_0 is a dimensionless quantity, called a shape factor, which depends only upon the shape of the channel.

In general, k_0 must be found by experiment. There are, however, several special cases for which the value of k_0 may be determined rigorously from the laws of hydrodynamics and viscosity. Examples of these special cases are (1) smooth circular pipes and (2) pipes with cores. One special case of particular interest in connection with porous media is that treated by Emersleben (38), where the channel was comprised of the inter-spaces in a bed of long equally spaced cylinders. The multiply connected channel thus formed has more in common with the multiply connected region in a porous medium than do the simply connected channels of pipes. Emersleben's treatment

(38), consisted in solving the hydrodynamical equations for the viscous flow of an incompressible fluid through the bed of cylinders parallel to their axes, where the equally spaced cylinders were all alike and nearly circular in cross section. From his solution, values of the shape factor k_0 for different relative spacings of the cylinders have been determined (114). Curve A of Fig. 2 gives values of k_0 for different porosities of the arrangement. Table I gives values of k_0 for various singly connected channels.

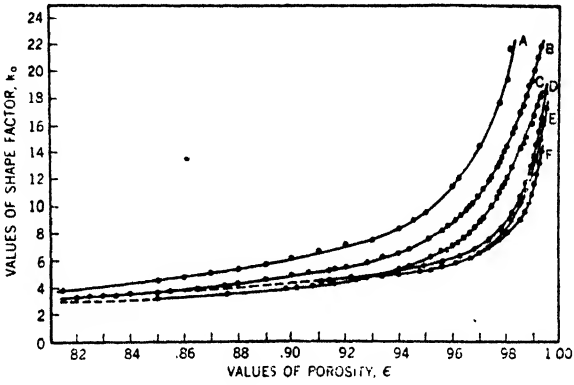

Fig. 2.—Shape factors are shown for different values of porosity. Curve A is for the theoretical case treated by Emersleben. Curves B, C, D, E and F are experimental curves for Welsh wool, fine noil wool, B-38-$^7/_8$-in. cotton, B-38-$1^3/_{16}$-in. cotton and Sea Island-C-38 cotton, respectively.

When attempting to compare the viscous flow through porous media with the laminar flow through straight channels, one is at once confronted with the situation that the streamlines for the flow through a porous medium are in general not straight but represent tortuous paths through the inter-spaces in the medium. It would appear, however, that for the flow which follows Darcy's law, inertial effects are quite negligible, and the chief effect of the tortuosity of the flow paths is to divert the directions of microscopic flow away from the direction of macroscopic flow and hence away from the direction of the applied pressure gradient. Since equation (5) holds for viscous flow through the multiply connected channel of the Emersleben case, it might be expected to hold for the viscous flow through a cylindrically confined porous medium where the inter-connected void of the

medium constitutes the multiply connected channel. The net rate of flow in the direction of the cylinder axis along which the pressure gradient is applied would be somewhat modified, however, by the tortuosity of the streamlines.

Consider a streamline at a point P (Fig. 3) making an angle θ with the x-direction (taken as the direction of the cylinder axis) and hence with the applied pressure gradient, $\Delta p/L$. The pressure gradient will have a component $(\Delta p/L) \cos \theta$, along the streamline. The actual velocity along the streamline must furthermore be multiplied by $\cos \theta$ to obtain its x-component. Thus the x-component of the velocity

TABLE I

VALUES OF k_0 FOR STREAMLINE FLOW IN VARIOUS CROSS SECTIONS[a]

Shape	k_0	Remarks
1. Circle	2.0	Hagen-Poiseuille's law
2. Ellipses		
(*a*)	2.13	Major axis = 2 × minor axis
(*b*)	2.45	Major axis = 10 × minor axis
3. Rectangles		
(*a*)	1.78	Length = breadth
(*b*)	1.94	Length = 2 × breadth
(*c*)	2.65	Length = 10 × breadth
(*d*)	3.00	Length = infinite
4. Triangle	1.67	Equilateral
5. Pipes with cores		
(*a*)	2.0–3.0	Cores set concentrically
(*b*)	1.7–3.0	Cores set eccentrically (eccentricity < 0.7)
(*c*)	1.2–2.0	Cores set eccentrically (eccentricity > 0.7)

[a] These values taken from Carman's paper (24).

of flow at the point P will be $\cos^2 \theta$ times what it would have been had the streamlines not been tortuous. (In this connection see Fowler and Hertel (47).) Thus if equation (5) is to give the over-all axial rate of flow through the void in a cylindrically contained porous medium, its right-hand member should contain $<\cos^2 \theta>_{AV}$ as a factor, where $<\cos^2 \theta>_{AV}$ is the average value of $\cos^2 \theta$ for all points P throughout the medium. The exact orientations of the streamlines are not known except in the trivial case of flow through a straight channel. It appears likely from symmetry considerations, however,

that where inertial effects are negligible the value of $\langle \cos^2 \theta \rangle_{AV}$ will be well represented by the value of $\zeta \equiv \langle \sin^2 \phi \rangle_{AV}$ where $\langle \sin^2 \phi \rangle_{AV}$ is the average of $\sin^2 \phi$ over the whole of the fluid-solid interface, ϕ being the angle a normal to the interface makes with the x-direction.

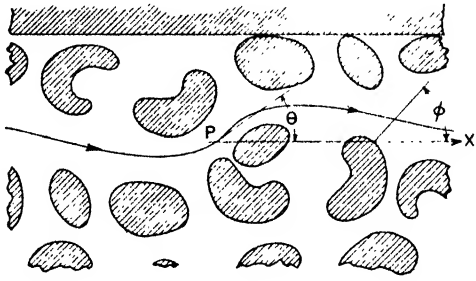

Fig. 3.—A portion of a cylindrically contained porous medium. The x-direction is parallel to the axis of the cylinder. The direction of the streamline at point P makes an angle θ with the x-direction. ϕ is the angle between a normal to the fluid-solid interface and the x-direction.

In adapting equation (5) for flow through a porous medium, the alternative definition of m is used. Thus, m is the volume of void divided by the total surface of particles. Let ϵ be the *porosity* of the medium, defined as the total volume of void divided by the gross space occupied by medium. Then $m = \epsilon/S_0 (1 - \epsilon)$, where S_0 is by definition the *specific surface* of the particles and is their total surface divided by their total volume. The rate of volume flow Q through the medium will be $A\epsilon V$ where A is the area of cross section and V is the average value of the x-component of velocity in the interspaces of the medium. This presupposes the medium to be of such a nature that the ratio of open area to total area in a cross section is sensibly constant and the same as the ratio of void volume to total volume occupied by the medium. With the foregoing considerations imposed on equation (5), the relationship for viscous flow of an incompressible fluid through a porous medium becomes

$$Q = \frac{A}{\mu S_0^2} \cdot \frac{\zeta \Delta p}{k_0 L} \cdot \frac{\epsilon^3}{(1 - \epsilon)^2} \qquad (6)$$

Equation (6) is a relationship which has come into fairly extensive use in the study of flow through porous media where, however, in most cases the disentanglement of the orientation factor ζ and the shape factor k_0 has not been accomplished, but rather a proportionality factor k ($=k_0/\zeta$ in this case) has been used to care for the combined effect of both quantities. The value of the development here given, where k has been separated into k_0 and $1/\zeta$, is twofold: On the one hand, a physical picture of the viscous flow through porous media and its relationship to laminar flow through straight channels is given; on the other hand, the flow through media where the particles have preferred orientations appears to verify experimentally the correctness of the orientation factor (114, 115). The usefulness of the separation of k into k_0 and $1/\zeta$ hinges upon the fact that k_0 as so used is practically constant and numerically equal to 3 for several multiply connected channels of practical interest.

In the work where orientation factors were not introduced, the equation for flow corresponding to equation (6) was

$$Q = \frac{A}{\mu S_0^2} \frac{1}{k} \cdot \frac{\Delta p}{L} \frac{\epsilon^3}{(1-\epsilon)^2} \tag{7}$$

Equation (7) is equivalent to the relationship arrived at by Kozeny in 1927 and by Fair and Hatch in 1933. Kozeny obtained the relationship by considering the flow through a porous medium to be equivalent to that through a group of similar parallel channels for which the total internal surface and the total internal volume were equal, respectively, to the particle surface and pore volume of the medium. A correction factor was then applied to take care of the extra length of the sinuous channels in the medium. The work of Fair and Hatch appears to have paralleled that of Kozeny.

Bartell and Osterhof (8) obtained a value of $k = 4.9$ by regarding the equivalent channels as circular ($k_0 = 2$) and using $\pi/2$ for the factor by which their lengths should be increased. Carman (24) believed that the correction for channel length should be $\sqrt{2}$ and thus obtained a value of $k_0 = 2.5$, since his average experimental value for k for certain types of media was 5.0. Although corrections based on simple increases in length of flow channels might properly apply to consolidated materials where actual, discrete, singly connected channels exist, such a correction appears to be fundamentally wrong for unconsolidated materials where the whole of the void space is interconnected and transverse pressure gradients do not exist (47). Sulli-

van and Hertel (115) found experimental values of k to be 3.07, 4.50 and 6.04 for flow through (1) a bed of glass fibers approximately parallel to flow ($\epsilon = 0.82$), (2) a compact bed of glass spheres ($\epsilon = 0.39$) and (3) a bed of glass fibers approximately perpendicular to flow ($\epsilon = 0.80$), respectively.

Since a large part of the usefulness of equation (7) for a specific surface determination is dependent upon an advance knowledge of the value of k in any particular case, any aid, even though not rigorously formulated, which will help predict k for the given case is of value. It was noted from Fig. 2 that values of the shape factor k_0 for the multiply connected channels occurring in wads of textile fibers do not vary over a wide range when the porosity is restricted to the lower values shown in the figure. Table I shows that several of the singly connected channels have values of k_0 comparable to those of the multiply connected channels. The differences in the values of k for beds of spheres and for beds of fibers noted in the last paragraph may, therefore, be regarded as largely due to differences in ζ rather than in k_0. Theoretically, $\zeta = 1, {}^2/_3, {}^1/_2$ for the cases, (1) flow parallel to cylinders, (2) flow through a bed of spheres and (3) flow perpendicular to circular cylinders, respectively. Using these values of ζ, the experimental values of k_0 will be 3 in each of the cases.

The difference between the average value of 5.0 for k, found experimentally by Carman (24) for the flow of liquids through a wide variety of sands, powders, etc., and the value of 4.50 found by Sullivan and Hertel, or the value of 4.65 found by Muskat and Botset (87) for the flow of air through beds of glass spheres, may perhaps be accounted for on the same basis. Sand particles and, in fact, most other particles not particularly selected, will not be perfectly round and will in any natural settling process show a preferred orientation transverse to the direction of settling. When the flow measurements are made transverse to this orientation the measured value of k (equation 7) will be higher than if flow measurements were made parallel to the orientation. Additional evidence of this effect is the case noticed by Muskat and Botset (87), where the flow perpendicular to the bedding plane of a piece of natural sandstone was only 70% as great for the same pressure drop as was the flow parallel to the bedding plane.

The foregoing theory has dealt rather exclusively with the flow of incompressible fluids. When a gas is used as the fluid, equation (6) must be altered to include the compressibility of the gas. An excellent discussion of the flow of gases through porous media has been

given by Muskat, "Flow of Homogeneous Fluids Through Porous Media," 1937, Chapter XI. From Muskat's treatment it is found that for viscous flow,

$$Q^* = Q \left\{ \frac{p_2^{1+\gamma} - p_1^{1+\gamma}}{(1+\gamma)(p_2 - p_1)p_1^{\gamma}} \right\} \tag{8}$$

where Q^* is the volume of gas delivered per second through a porous medium as measured under the pressure p_1; Q is the volume per second which would have been delivered for flow with constant density equal to that at p_2 (*i. e.*, had the gas been non-compressible); γ is a quantity which is determined by the thermodynamic character of the flow, and is equal to unity for isothermal flow; γ is, on the other hand, given by

$$\gamma = \frac{\text{specific heat at constant volume}}{\text{specific heat at constant pressure}}$$

for adiabatic flow; p_2 is the higher pressure while p_1 is the lower pressure (*i. e.*, $\Delta p = p_2 - p_1$).

It follows from equations (8) and (6) that the rate of volume delivery of a gas through a porous medium acting under a pressure difference $\Delta p = p_2 - p_1$ is given by

$$Q^* = \frac{A}{\mu S_0^2} \frac{\zeta}{k_0} \frac{\Delta p}{L} \frac{\epsilon^3}{(1-\epsilon)^2} \left\{ \frac{(p_2^{1+\gamma} - p_1^{1+\gamma}}{(1+\gamma)(p_2 - p_1)p_1^{\gamma}} \right\} \tag{9}$$

where γ is unity for isothermal flow, or γ is equal to the ratio of the specific heats for adiabatic flow. In practical cases, where the pressure difference $p_2 - p_1$ is quite small, the bracketed term of the right member of equation (9) may be sufficiently well approximated by unity, thus recovering equation (6) for use. Where $p_2 - p_1$ is not small, however, it will be necessary to determine the nature of the flow (isothermal or adiabatic) and use equation (9).

III. Experimental Confirmation of Theory

In order to verify equation (6) for porous media it is desirable to answer the following questions:

1. Is Q proportional to $A\,\Delta p/\mu L$ when all other quantities are constant?
2. Is Q proportional to $\epsilon^3/(1-\epsilon)^2$ when all other quantities are constant?
3. Is Q proportional to ζ when all other quantities are constant?

4. Is Q proportional to S_0^{-2} when all other quantities are constant?

These questions will be considered in the order listed.

The first question deals with the validity of Darcy's law along with a test of the effect of μ on the flow. The range of validity of Darcy's law is best represented in terms of a modified Reynolds' number. Reynolds' number was given as $(\rho/\mu)Va$ (see page 39). For a porous medium, the average forward velocity of flow V through the inter-spaces is given by u/ϵ where u is the macroscopic velocity of flow (37). In the case of a porous medium the characteristic linear dimension, a, is taken as the ratio of the pore space to the surface of the particles. Thus the modified Reynolds' number, R', becomes $R' = \rho u/[\mu S_0(1 - \epsilon)]$. As pointed out by M. King Hubbert (66), there are three values of the modified Reynolds' number which are "of particular significance: $R' = 0$, corresponding to zero flow; $R' = R'^*$, the point at which inertial forces become effective; and $R' = R'_{\text{crit.}}$, where the flow becomes turbulent." It is the value of R'^* which should be the upper limit of R' for the range of Darcy's law.

Lindquist (79) employing a medium composed of uniform lead shot with a porosity of 38 per cent found R'^* to be about 4 for different experiments for which the particle diameter ranged from 1 to 5 mm. Referring to Fig. 1, it will be seen that this agrees well with the value indicated by Hatfield's data (59) over a wide range of conditions of flow through porous carbon. Carman (24) indicates that R'^* is slightly in excess of 2.

Carman also discusses the fact, first pointed out by King (71), and later reviewed by Siegel (108), that for very low values of R' the flow sometimes increases faster than the drop in pressure. The explanation advanced for this was that when velocities were very low the fluid might form adsorbed stagnant layers whose thickness would decrease with increased velocity. Carman cited the work of Sven Erikson (40), who measured the actual velocity in the inter-spaces of a bed of sand by injecting a salt solution into water flowing through the bed and taking the time for the salt to appear at the outlet. By taking ϵ' as the ratio of the macroscopic velocity to the velocity in the inter-spaces, Erikson found ϵ' increased steadily from 0.14 to a final steady value of about 0.47 at $R' = 0.006$, the porosity 0.47 being the true porosity of the sand. Erikson further found that when the bed was drained and air was passed through, the fractional volume of water

retained by the wet sand was 0.33. It is noted that 0.33 = 0.47 − 0.14. The work of Darapsky is then cited. Darapsky (33) suggested that a small stationary ring of liquid is retained at each point of contact of the particles, the size of the ring being controlled by the velocity of the fluid. It has also been found that surface forces enter into the problem. Bozza and Secchi (17) found that a very fine quartz sand gave permeabilities about 1.3 times greater for aqueous solutions than for certain organic liquids, although the surface tensions of the organic liquids were lower than those of the aqueous solutions. The ratio of the permeabilities was increased further by the use of a bed of finely ground galena. In the work of Bozza and Secchi, values of R' ranged from about 1×10^{-3} to about 1×10^{-6}.

The use of air as a fluid is desirable for very fine media, since the formation of stagnant rings and layers is either absent or less pronounced. The following values, obtained by Lea and Nurse (78), using air and water in permeability measurements on fine powders, are examples which appear to indicate the decrease of permeability that may be occasioned by liquid layers:

Sample	Sq. cm. per gram by method:		
	(1) Air permeability	(2) Water permeability	(3) Andreasen (sedimentation)
Sand 120–150 B.S. sieve	290	270	....
Washed sand 80–25 μ	604	613	660
Washed sand 35–15 μ	1350	1640	1320
Washed sand 45–7.5 μ	1880	2210	1920
Washed sand 45–5 μ	1930	2360	....
Washed sand 22.5–7.5 μ	2270	2940	2230
Washed sand 17.5–7.5 μ	2790	3900	2720
Ground sand 45–0 μ	10,800	14,700	....

In applying Darcy's law to a porous medium it is tacitly understood that the medium does not undergo a mechanical deformation during the experiment. For deformable media care should be exercised (1, 126).

That the effect of viscosity is as given by equation (6) is indicated by the data of Fig. 1. Additional data for the effect of viscosity is given by Carman, who studied the flow of various liquids and of air through the same bed of sand. His results are presented in Table II.

In discussing Questions 2, 3 and 4 it is, of course, impossible to know precisely in all cases that the shape factor, k_0, is being held

TABLE II

RELATIONSHIP BETWEEN PERMEABILITY AND VISCOSITY

Sand, 60–90-Mesh I.M.M. Sieve Fraction, Used in All Experiments

Fluid	Porosity of sand, ϵ	Kinematic viscosity, ν, cm.^{2}/sec.	Measured value[a] of $K_2 = QL/Ah$, cm.^{2}/sec.	$K_2\nu\frac{(1-\epsilon)^2}{\epsilon^3} \times 10^3$
Ether	0.385	0.00342	0.0655	1.474
"	0.446	0.00342	0.1251	1.47
Acetone	0.383	0.00417	0.0552	1.555
"	0.386	0.00417	0.0582	1.575
Carbon tetra-	0.3705	0.0063	0.0312	1.52
chloride	0.391	0.0063	0.0399	1.555
"	0.411	0.0063	0.047	1.475
"	0.434	0.0063	0.0613	1.505
"	0.463	0.0063	0.0815	1.48
Benzene	0.40	0.0068	0.0399	1.515
"	0.378	0.0078	0.0274	1.52
"	0.383	0.0078	0.0279	1.47
"	0.427	0.0078	0.0451	1.475
"	0.466	0.0078	0.0689	1.555
Water	0.382	0.0116	0.01855	1.465
"	0.420	0.0116	0.0289	1.51
"	0.460	0.0116	0.0484	1.50
Tetrachloroethane	0.38	0.0119	0.0186	1.515
"	0.464	0.0119	0.0462	1.57
Ethyl alcohol	0.38	0.0162	0.0136	1.525
"	0.405	0.0162	0.0168	1.45
"	0.427	0.0162	0.0226	1.525
"	0.449	0.0162	0.0287	1.545
"	0.466	0.0162	0.0328	1.48
40% Glycerol	0.396	0.0371	0.00685	1.495
solution	0.450	0.0371	0.01238	1.515
Aniline	0.376	0.0478	0.00422	1.475
"	0.408	0.0478	0.00626	1.555
"	0.47	0.0478	0.0121	1.57
Air	0.39	0.157	0.00151	1.49
"	0.422	0.157	0.00225	1.51

[a] In the equation for K_2, h is the head of the liquid which causes the liquid to flow.

constant. One can only rely upon the evidence that shape factors for various types of channels, under certain conditions, have very nearly the same values. The demonstrated correctness of various relations

TABLE III

RELATIONSHIP BETWEEN PERMEABILITY AND POROSITY

Material of bed	Fluid	Porosity, ϵ	$K_{1\nu} \times 10^3$	Calculated value for specific surface, S_0, cm.$^{-1}$
Mixture fine sand B, and coarse sand C; 39% sand B	Ethyl alcohol	0.260	0.054	340
	" "	0.280	0.0715	340
	" "	0.320	0.1245	333
	" "	0.334	0.145	338
	" "	0.351	0.175	338
Mixture fine sand B, and coarse sand C; 13.3% sand B	" "	0.314	0.426	173
	" "	0.344	0.635	171
	" "	0.376	0.907	170
Sand A	Carbon tetrachloride	0.371	0.197	356
		0.391	0.252	358
	" "	0.411	0.296	363
	" "	0.434	0.386	359
	" "	0.463	0.513	361
Sand D	Water	0.425	0.493	303
	"	0.437	0.560	302
	"	0.460	0.720	300
	"	0.486	0.932	301
	"	0.502	1.06	303
Silica powder, mixed sizes, 2–80 μ	Air	0.375	0.0001305	14,200
	"	0.447	0.000287	14,100
	"	0.493	0.000499	13,500
Flaky flint sand, 0.0277 cm.	Water	0.452	0.217	527
	"	0.483	0.285	536
	"	0.496	0.350	519
	"	0.516	0.418	524
	"	0.523	0.417	543
	"	0.544	0.563	520
Black slate powder mixed sizes, 2–80 μ	Air	0.574	0.000481	20,600
	"	0.621	0.000733	21,100
	"	0.660	0.00115	20,600
Wire crimps	Glycerol solution	0.681	36.8	125
		0.722	61.6	122
	" "	0.757	85.0	126
	" "	0.765	100.0	123
0.6 cm. porcelain Berl saddles 5.01 cm.	" "	0.685	954.0	24.6
	" "	0.714	1360	23.9
	" "	0.746	1970	23.8

TABLE III (*Continued*)

Material of bed	Fluid	Porosity, ϵ	$K_2\nu \times 10^3$	Calculated value for specific surface S_0, cm.$^{-1}$
0.6 cm. porcelain Berl saddles 2.39 cm.	Glycerol solution	0.727	1285	24.9
	" "	0.750	1690	24.6
	" "	0.765	2020	24.5
	" "	0.794	2870	24.3
0.6 cm. porcelain Berl saddles 1.38 cm.	" "	0.794	2310	24.6
	" "	0.832	3840	23.7
6.6 cm. nickel Lessing rings	" "	0.870	1670	61.1
	" "	0.8815	2190	59.1
	" "	0.889	2730	59.4

being tested under assumed constancy of k_0 is, in a way, evidence that k_0 is essentially constant under the given range of conditions.

Concerning the correctness of the porosity factor $\epsilon^3/(1 - \epsilon)^2$, Donat (36) has tested it over a range of ϵ of 0.45 to 0.54 for a flint sand and found it to apply. Traxler and Baum (123) took data on the flow of air through fine silica powder and through pulverized black slate, which also confirmed the $\epsilon^3/(1 - \epsilon)^2$ relationship for the range used. Their results are:

Substance	Range of ϵ	Range of permeability (observed)	Range of permeability (calculated)
Black slate powder	0.574-0.660	1 : 2.39	1 : 2.39
Silica powder	0.375-0.493	1 : 3.59	1 : 3.47

Table III, taken from Carman's paper (25), shows a wide range of data for various materials, which are tabulated in a form to show that the function $\epsilon^3/(1 - \epsilon)^2$ is sufficiently accurate to care for the effect of porosity, within errors of the experiments from which the data were taken, over a range of 0.26 to 0.889 for ϵ.

Hatch (58) has used the same porosity function successfully in his studies of the viscous flow of water through beds of sand where the sand particles differed considerably in size and in size distribution. The range was 0.324 to 0.437 for ϵ.

Fowler and Hertel (47), for values of ϵ of 0.54 to 0.80, found $\epsilon^3/(1 - \epsilon)^2$ to be sufficient to account for the effect of porosity on the flow of air through wads of cotton fibers, kapok fibers, rayon fibers, glass wool and wool fibers, where the fibers were all packed in the same

manner. Their data are summarized in Fig. 4, where the linearity of the curves attest the correctness of the porosity function.

Sullivan (114) has shown that values of the shape factor, k_0, no longer can be considered constant in the case of flow through beds of cotton or of wool fibers for values of porosity greater than about 0.87. If, however, the porosity function $\epsilon^3/(1-\epsilon)^2$ is assumed, then

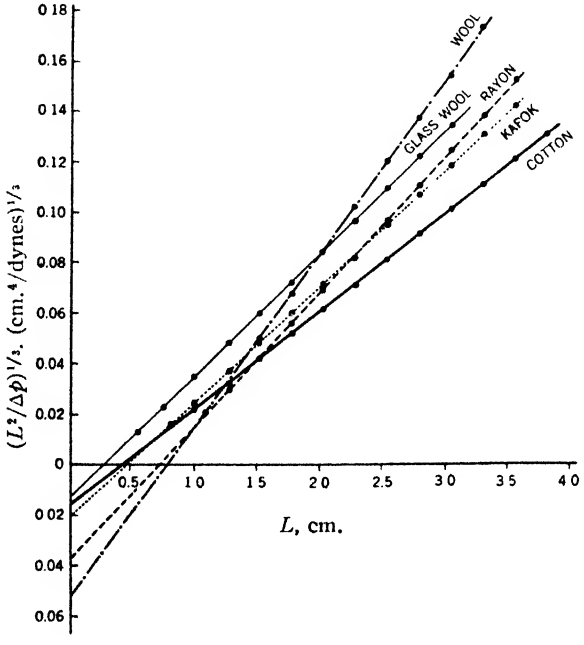

Fig. 4.—Wads of fiber were compressed to different values of tube length L in a given flow tube. When this is done $(L^2/\Delta p)^{1/3}$ *vs.* L should yield a straight line over the range of validity of the porosity function $\epsilon^3/(1-\epsilon)^2$, provided the shape factor k_0 and the orientation factor ζ of equation (6) remain constant.

calculated values of k_0 are in qualitative agreement with the theoretical values for the Emersleben case and vary in about the same way. In this connection, curves *B*, *C*, *D*, *E* and *F* are to be compared with curve *A* in Fig. 2.

For good results a porous medium should be fairly homogeneous with respect to porosity. This is exemplified by the works of Blaine

(13), Roller and Roundy (99) and others who find anomalies with very fine or with very hetero-disperse systems where agglomeration or channeling and bridging of particles may readily occur. Blaine noticed that the anomalies tended to disappear when the materials were compacted more strongly, thus destroying somewhat the possibility of large local values of porosity. Carman (24), using Coulson's data (31), found a variety of values for k (equation 7) when different

TABLE IV

COMPARISON OF RATES OF FLOW FOR FIBERS PARALLEL, AND FOR FIBERS PERPENDICULAR TO THE DIRECTION OF FLOW. PRESSURE DROP = 398.67 DYNES/CM.^{2} TUBE CROSS-SECTIONAL AREA = 3.12 CM.^{2} COTTON FIBERS AND GLASS WOOL FIBERS WERE USED

Wad length L, cm.	Porosity, ϵ	Fibers parallel $Q_{\parallel}$, cc./sec.	Fibers perpendicular $Q_{\perp}$, cc./sec.	Ratio $Q_{\parallel}/Q_{\perp}$
Cotton fiber staple $1^3/_{16}$ in., $S_0 = 4.22 \times 10^3$				
7.96	0.9941	75.3	38.5	1.96
7.45	0.9937	73.2	37.2	1.97
6.70	0.9930	69.9	35.6	1.96
5.95	0.9921	66.6	33.7	1.97
5.21	0.9910	62.8	31.7	1.98
4.46	0.9895	59.9	30.0	1.99
3.72	0.9874	55.3	27.4	2.01
2.98	0 9843	51.0	24.6	2.07
2.235	0.9791	45.0	21.2	2.12
1.49	0.9686	35.8	17.4	2.06
1.117	0.9581	30.2	15.5	1.95
0.745	0.9372	21.9	12.2	1.80
0.372	0 8741	12.48	6.24	2.00
Glass wool fibers, $S_0 = 5.25 \times 10^3$				
5.00	0.8025	0.2094	0.1064	1.97

percentages of the larger size spheres were used in mixtures of spheres where the two sizes of spheres present had diameter ratios of 1:5. Thus, for such mixtures it appeared that k, and hence k_0 (for spheres, ζ has the constant value of $\zeta = {}^2/_3$) varied with mode of packing. However, Coulson's spheres, which were of $^5/_{16}$-in. and $^1/_{16}$-in. diameters, respectively, were packed in a tower of 2-inch diameter, and since the nature of the wall correction in such a case is

somewhat uncertain (see page 61) the interpretation to be placed upon the anomaly mentioned in this case is none too clear.

In connection with Question 3 it may be said that not many materials lend themselves to a direct test of the effect of particle orientation. Fibers and spherical particles are exceptions, although a positive knowledge of shape factors k_0 is not available even for beds of these substances. The approximately constant value of k for flow

TABLE V

SCHRIEVER'S DATA FOR SMALL GLASS SPHERES

Diameter of spheres, cm.	Porosity, ϵ	Specific surface by permeability (using $k = 5.0$ in eq. (7)), cm.$^{-1}$	Specific surface calculated from diameter, cm.$^{-1}$
0.1025	0.387	50.64	50.84
	0.3777	49.96	50.84
	0.3653	49.90	50.84
	0.3533	49.81	50.84
0.0528	0.3889	112.96	113.63
	0.3779	114.78	113.63
	0.3689	112.85	113.63
	0.3603	112.63	113.63
0.0443	0.3958	135.98	135.44
	0.3849	133.84	135.44
	0.3715	136.12	135.44
	0.3552	133.57	135.44
0.0252	0.3934	241.9	238.1
	0.3806	236.7	238.1
	0.369	239.3	238.1
	0.3597	234.4	238.1

The hot gas-free oil used (Nujol) had a viscosity at 99° C. equal to 0.05 poise. (Recalculated from Carman's paper, values not corrected for wall effect.)

through a fairly compact bed of glass spheres, lead shot, randomly mixed sand grains, powders and other porous media where the particle surfaces are oriented at random and where ζ, therefore, has the theoretical value of $^2/_3$, lends support to the use of a constant value for an orientation factor where ζ has a constant value. The experimentally demonstrated fact (114) that, over a range of 0.80 to 0.994 for ϵ, the flow through a bundle of textile fibers parallel to the fibers is twice as great (see Table IV), other things being equal, as is the flow through a bundle of textile fibers whose axes are perpendicular

to the direction of flow but otherwise at random, is in agreement with the ratio of the ζ's for the two cases. Further support for the essential correctness of form of the orientation factor is obtained when shape factors calculated for the two cases (by use of equation 6 com-

TABLE VI

CARMAN'S DATA FOR WIRES, SADDLES AND RINGS

Material of bed	Diameter of container, D, cm.	Porosity, ϵ	Kinematic viscosity, ν	S_0 (uncorr.), cm.$^{-1}$	Wall corr., cm.$^{-1}$	S_0 (corr.), cm.$^{-1}$	S_0 (true value), cm.$^{-1}$
Steel wire crimps	2.39	0.688	0.84	125.2	2.7	123	126
	2.39	0.722	0.84	124 8	3.0	122	126
	2.39	0 765	0.84	126.2	3.6	123	126
	1.91	0.681	0.0386	128.5	3.3	125	126
	1.91	0.731	0 0386	128 0	3.9	124	126
	1.91	0.757	0.0386	130.2	4.3	126	126
0.6 cm. porcelain Berl saddles	5.01	0.685	3.10	25.9	1.3	24.6	24.5
	5.01	0.714	3.12	25.3	1.4	23.9	24.5
	5.01	0.746	3.18	25.4	1.6	23.8	24.5
	2.39	0 724	2 98	28.0	3.1	24.8	24.5
	2.39	0.750	2 97	28.0	3.4	24.6	24.5
	2.39	0.765	3.00	28.1	3.6	24.5	24.5
	2.39	0.714	0.87	27.7	2.9	24.8	24.5
	2.39	0.725	0.87	27.4	3.0	24.4	24.5
	2.39	0.738	0.87	28.4	3.3	25.1	24.5
	2.39	0.754	0.87	27.4	3.4	24.0	24.5
	2.39	0.771	0.87	28.7	3.7	25.0	24.5
	2.39	0.794	0.87	28.4	4.1	24.3	24.5
	1.38	0.794	0.85	31.6	7.0	24.6	24.5
	1.38	0.832	0 85	32.2	8.5	23.7	24.5
0.6 cm. nickel Lessing rings	2.39	0.870	2.96	67.6	6.5	61.6	59.5
	2 39	0.8815	2 96	66.2	7.1	59.1	59.5
	2.39	0.889	2.96	67.0	7.6	59.4	59.5

The values of S_0 (uncorr.) were obtained with equation (7), a value of $k = 5.0$ being used.

The wall corr. was $2/D(1 - \epsilon)$, *i. e.*, half the wall surface per unit volume of solid medium is subtracted from the permeability value of S_0.

The true value of specific surface was obtained from the geometry of the particle.

bined with $\zeta = <\sin^2 \phi>_{AV}$) are found to be in good qualitative agreement with the Emersleben case. The two cases of flow through bundles of textile fibers, however, represent only the end points of the

TABLE VII

CARMAN'S DATA FOR SPECIFIC SURFACE BY METHOD OF MIXTURES (SEE TEXT)

Material of bed	Porosity, ϵ	Kinematic viscosity, ν	Specific surface (calc.), cm.$^{-1}$	Specific surface (true value), cm.$^{-1}$
Sand B	0.402	0.0163	672	...
	0.431	0.0163	670	...
	0.436	0.0163	680	...
	0.474	0.0163	669	...
Sand C	0.359	0.113	88	...
	0.364	0.113	88	...
	0.370	0 113	90	...
	0.420	0.113	90	...
	0.424	0.113	89	...
Mixture 5.5% B and 94 5% C	0.351	0 0149	120	121
	0.370	0.0149	120	121
	0.399	0.0149	121	121
Mixture 13 3% B and 86.7% C	0.314	0.0147	173	167
	0.344	0.0147	171	167
	0.376	0.0147	170	167
Mixture 23% B and 77% C	0.288	0.0149	222	224
	0.326	0.0149	228	224
	0.349	0.0149	231	224
Mixture 39% B and 61% C	0 260	0.0163	340	317
	0 280	0.0163	340	317
	0 320	0.0163	333	317
	0.334	0.0163	338	317
	0.351	0.0163	338	317
Sand D	0.425	0 0108	303	...
	0.437	0.0108	302	...
	0.460	0.0108	300	...
	0.486	0.0108	301	...
	0.502	0.0108	303	...
Sand E	0.374	0.0109	178	...
	0.401	0.0109	178	...
	0.444	0.0109	177	...
Mixture 33.3% D and 66.7% E	0.395	0.0114	214	219
	0.401	0.0114	221	219
	0 424	0 0114	219	219
	0.461	0.0114	219	219
Mixture 55% D and 45% E	0 405	0 0149	241	246
	0.429	0.0149	242	246
	0.465	0 0149	240	246

The specific surface (calc.) is obtained directly from the permeability measurements using equation (7) with $k = 5.0$. The specific surface ("true value") is obtained by combining, with proper weighting, the specific surfaces (calc.) for the two sands of which the mixture is composed.

range of ζ. Additional confirmation of the correctness of the orientation factor is obtained by use of the given form and calculation of shape factor for the bed of glass spheres (115). A value of $k_0 = 3$ is obtained, which is in excellent agreement with the value of the shape factor for the cases of flow through beds of fiber of medium porosity.

In connection with Question 4 many experiments have been directed at the all-important problem of whether the flow through a bed of particles is inversely proportional to the square of the specific surface. Because of the nature of the substances composing porous media it has not always been possible to test this relationship directly. It should be remarked that in some of the tests previously described the accuracy of the relation $Q \propto S_0^{-2}$ was tacitly assumed. Flows

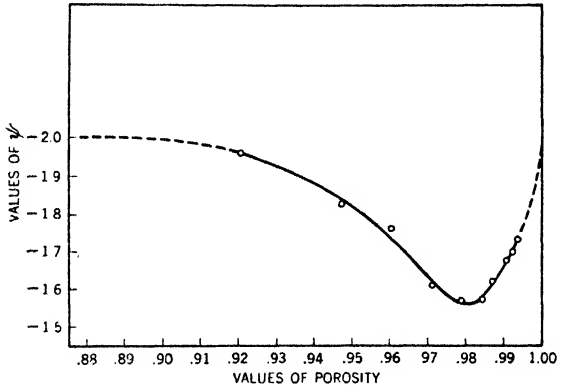

Fig. 5.—Experimental values of ψ, for different values of ϵ.

through beds of spheres where different beds consist of different sizes of spheres, and flows through wads of textile fibers where different sizes of fibers may be used, allow direct tests on these substances. In other cases where the specific surfaces of the substances are known, use may be made of the answers to the three previous questions to show whether or not this factor of equation (6) is correct. With the exception of data for fibers, Carman's papers give very extensive data along these lines. Table V gives Schriever's data for spheres. Table VI gives data for wires, saddles and rings. The "method of mixtures" also has been used (25) to show that mixtures of different-sized particles give final values of specific surface as measured by permeability methods, which agree with the calculated value for the mixture based on specific surface measurements on each fraction entering into the

mixture along with a knowledge of the per cent of a fraction of a given size in the mixture. Table VII gives data for mixtures.

Representative data obtained for textile fibers (115, 116) are given in Table IX.

The experimental failure, under laboratory conditions, of the simple $Q \propto S_0^{-2}$ relationship for cotton and for wool fibers for high values of ϵ is shown in Fig. 5. Thus, if the appropriate power of S_0 is designated by $\psi \equiv \psi(\epsilon)$, there exists the empirical relationship $Q \propto S_0^{\psi}$ for cotton and for wool fibers where Δp, A, L, μ and ζ are held constant (114). The apparent failure of the simple $Q \propto S_0^{-2}$ relationship is ascribed in this case to the varying value of k_0 shown in Fig. 2. It is not clear why k_0 should vary from wads of fiber of one size to wads of fiber of another size at the same porosity in such a way that Q is proportional to a power, different from -2, of the specific surface. The relationship was found to hold, however, for wool and cotton fibers simultaneously.

On the basis of all these experiments it may be safely concluded that equation (6) represents the viscous flow through porous media with sufficient accuracy for many purposes. When the porosity is less than about 0.87 and nothing is known concerning the shape or orientation of the particle surfaces, the extensive evidence compiled by Carman and others indicates that a value of $k = 5.0$ may be used. When, however, as in the case of spheres or in the case of fibers occurring within the tested range of porosities, the orientations of the particles are well enough known to allow the calculation of ζ, it should be so calculated and used with $k_0 = 3$. For arrangements of particles or ranges of porosity which do not include those previously tested, the value of k_0 may be somewhat different and it may be necessary to determine the appropriate value before accurate specific surface determinations can be made. As an example, the value of k_0 for parallel flow through a bed of equal circular cylinders arranged in the tightest mode of parallel alignment ($\epsilon = 0.093$) appears to be 0.81.

IV. Experimental Considerations

In a specific surface determination by the permeability method it is necessary to know accurately the length and cross-sectional area of the porous medium, the pressure drop across the medium, the porosity of the medium and the macroscopic rate of volume flow through the medium.

The choice of a fluid depends to some extent upon the medium. Many workers have used liquids of various types. In the choice of a liquid care should be exercised to select one which will not form stagnant layers on the particle surface. Lea and Nurse (78) and also Blaine (13) found air to be particularly useful for flow through Portland cement and through ground sands. Fowler and Hertel (47) and Sullivan and Hertel (116) used air exclusively in their studies on textile fibers, where, however, in view of the hygroscopic nature of the fibers, due regard was given to the moisture content of the air. Lea and Nurse also tried hydrogen, nitrogen and dry carbon dioxide for their cements and obtained the same results as with air. They found, however, that the flow of water through carefully selected sand gave lower permeabilities and, hence, higher specific surfaces than did the use of air (see page 50). When a gas is used under such a pressure difference that it cannot be considered a non-compressible fluid, equation (9) should be used.

When permeabilities for beds of large particles are being determined, the wall surface of the container may contribute an appreciable amount to the total surface exposed to the flow. A perfectly general method of correcting for wall surface has not been developed. The wall surface contributes to the total surface in contact with the fluid, it alters the type of packing in its neighborhood and its orientation usually is different from that of the medium. Although some experimenters have simply added the wall surface to the particle surface for use in equation (6) or in equation (7), Carman has pointed out (25) that this is an over-correction and has concluded that it is more nearly correct to add half the wall surface to the surface of the particles. Sullivan and Hertel (115) measured the effect of the wall surface for the particular case of small glass spheres of diameter about 0.07 cm., in tubes of diameters 3.86 cm. and 0.821 cm., and found that the wall surface must be multiplied by 0.67 and added to the particle surface if the results for the two tubes were to be brought into agreement. For fine powders and for fine textile fibers in ordinary containers, however, the container wall surface is such a small fraction of the total surface present that it may be neglected.

The apparatus necessary for permeability measurements depends upon the type of porous medium and also upon the fluid to be used. Figure 6 shows a sketch of the apparatus used by Carman for studying the flow of liquids through powders. "The material constituting the bed is packed in the tube, *A*, and rests on the metal gauze, *B*,

carefully cut to fit into the tube. The gauze is supported horizontally by a loosely wound spiral, *C*, which is made from a rectangular piece of thin copper sheet, and, owing to its tendency to expand, fits neatly into *A*. Just below *C* is the manometer tube, *D*, graduated in cm., and below this again is a standard ground joint, *E*. This connects it by the bent tube, *F*, to the tap, *G*, which controls the flow, and delivers to a beaker. According to the viscosity of the liquid used, and to the nature of the grains it was required to study, the dimensions of *A* varied considerably, both in length and in diameter and in the type of gauze. Care was always taken to use a gauze which was sufficient to retain the bed efficiently, but gave no measurable resistance when tested at the same rate of flow without the bed. Thus they varied from $^1/_8$-in. holes to 100-mesh. In the case of every tube, *A*, the area of the cross section was tested for constancy along the whole length of the tube, and calibrated, by running out water and weighing, and following the change in level in *A* with a traveling microscope" (25). *J* was a constant-head apparatus.

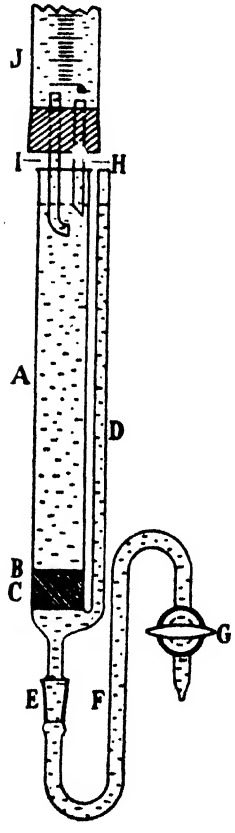

Fig. 6.—Carman's apparatus for liquid flow measurements.

Figure 7 shows a sketch of the apparatus used by Blaine (13), which is similar to that of Lea and Nurse (78), for determining specific surface by means of air permeability. "The permeability cell, *A*, was made of 1-in. (outside diameter) brass tubing and had an inside diameter of 2.38 cm., as compared to 2.54 cm. for the Lea and Nurse cell. The filter disk (Norton porous filter RA 225) sealed between the upper and lower parts of the cell with Duco cement was used in place of a perforated metal disk and filter paper. The outside edge of the filter disk was also sealed to insure against leakage. The plunger, *B*, used to compact the powder in the cell to a definite volume, had an adjustable collar with a set screw. The plunger was made to fit snugly inside of the permeability cell. The manometers, *C* and

D, 50 cm. long and half filled with kerosene, were used to measure the pressure drop across the bed of cement and that across the capillary, respectively. The capillary tube, E, was made of four 3-ft. lengths of capillary tubing having an average internal diameter of 0.675 mm.

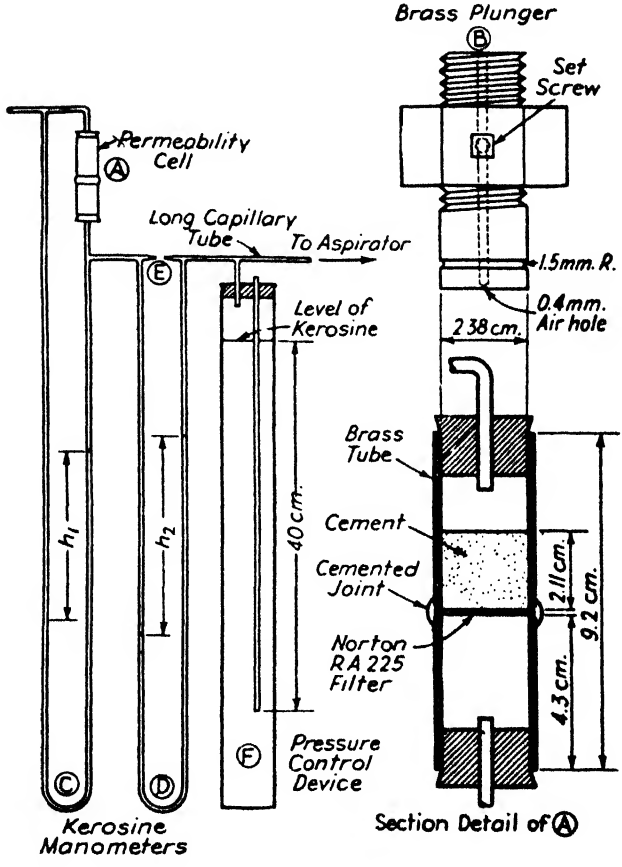

Fig. 7.—Blaine's apparatus for air permeability measurements on fine powders.

This average diameter was calculated from the weight and length of a column of mercury in the capillary. The value reported is the average for each of the capillary tubes. The several lengths were connected in series with rubber tubing and sealed with a rosin-paraffin mixture. The capillary was calibrated against a flow meter at pressures of from

4 to 27 cm. of kerosene. The equation constant, C, of the apparatus was 1.252×10^{-6}, as compared to 3.47×10^{-6} for the capillary used by Lea and Nurse. A constant pressure difference was obtained by use of a water aspirator and a kerosene release valve, F'' (13).

The equation used by Blaine for his apparatus was

$$S = \frac{14}{\rho'}\left(\frac{\epsilon^3}{(1-\epsilon)^2}\frac{Ah_1}{LCh_2}\right)^{1/2} \tag{10}$$

which is a reduced form of equation (7) where $k = 5.0$, and the rate of flow Q, the pressure drop Δp and the coefficient of viscosity μ all are represented indirectly by the manometer reading h_2 across the capillary, the manometer reading h_1 across the medium and the calibration constant C for the apparatus. In equation (10), ρ' is the density of the material which makes up the particles of the medium. The value of the left-hand member of equation (10), therefore, is

$$S = S_0/\rho' \tag{11}$$

and is not the specific surface (surface per unit volume) but is the surface per unit mass of the material. To know the surface per unit mass may frequently be more desirable than to know the surface per unit volume, since the mass of a quantity of the material is determined more easily than the volume. In using equation (10), care should be taken that the gas is not too greatly compressed; otherwise, the additional term given by equation (8) must be used.

An interesting apparatus for air flow through powders has been described by Gooden and Smith (53). It is calibrated to give directly the "surface-weighted average particle diameter"* for a powder.

An apparatus found convenient for specific surface measurements on textile fibers (116) is given in Fig. 8. A sample of fiber weighing 0.1 gram is rendered very fluffy and then placed in the tube. By means of piston A it is compressed from a wad length of about 16 cm. down to a wad length of 0.5118 cm. The same wad length for all wads is assured by the collar, B, which is rigidly attached to the piston. The tube in which the piston moves has an inside diameter of 0.8165 cm. The position of the compressed wad of fiber is indicated by C. Light mineral oil, G, is allowed to flow through the jet, K. The pressure drop caused by the flow of air through the fiber wad is obtained from the kerosene manometer by reading with a traveling

* The "surface-weighted average particle diameter" is given by six times the total solid volume of the medium divided by its total surface.

microscope the rise of the meniscus, E, and then multiplying by a factor to take care of the kerosene density and the fall of level in the large bulb, F. The rack and pinion, J, allows a constant head to be manually maintained as the supply of mineral oil, G, is decreased. Oil is delivered from the jet, K, to a volumetric flask (50 ml.), the time necessary to fill the flask being obtained with a stopwatch. D is a thermometer.

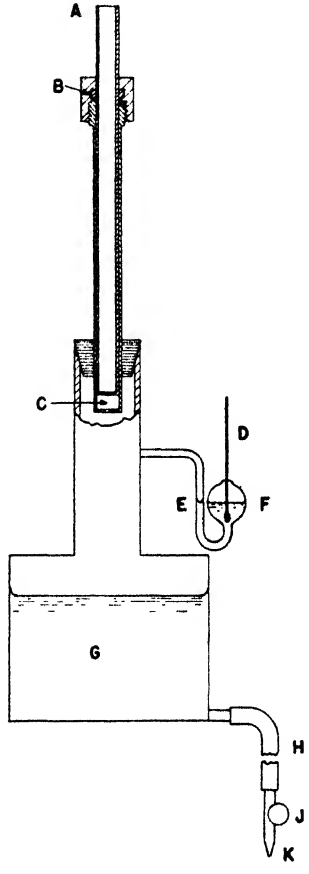

Fig. 8.—Sketch of apparatus used by Sullivan and Hertel for specific surface measurements on textile fibers.

V. Accuracy and Reproducibility of Results

In his paper entitled "Determination of the Specific Surface of Powders" Carman (25), considering the flow of liquids, states that the permeability method gives "an accuracy within ± 5% down to an average particle-size of 2–3 μ," whereas, in his paper presented before the A.S.T.M. (28) he says: "While the present experimental evidence is inconclusive it would appear that the method tends to give somewhat high values of specific surface for very fine particles, particularly for very hetero-disperse powders extending down to collodial dimensions."

Hatch (58) concludes, from his work with the flow of water through sands, "For normally accurate work over a substantial range of particle assemblage, the margin of error may well exceed ±10 per cent."

Lea and Nurse (78) found a high reproducibility for their air-permeability measurements on Portland cement. Table VIII gives their measurements for three cements where each value represents results of a single determination on a separate sample in each case.

Blaine (13) reports an average variation of only ±1.1 per cent from

the grand average for the results of eight operators, each of whom made five determinations on each of four cements which ranged from $S = 2490$ to 5130 cm.^{2}/gram.

Sullivan and Hertel (116) report a probable error of less than 2% per determination for relative values of specific surface for cotton fibers where the fibers were always oriented in the same manner, and where air was the fluid used. They estimated the specific surface values to differ from the true values by a probable error of $\pm 3\%$.

TABLE VIII

LEA AND NURSE'S DATA FOR REPRODUCIBILITY OF SURFACE PER GRAM MEASUREMENTS ON PORTLAND CEMENT

Cement	Surface per gram, cm.^{2}/g.	Mean value of surface per gram
P	4220	
	4180	
	4230	
	4240	
	4240	
	4240	4225
B	3430	
	3430	
	3450	
	3440	
	3430	
	3410	3432
C	2790	
	2790	
	2800	
	2730	
	2780	
	2770	2777

VI. Comparison with Other Methods

It is to be remembered that the permeability method gives the total exposed surface of the medium divided by the total solid volume of the medium, or divided by the total mass of the medium, depending upon whether the specific surface or the surface per unit mass is obtained. Where the medium is composed of particles of different sizes, therefore, the permeability method does not give the arithmetic average of the specific surfaces of the various particles. This is made

clear as follows: If s refers to surface, v to volume and subscripts to the various particles, then the value of specific surface obtained by permeability is, for n particles,

$$S_0 = \frac{s_1 + s_2 + s_3 + \ldots\ldots + s_n}{v_1 + v_2 + v_3 + \ldots\ldots + v_n} \tag{12}$$

TABLE IX

SULLIVAN AND HERTEL'S DATA FOR SPECIFIC SURFACE OF SPHERES AND OF TEXTILE FIBERS

Material	Porosity, ϵ	S_0, permeability method (equation (6) used)	S_0, calculated from microscopic values
Glass spheres[a]	0.3908	85.60 cm.$^{-1}$	85.56 cm.$^{-1}$
" "	0.3904	85.51 "	85.56 "
Glass fibers[b] ($\perp$ flow)	0.8075	5.16×10^3 cm.$^{-1}$	5.25×10^3 cm.$^{-1}$
" "	0.8025	5.07 " " "	5.02 " " "
Glass fibers[b] ($\parallel$ flow)	0.8661	5.62 " " "	5.27 " " "
" "	0.8179	4.77 " " "	4.92 " " "
Cotton fiber[c] ($\perp$ flow)			
(B-38-$^7/_8$ in.)	0.766	3.72×10^3 cm.$^{-1}$	3.69×10^3 cm.$^{-1}$
(B-38-$1^1/_{32}$ in.)	0.762	3.99 " " "	3.83 " " "
(B-38-$1^3/_{16}$ in.)	0.756	4.21 " " "	4.41 " " "
(Pima)	0.758	4.64 " " "	4.50 " " "
(Sea Island S-38)	0.756	5.20 " " "	4.93 " " "
(B-38-S-$1^3/_{16}$ in.)	0.758	4.33 " " "	....
(Sea Island-C-38)	0.758	6.40 " " "	....
(Sacaton No. 7)	0.760	4.40 " " "	....
(Hopi)	0.754	4.32 " " "	....
Wool fiber[c] ($\perp$ flow)			
(Welch wool)	0.709	1.205×10^3 cm.$^{-1}$	1.167×10^3 cm.$^{-1}$
(Fine Noil wool)	0.716	1.916 " " "	2.068 " " "

[a] Precision determination for spheres (115).

[b] Results are averages of six determinations (115).

[c] Flow determinations are averaged from three samples. Microscope determinations are averaged from five slides of 500 fibers each for each cotton or wool (116).

whereas the arithmetic average of the specific surfaces of the n particles would be

$$\frac{1}{n}\left(\frac{s_1}{v_1} + \frac{s_2}{v_2} + \frac{s_3}{v_3} + \cdots\cdots + \frac{s_n}{v_n}\right) \tag{13}$$

With the distinction indicated by equations (12) and (13) in mind, values of specific surface by the permeability method have been

compared for fibers (116) and for spheres (115) with those calculated from microscopic measurements upon the fibers and the spheres. The microscopic method consisted of obtaining the cross-sectional perimeter and the cross-sectional area for the fibers, and the projected diameter for the spheres. From these measurements the value of S_0 for a given medium was then calculated in conformity with equation (12). This comparison is set forth in Table IX where S_0 by the permeability method is calculated from equation (6) using k_0 equal to 3 and ζ equal to 1, $^2/_3$ or $^1/_2$ for fibers parallel to flow, beds of spheres or fibers perpendicular to flow, respectively.

Other cases where the specific surface of the bed could be calculated from its geometry were given in Table VI for wires, rings and saddles.

Specific surfaces by water permeability have been calculated from Hatch's data on sands (58) and are shown in Table X along with the mesh of the screens used in selecting the sands.

Carman (25), using acetone and ethyl alcohol as the fluids, measured the specific surface of "Asarco" zinc dust and then obtained an "equivalent size" ($d_m = 6/S_0$) of $d_m = 3.1$ μ. He then pointed out that a combined elutriation and microscopic examination of a sample of the same material had given an equivalent size of 3.6 μ. The specific surface of a sample of Merck's zinc dust was found by the same permeability method to have an equivalent size of 5.5 μ.

Lea and Nurse (78) have compared the values of surface per gram indicated by various methods, for Portland cement and ground sand. The comparison is set forth in Table XI.

Table XII gives Blaine's (13) comparison between air permeability and Wagner turbidimeter (129) values of surface per gram for various materials. Blaine also points out that a sample of hydrated lime which had an air permeability value for the surface per gram of 10,700 cm.^{2}/g. gave a value of 12,000 cm.^{2}/g. when tested by means of a sedimentation apparatus used by Bishop (12).

Table XIII, taken from the work of Roller and Roundy (99), shows a comparison of results obtained by different methods of specific surface determination. The values in the column headed "Statistical calculation" were obtained by a statistical treatment (98) of the results from an air-stream particle analysis (96) in which an oscillating U-tube, containing 15 grams of the cement, passed air whose velocity was regulated in accordance with Stokes' law for the fraction desired. The values in the column labeled "Air permeability" were

obtained by Gooden, using the air permeability method in the manner of Gooden and Smith (53). The values for the Wagner turbidimeter were calculated from size distribution data obtained by use of the turbidimeter.

TABLE X

COMPARISON OF SCREEN MESH, AND MEASURED SIZE WITH PERMEABILITY MEASUREMENTS FOR SANDS. (REDUCED FROM THE DATA OF HATCH (58))

Screen mesh[a]	Measured[b] size, mm.	Porosity[c] range, ϵ	Averaged[d] specific surface by water permeability, S_0, cm.^{2}/cm.^{3}	Surface-weighted[e] average diameter, d_m, by water permeability, mm.
20–28	1.00	0.373–0.415	86.2	0.696
28–35	0.685	0.386–0.428	124.3	0.482
35–48	0.417	0.396–0.438	202.0	0.297
48–60	0.359	0.406–0.443	224.5	0.267
60–100	0.215	0.391–0.439	383.0	0.157
20–100[f]	0.406	0.324–0.354	217.0	0.276
20–60[g]	0.455	0.385–0.428	186.6	0.322
20–60[h]	0.486	0.340–0.373	173.5	0.346

[a] Samples passed by screen of lower mesh but retained by that of the higher mesh.

[b] Measured size refers to values obtained by projection methods where the particles lie at random and the linear measure is always parallel to a given direction and is the maximum value in this direction for the particle being measured.

[c] Several runs were taken at different values of porosity.

[d] Average for all runs on the particular fraction considered. Equation (7) used with $k = 5.0$.

[e] Obtained from $d_m = 6/S_0$.

[f] Equal portions of (20–28), (28–35), (35–48), (48–60), (60–100) unstratified packing.

[g] Equal portions of (20–28), (35–48), (48–60) stratified packing.

[h] Equal portions of (20–28), (35–48), (48–60) unstratified packing.

A very favorable comparison between the surface-weighted average diameter of particles of silica powder as determined from microscopic measurements and from air permeability measurements is given in Table XIV, where the results of Gooden and Smith (53) are set forth.

VII. Conclusions

From the rather extensive data supplied by the various workers in the field, it appears that where proper technique is employed, the

specific surface, the surface per gram or the surface-weighted average particle diameter may be calculated with high reproducibility and good accuracy from permeability measurements on powders, sands, textile fibers and other non-consolidated porous media. Where the

TABLE XI

COMPARISON OF VARIOUS METHODS FOR DETERMINATION OF SURFACE PER GRAM. (LEA AND NURSE (78))

Sample		Surface per gram by method: (cm.²/g.)			
		(1) Air permeability	(2) Andreasen cubical dimension[a]	(3) Spherical dimension[b]	(4) Wagner, Stokes' law dimension[c]
Portland cement	A	3895	3860	3110	2270
	B	3430	3425	2760	1890
	C	2775	2860	2310	1790
	D	2430	2540	2045	1540
	E	3045	3045	2450	1710
	F	2130	2205	1770	1290
	G	1270	1350	1085	....
	H	2675	2780	2240	1500
Ground sand	J	3900	3920	3145	2160
	K	604	660	532	....
	L	1880	1920	1550	....
	M	2270	2230	1800	....
	N	2970	2720	2190	....
	O	1350	1320	1065	....
		Average ratio of (1) to (2)			0.98
		Average ratio of (1) to (3)			1.22
		Average ratio of (1) to (4)			1.70

[a] Values given are for surface per gram of a cube with the same volume as that of a sphere having a density and a falling velocity equal to those of the actual particles in the sedimentation pipette.

[b] Values given are for surface per gram of a sphere having a density and falling velocity equal to those of the actual particles in the sedimentation pipette.

[c] Values given are for surface per gram of spheres of same density and falling velocity as the particles in the Wagner photo-electric turbidimeter.

media are consolidated (such as porous carbon, natural sandstone and the like) or where the media contain bridging, agglomeration or considerable channelling, it is not certain how much of the surface is actually exposed to flow. Therefore specific surface calculations for such media are likely to be in error or of doubtful significance.

A correct interpretation of permeability measurements made on highly porous media ($\epsilon > 0.88$) will not always be possible, since for higher values of ϵ, k_0 changes rapidly with ϵ and also with the type of medium (see Fig. 2).

TABLE XII

COMPARISON OF SURFACE PER GRAM BY TWO METHODS (BLAINE (13))

Material	Surface per gram by method: (cm.²/g.)		
	(1) Air permeability	(2) Wagner turbidimeter	Ratio, (1) to (2)
Cement A	3720	1940	1.92
B	2490	1320	1.89
C	2980	1650	1.81
D	5130	2890	1.77
White Portland cement	3120	1620	1.92
Raw Mix No. 1	5160	2960	1.74
No. 2	5160	2980	1.73
No. 3	4860	2850	1.70
Potters flint	4710	3100	1.52

TABLE XIII

COMPARISON OF SURFACE AREA[a] VALUES BY DIFFERENT METHODS (ROLLER AND ROUNDY (99))

Cement	Statistical calculation	Air permeability	Wagner turbidimeter
L	2260 ± 110	2130	1790
N	2380 ± 180	2320	1800
M	2780 ± 190	2310	1880
H_1	3740 ± 150	3640	2860
H_2	5200 ± 270	3740	2940

[a] The expression, *surface area*, abbreviated as S. A., has been used by some authors to designate the cm.²/g. of the material.

Where the medium is not too hetero-disperse the permeability method used with an appropriate fluid (preferably air for the smaller fraction) appears to be suitable for particles ranging in average diameter from 1 or 2 μ upward.

The permeability method does not give information concerning the ***distribution*** of particle size in the medium.

TABLE XIV

COMPARISON OF DIAMETER MEASUREMENTS BY AIR PERMEABILITY AND BY MICROSCOPE MEASUREMENTS. (GOODEN AND SMITH (53))

(*a*) On separate fractions of silica powder

Microscope method (original values adjusted for third dimension)		Air permeability method (original readings), surface-weighted average, microns
Range, microns	Surface-weighted average, microns	
33–97	59	52
27–59	43	40
7–27	15	14
5–12	8	7
3–9	5	5
0.3–3	1.2	1.9

(*b*) On mixtures of fractions of silica powder: (Equal parts by weight)

Diameter of component fractions		Average diameter of mixture by air permeability method	
Microscope range, microns	Air permeability (average), microns	Calculated microns	Observed microns
7–27	13.6	7.1	6.9
3–9	4.8		
27–59	40	3,6	3.7
0.3–3	1.9		
All fractions combined	.....	4.8	4.7

Bibliography

1. C. Almy, Jr., and W. K. Lewis, *Ind. Eng. Chem.*, 4, 528 (1912). Study of flow through deformable beds.

2. A. H. M. Andreasen, *Kolloid-Z.*, 48, 175–179 (1929). On basis of comparison of sedimentation with microscope values for calcined flint, concludes that cube dimension is preferable to spherical dimension.

3. A. H. M. Andreasen, *et al.*, *Ibid.*, 49, 48–51, 253–265 (1929). Liquid sedimentation method by pipette sampling.

4. J. Arnould, *Chimie & industrie*, **21**, 478–482 (1929). Studied flow through bed of wire spirals.

5. P. J. Askey and C. G. P. Feachem, *J. Soc. Chem. Ind.*, **57**, 272–276 (1938). Argon adsorption method for getting total surface.

6. B. A. Bakhmeteff and N. V. Feodoroff, *J. Applied Mechanics*, **4**, A-97 (1937). Made a study of flow through porous media and concluded that the porosity function should be $\epsilon^{4/3}$ rather than $\epsilon^3/(1-\epsilon)^2$ for laminar flow.

7. F. E. Bartell, *J. Phys. Chem.*, **15**, 659–674 (1911); **16**, 318 (1912). Permeability of disks and membranes.

8. F. E. Bartell and H. J. Osterhof, *Ibid.*, **32**, 1553–1571 (1928). Obtained a value of k for Kozeny's equation by considering equivalent channels to be circular. Also studied capillary rise in sands.

9. S. H. Bastow and F. P. Bowden, *Proc. Roy. Soc. London*, **A151**, 220–233 (1935). The viscosities of simple liquids show no change in rectangular channels down to 1 μ in width.

10. S. L. Bigelow, *J. Am. Chem. Soc.*, **29**, 1675–1693 (1907). Finds Darcy's law to hold for collodion membranes.

11. Dana L. Bishop, *Bur. Standards J. Research*, **12**, 173–183 (1934) (Research paper 642). A sedimentation method for particle size of finely divided materials such as hydrated lime.

12. Dana L. Bishop, *Ibid.*, **23**, 285–292 (1939) (Research paper 1232). Particle size and plasticity of lime by sedimentation.

13. R. L. Blaine, *A. S. T. M. Bull.*, No. 108, p. 17, Jan. (1941). Specific surface of cement and of lime by air permeability. Comparison with other methods.

14. F. C. Blake, *Trans. Am. Inst. Chem. Engrs.*, **14**, 415 (1922). First use of dimensional group correlation for porous media, later adopted by Hickox and by Carman, which leads to the Kozeny treatment in special case of viscous flow.

15. C. F. Bonilla, *Ind. Eng. Chem.*, **31**, 618 (1939). Solution of isothermal flow in long pipes.

16. J. Boussinesq, *Compt. rend.*, **159**, 390, 519 (1914). Gives an equation for flow through porous media but does not include a general expression for porosity.

17. G. Bozza and I. Secchi, *Giorn. chim. ind. applicata*, **11**, 443–448, 487–492 (1929). Study of flow of organic liquids through fine sands.

18. W. Buche, *V. D. I. Beih. Verfahrenstechnik*, No. 5, p. 155 (1937). Review of recent advances in interpretation of "filter effect."

19. A. Burmester, *Z. angew. Math. Mech.*, **4**, 33 (1924). Study of packing of spheres.

20. S. P. Burke and W. B. Plummer, *Ind. Eng. Chem.*, **20**, 1196–1200 (1928). Propose the theory that total resistance to flow is equivalent to sum of resistances of individual particles to free fall.

21. H. B. Bull and J. P. Wronski, *J. Phys. Chem.*, **41**, 463–468 (1937). Anomalous relationships between permeability and viscosity for flow of various liquids through fine-pored media.

22. W. F. Carey and C. J. Stairmand, *Trans. Inst. Chem. Engrs., London*, **16**,

57 (1938); *Ind. Chem.*, **14**, 141 (1938). Show how to use sedimentation methods for very small particles down to 1 or 2 μ.

23. P. C. Carman, *J. Soc. Chem. Ind.*, **52**, 280–282T (1933); **53**, 159–166T, 301–309T (1934). A study of the mechanism of filtration.

24. P. C. Carman, *Trans. Inst. Chem. Engrs., London*, **15**, 150 (1937). Discusses critically the Kozeny equation for flow through porous media.

25. P. C. Carman, *J. Soc. Chem. Ind.*, **57**, 225–234 (1938); **58**, 1–7 (1939). Discusses critically the permeability method for specific surface of powders.

26. P. C. Carman, *Trans. Inst. Chem. Engrs., London*, **16**, 168–188 (1938). A critical review of the problems of filtration. Extensive bibliography for porous media and for filtration.

27. P. C. Carman, *Ind. Eng. Chem.*, **30**, 1163–1167 (1938); **31**, 1047–1050 (1939). Shows that the Kozeny equation will satisfactorily explain the effect of kieselguhr as a filter aid when porosity and specific surface are taken into account.

28. P. C. Carman, *A.S.T.M. Bull.*, No. 108, p. 8, Jan. (1941). Abstract of paper before A. S.T.M. meeting of March 4–5, 1941.

29. J. Chalmers, D. B. Taliaferro, Jr., and E. L. Rawlins, *Trans. Am. Inst. Mining Met. Engrs.* (Petroleum Div.), **98**, 375–400 (1932). Study of sand.

30. T. H. Chilton and A. P. Colburn, *Ind. Eng. Chem.*, **23**, 913–919 (1931). Do not agree with Dupuit's assumption.

31. C. A. Coulson, Univ. of London Ph.D. Thesis (1935). Laminar flow of a light oil through beds of steel ball bearings.

32. J. N. DallaValle, *Chem. Met. Eng.*, **45**, 688–691 (1938). Determines surface area of coarse sand by permeability method.

33. Darapsky, *Z. Math. Physik.*, **60**, 170 (1912). Theoretical calculation of permeability for tightest mode of packing of uniform spheres. Shows that Slichter's mode of packing for spheres is impossible.

34. H. P. G. Darcy *Les Fountaines Publiques de la Ville de Dijon*, Victor Dalmont, Paris, 1856. Describes the laws for flow of water through sand.

35. S. J. Davies and C. M. White, *Engineering*, **128**, 69, 98 (1929). Give shape factors for pipes.

36. J. Donat, *Wasserkraft u. Wasserwirtsch.*, **24**, 225–229 (1929). Tests Kozeny's equation using flint sand.

37. A. J. E. J. Dupuit, *Études Théoretiques et Pratiques sur le Mouvement des Eaux*, Paris, 1863. Points out that velocity in the pore space is u/ϵ.

38. O. Emersleben, *Physik. Z.*, **26**, 601–610 (1925). Studies analytically the axial flow through equally spaced parallel cylinders of equal size.

39. P. H. Emmett and Thomas DeWitt, *Ind. Eng. Chem., Anal. Ed.*, **13**, 28–33 (1941). P. H. Emmett, this volume, p. 1. Surface area determinations by adsorption methods.

40. Sven Erikson, *J. Gasbeleucht.*, **63**, 615 (1920). Studies the rate of flow of a salt solution in the pore space of a porous bed.

41. W. W. Ewing, *J. Am. Chem. Soc.*, **61**, 1317–1321 (1939). Obtains molecular surface by adsorption of gas molecules.

42. G. M. Fair, *Civil Eng.*, **4**, 137 (1934).

43. G. M. Fair and L. P. Hatch, *J. Am. Water Works Assoc.*, **25**, 1551–1565 (1933). Derive a flow equation equivalent to that of Kozeny.

44. G. H. Fancher and J. A. Lewis, *Ind. Eng. Chem.*, **25**, 1139–1147 (1933). Test Darcy's law for sands.

45. C. V. Fishel, *Trans. Am. Geophys. Union*, Part 2, 449–503 (1933); Part 2, 405 (1934). Verifies Darcy's law for sands when pressure gradient is very small.

46. P. Forchheimer, *Hydraulik*, 3 Aufl., Teubner, Leipzig and Berlin, 1930 Suggests a relation for flow through porous media when flow is no longer viscous.

47. J. L. Fowler and K. L. Hertel, *J. Applied Phys.*, **11**, 496–502 (1940). Applies the Kozeny equation to wads of textile fibers.

48. H. J. Fraser, *J. Geol.*, **43**, 910–1010 (1935). Experimental study of porosity and permeability of plastic sediments.

49. S. S. Fritts, *Ind. Eng. Chem., Anal. Ed.*, **9**, 180–181 (1937). Discusses turbidimeter methods.

50. C. C. Furnas, *U. S. Bur. Mines Bull.* **307** (1929). Does not agree with Kozeny's treatment.

51. L. C. Graton and H. J. Fraser, *J. Geol.*, **43**, 785–909 (1935). Extensive study of the geometry of packing of spheres.

52. C. V. Givan, *Trans. Am. Geophys. Union*, **15**, 572 (1934). Study of the flow of water through beds of lead shot.

53. E. L. Gooden and C. M. Smith, *Ind. Eng. Chem., Anal. Ed.*, **12**, 479–482 (1940). An apparatus for air permeability measurements on powders is used on silica powder.

54. H. Green and G. A. Ampt, *J. Agr. Sci.*, **5** (Part 1), 1–26 (1912–13). Compare permeabilities of glass spheres to air and to water.

55. A. G. Greenhill, *Proc. London Math. Soc.*, **13**, 43 (1881). Theoretical treatment of flow through channels of non-circular cross section.

56. F. E. Hackett and J. S. Strettan, *J. Agr. Sci.*, **18**, 671–682 (1928). Study capillary rise through a bed of spherical grains.

57. L. P. Hatch, *J. Applied Mechanics*, **5**, A-86 (1938). Criticizes the results of Bakhmeteff and Feodoroff of 1937.

58. L. P. Hatch, *Ibid.*, **7**, A-109 (1940). Reviews the theory and gives data for the flow of water through sand beds where particle size is determined by screening.

59. M. R. Hatfield, *Ind. Eng. Chem.*, **31**, 1419–1424 (1939). Studies flow of air, water, corn syrup, paraffin oil and glycerine through porous carbon.

60. E. A. Hauser and J. E. Lynn, *Experiments in Colloid Chemistry*, McGraw-Hill Book Co., New York, 1940. Chap. XII deals with methods of particle size determination.

61. H. Heywood, *Proc. Inst. Mech. Engrs. London*, **125**, 383–416 (1933). Microscopic measurements on particles of powders.

62. H. Heywood, *Ibid.*, **140**, 257 (1938). Discusses air-elutriation and liquid-sedimentation methods of specific surface determination from particle size.

63. G. H. Hickox, *Trans. Am. Geophys. Union*, Part 2, 567 (1934). Studies both viscous and turbulent flow through granular media.

64. D. I. Hitchcock, *J. Gen. Physiol.*, **9**, 755–762 (1926). Assumes that actual channel length through media = $(\pi/2) \times$ (apparent length).

65. Howe and Hudson, *J. Am. Ceram. Soc.*, **10**, 443 (1927). Permeabilities of porous plates with different amounts of binding agents.

66. M. King Hubbert, *J. Geol.*, **48**, 785–944 (1940). An extensive discussion of the physical basis of Darcy's law and its relation to the movement of ground water.

67. R. Hulbert and D. Feben, *J. Am. Water Works Assoc.*, **25**, 19–65 (1933). Permeabilities of sands.

68. K. Kammermeyer and J. L. Binder, *Ind. Eng. Chem., Anal. Ed.*, **13**, 335–337 (1941). Particle size determination by sedimentation.

69. F. B. Kenrick, *J. Am. Chem. Soc.*, **62**, 2838 (1940). Gives a method of analysis for obtaining total particle surface from random projection.

70. D. W. Kessler, *Bur. Standards Tech. Paper*, No. 305, 155–172 (1926). Permeabilities for many porous rocks.

71. F. H. King, *Nineteenth Ann. Rep., U. S. Geol. Survey*, **2**, 59–294 (1897–98). Points out that for very slow flow of liquid through medium, the permeability is sometimes less than for faster flow.

72. C. Koeppel, *Glückauf*, **73**, No. 17, 369–378 (1937). Experimental study of porosity for mixed sizes.

73. J. Kozeny, *Sitzber. Akad. Wiss. Wien, Math. naturw. Klasse*, (Abt. IIa), **136**, 271–306 (1927); *Wasserkraft u. Wasserwirtschaft*, **22**, 67, 86 (1927). Derives a formula for flow through porous media which involves specific surface and porosity.

74. J. Kozeny, *Kulturtechniker*, **35**, 478 (1932). Revises his earlier equation (1927) to take care of the permeabilities of clays where adsorbed layers of liquid exist.

75. E. O. Kraemer and A. J. Stamm, *J. Am. Chem. Soc.*, **46**, 2709–2718 (1924). New and simple method for determining distribution of size of particles in emulsions.

76. E. Krüger, *Intern. Mitt. Bodenk.*, **8**, 105 (1918). Introduces specific surface rather than particle size into a form of Darcy's law.

77. F. M. Lea, *J. Soc. Chem. Ind.*, **58**, 146 (1939). Shows that there is fair agreement between the sedimentation methods of Wagner and of Andreasen down to about 7.5 μ.

78. F. M. Lea and R. W. Nurse, *J. Soc. Chem. Ind.*, **58**, 277 (1939). Compares air permeability values of specific surface with Wagner photo-electric sedimentation and the Andreasen sedimentation values for cements and sands.

79. E. G. W. Lindquist, *Reports of the First Congress of Large Dams*, Stockholm, Sweden, pp. 81–102 (1933). "On the Flow of Water Through Porous Soil."

80. F. Mach, *Dechema Monographien*, **6**, 38 (1934). Studies flow through bed of porcelain saddles.

81. F. Mach, *Forschungsheft V. D. I.*, No. 375 (1935). Data on flow through lead shot.

82. E. Manegold, R. Hofmann and K. Solf, *Kolloid-Z.*, **56**, 267 (1931); **57**, 23 (1931). Permeabilities of ceramic filters and sintered glass filters to liquids.

83. G. Marten, C. E. Blyth and H. Tongue, *Trans. Ceram. Soc.*, **23**, 61 (1923–24). Get specific surface by rate of dissolution in a corrosive medium.

84. R. Meldau and E. Stach, *J. Inst. Fuel, Trans.*, **7**, 336–354 (1934). Show that anthracite powders tend to bridge large cavities and also to form small voids by juxtaposition of faces.

85. W. G. Meyer and L. T. Work, *Trans. Am. Inst. Chem. Engrs.*, **33**, 13 (1937). Laminar flow of air through broken rock.

86. M. Muskat, *J. Applied Phys.*, **8**, 274 (1937). Applications of permeability measurements.

87. M. Muskat and H. G. Botset, *Physics*, **1**, 27–47 (1931). Force air under high pressure through a bed of glass particles.

88. M. Muskat, *The Flow of Homogeneous Fluids Through Porous Media*, McGraw-Hill Book Co., New York, 1937. An extensive treatise which, however, does not analyze the permeability into other factors such as porosity and specific surface.

89. C. M. Nevin, *Bull. Am. Assoc. Petroleum Geol.*, **16**, 373 (1932). Finds that the average "pore diameter" of a compacted sand is one-fifth the diameter of the particle of modal size.

90. P. G. Nutting, *J. Franklin Inst.*, **203**, 313–324 (1927). Movement of fluids in porous solids.

91. N. A. V. Piercy, M. S. Hooper and H. F. Winney, *Phil. Mag.*, **15**, 647–676 (1933). Give shape factors for pipes with cores.

92. L. Prandtl and O. G. Tietjens, *Applied Hydro- and Aero-Mechanics; Fundamentals of Hydro- and Aero-Mechanics*, Engineering Society Monographs, McGraw-Hill Book Co., New York, 1934.

93. W. T. Ray and H. Kreisinger, *U. S. Bur. Mines Bull.*, **21** (1911). Study flow through bed of lead shot.

94. Osborne Reynolds, *Trans. Roy. Soc. London*, **A174**, 935–982 (1883), or *Sci. Papers*, Vol. 2, p. 51. Shows that transition between laminar and turbulent flow depends on the dimensionless expression called Reynolds' number.

95. H. Richter, *Forschungsarbeiten, V. D. I.*, No. 338 (1930). Study of flow through smooth curved copper tubes.

96. P. S. Roller, *Proc. Am. Soc. Testing Materials*, **32**, 607 (1932). Describes an air velocity particle analyzer for powders.

97. P. S. Roller, *Ibid.*, **38**, 458 (1938). Concerning limiting values for Wagner turbidimeter method.

98. P. S. Roller, *J. Phys. Chem.*, **45**, 241 (1941). Describes a statistical method of determining the total particle surface of a powder from the results of the air velocity analyzer.

99. P. S. Roller and P. V. Roundy, Jr., Paper presented at Symposium on

Fineness before A.S.T.M. at the March, 1941, meeting in Washington, D. C. Compares permeability method with the Wagner turbidimeter and with the Roller air analyzer method. Abstract in *A.S.T.M. Bull.*, No. **108**, 19, Jan., 1941.

100. P. Rosin and E. Rammler, *J. Inst. Fuel*, **7**, 29–36 (1933). Discuss a combination of sieve-analysis and elutriation method for particle size distribution for a powder.

101. H. Ruoss, *Kolloid-Z.*, **74**, 221 (1936). Gives method for obtaining equivalent channel diameter.

102. B. F. Ruth, *Ind. Eng. Chem.*, **31**, 985 (1939) Improved method of plotting dimensionless groups for pipe flow problems.

103. Karl Schaum, *Kolloid-Z.*, **34**, 1 (1924). Finds Darcy's law to hold for porous media.

104. L. Schiller, *Z. angew. Math. Mech.*, **3**, 2 (1923). Studies relationships for dimensionless groups for flow through non-circular pipes.

105. W. Schriever, *Trans. Am. Inst. Mining Met. Engrs.* (Petroleum Div.), **86**, 329–336 (1930). Studies flow of hot Nujol through bed of glass spheres.

106. K. Schultze, *Kolloid-Z.*, **36**, 65 (1925); **37**, 10 (1925). Studies capillary rise in non-circular channels.

107. Seelheim, *Z. anal. Chem.*, **19**, 387 (1880). Develops Darcy's law to include a term for particle size.

108. W. Siegel, *Der Chemie Ingenieur*, Band I, Zweiter Teil, Leipzig, 1933. Comprehensive review of flow through porous media.

109. C. S. Slichter, *Nineteenth Ann. Rep. U. S. Geol. Survey*, Part 2, 295–384 (1897–98). Extensive treatment of flow through a bed of equal sized spheres.

110. W. O. Smith, *Physics*, **3**, 139–146 (1932). Summarizes and revises Slichter's treatment of 1897–98.

111. W. O. Smith, P. F. Busang and P. D. Foote, *Ibid.*, **1**, 18–26 (1931). Study capillary rise of several liquids through a bed of spherical particles.

112. W. O. Smith, P. D. Foote and P. F. Busang, *Phys. Rev.*, **34**, 1271–1274 (1929). Count the number of points of contact for a sphere in random packing with other spheres.

113. T. E. Stanton and J. R. Pannell, *Natl. Phys. Lab., Collected Researches*, **11** (1914). Study of relationships for dimensionless groups for flow through smooth circular pipes.

114. R. R. Sullivan, *J. Applied Phys.*, **12**, 503–508 (1941). Flow through highly porous plugs of textile fibers is studied and compared with the work of Emersleben.

115. R. R. Sullivan and K. L. Hertel, *Ibid.*, **11**, 761–765 (1940). Finds different values of the k in Kozeny's equation for glass beads than for glass fibers.

116. R. R. Sullivan and K. L. Hertel, *Textile Research*, **11**, 30–38 (1940). Compares specific surface determinations by permeability method with those by microscope method for wool and for cotton fibers.

117. The Svedberg, *Colloid Chemistry*, Chemical Catalog Co., New York, 1928, p. 148. Data for comparing rates of fall of ellipsoids and spheres in sedimentation.

118. C. Terzaghi, *Eng. News-Record*, **95**, 832 (1925). Gives a modified form of Slichter's treatment.

119. F. V. Tooley and C. W. Parmalle, *J. Am. Ceram. Soc.*, **23**, 304 (1940). Give a method of analysis for obtaining total geometrical surfaces from results of random projection. Also give a method of obtaining total molecular surface by adsorption of organic molecules.

120. P. M. Travis, *A.S.T.M. Bull.*, No. 102, p. 29, Jan. (1940). Compares sedimentation method with microscopic method for particle size determination for zinc dust and for barium sulfate pigment.

121. R. N. Traxler, L. A. H. Baum and C. U. Pittman, *Ind. Eng. Chem., Anal. Ed.*, **5**, 165 (1933). Describe method of preparing briquettes of powders for permeability study.

122. R. N. Traxler and L. A. H. Baum, *Proc. Am. Soc. Testing Materials*, **35** (II), 457 (1935). Discuss difficulties of Wagner method as applied to cements.

123. R. N. Traxler and L. A. H. Baum, *Physics*, **7**, 9–14 (1936). Data on permeability of powders.

124. Tunstall, *Proc. Inst. Mech. Engrs. London*, **125**, 455 (1933). Obtains specific surface by adsorption of dyes.

125. S. Uchida and S. Fujita, *J. Soc. Chem. Ind. Japan* (Suppl. binding), **37**, 724B, 791B (1934). Study flow through bed of Lessing rings.

126. A. J. V. Underwood, *J. Soc. Chem. Ind.*, **47**, 325T (1928). Studies flow through deformable material.

127. A. J. V. Underwood, in *Filtration and Filters*, by J. A. Pickard, Ernest Benn, Ltd., London, 1929. Gives brief review of filter aspects of flow through porous media.

128. H. Wadell, *J. Franklin Inst.*, **217**, 459–490 (1934). Applies theory of dimensionless groups to motions of particles through fluids.

129. L. A. Wagner, *Proc. Am. Soc. Testing Materials*, **33** (II), 553 (1933). Photoelectric turbidimeter.

130. A. M. White, *Trans. Am. Inst. Chem. Engrs.*, **31**, 390 (1935).

131. C. M. White, *Proc. Roy. Soc. (London)*, **A123**, 645–663 (1929). Studies flow through curved pipes by means of dimensional analysis.

132. E. J. Wiggins, W. B. Campbell and O. Maass, *Can. J. Research*, **17**, 318–324 (1939). Applies Kozeny's equation to flow through wool and Celanese fibers.

133. H. D. Wilder, Jr., and T. V. Moore, *Oil Weekly*, **67**, 34 (1932). Find mean effective pore diameter to be independent of fluid.

134. R. E. Wilson, W. H. McAdams and M. Seltzer, *Ind. Eng. Chem.*, **14**, 105 (1922). Study flow through standard elbows.

135. L. T. Work, *Proc. Am. Soc. Testing Materials*, **28**, 771 (1928). Finds that the equivalent spherical diameter of a sieved particle may lie between 0.8 and 1.2 or more times the sieve aperture.

136. R. D. Wyckoff, H. G. Botset, M. Muskat and D. W. Reed, *Rev. Sci. Instruments*, **4**, 394 (1933).

137. F. Zunker, *Handbuch der Bodenlehre*, **VI**, p. 152, Breslau, 1930. Development of ideas concerning flow through porous media.

138. F. Zunker, *Z. Pflanzenernähr. Düngung Bodenk*, **A25**, 1 (1932). Finds that for plastic clays the Kozeny equation as originally developed is inadequate for very small clay particles, $d_m \sim 1\ \mu$. (Adsorbed stagnant layers of liquids cause trouble.)

A NEW METHOD OF ADSORPTION ANALYSIS AND SOME OF ITS APPLICATIONS

ARNE TISELIUS

Institute of Physical Chemistry, Upsala University, Upsala, Sweden

CONTENTS

Adsorption methods are of great importance in preparative organic and bio-chemistry. The differentiation of various enzymes by Willstätter and his school and, perhaps still more, the rapidly increasing application of the Tswett chromatographic analysis in various branches of organic chemistry demonstrate the usefulness of such procedures. The recent development of carotinoid chemistry is to a large part based upon the successful application of adsorption methods.

In the following an account will be given of some considerations and experiments which represent an attempt to widen the scope of application of adsorption analysis and to put it on a more quantitative basis than has been possible before. This work had as its origin the search for improved methods for the differentiation and separation of split products of proteins. The strikingly high specificity of the adsorption methods, as demonstrated in the work referred to above, made it seem worth while to investigate their application in this field. The procedure developed for this purpose appears to have a very wide applicability in the study of mixtures in various solvents, but so far

our experiments have been limited mainly to amino acids and peptides, and only a few orientation experiments have been made with other substances. A brief description of the method and its application has been given in a number of recent publications (12, 13, 14, 15).

Previous investigators have shown that the chromatography of colorless substances is possible in a number of cases by means of observations of the various layers in the Tswett column by their fluorescence, or by testing with different specific reagents, either on the column directly or after it has been cut into sections and extracted (see the monographs by Zechmeister and von Cholnoky or by Strain (7, 18)). In the present work a new method of observation possessing a more general applicability has been developed. After passing through the column of adsorbent and before any mixing has taken place, the solution is allowed to flow through an arrangement for determining continuously the total concentration of each volume element passing through. This can be done by connecting to the outlet of the column a suitable cell (of a small volume as compared to the total volume of solution to be investigated) in which the refractive index, light absorption, conductivity or some other suitable property of the solution is observed continuously. The readings are plotted against the volume of flow. An arrangement of this type is referred to below, using conductivity observations, and a similar arrangement with interferometric registration is now being built. A comparatively simple observation method, however, may be based upon the optical arrangement (the Toepler schlieren method and its modifications) used in electrophoresis (2, 5, 8, 9, 10, 11). Immediately after leaving the column, the solution enters the bottom of an optical cuvette with rectangular cross section, in which it is allowed to rise slowly. The variation of concentration (or rather the variation of refractive index) with height in the cuvette, which is recorded on the schlieren photograph, is equivalent to the concentration-volume function as obtained in the first-mentioned arrangement. Each component gives rise to a separate boundary in the cuvette, the distance of which from the meniscus depends upon the degree of adsorption.

I. Theory of the Procedure

The last-mentioned process lends itself to a particularly simple theoretical treatment. It represents the initial stage (before develop-

ment) in ordinary chromatography, as "transferred" to the liquid phase. (A general treatment of the phenomena in the chromatographic column has been given recently by Wilson (17).)

Figure 1 shows diagrammatically the adsorption process with a solution containing only one component. The left figure shows the solution just about to enter the adsorbent layer (dotted); in the next figure it has advanced so far that the boundary of the solute has reached the upper end of the filter, leaving a layer of pure solvent in the bottom of the cuvette. If the permeation of an adsorbable substance takes place with a sharp boundary (see (17)) a relation between the "retardation" and the adsorption is easily deduced in the following way. Suppose the layer of adsorbent has a cross-section area of 1 sq. cm. and a length of a cm., a weight per cc. of s grams and a pore volume of Δcc. Also suppose the adsorbent is initially completely wet with solvent and that the top boundary of the solution of adsorbable substance A is in contact with the lower surface of the adsorbent layer. Let us assume that when the boundary of A sweeps through the entire length a of the column, the meniscus in the observation tube on top of the column will have to rise l cm. ($l \geq \Delta$). If c_A is the concentration per cc. of A in the solution, this means that the quantity lc_A has entered into the column from below, which therefore represents the total increase of A in the column. Of this, Δc_A is in solution and the rest $(l - \Delta)c_A$ in the adsorbed form. The adsorbed quantity per gram of dry adsorbent is therefore

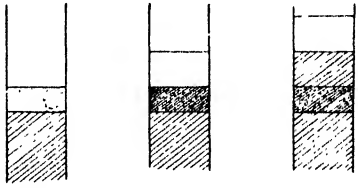

Fig. 1.—Diagram of adsorption analysis with only one component.

$$m_A = \frac{(l - \Delta)c_A}{as}$$

If $m_A = \alpha_A c_A$ (α_A = adsorption coefficient for A, and will of course vary with the concentration) we obtain

$$l = \Delta + \alpha_A as$$

This equation gives a significant meaning to the volume $(l - \Delta)$ (which may be called the "retardation volume") as this volume multiplied by the concentration c_A is the amount $\alpha_A c_A as$ of A adsorbed in the column. If the Langmuir adsorption isotherm is valid, α_A and, therefore, the retardation volume are independent of concentration

at low concentrations. If in a mixture of several components the adsorption isotherms are mutually independent, the retardation volumes are also independent and the boundaries and concentrations in the observation region are simply the superposition of those observed in experiments with single components. Usually, however, there is a mutual influence so that the adsorption coefficient α_A for A when it is alone in the solution is different from its value α'_A in presence of another substance, B. Let us consider the conditions in the solutions when an experiment similar to that demonstrated in Fig. 1 is performed with a mixture of A and B, in which B is more strongly adsorbed than A. We assume that the boundary of B has just reached the top of the adsorption layer and is at a distance l_B from the meniscus, whereas the A boundary is higher up in the observation tube at a distance l_A from the meniscus. (Fig. 2.) The volume between l_A and l_B contains only A and we will assume that its concentration is c_A whereas the concentrations of A and B in the original solution are c_A and c_B, respectively. By reasoning as above we obtain:

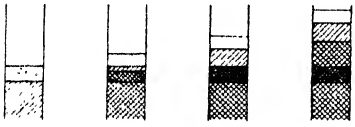

Fig. 2.—Diagram of adsorption analysis with two components.

$$l_B c_A = \Delta c_A + as\alpha' c_A + (l_B - l_A)c'_A$$

from which it follows that

$$\frac{c'_A}{c_A} = \frac{l_B - (\Delta + as\alpha')}{l_B - l_A}$$

As expected, this gives $c'_A = c_A$ for $\alpha = \alpha'$, but c'_A will usually exceed c_A since the adsorption of A is generally smaller in the presence of the more strongly adsorbed B. The solution following the B boundary in the observation tube will, however, have the same composition as the original solution.

It has been assumed above that the adsorption equilibrium is established sufficiently rapidly as compared to the rate of flow. This is a necessary assumption in any simple theory of chromatography. In the experiments to be described below the following observations justify this assumption: the retardation volume is independent of the rate of flow (within an interval of 30 min. to 10 hours for glucose solutions on active charcoal), the boundaries are reasonably sharp

and show a symmetrical concentration gradient, and the concentration gradient drops to zero between the boundaries. A direct verification was obtained in the case of glucose and lactose solution on charcoal, as direct measurements of the amounts adsorbed gave the same isotherms as obtained from the retardation volumes determined at a number of different concentrations (see below).

It may be seen from the last equation that a quantitative analysis of a mixture may be performed by determining the total concentration for each layer between two adjacent boundaries and taking the successive differences, provided that for each component $c = c'$. This is the case only if adsorption displacement is negligible, that is, for low concentrations or for adsorbents with low affinity and large adsorption area. Even when the conditions do not allow a quantitative analysis, detailed information is obtained about the adsorption properties of the mixture which is valuable as a guide for detecting the presence of unknown components and in attempts to make separations by adsorption.

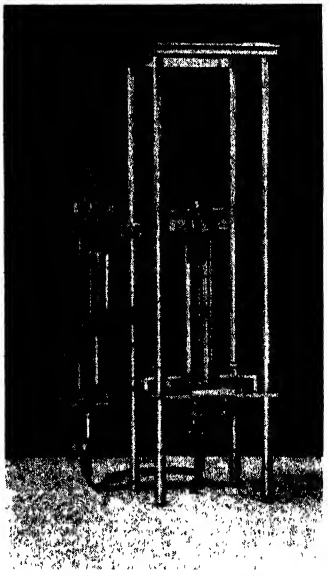

Fig. 3.—Apparatus for adsorption analysis of aqueous solutions.

II. Experimental Arrangement

The apparatus used in most of the experiments to be described is shown in Fig. 3. The solution to be investigated (volume of 25–50 cc.) is filled into the container to the left, and is pressed at a rate of about 50 cc. per hour through a "filter cell" packed with the adsorbent. The optical observation cell or cuvette is a rectangular vessel made of a transparent resin (Perspex, Lucite or Plexiglas) with 5 × 50-mm. cross section and 150-mm. height. The top surface of the filter cell is pressed against the bottom plate of the observation cell, which has a circular hole of the same diameter as the filter. After

passing through the apparatus the solution may be collected in a container connected to the outlet shown on top of the cuvette.

A number of filter cells have been used with diameters of 20, 10 and 5 mm., and lengths of 40, 20, 10 and 5 mm. For most experiments with amino acids in the apparatus described, a quantity of about 1 g. of charcoal is sufficient (corresponding to a filter cell of 20 mm.-diam. and 10 mm.-length). Figure 4 shows a diagram of a filter cell. It is also made of transparent resin, the adsorbent being packed between filter papers supported by perforated disks.

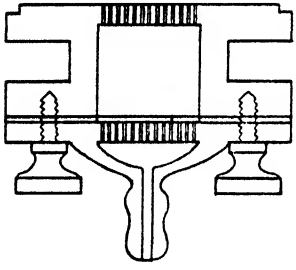

Fig. 4.—Filter cell for the apparatus of Fig. 3.

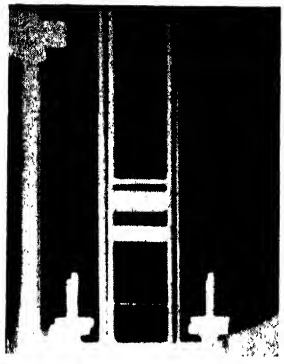

Fig. 5.—Schlieren photograph of the adsorption analysis of a mixture of 1% NaCl, 1% glucose and 1% lactose.

Pressures of about 0.1–1 atm. give a suitable rate of flow for the filter cells described with various active carbons as adsorbents. During an experiment the apparatus is kept in a water thermostat.

The optical arrangement is identical with that described earlier in connection with electrophoresis work (2, 5, 8, 9, 10, 11). Figure 5 shows a photograph obtained by the Toepler schlieren arrangement (a larger cuvette than that described above was used in this case); Fig. 6 shows a gradient-curve photograph by the Philpot-Svensson method.

The above apparatus cannot be used with organic solvents. For this purpose, Claesson in the author's laboratory has constructed an apparatus made entirely of metal and glass, shown in Figs. 7 and 8. The filter cells are made of metal. The glass windows are remov-

able, and are sealed with thin Cellophane or Mipolam gasket rings. As in many cases the solution may have a lower density than the solvent, the apparatus may be arranged for the solution to enter at the top of the cuvette instead of at the bottom.

III. Typical Results Obtained by the Method

1. Verification of the Relation Between the Adsorption Isotherm and the Retardation Volume

For this purpose adsorption measurements were made directly by the ordinary method on solutions of glucose or lactose of varying con-

Fig. 6.—Gradient-curve photograph of the adsorption analysis of a mixture of 0.5% NaCl (right side) and 0.5% glucose (left side).

centration, using Kahlbaum's Carbo Active as adsorbent. The samples were shaken for about one hour at 20°. Parallel with these experiments retardation volumes were determined by the new method and the adsorbed quantity calculated by the relation deduced above. In Fig. 9 the amounts adsorbed, as determined by the two independent methods, have been plotted against the equilibrium concentrations. Evidently the agreement is satisfactory, indicating also that there is no appreciable lag in the establishment of equilibrium during the flow of the solution through the filter. Naturally this cannot always be expected to be the case. Apparently the various active carbons tried are very satisfactory in this respect, whereas other adsorbents in certain cases may react more slowly, *e. g.*, aluminium oxide in aqueous solutions.

It has been found advisable to start an experiment with a moist filter; a dry filter may give diffuse boundaries. Instead of correcting for the volume of solvent thus contained in the filter a suitable substance of negligible adsorption may be added as a reference substance, *e. g.*, sodium sulfate or sodium chloride. The retardation distances

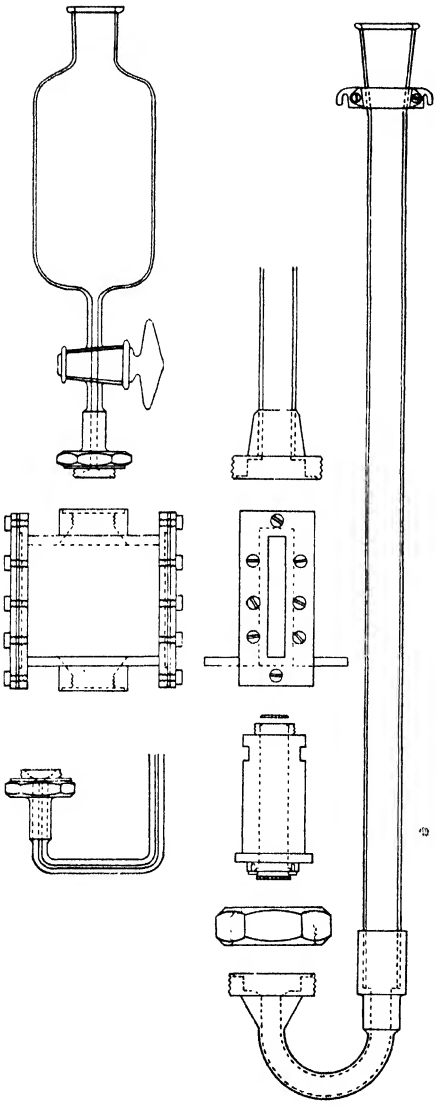

Fig. 7.—Apparatus for adsorption analysis in organic solvents.

are thus measured from the salt boundary rather than from the meniscus.

Figure 10 shows the specific retardation volumes (cc. per gram adsorbent) for lactose and glucose, as measured with Carbo Active Kahlbaum. In agreement with the shape of the adsorption isotherm, the retardation volume of lactose shows a large increase at low concentrations. Measurements on the mixtures show a marked displacement effect on the more weakly adsorbed glucose, whereas the lactose values are not appreciably changed.

Evidently the method can be used for determinations of adsorption, the adsorbed amount being obtained from distance measurements which can be performed with great accuracy.

2. *Quantitative Adsorption Analysis*

Table I gives the results of concentration determinations on the layers in the observation cuvette in a number of experiments with glucose-lactose mixtures of different total concentrations. Comparison of the last and the first columns shows the increased

concentration in the glucose layer, resulting from the displacement effect as predicted by the theory (see above). Only at concentrations below 0.2% is this effect negligible. It is a definite drawback of the present arrangement that experiments at lower concentrations than 0.1% are difficult on account of the low stability of the boundaries. From the results in the table it would appear that the displacement correction is roughly proportional to the concentration, so that a linear extrapolation to zero concentration might be permissible. It is also possible, of course, to make an empirical calibration of the observed and the true values for a given adsorbent; in this way mixtures of leucine and valine of total concentrations up to 2% have been analyzed with satisfactory results.

TABLE I

ADSORPTION ANALYSIS OF GLUCOSE AND LACTOSE SOLUTIONS

Concns of glucose and lactose, %	Sp. retard. vol., cc./g		Observed concentration in	
	glucose	lactose	lactose + glucose layer	glucose layer
0.10 + 0.10	5.04	76.0	0.20	0.10
0.22 + 0.22	4.51	48.2	0.41	0.21
0.60 + 0.60	4.01	25.0	1.21	0.64
1.00 + 1.00	3.32	15.2	1.98	1.16
2.00 + 2.00	2.92	9.75	4.02	2.61

3. *Examples of Applications on Various Solutions*

In the following, the specific retardation volume, $\bar{v}$, is given in cc. per gram of adsorbent at 20°.

Saccharides show strong adsorption on various active charcoals, *e. g.*, Carbo Active Kahlbaum, Carboraffin, Supranorit, Carbo animalis (Merck), blood charcoal (Merck). The retardation volumes vary surprisingly little for these adsorbents (less than 50%) and the relative order for the different saccharides is the same. Mono- and disaccharides are separated easily, and also di- and trisaccharides (raffinose). Otherwise the specificity is not so great as for other substances, *e. g.*, the aliphatic acids (see below). Thus it is not possible to separate sucrose and lactose, or glucose and fructose. Glucose and arabinose give a small but distinct separation.

It should be observed that the displacement effects referred to above also tend to merge the boundaries of two substances of nearly the same retardation volume into each other, so that the resulting diagram is not simply the superposition of the diagrams obtained for each component alone. This is in analogy to the simplest case of adsorption displacement, namely, when a substance displaces itself, which may

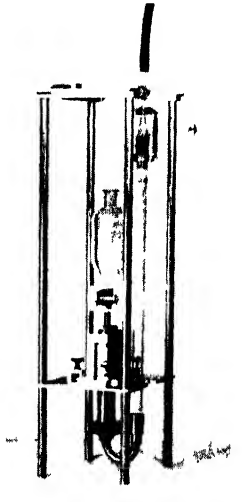

Fig. 8.—Apparatus for adsorption analysis in organic solvents

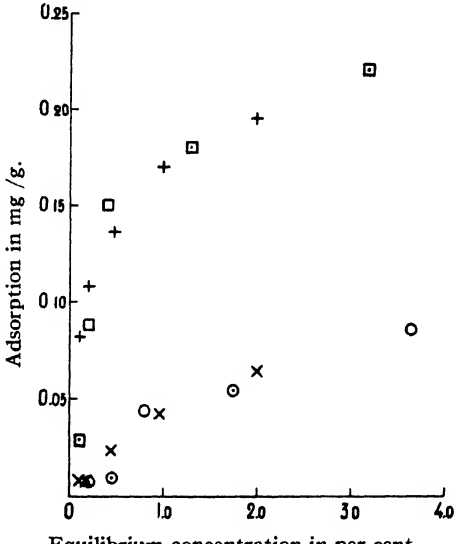

Fig. 9.—Adsorption isotherms for glucose and lactose obtained by equilibrium measurements (○ ⊡) and calculated from the observed retardation volumes (× +). Lower curve—glucose; upper curve—lactose.

be said to be the reason for the deviation of the adsorption isotherm from a straight line (supposing the adsorption affinity to be constant). Thus, in one experiment, a 1% solution of glucose gave a retardation distance of 20 mm.; in 2% solution, 14 mm. A 1% solution of galactose gave 19 mm., but a mixture of 1% glucose and 1% galactose gave only one boundary at 14 mm. instead of two boundaries at 20 and 19 mm., respectively. Evidently the glucose and galactose molecules are so similar in their adsorption behavior that they may substitute for each other in the isotherm. Such effects do not seem to depend

upon a similarity in adsorption isotherms solely; much smaller displacement effects are observed in mixtures of chemically dissimilar substances of nearly the same adsorption, *e. g.*, in mixtures of saccharides with amino acids. It is reasonable to assume that the active surface of the adsorbent contains affinity patterns of a large number of types and that displacement effects occur most markedly when there is a competition for similar patterns, as must be the case in mixtures of substances of similar constitution. One may perhaps even use the adsorption analysis in the manner described for detecting similarities in constitution, since the effects like those just described for the glucose-galactose mixture are very marked and easy to observe.

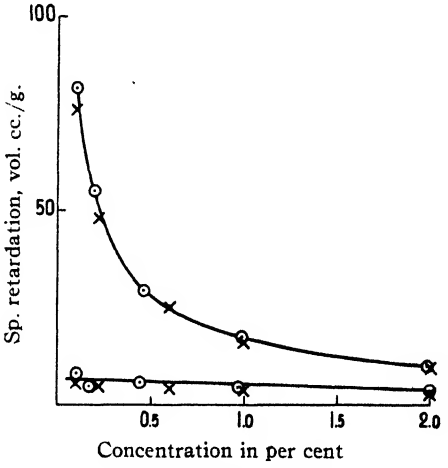

Fig. 10.—Specific retardation volumes for glucose (lower curve) and lactose (upper curve) alone (⊙) and mixed (×).

A number of organic acids and their mixtures have been investigated. Some of the results are given in Table II below. A number of mixtures were also tried, *e. g.*, acetic and succinic acids, which gave a nice separation. The higher fatty acids were investigated in various organic solvents with the metal and glass apparatus (Figs. 7 and 8). The differences were most marked in ether solutions; non-polar solvents like hexane give good adsorption but poor differentiation (Claesson, to be published).

TABLE II

SPECIFIC RETARDATION VOLUMES IN CC. PER GRAM OF CARBO ACTIVE FOR ACIDS IN 0.5% AQUEOUS SOLUTIONS

Acetic acid	5.5
Propionic acid	7.6
Butyric acid	11.0
Succinic acid	13.0
Tartaric acid (rac.)	11.4
Tartaric acid (meso)	7.0

It is interesting that mesotartaric acid and the racemic form show a difference in retardation volume sufficient to make a separation possible (Fig. 11). This is in agreement with adsorption data in the literature (see, for example, Ref. 6). It should therefore be expected that some difference might be observed in the adsorption of salts of optically active acids with alkaloids, but this has not yet been tried.

In adsorption analysis of electrolytes the dissociation may influence the result. The salts of organic acids are adsorbed much less than the acids themselves; sodium acetate, for example, does not give any ap-

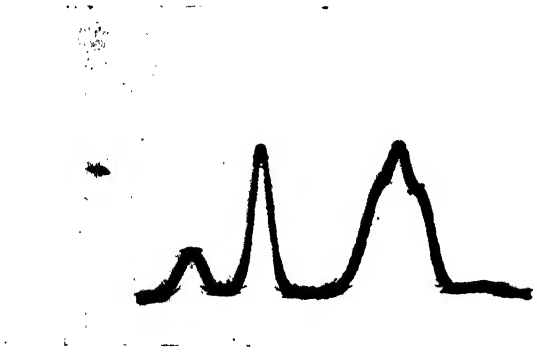

Fig. 11.—Adsorption analysis of a mixture of 0.5% rac. tartaric acid + 0.5% mesotartaric acid + 0.08 *N* sulfuric acid (left to right).

preciable retardation volume. Therefore the experiments on acids were mostly made in 0.05–0.1 *N* sulfuric acid medium, in which the dissociation is negligible. The sulfuric acid itself is not markedly adsorbed. In a mixture of sodium chloride and acetic acid some sodium acetate goes with the salt boundary and a weak hydrochloric acid boundary may be discovered, as hydrochloric acid shows a small but measurable adsorption.

The results on amino acids and peptides are summarized in Table III and in Fig. 12. The *p*H dependence of the retardation volume for leucine is shown in Table IV.

It is known from earlier work of Abderhalden and Fodor (1) and of Warburg and Negelein (4, 16) that many amino acids are markedly adsorbed by charcoal. The latter authors found that the carbon may catalyze the oxidation of amino acids. In order to avoid difficulties of this kind a trace of hydrocyanic acid was added to all solutions

investigated in the present work, and only air-free water was used as a solvent. As the retardation volume is strongly dependent upon concentration all experiments were made with 0.5% solutions, unless otherwise stated. The amino acids and peptides were preparations

TABLE III

SPECIFIC RETARDATION VOLUMES IN CC. PER GRAM OF ADSORBENT FOR 0.5% SOLUTIONS OF VARIOUS AMINO ACIDS AND PEPTIDES

Substance	Medium	Adsorbent	Sp. retard. vol.
Glycine	0.1 *M* NaCl	Carbo Active	0
Alanine	" " "	" "	0.3
Valine	" " "	" "	3.2
Leucine	" " "	" "	7.7
Iso-leucine	" " "	" "	9.2
Proline	" " "	" "	2.5
Oxy-proline	" " "	" "	1.9
Asparagine	0.05 *M* Na_2SO_4	" "	2.0
Betaine-HCl	" " "	" "	2.3
Phenylalanine	0.1 *M* NaCl	" "	62.5
Tryptophane	" " "	" "	76.5
Hippuric acid (0.29%)	0.1 *M* Na_2SO_4	" "	122
Histidine-HCl	0.1 *M* NaCl	" "	15.1
Aspartic acid (satd. soln.)	Glycine buff. *p*H 2 96	" "	3.6
Glutamic acid	" " " "	" "	5.5
Glycyl-glycine	0 1 *M* NaCl	" "	3.5
Leucyl-glycine	" " "	" "	18.2
Leucyl-glycyl-glycine	" " "	" "	29.8
Ornithine	Glycine buff. *p*H 9.92	Eponit 3n	2 7
Lysine	" " " "	" "	9.7
Histidine	" " " "	" "	15.4
Arginine	" " " "	" "	23.6

TABLE IV

SPECIFIC RETARDATION VOLUMES IN CC. PER GRAM OF ADSORBENT FOR 0.5% LEUCINE SOLUTIONS AT DIFFERENT *p*H'S. ADSORBENT: EPONIT 3N

Medium	*p*H of soln.	Sp. retard. vol.
0.2 *N* H_2SO_4	1.08	7.9
0.1 *N* glycine + 0.1 *N* H_2SO_4	2.18	11.2
M/40 Na_2HPO_4 + *M*/40 NaH_2PO_4	6.87	12.5
M/40 Na_2HPO_4 + 0.01 *N* NaOH	11.0	12.2
0.2 *N* NaOH	13.2	7.2

from Fraenkel and Landau and from Kahlbaum, the adsorbent was Carbo Active Kahlbaum, except for the experiments at alkaline and acid reactions, in which some material was dissolved from this adsorbent. Therefore a steam-activated carbon (Eponit 3n, Lurgi Gesellschaft, Frankfurt a. M.) was used in these cases. Of the other adsorbents tried Frankonit showed marked effects with the basic

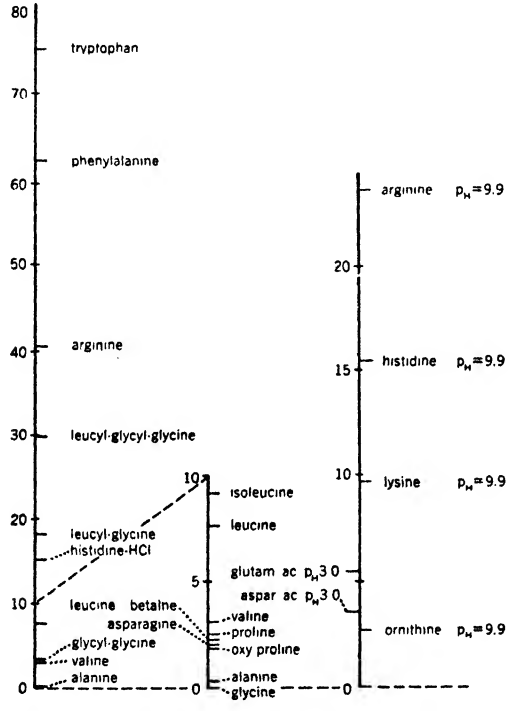

Fig. 12.—Retardation volumes for amino acids and peptides.

amino acids, but did not give as sharp boundaries as were obtained with charcoal.

Obviously the amino acids show great individual variation in their adsorption properties, which indicates that the adsorption analysis may be a valuable tool for their differentiation. The carbon chain length has a decisive influence and a difference of only one CH_2 group is sufficient to cause a marked difference in retardation volume (see leucine, valine, and lysine, ornithine, and aspartic acid, glu-

tamic acid). The appreciable difference between leucine and iso-leucine should also be noted. The aromatic and heterocyclic groups cause very large adsorption, in accordance with general experience (see phenylalanine and tryptophane. Tyrosine could not be investigated at neutral reaction on account of its insolubility). The mono-amino-dicarboxylic acids and the di-amino-mono-carboxylic acids were investigated in buffer solutions in the neighborhood of their respective isoelectric points, as their retardation volumes show strong dependence upon *p*H, whereas the neutral amino acids could be studied in simple salt media (NaCl, Na_2SO_4), the *p*H influence in this case being marked only at extreme acidity or alkalinity (see

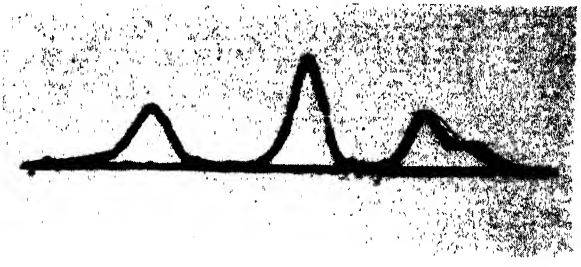

Fig. 13.—Gradient-curve diagram for a mixture of 0.5% leucine, 0.5% valine and 0.5% alanine (arranged in this order from left to right).

Table IV). This is in agreement with the well-known fact that the latter show a much more flat dissociation residue curve (Michaelis, 3) than the former.

Only the following dipeptides have so far been investigated: glycyl-glycine, leucyl-glycine and leucyl-glycyl-glycine. They gave excellent diagrams and seem to fit well into the general scheme (Fig. 12). Of all the amino acids investigated only glycine showed no measurable adsorption, in agreement with earlier findings (1). Glycine buffers could therefore be used with advantage in those experiments in which a definition of *p*H was required. (Acetate and citrate buffers are not so suitable since the corresponding acids are markedly adsorbed.) The ethyl ester of glycine, however, gave a marked effect (not shown in the figure; specific retardation volume in 0.5% solution on Carbo Active: 5.1 cc.).

In Fig. 13 a gradient diagram for a mixture of 0.5% leucine, 0.5% valine and 0.5% alanine is shown. These amino acids belong to a group in which separation by ordinary methods is rather troublesome. The adsorption method easily gives a distinct separation. Integration of the diagram gives the following concentrations: leucine 0.45%, valine 0.59%, alanine 0.48%. The high value for valine indicates that displacement effects play a role at this concentration and an experiment was tried using only 0.25% concentrations with the following result: leucine 0.24%, valine 0.26%, alanine 0.25%. In these experiments as well as with mixtures of saccharides or acids it was found that low concentrations of the more strongly adsorbed component were difficult to detect in the presence of high concentrations of components of low adsorption, the boundaries of the former usually becoming rather diffuse. This is also probably a consequence of the displacement effect. On the other hand, a small amount of a poorly adsorbed substance is easily discovered, even in the presence of a very large excess of a more strongly adsorbed component.

Fig. 14.—Adsorption analysis of a 5% casein solution digested with trypsin.

Only a few orientation experiments have been made with proteins. Surprisingly, the retardation volumes for egg albumin and casein on charcoal are small (smaller than that for leucine); probably the molecules are too large to enter into the finest pores of the adsorbent. Frankonit and floridin seem to be more suitable adsorbents in this case, but so far it has not been decided to what an extent real equilibrium is attained.

The investigation of digests obtained with proteolytic enzymes has only just begun. Figure 14 shows a diagram obtained after digesting a 5% casein solution with trypsin for 80 hours at 37°. A number of partially separated peaks may be observed, corresponding to a very complicated mixture.

It is a definite drawback of the method outlined here that the "development" as used in ordinary chromatographic analysis cannot be applied. A layer of lower density would follow each band in the column and would give rise to convection currents in the observation tube. Attempts are now being made to work out an arrangement which is independent of the density differences according to the general principle mentioned in the introduction to this paper. If sensitive enough such an arrangement would also make possible the study of more dilute solutions. A microconductivity cell connected to the outlet of the filter provides the simplest arrangement of this type, and has been found to work satisfactorily with mixtures of acids (*e. g.*, acetic acid and succinic acid), but it has, of course, a rather limited field of application. A micro-interferometric arrangement for the same purpose is now being constructed.

Thus our experiments have not yet led us to a procedure which is sufficiently free from complications to be capable of general application. On the other hand, it was thought that the results obtained so far might be of some interest as a demonstration that adsorption analysis methods may become of great importance in many fields in which they have hardly yet come into use. This is particularly true for protein degradation products with molecular sizes between those of native proteins and amino acids.

The work described here has been supported by a grant from the Swedish National Tuberculosis Association.

Bibliography

1. E. Abderhalden and A. Fodor, *Fermentforschung*, **2**, 74 (1919).
2. L. G. Longsworth, *J. Am. Chem. Soc.*, **61**, 529 (1939).
3. L. Michaelis, *Die Wasserstoffionen-Konzentration*, *I*, 2nd edition, Springer, Berlin, 1927, p. 54.
4. E. Negelein, *Biochem. Z.*, **142**, 493 (1923).
5. J. St. L. Philpot, *Nature*, **141**, 283 (1938).
6. N. Schilow and B. Nekrassov, *Z. physik. Chem.*, (A) **130**, 65 (1927).
7. H. H. Strain, *Chromatographic Adsorption Analysis*, Interscience Publishers, Inc., New York, 1941.
8. H. Svensson, *Kolloid-Z.*, **87**, 181 (1939).
9. H. Svensson, *Ibid.*, **90**, 141 (1940).
10. A. Tiselius, *Trans. Faraday Soc.*, **33**, 524 (1937).
11. A. Tiselius, *The Harvey Lectures*, Series XXXV, p. 87 (1939–40).
12. A. Tiselius, *Arkiv Kemi, Mineral. Geol.*, (B) **14**, No. 22 (1940).
13. A. Tiselius, *Ibid.*, (B) **14**, No. 32 (1941).
14. A. Tiselius, *Ibid.*, (B) **15**, No. 6 (1941).

15. A Tiselius, *Science*, **94**, 145 (1941).
16. O. Warburg and E. Negelein, *Biochem. Z.*, **113**, 257 (1921).
17. J. Norton Wilson, *J. Am. Chem. Soc*, **62**, 1583 (1940).
18. L. Zechmeister and L. von Cholnoky, *Die chromatographische Adsorptionsmethode*, 2nd edition, Springer, Wien, 1938. English Edition, London, 1941.

SOLUBILIZATION AND OTHER FACTORS IN DETERGENT ACTION

JAMES W. McBAIN

Department of Chemistry, Stanford University, California

CONTENTS

I. Introduction: Detergency a Complex of Many Diverse Factors*

Detergency is a broad term, covering many factors, some of which may be trivial while others are most intriguing and of the greatest

* An important symposium on *Wetting and Detergency* was held in London in 1937. American publisher: Chemical Publishing Co., New York, N. Y.

scientific interest. The American Society for Testing Materials defines a detergent as "any material which cleans." Thus water, through solvent and especially mechanical action, is an important detergent.

However, it is much more interesting to turn to little known but important factors. For example, many surfaces, such as glass or cellulose, are not wetted by water or aqueous solutions unless they are suitably charged. Thus, if the surface is made isoelectric by previous treatment with a very dilute solution of a polyvalent cation, water will simply roll off. A dilute solution of a cation-active agent, for this reason, does not wet glass, whereas lower concentrations and higher concentrations do so readily. Thus one of the first functions of a detergent or textile assistant or wetting-out agent is suitably to charge the surface. Non-aqueous detergents will be only briefly referred to in this review, but here we are confronted with such facts as that metals are preferentially wet by non-polar compounds, which agrees with studies of adhesive action.

It appears then that for most purposes there must be some affinity between the surface to be cleaned and the detergent used, in addition of course to some interaction between detergent and soil. The main inquiry here is as to the nature of this interaction.

We may leave to treatises on erosion such prominent factors in detergency as mechanical dislodgment, frictional carrying away by moving liquid, chemical attack and direct solution. This still leaves us with at least four important factors in detergent action, each of which calls for scientific recognition and much further study.

II. Early Studies of the Theory of Detergents*

Earlier theoretical writers gave their attention almost exclusively to ordinary soaps. The only alternatives at that time were the Turkey red oils and the saponins, whereas now we have thousands of synthetic and other substances, ranging from laboratory curiosities, such as nonyl glucoside, through the innumerable patented products to the physiologically vital substances, such as bile salts and blood proteins.

Chevreul (10), Berzelius (8), Persoz (69), von Bussy (89), Waren-Delarue (93), Knapp (34), Stiepel (82) and Moride (67) emphasized the emulsifying powers of soap solutions and of soap foam

* See Reference 43.

toward fats and fatty materials. The capacity of soap solutions to wet oily matter was also emphasized, while the unknown amount of hydrolysis alkali was credited with powers of saponification.

Hirsch (28), in 1898, showed experimentally that fatty oils were not more readily emulsified than were various other organic liquids, and he demonstrated also that the large amount of oil emulsified was quite out of proportion to the small amount of soap present. This showed that the effects produced were ascribable to the soap itself and not to any alkali present.

Donnan (13) in 1899 showed experimentally that emulsification and lowering of surface tension went hand in hand in the case of solutions of different soaps. However, Plateau (72) had pointed out that, in general, formation of solid surface films might be quite as effective as low surface tension in emulsification.

Hillyer (27) in 1903 showed experimentally that the emulsifying properties of soap could not be attributed to hydroxyl ions from hydrolysis alkali, nor did alkali possess the power of wetting oily matter that soap did. Hence both these factors in detergent action must be due to the soap itself. Of course, as Donnan had pointed out, the free fatty acid contained in all natural fats and fatty oils could be neutralized with formation of soap. This would be quite different from saponification of glycerides, which is an extremely slow reaction. Hillyer demonstrated again the parallelism of low surface tension and emulsification in the case of soaps, and incidentally showed that saponin emulsified through formation of solid surface film instead of through low surface tension. Hillyer also demonstrated the power of penetration into capillary interstices which is supposedly conferred upon soap solutions by their very low surface tension.

There was then experimental proof of the operation of two factors of detergent action, emulsification (parallel to low surface tension) and wetting power, both ascribable to the undecomposed soap itself. A third suggested factor, the action of soap in making tissue and impurities less adhesive to one another, was also put forward again by Hillyer, but the experimental evidence was entirely due to Spring (80) in 1909. Goldschmidt (21) had already postulated a protective action of the colloidal soap upon dirt particles, since Zsigmondy (98) had shown that the gold number of sodium stearate (the minimum quantity to protect 10 cc. of red gold sol from color change upon addition of 1 cc. of 10% sodium chloride solution) was 10 mg.

at 60° and 0.01 mg. at 100°. The value for sodium oleate was 0.6 to 1 mg.

Spring pointed out that all previous workers had been imbued with the conception of dirt as being of a fatty or oily nature, or covered with a coating of such nature. In his experiments, therefore, he carefully eliminated all fatty matter, which leaves the detergent action of soap quite unimpaired. His striking and original experiments dealt with purified lampblack, silica, alumina and iron oxide.

Spring's conception was that carbon promotes the hydrolysis of a soap solution and forms a stable non-adhesive sorption compound with the acid soap produced. Dirt upon a fabric he regarded as being combined with the fabric in an analogous way. Cleansing by soap is simply the formation of a sorption compound of dirt and soap in place of the sorption compound of dirt and fabric by direct substitution. A more logical alternative proposed by the present writer was that of double decomposition in which two sorption compounds are formed, fabric.soap and dirt.soap:

$$\text{fabric.dirt} + \text{soap} = \text{fabric.soap} + \text{dirt.soap}$$

As a matter of fact it is often extremely difficult to remove soap from a fabric after the operation of washing. Spring pointed out that alcoholic solutions possess poor detergent power because hydrolysis is not so great; this is not true if the alcoholic soap is used in water. However, he found that while lampblack took up acid soap, ferric oxide, silicic acid and cellulose take up soap containing an excess of alkali, so that his results in some cases might be more logically attributed to soap itself. The basic soaps of which he spoke do not in fact exist. The poor detergent action of alcoholic soaps on this view would simply be ascribable to the fact that in alcohol the soap contains only traces of colloid.

Jackson (31) in 1908 called attention to the influence which soap exerts upon the state of subdivision of the dirt, and he observed under the microscope dirt particles and fibers of linen being brought first into oscillation and then completely loosened by a soap. This spontaneous action was best exhibited by an alkaline oleate. He also pointed out that the presence of glycerine in soaps had only an unimportant influence upon their detergent action.

Krafft (36) insisted that the soaps must be in solution to exhibit appreciable detergent action. Thus in cold water sodium palmitate and stearate are insoluble, while the soluble oleate is an ideal deter-

gent, and even the only moderately soluble laurate and rosinate wash fairly well. The potassium soaps are distinctly more soluble. This necessity that the detergent itself be soluble is frequently overlooked. It is worth while emphasizing that it should always be held in mind in selecting detergents either for aqueous or non-aqueous applications. The colloidal nature of the lower soaps does not persist into very dilute solutions and is even less at high temperatures, which explains why stearate soaps are the best at the boiling point.

Moride (67) in 1909 emphasized the importance of wetting power. In particular he emphasized that soap solutions penetrate between the surface of the material to be cleansed and the layer of dirt or grease thereon. This conception was again emphasized by N. K. Adam (1) in 1937. Next to mechanical scraping, this wetting action may be the most important factor of detergency in removing thick layers of grease, as in washing dishes.

This earlier discussion may be summed up as a conclusion that detergent action of soap involved at least five factors: first, the necessity of having the soap in solution; second, power of emulsification, which goes parallel with low surface tension and the formation of surface films; third, wetting power which, like the last, is ascribable to the undecomposed soap itself and brings about penetration of the fabric and also detachment of grease therefrom; fourth, the formation of non-adhesive colloidal sorption compounds with tissue and impurities due sometimes to acid soap, but more often to soap itself, and capable of remaining in stable suspension; and fifth, the colloidal state of soap in solution.

III. Three Classes of Detergents

The three main classes of detergents are anion active, cation active and non-electrolytic.

Soaps are the best known examples of anion active detergents. Here the negative radical is responsible for the surface activity and for the colloidal behavior. The sulfonated or sulfated soaps, or Turkey red oils, are similar and have been known and used for a century. A decade ago synthetic substitutes were introduced to avoid hydrolysis or formation of insoluble heavy metal soaps. Incidentally some of the latter effect is not due to great insolubility, but partly to the action of the detergents themselves upon such products of reaction with hard water. The best known naturally occurring

examples, other than soap, are the salts of the bile acids such as sodium deoxycholate. All of these are colloidal electrolytes, as originally defined by the writer from 1912 onward. One of the ions is simple, say, sodium ion, while the other is partly or largely replaced by one or more kinds of colloidal particle or micelle by association of ions or ion pairs. The equilibria between the various forms in solution depend upon concentration and temperature and size of radical. In extreme dilution at low temperature, or in less dilution at higher temperature, even the substances of highest molecular weight dissociate into simple ions, save for effects of hydrolysis as in ordinary soaps and some other detergents.

The cationic analogs, such as cetyl ammonium chloride, were first studied by Krafft (36) in 1896 and later by Reychler (74) in 1913, who studied diethyl cetyl ammonium chloride and iodide, and now they may be typified by alkyl substituted pyridinium or ammonium chlorides, bromides or iodides. These again are colloidal electrolytes, but with the positive ion surface-active.

The non-electrolytic detergents are of the type of polyglycerol esters of fatty acids, or of condensation products of ethylene oxides with other substances. They therefore cannot be called colloidal electrolytes and indeed the constitution of their solutions in water and other solvents has scarcely begun to be investigated. The same comment applies to the study of the constitution of the colloidal electrolytes in non-ionizing and other non-aqueous solvents. This leaves a vast field open for investigation. The substances, such as triethyl cetyl ammonium cetyl sulfonate prepared by Reychler (74), which have both positive and negative radicals of high molecular weight, are as a rule insoluble in water, but they have not been investigated in non-aqueous solvents.

Since the term "colloidal electrolytes" does not include the third group, several other terms have been suggested, such as "paraffin chain salts" or "amphipathic" substances (Hartley, 25), a sub-group of what have been commonly referred to as polar substances. "Nearly all organic ions are to some extent amphipathic, but no others in so high a degree as the paraffin chain ions" (25). The term "paraffin chain salts" is no longer applicable to large categories of the newer much more complicated detergents, or indeed to bile salts or proteins. Similarly, although the term "amphipathy" reminds us that these chemicals must serve two masters, or have affinity for both solvent and soil, it is not general enough to describe the numerous com-

plicated molecules with all sorts of groupings in various positions serving different purposes, some but little understood; while the term "polypathic" would have an unfortunate connotation. "Polar," although inadequate, is probably still the best general term. Probably there will be no satisfactory designation until we understand such facts as that in a five-ring system a very slight change in a few atomic groupings changes a colloidal electrolyte such as sodium deoxycholate from a typical solubilizing detergent to sodium dehydrocholate which is not.

To suggest the manifold variety of the many thousands of substances to which we are referring, and their applications in industry, we may list some of the terms in common use: detergents, solubilizers, aquasolufacients, additives, emulsifiers, protective colloids, textile assistants, scouring, dyeing or finishing agents, wetting or wetting-out or spreading agents, penetrants, soaps. The terms solutizer and hydrotropic substances refer to a different class of substances which must be added in larger amounts and change the nature of the solvent to be effective; whereas a typical detergent is fully operative at a concentration of only one- or two-tenths of one per cent. This will be discussed more fully in a later section.

IV. Four Selected Factors in Detergent Action

There appear to be four inherently different factors in detergent action, all of which may or may not be exhibited by a single soap or detergent. Even when they occur together, it is important to discriminate between them. They are protective action, solubilization, base exchange and suspending action. Of these, protective action has been longest recognized; Engler and Dieckhoff (15) gave *prima facie* evidence of solubilization in 1892, although it was not proved until very recently; base exchange as a factor was discovered at Stanford University in 1940; and suspending action has only been discussed theoretically in a radio broadcast by the author ("Unlimited Horizons") in 1941. All are related to sorption.

Protective action and suspending action both imply pre-existing particles or such particles or droplets as may be formed by mechanical action. In protective action they are coated with a film supplied by the colloid. In suspending action no colloid need be present; the particle is charged and its sedimentation under the influence of gravity is retarded by the free ions of opposite sign which

are held in its neighborhood by electrostatic attraction. Protective action enables fine particles to go through a filter, whereas mere suspending action has no essential effect upon the dimensions or filterability of those particles. Protective action may be brought about by non-electrolytes, but suspending action requires free ions. Base exchange and solubilization are far more drastic. They take away the dirt, ion by ion or molecule by molecule, instead of taking pre-existing particles or droplets. A glass surface that has been stained with a polar dye is rendered colorless by exchange with an appropriate ion of a colloidal electrolyte such as a soap or a saponin. However, it may equally well be removed by sodium chloride, where there is no colloid. Solubilization can occur where there are no ions, *i. e.*, with a non-electrolyte or in non-ionizing media. In solubilization, molecules or ions are attached to the colloidal particles of detergent or sometimes definitely incorporated within them. The solubilization or enhancement of solubility of a hydrocarbon under reduced pressure can by no stretch of terminology be called peptization.

V. Protective Action

Spring's (80) experiments on protective action of soap make a good lecture demonstration. Lampblack or iron oxide, even though very finely subdivided, is not carried through filter paper by water, whereas when soap is present the filtrate is deeply colored. Elford (17) has emphasized the importance of such protective action, even in ultrafiltration, in coating not only particles or large molecules so as to render them independent of each other (peptization), but in similarly coating the pores of the ultrafilter to make them also indifferent. Again we are reminded of the equation

$$\text{fabric.dirt} + \text{soap} = \text{fabric.soap} + \text{dirt.soap}$$

However, Spring showed that it is not always quite so simple, since some materials take up an excess of acids and some others an excess of base, while still other detergents may be taken up unchanged. The equation is correct only if we remember that the word soap on the right-hand side often refers largely to the surface-active portion or derivatives thereof, formed by hydrolysis or base exchange.

Innumerable examples of protective action are to be found in the literature on emulsions and protected colloids, although in the greater

number of cases this factor has not been isolated from the others mentioned.

VI. Suspending Action

All suspensions and all emulsions should sediment under the influence of gravity. If they are lighter than the liquid system, they should cream, if heavier they should go to the bottom. If they can coalesce or stick to the bottom, the system should be progressively impoverished. If they cannot, the system should exhibit a logarithmic gradient of concentration upwards or downwards. All this is in accord with the well-known principles and equations worked out for the gravitational field by Mason and Weaver (66) and by many writers for the ultracentrifuge.

However, this is not commonly observed. Unless the particles are very coarse and heavy or the droplets large and light, the system may appear sensibly homogeneous for long periods. This, as has been shown, for example, by McDowell and Usher and by Johnston and Howell (65), is due to convection and stirring caused by vibration and especially by even minute irregularities of temperature. Thus the finer particles are kept mixed in spite of the forces that are continually tending to sediment them. For example, even for the heavy particles in a gold sol free of vibration, stirring is effective whenever there is a temperature change of more than 0.001° per hour (65).

Now we approach the problem as to how coarse heavy particles may be made to behave like fine particles without changing their actual size. The answer is simple. It depends merely upon imparting a charge to the particle so that charges of opposite sign to those on the particle must remain in the vicinity through electrostatic attraction. It is not even necessary that all the charges on the particle have the same sign. Then when the particle tries to settle, it must carry along with it all its atmosphere of free ions. Then the effective weight of each discrete unit in the system, that is, particle plus each ion, is the average of all. For example, if there are n charges on a particle, say 100, and n corresponding free ions, the average weight would be approximately $1/(n + 1)$ or $^1/_{101}$ of that of the original uncharged particle, since the ions are so small in comparison with the particle that their individual weights can be neglected. The effect is similar to a stone falling in water, but attached to a large number of small floats not sufficient actually to buoy it up, but enough to keep it held up in eddy currents.

We have to turn to some such explanation of suspending action in the numerous cases where such suspension is observed in the absence of colloids, as, for example, with various powders in sodium hydroxide or other ordinary electrolytes. Naturally soap can combine protective action with this suspending action and therefore be much more effective. This hypothesis, while apparently inevitable, needs quantitative investigation, for it is of the greatest importance in all suspensions, emulsions and lyophobic colloids.

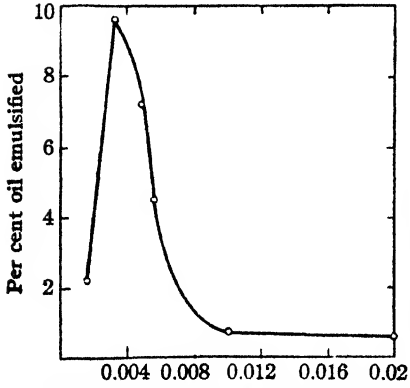

Fig. 1.—Emulsification of a hydrocarbon oil in water.

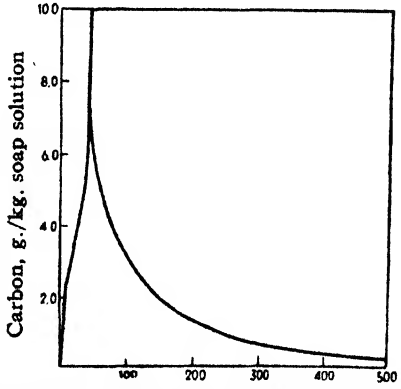

Fig. 2.—Influence of added alkali upon the suspending power of 0.0125 N_W (or 3.22 per cent) solutions of potassium myristate at 15° C.

Suspending action is not perfectly simple, for it is influenced by any change affecting the charge or charges, such as change in ionic concentrations, which may also drive back the dissociation of surface molecules or sessile ion pairs, and it is always steadily lessened by presence of increasing amounts of other indifferent ions.

Thus it is not surprising that Spring found the rate of sedimentation to be a function of the concentration of soap, or indeed of alkali, present. Lampblack sedimented as fast in 2% soap solution as in water; whereas in 1% solution it remained suspended for months, and in $^1/_2$% solution for days. For ferric oxide the optimum concentration was $^1/_2$% soap, and for potter's clay $^1/_{32}$% soap. Alumina

showed remarkable periodic optima in $^1/_4$, $^1/_8$ and $^1/_{16}$% soap, with a similar numerical periodicity of coagulation. Such phenomena have not been adequately studied or explained.

Donnan and Potts (14) found a similar optimum concentration in the emulsification of paraffin oil by soap solutions of $N/300$. In laundry practice optimum results are often obtained with 0.1 to 0.2% soap, although this has sometimes been found as high as 0.2 to 0.4%.

It is worth presenting diagrams showing, respectively, a maximum emulsifying power for oil in 0.9% sodium laurate (14), an extremely sharp optimum concentration of added alkali in the carbon number of 3.22% potassium myristate (49), and the broad optimum at 0.4% sodium oleate for the suspension of manganese dioxide (16) (Figs. 1, 2 and 3).

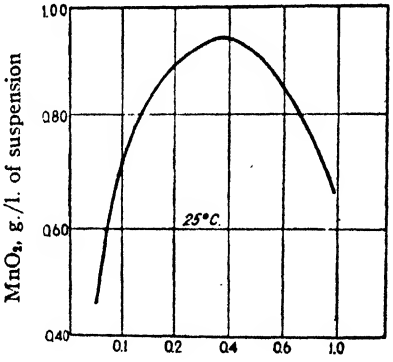

Fig. 3.—Suspension of manganese dioxide particles by aqueous sodium oleate solutions.

VII. Some Properties That Have Been Taken as Indirect Measurements of Detergent Power

Frothing (both as regards amount and stability of foam) lowering of surface tension, gold number, carbon number, dye number, Congo rubin number, etc., and similar properties have been put forward as indexes of detergent power. However, the foregoing discussion makes it obvious that no one property is likely to reflect all the complicated factors of detergency.

Gold number, for example, is a single number for a single soap. It is the number of milligrams added to ten cubic centimeters of standard red gold sol which just fails to prevent change to blue on the addition of one cubic centimeter of 10% sodium chloride solution. This one number omits all reference to effects of concentration, of the value of the detergent without salt or in other solutions, and all other factors.

Soap and beer are popularly appraised by the amount and stability of the foam they produce. However, some good detergents do not

foam. Other detergents may be excellent foamers, but exhibit no washing power under laundry conditions, because of cation-active effects. *Foam may be of mechanical importance in carrying off loosened dirt. There are, of course, definite relations between foam and some other properties of detergents, and Dr. R. D. Vold has pointed out relations to unsaturation and chain length of ordinary soaps.

In this connection attention may be called to the remarkable parallelism which the writer has noted between the reagents used in tanning, and in the treatment of drilling muds, and in the control of foam.

The carbon number has been extensively investigated by the writer and his collaborators (49), using refinements of Spring's technique, although the work of Maggs is still unpublished. It is only necessary to call attention to the complexities of the factors in carbon number—the effects of suspended carbon, of the excess of carbon, and of the filter paper upon the soap solution, as well as the interplay of protective and suspending actions. The optimum carbon number is observed at a much higher concentration of soap than that for laundry practice and still higher concentrations often show recurring optima.

The extensive measurements of dye numbers by McBain and Woo (61) are of great interest in themselves, but they used such finely divided dye that suspending action, protective action and solubilization are superimposed in the same numbers. In some cases this may be of more direct importance than a separate evaluation of each of the factors. Naturally they refer strictly to this one specific soil only.

The "launderometer" is a method of obtaining definite numerical values for detergent solutions with all their factors together, includir mechanical effects, but only at 60° C. with one particular fabric a: one standardized soil. If any one of these factors is varied, a: practical applications, the results can be very different. The effect of choice of fabric is illustrated by certain detergents which are remarkably efficient for wool but are of little value for cotton. Such specific effects still go unexplained. For their examination a breakdown of the detergent action into its separate factors will be requisite.

The surface tension relations of detergents open up whole fields of investigation, as yet very incompletely explored. Nearly everything here still remains to be done.

Careful measurements of surface tension of many alkyl sulfates have been made by Lottermoser and collaborators (42), a few with

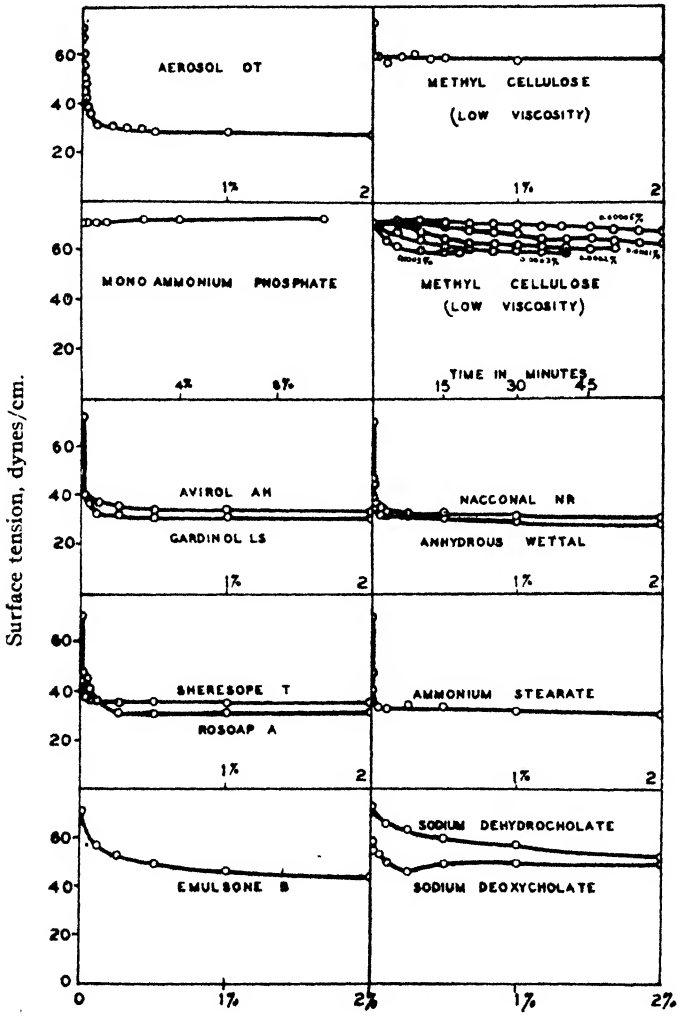

Fig. 4.—Surface tension-concentration curves by H. D. Bruce.

intriguing multiple maxima and minima for different concentrations of the same detergent, but sometimes with only one or none (E. K.

Washburn and collaborators (95) report similar effects). References to a hundred such cases are given by McBain and Mills (56). Other

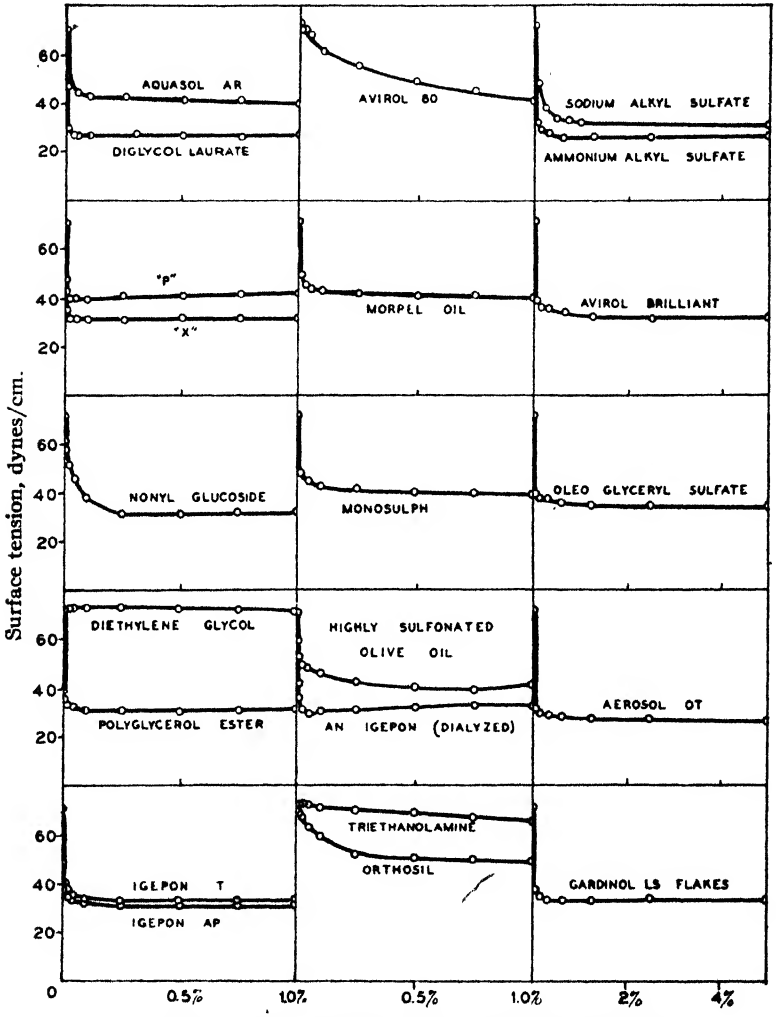

Fig. 5.—Surface tension-concentration curves by Ts-Ming Woo.

typical data are given by Powney and Addison (73), Wark (94), Cupples (12) and in International Critical Tables. Establishment of the surface tension is often practically instantaneous, but, also, often ex-

ceedingly slow. Sometimes for one range of concentrations it is instantaneous, but in another, for the same substance, requires very long periods. (For a recent paper on the still unexplained phenomena, see Alexander (3) or McBain and Sharp (59).)

Interfacial tensions against such a hydrocarbon oil as kerosene have been found, in unpublished work by Ts-Ming Woo at Stanford, usually to parallel the surface tension against air, with, of course, lower values. However, for ordinary soaps the curves differ greatly since the interfacial tension gradually sinks toward zero. We here reproduce some typical otherwise unpublished surface tension measurements made by Woo and H. D. Bruce with the du Nouy tensiometer at approximately 25°, mostly at an age of five minutes (Figs. 4 and 5).

Triethanolamine is not a detergent and has a Type I curve, in which the surface tension is steadily lowered with increase in concentration. Diethylene glycol is not a detergent and has a Type II curve, in which the surface tension of water is raised; so has monoammonium phosphate. The non-electrolytic detergents are nonyl glucoside, methyl cellulose, polyglycerol ester, "X," Product P and diglycol laurate. Aquasol AR, Monosulph and Morpel oil are Turkey red oils. The per cent refers to grams of the material as received in 100 cc. of water. Some of the substances were pure; some of the commercial materials contain a large proportion of diluents, such as water and salt.

All the typical detergents have Type III curves; that is, in very dilute solutions the surface tension of water is drastically reduced, sometimes to a third of its value, sometimes passing through a minimum and then remaining roughly constant with further concentration. For many applications this is most valuable. The non-electrolytic detergents lower the surface tension similarly but without the minimum, most of the curve, like those for Lottermoser's saponin, gelatine or gums, running appreciably horizontal. It is now notorious that the adsorption in the surface may in some concentrations differ from that calculated from the Gibbs equation as usually applied, sometimes even in sign (20, 62). According to that theorem, when the surface tension concentration curve is horizontal and therefore has no slope, the substance that is lowering the surface tension to a fraction of the value for the solvent (or for the well-mixed or dynamic surface tension) is not even adsorbed in the surface. The mystery is not lessened if one assumes adsorption upon the surface, because

then the theorem demands that for some unknown reason a very deep layer of solution below it is correspondingly impoverished as compared with the main bulk of the liquid below that.

VIII. The Perfect Triangle in Detergency

It takes three materials to make a complete example of detergency: namely, soap solution, dirt and fabric. Each then can react with, and compete for, the others and their products. Likewise, it is then easy to add the mechanical effects, thus to evaluate these as well. It can be demonstrated that an equilibrium, either static or dynamic, can be attained. For example, excess dirt could be extracted or deposited from the soap solution by fresh fabric; similarly, more deeply soiled fabric will give up some dirt to the soap-dirt solution. The effects of concentrations, temperature, added substances, so-called builders (such as silicates or phosphates) can be systematically studied, and if the experiment is properly carried out, the result is a complete empirical answer corresponding to the conditions chosen. Both time effects and equilibria need study. However, to establish a theory, the factors must be separately isolated. For scientific elucidation each side of the triangle must be separately studied, the solvent being taken for granted. Moreover, a complete scientific grasp of the field can hardly be obtained without appropriate variation of the solvent.

The fundamental approach must be applied in turn to each of the separate factors in detergency and to the influence of typical added substances on each. It appears self-evident that in this way each and every factor may not only be discovered and recognized but quantitatively characterized and formulated.

This systematic investigation is necessary because the theory is so incomplete and some of that which is universally taught has been demonstrated to be erroneous. We have already mentioned the conflict between the formulation of the Gibbs theorem and some carefully established facts. Again, under the influence of Langmuir's classical studies of insoluble films and of his simplified interpretation in terms solely of short range, unrelayed forces, it has been commonly considered impossible to lower the surface tension of paraffins and similar derivatives because their exterior already consisted of indifferent methyl groups. However, surface tensions of paraffins actually do differ greatly from each other; and M. E. L. McBain and Perry (64) showed that the surface tensions can be considerably reduced, even below that of any insoluble film on water. Likewise, we

have barely alluded to the many anomalies in surface behavior found in the writer's laboratory (48), often much delayed in publication, and now confirmed in many other places, especially in England, none of which fit into accepted theory or have received adequate explanation.

IX. Ion Exchange

In attempting to set up this detergent triangle for soap, dye and glass or cotton, confining it to the factor of solubilization alone by using a soluble dye, we (51) immediately discovered that ion exchange is a factor in detergency. When a large glass flask is wetted with a solution of methylene blue or crystal violet and then rinsed out with water until the washings are colorless, a bright blue solution is obtained with one further rinsing of soap solution or of sodium chloride or other ordinary electrolyte. Thus ion exchange is a real factor in removing soil that is in itself electrolytic or is derived from ionizable material. Cation-active and anion-active substances both are capable of ion exchange. Commercial detergents that are non-electrolytes may produce ion exchange by virtue of their contamination or dilution with electrolytes.

Ion exchange is not a cleansing in the sense of absolute removal of all material from the surface, but is merely a process of substitution. This again gives still further content to the diagrammatic equation

$$\text{fabric.dirt} + \text{soap} = \text{fabric.soap} + \text{dirt.soap}$$

We have found that salts most commonly used as soap builders, although themselves devoid of solubilizing power, are among the most effective in ion exchange.

In one per cent solution, sodium oleate, lauryl pyridinium iodide or synthetic detergent sulfates extract more dye than these salts, because the detergents have the additional advantage of solubilization as well as ion exchange. Basic dyes are more affected by anion-active detergents than are acid dyes.

After soaps and other synthetic detergents, the best salts for removing dyes from cotton or glass are aluminum chloride or hydrochloride, followed by barium chloride, several sodium silicates and hexametaphosphate (Calgon), then sodium sulfate or potassium hydroxide and trisodium phosphate, borax, hypo, potassium bromide, sodium chloride and potassium chloride. This shows the usual effects of valency and of preferential sorption of H^+ and OH^-. Of

course, such solutions as sucrose and methyl cellulose are completely non-effective unless a salt is added.

Dyes which are sodium salts, such as Congo Red, Calcomine Orange 2R, Calcomine 5RS and Pontamine Sky Blue 6BX, are very weakly sorbed by ordinary glass, or, if so, are almost completely removed by rinsing with distilled water.

However, all these acid dyes are sorbed if the glass is first exposed to aluminum ions. As long as there is any aluminum chloride in solution no basic dye is sorbed. Even after several rinsings the glass sorbs very little of the basic dyes. The aluminum ions are very slowly removed by rinsing, but the glass is readily changed back to normal by washing with sodium oleate or with sodium carbonate followed by oleate.

This process of ion exchange is rendered much more important by the recent findings of Harris, Steinhardt, Sookne and others (79, 81), who showed that the acid and base binding capacities of cotton and wool are determined by their content of electrolytic ash.

Consideration of the factors here discussed should lead to an explanation of the difference in detergents toward cotton and wool, respectively. Some suggested cases of ion exchange may finally be interpreted as instances of coacervation dispersed by salts.

Finally, it may be pointed out that an important application of a detergent, especially a cation-active one, is the opposite of that here discussed. It consists of the fixation of the opposite ion of soluble dyes by forming insoluble salts on the fabric. Similarly, instead of a detergent ion replacing charged particles in the delustering of rayon, it is used to attach such particles.

X. Solubilization

Definition.—Solubilization consists in the spontaneous passage of molecules of a substance insoluble in water into a dilute aqueous solution of a detergent, to form a thermodynamically stable solution. The thermodynamic stability is attested by the fact that the same equilibrium is attained from the side of undersaturation and of supersaturation; that is, a stable reversible equilibrium is attainable. Furthermore, the thermodynamic stability of such a system is proved by its being formed from the components with a decrease of free energy.

McBain and O'Connor (57) showed that when a volatile, insoluble hydrocarbon is solubilized or dissolved in an excess of aqueous de-

tergent, the vapor pressure is far less than that of the volatile liquid alone. It is clear that under these conditions there can be no droplets of emulsion present. The partial pressure of the hydrocarbon rises to approximately that of the volatile liquid only at saturation, and above this, emulsion may appear, if excess of hydrocarbon is mechanically dispersed in the saturated solution. Clearly, then, there is a sharp distinction between solubilization and mere stabilization of droplets as emulsion. Both processes, of course, can occur simultaneously.

Incidentally, it may be mentioned here that emulsification can be spontaneous without external mechanical agitation or work. McBain and Woo (60) provided a number of new demonstrations of this little-known phenomenon, which was discovered in 1878 by Gad (19). It occurs when diffusion across an interface drives solvent with it, or when a detergent is being formed in the interface. Such spontaneous emulsification naturally overshoots any equilibrium and must be partly or wholly reversed before true equilibrium is attained.

O'Connor investigated solubilization of hexane, methylcyclopentane, petroleum ether and diethyl ether, showing both the increase in solubility and the lowering of vapor pressure. It is significant that highly unsaturated vapor is dissolved by soap solution with further reduction in vapor pressure. Using potassium oleate, 100 cc. of solution containing 5.62 g. solubilized nearly 2 cc. of hexane or methylcyclopentane at 25° C. This amount is definitely increased by very small additions of either potassium hydroxide or of sodium silicate of ratio $SiO_2/Na_2O = 3.19$.

Historical Development.—It has been known since 1874 (see reference 15) that *concentrated* soap solutions dissolve cresols and tar oils. In 1892 Engler and Dieckhoff (15) published an important paper which appears to be known only in very restricted circles. They made a clear distinction between solution and emulsification, relying solely on the visual appearance of their systems. They made numerous measurements of the dissolving power of soap solutions for hydrocarbons, fatty acids, phenols and mixtures, some of the latter enhancing each other's solubilization.

Pickering's often quoted experiments (70) in 1917 were inconclusive because he used mechanical working of concentrated pastes of semi-solid soap. In 1918 and 1921 McBain, Beedle and Bolam (46, 7) made the obvious suggestion that a water-soluble substance could be sorbed by a soap particle in aqueous solution. In 1932, Lester

Smith, in a series of important and significant papers (77), showed that the solubility of various liquids was much increased by the presence of 10% of soap, and, like Weichherz (96) in 1929, he suggested that the increase was sorbed upon the soap micelles, possibly displacing water of hydration. The results depended upon the procedure and did not strictly demonstrate the existence of any true reversible equilibrium.

Lester Smith's explanation of solubilization has been repeatedly misquoted (25) in recent years. His actual words are, "The results are explained by postulating adsorption of the dye on the colloidal soap," and "the solvent powers of soap solution can only be accounted for by postulating adsorption of the organic solute on the colloidal soap particles." On page 1682 Smith cites the present references 46 and 7 as an example of this.

In Smith's second paper of 1932 he used a water-insoluble indicator dye, methyl yellow (0.32 part in 10^7 water), but (p. 1673) he first dissolved it in ether along with free fatty acids, and afterward produced soap by adding aqueous alkali and more ether (and usually methyl alcohol). This procedure too closely resembles von Weimarn's technique of forming unstable colloids *in situ* to carry any conviction as to the spontaneous formation of an inherently stable protected colloid.

McBain and McBain (52) in 1936 were the first to show that stable reversible equilibria are involved, and that dilute soap solution will extract water-insoluble dyes not only from pure crystals but even from unsaturated solutions thereof in kerosene, medicinal paraffin oil, paraffin wax or benzene. Each of the latter solvents will extract some of the dye from the soap solution.

XI. Mechanism of Solubilization

There are five general suggestions to explain solubilization, one or more of which may be true. First is hydrotropy; second, the "choleic acid principle" of the bio- and organic chemists; third, sorption upon or by micelles of detergent; fourth, ordinary solution in the hydrophobic portion of the micelles; and fifth, layers within lamellar micelles of detergent. Each of these must be discussed in turn, eliminating the first, casting doubt upon the second and fourth, and giving conclusive x-ray evidence that the fifth suggestion definitely occurs with soaps and lecithin.

1. Hydrotropy, or Change in Solvent

In 1916 Neuberg (68) introduced the term "hydrotropy" as a designation for the effect of large additions of various substances to water in increasing the solubility of other substances therein. Twenty-five per cent solutions of various sodium salts, such as benzoate, salicylate, benzene sulfonate and forty others, increased the solubility of twenty-one organic liquids, such as amyl alcohol, aniline and toluene, and the solubility of magnesium carbonate and phosphate. Von Hahn (90) showed that such substances as ethyl alcohol, acetone, pyridine, acetic acid and propyl alcohol increase these solubilities to the same extent as does benzoate or salicylate. Lithium iodide and triethanolamine borate are strongly hydrotropic. Sodium benzene sulfonate in 2 *N* or 50% solution (18) increases the solubility of benzoic acid from 0.29 g. per 100 g. water to 0.87.

Contrast with these cases of hydrotropy in concentrated solutions our statement that a good detergent should be effective even in a concentration as low as one- or two-tenths of a per cent.

It would indeed be miraculous if slight additions could greatly change the thermodynamic environment or essential properties of a solvent, so that substances which were previously insoluble therein now could dissolve in large amounts as ordinary simple molecules in true solution. It does not happen. M. E. L. McBain (61) found that the water-insoluble dye, Yellow AB, is still insoluble in 1% ethyl alcohol, or 5% ethyl alcohol, and it is still only 0.1% in 30% alcohol. Only above 50% alcohol does the solubility rise rapidly to substantial amounts, to become 2.4% in pure alcohol. Triethanolamine behaves similarly. On dilution with water, both of these soon deposit almost all their dye, whereas a good detergent would not.

To show that solubilized hydrocarbon does not go into true molecular solution, S. A. Johnston measured the freezing-point lowering of potassium oleate, finding that it was not affected when iso-octane was solubilized therein.

When glass stained with methylene blue is rinsed with 3% acetone, no dye is removed and the rinsing liquid is colorless, whereas the rinsing with 1% salt is blue through ion exchange, and a rinsing with a dilute detergent is blue through both ion exchange and solubilization.

Large additions of a good solvent are required to give appreciable solvent action to a non-solvent. Conversely, a comparatively small amount of diluent spoils a good solvent.

Attempts to explain hydrotropy either on the basis of surface activity or the formation of chemical reactions or addition compounds have been incompletely successful. It seems unreasonable to postulate complex compounds between sodium benzoate and such widely different substances as cetyl alcohol, aniline, uric acid, ethyl acetate, toluene and acetophenone.

All cases of heterogeneous equilibrium, no matter what the mechanism involved, may be represented by phase rule diagrams. It is remarkable that some think, following Lindau (41), that hydrotropy can be "explained" by the phase rule! All that is emphasized is that the systems are so concentrated that they fall well within a ternary diagram, in the same way that large additions of alcohol render benzene less immiscible with water.

Albert (2) in 1939 prepared clear systems of oil of eucalyptus, pine, citronella, tea tree and clove in concentrated soap solutions, of which the best was a Turkey red oil consisting of ammonium ricinoleosulfate. These were distinguished from similar solutions in strong aqueous alcohol because they remained clear on dilution instead of being redeposited. In certain instances cyclohexanol, menthol and oil of turpentine were likewise incorporated and occasionally increased the solubilization.

2. *The Choleic Acid Principle* of Wieland and Sorge*

Wieland and Sorge (97) found in biliary choleic acid approximately one molecule of higher fatty acids (palmitic, stearic and oleic) to about eight molecules of deoxycholic acid. They conceived it to be a new kind of coordination compound, supporting this by the fact that it had a higher melting point than either deoxycholic acid or the fatty acid. Over one hundred substances are listed as giving similar compounds with deoxycholic acid, including hydrocarbons, alcohols, ethers, acids, esters, ketones, etc., and the so-called coordination number is usually 4, 6 or 8, and occasionally 2 and 3. "Choleic acids contain on the average 88–95% by weight of the bile acid and 12–5% of acholic component."

"The formation of compounds of this nature was connected with the important physiological function of the bile acids to render all sorts of water-insoluble substances water-soluble. Since the alkali salts, *e. g.*, of naphthalene choleic acid or camphor choleic acid, are water-soluble,

* See Reference 78.

naphthalene, camphor, etc., can thus be held in aqueous solution." "The capacity of free bile acids to keep fatty acids and other acholic components in aqueous solution, whether due to the formation of coordination compounds or to other forces, is confined to the alkaline side of the neutral point;" that is, to the bile *salts* and not to the bile acids. The bile acids and choleic acids proper are completely insoluble in water.

The binary diagrams adduced for choleic *acids* probably indicate some form of combination with those acids in spite of many thermodynamic impossibilities in the diagrams as recorded. Even though such acid compounds may exist in the crystalline state, the corresponding salts can scarcely be responsible for solubilizing action if they are completely dissociated in solution. The phase diagram (91) for sodium deoxycholate and water shows that an octahydrate exists, which, however, is completely dissociated in the dissolved state.

The work of the past few years on solubilizing by detergents has shown that this property is common to very many detergents and not peculiar to bile salts. Likewise our unpublished studies (50) of the aqueous solutions of the bile salts show, in agreement with Roepke and Mason (75), that they too are colloidal electrolytes in aqueous solution. Hence we concur with these workers and with Anson (5) that the bile salts are no different from all the other detergents we are discussing. Ordinary soap has such a universal affinity for all substances tested that no completely indifferent reference substance has yet been found for testing such properties as hydration, glycerine being the best.

3. *Sorption by Micelles of Detergent*

Sorption occurs so readily at interfaces between liquids or between liquid and solid that it is difficult to imagine it not occurring to some extent on most colloidal particles, including those of soaps and other detergents. The only question is as to whether it is a relatively major or a negligible fraction of the interactions observed.

Soap curd fibers, according to the as yet unpublished vapor pressure measurements of W. W. Lee, definitely adsorb water vapor. Likewise the as yet unpublished x-ray measurements of A. de Bretteville, Jr., show that the addition of water causes a lengthening in the long spacings in the stable B monoclinic form, without appreciable alteration in the side spacings between the soap molecules. This shows that some of the water goes in between the ends of the soap molecules,

which are themselves laid end to end in pairs, and not between the soap molecules themselves. Any further water must therefore be sorbed on the exterior of the fibers. Soap curd fibers bear such a close relation to the lamellar micelles which exist in soap solutions that these results must be taken as fully relevant.

The sorption, by such curd fibers, of methylene blue from aqueous solution was studied by McBain, McDowell and Worden (53) and gave reasonable results for the size of the curd fibers, on the assumption that the dye was sorbed on the exterior of the soap fibers. The amount of methylene blue in the curd seems to be independent of whether the fibers are formed before the dye is added or are allowed to form in the presence of the dye. It should be mentioned that the soap molecules lie at right angles to the soap fibers, so that a continuous sheet of polar groups can be exposed on each of two sides. The other two sides have to be hydrocarbon chain. These dyed curds are now under x-ray examination.

McBain and McBain (52) pointed out that hydrophobic substances should as a rule tend to be incorporated within the micelle rather than remain in such large proportion upon the exterior as to render the micelles unstable. Brintzinger and Beier (9) assumed chemical combination, solution in and adsorption by colloidal particles of gelatine and in gum arabic, all occurring together, but their work included suspensions such as charcoal in addition to soluble acids and bases. Gurwitsch (22), in showing that the amounts of oil which could be incorporated in soap solutions without turbidity were parallel to the known ease and extent of association of the soap molecules, assumed that the oil molecules formed thick coatings around the soap micelles and made the micelles hydrophobic (that is, unstable). Such external sorption is much more likely for soluble dyes than for water-insoluble dyes.

4. *Ordinary Solution Within the Micelle*

Hartley and Lawrence adopted the spherical micelle (25, 39) originally proposed for soaps by Reychler (74) in 1913, and assumed by the writer for the small ionic micelle. They considered their micelle sufficiently large for the interior to be regarded as liquid hydrocarbon, and that this could dissolve amounts comparable to those soluble in an equal weight of hydrocarbon, subject to some modifications for the polar environment. There are considerable geometrical difficulties involved in this picture since soap molecules are

only three to five times longer than they are thick, and every molecule has to have one end on the surface. They also assume a minimum of fifty such molecules to make a close packed (not hollow or vacuous) sphere, whose greatest diameter is not more than twice the chain length. All published diagrams are a travesty on well-known atomic and molecular dimensions. Even if such short thick rods could be close packed radially, which is impossible as Ward (92) admits, over seven-tenths of the external exposed surface would have to be hydrocarbon. Further, dimensions have to be harmonized with observed conductivity and freezing-point lowering and with surface density of charge. Incidentally, their micelles have to be still larger and still less dissociated to conform to the conductivity of typical solutions (88).

Miss Parsons (25) found that *p*-dimethylaminoazobenzene was proportionately five times more soluble than in pure hexadecane, according to this hypothesis. McBain and O'Connor (58) found that potassium oleate in solution dissolved only about one-quarter as much as would an equal weight of olein. In Hartley's more careful work (26) there is better concordance. However, a survey of the extraordinarily diverse nature of all the detergents that solubilize in aqueous or non-aqueous solutions, and of the equally remarkable variety of the materials which they solubilize, renders it almost impossible to accept the solution hypothesis as a general explanation.

Most recently Ward (92) in a study of sodium dodecyl sulfate states, "It is shown that alcohol molecules are not in solution in the paraffin interior of the micelles in the mixed solvents, but are strongly adsorbed on the micelle surfaces." Toms (86) in discussing hydrated stearanilide and palmitanilide distinguishes between two kinds of bound water held by hydration of the micelles in solution. "This 'primary' bound water is difficult to remove by ordinary desiccation." "Easily removed by ordinary drying methods, this 'secondary' bound water is probably held loosely on the outer surfaces of the swollen micelles." Similarly Angelescu and collaborators (4) regard aromatic hydroxy compounds in soap solutions as being distributed outside and inside the micelles, in accordance with dipole moments and affinity for the hydrophobic portion of the soap, respectively.

5. *X-Ray Proof for Organized Lamellar Micelles*

The existence of lamellar micelles in soap solutions was long ago suggested by the writer in order to harmonize the different kinds of

physical chemical data. These lamellar, weakly conducting micelles were unhappily named "neutral" to contrast them with the small, highly charged and very highly conducting ionic micelles. M. E. L. McBain (63) showed in 1924 and in 1935 that the lamellar micelle conducts as well as crystallized soap curd fibers; that is, about seven per cent as well as an equivalent concentration of sodium chloride. A brief statement of the writer's conception of soap solutions was given in 1940 (44).

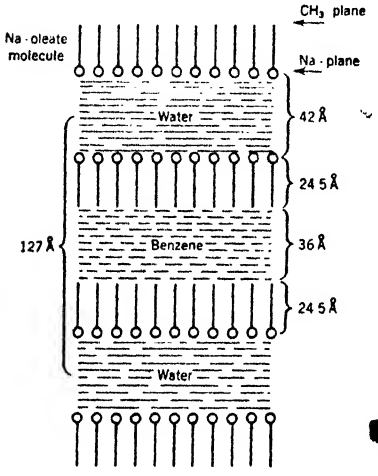

Fig. 6.—Schematic diagram of a micelle in 9.12 wt.% sodium oleate solution with 0.791 g. benzene/g. oleate.

Direct x-ray evidence has been obtained for the presence of the lamellar micelles in aqueous soap solutions, the soap molecules being close-packed side by side and placed in pairs end to end, just as in soap curd, except that Stauff (84) finds that the sideways packing may correspond to liquid crystal rather than crystal. His "Grossmizellen" are identical with McBain's neutral or lamellar micelle. Hess, Kiessig and Philippoff (29) find further x-ray results in 5% solutions of mercury sulfosalicylate. This work has mostly come from Germany (37, 29, 84), and is commonly ignored by writers in England (3, 92). However, there is no alternative explanation if x-rays do actually produce such photographs.

X-rays and electron diffraction likewise show regular spacings for surface-active materials dissolved in lubricating oils in the neighborhood of metal surfaces, as reported by Trillat (87) in France, Clark (11) in America and Tausz (83) in Germany. Indeed, they indicate that the oriented layers are many thousands of Ångström units deep.

Kiessig and Philippoff (32) find that the long x-ray spacings of the lamellar micelles correspond to the layers of soap molecules placed end to end at right angles to the lamellae and amount to 91 Å. Comparison with the length of the anhydrous sodium oleate molecule shows presence of some water which must be in sheets between the ends of the molecules as in de Bretteville's work referred to above.

6. *X-Ray Evidence for Deep Layers of Liquid Within Lamellar Micelles*

Now comes one of the most significant developments in the field of colloid and surface chemistry. When benzene is solubilized in the

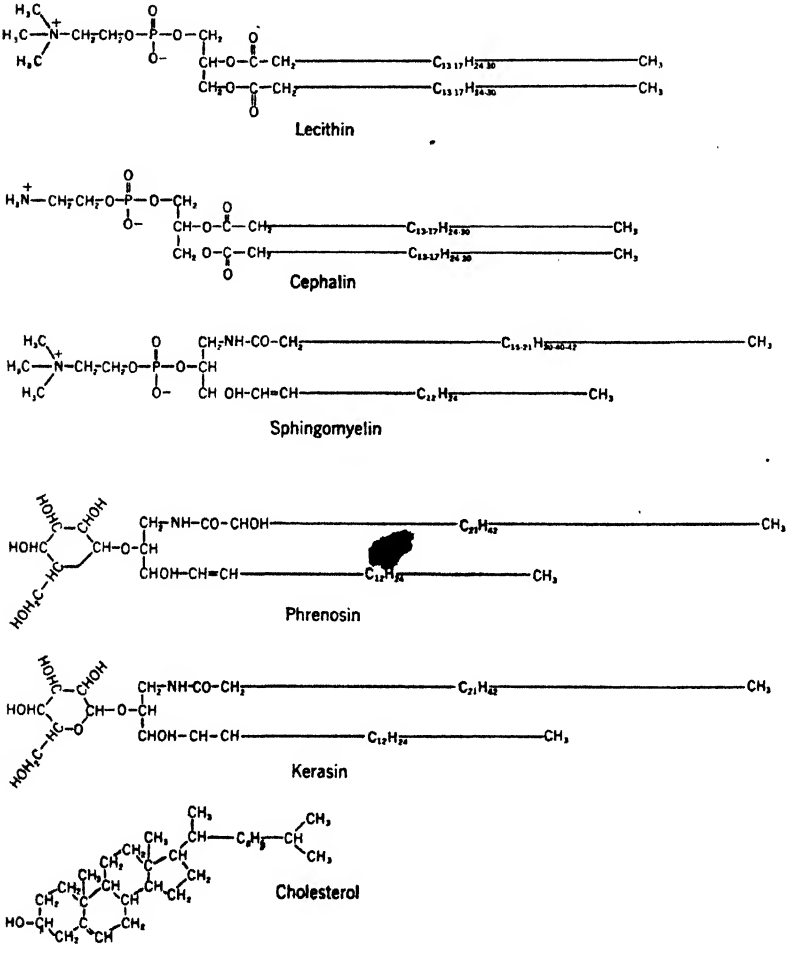

Fig. 7.—Stereochemical formulas of certain nerve lipides.

sodium oleate solution, the lamellar micelles expand to incorporate sheets of the hydrocarbon, just as they normally contain sheets of water (32), and the x-ray spacing increases from 91 to 127 Å. This is shown in Fig. 6.

Confirming these conclusions with an extremely different system is the x-ray work of Palmer (76, 6) on nerve lipide emulsions containing cephalin. Figure 7 shows the formulation of the bimolecular leaflets of typical lipides and Fig. 8 shows the expansion as water is progressively taken up as a layer within the bimolecular leaflet. The thickness of the water layer in the case of the 25% emulsion is no less than 85 Å., since the total long spacing is 150 Å., of which only 65 Å. are accounted for by the lipide molecules.

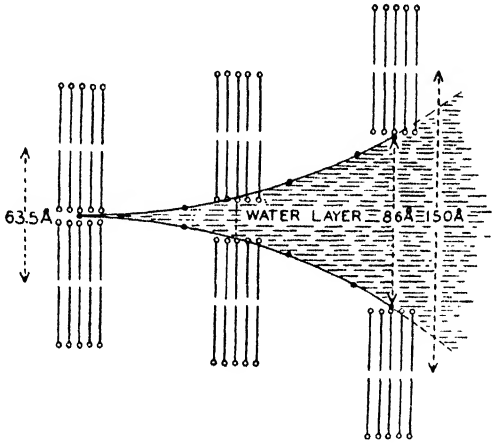

Fig. 8.—Schematic representation of the thickness of the water layers between bimolecular leaflets of mixed lipides as a function of the relative amount of water with which the lipides were emulsified. Points represent values obtained when the water content was 0 (dry), 25, 50, 67 and 75%.

According to Palmer and collaborators "apparently the first step in the recruitment into a homogeneous mixed phase of the lipides incompatible in the dry condition is the solvation of the polar groups and perhaps also the unsaturated or partially oxidized double bonds of the fatty acids." They also find that the side spacings point to lack of crystal regularity. Addition of potassium chloride reduces the water in the sandwich and 0.076 *N* calcium chloride expels it.

All these remarkable x-ray and electron diffraction results dealing not only with water but especially with non-aqueous layers constitute a definitive proof that short range forces may be relayed over long distances by successive polarization, just as a long row of iron filings

may be held to a magnet. This fully confirms the general view of Sir William Hardy (23) summarized at the Sixth Colloid Symposium in 1928 to the effect that surfaces and surface forces are extremely deep (24, 47). Likewise for ionizing solvents all surfaces are as deep as the diffuse double layer (48, 56). It is of fundamental importance in biology that most of the water in cells and in gels and jellies is within the reach of surfaces, and must therefore be polarized or in a sense "bound."

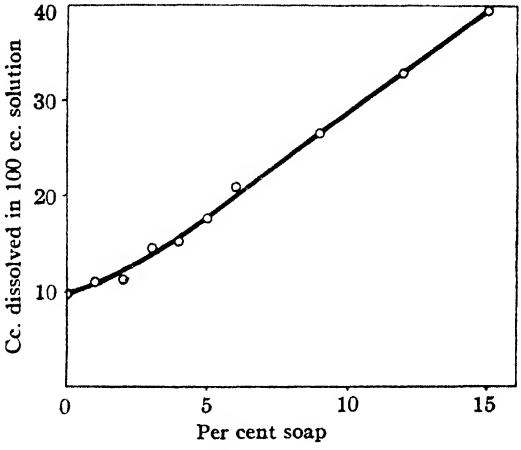

Fig. 9.—Effect of addition of potassium oleate in enhancing the solubility of propylene in water.

We may sum up this section by stating that it has been definitely proved for a few particular, but typical, cases that solubilization is due to sandwich-like layers between bi- or polymolecular leaflets in detergent micelles. Sorption is also of probably general occurrence, whereas compound formation or "choleic acid principle" must be confined to specific cases. Solution in the actual fabric of the micelles has not been proved; it may sometimes occur but cannot be a general explanation.

XII. Measurement of Solubilization

To set up the triangle for measuring the solubilization factor in detergent action, it is necessary to avoid all possibility of peptization or protective action or emulsification or suspension, by using either an unsaturated solution of soluble non-electrolytic substance or a

volatile vapor. Tjutjunnikow and Pleschkowa (85) used the soluble dye "Gelb echt" as soil and charcoal as fabric with five types of soap as detergent. This is the only such study, and it does not exclude ion exchange.

We have attempted only one side of such a triangle. The very simplest case is to measure the enhancement of the solubility of an indifferent hydrocarbon vapor through presence of detergent. This has been done by McBain and O'Connor (58), supplemented by unpublished data of A. M. Soldate. Butadiene and isobutane are appreciably solubilized by 1% potassium oleate. O'Connor's data for the increase in solubility of propylene in water caused by progressive addition of potassium oleate are shown in Fig. 9.

Soldate's data with propylene are given in Table I, where K = g. propylene per g. water $\times 10^5$/mm. Hg equilibrium pressure.

TABLE I

SOLUBILITY OF PROPYLENE IN AQUEOUS SOLUTIONS

Liquid	K	Solubilization
Water	0.034	0
1.5% Aerosol OT	0.075	+
15% Aerosol AY	0.09	+
12% Potassium oleate	0.148	++
0.4 to 5% Calgon	0.033–0.038	0

The method is not sensitive enough to measure any increase due to additions of potassium carbonate, tetrasodium phosphate or Calgon to the water or to the soap solution, but O'Connor (57) had previously shown that silicate or alkali may have some effect on the other hydrocarbons studied in a different method. The large effects obtained by Woo with a dye are mostly to be ascribed to factors other than solubilization proper, since his dye was used in the form of very finely divided particles.

The first study with recrystallized dye free from particles was made by Hartley (26), using cetyl pyridinium chloride, acetate, sulfate and bromide with transazobenzene. The solubility in water alone at 25° was 2.4×10^{-5} mols per liter, which was reduced to 2.0 and 1.8×10^{-5} by 0.1 N and 0.32 N sodium chloride, respectively. One normal sodium sulfate brought it down to 1.0×10^{-5}. The solubility in water was subtracted from that observed in the presence of the pyridinium salt with or without added sodium chloride or sulfate. The

lowest concentration investigated was 0.00072 N pyridinium chloride, which raised the solubility only to 2.6×10^{-5}, while 0.00095 N and 0.00104 N raised it to 3.5 and 4.8×10^{-5}, respectively. The highest concentration, 0.498 N, raised it to $10{,}000 \times 10^{-5}$, making the ratio between excess dye and added detergent 0.2. For the intermediate concentration, 0.05 N, the solubility was 816×10^{-5} and the ratio 0.16. Thus in the most concentrated solution, the ratio was still far

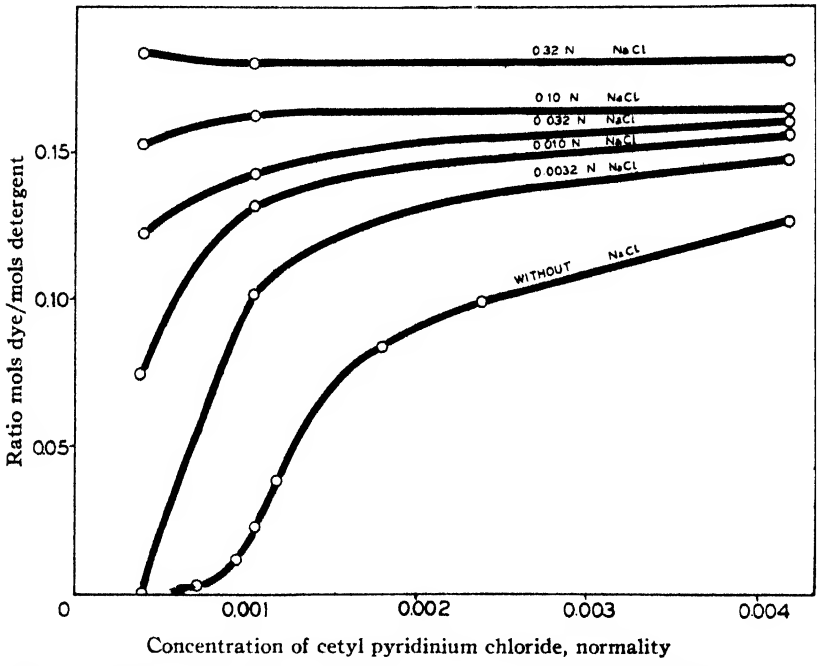

Fig. 10.—Effect of electrolyte additions on the solubilization of azobenzene by cetyl pyridinium chloride.

below the value 0.438 corresponding to the solubility in anhydrous pyridine.

Hartley's most interesting result is that although the ratio of solubilized dye to detergent becomes very small (although not negligible) in very dilute solution, it is greatly increased by the addition of electrolytes. This is well brought out in Fig. 10 (not identical with Hartley's graph), replotted from Hartley's numerical data, in which it appears that addition of 0.32 N sodium chloride brings up the ratio, even for 0.00031 N detergent, to that exhibited by the most concen-

trated solution of the detergent alone. This is explained by Hartley as proof of the effect of salt in forming micelles at the lowest concentration of detergent. R. C. Merrill, Jr., in this laboratory, suggests that additions of salts or builders in solutions where the detergent

TABLE II

THE SOLUBILITY OF YELLOW AB IN 1.0% AQUEOUS SOLUTIONS OF VARIOUS PURE AND COMMERCIAL SOLUBILIZING SOAP-LIKE DETERGENTS AT 25° IN MG. OF DYE/100 CC. OF SOLUTION

Soap or detergent	From super-satn.	From under-satn.	pH	Mols dye / Mol solubilizer
Merck sodium oleate	3.6	3.4	10.1	0.0042
Sodium laurate[a]	3.0	3.6	12–13	0.0034
Na salt of dioctyl ester of sulfo-succinic acid	12.2	11.8	7.1	0.022
Lauryl pyridinium iodide	32.4	31.5	6.8	0.048
A Na naphthenate	3.4	2.8	8.0	....
Commercial detergent of the type $RCONHCH_2CH_2N(C_2H_5)_2 \cdot HCl$	54.0	53.0	2.5	....
Commercial non-electrolytic detergent	62.5	58.0	5.0	....
Mixture of C_8 to C_{12} sulfonates	21.2	20.5	9.1	About 0.02
Sulfonated castor oil 75% pure	83.8	77.5	7.0	....
Sulfonated castor oil 4.3% SO_3, 29.6% H_2O	65.0	59.0	6.0	....
Sulfonated castor oil 30% water	75.0	75.0	6.5	....
Sulfonated castor oil 32.5% SO_3, 48% pure	37.2	36.5	5.1	....
Sodium cholate	2.5	2.3	10.7	0.0042
Sodium deoxycholate	6.2	6.0	8.0	0.011
Sodium deoxycholate + excess NaOH	7.4	7.3	9.0	0.012
Sodium dehydrocholate	0.0	0.0	9.0	0.00
Sodium taurocholate	6.0	5.2	6.3	0.011

[a] From pure Eastman Kodak Co. lauric acid (0.0361 g. excess NaOH per 40.0 cc.).

would otherwise be almost fully ionized produce micelles, and therefore solubilization, whereas in more concentrated solution, if all the detergent is in colloidal form, they reduce solubilization. Hartley considers that salts penetrate into these micelles.

A more careful study of the solubilization of water-insoluble dye, avoiding as far as possible all the sources of error in previous work, including that of Hartley, has been published by McBain, Merrill and

Vinograd (55). They used the water-insoluble dye Yellow AB (F. D. & C. Yellow No. 3) (phenylazo-β-naphthylamine), and also chloro-

TABLE III

THE SOLUBILITY OF YELLOW AB IN AQUEOUS SODIUM DEOXYCHOLATE SOLUTIONS AT 25° IN MG. OF DYE PER 100 CC. OF SOLUTION

Concn. NaDe, *M*	From supersatn.	From undersatn.	Mols dye / Mol NaDe
0.45	335.5	335.5	0.0302
0.225	165.0	165.0	0.0297
0.090	54.9	51.6	0.0239
→			
0.063	32.6	31.9	0.0207
0.045	15.1	15.0	0.0135
0.027	8.6	6.0	0.0109
0.0090	0.60	0.60	0.0027
0.0063	0.38	0.36	0.0024
→			
0.0045	0.24	0.22	0.0020
0.0036	...	0.13	0.0014
0.0027	0.095	...	0.0014
0.0018	0.07	0.06	0.0013
0.0009	0.03	0.027	0.0012

TABLE IV

THE SOLUBILITY OF YELLOW AB IN MG. OF DYE PER 100 CC. OF SOLUTION IN 0.009 *M* AQUEOUS SODIUM DEOXYCHOLATE AS AFFECTED BY THE ADDITION OF SALTS WHICH ARE BY THEMSELVES NON-SOLUBILIZING

Salt, concn. equiv. *N*	*p*H	From supersatn.	From undersatn.
NaDe alone	7.2	0.60	0.60
NaCl, 0.0250	..	1.16	1.16
NaCl, 0.050	7.6	1.81	1.80
Silicate, 0.025, Na_2O/SiO_2 = 0.310	10 4	1.07	1.07
$NaNO_3$, 0.025	6.8	..	1.14
NaBr, 0.025	7.0	1.07	1.04
NaI, 0.025	7.1	1.18	1.18
Na_2SO_4, 0.025	8.2	1.17	1.12
Na_2CO_3, 0.025	10.5	1.20	1.25
Na_3PO_4, 0.025	10.9	0.74	0.84
Urea, 0.025	7.0	0.56	0.53

phyll. Their results are reproduced in the following tables (II–V). In reading all these tables, it must be remembered that the commercial detergents were taken "as is," so that some that contain large

amounts of water or water and salts are being tested in correspondingly more dilute solution than those that are chemically pure. In Tables III and V the range between "critical concentrations" for initiation and complete formation of micelles is indicated by arrows.

TABLE V

THE SOLUBILITY OF CHLOROPHYLL IN AQUEOUS SOLUTIONS OF SODIUM DEOXYCHOLATE AT 25° IN MG. PER 100 CC. OF SOLUTION

NaDe, *M*	From supersatn.	From undersatn.	Mols chlorophyll / Mol NaDe
0.090	4.0	3.84	0.00048
→			
0.063	2.02	1.98	0.00035
0.027	0.32	0.28	0.00012
0.009	0.09	0.09	0.00011
0.0063	0.04	..	0.00007
→			
0.0027	..	0.01	0.00004

TABLE VI

SOLUBILIZATION OF YELLOW AB IN POTASSIUM OLEATE

N_W	Mg. dye/100 cc.	Mols dye/mol solvent
0.134	141	0.0041
0.067	68	0.0041
0.033	38	0.004
0.016	19	0.004
0.010	5.6	0.002

For comparison with the graph of Hartley's results we reproduce ours for Yellow AB in aqueous lauryl sulfonic acid (Fig. 11). Both show measurable solubilization below the so-called "critical concentration for initial formation of micelles."

Tables VI to X are supplied from unpublished work by R. C. Merrill, Jr., and include not only Yellow AB but also Orange OT (F. D. & C. Red No. 2) (orthotolylazo-β-naphthol). The measurements were made at 25° C. except where otherwise stated. Five per cent solutions of the solvents Butyl Cellosolve, Butyl Carbitol, Morpholine, acetone and isopropyl alcohol dissolved no dye, although 5% pyridine solution dissolved less than 0.05 mg./100 cc.*

*Examples of solubilization of carvacrol, cresol, ethylene dichloride, chloroform, lecithin, and fungicide are given in *Aerosol Wetting Agents*, by American Cyanamide and Chemical Corp., N. Y., 1941, p. 15.

An important note may be added here. M. E. L. McBain (55, 61) has demonstrated that when the detergent is not too concentrated or is not too lightly loaded with insoluble material, there always appear multitudes of colloidal particles visible in the ultramicroscope. This is true not merely with solubilized solids, such as dyes, but also with unsaturated vapors of hydrocarbons, as studied by O'Connor. It would appear that the affinity of the detergent and the substance to be solubilized for each other favors the formation of colloidal particles,

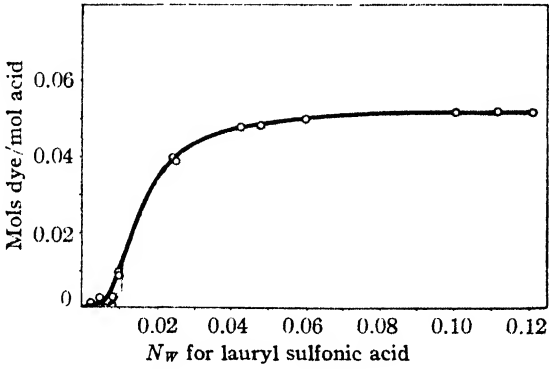

Fig. 11.—Solubility of recrystallized Yellow AB in lauryl sulfonic acid solutions at 25°.

not only by extending the region below which they normally would not form in the detergent alone, but also by forming these coarser colloidal particles. Particles of the size of Hartley's spherical micelle only two molecules in diameter could never be seen in the ultramicroscope, even with dye dissolved within them.

XIII. Passage of Solubilized Material Through Membranes

The observations on solubilization open important physical chemical questions in connection with the biologically vital problem as to the passage of material through membranes, cell walls and organisms. (See Sobotka's book, p. 128 (78), also H. N. Holmes (30), etc.)

Merrill has here found that solubilizers are effective in bringing insoluble substances into aqueous solution, even though separated from them by a membrane permeable only to ions. Sudan III dissolved in toluene, contained in a Visking cellulose sausage membrane swollen in 65% zinc chloride, when placed in a 1% solution of sodium

deoxycholate, or Aerosol OT, gradually allowed the color to permeate the aqueous liquid.

Similarly the dye in toluene passed through the membrane into fresh toluene containing a solubilizer such as Ninol 700.

Vinograd, also in this laboratory, found that Yellow AB in 1% aqueous Aerosol does not pass through a Cellophane membrane into

TABLE VII

SOLUBILIZATION OF YELLOW AB BY 0.1 *N* SODIUM DEOXYCHOLATE AND EFFECT OF ADDED SALTS

Salt added	Mg. dye/100 cc. solution	
	at 25°	at 62°
Sodium deoxycholate alone	71.2	175
+ 0.025 *N* Na_2SO_4	42.2	128
+ 0.025 *N* Na_3PO_4	37.0	113
+ 0.025 *N* Na_2CO_3	44.0	144
+ 0.025 *N* NaCl	41.5	119
+ 0.025 *N* sucrose	32*	121*

* Sodium deoxycholate decomposed in these experiments, possibly because of bacterial action.

TABLE VIII

SOLUBILIZATION OF YELLOW AB IN 1% OF VARIOUS DETERGENTS

Detergent	Mg. dye/100 cc.	Detergent	Mg. dye/100 cc.
Aerosol OT	12.0	Sodium dehydrocholate	0.0
Anhydrous Wettal	60.2	Sodium deoxycholate	6.1
Aquasol AR, 75%	62.0	Sodium laurate	3.3
Duponal WA	20.8	Sodium naphthenate	3.1
Igepal CTA (2%)	40.3	Sodium oleate (Merck)	3.5
Lauryl pyridinium iodide	31.9	Sodium taurocholate	5.6
Monosulph	75.0	Sapamine MS	53.5
Morpeltex	36.8	Triton B	0.9
Polysavox + 5% NaOH	3.0	Turkey red oil 75% (BKH)	80.6
Sodium cholate	2.4		

water although the Aerosol OT does. The dye is dropped at the membrane. However, if instead of water 0.5% Aerosol is used, the dye comes through into it.

Vinograd finds that Yellow AB does not affect the velocity of diffusion of Aerosol OT through water. The dye is found to move with the original Aerosol partner with which it was first associated and

TABLE IX

SOLUBILIZATION OF ORANGE OT IN VARIOUS DETERGENTS, 1% SOLUTION EXCEPT WHERE OTHERWISE NOTED

Detergent	Mg. dye/ 100 cc.	Detergent	Mg. dye/ 100 cc.
Aerosol AY	0.78	Octyl tripolyphosphate	0.27
Aerosol IB	0.07	Oleic acid soap (0.1%)	1.72
Aerosol MA (0.5%)	0.40	Olive oil soap (0.1%)	1.51
Aerosol MA (1%)	1.12	"P" (non-electrolyte)	0.82
Aerosol MA (16%)	24.2	Palm oil soap (0.1%)	1.62
Aerosol MA (30%)	34.1	Peregal O (non-electrolyte)	1.10
Aerosol MA (40%)	48.5	Polyglycerol ester (0.5%)	3.00
Aerosol OT	1.62	Product Q paste	17.75
Anhydrous Wettal	10.4	Product QB liquid	1.20
Aquasol AR	10.0	Santomerse D	4.86
Cetyl pyridinium chloride	22.7	Santomerse 3	7.00
		Sapamine A	0.63
Cetyl trimethyl ammonium bromide (0.08%)	0.31	Sapamine CH, 16.3% active	0.38
		Sapamine MS	7.00
		Saponin (Brit. Drug Houses)	0.70
Damol	12.7	Sodium deoxycholate	1.52
Daxad No. 11	2.87	Sodium heptadecyl sulfonate, 50% active	1.53
Duponal WA	8.0		
Emulphor O	4.90	Sodium lauryl sulfate	0.35
Emulsol 605 (0.5%)	2.51	Sodium lauryl sulfate + Triton 720 (0.5% each)	0.74
Emulsol 606 (0.5%)	4.24		
Igepal C	1.87	Sodium lignin sulfonate	0.85
Igepal CTA	1.80	Sodium novenate	4.69
Lamepon 4C	1.10	Sodium taurocholate	1.45
Laurel Conc. Textile oil	9.92	Syntex	3.65
Lauryl ester of α-alanine hydrochloride (0.5%)	3.98	Tallow soap (0.1%)	2.43
		Tergitol 4	0.38
Lauryl ester of 2-NH_2. HCl isobutyric acid (0.5%)	3.70	Tergitol 7	0.94
		Tergitol 08	0.10
		Triton B, 40% active (2.5%)	0.12
Lauryl pyridinium iodide	12.40	Triton K-12	4.72
"M" (non-electrolyte)	3.65	Triton 720	1.12
Monopol oil	4.50	Triton K-12 + Triton 720 (0.5% each)	4.05
Morpel oil	8.45		
Monosulph	8.62	Triton NE (non-electrolyte)	1.67
Nacconal FSNO	3.75	Turkey red oil A	13.50
Nacconal NR	16.15	"X" (non-electrolyte)	4.87
Ninol 555 (0.5%)	3.14	Zephiran, 10% active	0.40
Ninol 700 (0.5%)	4.55		
Ninol 967 (0.5%)	2.97		
Nopco 1440	7.75		

these are somewhat slowed. When dye in 1% Aerosol OT is allowed to diffuse into 1% Aerosol OT, its diffusion coefficient corresponds to that of a spherical particle of radius 34 Å. This is more than six times slower than the net rate of diffusion of Aerosol alone into water.

TABLE X

SOLUBILIZATION OF ORANGE OT IN AEROSOL OT

N	Mg. dye/100 cc.	Mols dye/mol Aerosol OT
0.0330	2.45	0.00283
0.0225	1.61	0.00273
0.0200	1.12	0.00214
0.0150	0.76	0.00193
0.0125	0.58	0.00178
0.0100	0.47	0.00179
0.0050	0.13	0.00099
0.0020	0.04	0.00038
0.0010	0.02	0.00038

These results show that solubilizing detergents can carry otherwise insoluble materials through membranes, even through such membranes as are molecular sieves.

XIV. Detergents in Non-Aqueous Solvents

So much attention has been given to aqueous systems that it is important to remember that practically all colloid and surface phenomena can be observed in non-aqueous non-ionizing media.

TABLE XI

SOLUTIONS OF $C_{12}H_{25}SO_3H$ IN HYDROCARBONS SHOWING SURFACE TENSION OF SOLVENT, σ_0; OF 1% SOLUTION, σ_1; AT MINIMUM, $\sigma_{min.}$, IF ANY; AND TYPE OF SURFACE TENSION CURVE

Solvent	σ_0	σ_1	$\sigma_{min.}$	Type
Nujol	33.5	25.9	24.8 at 0.2%	III
Mineral oil	33.0	27.8	27.4 at 0.18%	III
Benzene	29.7	29.3	None	I
Xylene	27.8	27.3	None	I
Tetraisobutylene	25.3	22.5	22.3 at 0.15%	III
Hydrogenated tetra-isobutylene	25.0	19.5	19.4 at 0.8%	III
Decane	23.7	22.3	None (?)	I, III (?)
Heptane	22.2	22.2	None	...
Iso-octane	19.5	19.2	None	I

M. E. L. McBain and Perry (64) found that Type III surface tension curves with a pronounced minimum are to be observed in solutions in various hydrocarbons. Their graphs (Figs. 12 and 13) and table (Table XI) are quoted here, but reference must be made to their publication for their comments on numerous other data. The only explanation so far put forward to account for the minimum found in such Type III curves is that suggested by the writer (48), based upon the electrical double-layer, whether partly diffuse, as in

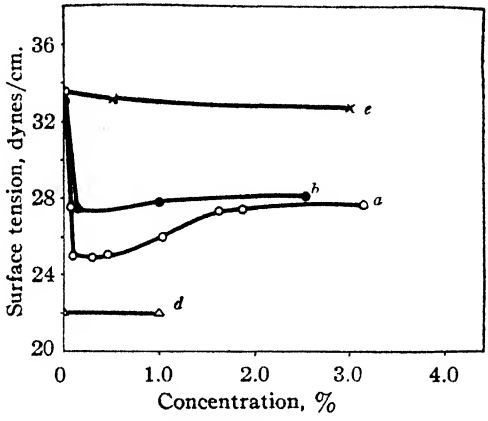

Fig. 12.—Surface tension curves for hydrocarbon solutions: Type III curves for lauryl sulfonic acid in (*a*) Nujol and (*b*) mineral oil; Type I curves for (*d*) lauryl sulfonic acid in heptane and (*e*) butyric acid in Nujol.

water, or the classical condensed Helmholtz type in these non-ionizing solvents.

McBain, Merrill and Vinograd (54) have adduced some hundreds of observations which show that solubilization can occur in non-aqueous solvents. This has great industrial importance. For example, an oil may be used in an engine with a detergent to solubilize and peptize the sludge or other dirt, to prevent ringing, sticking, formation of varnish, and to keep the engine clean. Other desirable materials may likewise be solubilized in petroleum product.

Pink (71) found that solutions of ethanolamine oleate in benzene and other organic solvents dissolve relatively large amounts of water. Here again small additions of substances, in this case, phenols and

cresols, greatly increase the amounts of water taken up by the detergent solution. In Kistler's (33) experiment some of the water emulsified in kerosene with aluminum palmitate that did not freeze may have been solubilized.

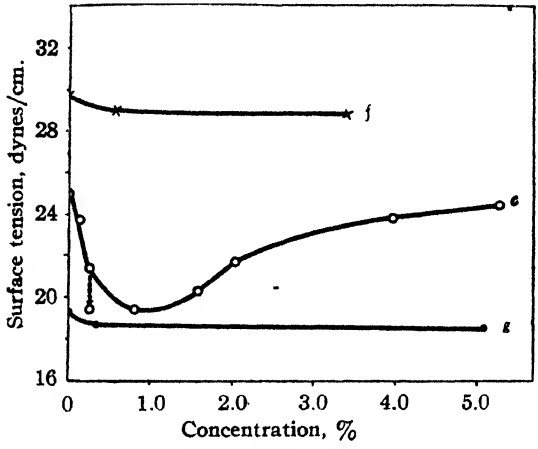

Fig. 13.—Surface tension curves for hydrocarbon solutions of lauryl sulfonic acid: Type I curves for (*f*) benzene and (*g*) iso-octane; Type III curve for (*c*) hydrogenated tetraisobutylene, showing with vertical dashed line the time effect in lowering of surface tension in very dilute solutions only.

XV. Engler and Dieckhoff's Classical Paper on Solubilization

Since Engler and Dieckhoff's interesting paper of 1892 is comparatively inaccessible and very seldom referred to, we may conclude this survey of some of the factors in detergent action by quoting two

TABLE XII

SOLUBILITY IN ONE HUNDRED CC. OF 10% HOT SODIUM STEARATE SOLUTION

		With addition of 10 cc. phenol
Benzene	1.6 cc.	9.2 cc.
Toluene	1.5 cc.	13.9 cc.
Xylene	1.0 cc.	37.0 cc
Turpentine	0.8 cc.	101.0 cc.

of their tables, even if some of the experiments merely serve as a reminder of the large number of factors that may contribute to total effective detergent action.

TABLE XIII

SOLUBILITY OF HYDROCARBONS IN ONE HUNDRED CC. SOAP SOLUTION AT ROOM TEMPERATURE

	Benzene	Toluene	Xylene	Turpentine
Na acetate satd. cold	0.1 cc.	2 drops	1 drop	1 drop
Na acetate + 13.47 g. HAc	0.2 cc.	4 drops	2 drops	1 drop
Na butyrate 50%	1.6 cc.	0.8 cc.	0.5 cc.	0.4 cc.
Na butyrate + 46 g. butyric acid	58.4 cc.	47.6 cc.	38.2 cc.	19.8 cc.
Na isobutyrate 50%	2.4 cc.	1.2 cc.	0.4 cc.	0.3 cc.
Na isobutyrate + 46 g. isobutyric acid	50.0 cc.	41.4 cc.	31.2 cc.	17.7 cc.
Na isovalerate 50%	3.6 cc.	2.4 cc.	1.2 cc.	0.7 cc.
Na isovalerate + 45.2 g. isovaleric acid	84.4 cc.	76 cc.	49.6 cc.	68.7 cc.
Na stearate 10%[a]	1.6 cc.	1.5 cc.	1.0 cc.	0.8 cc.
Na palmitate 10%[a]	1.8 cc.	1.3 cc.	1.4 cc.	0.4 cc.
Na oleate 10%	10 cc.	9.6 cc.	7.4 cc.	7 cc.
Na rosin soap 10%	5.2 cc.	4.4 cc.	3.6 cc.	5.8 cc.
Na rosin soap 15%	8.8 cc.	8.2 cc.	8.0 cc.	11.2 cc.
K rosin soap 15%	8.4 cc.	8.0 cc.	6.8 cc.	9.0 cc.
Na rosin soap 25%	20 cc.	18 cc.	17 cc.	32 cc.

[a] At elevated temperature.

Solutions in rosin soap clouded on warming, cleared again on cooling; *e. g.*, heating cold 25% sodium rosin soap saturated with 32 cc. of turpentine (see Table XIII) at 100° separated 20 cc. oil, which completely dissolved again on cooling. Excess of rosin greatly increased the solubility.

Bibliography

1. N. K. Adam, *J. Soc. Dyers Colourists*, **53**, 121 (1937).
2. A. Albert, *J. Soc. Chem. Ind.*, **58**, 196 (1939).
3. A. Alexander, *Trans. Faraday Soc.*, **37**, 15 (1941).
4. E. Angelescu and T. Manolescu, *Kolloid-Z.*, **94**, 319 (1941).
5. M. L. Anson, *J. Gen. Physiol.*, **23**, 239 (1939).
6. Bear, Palmer and Schmitt, four studies communicated to the *J. Cellular Comp. Physiol.* (1941).
7. Beedle and Bolam, *J. Soc. Chem. Ind.*, **40**, 27T (1921).
8. Berzelius, *Lehrbuch der Chemie.* 2. Aufl., Bd. III (1828).
9. H. Brintzinger and H. G. Beier, *Kolloid-Z.*, **64**, 160, 300 (1935); *Ibid.*, **68**, 271 (1934); *Naturwissenschaften*, **20**, 254 (1932), includes even suspensions like charcoal.
10. Chevreul, *Recherches sur les corps gras d'origine animale*, Paris, 1823, p. 376.

11. G. L. Clark, B. H. Lincoln and R. R. Sterrett, *Proc. Am. Petroleum Inst.*, (III) **16,** 81 (1935).

12. Cuoples, *Ind. Eng. Chem.*, **27,** 1219 (1935); **28,** 60, 434 (1936); **29,** 924 (1937); **31,** 1307 (1939).

13. Donnan, *Z. physik. Chem.*, **31,** 42 (1899).

14. Donnan and Potts, *Kolloid-Z.*, **7,** 208 (1910).

15. C. Engler and E. Dieckhoff, *Arch. Pharm.*, **230,** 561 (1892).

16. Fall, *J. Phys. Chem.*, **31,** 801 (1927).

17. J. D. Ferry, *Chem. Rev.*, **18,** 413 (1936). Fig. 15*b*.

18. H. Freundlich and Slottman, *Biochem. Z.*, **188,** 101 (1927).

19. J. Gad, *Arch. Anat. Physiol.*, **1878,** 181.

20. C. W. Gibby and C. Argument, *J. Chem. Soc.*, **1940,** 596.

21. Goldschmidt, *Chem. Ztg.*, **1904,** 302; Goldschmidt and Weissmann, *Kolloid-Z.*, **12,** 18 (1913); *Seifensieder Ztg.*, **41,** 337 (1914); *Z. Elektrochem.*, **18,** 380 (1912).

22. L. Gurwitsch, *Kolloid-Z.*, Ergänzungband, **36,** 196 (1925); see also *The Scientific Principles of Petroleum Technology.* Translated by Moore, D. Van Nostrand Co., New York, 1927, p. 95.

23. W. B. Hardy, *Colloid Symposium Monograph*, **6,** Chem. Catalog Co., New York, 1928, p. 7.

24. W. B. Hardy, *J. Gen. Physiol.*, **8,** 641 (1927).

25. Hartley, *Aqueous Solution of Paraffin-Chain Salts*, Hermann et Cie, Paris, 1936, p. 41; also article in *Wetting and Detergency*, Harvey, London, 1937, p. 153.

26. G. S. Hartley, *J. Chem. Soc.*, **1938,** 1968.

27. Hillyer, *J. Am. Chem. Soc.*, **25,** 511, 524, 1256 (1903).

28. Hirsch, *Chem. Industrie*, **1898,** 509.

29. Hess, *et al.*, *Ber.*, **70,** 1808 (1937); *Naturwissenschaften*, **26,** 184 (1938); **27,** 593 (1939); *Kolloid-Z.*, **88,** 40 (1939).

30. H. N. Holmes, *J. Phys. Chem.*, **43,** 1159 (1940).

31. Jackson, *J. Soc. Arts*, **55,** 1101, 1122 (1908) (Cantor Lectures).

32. H. Kiessig and W. Philippoff, *Naturwissenschaften*, **27,** 593 (1939).

33. S. S. Kistler, *J. Chem. Soc.*, **1939,** 53.

34. Knapp, *Lehrbuch der Chem., Technol.*, Bd. I, Abt. 2, 2. Aufl., p. 625.

35. Kortüm, *Z. Elektrochem.*, **42,** 289 (1936).

36. F. Krafft, *et al.*, *Ber.*, **27,** 1747, 1755 (1894); **28,** 2566 (1895); **29,** 1328 (1896); **32,** 1584 (1899).

37. Krishnamurti, *Indian J. Phys.*, **3,** 307 (1929).

38. I. Langmuir, *J. Chem. Phys.*, **6,** 873 (1938), see reference 40.

39. Lawrence, *Trans. Faraday Soc.*, **33,** 325 (1937).

40. S. Levine, *Proc. Roy. Soc. London*, **A170,** 145 (1939); S. Levine and G. P. Dube, *Trans. Faraday Soc.*, **35,** 1125 (1939).

41. G. Lindau, *Naturwissenschaften*, **20,** 396 (1932).

42. Lottermoser and Stoll, *Kolloid-Z.*, **63,** 57 (1933); Lottermoser and Püschel, *Ibid.*, 191; Lottermoser and Winter, *Ibid.*, **66,** 286 (1934).

43. J. W. McBain, *Third Report of the British Association for the Advancement of Science on Colloid Chemistry, D. S. I. R., H. M.* Stationery Office, London, 1920, p. 24.

44. McBain, *Nature*, **145**, 702 (1940).
45. *Cf.* McBain's diagram, *J. Chem. Education*, **6**, 2121 (1929).
46. McBain and Bolam, *J. Chem. Soc.*, **113**, 825 (1918).
47. McBain and G. P. Davies, *J. Am. Chem. Soc.*, **49**, 2230 (1927).
48. For a review see, for example, McBain, Ford and Wilson, *Kolloid-Z.*, **78**, 1 (1937).
49. McBain, Harbourne and King, *J. Soc. Chem. Ind.*, **42**, 373T (1928).
50. J. W. McBain and S. A. Johnston, to be communicated to the *J. Am. Chem. Soc.*
51. McBain, Lee, Merrill and O'Connor, *Chem. Prod.* (*London*), **4**, 19 (1941).
52. McBain and McBain, *J. Am. Chem. Soc.*, **58**, 2610 (1936).
53. McBain, McDowell and Worden, *J. Am. Chem. Soc.*, **61**, 2540 (1939).
54. McBain, Merrill and Vinograd, *Ibid.*, **62**, 2880 (1940).
55. McBain, Merrill and Vinograd, *Ibid.*, **63**, 670 (1941).
56. McBain and Mills, *Reports on Progress in Physics*, **5**, 30 (1939).
57. McBain and O'Connor, *J. Am. Chem. Soc.*, **62**, 2855 (1940).
58. McBain and O'Connor, *Ibid.*, **63**, 875 (1941).
59. McBain and Sharp, *Ibid.*, 1422.
60. McBain and Woo, *Proc. Roy. Soc. London*, **A163**, 182 (1937).
61. McBain and Woo, *J. Am. Chem. Soc.*, **60**, 223 (1938); *J. Phys. Chem.*, **42**, 1099 (1938); *Kolloid-Z.*, **87**, 74 (1939).
62. McBain and Wood, *Proc. Roy. Soc. London*, **A174**, 286 (1940).
63. M. E. L. McBain, *J. Phys. Chem.*, **28**, 673 (1924); *Trans. Faraday Soc.*, **31**, 153 (1935).
64. M. E. L. McBain and L. H. Perry, *J. Am. Chem. Soc.*, **62**, 989 (1940).
65. McDowell and Usher, *Proc. Roy. Soc. London*, **A138**, 133 (1930); Johnston and Howell, *Phys. Rev.*, **35**, 274 (1930).
66. Mason and Weaver, *Phys. Rev.*, **23**, 412 (1924).
67. Moride, *Traité de Savonnerie*. 3rd edition, Paris, 1909.
68. C. Neuberg, *et al.*, *Biochem. Z.*, **76**, 107 (1916); **171**, 485 (1926); **188**, 227 (1927); **199**, 498 (1928); **229**, 467 (1930); for later references see reference 35.
69. Persoz, *Traité Théorique et Pratique de l'Impression des Tissus*, 1846.
70. S. U. Pickering, *J. Chem. Soc.*, **111**, 86 (1917).
71. R. C. Pink, *Ibid.*, **1939**, 53.
72. Plateau, *Pogg. Ann.*, **44**, 141 (1888).
73. Powney and Addison, *Trans. Faraday Soc.*, **33**, 1246 (1937).
74. A. Reychler, *Kolloid-Z.*, **12**, 277 (1913); **13**, 252 (1913); *Bull. soc. chim. Belg.*, **27**, 217, 300 (1913).
75. R. R. Roepke and H. L. Mason, *J. Biol. Chem.*, **133**, 103 (1940).
76. F. O. Schmitt and K. J. Palmer, *Cold Spring Harbor Symposium on Quantitative Biology*, **8**, 94 (1940).
77. E. Lester Smith, *J. Phys. Chem.*, **36**, 1401, 1672, 2455 (1932).
78. H. Sobotka, *The Chemistry of the Sterids*, Williams and Wilkins Co., Baltimore, 1938.
79. Sookne and Harris, *J. Research Natl. Bur. Standards*, **23**, 299 (1939); *Textile Research*, **9**, 437 (1939); Sookne, Fugitt and Steinhardt, *J. Research Natl. Bur. Standards*, **25**, 61 (1940).
80. Spring, *Kolloid-Z.*, **4**, 161 (1909); **6**, 11, 109, 164 (1909); *Arch. sci. phys.*

nat., **28**, 569; **29**, 41; **36**, 80; *Rec. trav. chim.*, **29**, 1; *Bull. acad. roy. méd. Belg.*, **1909**, 187, 949; **24**, 17 (1911).

81. Steinhardt and Harris, *J. Research Natl. Bur. Standards*, **24**, 335 (1940); Steinhardt, Fugitt and Harris, *Ibid.*, **25**, 519 (1940).

82. Stiepel, *Seifensieder Ztg.*, **41**, 347 (1914); **51**, 647 (1924).

83. J. Tausz, *et al.*, *Z. angew. Chem.*, **43**, 570 (1930); *Erdöl u. Teer*, **9**, 331 (1933).

84. Thiessen, Stauff, *et al.*, *Naturwissenschaften*, **27**, 213 (1939); *Kolloid-Z.*, **89**, 224 (1939).

85. B. Tjutjunnikow and S. Pleschkowa, *Allgem. Oel- und Fett-Ztg.*, **31**, 59 (1934).

86. B. A. Toms, *Nature*, **146**, 266 (1940).

87. J. J. Trillat, *Rev. sci.*, **64**, 552 (1926); *Ann. Physik*, **10**, 5 (1926); *Compt. rend.*, **182**, 843 (1926); **187**, 168 (1928); *Mech. Eng.*, **50**, 471 (1928); *Halle aux cuirs*, Suppl. tech. 1927, 137; *Metallwirtschaft*, **7**, 101 (1928).

88. P. Van Rysselberghe, *J. Phys. Chem.*, **43**, 1054 (1939).

89. Von Bussy, see reference 67, p. 15.

90. F. von Hahn, *Kolloid-Z.*, **62**, 202 (1932).

91. R. D. Vold and J. W. McBain, *J. Am. Chem. Soc.*, **63**, 1296 (1941).

92. Ward, *Proc. Roy. Soc. London*, **A176**, 412 (1940).

93. Waren-Delarue, see reference 67, p. 15.

94. Wark, *J. Phys. Chem.*, **40**, 666 (1936).

95. Washburn and Berry, *J. Am. Chem. Soc.*, **57**, 975 (1935).

96. Weichherz, *Kolloid-Z.*, **47**, 133; **49**, 158 (1929).

97. Wieland and Sorge, *Z. physiol. Chem.*, **97**, 1 (1916).

98. Zsigmondy, *Lieb. Ann.*, **301**, 29 (1898); *Z. anal. Chem.*, **40**, 712 (1901); see also *Z. deut. Öl- u Fett-Ind.*, **44**, 297–366 (1924).

RECENT DEVELOPMENTS IN STARCH CHEMISTRY

KURT H. MEYER*

Chemical Laboratory, University of Geneva, Geneva, Switzerland

CONTENTS

The great interest which starch holds for chemists, botanists and technologists accounts for the vast number of publications which have appeared on the subject. This rich literature, however, is of such perplexing variety and so full of contradictions that a clear comprehension of the structure and reaction mechanism of starch is very

* Translated by J. Edmund Woods, Queens College, New York.

difficult to acquire. Part of the blame for this is due to unfortunate terminology which is not employed uniformly. For example, various authors apply the term "amylose" to entirely different preparations. The chief reason, however, is that, in researches upon starch, we have not yet, in many cases, come to make the same demands upon the preparative methods and the physico-chemical investigations as have proved indispensable in the study of other high polymers such as cellulose.

In discussing the present subject a critical survey of the methods in use is, therefore, absolutely necessary. At the same time such an examination will naturally provide a test and contribute to the understanding of the results, which will demonstrate how much is really known about starch. The picture thus produced will necessarily be clearer and more comprehensible than one might expect from a first impression of the copious literature. In our discussion we can dispense with a complete survey of previous investigations as Samec and Blinc (77, 78) have recently reported them collectively in a series of publications entitled "Die neueren Ergebnisse der Stärkeforschung" (see also (79)). Naturally, the work done recently at the University of Geneva was not considered in these publications.

I. The Chemical Constitution of Starch

1. Introduction and Synopsis

The term starch refers to polysaccharides occurring in plants in the form of grains which, upon complete hydrolysis, yield glucose and, upon partial enzymatic hydrolysis, yield principally maltose. Granules of "transitory" starch form in the green leaves as the first identifiable product of assimilation. Notwithstanding its considerable biological importance, it has not yet been definitely characterized. Only the starches of the grass-like plants (cereal starches) and those of roots and tubers, especially of potatoes, have been investigated thoroughly.

In addition to polysaccharide, the cereal starches contain small amounts of fatty acids, among which Taylor and Lehrmann (90) have identified palmitic, oleic and linoleic acids in cornstarch; Posternak (71) has also detected α- and β-glyceryl phosphoric acid. It is certain that neither class of substance is combined with the polysaccharide by primary valence linkage, for they can be removed by treatment with neutral solvents. It is probable, however, that they

are united with one another as fatty acid esters of glyceryl phosphoric acid.

The behavior of starch toward hot water, whereby a small, rather sharply limited portion goes into solution homogeneously, while the bulk remains as swollen grains or fragments which do not dissolve homogeneously, long ago led to the conclusion that starch consists of two different polysaccharides, water-soluble "amylose" and insoluble, paste-forming "amylopectin." Recently, to be sure, the composite nature of starch has been questioned by Alsberg (1) and by Badenhuizen (2). On the other hand, as will be fully explained later, the physical and chemical differences of the two constituents arise from differences in constitution (47). The so-called amylose consists essentially of a polymeric homologous mixture of unbranched chains (48) in which 100 to 700 glucose residues are united in α-1:4-glucosidic arrangement. Thus:

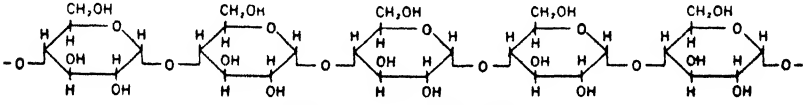

Section of amylose chain.

Amylopectin consists of giant, branched molecules of 500 to more than 2000 glucose residues in which branching occurs on the average at every 25th glucose unit, as represented by the following formula:

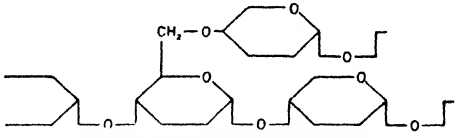

Branch point of amylopectin.

Accordingly we shall adopt a terminology based upon constitution, in agreement with prevailing chemical usage, and shall designate as *amylose* the unbranched chains and as *amylopectin* the branched molecules. In this to be sure, we depart from common usage, for Maquenne (46), who introduced these terms, employed them with entirely different meanings. Thus, he understood amylose to be the part of starch decomposed by malt and amylopectin the part not decomposed by malt. He supposed that starch consists of 80 per cent amylose and 20 per cent amylopectin. We now know, however, that there is no constituent of starch which is unaffected by malt, the

unbranched part being completely broken down and the branched part incompletely broken down. Hence, Maquenne's definition cannot stand in its original form. In more recent writings the term amylose has been used chiefly for that constituent which remains in aqueous solution when, after preparation of a paste with hot water, the bulk of the material is coagulated by freezing (Ling and Nanji (45)) or by electrodecantation (Samec (79, 81)). This amylose, called "amyloamylose" by Samec, really consists principally of unbranched constituents, although it is not entirely free from branched ones. For that reason we shall designate it as crude amylose. In many cases, however, "amylose" is also used simply to mean a degraded starch. This is done, for example, by Baird, Haworth and Hirst (3).

2. *The Separation of Starch Into Its Components*

In order to separate and examine the components of starch grains without altering them chemically, it is necessary to use means by which the cohesive bonds (secondary valence bonds) holding the molecules together in the grains are severed, while leaving the primary valence bonds intact. It is not altogether easy to find such means, for even agents which are very slow to hydrolyze the glucoside bonds and which have scarcely any noticeable effect upon maltose, for example, can nevertheless break down starch to a considerable degree. Thus, inasmuch as the polysaccharides of starch possess on the average more than 1000 glucoside links to the molecule, breaking 0.1 per cent of the glucoside links reduces the size of every starch molecule, on the average, to a half, whereas under comparable conditions only 0.1 per cent of maltose molecules are involved. Reagents which are considered harmless for glucoside bonds in sugar chemistry can therefore be unsuitable in starch chemistry. One should, above all, eliminate all hydrolytic agents, the degrading action of which has been recognized in cellulose chemistry. Moreover, the methods of cellulose chemistry should be used to test for decomposition.

A more reliable, though not very sensitive, method to test for decomposition is that of following the changes in reducing power, which increases in proportion to the number of bonds split hydrolytically. Much more delicate is the observation of the viscosity, which surpasses in sensitivity every chemical method for estimating degradation, for the ratio η_{sp}/c (*i. e.*, specific viscosity/concentration) is

approximately proportional to the molecular weight in the case of polymeric homologs of the same series, provided they do not differ too greatly. Thus, if a molecule containing 1000 glucose residues is broken by any agency whatsoever into two molecules of 500 units, only 0.1 per cent of the glucoside bonds are hydrolyzed; although the reducing aldehydic groups thus liberated are scarcely detectable analytically, the ratio η_{sp}/c falls to about one-half. Again, if, after a certain treatment, a starch preparation exhibits the same value of η_{sp}/c in a suitable solvent as before, no breakdown has occurred. The solvent must give a clear solution so as to be entirely homogeneous; aqueous solutions are unsatisfactory because unstable. In our laboratory hydrazine hydrate is used as solvent for starches or their components (53). The viscosity of acetyl derivatives is determined in chloroform or in tetrachloroethane and that of methyl derivatives in chloroform or in benzyl alcohol.

Fractionation of Starch (with Degradation). The following still widely used methods for separating starch into its components do not completely fulfill the necessary requirement of protecting the molecules of the starch constituents from degradation.

Treatment with Superheated Water. Starch is only partly dissolved by boiling water; the bulk of it remains in the form of swollen grain fragments. For this reason Ling and Nanji (45), Samec (77, 79) and many other investigators treat starch with water at 120° to 140°, whereby gradual dissolution occurs or, at least, a better homogenization or "peptization" is obtained. However, this technique, which is very popular in starch chemistry, destroys the starch molecules by hydrolysis of glucosidic linkages. This is evident from the reduction of viscosity as well as from the following observations (63). The reducing power of a starch solution increases after two hours' heating at 126° with water of *p*H 6 by about 3 units of the so-called copper number. That is, additional aldehyde groups are liberated by hydrolysis, specifically, one to every 600 glucose units. The degradation goes as far as molecules about 100,000 units in weight (78*a*).

The decomposing effect of superheated water may also be observed with so-called erythrogranulose, the high molecular dextrin which remains behind upon hydrolyzing starch with β-amylase, being unattacked by this enzyme. If erythrogranulose is exposed to superheated water, it can be hydrolyzed afterward by β-amylase (Hanes (21)), signifying, therefore, that new points of attack have been

formed; these result from cleavage of bonds within the molecules, as will be shown later. Products and peptized solutions obtained with superheated water cannot be considered, therefore, as consisting of intact starch components. In this category belongs, among others, the "erythroamylose" of Samec, which he regards as made up of unchanged starch components.

Treatment with Acids or Acid Salts. As the hydrolyzing action of hydrogen ions is generally recognized, the "soluble" starches obtained with acids are correctly regarded as degradation products. However, many other substances not designated by authors as "breakdown products" are also the results of hydrolytic decomposition. Among these is the "simplified starch" of Haworth, prepared with hydrochloric acid, as well as the "simplified amylose" or the soluble glycogen described by English writers (3, 26). Moreover, the preliminary treatment of starch with cold hydrochloric acid and subsequent drying, whereby starch is made "peptizable," is nothing else than a degradation into easily soluble fragments of lower molecular weight.

Again, acidic salts like zinc chloride or mercury-potassium iodide act hydrolytically, as is known from cellulose chemistry and otherwise. Zinc chloride has been used, among other reagents, by Lamm (44) for dissolving starch, in order to determine the molecular weight of starch by the ultracentrifuge method.

Alkalies, in the presence of oxygen, lead to degradation. (See Staudinger (87); K. H. Meyer (54).) When oxygen is excluded, even concentrated alkalies seem to have no degrading action.

Superheating with glycerol degrades starch, through a soluble breakdown product, the so-called "Zulkowski starch," to lower molecular weight products ("trihexosane," etc.), which have been investigated by Pringsheim (72) and Pictet (70).

Hydrolytic enzymes have often been employed for breaking down starch, as by Naegeli and by Maquenne. Yet the amylatic enzymes attack all starch components; the compounds remaining after attack by amylases are themselves degraded (see below).

Fractionation of Starch (without Degradation). By the following procedures starch is not degraded or hydrolyzed, according to our experience; they can therefore be used for the isolation of starch components.

Water below 80° effects practically no degradation, even in the course of several hours; it has been estimated that the velocity of

hydrolysis at 80° is some hundred times smaller than at 120°, so that the decomposition at 80° is negligible. To be sure, starch cannot be dissolved by water at 80° but merely swelled; from the swollen starch grains crude amylose diffuses out in water-soluble form, so this mild treatment is satisfactory for the separation of amylose and amylopectin (52).

For the fractionation of that portion which is insoluble in hot water, it is satisfactory to use an aqueous solution of one part by weight of chloral hydrate in two parts of water (52, 53), the acidity of which has been neutralized by addition of bicarbonate. At room temperature only crude amylose dissolves, more and more dissolving as the temperature rises. Solution is complete at 80°. Dilute and concentrated caustic soda solutions do not split the amylose at room temperature in the absence of oxygen. Difficultly soluble preparations, *e. g.*, of amylose, can be brought into solution with dilute sodium hydroxide and they are slow to precipitate again after neutralization. Formamide dissolves starch at temperatures above 100°, but the possibility of degradation is not excluded because of the increasing acidic activity of formamide when heated. Hydrazine hydrate is our preference as a solvent for viscosimetric investigations. Ethylenediamine hydrate is also useful.

In order to convert starch or difficultly soluble starch components into water-soluble form, they are heated with one part chloral hydrate and two parts water to 80°, filtered through a G3 Jena filter and the solution sprayed into stirred acetone in a very fine stream. The precipitate is separated by decantation, washed several times with acetone and extracted in a Soxhlet, first with acetone and then with ether. The freshly prepared material is soluble in warm water but it rapidly loses its solubility (50, 53).

In 1 to 2 per cent suspensions of starch, the grains of which are well swollen but not excessively disintegrated into small fragments, the liquid, amylose-containing phase can be separated from the paste by settling and decantation or by centrifuging. If the grains have been fractured by boiling, clarification with the ordinary laboratory centrifuge cannot be accomplished. Nevertheless the suspended particles coagulate if the solution is frozen; after melting, the previously suspended particles form a coherent mass which can be removed by the method of Ling and Nanji (45). Separation of the suspended particles succeeds particularly well by electrodialysis (really electrodecantation), which was introduced into starch chem-

istry by Samec (79, 81). Those particles which consist mainly of amylopectin then migrate to the anode and there fall to the bottom, while the solution, containing the amylose as well as the lower molecular weight breakdown products, becomes clear. According to Samec, electrodialysis should effect a separation into a part containing phosphoric acid (amylopectin), which settles out, and a phosphorus-free amylose. This may be correct in many cases, yet for the anodic separation it is not the phosphoric acid content but the particle size which is important. Large carbohydrate particles, which produce turbidity, always separate, even if they are phosphorus-free, *e. g.*, the amylopectin-containing residue of boiled maize starch; see Meyer and Bernfeld (55). Conversely, the phosphorus-containing amylopectin of potato starch can remain in solution for a long time, even on electrodialysis, if it has previously been converted into water-soluble form by treatment with chloral hydrate and then dissolved in water (63).

Isolation of Amylose. Starch grains of maize and wheat, as well as of potato, swell in water at 60° to 80° without being fractured and crude amylose diffuses out of them. The solution can be freed of the swollen grains by settling or centrifuging. At 100° the grains disintegrate and the turbid solution must first be cleared by electrodialysis. Most of the polysaccharide separates from the solution in the course of a few weeks at 5°. The precipitate is crystalline, for it gives a powder diagram with x-rays. We designate this kind of separation, therefore, as a crystallization, although it is often referred to by the superficial term, "retrogradation."

3. *Amylose, Its Properties and Constitution*

Properties of Amylose. Amylose contains no phosphorus (Samec (79)). It can be separated into fractions having different solubilities in water (53). With increasing purity all fractions become less water-soluble. By precipitation from chloral hydrate, amylose is obtained in finely divided, water-soluble form; this product gradually becomes insoluble again. It appears that purification lowers the solubility and that the solubility diminishes further by slow increase in crystallite size, just as in the aging of inorganic precipitates. The influence of crystallite size can be very important in the case of amylose with its high molecular weight (10,000 to 60,000) and small crystallite size, which is estimated to be about 100 Å units

from the width of x-ray diffraction lines. For small crystals of spherical form the familiar relationship

$$\frac{RT}{M} \ln \frac{L_2}{L_1} = \frac{2\sigma}{\rho}\left(\frac{1}{r_2} - \frac{1}{r_1}\right)$$

is valid, where M is the molecular weight, L_2/L_1 is the ratio of solubilities of particles having radii r_2 and r_1, ρ is the density and σ is the free surface energy. When r_1 is large, we may disregard $1/r_1$ in comparison with $1/r_2$ and obtain

$$\frac{L_2}{L_1} = e^{2M\sigma/RT\rho r_2}$$

The variation in solubility with the radius r is greater the greater the molecular weight; in the case of amylose even a threefold increase in crystallite size can lower the solubility to a small fraction of its initial value.

Amylose occurs in a much more readily soluble form in starch than it does when crystallized out as purified amylose. This may well be attributed to the smaller size of the crystalline micelles in the grains. Also it may be that in native starch mixed crystallites containing both large and small molecules may exist which are more easily soluble than the uniform fractionated product.

Aqueous solutions of amylose, either freshly extracted from starch or converted into soluble form, exhibit changes which signify aging and which are traceable to supersaturation effects. The aging reveals itself, first, by a rapidly increasing resistance toward β-amylase, next ultramicroscopic particles appear, the solution then becomes turbid, and finally a precipitate separates out. The aging consists, therefore, of an association which leads first to invisible and enzyme-resistant aggregates and ends finally in a separation of the solid phase. The more uniform the preparation, the faster the aging and the precipitation proceed. Whereas crude amylose crystallizes out only in the course of several weeks, pure fractionated amylose precipitates within a few hours or even minutes. What is particularly important for enzymatic reactions, one can "rejuvenate" amylose solutions or suspensions by treatment with dilute alkali followed by neutralization, for amylose is liberated at first in molecularly dissolved form from alkaline solutions (58).

The Constitution of Amylose may be determined by methylation and hydrolysis. This method will be described below in detail; here

we give only the results. Separation of the methylated sugars after complete hydrolysis gives 0.4 per cent of 2:3:4:6-tetramethylmethylglucoside, corresponding to 0.4 per cent of the total glucose residues as end-groups. (See K. H. Meyer, Wertheim and Bernfeld (54, 63); also Hess and Krajnc (29).) Most of the sugar formed by hydrolysis consists of 2:3:6-trimethylmethylglucoside, from which it follows that the glucose residues are combined by 1:4-linkages. (See Irvine (34*a*).) The molecular weight of the methylated amylose amounts to 50,000, which corresponds to 250 glucose units. This was determined in water as well as in benzyl alcohol from the osmotic pressure, reduced to zero concentration by extrapolation (63). Since only 0.4 per cent of the glucose units, *i. e.*, 1 out of 250 units, possess four free hydroxyl groups and may be regarded as an end group, and since the molecule contains 250 units, it cannot be branched.

Crude amylose from maize can be separated into fractions having molecular weights from 10,000 to 60,000 (53); potato amylose behaves similarly. The amylose present in starches is, therefore, a mixture of polymeric, homologous, unbranched chains having successive 1:4-linkages; (*cf.* formula of amylose chain, page 145).

From the optical rotation one can determine whether α- or β-glucosidic linkages are present. Obviously the optical rotation in water can be measured only with difficulty because of the aging phenomenon. In one per cent solution (made alkaline and again acidified) we obtained a rotation of 220 $\pm$ 5°, referred to $C_6H_{10}O_5$. This value agrees very closely with that of 230° which is calculated on the basis of Hudson's rule for a chain with continuous α-linkages (so-called maltose linkage). That is to say, if β-maltose and β-glucose are split up into separate rotational groups, as shown in the following scheme, it is ap-

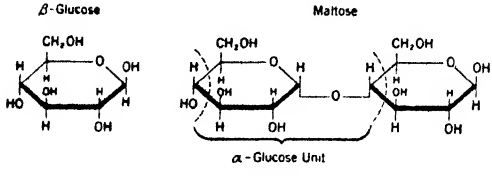

Calculation of optical rotation of amylose.

parent that all the groups found in the β-glucose are also present in the β-maltose, and that the latter also includes the groups of an α-glu-

cose unit whose configuration is the same as that of a glucose unit in a chain having continuous α-1:4-linkages. Accordingly, by subtraction of the molecular rotation of β-glucose from that of β-maltose, one can get the molecular rotation of a compound consisting of 1:4-glucose residues united by α-bridges. The molecular rotation of β-maltose in water amounts to $+403.5°$, that of β-glucose $31.5°$; the 1:4-glucose residue therefore has a rotation of $372°$, from which a specific rotation of $230°$ is calculated. (See Meyer and Mark (47); also Meyer, Hopff and Mark (51).)

Determination of Free Aldehyde Groups. The terminal aldehyde group of the amylose is free and can be quantitatively estimated by reduction by means of alkaline silver oxide or with alkaline copper oxide solution; but obviously no great reliance can be placed upon the exactness of the analysis. Fehling's solution is unsatisfactory for the determination of aldehyde groups in very small amounts. On the one hand, the Fehling solution can undergo self-reduction to yield cupric oxide; on the other hand, a very small amount of cuprous oxide formed by reduction can remain undetected because of its appreciable, though slight, solubility. We use the reduction of an alkaline suspension of silver hydroxide (54). After warming and dissolving the silver hydroxide in ammonium hydroxide, the colloidal silver solution is compared colorimetrically with a colloidal silver solution of known silver content. In pure amylose we found one aldehyde group to 200 glucose residues; in amylopectin there was one aldehyde group to more than 2000 residues.

According to Fargher and Probert (10) and also Richardson, Higginbotham and Farrow (76), the free aldehyde groups of starch and its components can be determined by the Schwalbe-Braidy reduction by means of a concentrated solution of sodium carbonate and bicarbonate to which copper sulfate has been added. Since the cuprous oxide formed by reduction is likely to be somewhat soluble in the reagent, a little glucose (two milligrams per gram of starch) is added. Its reducing power is determined in a blank test and the reducing power of the starch is found by subtracting this blank value from the figure obtained with starch and glucose. Four atoms of oxygen are consumed for each aldehyde group. The cuprous oxide is removed by centrifuging, dissolved in ferric sulfate and titrated with $N/25$ or $N/100$ ceric sulfate, using o-phenanthroline as an indicator.

Richardson and Higginbotham (76), working with maize starch, obtained 2.8 to 8.9 mg. of copper per gram of starch, *i. e.*, one alde-

hyde group for 460 to 1470 glucose units. In the water-soluble portion of maize starch, consisting principally of amylose, they found 27 mg. of copper per gram, corresponding to one aldehyde group for about 150 glucose units.

Chemical Properties of Amylose. With alkalies amylose forms salt-like compounds which are rather sparingly soluble in water and separate out from normal NaOH solutions. The dissociation constant of amylose (as an acid) is about 5×10^{-12} (54). A loose addition compound forms with chloral hydrate. For the addition compound with iodine see Section VI, page 177.

The hydroxyl groups of amylose can be esterified and etherified. With the formation of nitrates, considerable degradation always occurs, as Staudinger (88) has shown. Even the nitrates obtained under the mildest conditions, with phosphoric-nitric acids, have a viscosity about 30 per cent less in formamide after denitration than they had before nitration. Acetates of starches and their components can be obtained without degradation by means of pyridine-acetic anhydride; by starting with solubilized starch, a triacetate is formed without difficulty. The statement by Reich and Damanski (75) that native starch yields only a diacetate contradicts the experience of all other investigators—Friese and Smith (20), Hess and Smith (27), Brigl and Schinle (7), Karrer and Krauss (35), Higginbotham and Richardson (31), Staudinger and Husemann (88)—and could not be confirmed by us. Because of its importance in establishing constitution, methylation will be treated separately.

Triacetylamylose and trimethylamylose form solid, elastic films on evaporation from solvents. When partially swollen, they can be stretched to form birefringent fibers. The films closely resemble those of the corresponding acetyl- and methylcelluloses. (See K. H. Meyer (56) and Samec (80).)

Enzymatic decomposition will be treated later in detail. Here it suffices to state that amylose is completely hydrolyzed by β-amylase. (See Samec and Waldschmidt-Leitz (82).)

4. The Determination of End-Groups by Methylation and Hydrolysis

The methylated sugars obtained by acid hydrolysis of methylated polysaccharides reveal which hydroxyls of the glucose residues were free, for only these can undergo methylation. The 2:3:4:6-tetramethylglucose found among the sugars formed by hydrolysis comes

from terminal glucose units having free 2:3:4:6-hydroxyls, which were united to the other residues of the molecule only through number 1 carbons. From the amount of 2:3:4:6-tetramethylglucose found, the "end-group content" can, therefore, be estimated. From the unbranched parts of the chain 2:3:6-trimethylglucose is derived and dimethylglucose from the points of branching or from incompletely methylated residues according to the following scheme.

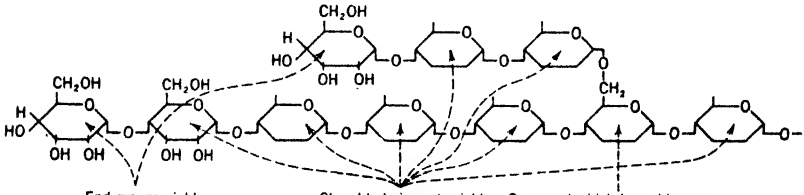

Hydrolysis of methylated branched chain of glucose units with α-1:4 linkages.

Starch can be methylated directly if dissolved in 45 per cent sodium hydroxide solution and treated with dimethyl sulfate, according to Hess (28). We ourselves have failed to get good results by this method. Haworth (3, 24) first converts the starch into an acetyl derivative with pyridine and acetic anhydride; the acetyl derivative is then methylated in acetone with alkali and dimethyl sulfate. We start with starch, amylose or preparations which have been freshly precipitated from chloral hydrate; these products are soluble in dilute alkali and can be methylated easily. By many repeated methylations the methoxyl content can reach 42 to 43 per cent instead of the 45.6 per cent to be expected from complete methylation. In earlier work Haworth and his co-workers (24) often used the so-called Barnett process of acetylation in which SO_2Cl_2 and acetic anhydride are employed. In this procedure, however, considerable hydrolytic breakdown takes place, as Higginbotham and Richardson (31) have shown.

Complete methylation can be accomplished in several ways. Freudenberg and Boppel (17) suspend well-dried starch in liquid ammonia, adding metallic sodium and methyl iodide to it. If the treatment is repeated several times, a methyl starch containing 45.5 per cent methoxyl is obtained. A very considerable reduction in chain length results from this treatment, however, which is recognizable by the sharp decrease of the viscosity in chloroform. It is probably due to reductive splitting of glucosidic linkages. We cannot accept Freud-

enberg's explanation that this represents a reduction of molecular entanglements. Hess and Lung (28) methylate first with dimethyl sulfate, dissolve the methylated starch in anisole, add sodium dissolved in liquid ammonia, and methylate with methyl iodide after evaporation of the ammonia. Here also degradation takes place.

The hydrolytic splitting of methyl starch is accomplished, according to Hirst and Young (32), with a hot mixture of 30 per cent acetic acid and 70 per cent of a 5 per cent aqueous solution of hydrochloric acid. According to Hirst, Plant and Wilkinson (32*a*), it can be done in the cold with concentrated hydrochloric acid. After neutralization with barium carbonate, the tetramethylglucose and part of the trimethylglucose can be extracted by repeated shaking with chloroform. Such preliminary separation is advantageous in case only a small amount of tetramethylglucose is present. The rest of the sugars, namely, tri- and dimethylglucose, are extracted with chloroform from the residue left after evaporation of the aqueous solution to dryness. For definitive fractionation, the sugars are converted into methylglucosides and then fractionated. Glucosidifying is effected by 12 hours' boiling with methanol plus one per cent hydrochloric acid. A small part of the methoxyl is split off by this method, so that loss occurs. For this reason Freudenberg and Jacob (18) have recently recommended glucosidifying with methyl silicate, methanol and some acetyl chloride; the operation is carried out in the cold and no loss should occur. The mixture of methyl glucosides can be treated in various ways. Haworth, and Hirst and Young (32) fractionally distill in high vacuum, and in the fractions, the weights of which are determined precisely, they measure the content of tetra- or trimethyl derivatives with the aid of the refractive index. The total content of tetramethylmethylglucoside gives the "end-group content."

Freudenberg and Boppel (17) benzoylate the glucoside mixture in pyridine, thus converting di- and trimethylglucosides into relatively non-volatile benzoates. The tetra-product can then be easily distilled off. Hess (28) prepares phosphoryl derivatives of the glucoside mixture with phosphorus oxychloride in pyridine for the same purpose, but the losses in Hess' procedure are particularly large, amounting to about 50 per cent of the tetra-product. We (54) use the Haworth method with the modification of Hirst and Young, although the error is rather high. One can estimate the end-group content to ± 0.1 per cent when the content is as small as 0.3 to 0.4 per cent but

only to ±1 per cent when the content runs to as much as 4 to 10 per cent. In comparative experiments, therefore, exactly the same methods should always be used.

The constitution of the 2:3:4:6-tetramethylmethylglucoside and of the 2:3:6-trimethylmethylglucoside which distill over is verified by comparison with synthetic products. The constitution of the dimethylglucose remaining behind after the distillation has been determined in various ways. Haworth, Hirst and Isherwood (25) obtained dimethyl-*d*-tartaric acid by oxidation of a dimethylglucose obtained from methylated glycogen. The two methoxyl groups must, therefore, be on adjacent carbon atoms, suggesting 2:3-dimethylglucose. The 4 and 6 positions were, therefore, bound in the glycogen. Freudenberg and Boppel (17), using the reaction of dimethylglucose (obtained from methylated starch) and azobenzene-*p*-carboxylic acid chloride in pyridine, were able to isolate a mixture of the α- and β-forms of the azobenzene carboxylic ester of 2:3-dimethylglucose, which was identified by comparison with the synthetic substances.

As already mentioned, the end-group content of amylose amounts to 0.4 per cent; that of amylopectin is about ten times as large (55, 63); that of glycogen amounts to 9 per cent and that of a dextrin obtained from glycogen by β-amylatic breakdown even 18 per cent (62). These examples show how important the end-group method is for characterizing polysaccharides.

5. *Amylopectin, Its Properties and Constitution*

After extraction of the amylose, the bulk of the starch (85 to 95 per cent) remains behind. Depending upon the previous treatment, it is either in the form of highly swollen grains or, if electrodialysis was used for separation, as a hydrous flocculent precipitate. The polysaccharide (amylopectin) contained in it is less water-soluble than amylose and, unlike the latter, it is not fully broken down by β-amylase but only to about 60 per cent. Amylopectin may be resolved into fractions by fractional extraction with 33 per cent aqueous chloral hydrate solution. The fractions are indistinguishable in their susceptibility to attack by β-amylase; they probably are similarly constituted but possess different molecular weights. Amylopectin can be converted into a finely divided, water-soluble form by precipitation with acetone from solution in aqueous chloral hydrate; the aqueous solution clouds up very quickly, however. Somewhat more stable are the solutions of this amylopectin in dilute alkali (55).

The amylopectin of cereal starches does not contain any chemically bound phosphoric acid (71); preparations which contain phosphorus because of admixed phosphatides can be freed of phosphorus by solvents or by precipitation. On the other hand, the amylopectins of reserve starches, such as potato or arrow root, do contain small amounts of phosphoric acid as phosphoric esters of hydroxyl 6, for Posternak (71) was able to obtain glucose-6-phosphoric acid from them by enzymatic hydrolysis.

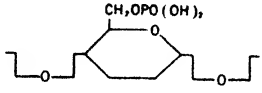

Phosphorus-containing glucose unit.

The constitution of amylopectin is distinctly different from that of amylose. As is proved by the Haworth end-group method together with molecular weight values and determinations of aldehyde groups, it has a branched structure. A branched structure was first proposed for starch by Meyer and Mark (47); the strongest argument for this branching was furnished by Haworth (24), who showed that the end-group content (content of glucose units with free 2:3:4:6 hydroxyls) of some 4 or 5 per cent corresponded to one terminal unit per 25 residues. For many years, however, Haworth attached another significance to his results. He supposed that the starch molecule consisted only of small chains of 25 glucose units, which associated to give larger, supermolecular complexes. Only after other investigators, namely, Staudinger, Freudenberg, Hirst and Young, and K. Hess, had explained the high content of terminal groups as a consequence of branched structure in large molecules did Haworth (23) finally accept this view also. It must be emphasized, however, that the statement that "starch" is branched is incorrect. Only the main constituent, amylopectin, is branched.

The earlier assumption of Haworth that starch is made up of associated molecules consisting of about 25 glucose units each and possessing a molecular weight of about 4000 is in contradiction to the entire behavior of starch, which points to a much higher molecular weight. Osmotic determinations on soluble amylopectin derivatives (esters and ethers) give molecular weights in excess of 300,000. Also, in a straight chain molecule, for each tetra-OH "end-group" there is a free aldehyde end-group, but this is not true of amylopectin. The

slight reducing power of amylopectin toward alkaline silver or copper solutions indicates that there is only one aldehyde group to about 1500 to 3000 glucose units. For each free aldehyde group, therefore, there occur on the average some 100 tetra-OH end-groups, a fact which is explainable only by a branched structure for the molecule.

Maize amylopectin contains 3.8 per cent tetra-OH groups (Meyer, Wertheim and Bernfeld (54)). Potato amylopectin seems to contain somewhat more end-groups and to have a higher average molecular weight (63). The branch positions are formed by α-1:6 bonds, for the dimethylglucose found among the sugars split from highly methylated starch is 2:3-dimethylglucose, as was established by Freudenberg and Boppel (17). Accordingly, hydroxyls 4 and 6 of the corresponding glucose residues of the starch were bound. Furthermore, Myrbäck (67) obtained among the products of decomposition with malt-amylase a trisaccharide in which one of the number 6 hydroxyls was not free and this he concluded was a 4[iso-maltosido] glucose (I) or a 6[maltosido] glucose (II) or a mixture of both.

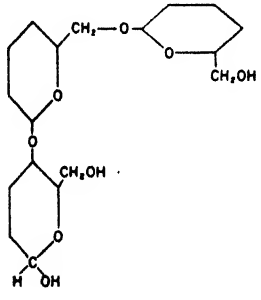

I

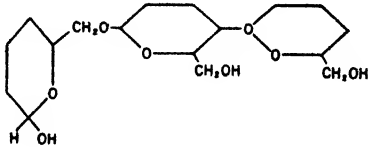

II

Further conclusions about the structure of amylopectin are furnished by investigations with enzymes (Meyer and Bernfeld (55, 61). Amylopectin is broken down by β-amylase, giving a high molecular weight residual substance, which amounts, in the case of maize amylopectin, to about 45 per cent of the original material. This residue, called residual-dextrin I* or erythrogranulose, contains 9 per cent of tetra-OH end-groups; all the end-groups of amylopectin are, there-

* In German, "Grenzdextrin I."

fore, still present and no branch positions can have disappeared. It therefore contains groups of the following kind, which are due to the degraded branches of the amylopectin:

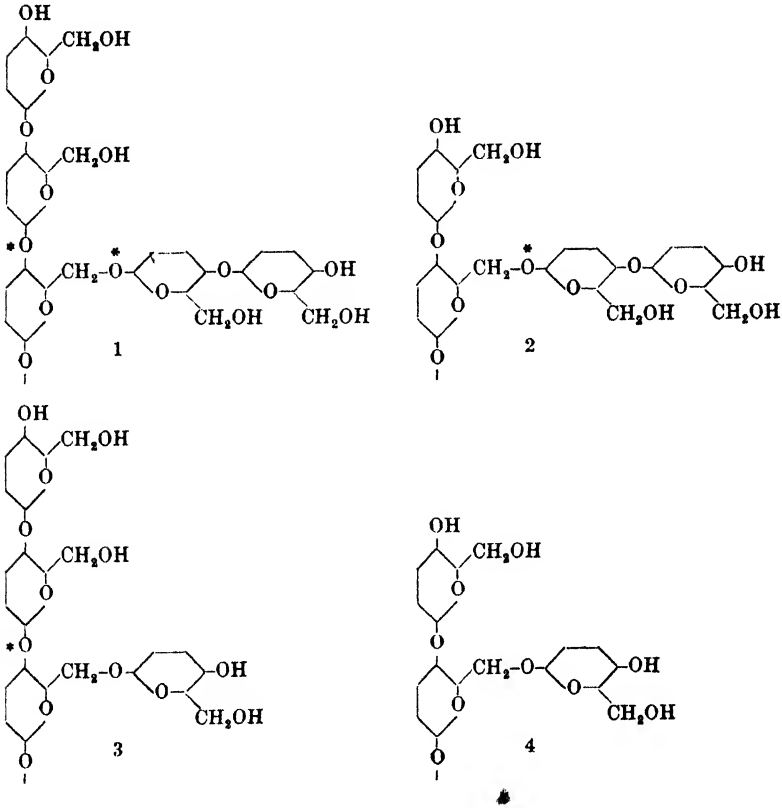

End-groups of residual-dextrin I.

Residual-dextrin I or its end-groups are now attacked, not by β-glucosidase (emulsin), but by α-glucosidase (maltase from yeast), with glucose breaking off. The branching link is, therefore, an α-bond. The substance remaining, which is still a very high molecular weight dextrin (dextrin II), is now no longer resistant toward β-amylase, but is hydrolyzed by it into maltose and a residue (residual-dextrin III), which, like glycogen, gives a light, reddish brown color with iodine.

These facts can be explained only by a ramified structure, as is indicated in Fig. 1. They are not consistent with the picture of a prin-

cipal chain carrying unbranched side chains, as has been proposed by Staudinger and by Hirst and Young. As one end-group and, consequently, a branch as well occur for every 28 glucose units, 55 per cent (*i. e.*, 16 glucose units per end-group) is broken down by β-amylase with 1.5 units per end-group being left over (*cf.* with formulas for end-groups of residual-dextrin I); it can therefore be inferred that

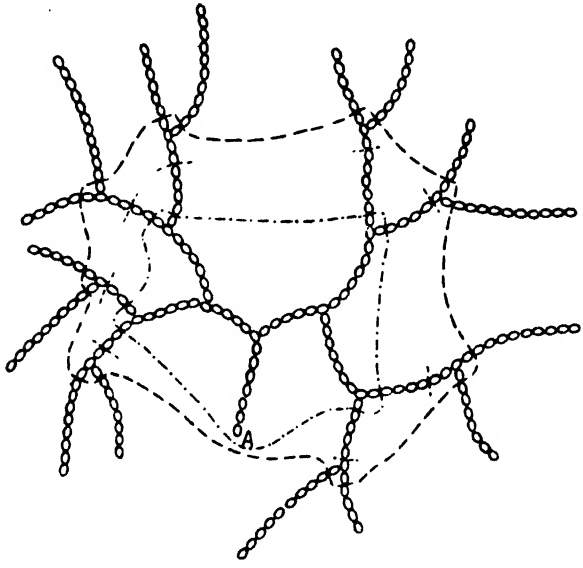

Fig. 1.—Schematic structure of amylopectin, showing successive stages in its enzymatic hydrolysis. A, aldehydic end-group; o, glucose unit.
– – – End of initial degradation by β-amylase, yielding residual-dextrin I.
- - - - - Hydrolysis continued by α-glucosidase, giving dextrin II, hydrolyzable by β-amylase.
– · – · – End of further attack by β-amylase, yielding residual-dextrin III.

the outside branches of amylopectin consist of 15 to 18 glucose units, whereas the inside parts of the chains, between branch positions, are about 8 to 9 units long.

The differences between amylose and amylopectin can be summarized as follows:

Amyloses are unbranched and have molecular weights between 10,000 and 100,000. The tetra-OH end-group content is 0.4 per cent; it does not form the characteristic starch paste. It is hydrolyzed completely by β-amylase. Its ethers and esters form strong extensible films.

Amylopectin is branched; its molecular weight exceeds 300,000. The tetra-OH end-group content is 4 per cent; it is the paste-forming substance in starch. β-Amylase breaks it down to a residual substance (residual-dextrin I) of high molecular weight; the ethers and esters form brittle, inextensible films.

II. Physico-Chemical Investigation of Solutions of Starch and Its Components

1. Osmotic Measurements for the Determination of Molecular Weight

Physical measurements on solutions for the determination of material constants are limited, practically, to homogeneous solutions which do not undergo changes with time, as otherwise the results are extremely difficult to evaluate. Among starches and their derivatives, however, alterations in solution are very frequent. Aqueous solutions of starches and their components are particularly unstable, exhibiting a series of phenomena which are spoken of collectively as aging.

A sensitive test for aging effects is the degree of digestion by β-amylase. This value is greatest in fresh amylose solutions or freshly prepared starch pastes (59, 80). By boiling up aged solutions, or by making alkaline and then neutralizing, the initial condition can be restored again. On further aging, ultramicroscopic particles appear, then the solutions become turbid. In the course of weeks, amylose separates from amylose solutions as a crystalline precipitate, while a starch paste gelatinizes or becomes very cloudy. This behavior, like the precipitation of amylose, is attributable to association to supermolecular aggregates. The fundamental reason for all these aging phenomena is possibly that the carbohydrates of starch are practically insoluble in water and they disperse in water to give a supersaturated solution of the mixtures present in native starch; in these solutions soluble aggregates first form, then insoluble ones, which either flocculate or develop into a loose network of felted micelles, to appear macroscopically as a jelly or gel. Solutions in formamide are also unstable,

as is shown by the rapid increase in viscosity followed by gelatinization (53, 57).

From the foregoing it is apparent that the measurement of the osmotic pressure of aqueous starch solutions or amylose solutions can give the pressure only for a certain stage in the association or aging process and that the molecular weight of the parent molecule cannot be obtained from this. Only in the stable solutions of highly degraded starches can osmotic determinations of molecular weight be made in water. They are also possible, however, for solutions of ethers or esters in suitable solvents, such as tetrachloroethane and benzyl alcohol. In such measurements, however, the following is to be noted: as the experience of recent years has demonstrated, high polymeric substances with chain-like structures show considerable deviations from van't Hoff's Law, even at very low concentrations. The osmotic pressure is not proportional to concentration but increases faster than concentration and conforms for the most part to the relationship

$$p = ac + bc^2; \text{ or } \frac{p}{c} = a + bc$$

One must, therefore, measure the osmotic pressure at different concentrations and, as the simplest way, extrapolate p/c, the so-called reduced osmotic pressure, graphically to zero concentration, at which the van't Hoff relationship holds.

In measurements with the ultracentrifuge also it turns out that deviations occur even at very small concentrations, and, as in the case of osmotic pressure, these lead to particle weights which are too low. In this case also, for exact determinations of molecular weight, it is necessary to use several concentrations and then extrapolate to zero concentration. In this connection compare Signer's (85) measurements on polystyrene. Only a few of the numerous molecular weight determinations made by osmotic pressure measurements can withstand the foregoing criticism. This is true also of the painstaking ultracentrifuge measurements of Lamm (44). Using an aqueous solution which had been prepared by dissolving starch in concentrated, aqueous $ZnCl_2$ solution, diluting with water and then removing the $ZnCl_2$ by dialysis, Lamm found particles having molecular weights from 100,000 to 1,000,000; in an amylose solution prepared according to Samec's directions particles having molecular weights from 300,000 to 1,800,000 were detectable. But unquestionably the

solutions involved were not molecularly dispersed; rather, they represented an indefinite degree of aging (association). As the molecular weights of molecularly dissolved amylose are from 10,000 to 60,000, the particles in Lamm's solutions were in fact rather highly associated.

The molecular weight of about 200,000, which was calculated by Samec (80) from osmotic pressure measurements, using aqueous solutions of amylose, is also open to question as referring to aggregates at some stage of aging. Measurements made upon solutions of starch in formamide, in which viscosity shows that aggregation is occurring, are likewise unreliable. The molecular weights of aggregates are of course unsuitable for the characterization of chemical constitution. For that purpose one needs the molecular weight in molecularly dispersed solutions. Measurements of osmotic pressure in hydrazine hydrate or in ethylenediamine, which give stable solutions of amylose, have not yet been carried out.

We have confined ourselves to determining the molecular weights of esters and ethers. Thus, one can convert amylose into triacetylamylose with acetic anhydride-pyridine, without any degradation. The osmotic pressure of triacetylamylose in tetrachloroethane gave a molecular weight of about 78,000, which corresponds to a molecular weight of 45,000 for the parent amylose (56). A methylated amylose which forms stable aqueous solutions at room temperatures gave a molecular weight of 50,000 (63). Triacetylamylopectin showed a molecular weight of more than 300,000 but precise data cannot be given at the present time. It seems probable to us that molecules of amylopectin occur having weights of from 100,000 to 1,000,000. Measurements by Carter and Record (8) on methylated starch products prepared by Baird, Haworth and Hirst (3) from starch which had been degraded by hot, alcoholic hydrochloric acid (the authors called this "amylose"), gave values between 40,000 and 124,000 in chloroform. Staudinger and Husemann (88) found molecular weights from 40,000 to 250,000 for degraded methyl- and triacetylstarches.

Finally, the available measurements on glycogen should be mentioned. Methylated glycogens from the livers of various kinds of animals give molecular weights from 300,000 to 800,000 in chloroform, according to Carter and Record (8). Larger values obtained by the same workers using acetylated glycogen were declared by the authors themselves to be uncertain. Husemann and Ruska (34)

found that by fractional precipitation Merck's glycogen could be separated into fractions of very different molecular weights.

2. *Determination of Molecular Weight and of Molecular Shape with the Aid of Viscosity*

As is well known, the limiting viscosity of chain polymers of a given series in the same solvent should, according to Staudinger, be proportional to the molecular weight

$$\lim_{c \to 0} \left[\frac{\eta_{sp}}{c} \right] = K_m M$$

where M is the molecular weight and K_m is a constant.

Staudinger (89) himself, however, has found recently that this relationship does not hold for a large number of chain polymers and K. H. Meyer (49) was unable to confirm the law in a critical survey of all the available data, and could only establish that the limiting viscosity increases continuously with the molecular weight, just as the density and the boiling point do in a homologous series. Only recently G. V. Schulz (84), a co-worker of Staudinger's, has come to the same conclusion. If, therefore, the molecular weights and the limiting viscosities of several members of a series are known, the molecular weight of another member can be interpolated from the viscosity. This method is applicable, however, only to unbranched polymers; *i. e.*, in the present study only to amylose and even then only if products of equal uniformity are compared. The viscosity of a uniform product is lower than that of a less uniform one of the same average molecular weight.

The comparison of viscosities in the case of amylopectin affords only the roughest estimate of molecular weight. In general, the limiting viscosity in the case of isomers is less for branched than for normal isomers. If, therefore, one finds that substances of the same molecular weight and apparently of the same or very similar constitution exhibit quite different viscosities, the inference is permissible that the less viscous substance possesses a branched structure. By comparison of cellulose acetates with starch acetates of equal molecular weight, Staudinger (87) concluded that the latter were branched and K. H. Meyer (50) was able to show that amylose and its derivatives exhibit a considerably higher viscosity than amylopectin of equal molecular weight.

It seems particularly difficult to us to evaluate viscosity measurements on aqueous starch pastes and starch solutions intelligently. In pastes the structure of the grains has not yet been destroyed completely; giant supermolecular networks are present and these inhomogeneities give the paste a high viscosity. Solutions of starch which has been made soluble according to our methods are much less viscous. The instability of all starch solutions must also be remembered. By changes in aggregation and crystallization the viscosity is usually increased, although, under certain conditions, it may even be lowered. The great sensitiveness which the viscosity of dilute potato starch paste exhibits toward salts seems to us to be very remarkable and, for the present, inexplicable. A one per cent paste, prepared at 100°, has a relative viscosity ($\eta_{rel.}$) of 90 at 20°; after addition of one per cent sodium chloride, $\eta_{rel.}$ is only 9.

III. The Fine Structure of Starch Grains and of Starch Paste

Starch grains consist of concentric layers. These layers separate from one another when heated starch is treated with water (Badenhuizen). The layers consist (according to Nägeli and to A. Meyer) of elongated, crystalline micells, arranged radially, as in spherulites. The radial structure is revealed by the double refraction of the grains. X-ray diagrams reveal the lattice-like arrangement. The interference lines of native starch are rather broad and show that the crystallites are small, probably not exceeding 100 Å units in size. The diagrams vary with the kind of starch. Notwithstanding many years of investigation by J. R. Katz (36, 37), nothing more than the fact of crystallinity and the existence of different modifications has been established. On complete dehydration the diagram indicates an amorphous condition (51). The single molecule of water associated with each glucose unit is thus indispensable to the building-up of the crystal structure. The double refraction of the grains amounts to 0.0155, according to Frey-Wyssling (19) and is about one-fourth that of cellulose. The planes of the glucose rings cannot, therefore, have the same arrangement as in cellulose, where they lie parallel to the long axis of the crystallite, but must make a definite angle with the axis. If the glucose units are arranged, as in cellulose, in a diagonal screw sequence, a chain-structure such as that in Fig. 2 is obtained. This would be consistent with the other properties and would also provide space to accommodate the water molecules between the chains as they extend parallel to the crystallite (51). A screw-like

arrangement of glucose residues was proposed by Freudenberg but this model is in disagreement with the evidence of double refraction, for if the screw axes lie radially, the uniaxial birefringence would have to be negative, which is not the case (Frey-Wyssling).

The starch grain, however, is no ordinary spherocrystal, for it can be deformed elastically. If we seek other examples of similar behavior, we discover one in crystallized gutta percha, where the crystallites comprise only part of the chains, while other parts are free, passing from one crystallite to another and joining them together, (50). The same explanation appears to be plausible in this case; the crystallites are held together by free parts of the primary valence chains, which act as an amorphous, elastic cement. This conception serves also to account for the swelling phenomenon.

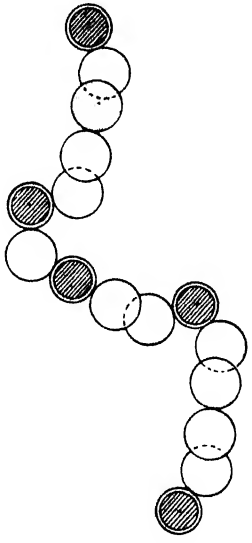

Fig. 2.—Model of starch chain. Glucose units arranged as diagonal screw. Cross-hatched circles = oxygen. Open circles = carbon.

The starch grains exhibit a limited swelling in hot water, *i. e.*, they take in from 30 to 50 times their volume of water and form an elastic jelly. Such limited swelling is characteristic of chain polymers which are held together in loose, 3-dimensional giant molecules by network cross linkages. A familiar example is the swelling of slightly vulcanized rubber, in which the polyprene chains are linked together by sulfur bridges. There are now a number of chemically inert solvents which break the network linkages of starch and dissolve it, *e. g.*, concentrated aqueous solutions of chloral hydrate, sodium trichloroacetate and thiourea. Network linkages which are dissolved in this way can only be secondary valence bonds (57). All substances which burst the network linkages of starch are also good swelling agents for starch and good solvents for amylose. The bridge bonds are, therefore, of the same type as the lattice forces of starch or amylose. In the paste from highly swollen starch grains the giant branched molecules of amylopectin are also united into loose 3-dimensional networks by regions having a lattice-like arrangement. In these regions, sections of several chain molecules are linked to-

gether into crystallites. Conversely, these micellar regions are connected to one another by molecular filaments (cohering "fringe micelles"). Figures 3 and 4 illustrate this concept.

If starch is actually dissolved after complete destruction of the grain structure, *e. g.*, by chloral hydrate, the polysaccharide which is recovered by precipitation from such a solution no longer gives a paste. The typical properties of pastes are, therefore, bound up with the morphological structure of the swollen grains, which have loosened up to form large inflated units.

The formation of the loose, 3-dimensional net, which is responsible for the limited swelling capacity and with it the paste production, is, therefore, connected with the size and the highly ramified structure of the amylopectin molecule. It is this which makes it possible for part of the molecule to remain in lattice-like micelles and another part of the same molecule to be surrounded by solvent (*i. e.*, "dissolved"). On the other hand, the amylose molecule, the unbranched constituent of starch, is either completely dissolved or else tied up as a whole in the lattice union with other molecules to form a solid body incapable of swelling and, therefore, not capable of paste production.

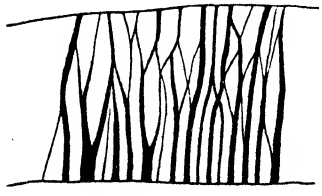

Fig. 3.—Layer of a starch grain; crystalline micelles shown by thick lines.

Undamaged starch is not attacked by cold water; in warm water part of the crystallite is liquefied by the solvent and the grain absorbs water with an increase in volume. The degree of swelling depends upon the temperature. With maize starch scarcely any action is noticeable below 55°; at 80° the grains swell to 25 times their initial volume. In consequence of the loosened structure, the smaller unbranched molecules can diffuse out, while the very large branched molecules of amylopectin are still held together in micelle-like bundles, thus preserving the shape of the highly swollen grains. Within the swollen grains, the layers of which now form loose, water-filled, 3-dimensional nets, an equilibrium must exist between the chain parts "dissolved" in water (*i. e.*, surrounded by water) and the "undissolved" chain parts, *i. e.*, those which are bound together in crystalline micelles. The saturation concentration of dissolved chain parts

corresponding to this equilibrium increases with rising temperature up to 120°, when complete destruction of the grains occurs. The fraction of the starch grain which is regarded as "dissolved" depends now, not only upon the saturation concentration, which is controlled by the temperature, but also upon the amount of absorbed water, which, for its part, is determined by the mesh-width of the system. The structure becomes loosened by the dissolution of crystallites at the beginning of the swelling process; thus more water can penetrate, and then additional crystallites may dissolve. For this reason the temperature change from the beginning of the process to the stage

Fig. 4.—Layer of a swollen starch grain; the connected crystalline micelles shown by thick lines.

of very marked swelling, with 2000 to 4000 per cent water absorption, is rather small, amounting to scarcely 30°. The unbranched and weakly bound amylose molecules diffuse out of the swollen starch grains and ultimately also the lower molecular weight amylopectin. Consequently the osmotic pressure within the grains diminishes and the swollen grains finally shrink noticeably.

The most recent measurement of the heat of swelling is due to Küntzel and Doehner (43). They obtained 36.75 cal. per g. This heat comprises the heats of fusion and of solution of the "molten" polysaccharide. On melting, 39.35 cal. per g. is absorbed and on dissolving, with the accompaniment of hydration, 2.6 cal. per g. is evolved. The heat of fusion of roughly 40 calories is about equal to that of α-glucose.

When starch swells in a limited amount of water, the shells touch and adhere together so that they can no longer be separated without

rupture; the "starch-paste" is thus formed. Evidently, sections of the chains in some grains penetrate into other shells and, due to this entangling, the macroscopic effect of adhesion is exhibited. The analogous phenomenon occurs when fresh surfaces of unvulcanized rubber come into contact.

On cooling a paste it congeals. X-ray investigation shows that this solidification is traceable to the formation of crystallized regions. Matted crystallites, united by molecular filaments, form a coherent, elastic structure and the heat of crystallization is evolved. The velocity of crystallization varies with the kind of starch. Maize and rice pastes crystallize rapidly, potato paste very slowly (63). It is not entirely clear what causes this difference. However, according to Fischer and Seck (11), by previous mild degradation with acids or with sodium peroxide, one can get, even from potato starch, a product which congeals rapidly. Accordingly, this suggests that the extraordinary size of the molecules of potato amylopectin represses the crystallization.

According to all the foregoing facts, it is evident that the paste-forming properties of starch or of amylopectin do not depend upon the electrochemical character of the starch components nor upon their phosphorus content—a conception which Samec advanced. The molecular-morphological consideration of the swelling and paste-forming processes demonstrates an immediate and clear connection between the branched structure of the huge amylopectin molecules and the formation of loose, 3-dimensional nets, such as we have supposed to exist in swollen grains or paste.

IV. The Enzymatic Degradation of Starch

Starch can be degraded by enzymes in various ways. Two enzymes, α- and β-amylase, yield chiefly maltose, which is liberated by the former as α-maltose with negative mutarotation and by the latter as β-maltose. (See Kuhn (42).) In the presence of inorganic phosphates starch is converted by phosphorylase into glucose-1-phosphoric acid (see Hanes (22)); α-glucosidase yields glucose.

1. Degradation by Amylases

α-Amylase occurs in animal fluids and organs (*e. g.*, saliva, liver, leucocytes, pancreas); also in certain bacteria (*e. g.*, *Bacillus mesan-*

thericus subtilis); it is also found in malt along with large amounts of β-amylase. β-Amylase is present in cereal grains as well as in malt.

In order to get an insight into the course of enzymatic breakdown, it is necessary to study the action of purified enzyme (*e. g.*, α-amylase which is free from β-) upon purified starch components. In this way, however, one departs radically from the conditions of biological hydrolysis, for the purified components are much less readily soluble or capable of swelling in water than the mixtures occurring in starch. Moreover, an enzyme mixture, such as the one present in malt amylase, can behave differently from the pure enzymes.

Animal amylase seems to be free from β-amylase. In malt amylase the β-amylase is destroyed by 20 minutes' heating of the aqueous extract at 70°; see Wijsman (92), Ohlsson (68), Klinkenberg (39), Blom, Bak and Braae (6). Hence a purified α-amylase can be prepared by heat treatment. β-Amylase occurs almost free from α- in ungerminated grain and by permitting the aqueous grain extract to stand for several days at a *p*H of 3.6, the residual α-amylase is destroyed. (See Blom, Bak and Braae (6).) This method is suitable for the preparation of pure β-amylase. Additional methods are described in the new treatise of Bamann and Myrbäck, "Die Methoden der Fermentforschung."

According to Ohlsson (68), α-amylase splits starch first into large fragments (dextrin) and thereby destroys the starch shells or "liquefies" them. The supposition that liquefaction can set in without hydrolytic cleavage is false and is due to the circumstance that the slight hydrolysis of less than 0.1 per cent of the glucosidic links, which suffices to destroy all the amylopectin and produce liquefaction, may easily be overlooked. The dextrin hydrolyzes further into maltose for the most part, with some glucose formed at the same time, a circumstance which was unnoticed for a long time; see Hanes (21), Somogyi (86), Myrbäck (65, 66). Since maltose is not the only degradation product, it is not possible to calculate the amount of maltose formed in an enzymatic reaction merely on the basis of optical rotation or from the reducing power reckoned for maltose. It is in this way that many errors have been made—among others, the claim of Pringsheim (73, 74) that under certain conditions starch can be hydrolyzed quantitatively into maltose by enzymes, which is not true.

The breakdown products can be analyzed completely by examining four aliquots. In one sample the reducing power is determined

directly by titration according to Bertrand; in the second sample the glucose is eliminated by fermentation either according to Harding and Hanes (21) with the yeast *monilia krusei*, or according to Somogyi (86) with baker's yeast at *p*H 8. Under the latter conditions maltose and dextrin are not attacked and the reducing power is determined by titration. In the remaining samples glucose and maltose are removed with *monilia tropicalis* or with baker's yeast without addition of buffer; the reducing power is determined in one sample and the other is hydrolyzed with hydrochloric acid and then titrated. The difference between samples 1 and 2 gives the content of glucose; that between samples 2 and 3 the maltose. The balance consists of dextrin, the quantity of which is obtained from sample 4 and the reducing power from sample 3. The ratio of the values from samples 3 and 4 gives the average degree of polymerization of the dextrin, *i. e.*, the number of glucose units per molecule.

Using an amylase from leucocytes, Somogyi obtained the following results with maize-starch paste: at the beginning only unfermentable dextrin formed; then maltose and finally even some glucose appeared, while the dextrin partially disappeared. The glucose did not come, therefore, from the maltose. In preliminary researches we have studied the action of α-amylase and bacterial amylase upon amylose. The hydrolysis proceeded in a similar way. The end-products were likewise low molecular-weight dextrin, maltose and glucose. It is probable that the dextrin from amylose hydrolysis differs from that from starch. The action of α-amylase upon amylopectin has not yet been investigated thoroughly.

The action of β-amylase has been studied carefully. According to Ohlsson (68), maltose is produced immediately, on the one hand; while, on the other, a very high molecular-weight breakdown product results and, above all, no liquefaction or marked change in viscosity occurs. The enzyme must, therefore, remove the maltose from the ends of the starch chains. The point of attack is the end which is not aldehydic. (See Ohlsson (68), Hanes (21), Myrbäck (66).) Amylose is completely hydrolyzed by β-amylase. (See Samec and Waldschmidt-Leitz (82), Meyer and Bernfeld (54).) At the same time very small amounts of glucose form in addition to maltose; see Hanes (21). Up to 80 per cent hydrolysis the reaction is of zero order, which indicates that only the end-groups of the starch are reactive and that on splitting off a maltose unit, another end-group forms, so that the concentration of the substrate is not at first changed

(58, 59). It changes only after some chains are fully hydrolyzed off, thus altering the concentration of the substrate. Aqueous solutions of amylose lose their initial sensitiveness toward β-amylase rather quickly through aging (association). In aged solutions only a part is hydrolyzed, while another part escapes breakdown by coagulation. The micells are evidently protected against attack by enzymes. After the low molecular-weight dissolved part of the amylose, which acts as protective colloid, has been hydrolyzed, the rest coagulates and separates out.

Amylopectin yields a high molecular-weight residual substance with β-amylase; this substance is further attacked by β-amylase only with extreme slowness, the reduction in velocity being to $^1/_{300,000}$. The

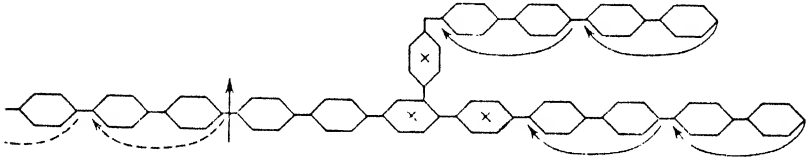

Fig. 5.—Enzymatic degradation of amylopectin.

⌒ Attack by β-amylase.

× Branch-points prevent continued hydrolysis and residual-dextrin I remains.

↑ Cleavage by α-amylase or superheated water.

⌒ Subsequent attack by β-amylase.

enzyme must, therefore, encounter an obstacle while it is hydrolyzing the chain, as Hanes (21) first concluded. The obstacle may consist of points of branching and even of phosphorylated residues in the case of potato amylopectin. The constitution of the residual substance (residual-dextrin I or erythrogranulose), its structure, and the branch stubs present in it were discussed above. Residual-dextrin I is attacked by α-amylase, α-glucosidase, and by superheated water; the product of the reaction is further broken down by β-amylase. By this reaction, therefore, points of attack for the β-amylase are exposed as depicted in the accompanying scheme, Fig. 5.

In the case of hydrolysis by malt amylase, which contains both α- and β-amylase, the large molecules are first broken down by the α-amylase, whereupon liquefaction occurs and, at each point of fracture, a new point of attack for the action of β-amylase is produced. Con-

sequently, this combined hydrolysis proceeds faster than hydrolysis by pure enzymes. The end-products of the action of malt amylase include, besides much maltose, some glucose as well as about 20 per cent of low molecular-weight, unfermentable dextrins, mainly trisaccharides. These, according to Myrbäck (65, 66, 67), come from the branching points and in part possess a branched structure. (See p. 160.) If glucosidase is present, as, *e. g.*, in takadiastase, trisaccharides and branched dextrins are also attacked with the formation of glucose. Pringsheim (73, 74) considered the added effect of a small amount of α-glucosidase from yeast as an activation of the amylase (in this connection see Holmbergh (33) and Weidenhagen (91)) and he designated it "complementary action." It is better to drop this designation.

2. *Degradation and Synthesis by Phosphorylase*

In the juices of peas and potatoes Hanes (22) was able to detect an enzyme which hydrolyzes soluble starch in the presence of phosphates to glucose-1-phosphoric acid. The reaction reached an equilibrium. It can therefore serve also for the synthesis of a starch-like polysaccharide in which one proceeds from glucose-1-phosphate. Hanes succeeded in effecting such a synthesis with suitably treated potato juice. The product formed was similar to amylose and gave a blue color with iodine. Hassid and McCready (22*a*) claim, however, that the synthetic product differs from native starch in that it is completely hydrolyzed to maltase by β-amylase and has no detectable tetra-OH end-groups.

3. *Degradation by the Enzyme of Bacillus macerans*

Upon hydrolyzing starch with *Bacillus macerans*, F. Schardinger (1903) obtained crystalline dextrins, the so-called α- and β-dextrin and, in addition, a small amount of other dextrins (Freudenberg). The Schardinger dextrins do not reduce Fehling's solution. Tilden and Hudson (90*a*) found that similar, singular dextrins are also obtained with a cell-free enzyme prepared from *Bacillus macerans*. According to recent investigations by Freudenberg and his co-workers (14, 15, 16), the α- and β-dextrins probably consist of closed rings of 5 or 6 glucose units joined together by maltose-type linkages. The x-ray study of Schardinger α-dextrin supports this assumption; see Kratky and Schneidmesser (40).

V. Glycogen, Its Constitution, Degradation and Synthesis

1. Occurrence and Constitution

Under the name glycogen are included various carbohydrates which give a brown to red-violet color reaction with iodine and on complete hydrolysis yield glucose. Partial enzymatic hydrolysis gives, among other products, maltose. As a rule glycogen in its native state is not differentiated morphologically and is not detectable by color reaction, since it is dispersed in the protoplasm. Only in embryos and in the liver and muscle cells of diabetic sufferers does it occur in the form of granules or flakes of varying size (1 to 10 μ), both in the nucleus and in the cytoplasm. Glycogen occurs in the cells of many higher and lower animals (*e. g.*, in muscle and in liver cells), and in fungi, such as yeast, in algae (*cyanophycea* and *rhodophycea*) and in bacteria. The expression "animal starch" is not, therefore, particularly appropriate.

According to Willstätter and Rohdewald (93) glycogen exists both in a variety which is extractable by hot water (lyoglycogen) and in one which at first is insoluble in hot water (desmoglycogen). The latter dissolves only after the protein material has been destroyed, *e. g.*, with alkali. Willstätter and Rohdewald assume that this glycogen is combined with protein as an addition compound "symplex." We have found (60) that the lyoglycogen which is dissolved out of muscle with hot water is also combined with protein, for it is resistant toward β-amylase, but is attacked by the latter as soon as the protein has been precipitated by tungstic acid. Glycogen which has been prepared by Brücke's process is exceedingly heterogeneous. Upon electrodialysis a large fraction of high molecular-weight polysaccharide precipitates out, the low molecular-weight material remaining in solution (60, 62). According to Husemann and Ruska (34), one can get fractions of greatly different molecular weight by fractional precipitation from aqueous solutions with alcohol.

As Haworth, Hirst and Isherwood (25) have found, acid hydrolysis of methylated glycogen gives 2:3:6-trimethylglucose, as well as a considerable amount of 2:3:4:6-tetramethyl- and 2:3-dimethylglucose. The tetra-OH end-group content fluctuates between 7 and 9 per cent. Haworth and his co-workers (25, 26) deduced from this a highly ramified structure for glycogen; α-1:4-linkages preponderate as in starch, and the attachment of branches takes place through α-1:6-linkages, as the English authors assumed and as is generally agreed upon

today. Our investigation (62) of the residual substance formed by hydrolysis with β-amylase gave further insight into the constitution. Glycogen from edible mussel having an end-group content of 9 per cent (one terminal group per 11 glucose units) loses 47 per cent by weight as maltose on hydrolysis with pure β-amylase; that is, about five glucose units per end-group are thereby removed. All the end-groups are still present in the remaining dextrin. It contains 18 end-groups, *i. e.*, one end-group to 5.5 glucose units. From this one can conclude that the outside branches of the glycogen molecule, which are exposed to attack by the enzyme, consist on the average of 6 to 7

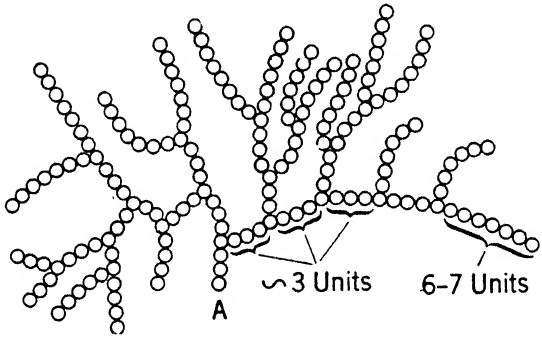

Fig. 6.—Structure of glycogen. A, aldehydic end. o, glucose units.

glucose units in α-1:4-glucosidic combination, and that of these 5.5 are split off by β-amylase, while 1 to 2 remain at the points of branching to furnish the end-groups of the residual-dextrin. Between those glucose residues whose 6-position is occupied by a branch there can be only very short chains, averaging 3 glucose units, with free hydroxyls at 2, 3, 6. Figure 6 represents the arrangement of the glucose units.

It is understandable that with such a structure, the parallel arrangement of long-chain parts in crystalline micelles is impossible; this explains why glycogen is always amorphous, whereas starch shows crystalline x-ray interferences.

The distinction between glycogen and starch can be summarized as follows: Starch is a polymeric homologous mixture of unbranched molecules (amylose) and of branched ones (amylopectin). The exterior branches of amylopectin consist of 15 to 18 glucose units; the

interior chain sections between the branch points consist of 8 to 9 glucose units on the average. Glycogen consists only of branched molecules, which can be of very different sizes and which in the natural state are united with protein to form "symplex." The outside branches of the ramified glycogen molecules are 6 to 7 units long; in the interior between the points of branching only very short links averaging 3 glucose units occur.

2. *Degradation and Synthesis of Glycogen by Enzymes*

The enzymatic hydrolysis of glycogen is analogous to the hydrolysis of starch. It is split by α-amylase, first into large, then into smaller fragments, among which, besides maltose, other di- and oligosaccharides are also found. As explained above, β-amylase yields considerable amounts of maltose besides a high molecular-weight residue; here also it is to be assumed that the enzyme encounters an obstacle at the branch points. Phosphorylase in particular, which can be obtained from yeast as well as from muscle and liver, breaks glycogen down into glucose-1-phosphoric acid (Cori's ester) in the presence of inorganic phosphates. This reaction reaches an equilibrium. Conversely, with the help of the same enzyme, glucose-1-phosphoric acid can be converted into glycogen. (See Schäffner (83), Kiessling (38), and Cori (9).) The biological breakdown of glycogen always yields glucose-1-phosphoric acid, according to Parnas (69).

VI. The Color Reactions of Starch and of Glycogen with Iodine

As Barger (4) in particular has shown, a large number of compounds give color reactions with iodine similar to that of starch, so that it is erroneous to consider the iodine reaction as a unique one, characteristic only of starches. Contrary to the recently advanced theory of Freudenberg (12, 17) that the iodine is deposited in the spirally coiled starch molecules, the spaces between which are just the size required by the iodine molecules, it must be objected that even compounds which are extended in the crystalline state and which are therefore certainly not coiled spirally in any definite manner in solution (polyvinyl alcohol and methyl cellulose) give a deep blue color reaction with iodine. Moreover, in addition to these two substances, trimethyl starch, cellulose swollen by means of $ZnCl_2$ and certain colloidal suspensions and finely divided precipitates, such as basic lanthanum and praseodymium acetate (4), the sodium compound of

carbethoxyhydrindene (4), *o*-oxychalcone (4), benzylidene phthalide (4), acetocoumarin and the methylcycloacetals of acetone and acetoin (5) all give colors with iodine similar to that of starch. None of these substances gives the color reaction either in molecularly dispersed solutions or in the state of well-formed crystals. Rather, it occurs only with colloidal precipitates having greatly distorted lattices. From this it may well be inferred that the iodine molecule is deposited in the interstices of these particles and that the change of light absorption of the iodine is connected with this deposition. Moreover, such colored compounds are not restricted to iodine-containing systems. The case of ultramarine may be recalled in this connection.

Accordingly, the question arises as to whether the blue color with starch is also due to a similar phenomenon, *i. e.*, if here, too, supermolecular aggregates or micells of starch are formed in the fissures of which iodine produces an effect similar to that in the above-mentioned precipitates. If the dependence of light absorption, which serves as a measure of the concentration of blue material, upon the concentration of the components is investigated colorimetrically, it is found (64) that the concentration of blue compound is proportional to higher powers of both starch and iodine concentrations

$$K[\text{Starch-iodine}] = [\text{Starch}]^n \cdot [I_2]^m \quad (n, m \sim 2)$$

From this it follows that several molecules of iodine unite with several molecules of starch to give the blue substance. The same result is obtained with solutions of pure maize amylose and aqueous solutions of iodine. If iodine is allowed to act upon dilute aqueous solutions of amylose, a pure blue color results. This solution shows the characteristics of an unstable colloidal dispersion. It is flocculated by addition of electrolytes, such as hydrochloric acid or sodium sulfate. The composition of the blue-black precipitate changes with the composition of the solution. With excess iodine it is approximately $I_{2n}(C_6H_{10}O_5)_{10n}$; with excess amylose it is approximately $I_{2n}(C_6H_{10}O_5)_{20n}$. Iodide ions are not necessary either for the color reaction or for the precipitation of the iodine compound (64). Water is essential, however, for although starch in contact with atmospheric moisture becomes colored by iodine vapor, bone-dry starch remains colorless. According to all these observations, starch-iodine can be grouped with other colored colloidal addition (or "deposition") compounds.

The shade of the iodine addition compound depends, above all, on the constitution of the polysaccharide, as is apparent from the following classification: the unbranched amylose yields a pure blue color reaction; that of the branched amylopectin from potato has a tinge of violet; the more highly branched erythroamylose and residual-dextrin (erythrogranulose) give a red shade; the still more highly branched glycogen gives a red-brown color; while the most irregularly built compounds, such as residual-dextrin from glycogen, produce only a deepening of the iodine color from yellow to brown. It can hardly be an accident that the shade of the iodine color reaction shows a definite relationship to the crystallizing power, which decreases from amylose to amorphous glycogen. Molecules whose form permits the building up of crystallites associate in aqueous solutions to give micelles, and form blue colloidal addition complexes with iodine. The reaction with iodine is feebler the smaller the tendency to micelle formation. It is clear, therefore, that a connection exists between the shade of color and the length of the unbranched parts of the chains, for the longer these links are, the more readily can crystallization and micelle formation occur. Here it may be recalled that even the unbranched amylose is converted by α-amylase or by acids into intermediate products which give a red color reaction with iodine. The chains are so broken up that the short chains still remaining no longer suffice for the formation of well-arranged micells.

Aside from the constitution, however, the shade depends also upon certain purely physical considerations. *E. g.*, the color frequently changes from blue to red-brown on drying, whereupon addition of water restores the original color. This observation is also consistent with the idea here presented of the nature of the colored compound.

Bibliography

1. Alsberg, *Plant Physiol.*, **13**, 295 (1938).
2. Badenhuizen, *Rec. trav. botan. néerland.*, **35**, 559 (1938); *Protoplasma*, **33**, 440 (1939).
3. Baird, Haworth and Hirst, *J. Chem. Soc.*, **1935**, 1201.
4. Barger and Eaton, *Ibid.*, **1924**, 2407.
5. Bergmann, *Ber.*, **57**, 755 (1924).
6. Blom, Bak and Braae, *Z. physiol. Chem.*, **241**, 273 (1903).
7. Brigl and Schinle, *Ber.*, **62**, 99 (1929).
8. Carter and Record, *J. Chem. Soc.*, **1939**, 662.
9. Cori and Cori, *J. Biol. Chem.*, **131**, 397 (1939).
10. Fargher and Probert, *J. Textile Inst.*, **18**, 559 (1927).

11. Fischer and Seck, *Kolloid-Z.*, **93**, 207 (1940).
12. Freudenberg, Schaaf, Dumpert and Ploetz, *Naturwissenschaften*, **27**, 841 (1939).
13. Freudenberg and Jacobi, *Ann.*, **517**, 102 (1933).
14. Freudenberg, Blomquist, Ewald and Soff, *Ber.*, **69**, 1258 (1936).
15. Freudenberg and Rapp, *Ibid.*, **69**, 2041 (1936).
16. Freudenberg and Meyer-Delius, *Ibid.*, **71**, 1596 (1938).
17. Freudenberg and Boppel, *Ibid.*, **71**, 2505 (1938); *Ibid.*, **73**, 609 (1940).
18. Freudenberg and Jacob, *Ibid.*, **74**, 162 (1941).
19. Frey-Wyssling, *Naturwissenschaften*, **28**, 78 (1940); *Ber. Schweiz. Bot. Ges.*, **50**, 321 (1940).
20. Friese and Smith, *Ber.*, **61**, 1975 (1928).
21. Hanes, *Can. J. Research*, **B13**, 185 (1935); *New Phytologist*, **36**, 101 (1937).
22. Hanes, *Proc. Roy. Soc. London*, **B128**, 421 (1940); **B129**, 174 (1940).
22*a*. Hassid and McCready *J. Am. Chem. Soc.*, **63**, 2171 (1941).
23. Haworth, *Chemistry & Industry*, **58**, 917 (1939).
24. Haworth, Hirst and Webb, *J. Chem. Soc.*, **1928**, 2681.
25. Haworth, Hirst and Isherwood, *Ibid.*, **1937**, 577.
26. Haworth, Hirst and Smith, *Ibid.*, **1939**, 1914.
27. Hess and Smith, *Ber.*, **62**, 1619 (1929).
28. Hess and Lung, *Ibid.*, **71**, 815 (1938).
29. Hess and Krajnc, *Ibid.*, **73**, 976 (1940).
30. Hess and Steurer, *Ibid.*, **73**, 1076 (1940).
31. Higginbotham and Richardson, *J. Soc. Chem. Ind.*, **57**, 234 (1938).
32. Hirst and Young, *J. Chem. Soc.*, **1939**, 951.
32*a*. Hirst, Plant and Wilkinson, *J. Chem. Soc.*, **1932**, 2375.
33. Holmbergh, *Z. physiol. Chem.*, **134**, 96 (1924).
34. Husemann and Ruska, *J. prakt. Chem.*, **156**, 1 (1940).
34*a*. Irvine and Macdonald, *J. Chem. Soc.*, **1925**, 1502.
35. Karrer and Krauss, *Helv. Chim. Acta*, **12**, 1551 (1929).
36. Katz and Derksen, *Z. physik. Chem.*, **A150**, 100 (1930).
37. Katz and v. Itallie, *Ibid.*, **A155**, 199 (1931); **A166**, 27 (1933).
38. Kiessling, *Biochem. Z.*, **298**, 421 (1939); *Naturwissenschaften*, **27**, 129 (1939).
39. v. Klinkenberg, *Proc. Acad. Sci. Amsterdam*, **34**, 893 (1931).
40. Kratky and Schneidmesser, *Ber.*, **71**, 1413 (1938).
41. Krüger and Tschirch, *Ibid.*, **63**, 828 (1930).
42. Kuhn, *Ann.*, **443**, 1 (1925).
43. Küntzel and Doehner, *Kolloid-Z.*, **88**, 209 (1939).
44. Lamm, *Nova Acta Regiae Soc. Sci. Upsaliensis*, (4) **10**, Nr. 6 (1937).
45. Ling and Nanji, *J. Chem. Soc.*, **123**, 2666 (1923).
46. Maquenne and Roux, *Compt. rend.*, **140**, 1303 (1905); *Ann. chim.*, **9**, 179 (1906).
47. K. H. Meyer and Mark, *Der Aufbau der hochpolymeren org. Naturstoffe*, Akadem. Verlagsges, Leipzig, 1930.
48. K. H. Meyer, *Naturwissenschaften*, **28**, 397 (1940).

49. K. H. Meyer, *Kolloid-Z.*, **95**, 70 (1941).
50. K. H. Meyer, *Die hochpolymeren Verbindungen*, Akadem. Verlagsges., Leipzig, 1941. Engl. ed. in preparation.
51. K. H. Meyer, Hopff and Mark, *Ber.*, **62**, 1103 (1929).
52. K. H. Meyer, Brentano and Bernfeld, *Helv. Chim. Acta*, **23**, 845 (1940)
53. K. H. Meyer, Bernfeld and Wolff, *Ibid.*, **23**, 854 (1940).
54. K. H. Meyer, Wertheim and Bernfeld, *Ibid.*, **23**, 864 (1940).
55. K. H. Meyer and Bernfeld, *Ibid.*, **23**, 875 (1940).
56. K. H. Meyer, Bernfeld and Hohenemser, *Ibid.*, **23**, 885 (1940).
57. K. H. Meyer and Bernfeld, *Ibid.*, **23**, 890 (1940).
58. K. H. Meyer, Bernfeld and Press, *Ibid.*, **23**, 1465 (1940).
59. K. H. Meyer and Press, *Ibid.*, **24**, 50 (1941).
60. K. H. Meyer and Press, *Ibid.*, **24**, 58 (1941).
61. K. H. Meyer, Wertheim and Bernfeld, *Ibid.*, **24**, 212 (1941).
62. K. H. Meyer and Fuld, *Ibid.*, **24**, 375 (1941).
63. K. H. Meyer, Wertheim and Bernfeld, *Ibid.*, **24**, 378 (1941).
64. K. H. Meyer and Bernfeld, *Ibid.*, **24**, 389 (1941).
65. Myrbäck, *Biochem. Z.*, **307**, 132, 140 (1941).
66. Myrbäck and Ahlborg, *Ibid.*, **307**, 69 (1940).
67. Myrbäck, Ortenblad and Ahlborg, *Ibid.*, **307**, 53 (1940).
68. Ohlsson, *Z. physiol. Chem.*, **189**, 17 (1930).
69. Parnas, *Die Glykogenolyse*, in *Handbuch der Enzymologie*, edited by Nord and Weidenhagen, Akadem. Verlagsges, Leipzig, 1940.
70. Pictet, *Helv. Chim. Acta*, **9**, 33 (1926); **12**, 700 (1929).
71. Posternak, *Ibid.*, **18**, 1351 (1935).
72. Pringsheim and Wolfsohn, *Ber.*, **57**, 887 (1924).
73. Pringsheim, Bochardt and Hupfer, *Biochem. Z.*, **250**, 109 (1932).
74. Pringsheim and Fuchs, *Ber.*, **65**, 1762 (1932).
75. Reich and Damanski, *Bull. soc. chim. biol.*, **19**, 158, 357 (1937).
76. Richardson, Higginbotham and Farrow, *J. Textile Inst.*, **37**, 131 (1936).
77. Samec and Blinc, *Kolloidchem. Beihefte*, **47**, 371 (1938); **49**, 75 (1939); **52**, 57 (1940).
78. Samec, *Ibid.*, **51**, 359 (1940).
78*a*. Samec, *Ibid.*, **51**, 438 (1940). See tables.
79. Samec and Blinc, *Die neuere Entwicklung der Kolloidchemie der Stärke*, Steinkopff, Dresden, 1940. (Reprint largely of *Kolloidchem. Beihefte* articles, of Ref. 77, 78.)
80. Samec, *Z. physiol. Chem.*, **263**, 17 (1940); *Ber.*, **73**, 1076 (1940).
81. Samec, *Kolloid-Z.*, **94**, 350 (1941).
82. Samec and Waldschmidt-Leitz, *Z. physiol. Chem.*, **203**, 16 (1931).
83. Schäffner and Specht, *Naturwissenschaften*, **26**, 494 (1938).
84. Schulz and Imglingerd, *J. prakt. Chem.*, **158**, 136 (1941).
85. Signer, *Trans. Faraday Soc.*, **32**, 296 (1936); *Helv. Chim. Acta*, **18**, 701 (1935).
86. Somogyi, *J. Biol. Chem.*, **134**, 301 (1940).
87. Staudinger and Eilers, *Ber.*, **69**, 819 (1936).
88. Staudinger and Husemann, *Ann.*, **527**, 207 (1937); *Ber.*, **71**, 157 (1938).

89. Staudinger and Fischer, *J. prakt. Chem.*, **157**, 19 (1940).
90. Taylor and Lehrmann, *J. Am. Chem. Soc.*, **48**, 1739 (1926).
90*a*. Tilden and Hudson, *Ibid.*, **61**, 2900 (1939).
91. Weidenhagen and Wolf, *Z. Ver. deut. Zucker-Ind.*, **80**, 866 (1931); **81**, 644 (1931).
92. Wijsman, *Rec. trav. chim.*, **9**, 1 (1890); *Diss. Amsterdam*, 1889.
93. Willstätter and Rohdewald, *Z. physiol. Chem.*, **225**, 103 (1934).

FRICTIONAL AND THERMODYNAMIC PROPERTIES OF LARGE MOLECULES

R. E. POWELL AND HENRY EYRING

Princeton University, Princeton, N. J.

CONTENTS

In the statistical approach to thermodynamics, one formulates a molecular model and can derive from it all the colligative properties of matter in bulk (22). It is equally easy to start with a model of how two molecules interact, and utilize the statistical method of absolute reaction rates to predict chemical reaction rates and dynamic

properties. Recently these methods have been used to investigate a field of considerable technical importance—including long molecules and their behavior in solution, flow behavior and dielectric behavior. It is the purpose of the present paper to sketch the method of absolute reaction rates and its application to simple systems, and more particularly its extension to large molecules.

I. Thermodynamics of Simple Molecules

A satisfactory physical model for a liquid should possess the feature that from the single model may be derived not only the equilibrium properties but also the properties that measure rate processes. Thus the experimental study of diffusion or viscosity should give an improved model of the liquid state, which in turn should permit the prediction of the heat capacity or the vapor pressure. It will be of interest to show, then, that the models suggested for rate processes in simple liquids and in solutions are quite adequate to reproduce the thermodynamic properties (95).

From analysis of the data on diffusion and viscosity, it has been concluded that a simple liquid must possess the following properties:

1. A molecule which is flowing or diffusing does so by moving into adjacent empty equilibrium positions or "holes." For non-associated liquids, the presence of these holes is the all-important factor determining flow. A liquid is thus to be considered as a binary mixture of molecules and holes.

2. The heat of activation for viscous flow or diffusion is only about one-third the heat of vaporization for normal liquids. Since the entire heat of vaporization would be required to make a cavity the size of a molecule, it is clear that a hole is considerably smaller than a molecule. The actual volume required to provide a new equilibrium position can be calculated from the pressure effect on viscosity. It is found in this way that a hole, for normal non-metallic liquids, is about one-seventh the volume of a molecule.

3. If the expansion on melting (about 10% for a typical non-metal) is due to the introduction of new equilibrium positions into the solid, the substance acquires on melting about 0.7 mole of new equilibrium positions per mole of molecules. The random distribution of the mole of molecules among the 1.7 moles of equilibrium positions would be sufficient to reproduce the entropy of fusion of 2 E. U. observed for many simple substances.

From the hints furnished by the rate studies, Walter and Eyring (95) have formulated and tested a partition function for the liquid state. The liquid is assumed, first, to be made up of N molecules distributed at random over the original N equilibrium positions of the solid plus n_h new equilibrium positions. Of the $3N$ translational degrees of freedom of the N molecules, the fraction V_s/V of them is taken as solid degrees of freedom and the remaining $(V - V_s)/V$ of the $3N$ degrees of freedom are taken as gas-like. Here V is the actual volume occupied by a mole of liquid, and V_s is the volume of the solid at the melting point. It is to be noted that this is a departure from the conventional model for a liquid, in which all the molecules occupy equivalent equilibrium positions and each molecule is allowed an average free volume and moves in an averaged potential field. It also differs from the model of Lennard-Jones and Devonshire (52), who postulated that, on melting, as many new equilibrium positions entered as there are molecules, *i. e.*, $N = n_h$ for the entire liquid range. Here it is assumed that n_h is a linear function of $V - V_s$, increasing with V without limit.

The partition function for one molecule in a solid-like equilibrium position is

$$f_s e^{E_s/RT} = \left(\frac{e^{-\theta/2T}}{1 - e^{-\theta/T}} \right)^3 e^{E_s/RT} \tag{1}$$

where E_s is the potential energy of the solid, and $\theta = {}^3/_4\theta_{\text{Debye}}$. For a molecule in a gas-like equilibrium position, the partition function is

$$f_g e^{-\delta E_s/RT} = \left\{ \frac{(2\pi mkT)^{3/2}}{h^3} \frac{V_s}{n} \right\} e^{-\delta E_s/RT} \tag{2}$$

where the volume of a hole is $1/n$ the volume of a molecule, and δE_s is the interaction energy between molecules. Before final application of the equation, a numerical value must be assigned to n and a suitable function chosen for δ.

If the N molecules are distributed at random over the $N + n_h$ equilibrium positions, there is a term $(N + n_h)!/N!n_h!$ in the partition function. The complete partition function is

$$f = \left\{ \left(f_s e^{E_s/RT} \right)^{V_s/V} \left(f_g e^{-\delta E_s/RT} \right)^{(V - V_s)/V} \right\}^N \frac{(N + n_h)!}{N!n_h!} \tag{3}$$

which extrapolates smoothly to the partition function for the solid, and to that for the gas if $\delta \rightarrow 0$ when $V \rightarrow \infty$.

Equation (3) was tested by application to argon, nitrogen and benzene. From the observed entropy and volume change of fusion, n was evaluated as 8.35 for all three liquids. The simplest form of the function δ which would give fair agreement with the experimental data was $\delta = (V_s/V)^2/(2\gamma + 0.18)$ for argon, with similar equations for nitrogen and benzene, where $\gamma \equiv n_h/N = (V - V_s)/(V_s/n)$.

The partition functions permit the successful calculation of melting-point constants, critical constants, volumes and vapor pressures over the entire liquid range, heat capacities, compressibilities and second virial coefficients. Table I lists some of the values so computed for argon.

TABLE I

OBSERVED AND CALCULATED PROPERTIES FOR ARGON

T ° K.	Volume, cc.		Vapor pressure, atmos.	
	Calcd.	Obsd.	Calcd.	Obsd.
83.85	28.27	28.03	0.660	0.674
87.44	28.81	28.69	1.000	1.000
89.95	29.17	29.07	1.310	1.323
97.71	30.42	30.15	2.735	2.671
111.87	32.9	32.63	8.02	7.40
122.34	35.9	35.08	15.04	13.58
137.59	43	41.02	33.14	28.29
147.93	52	51.68	48	43.19

Melting Point Constants		Critical Constants	
Calcd.	Obsd.	Calcd.	Obsd.
T_m 82.9°	83.85°	T_c 154.2°	150.66°
V_m 3.14 cc.	3.05 cc.	V_c 78.7 cc.	75.26 cc.
S_m 3.40	3.35	P_c 59.4 atm.	48.00 atm.

II. Thermodynamics of Large Molecules

As for simple molecules, so also for macromolecules the study of rate processes has thrown light upon the problem of equilibrium thermodynamic properties (69). The experimental results of Flory (19) on the viscosity of polyester melts led Kauzmann and Eyring (40) to the conclusion that these long molecules flow by segments about 25 chain atoms long, instead of by whole molecules. This same "segment" model has been applied to the thermodynamic properties of long molecules. The concept that a long molecule is

made up of smaller "kinetic units" has been offered before for a qualitative description of the surface tension (55) and the osmotic pressure (34), but it has had leveled against it the criticism that it was merely an *ad hoc* explanation for the thermodynamic data, without any independent supporting evidence (36). It is therefore gratifying that investigations along an entirely different path—the viscosity studies—have led directly to the segment model of linear macromolecules. In fact, the segment model from viscosity studies is in quantitative agreement with the segment model from thermodynamic properties.

1. Melting

The melting process may be considered, from a statistical point of view (as we have seen in the theory for the simple liquid), as the introduction of new equilibrium positions into the solid. The heat of fusion is expended in deforming enough bonds between molecules and in providing the additional space to create these new equilibrium positions, and the entropy of fusion is gained partly from the disordered distribution of the molecules over the new and old equilibrium positions and partly from their increased possibilities of rotation. If a long molecule acts in segments, the equilibrium positions need be supplied only for the segments. The properties of the segments will then fix the values for the heat of fusion ΔH_f, the entropy of fusion ΔS_f and the melting point, which is equal to their ratio $\Delta H_f / \Delta S_f$. The melting points should approach a limiting value as we ascend a homologous series of compounds, and the limiting melting point should be the same for all series. Figure 1 presents experintental date on the convergence of melting points. The limiting melting point is about 122° C., or 395° K. Since the increase in melting point per CH_2 group is about 20° (determined from the lower homologs), the average length of a melting segment is 395/20 or about 20 carbon atoms.

Fuller, Baker and Pape (27) have made x-ray and elasticity studies of linear polyamides at temperatures below their melting point, and have found that when a sample is quenched or annealed at a temperature near its melting point instead of at room temperature, its x-ray photograph is sharper and it is less elastic. These authors conclude that in the solid polyamide at high temperatures, segments of the polymer molecule can rotate, and that amorphous portions of the solid are becoming crystalline.

2. *Osmotic Pressure*

Osmotic pressure is given for the ideal, dilute solution by van't Hoff's law,

$$\frac{\pi V_1}{RT} = N_2 \tag{4}$$

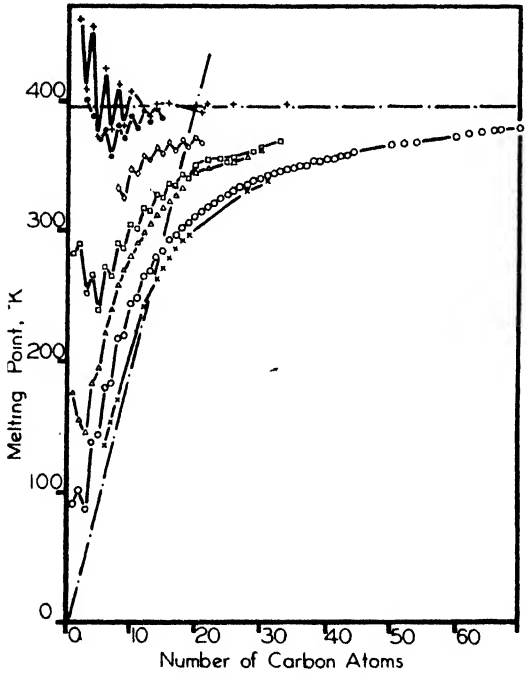

Fig. 1.—Melting points of homologous series.

Key: ○ *n*-paraffins
× *n*-α-olefines
△ *n*-prim.-alcohols
□ *n*-prim.-monobasic acids
◇ α-ω-hydroxy acids
● substituted malonic acids
+ α-β-dibasic acids

If a long molecule in solution moves in segments, its osmotic pressure may be assumed to be determined by the effective mole fraction, not the actual mole fraction:

$$\frac{\pi V_1}{RT} = N_2^* = \frac{n_2^*}{n_1 + n_2^*} \tag{5}$$

where n_1 is the number of molecules of solvent and n_2^* the effective number of molecules of solute. The effective number of molecules

of solute may be evaluated in terms of the actual number as follows: When the polymer segment is in an environment of other polymer molecules, it will be able to move into any cavity large enough for it. But if the polymer segment is in an environment of small solvent molecules, the statistical chances are overwhelming that any such cavity will be filled by the small molecules. The assumption is therefore made that the probability of the polymer molecule's moving by segments is a linear function of its environment, as expressed by the volume fraction of polymer. If a single molecule behaves in the pure polymer as Q segments

$$n_2^* = n_2[1 + (Q - 1)\phi_2] \tag{6}$$

where n_2 is the actual number of solute molecules, and ϕ_2 is the volume fraction of polymer. The resulting expression for the osmotic pressure is

$$\frac{\pi V_1}{RTN_2} = 1 + (Q - 1)\phi_2 \tag{7a}$$

$$\frac{\pi V_2}{RT\phi_2} = 1 + Q\phi_2 \tag{7b}$$

$$\frac{\pi M_2}{RTc_2} = 1 + Qc_2/d_2 \tag{7c}$$

where N_2 is the mole fraction, ϕ_2 the volume fraction, c_2 the concentration in g./cc., M_2 the molecular weight, V_2 the molal volume and d_2 the density of the polymer. Terms of higher order in ϕ_2 have been omitted. Equation (7) reduces to van't Hoff's law at the lowest concentrations, and predicts a linear increase of reduced osmotic pressure π/c with concentration c. An equation of this type represents the experimental data satisfactorily for a number of polymer solutions, as is illustrated in Fig. 2 for a series of cellulose acetates of different molecular weights (83). The intercept is a measure of the average molecular weight, while the slope is a measure of the size of a segment, so a family of approximately parallel lines is obtained for the cellulose acetates. From the slopes of the plots of π/c against c, the segment lengths have been determined for a number of types of polymers. In polystyrenes and polyethylene oxides the segment length is approximately 20–30 atoms. In cellulose nitrate, cellulose acetate and methyl cellulose the segment length of 9–14 chain atoms corresponds to about 2 glucose units. The segment lengths in rubber

vary from 42 to 460 chain atoms, and are, moreover, very sensitive to the treatment of the sample. Any branching or cross-linking will make the polymer molecule less like a flexible jointed rod and more like a single rigid molecule, so that the apparent segment length will increase. Probably most of the variation in segment lengths for rubber and for some of the other types of polymers is due to differences in the degree of branching or cross-linking (69).

The solvent in concentrated polymer solutions exhibits an abnormally high vapor pressure, as if the solvent contained a perfect solute of much smaller molecular weight. For example, oleyl oleate

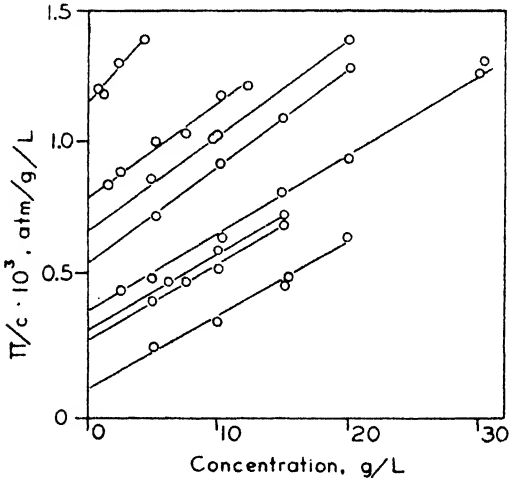

Fig. 2.—Osmotic pressure of cellulose acetate solutions.

(m. w. 532.5) has in carbon tetrachloride an apparent molecular weight of 242, and a sample of caoutchouc (m. w. 270,000) has in toluene an apparent molecular weight of 417. This behavior is explained by the segment model for the long molecules, and the segment length is again about 20 chain atoms.

A similar thermodynamic treatment may be offered for the surface tension of long molecules. As Table II shows, the surface tension of higher normal paraffin hydrocarbons becomes sensibly independent of length, showing that the unit responsible for surface tension is of the same size for all the higher hydrocarbons. The actual size of a segment may be estimated from the temperature coefficient of surface

tension by applying Eötvös' equation, $d/dT(\sigma V^{2/3}) = 2.12$. The apparent molecular weights so estimated are about 150–200 for compounds whose actual molecular weights are between 350 and 900.

TABLE II

SURFACE TENSION OF HIGHER NORMAL PARAFFIN HYDROCARBONS

Hydrocarbon	Surface tension, 20° C.
n-C_6H_{14}	18.43
n-C_8H_{18}	21.80
n-$C_{10}H_{22}$	23.91
n-$C_{18}H_{38}$	~28.1
n-$C_{26}H_{54}$	~29.4
n-$C_{60}H_{122}$	~29.1

It is worth noting that the segment lengths estimated from osmotic pressure data (18–33 atoms for polystyrene and polyethylene oxide) and from melting point data (20–25 atoms for hydrocarbons) are in agreement with the segment lengths from viscosity data (20–25 atoms for hydrocarbons, 28–34 atoms for polyesters) for long molecules of similar structure.

3. *Swelling*

The results on the viscosity of polymer melts indicate that the pure polymer contains unoccupied equilibrium positions large enough to permit the motion of segments. When a solvent is added to the polymer, and the polymer swells, some of these cavities will be filled by small molecules. Three qualitative conclusions may be drawn:

1. There will be a net decrease in volume.
2. The cavities, and therefore the swelling, will not depend upon the degree of polymerization.
3. The process will involve a *decrease* in entropy, since the polymer segments no longer possess the cavities into which to move.

Each of these conclusions is in accord with the experimental results; swelling is accompanied by a volume decrease (24); when cellulose nitrate swells in acetone, the swelling pressure for a given amount of acetone is independent of the molecular weight (75); and there is a negative entropy change of several E. U. when gases dissolve in synthetic rubbers, or when agar, casein, keratin or cellulose swells in water (3, 25, 79, 91).

III. Absolute Reaction Rates

The method of absolute reaction rates has been applied successfully to many chemical rate processes—gas reactions, reactions in solution, heterogeneous reactions (32). It offers an equally potent method of attack upon physical rate processes such as viscous flow, diffusion in liquids and solids or dielectric relaxation. The method has so many possible applications that it will be profitable to derive here its formulas and to present them in a usable form.

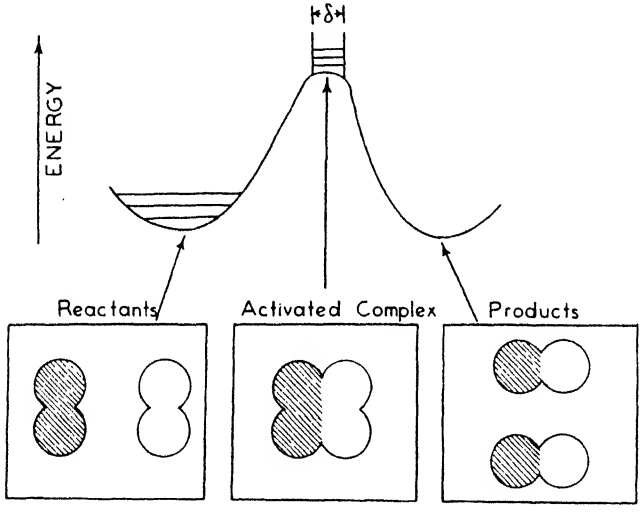

Fig. 3.—Energy profile for a typical reaction.

When two molecules are to undergo a chemical reaction with each other, they are at first separate. As they approach one another closer and closer, the potential energy of the system increases. At the summit of the "energy barrier" they have formed a quasi-molecule or "activated complex." This activated complex is much like an ordinary molecule, except that it is unstable in the one degree of freedom corresponding to completion of the reaction; the system thus crosses the energy barrier, and the activated complex flies apart to form the final products. The whole process is illustrated in Fig. 3, which is a schematic representation of a reaction such as $H_2 + I_2 \rightarrow 2HI$. The method of treatment will be formally the same no matter

how many molecules react or are produced, or if a physical rather than a chemical rate process is under discussion.

The rate of reaction will be given by the concentration of activated complexes per length δ along the reaction path multiplied by the rate at which they are crossing the top of the barrier:

$$\text{rate} = c_a \bar{u}/\delta \tag{8}$$

where c_a is this concentration of activated complexes, $\bar{u}$ their mean velocity across the top of the barrier and δ the distance across the top of the barrier. The mean velocity is given by

$$\bar{u} = \frac{\int_0^\infty u e^{-mu^2/2kT}\, du}{\int_{-\infty}^{\infty} e^{-mu^2/2kT}\, du} = \left(\frac{kT}{2\pi m}\right)^{1/2} \tag{9}$$

To find the concentration of activated complexes, it is necessary to know only the concentration of reactants and the equilibrium constant connecting the activated with the initial state:

$$\frac{c_a}{c_0} = K_a = K^\ddagger (2\pi m k T)^{1/2} \delta/h \tag{10}$$

The factor $(2\pi mkT)^{1/2}\delta/h$ which has been taken out of the equilibrium constant is the partition function for the one degree of translational freedom of the activated complex corresponding to completion of the reaction. The rate of reaction is then given by

$$\text{rate} = c_0 \frac{kT}{h} K^\ddagger \tag{11}$$

and the specific reaction rate, k', is given by the same expression without the factor c_0. This simple result may be stated in these words: The concentration of activated complex is determined by an equilibrium constant, $K^\ddagger$; the activated complex decomposes for all reactions at the same rate, which is the universal frequency kT/h, or numerically $\sim 10^{13}$ per second at room temperature.

The equilibrium constant of activation $K^\ddagger$ may be put into several equivalent forms. It may be written as the ratio of the partition functions of the activated and the normal states, in which case the rate equation becomes

$$k' = \frac{kT}{h}\frac{F_a}{F_0} \tag{12}$$

or it may be put into thermodynamic notation,

$$k' = \frac{kT}{h} e^{-\Delta F^{\ddagger}/RT} \tag{13a}$$

$$k' = \frac{kT}{h} e^{\Delta S^{\ddagger}/R} e^{-\Delta H^{\ddagger}/RT} \tag{13b}$$

where $\Delta F^{\ddagger}$, $\Delta H^{\ddagger}$ and $\Delta S^{\ddagger}$ are called the free energy, the heat and the entropy change of activation. It is equation (11), or (12) or (13), all equivalent to it, which is to be applied to a rate problem. The method may be applied synthetically if the reaction mechanism is known, *i. e.*, the heat of activation may be determined from "energy contour maps," the partition functions for the normal and activated states may be computed from force constants and moments of inertia, and so the rate of reaction may be obtained completely *a priori*. For a number of gas reactions this has been carried through. However, it it is always tedious and many times impracticable. An easier procedure is to use experimentally measured heats of activation, and to calculate only the non-exponential factors from known or estimated properties of the molecules. The alternative, which is often useful, is to apply equation (13) to the analysis of experimental data. From one measured rate, the free energy of activation is obtained; if measurements are made at two temperatures, the free energy of activation may be broken into a heat and an entropy term. In many instances an inspection of these quantities will suggest a new or more accurate picture of the reaction mechanism. For example, $\Delta F^{\ddagger}$ for viscous flow may be closely correlated with a thermodynamic property, the energy of vaporization; in the denaturation of proteins, the high positive value of $\Delta S^{\ddagger}$ means that many bonds are broken in the process; the value of $\Delta H^{\ddagger}$ for dielectric relaxation is higher than the value of $\Delta H^{\ddagger}$ for viscous flow of the same liquid, indicating that more bonds must be broken in the former process.

The method of absolute reaction rates, then, recommends itself as a simple and successful approach to rate problems. The following sections present some examples of its application, and it is to be hoped that the method will be directed at many problems as yet untouched.

IV. Viscosity of Simple Liquids

The model formulated for flow processes in the liquid is that illustrated in Fig. 4 (16). A given molecule is continually leaving its equilibrium position, squeezing past its neighbors (passing over the energy barrier), and dropping into an adjacent empty equilibrium position. This motion occurs in random directions. If now some force is applied to the molecule, it will jump slightly more often in the direction in which the applied force is helping, and slightly less often in the direction in which the applied force is hindering. This same model holds for several rate processes: (1) When the applied force is a shear gradient, the net process is viscous flow; (2) when the applied force is an activity gradient, the net process is diffusion; (3) when the applied force is a potential gradient acting on ions, the net process is ionic conductance; (4) when the applied force is gravitational or centrifugal, the net process is sedimentation.

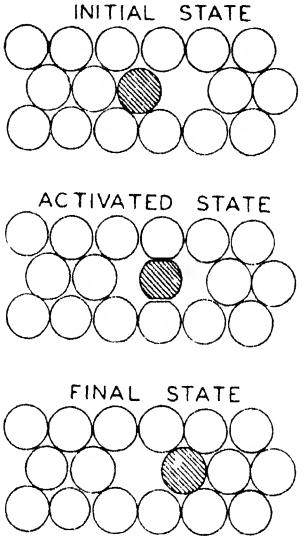

Fig. 4.—Model for flow processes.

The expression for viscosity is readily derived. Let a shearing force f be applied across the two layers of molecules. The distance between equilibrium positions is λ, the distance between molecules is λ_1 normal to the plane of shear, λ_2 along the direction of flow and λ_3 in the third direction. Fluidity, or reciprocal viscosity, is defined as the difference in velocity per unit distance normal to the plane of flow per unit shear:

$$\phi = \frac{1}{\eta} = \frac{\Delta u}{\lambda_1 f} \tag{14}$$

The difference in velocity is given by the distance a molecule moves in one jump multiplied by the net rate of jumping:

$$\Delta u = \lambda(k_f' - k_b') \tag{15}$$

If the free energy of activation for a molecule jumping under no

external force is $\Delta F^{\ddagger}$, the forward process is helped by the work due to a force f acting on an area $\lambda_2\lambda_3$ through a distance $\lambda/2$, and the reverse process is hindered by the same amount, so

$$k_f' = \frac{kT}{h} e^{-\Delta F^{\ddagger}/RT}\left(e^{-f\lambda_2\lambda_3\lambda/2kT}\right) \tag{16a}$$

$$k_b' = \frac{kT}{h} e^{-\Delta F^{\ddagger}/RT}\left(e^{-f\lambda_2\lambda_3\lambda/2kT}\right) \tag{16b}$$

Upon combining equations (14), (15) and (16), and expanding the second exponentials, the viscosity equation is obtained:

$$\phi = \frac{1}{\eta} = \frac{\lambda^2\lambda_2\lambda_3}{\lambda_1 h} e^{-\Delta F^{\ddagger}/RT} \tag{17}$$

To a close approximation, the factor involving the λ's is simply the volume of a molecule, so that equation (17) takes the form

$$\phi = \frac{V}{Nh} e^{-\Delta F^{\ddagger}/RT} \tag{18a}$$

$$= \frac{V}{Nh} e^{\Delta S^{\ddagger}/R} e^{-\Delta H^{\ddagger}/RT} \tag{18b}$$

The viscosity does well obey an equation like (18*b*), *i. e.*, good straight lines are obtained when log η is plotted against $1/T$. The equation has been further tested in several ways:

1. Correlation with Vaporization (74)

The free energy of activation may be estimated as some fraction of the total free energy change of a complete reaction which is similar. The bonds which are broken for flow to occur are of the same kind as the bonds broken in vaporization; however, the flowing molecule does not gain the entropy ΔS_{vap} per mole of expansion into the vapor state, nor does it do the work RT per mole of expansion against the atmosphere. Hence the free energy of activation is to be correlated with $\Delta F_{vap} + T\Delta S_{vap} - RT = \Delta E_{vap}$, and Fig. 5 shows values of $\Delta F^{\ddagger}$ plotted against ΔE_{vap} for a large number of liquids. The squares at the left of the diagram are the liquefied gases nitrogen, oxygen, argon; the circles in the intermediate portion are various typical organic liquids, and the triangles are water and various alco-

hols; the triangle at the far right is glycerol. The equation of the straight line is

$$\eta = \frac{Nh}{V} e^{\Delta E_{vap}/2.45\,RT} \tag{19}$$

Another useful correlation is that between the heat of activation for viscous flow and the energy of vaporization (15). For the typical organic liquids, $\Delta H^{\ddagger}$ is between one-fourth and one-third of ΔE_{vap}.

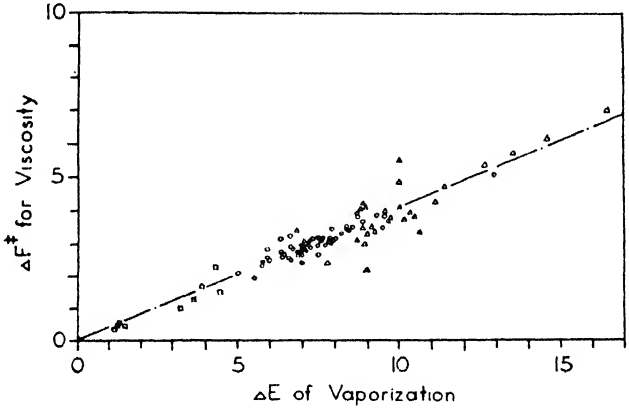

Fig. 5.—Relation of viscous flow to vaporization.

2. *Importance of Holes*

The question arises as to whether the presence of holes or the squeezing past neighboring molecules is the determining factor for flow of liquids. Batschinski found that for simple liquids compensating changes of temperature and pressure which left the volume unchanged had little effect on the viscosity (4). The investigations of Bingham lead to the same conclusion (5). Since the volume is a measure of the number of holes present, these results suggest that holes are all-important. A more detailed study has verified that for non-associated liquids the heat of activation for viscous flow at constant volume is indeed small, and satisfactory estimates of the viscosity at the melting points have been made for a number of liquids by use of the "hole" model (74). These results were incorporated into the partition function for normal liquids discussed in a preceding section.

3. *Size of Holes*

The viscosity equation for high pressures may be written (26)

$$\eta_p = \frac{Nh}{V} e^{(\Delta F^{\circ\ddagger} + P\bar{\Delta V}^{\ddagger})/RT} \qquad (20)^*$$

where P is the pressure and $\bar{\Delta V}$ is the mean volume change of activation. Strictly, $P\bar{\Delta V}^{\ddagger} = \int_0^P \overline{\Delta V^{\ddagger}} dP$; but since plots of log η_p/ log η_0 against pressure give good straight lines it is a good approximation to treat $\Delta V^{\ddagger}$ as independent of pressure. For simple liquids, the activation volume is found to be about one-sixth or one-seventh the volume of a molecule.

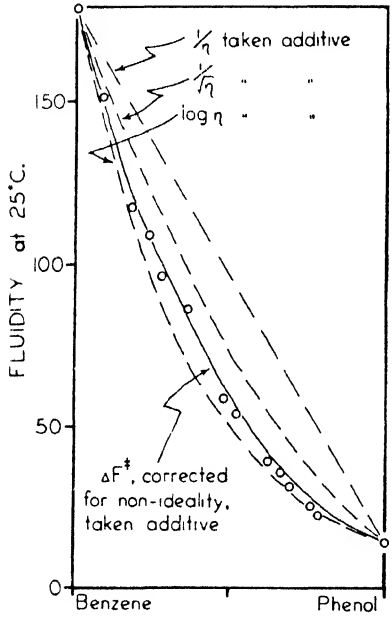

Fig. 6.—Effect of concentration on viscous flow of simple liquids.

4. *Viscosity of Mixtures (74)*

The flow-determining factor in simple liquids is the presence of holes, and the formation of these holes requires a certain amount of energy (about one-third the heat of vaporization). When the hole is formed in a mixed solvent, the energy must be taken at an intermediate value. The mixture law for viscosity becomes, for ideal solutions,

$$\eta = \frac{Nh}{V} e^{(N_1\Delta F_1^{\ddagger} + N_2\Delta F_2^{\ddagger})/RT} \qquad (21)$$

and this reduces, to a close approximation, to the empirical rule of Arrhenius or of Kendall:

$$\eta = \eta_1^{n_1}\eta_2^{n_2} \qquad (22)$$

* The superscript ° in $\Delta F^{\circ\ddagger}$ signifies substances ideal at all concentrations, *i. e.*, with activity coefficient γ equal to unity. (The same applies for equations 38–41, 43 and 44).

If imperfection in the free energy of vaporization is taken into account, equation (21) is in fact the mixture law for non-ideal solutions. Figure 6 illustrates the application of these and some empirical mixture laws to the system benzene–phenol.

V. Viscosity of Long Molecules

When the heat of activation for the viscous flow of the normal paraffins is plotted against the number of carbon atoms in the molecule, the heat appears to approach a limiting value (Fig. 7), just as the melting point does (Fig. 1). Thus when the hydrocarbon becomes large, it flows in segments of fixed size, independent of the total length of the molecule (40). The limiting value of $\Delta H^{\ddagger}$ is 6–7 kcal., which corresponds to a chain length of 20–25 carbon atoms.

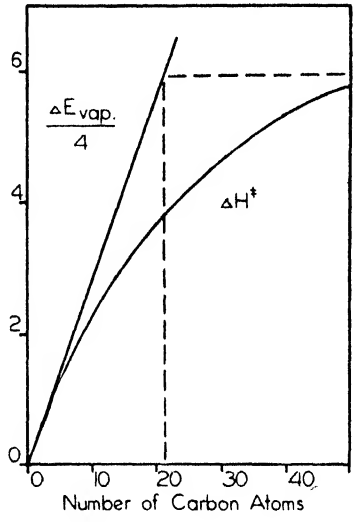

Fig. 7. Relation of heat of activation for viscous flow to chain length.

More evidence for flow by segments is offered by Flory's data on the viscosity of polyester melts (19). The heat of activation for viscosity is found to be independent of molecular weight, indicating that the unit of flow is the same for all molecular weights studied. The viscosity of a polyester of weight-average chain length Z_w is given by

$$\ln \eta = A/R + BZ_w^{1/2}/R + C/RT \qquad (23)$$

where the constants have the values $A = -28$, $B = 0.5$, $C = 8.3$ kcal. From equation (18) the viscosity equation should read

$$\ln \eta = \ln Nh/V - \Delta S^{\ddagger}/R + \Delta H^{\ddagger}RT \qquad (24)$$

The value of $\Delta H^{\ddagger}$ is seen to be 8.3 kcal. From the known heats of vaporization of similar molecules, and the relation $\Delta H^{\ddagger} = \Delta H_{vap}/4$, the segment lengths are estimated to be 28–34 chain atoms for the

several polyesters. Thus the molal volume of a segment is known (about 500 cc.) and the value of $\Delta S^{\ddagger}$ is found to be

$$\Delta S^{\ddagger} = 6.8 - 0.5Z_w^{1/2}$$

so that a segment on activation gains (rotational) entropy of 6.8 E. U., and loses an amount which depends on the total chain length. The latter term is interpreted as arising from the necessity of cooperation between segments in order that the molecule as a whole may progress. The square root of chain length enters exponentially into the viscosity equation, *i. e.*,

$$\text{fluidity} = \phi = 1/\eta = Ke^{-BZ^{1/2}/R} \tag{25}$$

The exponential may be written in the equivalent form $(1 - BZ^{1/2}/Rn)^n$ where n is a large number. But this is just the probability that n successive events shall all be successful, where $BZ^{1/2}/Rn$ is the probability of failure. A freely twisted hydrocarbon chain encloses on the average $3.4Z^{3/2}$ cubic Ångström units, $1/n$ of which volume is available to each segment, n being the number of segments. The chain itself occupies a volume of $20Z$ cubic Ångström units. The probability of a segment making an unprofitable jump is then

$$3.4Z^{3/2}/n \div 20Z = 0.17Z^{1/2}/n$$

It is seen that the value of the parameter B is calculated to be 0.34, to be compared with the value of 0.5 observed by Flory.

It is interesting to apply the same equation to liquid sulfur. The heat of activation for viscous flow is about 10 kcal., and from the known heat of vaporization the unit of flow is estimated to be 20 atoms. Such a segment length gives a value of $\Delta S^{\ddagger}$ of -37, and if this entropy is due to a $BZ^{1/2}$ term with $B = 0.5$, the average length of a sulfur chain is 5500 atoms.

VI. Viscosity of Solutions of Macromolecules (69)

For dilute solutions of long molecules, experiments of Staudinger (80) and others have shown that the viscosity equation is of the form

$$\eta = \eta_0(1 + kZ\phi) \tag{26}$$

where η_0 is the viscosity of the pure solvent, Z the chain length, ϕ the volume fraction of solute and k a constant for a given polymer type. An equation of this type can also be deduced from a model

in which the long molecule is taken as a series of spheres connected by rigid rods with the appropriate valence angles, moving in a continuous fluid (37).

For the molten polymer, the viscosity is given by Flory's equation,

$$\eta_P = \frac{Nh}{V_p} e^{-\Delta S_p^{\ddagger}/R} e^{BZ^{1/2}/R} e^{\Delta H_p^{\ddagger}/RT} \tag{27}$$

where Z is the chain length, and V_p, $\Delta S_p^{\ddagger}$ and $\Delta H_p^{\ddagger}$ are the volume, entropy of activation and heat of activation for a single segment.

The viscosity at intermediate concentrations may be estimated by combining these two equations in the following manner: The viscosity at either limit may be expressed, with complete generality, by the absolute rate expression

$$\eta = \frac{Nh\, F_0}{V\, F^{\ddagger}} \tag{28}$$

where $F^{\ddagger}$ is the partition function for the activated state and F_0 for the normal state, and the partition functions contain whatever factors are necessary for the expressions to reduce to the usual viscosity equations. If a long molecule is in a concentrated solution, some sections of it will be surrounded by other long molecules, some sections surrounded by small solvent molecules. To a first approximation, the parts which are in an environment of macromolecules will have such degrees of freedom as they would have in the molten polymer, and the parts which are in an environment of solvent will have such degrees of freedom as they would in the dilute solution, each part executing its own motion without undue hindrance from distant parts of the same molecule. Intermediate partition functions are then to be taken in equation (28):

$$\eta = \frac{Nh}{V_{av}} \left(\frac{F_0}{F^{\ddagger}}\right)_{\text{dilute}}^{1-\phi} \left(\frac{F_0}{F^{\ddagger}}\right)_{\text{polymer}}^{\phi} \tag{29}$$

Since Nh/V is numerically the least variable of the factors, it is insensitive to the method of averaging and may be included within the parentheses. The concentration unit, ϕ, which is a measure of the environment of a long molecule, is the volume fraction of polymer. The method of averaging of equation (29) does not specify the actual forms of the viscosity equations at the two limits. In the special case in which the viscosity of the dilute solution is expressed by Staudinger's equation (equation (26)) and the viscosity of the molten

polymer is given by Flory's equation (equation (27)), the viscosity of a concentrated solution is

$$\eta = \{\eta_0(1 + kZ\phi)\}^{1-\phi}\left\{\frac{Nh}{V_p}\, e^{-\Delta S_p^{\ddagger}/R}\, e^{BZ^{1/2}/R}\, e^{\Delta H_p^{\ddagger}/RT}\right\}^{\phi} \tag{30}$$

For the dilute solution, equation (30) may be put in the equivalent form

$$\begin{aligned}\frac{\ln \eta/\eta_0}{\phi} = \left[kZ + BZ^{1/2}/R + \frac{\Delta H_p^{\ddagger} - \Delta H_0^{\ddagger}}{RT} - \frac{\Delta S_p^{\ddagger} - \Delta S_0^{\ddagger}}{R} - \ln \frac{V_p}{V_0}\right] \\ + \phi\left[-\frac{k^2Z^2}{2} - kZ\right] \\ + \phi^2\left[\frac{k^3Z^3}{3} + \frac{k^2Z^2}{2}\right] + \ldots\end{aligned} \tag{31}$$

which gives the logarithmic viscosity increment; and when extrapolated to zero concentration, this is the "intrinsic viscosity" (46). It now remains to test the applicability of equations (30) and (31).

1. Dependence on Molecular Weight

Equation (31) relates the intrinsic viscosity to the molecular weight. The constant K_m of Staudinger is given (except for a proportionality constant for the units used) by

$$\frac{1}{Z}\left[\frac{\ln \eta/\eta_0}{\phi}\right]_{\phi=0} = k + \frac{B}{RZ^{1/2}} + \frac{P}{Z} \tag{32}$$

where the last three (small) terms in the first bracket of equation (31) have for convenience been collected into the symbol P. For very high molecular weights, the second and third terms of equation (32) will vanish and K_m indeed be a constant. However, at lower molecular weights the experimental K_m should show a marked drift to higher values. The experimental data do show this upward drift for polystyrenes and for polyvinyl chlorides (81, 85, 86). Additional examples, in which branching is more probably absent, are polymeric hydroxydecanoic acid (45), polyethylene oxides (21) and polyesters (20).

2. Dependence on Concentration

From equation (31), the logarithmic viscosity increment should not be constant, but should show a regular decrease with increasing concentration. This has been observed by many investigators, and

is clearly shown in Fig. 8, in which the data are plotted for cellulose acetate in cyclohexanone (54).

From the experimental viscosity curve, together with an independently measured value of the molecular weight, the parameters k and B can be evaluated separately. Table III lists the numerical values found in this way for several different types of polymers.

It will be observed that the values of the viscosity parameter k are in the same order as the values of the segment length determined from osmotic pressure. Increased rigidity of a polymer molecule appears to increase both of these quantities. However, the uncertainties in the data make it unsafe to draw more than a qualitative conclusion.

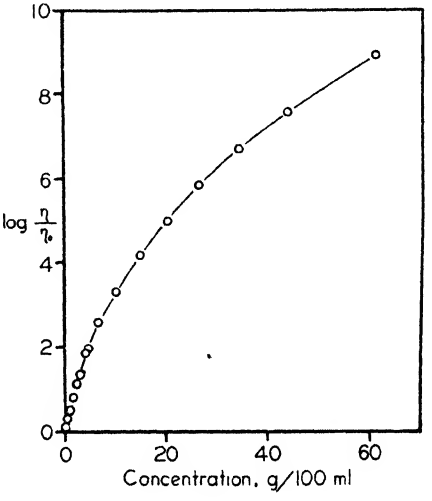

Fig. 8.—Effect of concentration on viscosity of polymer solutions (cellulose acetate in cyclohexanone).

Solutions of globular macromolecules may be investigated by the same method applied to linear macromolecules: (1) The logarithmic viscosity increment does not decrease, but increases with concentration. The mixtures obey closely the hydrodynamic equations derived by Einstein (14) and by Guth and Simha (33):

$$\eta = \eta_0(1 + 5/2\,\phi + 109/14\,\phi^2 + \ldots) \qquad (33)$$

TABLE III

VISCOSITY CONSTANTS FOR HIGH POLYMERS

Substance	k	B/R
Cellulose nitrate (1, 17, 18, 35)	0.00845	2.33
Cellulose acetate (17, 35, 54)	0.0194	2.21
Polyesters (19)	0.025	0.62
Polystyrene (84)	0.0447	0.845
Rubber (17, 18)	0.0835	3.27

Sulfur sols (64) or phenol-aldehyde resin sols (44) are examples. (2) The viscosity is lower by one or two orders of magnitude than that of linear molecules, because the large terms in kZ and $BZ^{1/2}$ are absent. Thus a 2% solution of rubber or of cellulose nitrate may be extremely viscous, but it is not difficult to work with a 70% solution of Batavia dammar, a natural resin (53). (3) There is a perceptible increase in viscosity of phenolic resin solutions with increasing degree of polymerization, indicating that the viscosity contribution between solute molecules should again be taken into account (44).

3. *Dependence on the Solvent*

It was early proposed that the intrinsic viscosity is the same for all solvents, if the investigator limits himself to good, homopolar solvents. However, it is a well-known fact, and one of industrial importance, that one solvent will give a considerably less viscous solution of a given polymer than another solvent. From the point of view of a polymer molecule, a "good" solvent is clearly one in which the solvent molecules seek the company of the polymer molecule and cluster about it, so that the polymer molecule is effectively in a more dilute solution. The polymer molecule will meet so few other polymer molecules that it will seldom act in segments, its osmotic pressure will become more ideal and its viscosity less. The intrinsic viscosity of a solution of rubber in benzene is decreased 40% by the addition of 15% of methyl alcohol, and the osmotic pressure becomes practically ideal (30).

The effective volume-fraction of polymer in a non-ideal solution may be written $\gamma\phi$, where γ is an activity coefficient. The viscosity of a solution is now given by

$$\eta = \{\eta_0(1 + kZ\phi)\}^{1-\gamma\phi}\{\eta_p\}^{\gamma\phi} \tag{34}$$

For solutions of the same concentration in two different solvents, equation (34) may be written

$$\ln \frac{\eta_1/\eta_{01}}{\eta_2/\eta_{02}} = \phi \left\{(\gamma_1 - \gamma_2) \ln \frac{\eta_p/\eta_{01}}{1 + kZ\phi} - \gamma_2 \ln \frac{\eta_{01}}{\eta_{02}}\right\} \tag{35}$$

The second term inside the brackets is negligibly small; $(\gamma_1 - \gamma_2)$ will be positive or negative, depending on which solvent is the better;

and the function will be linear in ϕ since $(\gamma_1 - \gamma_2)$ and its logarithmic coefficient will be sensibly constant over a small concentration range. It is possible that the segment length Z may vary somewhat from solvent to solvent, but such an effect would not change the qualitative picture. If several solvents are compared, a family of curves will be obtained (Fig. 9). Kurtz, Harvey and Lipkin have investigated the viscosity of phenolics and of natural resins in selected technical solvents, and have obtained curves of this type by plotting (Kinematic viscosity of solution 1/Kinematic viscosity of solution 2) against concentration (49).

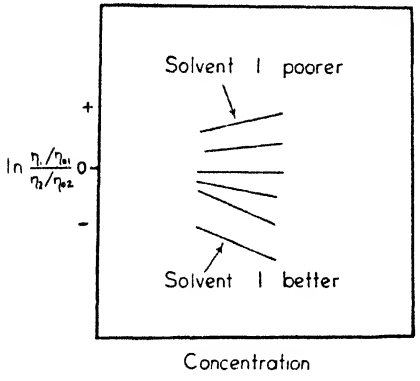

Fig. 9.—Effect of solvent on viscosity of polymer solutions.

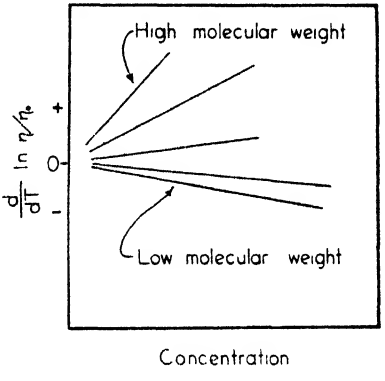

Fig. 10.—Effect of temperature on viscosity of polymer solutions.

4. *Dependence on Temperature*

Each of the limiting viscosities depends on the temperature in the manner $\eta = \text{const. exp}\,(\Delta H^{\ddagger}/RT)$, so they both must decrease with increasing temperature. For non-ideal solutions there is an additional effect. If the solvent is good, each polymer molecule is surrounded by more solvent molecules than would be expected for random mixing, *i. e.*, $\gamma < 1$. An increased temperature tends to bring about more randomness, *i. e.*, γ approaches unity. But increased ideality means in this case that more polymer molecules meet polymer molecules and contribute the pure-polymer type of viscosity. The viscosity may even increase with increasing temperature. Explicitly,

$$\frac{d}{dT} \ln \eta/\eta_0 = \phi \left\{ \frac{d\gamma}{dT} \frac{\ln (\eta_P/\eta_0)}{\ln (1 + kZ\phi)} - \gamma \frac{\Delta H_p^{\ddagger} - \Delta H_0^{\ddagger}}{RT^2} \right\} \qquad (36)$$

The second term gives the usual negative temperature coefficient of the limiting viscosities, where $\Delta H_p^{\ddagger}$ is about 10 kcal. and $\Delta H_0^{\ddagger}$ is about 2 kcal. If γ is less than unity, $a\gamma/dT$ is positive; the numerator of the coefficient of $d\gamma/dT$ increases rapidly with increasing chain length, so that for polymers of high molecular weight the positive term becomes decisive. The predicted temperature dependence is illustrated in Fig. 10. Experimental results of this type have been obtained for polystyrenes and for polyvinyl chlorides (84, 85). For spherical or highly branched molecules, where movement by segments is of no or of minor importance, the viscosity should always decrease with increasing temperature, as in the lower curves of Fig. 10.

5. *Dependence on Velocity Gradient*

Under the influence of a finite rate of shear, intermolecular bonds are constantly being broken and reforming. The small molecules are

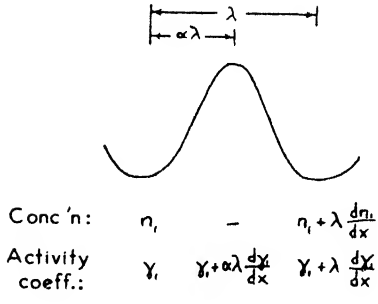

Fig. 11.—Model for diffusion.

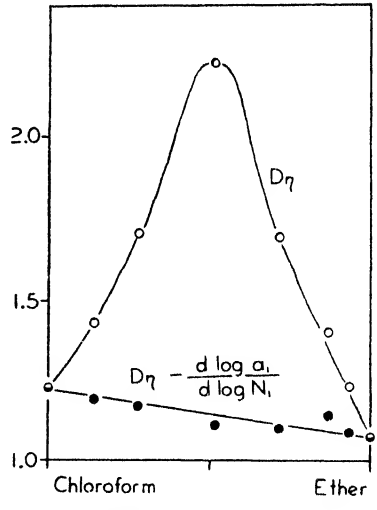

Fig. 12.—Effect of concentration on diffusion.

able to resume their normal equilibrium positions almost instantaneously, but when two polymer molecules are disentangled they may be carried apart by the solvent before the bonds can form again. A steady state is set up, in which the number of bonds being broken is equal to the number of bonds forming. At this steady state the num-

ber of polymer molecules surrounded by solvent molecules is somewhat greater than under static conditions, *i. e.*, the sign of $d\gamma/d\sigma$, σ being the rate of shear, is negative. Then

$$\frac{d}{d\sigma} \ln \eta/\eta_0 = \phi \left\{ \frac{d\gamma}{d\sigma} \frac{\ln (\eta_P/\eta_0)}{\ln (1 + kZ\phi)} + \gamma \frac{d}{d\sigma} \ln \frac{(\eta_p/\eta_0)}{(1 + kZ\phi)} \right\} \tag{37}$$

The second term, representing the dependence on shear of the limiting viscosities, is probably small. Then (1) the thixotropic effect will increase with increasing concentration, and (2) since the numerator of the coefficient of $d\gamma/d\sigma$ increases rapidly with chain length, the thixotropic effect will increase with increasing molecular weight. These predictions are in accord with the experimental results on polystyrenes (80).

VII. Diffusion of Simple Liquids

The expression for the diffusion of liquids can be derived from the same model that is used for viscous flow (Fig. 4) (88). The concentration and the activity coefficient of the solute at various positions of the diffusing molecule are given in Fig. 11. The general rate expression when activities are taken into account is

$$k' = \frac{kT}{h} e^{-\Delta \mathring{F}^{\ddagger}/RT} \frac{\gamma_n}{\gamma^{\ddagger}} \tag{38}$$

The forward and backward rates of transport are then

$$\text{rate}_f = n_1 \lambda \frac{kT}{h} e^{-\Delta \mathring{F}^{\ddagger}/RT} \frac{\gamma_1}{\gamma_1 \left[1 + \frac{\alpha\lambda}{\gamma_1} \frac{d\gamma_1}{dx} \right]} \tag{39}$$

$$\text{rate}_b = \left(n_1 + \lambda \frac{dn_1}{dx} \right) \lambda \frac{kT}{h} e^{-\Delta \mathring{F}^{\ddagger}/RT} \frac{\gamma_1 \left[1 + \frac{\lambda}{\gamma_1} \frac{d\gamma_1}{dx} \right]}{\gamma_1 \left[1 + \frac{\alpha\lambda}{\gamma_1} \frac{d\gamma_1}{dx} \right]} \tag{40}$$

and the net rate is, upon simplifying,

$$\text{rate}_{\text{net}} = -\frac{dn_1}{dx} \lambda^2 \frac{kT}{h} e^{-\Delta \mathring{F}^{\ddagger}/RT} \left[1 + \frac{d \ln \gamma_1}{d \ln n_1} \right] \tag{41}$$

The diffusion coefficient D is defined by the relation

$$\text{rate}_{\text{net}} = -D \frac{dn_1}{dx} \tag{42}$$

and upon combining equations (41) and (42),

$$D = \lambda^2 \frac{kT}{h} e^{-\Delta \mathring{F}^{\ddagger}/RT} \left[1 + \frac{d \ln \gamma_1}{d \ln n_1}\right] \tag{43}$$

If V_1, the molal volume of "solute," and V_2, the molal volume of "solvent," are not too different, equation (43) becomes

$$D = \lambda^2 \frac{kT}{h} e^{-\Delta \mathring{F}^{\ddagger}/RT} \left[\frac{d \ln a_1}{d \ln N_1}\right] \tag{44}$$

$$D\eta = \frac{\lambda_1 kT}{\lambda_2 \lambda_3} \left[\frac{d \ln a_1}{d \ln N_1}\right] \tag{45}$$

The close relation between the processes of viscous flow and diffusion is well confirmed by the correspondence of the heats of activation for the two processes. A check of the concentration dependence expressed by equation (45) is presented in Fig. 12, where $D\eta$ and $D\eta \div (d \ln a_1/d \ln N_1)$ are plotted for the system chloroform–ether. The term in brackets is seen to bring the experimental data into a straight line (51).

Absolute values of the diffusion coefficient predicted from equation (45) are consistently higher than the values observed by a factor of from 2 to 5. This can be explained if the flowing molecule so orients itself that λ_1 is its smallest dimension and $\lambda_2\lambda_3$ its largest area. Pure liquids in motion are indeed known to exhibit optical anisotropy (Maxwell effect). An expression for this effect may be derived easily (74). Suppose that if a molecule takes a particular orientation so that its area exposed to shear is $\lambda_2'\lambda_3'$ its index of refraction is n'; the average molecule, with area $\lambda_2^0\lambda_3^0$, has an index of refraction n^0. Then the two kinds of molecules will differ in energy, and the fraction of oriented molecules will be given by the Boltzmann factor

$$\begin{aligned} \frac{n'}{n^0} &= \exp[-f(\lambda_2'\lambda_3' - \lambda_2^0\lambda_3^0)x/kT] \\ &= 1 - f(\lambda_2'\lambda_3' - \lambda_2^0\lambda_3^0)x/kT \end{aligned} \tag{46}$$

which must be averaged over all x's from zero to the top of the potential barrier. The experimentally measured quantity, $\Delta n/n$, is given by

$$\frac{\Delta n}{n} = \frac{n^0 - n'}{n^0} = 1 - \frac{n'}{n^0} = f(\lambda_2'\lambda_3' - \lambda_2^0\lambda_3^0)/kT \times \left\{ \frac{\int_0^{\lambda/2} x\, e^{-E/RT}\, dx}{\int_0^{\lambda/2} e^{-E/RT}\, dx} \right\} \tag{47}$$

which may be compared with Maxwell's experimental formula

$$\frac{\Delta n}{n} = fM \tag{48}$$

where M is constant for a given substance. We may estimate the value of M for benzene at 300° K.: $\lambda_2'\lambda_3'$ is about 16×10^{-16} cm.^{2}; $\lambda_2^0\lambda_3^0$, 11×10^{-16} cm.^{2}; the quantity in brackets is found by numerical integration carried out for a 3 kcal. barrier to be about $(\chi/2)$ (0.145). The calculated Maxwell constant is 0.52×10^{-10}. For comparison, Table IV lists experimental values of the Maxwell constant for several liquids (8).

TABLE IV

MAXWELL CONSTANTS FOR VARIOUS LIQUIDS

Substance	$M \times 10^{10}$
o-Dichlorbenzene	1.85
p-Xylene	1.84
Mesitylene	1.31
m-Xylene	1.29
Chlorbenzene	1.22
o-Xylene	1.21
Toluene	1.04
Phenyl ethanol	0.67
Benzene	0.64
Heptanol-1	0.41
Carbon tetrachloride	0.06
Cyclohexane	0.03

VIII. Diffusion of Macromolecules

Much of the experimental work on the diffusion of large molecules has been carried out on globular macromolecules (*e. g.*, proteins) for which a hydrodynamic treatment may be expected to be valid (50, 62, 63, 68). Not many measurements have been made of the diffusion coefficient of linear macromolecules. Table V presents the diffusion data of Polson on the diffusion of cellulose derivatives (67). It is seen that there is a rough inverse proportionality between diffusion coefficient and molecular weight, but the diffusion coefficient changes less rapidly than the molecular weight. As would be expected, it is the product $D\eta$ which must be taken to compare methyl celluloses even approximately with cellulose acetates. The diffusion coefficient does not show any regular trend with concentra-

tion for the concentrations in this table, but may show deviations at lower concentrations.

TABLE V

DIFFUSION CONSTANTS FOR HIGH POLYMERS

	Concn., g./100 cc.	$D \times 10^7$, cm.²/sec.	$D\eta_{rel} \times 10^7$	Mol. wt.
Methyl cellulose	0.5	4.38	4.45	14,100
Methyl cellulose	0.5	3.00	3.05	24,300
Methyl cellulose	1.0	3.07	3.11	24,300
Methyl cellulose	0.5	2.43	2.47	38,100
Methyl cellulose	1.0	2.26	2.31	38,100
Cellulose acetate	0.61	10.85	3.46	20,000
Cellulose acetate	1.15	10.9	3.48	20,000
Cellulose acetate	0.5	4.48	1.43	53,000
Cellulose acetate	1.46	4.30	1.37	53,000
Cellulose acetate	0.516	3.29	1.05	90,000

IX. Sedimentation Velocity

When the jumping molecule of Fig. 4 is in a centrifugal field, it is helped in its forward motion by the force $m\omega^2 x$ acting through a distance $\alpha\lambda$, and hindered in its backward motion by the same force acting through a distance $(1 - \alpha)\lambda$. Here x is the distance from the axis of rotation, ω is the angular velocity and m has been written for the difference in mass between a molecule and the same volume of solvent. The forward and backward rates of transport are

$$\text{rate}_f = n_1\lambda \frac{kT}{h} e^{-\Delta F^\ddagger/RT}\left(e^{m\omega^2 x\alpha\lambda/kT}\right)\frac{\gamma_1}{\gamma_1\left[1 + \frac{\alpha\lambda}{\gamma_1}\frac{d\gamma_1}{dx}\right]} \tag{49}$$

$$\text{rate}_b = \left(n_1 + \lambda\frac{dn_1}{dx}\right)\lambda\frac{kT}{h}e^{-\Delta F^\ddagger/RT}\left(e^{-m\omega^2 x(1-\alpha)\lambda/kT}\right)\frac{\gamma_1\left[1 + \frac{\lambda}{\gamma_1}\frac{d\gamma_1}{dx}\right]}{\gamma_1\left[1 + \frac{\alpha\lambda}{\gamma_1}\frac{d\gamma_1}{dx}\right]} \tag{50}$$

and the net rate is, upon simplifying,

$$\text{rate}_{net} = \frac{n_1\lambda^2 m\omega^2 x}{h} e^{-\Delta F^\ddagger/RT} - \frac{dn_1}{dx}\lambda^2\frac{kT}{h}e^{-\Delta F^\ddagger/RT}\left[1 + \frac{d\ln\gamma_1}{d\ln n_1}\right] \tag{51}$$

But the second term of equation (51) is simply the diffusion equation, equation (43). Further, the first term of equation (51) is equivalent to

the usual Svedberg sedimentation equation, as may be seen by writing it in the form

$$s \equiv \frac{dx/dt}{n_1\omega^2 x} = \frac{m\lambda^2}{h} e^{-\Delta F^{\ddagger}/RT} \tag{52a}$$

$$= \frac{m\lambda_1}{\eta h \lambda_2 \lambda_3} \tag{52b}$$

$$= \frac{mD}{kT} \Big/ \left[\frac{d \ln a_1}{d \ln N_1}\right] \tag{52c}$$

where s is the "sedimentation constant" for a molecule (89). It is

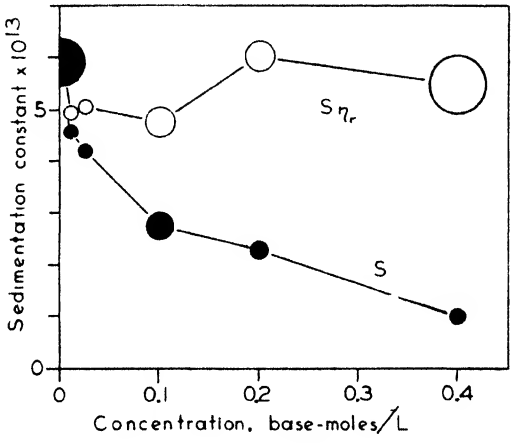

Fig. 13.—Sedimentation constant of polystyrene in chloroform.

seen from equation (52) that the sedimentation constant varies with the reciprocal of the viscosity, and it is in fact customary to correct observed values of the sedimentation constant by multiplying by the viscosity (89). Figure 13 presents the results of a typical experiment on the sedimentation velocity of polystyrene in chloroform (76). The sedimentation constant (filled circles) and the sedimentation constant multiplied by the viscosity (open circles) are plotted against concentration; the radius of a circle represents its estimated probable error. It is seen that correcting for the viscosity does improve the constancy of the data. It is worth pointing out that the sedimentation constant should not show exactly the same concentration dependence as the diffusion coefficient.

In making ultracentrifugal calculations, it is usually assumed that s (or D, or η) is constant for a given experiment. However, the solution in the ultracentrifuge is under a hydrostatic pressure which varies within the cell from zero to several hundred or, in extreme cases, even several thousand atmospheres. Under such a pressure the viscosity of water is greater by some 50%, and of organic solvents by several-fold (6). Thus the value of s differs from point to point

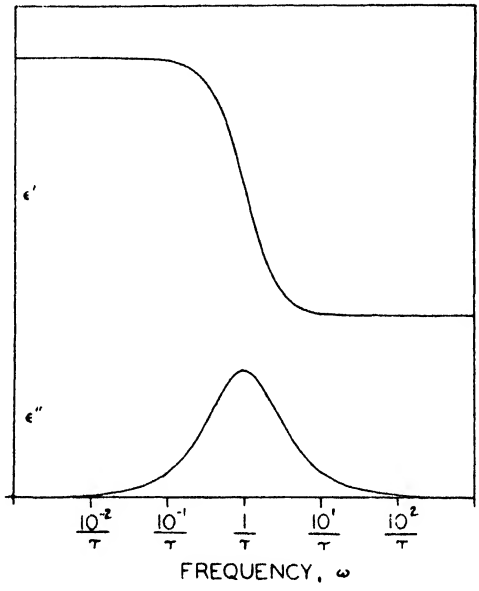

Fig. 14.—Anomalous dispersion of the dielectric constant.

within the cell. Such an effect can be detected by measuring the sedimentation velocity at different speeds of the rotor; if s decreases with increasing speed, the variation of viscosity with speed (see equation 20) should certainly be taken into account before integrating the ultracentrifugal equation (90).

In sedimentation measurements on methyl cellulose, cellulose acetate and polychloroprene, the sedimentation constant shows only small changes for large changes in the molecular weight (47, 77). This result suggests that the polymer molecules are acting in segments, and that each segment sediments more or less independently.

X. Dielectric Relaxation

When the dielectric constant of a polar substance is measured over a range of frequencies, at sufficiently high frequencies the dielectric constant will show an abrupt decrease (Fig. 14, top curve). To explain this "anomalous dispersion" Debye postulated that dipoles are oriented by the applied field, and that at high frequencies the dipoles can no longer follow the field because of the viscous drag of the medium (12). The familiar equation derived by Debye is

$$\alpha = \alpha_\infty + \frac{\mu^2}{3kT} \frac{1}{1+ i\omega\tau} \tag{53}$$

where α is the polarizability, α_∞ is the "optical" polarizability, μ is the permanent dipole moment of a molecule, i is $\sqrt{-1}$, ω is the frequency in radians sec.$^{-1}$ and τ is the "relaxation time" of a molecule. The relaxation time is the mean time required for a molecule to revert to random distribution after the orienting field is removed. Debye assumed Stokes' law for the frictional drag on a sphere rotating in a viscous liquid, and obtained for the relaxation time

$$\frac{1}{\tau} = \frac{kT}{4\pi r^3 \eta} \tag{54}$$

where r is the radius of the sphere and η is the viscosity of the medium.

Among the number of other models that have been proposed to explain anomalous dispersion are:

(*a*) Displacement of a charged particle against elastic and frictional forces (13, 61).

(*b*) Ionic polarization in a two-layer dielectric (94).

(*c*) High-resistance blocking layer at electrode/dielectric boundary (39).

(*d*) Suspension of dielectric spheres in a dielectric medium (31, 93).

(*e*) Conducting spheres in an insulating medium (93).

(*f*) Conducting shells in an insulating medium (56).

Each of the equations for the dielectric constant derived from the foregoing models contains the factor $1/(1 + i\omega\tau)$. It is striking that such a variety of mechanisms lead to the same dependence on frequency. This Debye type of frequency dependence can in fact be derived from a very general model, as follows (48).

Assume that a molecule can be in either of two states. Then the rate of change from the first to the second state will be given by

$$-\frac{dN_1}{dt} = N_1k_1 - N_2k_2 \tag{55}$$

where there are N_1 molecules in the first state, N_2 in the second, and k_1 and k_2 are the specific rates for the forward and reverse reactions.

Let the number of molecules in the two states, and also the two rates, be perturbed by an applied force, X. Assume that the new numbers and rates may be expressed by the first two terms of a series (this assumption is easily valid for the cases in which we are interested):

$$\begin{aligned} N_1 &= N_1^0 + X\frac{dN_1}{dX} & k_1 &= k_1^0 + X\frac{dk_1}{dX} \\ N_2 &= N_2^0 - X\frac{dN_1}{dX} & k_2 &= k_2^0 + X\frac{dk_2}{dX} \end{aligned} \tag{56}$$

Since the system in the absence of an applied force is at equilibrium,

$$\frac{N_2^0}{N_1^0} = \frac{k_1^0}{k_2^0} = e^{\Delta F/RT} \tag{57}$$

where ΔF is the difference in free energy between the two states. From equation (57),

$$\begin{aligned} \frac{dk_1}{dX} &= k_2^0 e^{\Delta F/RT}\left(\frac{d}{dX}\frac{\Delta F}{RT}\right) + e^{\Delta F/RT}\frac{dk_2}{dX} \\ &= k_2^0\frac{N_2^0}{N_1^0}\left(\frac{d}{dX}\frac{\Delta F}{RT}\right) + \frac{N_2^0}{N_1^0}\frac{dk_2}{dX} \end{aligned} \tag{58}$$

Upon substituting equations (56) and (58) into (55), the rate equation becomes

$$\begin{aligned} -\frac{dN_1}{dt} = &\left[N_1^0 + X\frac{dN_1}{dX}\right]\left[k_1^0 + Xk_2^0\frac{N_2^0}{N_1^0}\left(\frac{d}{dX}\frac{\Delta F}{RT}\right) + X\frac{N_2^0}{N_1^0}\frac{dk_2}{dX}\right] - \\ &\left[N_2^0 - X\frac{dN_1}{dX}\right]\left[k_2^0 + X\frac{dk_2}{dX}\right] \\ = &X\left[k_1^0\frac{dN_1}{dX} + k_2^0\frac{dN_1}{dX} + k_2^0N_2^0\left(\frac{d}{dX}\frac{\Delta F}{RT}\right)\right] \end{aligned} \tag{59}$$

If the applied force is periodic, $X = X_0 e^{i\omega t}$, equation (59) becomes a familiar type of differential equation

$$\frac{d}{dt}\left(X\frac{dN_1}{dX}\right) + (k_1^0 + k_2^0)\left(X\frac{dN_1}{dX}\right) = -k_2^0 N_2^0\left(\frac{d}{dX}\frac{\Delta F}{RT}\right)X_0 e^{i\omega t} \quad (60)$$

the solution of which is at once

$$-X\frac{dN_1}{dX} = \frac{k_2^0 N_2^0\left(\frac{d}{dX}\frac{\Delta F}{RT}\right)X_0 e^{i\omega t}}{i\omega + (k_1^0 + k_2^0)} \quad (61)$$

Equation (61) may be rewritten in the equivalent form

$$-\frac{dN_1}{dX} = \frac{N\left(\frac{d}{dX}\frac{\Delta F}{RT}\right)}{2[1 + \cosh(\Delta F/RT)]}\frac{1}{1 + i\omega/(k_1^0 + k_2^0)} \quad (62)$$

The Debye frequency dependence will thus be shown by any property which measures how much a system changes from one state to another when a periodic force is applied, *e. g.*,

$$A = A_1 + \frac{A_2}{1 + i\omega\tau} \quad (63)$$

where A is the property, A_2 is the frequency-dependent contribution and A_1 is the frequency-independent contribution. The constants are usually evaluated in terms of the limiting values. At infinite frequency $A_\infty = A_1$ and at zero frequency $A_0 = A_1 + A_2$. Then,

$$A = A_\infty + \frac{(A_0 - A_\infty)}{1 + i\omega\tau} \quad (64)$$

The polarizability, which measures the amount of dipole moment induced per unit volume, is such a property. Hence,

$$\alpha = \alpha_\infty + \frac{(\alpha_0 - \alpha_\infty)}{1 + i\omega\tau} \quad (65)$$

The dielectric constant, and not the polarizability, is the quantity experimentally measured. If the Clausius-Mosotti relation between polarizability and dielectric constant is valid, $4\pi\alpha/3 = (\epsilon - 1)/(\epsilon + 2)$, and equation (65) becomes

$$\epsilon = \epsilon_\infty + \frac{(\epsilon_0 - \epsilon_\infty)}{1 + i\omega\tau\left(\frac{\epsilon_0 + 2}{\epsilon_\infty + 2}\right)} \quad (66)$$

The quantity $\tau(\epsilon_0 + 2)/(\epsilon_\infty + 2)$ is sometimes called the relaxation time of the dielectric, τ^*. For many substances τ^* is only slightly greater than τ; but for water, $\tau^* = 23\tau$. Several authors have investigated the validity of the Clausius-Mosotti relation in polar liquids, and have concluded that ϵ should be more nearly linear with α (10, 38, 66, 72, 73, 92, 99). If ϵ were linear with α, the factor $(\epsilon_0 + 2)/(\epsilon_\infty + 2)$ would be replaced by unity.

Upon rationalizing equation (64), the dielectric constant breaks into a real and an imaginary part,

$$\epsilon = \epsilon_\infty + \frac{(\epsilon_0 - \epsilon_\infty)}{1 + \omega^2\tau^{*2}} - i\frac{(\epsilon_0 - \epsilon_\infty)\omega\tau^*}{1 + \omega^2\tau^{*2}} \tag{67}$$

which may also be written

$$\epsilon = \epsilon' - i\epsilon'' \tag{68}$$

The real part of the dielectric constant, ϵ', is shown in the upper curve of Fig. 14, and the imaginary part or loss factor, ϵ'', is shown in the lower curve. At the frequency $\omega = 1/\tau^*$ the loss factor reaches its maximum value, $\epsilon'' = (\epsilon_0 - \epsilon_\infty)/2$, and the dielectric constant is in the middle of its dispersion region, $\epsilon' = (\epsilon_0 + \epsilon_\infty)/2$. From either of these measurements the relaxation time may conveniently be evaluated.

The imaginary part of the dielectric constant is not measured directly, but is determined through the alternating-current conductivity (61). The conductivity is defined as

$$\gamma = \frac{1}{E}\frac{dq}{dt} \tag{69}$$

where E is the potential gradient and q is the charge per unit area. For a parallel plate condenser,

$$4\pi q = \epsilon E \tag{70}$$

The conductivity is then given by

$$\gamma = \frac{1}{E_0 e^{i\omega t}} \frac{\epsilon' - i\epsilon''}{4\pi} \frac{d}{dt} E_0 e^{i\omega t}$$

$$= \frac{i\omega}{4\pi}(\epsilon' - i\epsilon'') \tag{71}$$

$$= \frac{\epsilon''\omega}{4\pi} + i\frac{\epsilon'\omega}{4\pi}$$

It is seen that the real part of the conductivity gives the imaginary part of the dielectric constant.

If the dielectric dispersion is the result of more than a single rate process, the dielectric constant will be given by a sum of terms like equation (62), with different relaxation times, τ. When there is a distribution of relaxation times, the maximum loss factor will be lower than $^1/_2(\epsilon_0 - \epsilon_\infty)$ and the loss factor curve will be broader; also, the dispersion region of the dielectric constant will be wider than two logarithmic units of frequency. A plot of ϵ'' against ϵ', with temperature or frequency as a parameter, will give a circular arc less than the theoretical semicircle (9). Fuoss and Kirkwood have succeeded in reversing the summation and obtaining from the dielectric data the distribution of relaxation times (29, 100).

The second conclusion to be drawn from equation (58) is that the dielectric constant or other property will be small if the two states differ much in energy. The hyperbolic cosine in the denominator increases rapidly if ΔF is more than about 1 kcal. White has come to the same qualitative conclusion, from a somewhat different model (96). It is an experimental result that the dielectric constant of polar substances is less in the solid state than in the liquid.

Thirdly, equation (62) shows that the relaxation time τ is the reciprocal of a specific rate constant. Since the frequency dependence of the dielectric constant does not uniquely determine the mechanism, the merit of a theoretical treatment must lie in its ability to predict the values of τ and $(\epsilon_0 - \epsilon_\infty)$ and their dependence on temperature and structure. A large amount of experimental work on polar substances in the vapor state and in dilute solution has verified Debye's expression for $(\epsilon_0 - \epsilon_\infty)$ in terms of the rotating dipole model (78). However, the Debye-Stokes expression (54) for τ gives viscosity values smaller than the macroscopic viscosity by a factor of from ten to several thousand. The absolute reaction rate method offers a particularly straightforward approach to the study of the relaxation time (16, 23, 87). The free energy of activation for dielectric relaxation may be obtained from the equation

$$\frac{1}{\tau} = \frac{kT}{h} e^{-\Delta F^{\ddagger}/RT} \tag{72}$$

and the free energy of activation for viscous flow from the equation

$$\frac{1}{\eta} = \frac{V}{Nh} e^{-\Delta F^{\ddagger}/RT} \tag{73}$$

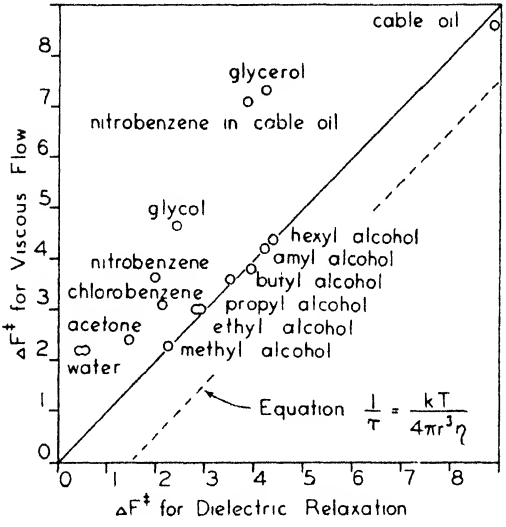

Fig. 15.—Relation of dielectric constant to viscosity.

G. Bäz, *Physik. Z.*, **40**, 394-404 (1939).
K. Schmale, *Ann. Physik*, **35**, 671–689 (1939).
E. Keutner, *Ibid.*, **27**, 29-48 (1936).
H. H. Race, *Phys. Rev.*, **37**, 430–446 (1931).
W. Mueller, *Ann. Physik*, **24**, 99-112 (1935).
S. O. Morgan, *Trans. Electrochem. Soc.*, **65**, 109–118 (1934).

The two free energies calculated from some liquids are plotted against one another in Fig. 15. For many of the liquids, the points are seen to fall on a straight line of slope unity. The correspondence of the free energies suggests a close relationship between the two processes,

in agreement with Debye's postulated mechanism. For purposes of comparison, Debye's equation (54) is indicated by the broken line in Fig. 15. It is apparent that the data do not verify Debye's equation. A sphere rotating in a continuous viscous fluid evidently gives a less satisfactory picture of the process than a single molecule breaking bonds to its neighbors. Dipole rotation is considerably easier than viscous flow for such associated liquids as water and glycerol, and also for solutions of polar substances in viscous hydrocarbon solvents. (For some such solutions, no dispersion has been detected: the experimental points would fall somewhere in the far left portion of the graph (65).) A probable reason is that extra work is required in viscous flow to move the associated liquid or long hydrocarbon from one equilibrium position to the next, work which is not needed for dipole rotation.

Data for solid dielectrics, *e. g.*, isobutyl bromide and isoamyl bromide glasses (2), are not included in Fig. 15 because the viscosity can only be estimated by a long and uncertain extrapolation.

The dielectric dispersion of a dilute solution of polymeric hydroxydecanoic acid has been investigated, and as would be expected if the molecule moved by segments, no dispersion was found in the frequency region corresponding to orientation of the whole molecule (7). It is not certain how large the orienting unit is. Kirkwood and Fuoss have assumed in their calculations that each dipole can orient, being restricted only by the directions of the bonds to its neighbors (29).

Additional information about dielectric dispersion may be obtained by breaking the free energy of activation into a heat and an entropy term. Equation (72) may be written

$$\frac{1}{\tau} = \frac{kT}{h} e^{\Delta S^{\ddagger}/R} e^{-\Delta H^{\ddagger}/RT} \tag{74}$$

From the temperature coefficient of $1/\tau$, $\Delta H^{\ddagger}$ is evaluated, and $\Delta S^{\ddagger}$ is obtained by subtraction. Table VI lists the values so calculated for a number of liquid and solid dielectrics.

It will be observed that the heats of activation, $\Delta H^{\ddagger}$, are considerably higher than the heats of activation for viscous flow, which are usually 2–3 kcal. and rarely exceed 10 kcal. In terms of the physical model, a molecule undergoing dipole rotation must break more bonds to its neighbors than a flowing molecule. For the alcohols in Ta-

TABLE VI

DIELECTRIC DISPERSION FOR VARIOUS SUBSTANCES

	t, ° C.	$\Delta F^{\ddagger}$	$\Delta H^{\ddagger}$	$\Delta H^{\ddagger}$ visc.	ΔE, vap.	$\Delta S^{\ddagger}$	No. of rotating molecules
Liquids							
Ethyl alcohol (41)	25	2.90	5.7	3.44	8.93	9.40	
Propyl alcohol	25	3.57	6.1	4 53	9.1	8.50	
Butyl alcohol	25	3.90	6.4	4.61	9.7	8.40	<1
Amyl alcohol	25	4.18	6.6	6	10.1	8.11	
Hexyl alcohol	25	4.09	6.8	6	10.5	8.19	
Nitrobenzene in cable oil (59)	20	3.82	5.8			6.77	
Cable oil (71)	25	8.84	16.4			25.3	
Castor oil (43)	1	9.95	16.7			24.6	1
Wood rosin	101	15.5	23.8			22.2	
Solids							
Cetyl alcohol in paraffin (23)	14	4.45	12.6			28.4	1
dl-Camphor (101)	−132	4.85	10.2			38.0	
dl-Bornyl bromide	−100	5.75	10.3			26.3	
3,*x*-Dichlorocamphor (98)	− 61	7.00	20.4			63.2	2–5
Cyclopentanol	− 67	6.08	9.73			17.7	
Isobutyl bromide (2)	−157	3.79[6]	23.1			167.1	
Isoamyl bromide	−145	4.42[5]	18.0			106.1	~10
"Halowax," chlorinated naphthalene (57)	− 51.5	7.77	31.0			104.8	5
Glycol phthalate (42)	30	11.21	53.5			139.0	5
Polyvinyl chloride (28)	99	16.9	43.0			70.3	5–10
Rubber, 10% S (58)	30	9.69	27.0			57.0	?
"Permitol," tetrachlorodiphenyl (23)	8.5	11.85	56.5			158.6	
	12.5	11.22	56.7			159.1	
	16.7	10.57	53.2			147.0	
	19.9	10.00	40.8			104.8	~5
	25.3	9.50	42.0			108.9	
	29.8	9.05	37.5			122.0	
	34.5	8.67	34.6			84.4	
Glycerol (57)	− 65	9.10	38.2			140	5
	− 60	8.60	32.7			113	
	− 50	7.66	24.7			76.3	
	− 40	6.97	21.0			60.3	
	− 20	5.68	17.6			47.2	
	0	4.75	14.3			35.0	2
	20	4.22	11.1			23.5	....~1

TABLE VI (*Continued*)

	t, ° C	$\Delta F^{\ddagger}$	$\Delta H^{\ddagger}$	$\Delta H^{\ddagger}$ visc.	ΔE, vap.	$\Delta S^{\ddagger}$	No. of rotating molecules
Ice (60)	− 45.9	9.34	14.52			22.8	
	− 32.6	9.01	14.52			22.9	
	− 20.6	8.85	14.52			22.5	
	− 11.9	8.62	14.52			22.6	
	− 8.5	8.47	14.52			22.9	7
	− 7.5	8.49	14.52			22.7	
	− 3.9	8.40	14.52			22.7	
	− 2.8	8.39	14.52			22.7	
	− 0.9	8.39	14.52			22.5	

ble VI, dipole rotation requires about $^2/_3$ the heat of vaporization, where viscous flow requires only $^1/_3$ to $^1/_2$ the heat of vaporization.

An interesting feature of Table VI is the large positive entropy of activation shown by every substance, some entropies being as high as 150 E. U. A molecule in the activated state is rotating and has many more positions available to it than a molecule at rest, and this increase in rotational entropy shows itself in a positive value for $\Delta S^{\ddagger}$. When the entropy change is very large, it must represent the contributions of several rotating molecules. Probably when a single molecule is rotating, some of its neighbors are also permitted to rotate. The rotational entropy of a single molecule can be estimated from the entropy of fusion or from the molecular dimensions; then the approximate number of rotating molecules to give the observed $\Delta S^{\ddagger}$ can be calculated. The last column of Table VI lists the number of rotating molecules so computed. For the liquids, only about one molecule must rotate. For the alcohols, possibly less than one molecule, *e. g.*, the CH_2OH group, needs to rotate. For the solids, the number of rotating molecules can become about 5.

If the polar molecules were already rotating freely in the normal state, there should be little or no entropy increase in going to the activated state. Such behavior is, in fact, shown by the hexa-substituted benzenes investigated by White, Biggs and Morgan (97) (Table VII).

The entropy of activation is approximately zero down to the lowest temperatures employed. The conclusion that the molecules are rotating freely at the lowest temperatures is in agreement with the

TABLE VII

DIELECTRIC DISPERSION FOR HEXA-SUBSTITUTED BENZENES

	Frequency, kc	t, ° C.	$\Delta F^{\ddagger}$	$\Delta H^{\ddagger}$	$\Delta S^{\ddagger}$
Chloropentamethyl benzene	1	−89	8.88	8.53	−1.96
	3	−80	8.90		−1.92
	10	−68	9.00		−2.30
	30	−59	8.96		−2.01
	100	−42	9.13		−2.60
1,2-Dichloro tetramethyl benzene	1	−108	7.85	7.98	0.79
	3	−100	7.85		0.75
	10	−90	7.89		0.49
	30	−81	7.88		0.52
	100	−69	7.91		0.34
1,2,4-Trichloro trimethyl benzene	1	−85	9.09	9.01	−0.43
	3	−77	9.07		−0.31
	10	−64	9.19		−0.86
	30	−55	9.13		−0.55
	100	−40	9.22		−0.90
1,2,3-Trichloro trimethyl benzene	1	−90	8.76	8.80	0.22
	10	−70	8.83		−0.15
	100	−47	8.84		−0.18
1,2,3,4-Tetrachloro dimethyl benzene	1	−70	9.79	9.50	−1.43
	10	−46	9.95		−1.98
	100	−21	9.94		−1.74
1,2,3,5-Tetrachloro dimethyl benzene	1	−78	9.51	9.27	−1.23
	10	−56	9.61		−1.57
	100	−31	9.66		−1.61
Pentachloro methyl benzene	1	−42	11.34	11.27	−0.30
	3	−32	11.31		−0.25
	10	−18	11.39		−0.47
	30	− 6	11.38		−0.41
	100	11	11.48		−0.74

TABLE VIII

DIELECTRIC DISPERSION OF PLASTICIZED POLYVINYL CHLORIDE

Per cent tricresyl-phosphate	t, ° C. (f = 60 cycles)	$\Delta F^{\ddagger}$	$\Delta H^{\ddagger}$	$\Delta S^{\ddagger}$
0	98	16.7	40.7	64.7
10	80	15.9	29.2	37.7
20	65	15.2	22.7	22.2
30	48	14.4	17.6	10.0
40	32	13.6	14.2	1.97
50	16	12.88	12.6	− 0.97
60	3	12.88	12.1	− 0.65

results of White, Biggs and Morgan, who were able to detect no rotational transition for these substances.

The magnitude of the entropy of activation for dielectric relaxation would appear to be a sensitive criterion for rotation in the solid state. Table VI contains two examples: glycerol and Permitol. As the temperature is increased, $\Delta S^{\ddagger}$ decreases markedly, indicating that the molecules are rotating more and more freely in the normal state. A final example is provided by the system polyvinyl chloride plasticized with tricresylphosphate (Table VIII and Fig. 16) (11). The value of $\Delta S^{\ddagger}$ is 65 E. U. for pure polyvinyl chloride. It drops rapidly as tricresylphosphate is added, and at about 40% plasticizer, $\Delta S^{\ddagger}$ is approximately zero, or the dipoles are rotating almost freely. Further additions of tricresylphosphate produce little effect.

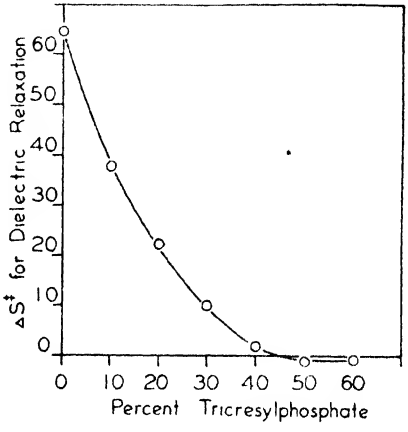

Fig. 16.—Dielectric relaxation for plasticized polyvinyl chloride.

Bibliography

1. F. Baker, *J. Chem. Soc.*, **103**, 1653 (1913).
2. W. O. Baker and C. P. Smyth, *Ann. N. Y. Acad. Sci.*, **40**, 447 (1940).
3. R. M. Barrer, *Trans. Faraday Soc.*, **35**, 628 (1939).
4. A. J. Batschinski, *Z. physik. Chem.*, **84**, 643 (1913).
5. E. C. Bingham, H. E. Adams and G. R. McCauslin, *J. Am. Chem. Soc.*, **63**, 466 (1941).
6. P. W. Bridgman, *The Physics of High Pressure*, New York, 1931.
7. W. B. Bridgman, *J. Am. Chem. Soc.*, **60**, 530 (1938).
8. W. Buchheim, H. A. Stuart and H. Menz, *Z. Physik*, **112**, 407 (1939).
9. K. S. Cole and R. H. Cole, *J. Chem. Phys.*, **9**, 341 (1941).
10. R. H. Cole, *Ibid.*, **6**, 385 (1938).
11. J. M. Davies, R. F. Miller and W. F. Busse, *J. Am. Chem. Soc.*, **63**, 361 (1941).

12. P. Debye, *Polar Molecules*, New York, 1929.
13. P. Drude, *Ann. Physik*, **64**, 131 (1898).
14. A. Einstein, *Ibid.*, (4) **19**, 289 (1906); **34**, 591 (1911).
15. R. H. Ewell and H. Eyring, *J. Chem. Phys.*, **5**, 726 (1937).
16. H. Eyring, *Ibid.*, **4**, 283 (1936).
17. H. Fikentscher, *Cellulosechem.*, **13**, 58 (1932).
18. H. Fikentscher and H. Mark, *Kolloid-Z.*, **49**, 135 (1930).
19. P. J. Flory, *J. Am. Chem. Soc.*, **62**, 3036 (1940).
20. P. J. Flory and P. B. Stickney, *Ibid.*, **62**, 3032 (1940).
21. R. Fordyce and H. Hibbert, *Ibid.*, **61**, 1912 (1939).
22. R. H. Fowler and E. A. Guggenheim, *Statistical Thermodynamics*, Cambridge, 1939.
23. F. C. Frank, *Trans. Faraday Soc.*, **32**, 1634 (1936).
24. H. Freundlich, *Kapillarchemie*, Leipzig, 1932, Vol. 2, p. 650.
25. R. Fricke and J. Lüke, *Z. Elektrochem.*, **36**, 318 (1930).
26. D. Frisch, H. Eyring and J. F. Kincaid, *J. Applied Phys.* **11**, 75 (1940).
27. C. S. Fuller, W. O. Baker and N. R. Pape, *J. Am. Chem. Soc.*, **62**, 3275 (1940).
28. R. M. Fuoss, *Ibid.*, **63**, 369 (1941).
29. R. M. Fuoss and J. G. Kirkwood, *Ibid.*, **63**, 385 (1941); Idem, *J. Chem. Phys.*, **9**, 329 (1941).
30. G. Gee, *Trans. Faraday Soc.*, **36**, 1171 (1940).
31. A. Gemant, *Die Elektrophysik der Isolierstoffe*, Berlin, 1930.
32. S. Glasstone, K. J. Laidler and H. Eyring, *The Theory of Rate Processes*, McGraw-Hill, New York, 1941.
33. E. Guth and R. Simha, *Kolloid-Z.*, **74**, 266 (1936).
34. W. Haller, *Ibid.*, **56**, 257 (1931).
35. K. Hess and W. Philippoff, *Ber.*, **68B**, 688 (1935); **70B**, 639 (1937).
36. E. Hückel, *Z. Elektrochem.*, **42**, 753 (1936).
37. M. L. Huggins, *J. Phys. Chem.*, **42**, 911 (1938); **43**, 439 (1939); *J. Applied Phys.*, **10**, 700 (1939).
38. G. Jaffe, *J. Chem. Phys.*, **6**, 385 (1938).
39. A. Joffe, *The Physics of Crystals*, New York, 1928.
40. W. Kauzmann and H. Eyring, *J. Am. Chem. Soc.*, **62**, 3113 (1940).
41. E. Keutner, *Ann. Physik*, **27**, 29 (1936).
42. R. H. Kienle and H. H. Race, *Trans. Electrochem. Soc.*, **65**, 87 (1934).
43. D. W. Kitchin and H. Mueller, *Phys. Rev.*, **32**, 979 (1928).
44. K. H. Klaasens and R. Houwink, *Kolloid-Z.*, **76**, 217 (1936).
45. E. O. Kraemer and F. J. Van Natta, *J. Phys. Chem.*, **36**, 3175 (1932).
46. E. O. Kraemer, *Ind. Eng. Chem.*, **30**, 1200–1203 (1938).
47. E. O. Kraemer and J. B. Nichols, *The Ultracentrifuge*. See Ref. 89.
48. R. de L. Kronig, *Physik. Z.*, **39**, 823–830 (1938).
49. S. S. Kurtz, W. T. Harvey and M. R. Lipkin, *Ind. Eng. Chem., Anal. Ed.*, **11**, 476 (1939).
50. O. Lamm and A. Polson, *Biochem. J.*, **30**, 538 (1936).

51. H. Lemonde, *Ann. Phys.*, **9**, 539 (1938).
52. J. E. Lennard-Jones and A. F. Devonshire, *Proc. Roy. Soc. London*, **A169**, 317 (1939).
53. C. L. Mantell and A. Skett, *Ind. Eng. Chem.*, **30**, 417 (1938).
54. E. W. J. Mardles, *J. Chem. Soc.*, **123**, 1951 (1923).
55. K. H. Meyer and R. Lühdemann, *Helv. Chim. Acta*, **18**, 1307 (1935).
56. J. B. Miles and H. P. Robertson, *Phys. Rev.*, **40**, 583 (1932).
57. S. O. Morgan, *Trans. Electrochem. Soc.*, **65**, 109 (1934).
58. F. H. Mueller, *Kolloid-Z.*, **77**, 260 (1936).
59. W. Mueller, *Ann. Physik*, **24**, 99 (1935).
60. E. J. Murphy, *Trans. Electrochem. Soc.*, **65**, 133 (1934).
61. E. J. Murphy and S. O. Morgan, *Bell System Tech. J.*, **18**, 502 (1939); **17**, 640 (1938).
62. H. Neurath, *Cold Spring Harbor Symposia Quant. Biol.*, **8**, 80 (1940).
63. H. Neurath, G. R. Cooper and J. O. Erickson, *J. Biol. Chem.*, **138**, 411 (1941).
64. Sven Odén, *Z. physik. Chem.*, **80**, 709 (1912).
65. J. L. Oncley and J. W. Williams, *Phys. Rev.*, **43**, 341 (1933).
66. L. Onsager, *J. Am. Chem. Soc.*, **58**, 1486 (1936).
67. A. Polson, *Kolloid-Z.*, **83**, 172 (1938).
68. Idem, *Ibid.*, **87**, 149 (1939).
69. R. E. Powell, C. R. Clark and H. Eyring, *J. Chem. Phys.*, **9**, 268 (1941).
70. Idem, *Ann. N. Y. Acad. Sci.* (1941).
71. H. H. Race, *Phys. Rev.*, **37**, 430 (1931).
72. W. H. Rodebush and C. R. Eddy, *J. Chem. Phys.*, **8**, 424 (1940).
73. W. H. Rodebush, C. R. Eddy and L. D. Eubank, *Ibid.*, **8**, 889 (1940).
74. W. E. Roseveare, R. E. Powell and H. Eyring, *J. Applied Phys.*, **12**, (1941); *Ind. Eng. Chem.*, **33**, 430 (1941).
75. G. V. Schultz, *Naturwissenschaften*, **25**, 346 (1937).
76. R. Signer and R. Gross, *Helv. Chim. Acta.*, **17**, 59 (1934).
77. R. Signer, *The Ultracentrifuge.* See Ref. 89.
78. Investigations of C. P. Smyth and co-workers.
79. A. J. Stamm and W. K. Loughborough, *J. Phys. Chem.*, **39**, 121 (1935).
80. H. Staudinger, *Die hochmolekularen organischen Verbindungen*, Berlin, 1932.
81. Idem, *Ibid.*, p. 179.
82. Idem, *Ibid.*, pp. 189–208.
83. H. Staudinger and G. Daumiller, *Ann.*, **529**, 219 (1937).
84. H. Staudinger and W. Heuer, *Z. physik. Chem.*, **A171**, 129 (1934).
85. H. Staudinger and J. Schneiders, *Ann.*, **541**, 151 (1939).
86. H. Staudinger and H. Warth, *J. prakt. Chem.*, **155**, 261 (1940).
87. A. E. Stearn and H. Eyring, *J. Chem. Phys.* **5**, 113 (1937).
88. A. E. Stearn, E. M. Irish and H. Eyring, *J. Phys. Chem.*, **44**, 981 (1940).
89. T. Svedberg and K. O. Pedersen, *The Ultracentrifuge*, Oxford, 1940.
90. Idem, *Ibid.*, p. 37.
91. A. R. Urquhart and A. M. Williams, *J. Textile Inst.*, **15**, 559 (1924); **20**, T125 (1929).

92. J. H. Van Vleck, *J. Chem. Phys.*, **5**, 556 (1937).
93. K. W. Wagner, *Arch. Elektrotech.*, **2**, 371 (1914).
94. K. W. Wagner, in Schering, *Die Isolierstoffe der Elektrotechnik*, Berlin, 1934.
95. J. Walter and H. Eyring, *J. Chem. Phys.*, **9**, 393 (1941).
96. A. H. White, *Ibid.*, **7**, 58 (1939).
97. A. H. White, B. S. Biggs and S. O. Morgan, *J. Am. Chem. Soc.*, **62**, 16 (1940).
98. A. H. White and W. S. Bishop, *Ibid.*, **62**, 8 (1940).
99. J. Wyman, *Ibid.*, **58**, 1482 (1936).
100. W. A. Yager, *Physics*, **7**, 434 (1936).
101. W. A. Yager and S. O. Morgan, *J. Am. Chem. Soc.*, **57**, 2071 (1935).

THE CONSTITUTION OF INORGANIC GELS

HARRY B. WEISER AND W. O. MILLIGAN

The Rice Institute, Houston, Texas

CONTENTS

For almost a quarter of a century investigations have been carried out in the chemical laboratories of The Rice Institute on the constitution of colloidal systems of inorganic compounds. At irregular intervals surveys have been made of the results of this work. The most recent of these reports dealing with the hydrous oxides was presented before the General Meeting of the American Chemical Society at Dallas in April, 1938, and published in the August, 1939, number of *Chemical Reviews* (23).

The constitution of gel systems was deduced from experimental evidence obtained by the application of the techniques of isothermal and isobaric dehydration and of x-ray and electron diffraction. The constitution of hydrosol systems was formulated from the results of the potentiometric "titration" of sols with electrolytes and from the direct examination of the sols by x-ray diffraction methods.

The phase rule and diffraction studies on hydrous oxide gels disclosed that, in general, they are not polymerized bodies or condensation products resulting from the splitting off of water from hypothetical metallic hydroxides. Instead, the gels are believed to consist of agglomerates of extremely minute crystals of oxide or simple oxide hydrate (or hydroxide), which hold large amounts of water by adsorption and capillary forces. Similarly, the direct examination of sols by x-rays discloses that the particles in typical oxide sols consist essentially of aggregates of minute crystals of hydrous oxide or of simple hydrate (or hydroxide). In typical positive sols containing anions such as chloride, the latter is not bound in the form of basic salts or Werner complexes in most cases, but is adsorbed in an amount which depends on the size and physical character of the primary particles.

In the following pages are summarized the results, both published and unpublished, of investigations, since 1938, concerning the constitution of oxide and salt gels using the well-established phase rule and diffraction techniques.

I. Gels of the Hydrous Oxides

1. Alumina

Alumina gel thrown down from an aluminum salt solution with alkali or ammonia consists of minute crystals of γ-$Al_2O_3 \cdot H_2O$ or γ-AlOOH. Under favorable conditions (cold precipitation and excess alkali) this more soluble and less stable modification of the hydrated oxide is transformed slowly, first into metastable α-$Al_2O_3 \cdot 3H_2O$ or α-$Al(OH)_3$ and finally into the less soluble and more stable γ-$Al_2O_3 \cdot 3H_2O$ or γ-$Al(OH)_3$ corresponding to the mineral gibbsite. Accordingly, freshly prepared alumina gels consist essentially of γ-AlOOH; on aging, especially in contact with alkali, the product is a mixture of γ-AlOOH with more or less α-$Al(OH)_3$, or under extreme aging γ-$Al(OH)_3$. The various transformations of precipitated alumina may be summarized as follows (19, 23):

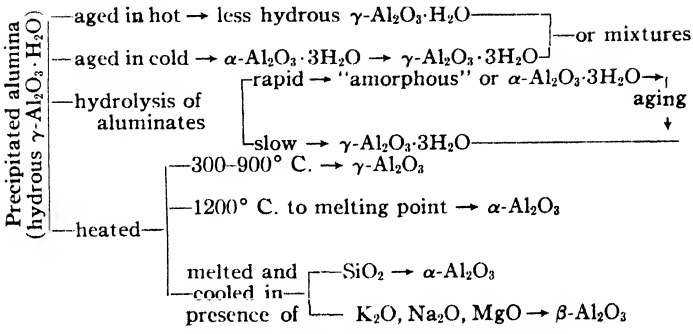

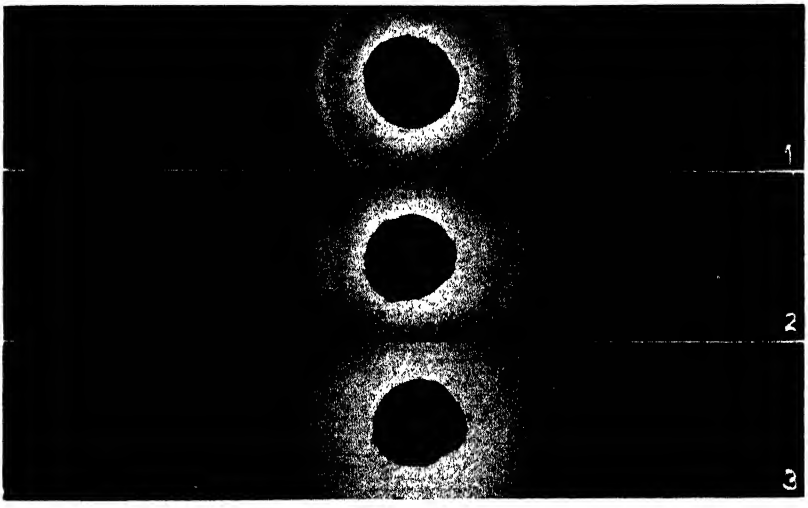

Fig. 1.—X-ray diffraction patterns for γ-AlOOH from: (1) nitrate, (2) chloride, (3) sulfate.

The size of the primary crystals of γ-AlOOH thrown down from aluminum salt solutions varies widely with the nature of the anion of the salt. This is illustrated by the photographs (Fig. 1) of the x-ray diffraction patterns of γ-AlOOH precipitated by ammonia from $N/10$ solutions of aluminum nitrate, chloride and sulfate (24). It will be noted that the diffraction bands for the gel from sulfate are very much broader than the lines for the gel from chloride or nitrate, demonstrating the much smaller crystal size of γ-AlOOH precipitated from

sulfate solution. Indeed, the x-ray diffraction bands of the gel from sulfate are so broad that such samples were identified tentatively as γ-AlOOH only because the position of the bands corresponded roughly to that of the sharpest lines in the pattern of the gels from chloride and nitrate. To establish definitely the constitution of the precipitate from sulfate, an electron diffraction pattern was obtained (24) for a gel precipitated at 25° from dilute solution with ammonia at a

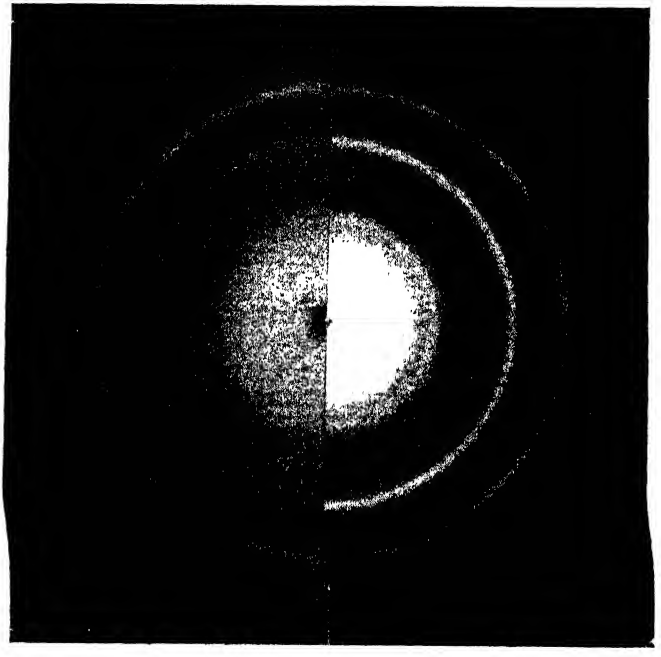

Fig. 2.—Electron diffraction patterns for γ-AlOOH precipitated at 25° C. from chloride (right) and sulfate (left).

*p*H value of approximately 6. Figure 2 (left) is a photograph of this electron diffraction pattern. It is obvious that the diffraction rings are in the same position as those from an aged sample of γ-AlOOH from chloride (Fig. 2, right). The freshly formed precipitate from the sulfate is therefore γ-AlOOH; the crystals are too small to give a sharp x-ray diffraction pattern but are large enough to give a sharp electron diffraction pattern.

The much smaller crystal size of γ-AlOOH from sulfate than from chloride or nitrate recalls that the highly dispersed, adsorptive alumina floc in water purification practice is obtained from aluminum sulfate. A study has been made (31) of the constitution of the alumina floc thrown down from highly dilute solutions using the techniques of x-ray and electron diffraction. The fresh floc precipitated at *p*H values of 5–8 consists of minute crystals of γ-AlOOH, the size of which increases with increasing *p*H value of the solution from which it separates. The primary crystals show a progressive increase in size on standing in contact with the mother liquor. Under otherwise constant conditions, the size of the crystals increases with decreasing concentration of the aluminum sulfate solution in accord with von Weimarn's precipitation rule and with the expected decrease in adsorption of sulfate ion as the concentration of this ion in the mother liquor falls off. By suitable changes in *p*H value, time of aging and concentration of aluminum sulfate, the floc of γ-AlOOH can be varied from primary crystals so small that the x-radiogram consists of two or three broad bands to primary crystals large enough to give well-defined lines. The use of aluminum sulfate and sodium carbonate at a *p*H value between 5.3 and 6.5 in the precipitation of alumina floc is favorable for the most highly dispersed crystals of γ-AlOOH. The transformation of colloidal γ-AlOOH crystals to coarser crystals of α-$Al(OH)_3$ takes place more rapidly the higher the *p*H value of the mother liquor.

In a study of the constitution of the alumina floc (32) over a *p*H range of 4 to 10.5, 0.04 *M* aluminum sulfate solutions were treated with varying amounts of alkali and the *p*H values of the mixtures were determined. A number of freshly formed gels, precipitated at slightly different *p*H values and aged in the mother liquor at 100° for 24 hours, were examined by x-ray diffraction methods. A few of the diffraction patterns are reproduced in Fig. 3. At a *p*H of 5.5 and slightly above, the gels gave broad patterns of γ-AlOOH which became gradually sharper as the *p*H value of the supernatant solution was increased. At relatively high *p*H values, sharp diffraction patterns of α-$Al(OH)_3$ were obtained. At *p*H values slightly below 5.5, the fresh gels gave a band diffraction pattern different from that of γ-AlOOH; at lower *p*H values the gels became gradually more crystalline as evidenced by the sharpness of the diffraction lines. Aging the gel in the mother liquor at *p*H values below 5 increased the primary crystal size until it gave a relatively sharp x-ray diffraction

pattern distinct from any known form of hydrated or anhydrous alumina. From an analysis of the aged crystalline material and a dehydration isobar, the new phase was identified as a basic salt that may be represented by the formula $Al_2O_3 \cdot SO_3 \cdot 1.5H_2O$. Similar investiga-

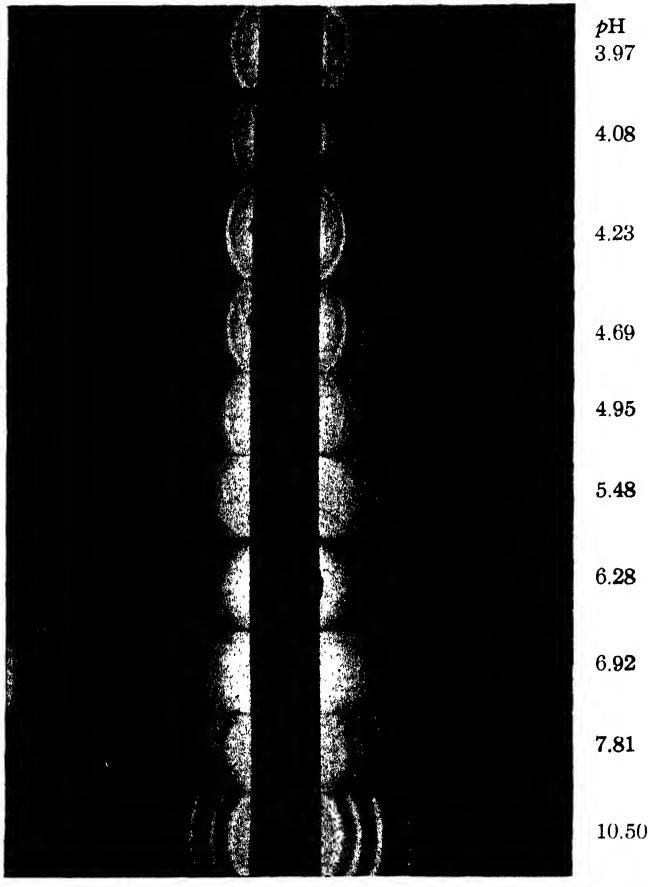

Fig. 3.—X-ray diffraction patterns for alumina gels precipitated at various *p*H values.

tions with gels thrown down from aluminum chloride and nitrate solutions show that between *p*H 4–8 no basic salts are formed. Potentiometric titration curves for the three aluminum salts all show breaks at a *p*H value of about 4. Accordingly, such breaks in titra-

tion curves do not furnish conclusive evidence of the formation of basic aluminum salts. The observed breaks probably result from the presence of free acid in the original aluminum salt.

2. *Oxides of Rarer Elements of the Third Group*

Gallia.—Gallium oxide gel, precipitated at 25° or 100° from a gallium chloride solution with a slight excess of ammonia, gives an x-ray diffraction pattern consisting of two broad but distinct bands. Since the bands are in the same position as the two sharp lines in the pattern obtained from relatively large crystals of α-Ga_2O_3, it was concluded (10) that the gel consisted of minute crystals of α-Ga_2O_3. The evidence was admittedly inconclusive and the deduction was questioned by Laubengayer and Engle (7). The problem has now been settled (24) by the observation that the sharper diffraction lines in the electron diffraction pattern of the gel correspond to the lines in the x-ray diffraction pattern of α-Ga_2O_3. The gel is therefore highly hydrous α-Ga_2O_3.

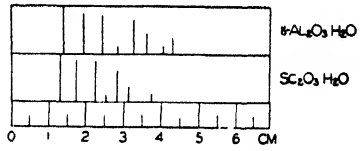

Fig. 4.—X-ray diffraction patterns for alumina and scandia.

Scandia and Yttria.—Scandia gel (22) gives a dehydration isobar characteristic of a hydrous monohydrate $Sc_2O_3 \cdot H_2O$ or ScOOH. In Fig. 4 are given diagrams of the x-ray diffraction patterns of γ-AlOOH and ScOOH. Except for a uniform displacement of the lines the patterns are very similar, indicating a definite similarity in crystal structure.

Yttria gel (22) gives a continuous dehydration isobar characteristic of a typical hydrous oxide that contains no water in definite stoichiometrical combination. The x-ray diffraction pattern consists of two diffuse bands.

Rare Earths.—The oxide gels of the rare earths (22) neodymium and praseodymium, precipitated at 100°, give dehydration isobars which definitely establish them as hydrous trihydrates $Nd_2O_3 \cdot 3H_2O$ or $Nd(OH)_3$ and $Pr_2O_3 \cdot 3H_2O$ or $Pr(OH)_3$. Diagrams of the x-ray diffraction patterns of the two hydrates and of the corresponding anhydrous oxides are given in Fig. 5. The dehydration isobars give indications of the formation of $Pr_2O_3 \cdot H_2O$ at about 400° and of $Nd_2O_3 \cdot H_2O$ at 400–500°. X-ray diffraction data likewise suggest the forma-

tion of monohydrates but the results to date are not conclusive on this point.

Samarium oxide gel (22), like yttrium oxide gel, appears to be a typical hydrous oxide, giving a continuous dehydration isobar and an x-ray diffraction pattern with but a single broad band.

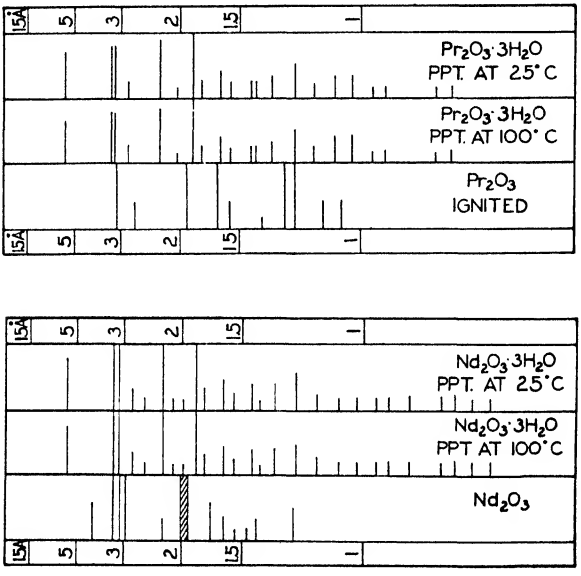

Fig. 5.—X-ray diffraction patterns for praseodymium and neodymium oxides and hydroxides.

3. *Chromic Oxide*

The gel formed by the addition of alkali or ammonia to a chromic salt is amorphous to x-rays whether precipitated cold or hot. Moreover, the gel, after being heated for days or weeks in contact with water at the boiling point, gives an x-ray diffraction pattern of the amorphous type. The freshly formed gel is readily obtained in thin coherent films which have been examined by the electron diffraction technique (24). The resulting diffraction pattern is of the amorphous type. We have been unable to confirm Baccaredda and Beati's (1) observations that a chromic oxide gel gives an electron diffraction

pattern similar to that of α-$Al_2O_3 \cdot 3H_2O$. If the fresh gel is heated in an autoclave for several hours at 100–250°, it gives the x-ray diffraction pattern for $Cr_2O_3 \cdot H_2O$.

4. *The Brown Gel of Ferric Oxide*

The brown gel of hydrous ferric oxide, frequently misnamed ferric hydroxide, is commonly prepared by the addition of a base to a ferric

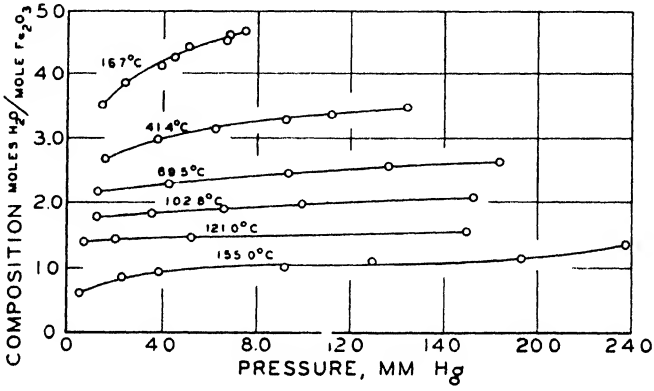

Fig. 6.—Dehydration isotherms for hydrous ferric oxide from ferric ethylate.

salt solution. The gel freshly formed in the cold (21) and dried in a vacuum is amorphous to x-rays, but after standing at room temperature in contact with water for several weeks, it gives a band x-ray diffraction pattern corresponding to α-Fe_2O_3 or hematite; after several months, the crystals have grown until the sample gives a sharp hematite diffraction pattern. Although the fresh gel is amorphous to x-rays, it is crystalline to electrons, giving the hematite diffraction pattern (24). If a fresh ferric chloride solution is the source of ferric ions, the gel precipitated therefrom is pure α-Fe_2O_3; but if an old solution is used, the gel is a mixture of α-Fe_2O_3 and β-FeOOH. The compound β-FeOOH is the product of the slow hydrolysis of ferric chloride (20).

Thiessen and Köppen (14) claim that the brown ferric oxide gel formed by the hydrolysis of ferric ethylate yields a series of no less than eight hydrates of ferric oxide on isothermal dehydration. Our

failure to confirm this result was attributed by Thiessen and Köppen to impurities in the sample and faulty technique. The experiments have recently been repeated with samples of special purity (30). No indication whatsoever of definite hydrates was observed during the isothermal dehydration process. This is evidenced by a typical set of isotherms reproduced in Fig. 6.

5. *Silica, Columbia and Tantala*

Silica Gel.—The x-ray diffraction pattern of silica gel thrown down either at room temperature or at 100° consists of very broad bands. The precipitated oxide readily forms thin coherent films which lend themselves to examination by electrons. The resulting electron diffraction pattern is clearly of the amorphous type (24). In accord with this observation, Germer and Storks (4) found that a silica film formed by condensation of vapors gives an electron diffraction pattern characteristic of an amorphous material.

Thiessen and Körner (15) and Spychalski (13) claim to have prepared a series of hydrates of silica during the isothermal dehydration of silica gel formed by hydrolysis of ethyl silicate. These experiments have been repeated (30) with silica gels prepared at low temperatures and with improved experimental technique made possible by the use of the McBain-Bakr silica spring balance. In accord with the observations on ferric oxide gel from ferric ethylate, the dehydration isotherm for silica from ethyl silicate is a smooth curve, which indicates the absence of hydrate formation in the dehydration process. A single point of inflection in the dehydration curve for silica gel is not due to a hydrate but to some kind of capillary structure in the gel which was recognized by van Bemmelen a half-century ago. The hysteresis phenomenon exhibited by silica gel on hydration following dehydration is in some way associated with the physical structure of the oxide gel.

Columbia and Tantala Gels.—The gels of columbium pentoxide and tantalum pentoxide resemble silica in being amorphous to x-rays and in exhibiting the hysteresis phenomenon on dehydration followed by subsequent hydration. Like silica also, both columbia and tantala gels give electron diffraction patterns of the broad-band amorphous type (24).

Hydrous oxides such as those of chromium, silicon, columbium and tantalum which give broad-band electron diffraction patterns are

considered to be amorphous in the sense that Zachariasen (33) assumes a glass to be amorphous, that is, the atoms are arranged in the form of a network lacking the periodicity and symmetry which characterize a crystal lattice.

6. *Titania, Zirconia and Thoria*

Titania.—Titania precipitated from a titanium salt solution with ammonia at room temperature is amorphous to x-rays and gives a smooth dehydration isobar (18). Aging the gelatinous precipitate under water for long periods of time at room temperature or for shorter periods of time at 100° gives hydrous anatase. In our first investigations of the product formed by hydrolysis of titanium salts, it was found that titanium sulfate yields anatase whereas titanium chloride and nitrate give rutile. Pamfilov and Ivancheva (11) confirmed these results except that they obtained anatase rather than rutile by hydrolysis of titanium nitrate. A comprehensive reinvestigation (29) of the problem of the hydrolysis products of titanium salts disclosed that the rate of transformation of the more soluble and less stable anatase modification of titania into the less soluble and more stable rutile modification is influenced by two opposing factors: (*a*) retardation of the transformation by an adsorbed layer of ions on the anatase which reduces its rate of solution and (*b*) acceleration of the transformation by an ionic environment in which anatase is more soluble.

Anatase formed by hydrolysis of titanium chloride or nitrate solutions is transformed fairly rapidly into rutile at 100°. The rate of transformation is slowed down enormously in the presence of a large excess of alkali chloride or nitrate because of the protective action of adsorbed anions. The rate of transformation is speeded up in the presence of excess hydrochloric or nitric acid because of increased solubility of anatase, in spite of the protective action of adsorbed ions. Anatase formed by hydrolysis of titanium sulfate is not transformed into rutile in any reasonable time even in strong sulfuric acid solutions since sulfate ions are adsorbed much more strongly than univalent chloride and nitrate ions.

An electron diffraction pattern of freshly precipitated titania was found to correspond neither to the anatase nor the rutile modification of the oxide (24). This problem is under investigation.

Zirconia and Thoria.—The minute crystals of precipitated zirconia and thoria grow more slowly on aging at 100° than the corre-

sponding titania crystals. On heating the respective precipitates for several hours at 100° in contact with the mother liquor, they give broad-band x-ray diffraction patterns corresponding to zirconia and thoria, respectively (2). Because of the difficulty of obtaining suitable films for electron diffraction studies, the gels have not been examined by this technique (24).

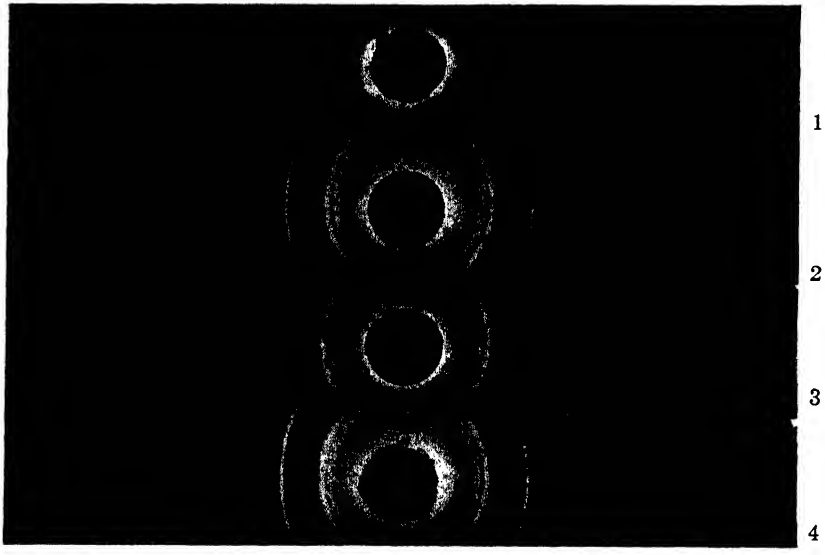

Fig. 7.—X-ray diffraction patterns for (1) cupric sulfide precipitated at 25° C. from cupric sulfate by hydrogen sulfide, (2) same precipitated at 100° C., (3) cupric sulfide mineral, (4) cupric sulfide precipitated at 100° C. from cupric chloride by hydrogen sulfide (pattern obtained at once).

II. Salt Gels

1. Copper Sulfides

The composition of the product formed by the interaction of a cupric salt solution with hydrogen sulfide has been questioned. Kolthoff and Pearson (5) claim that the precipitate formed at 25° or 100° is cupric sulfide but that some cuprous salt may form on standing. On the other hand, Sauer and Steiner (12) believe that the gel thrown down in the cold is chiefly cuprous sulfide and sulfur, which react to form cupric sulfide on heating.

An x-ray diffraction examination has been made (25) of samples prepared by the procedures of Kolthoff and Pearson and of Sauer and Steiner with the results shown in Figs. 7 and 8. These data indicate that fresh samples precipitated either in the hot or in the cold are essentially cupric sulfide, in agreement with Kolthoff and Pearson's

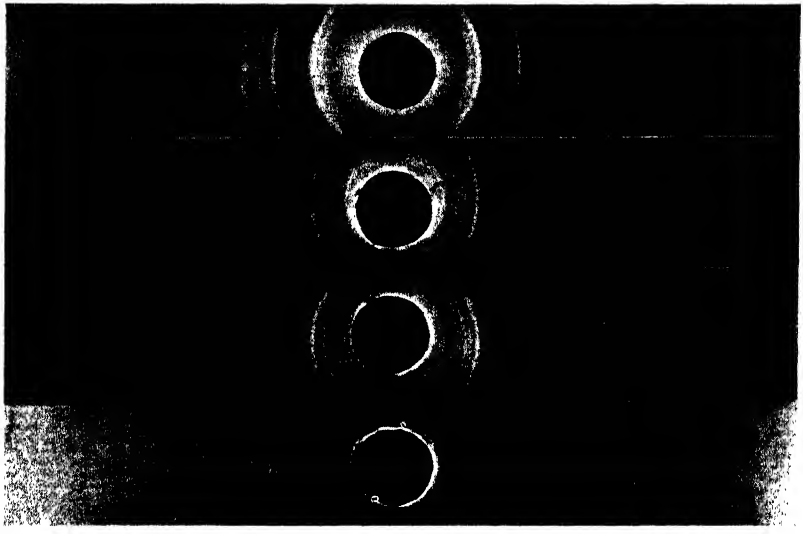

Fig. 8.—X-ray diffraction patterns for (1) cupric sulfide mineral, (2) cupric sulfide precipitated at 25° C. from cupric chloride by hydrogen sulfide, (3) same precipitated at 100° C. (sample aged at 100° C. for an hour), (4) cuprous sulfide mineral.

chemical evidence. Similarly, the samples prepared by the method of Sauer and Steiner give the x-ray diffraction pattern of cupric sulfide plus some additional unidentified lines. The crystalline phase responsible for the extra lines has not been identified; the lines do not correspond to CuO, $Cu(OH)_2$, Cu_2O, Cu_2S or to any known crystalline form of sulfur.

It has been observed further that cupric sulfide precipitated at 100° is distinctly more gelatinous than that thrown down at 25°, in agreement with the observations of Kolthoff. Since the x-ray diffraction patterns of the two samples indicate no difference in primary particle size, the difference in physical structure must result from

variation in size and nature of the surface of the secondary aggregates.

2. *Arsenic Trisulfide*

Ten years ago (16) it was demonstrated that precipitated and dried arsenic trisulfide varies in color continuously from yellow through

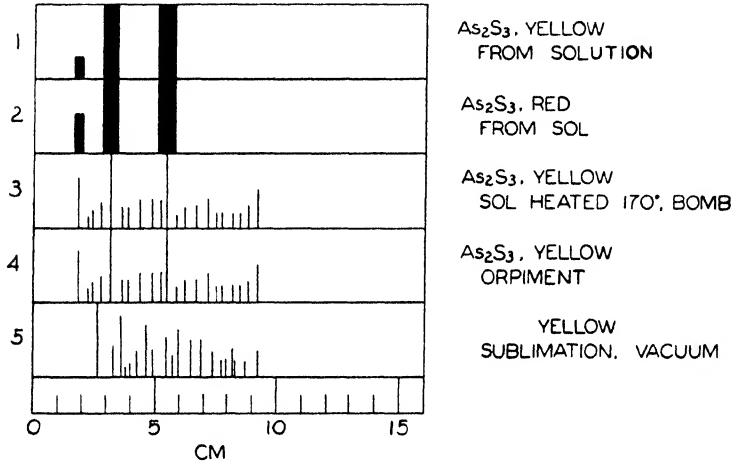

Fig. 9.—X-ray diffraction patterns for arsenic trisulfides.

orange-yellow, orange, red-orange to red depending on the conditions of precipitation. The lighter shades result by conducting hydrogen sulfide into a solution of arsenious oxide or an arsenate containing sufficient electrolyte to cause immediate precipitation. The darker shades result from the coagulation of freshly prepared arsenic trisulfide sol. The red color of the sulfide is not due to an allotropic change in the yellow sulfide, to the presence of red sulfarsenite or to As_2S_2. The yellow sulfide dries to an impalpable powder whereas the red sulfide dries to a glass. This difference in physical structure accounts for the variation in color. The red sulfide is rendered yellow on disintegrating the glassy mass by heating just below the sintering temperature or by grinding. The results of an x-ray diffraction examination (25) of various samples are given in chart form in Fig. 9. These results indicate that both the yellow and red gels are minutely crystalline, and that the broad bands are in a position corresponding

to the sharper lines in the mineral orpiment. A different crystalline product which may be a second modification of arsenic trisulfide is obtained by sublimation in a vacuum.

3. *Heavy Metal Ferro- and Ferricyanide Gels*

Copper Ferrocyanide.—Most heavy metal ferro- and ferricyanides are so insoluble that they come down in a highly gelatinous form by the interaction of even dilute solutions of metallic ion with ferro-

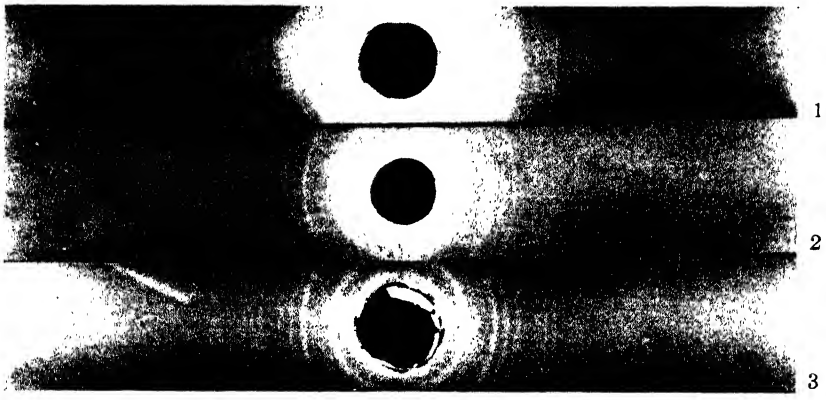

Fig. 10.—X-ray diffraction patterns for cupric ferrocyanide gels. (1) Moist gel, (2) air-dried gel from $K_4Fe(CN)_6$, (3) air-dried gel from $H_4Fe(CN)_6$.

or ferricyanide ion. The gels adsorb the common multivalent anion so very strongly that precipitation of the metal is incomplete on mixing equivalent amounts of the respective ions. An x-ray diffraction examination (26) of moist gels precipitated in the presence of excess potassium ferrocyanide disclosed that the potassium ferrocyanide is not combined to form a double or complex salt but is adsorbed, for the most part, on the surface of the highly dispersed crystals of copper ferrocyanide. The possibility that a small amount of alkali ferrocyanide dissolves in the copper salt is not excluded; but any such solid solution is insufficient to cause detectable distortion of the lattice of copper ferrocyanide. Typical x-ray diffraction patterns of copper ferrocyanide are reproduced in Fig. 10. Gels containing adsorbed

potassium ferrocyanide give x-ray diffraction patterns identical with those precipitated from a solution of hydroferrocyanic acid which is very weakly adsorbed. Relatively pure copper ferrocyanide gel is best obtained by precipitation with excess copper ion.

An x-ray diffraction study (26) of some common metallic ferrocyanide gels disclosed that the ferrocyanides of copper, cobalt, nickel

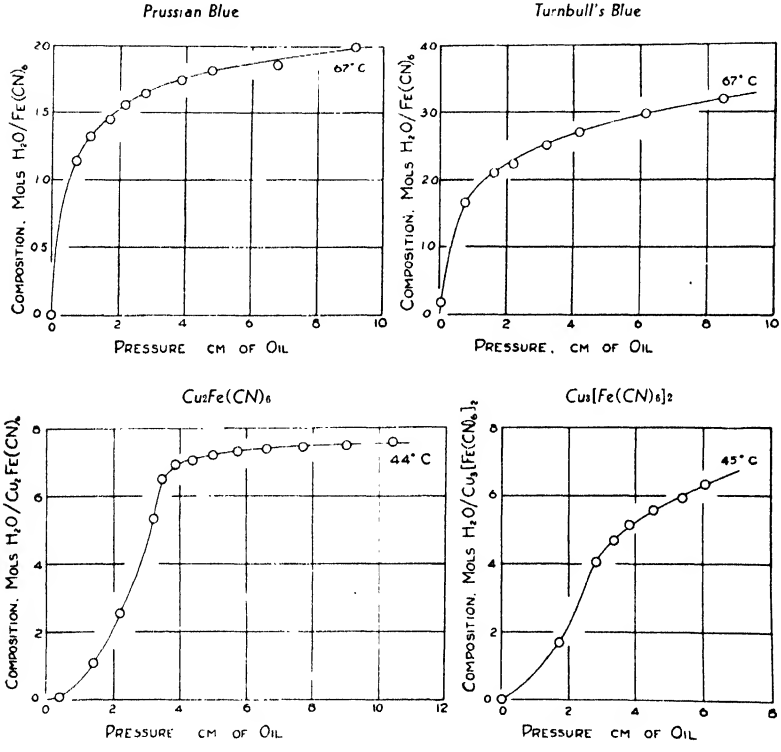

Fig. 11.—Dehydration isotherms for iron-cyanide gels.

and manganese, but not of lead, are isomorphous with lattice constants that are nearly the same. The ferrocyanides of zinc, cadmium and silver each give two distinct x-ray diffraction patterns, depending on whether the gel is thrown down with metal in excess or with potassium ferrocyanide in excess. The two diffraction patterns for each of these three salts may correspond, respectively, to the normal salt

and a double salt with potassium ferrocyanide. Cadmium ferrocyanide formed in the presence of excess ferrocyanide ion gives a diffraction pattern similar to copper ferrocyanide, suggesting that the cadmium salt formed under these conditions is $Cd_2Fe(CN)_6$.

The water in most heavy metal ferro- and ferricyanide gels is adsorbed and no definite hydrates are formed. This is illustrated (27)

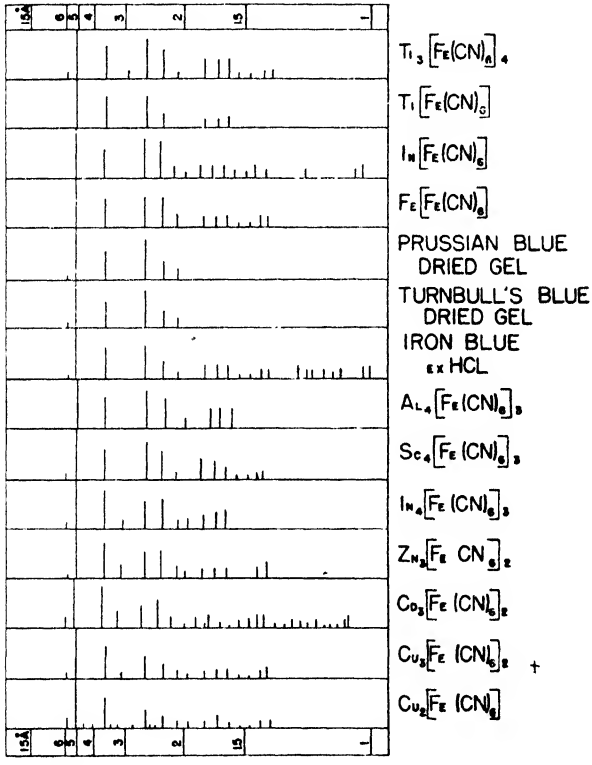

Fig. 12.—X-ray diffraction patterns for ferro- and ferricyanide gels.

by the smooth dehydration isotherms for cupric ferro- and ferricyanide and for Prussian blue and Turnbull's blue, shown in Fig. 11. Further support of the view that copper ferrocyanide, Prussian blue and Turnbull's blue form no hydrates is furnished by the observation

that the moist gels and the gels completely dehydrated in vacuum give identical x-ray and electron diffraction patterns. Quantitative studies of the structure of heavy metal iron cyanides must take into account the fact that, in general, these materials do not contain water in definite chemical combination.

Prussian Blue and Turnbull's Blue.—The freshman is usually told that the interaction of ferric salts and alkali ferrocyanides yields $Fe_4[Fe(CN)_6]_3$ or Prussian blue whereas the interaction of ferrous salts and alkali ferricyanides yields $Fe_3[Fe(CN)_6]_2$ or Turnbull's blue. Actually, the oxidation-reduction reactions which take place on mixing iron salts and alkali iron cyanides complicate the problem to such

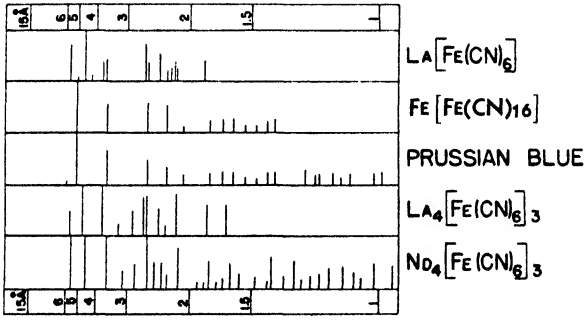

Fig. 13.—X-ray diffraction patterns for ferro- and ferricyanide gels.

an extent that certain investigators conclude from chemical analysis that all the blue gels are ferrocyanides whereas others arrive at the diametrically opposite conclusion that all the blue gels are ferricyanides (17). Levi (8) observed that the x-ray diffraction patterns of so-called Prussian blue and Turnbull's blue are identical and we have confirmed this observation by both x-ray and electron diffraction techniques. Moreover, it has been found that the densities of so-called Prussian blue and Turnbull's blue are the same within the limits of experimental error (28). Accordingly, a comprehensive x-ray diffraction study of the blue-complex cyanides and related compounds was undertaken (28) in an attempt to determine their probable structure. The results of the study are as follows:

From an analysis of the x-ray diffraction patterns in Figs. 12 and 13 it was deduced that the following heavy metal iron-cyanides possess isomorphous structures of face-centered cubic symmetry: $Ti_3[Fe(CN)_6]_4$, $Ti[Fe(CN)_6]$, $In[Fe(CN)_6]$, $Fe[Fe(CN)_6]$ Prussian blue, Turnbull's blue, "iron-blue ex-HCl," $Al_4[Fe(CN)_6]_3$, $Sc_4[Fe(CN)_6]_3$, $In_4[Fe(CN)_6]_3$, $Zn_3[Fe(CN)_6]_2$, $Cd_3[Fe(CN)_6]_2$, $Cu_3[Fe(CN)_6]_2$ and $Cu_2[Fe(CN)_6]$. On the other hand, $La_4[Fe(CN)_6]_3$, $La[Fe(CN)_6]$ and $Nd_4[Fe(CN)_6]_3$ do not belong to this isomorphous series, but exhibit a more complex type of structure. Since these x-ray diffraction studies show that definite trivalent heavy metal ferrocyanide (*e. g.*, $Sc_4[Fe(CN)_6]_3$) and definite divalent heavy metal ferricyanides (*e. g.*, $Zn_3[Fe(CN)_6]_2$) may possess the same isomorphous face-centered cubic structure, it follows that x-ray studies cannot be used to distinguish between $Fe_4[Fe(CN)_6]_3$ and $Fe_3[Fe(CN)_6]_2$ as possible formulas for the gels of Prussian blue and Turnbull's blue.

A consideration of oxidation-reduction potentials suggests that the ferric ions would be expected to react with ferrocyanide ions to give ferrous ions and ferricyanide ions. Confirming the work of Müller (9), ferricyanide ions are found in the filtrate after mixing ferric chloride with potassium ferrocyanide. This result indicates that an oxidation-reduction reaction has taken place. The lack of quantitative agreement between the amount of ferricyanide formed and the calculated quantity is attributed to adsorption of both ferrocyanide and ferricyanide ions by the blue gel. It is concluded that both Prussian blue and Turnbull's blue may be represented by the formula $Fe_3[Fe(CN)_6]_2$. This conclusion is not inconsistent with the x-ray diffraction work discussed above.

Bibliography

1. M. Baccaredda and E. Beati, *Atti X° congr. intern. chim.*, **2**, 99 (1938).
2. J. Böhm and H. Niclassen, *Z. anorg. allgem. Chem.*, **132**, 6 (1924).
3. W. C. Bray and A. V. Hershey, *J. Am. Chem. Soc.*, **52**, 2595 (1930).
4. L. H. Germer and K. H. Storks, *Ind. Eng. Chem., Anal. Ed.*, **11**, 583 (1939).
5. I. M. Kolthoff and E. A. Pearson, *J. Phys. Chem.*, **36**, 642 (1932).
6. I. M. Kolthoff and O. Tomicek, *Ibid.*, **39**, 945 (1935).
7. A. W. Laubengayer and H. R. Engle, *J. Am. Chem. Soc.*, **61**, 1210 (1939).
8. G. R. Levi, *Giorn. chim. ind. applicata*, **7**, 410 (1925).
9. E. Müller, *J. prakt. Chem.*, **84**, 353 (1911); **104**, 241 (1922).
10. W. O. Milligan and H. B. Weiser, *J. Am. Chem. Soc.*, **59**, 1670 (1937).
11. A. V. Panfilov and E. G. Ivancheva, *J. Gen. Chem., U. S. S. R.*, **8**, 1739 (1939).

12. E. Sauer and D. Steiner, *Kolloid-Z.*, **72**, 41 (1935).
13. R. Spychalski, *Z. anorg. allgem. Chem.*, **239**, 317 (1938).
14. P. A. Thiessen and R. Köppen, *Ibid.*, **189**, 113 (1930); **228**, 57 (1936).
15. P. A. Thiessen and O. Körner, *Ibid.*, **189**, 168, 174 (1930).
16. H. B. Weiser, *J. Phys. Chem.*, **34**, 1021 (1930).
17. For a survey see H. B. Weiser, *Inorg. Colloid Chemistry*, John Wiley & Sons, New York **3**, 343 (1938).
18. H. B. Weiser and W. O. Milligan, *J. Phys. Chem.*, **38**, 513 (1934).
19. H. B. Weiser and W. O. Milligan, *Ibid.*, **38**, 1175 (1934).
20. H. B. Weiser and W. O. Milligan, *J. Am. Chem. Soc.*, **57**, 238 (1935).
21. H. B. Weiser and W. O. Milligan, *J. Phys. Chem.*, **39**, 25 (1935).
22. H. B. Weiser and W. O. Milligan, *Ibid.*, **42**, 673 (1938).
23. H. B. Weiser and W. O. Milligan, *Chem. Rev.*, **25**, 1 (1939).
24. H. B. Weiser and W. O. Milligan, *J. Phys. Chem.*, **44**, 1081 (1940).
25. H. B. Weiser and W. O. Milligan (unpublished results).
26. H. B. Weiser, W. O. Milligan and J. B. Bates, *J. Phys. Chem.*, **42**, 945 (1938).
27. H. B. Weiser, W. O. Milligan and J. B. Bates, *Ibid.*, **45**, 701 (1941).
28. H. B. Weiser, W. O. Milligan and J. B. Bates, *Ibid.* (in press).
29. H. B. Weiser, W. O. Milligan and E. L. Cook, *Ibid.* (in press).
30. H. B. Weiser, W. O. Milligan and W. J. Coppoc, *Ibid.*, **43**, 1109 (1939).
31. H. B. Weiser, W. O. Milligan and W. R. Purcell, *Ind. Eng. Chem.*, **32**, 1487 (1940).
32. H. B. Weiser, W. O. Milligan and W. R. Purcell, *Ibid.*, **33**, 669 (1941).
33. W. H. Zachariasen, *J. Am. Chem. Soc.*, **54**, 3841 (1932).

THE CREAMING OF RUBBER LATEX

G. E. VAN GILS AND G. M. KRAAY

Department of Rubber Research, Experimental Station West-Java, Buitenzorg, Java, Netherlands East Indies

CONTENTS

I. Introduction

The study of the creaming of rubber latex by means of creaming agents is of importance not only for the technology of the creaming process as applied on estates in the Middle East, but it is also interesting from a scientific and, more especially, from a colloid-chemical point of view. This becomes clear when one takes into consideration the fact that the creaming process is not confined merely to rubber latex, but that milk, for example, can be creamed with the aid of suitable creaming agents, as can all synthetic dispersions. Also,

the sedimentation process is closely related to the creaming phenomenon. Being dependent only upon the difference in specific gravity of the dispersed phase and the dispersing medium, the addition of a "creaming agent" will result either in creaming or in sedimentation. A technically very important sedimentation process, for instance, is the clarification of coal-washery effluent by means of colloidal "creaming agents" such as starch and konnyaku meal (21). That we are dealing here with a process quite different from the flocculation of suspensions with electrolytes is evident from the fact that, with the use of "creaming agents," the sediment can be redispersed (reversibility of the process), although it has a much smaller volume than that obtained by flocculation with electrolytes.

II. The Creaming of Latex in Actual Practice

The literature (2) mentions many creaming agents for rubber latex, *e. g.*, gum arabic, gum tragacanth, gum karaya, alginic acid, alginates, tragon seed gum and many more. In recent times, in addition to the vegetable creaming agents, certain synthetic creaming agents have been recommended such as polyacrylic acid and salts, polyvinyl alcohol and esters, polymethylene oxide and derivatives, and also creaming agents prepared by modifying natural substances, such as methyl cellulose. However, these creaming agents are not all equally effective, even though this is implied in the literature on the subject, and, in addition, a serum may result which still contains rubber to a greater or lesser extent.

An effective creaming agent free from these defects, which is being applied in the Netherlands Indies, is konnyaku or Amorphophallus meal obtained from the bulbs of Amorphophallus species, especially *Amorphophallus Rivieri Durieu.* Research has shown (6) that a carbohydrate of high molecular weight, yielding on hydrolysis mannose and glucose, a so-called gluco-mannan, is the active constituent in the creaming agent.

The advantage of using konnyaku meal for the creaming of rubber latex on the estates lies in the fact that it dissolves readily in water, yielding a viscous liquid. It is customary to use a one per cent solution. To rubber latex containing 4 g. of ammonia per liter, 14 per cent of this solution is added while stirring thoroughly for about 15 minutes. Allowing the mixture to stand undisturbed for a few hours, one observes that two layers have formed. The lower layer

consists of serum distinctly separated from the supernatant layer of latex. Gradually the volume of the serum layer increases. The line of demarcation between latex and serum rises in the column of liquid. If the height of the serum layer is plotted against the time of creaming in hours one obtains the curve depicted in Fig. 1. In the first couple of hours no line of demarcation can be seen. This lapse of time must be regarded as an induction period. Thereafter the process continues at a more or less constant rate, until after a lapse of about 24 hours the process continues at a greatly reduced rate. The end of the curve runs asymptotically toward a certain maximum height of serum.

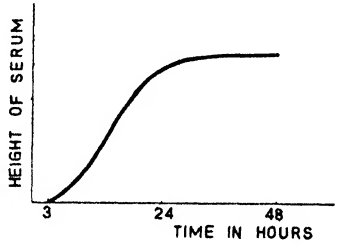

Fig. 1.—Creaming curve.

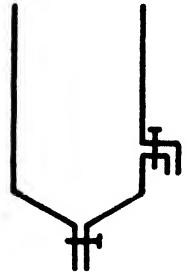

Fig. 2.—Creaming tank.

In actual practice the time of creaming varies between four and six times 24 hours, whereupon the cream is drawn off. To this end cylindrical tanks are used, provided with conical bottoms containing a discharge valve for the removal of the serum. A second valve, located at about one-quarter the height of the cylindrical body of the tank, provides an outlet for the cream. Over the total length of the body of the tank a narrow glass window is affixed so as to permit control of the ascending line of demarcation between the cream and the serum. The advantage of drawing off the cream by means of the valve in the cylindrical body of the tank lies in the fact that the liquid is thus decanted. Sludge, consisting of particles of sand, crystalline magnesium ammonium phosphate, etc., settles on the conical bottom. See Fig. 2.

The serum, containing a considerable proportion of the proteins from the original latex, is discarded. When using konnyaku meal as a creaming agent the rubber content of the serum is practically nil.

The cream, the dry rubber content* of which may vary between 55 and 60 per cent, depending on the latex used, cannot be employed as such for all purposes since it contains swollen particles of konnyaku meal. These particles are separated by centrifuging the cream by means of a clarification centrifuge. The swollen particles of konnyaku meal settle in the machine on the wall of the bowl, together with a sludge consisting partly of proteins and lipins. The clarified cream has to be ammoniated in order to obtain an ultimate concentration of ammonia of 7 to 8 g. per liter, which guarantees a satisfactory preservation. The cream may be shipped either in drums or in bulk.

III. The Creaming Mechanism

Hevea latex may be considered to consist of small spherical rubber particles the dimensions of which may vary from one-tenth to several microns. These particles, forming the solid phase, are suspended in an aqueous medium (the serum) containing electrolytes, proteins and other organic substances in solution. Some of the proteins occurring in latex are adsorbed onto the surface of the rubber particles and control their behavior. The source of the negative electrical charge of the rubber particles is to be traced to the enveloping proteins. The particles show a lively Brownian movement.

The specific gravity of rubber is 0.9042, and that of the serum is about 1.024 (19). This difference in specific gravity is the reason for the tendency of the rubber particles to ascend within the liquid. The Brownian movement, however, opposes this tendency. When ammoniated latex is allowed to stand undisturbed for a while one can observe that natural creaming proceeds very slowly: only after a lapse of months is a distinct layer of cream to be distinguished (3).

The factors affecting the ascension velocity of a particle are expressed mathematically by the formula of Stokes:

$$v = \frac{2g(d_s - d_r)r^2}{9\eta}$$

where v = terminal velocity
g = acceleration due to gravity
η = viscosity of the medium
r = radius of the particle
d_s = density of the serum
d_r = density of rubber

In order to increase the sedimentation velocity so that the cream-

* Usual abbreviation for dry rubber content is DRC.

ing process may be used technically the formula of Stokes gives us two clues: 1. The enhancing of the force of gravity by means of centrifugal force. This is realized in actual practice (Utermark process). 2. The ascending velocity is largely dependent upon the radius of the particles (r^2). Now, if it is found possible to enlarge the radius of the particles by clustering them this would constitute a means of accelerating the creaming, thus making the phenomenon of technical importance.

Clustering of the particles occurs, for instance, in flocculation, which can be induced by lowering the stability of the particles (Fig. 3). However, in the case of rubber latex in general, flocculation is followed immediately by coalescence, which is an irreversible process. In order to obtain clusters which may be of use in the creaming process we have to find a means of causing the rubber particles to cohere in clusters in a reversible manner. This is accomplished by adding a "creaming agent" to the latex. Baker (2) was the first to describe the formation of clusters in rubber latex. Why the particles cohere in clusters in the presence of a creaming agent will be discussed later.

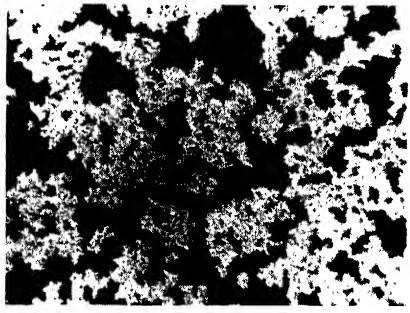

Fig. 3.—Cluster formation, photographed in dark-field illumination (latex = white).

In the creaming of very dilute latex (as of milk) the ascending clusters collect at the top of the liquid to form a cream layer which constantly thickens, whereas the lower liquid layer, from which the rubber is being continuously withdrawn, becomes clearer (Fig. 4-*a*).

With latex of normal concentration (35% DRC), however, entirely different phenomena are to be observed. The concentration of the rubber particles is so high that the clusters unite to form a mass extending throughout the liquid. Now comes the mechanical ascension of the combined clusters, but after a certain period of time has elapsed a second phenomenon is to be observed, *i. e.*, a syneresis of the mass exuding a clear serum. In contradistinction to the phenomena of the creaming of milk or of very dilute latex, one will observe in this case that the line of separation between the serum and the cream moves upward (Fig. 4-*b*).

Of the two processes here discussed the ascension of the mass of clusters is purely mechanical, and can be accelerated by applying centrifugal force. The second process, that of syneresis, still to be discussed, is not purely mechanical and is not subject to the influence of a field of force.

The following experiment throws some light on these two phenomena. A freshly prepared mixture of latex and creaming agent is introduced into a graduated centrifuge tube, and centrifuging is

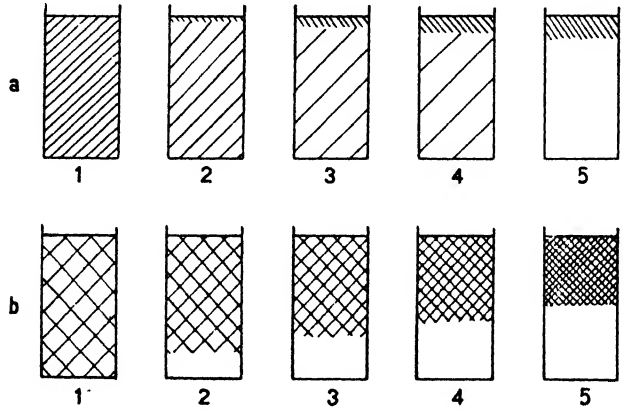

Fig. 4-*a* (top).—Creaming of extremely dilute latex.
Fig. 4-*b* (bottom).—Creaming of latex of normal concentration.

begun immediately. The cream and serum layers separate, and the cream volume may be read off. If, however, the mixture of latex and creaming agent is allowed to stand for a few hours before centrifuging, one obtains a cream layer much smaller than the one obtained in the preceding experiment. Since, in either case, the transparency of the serum so obtained is identical, the conclusion may be drawn that in the second experiment the packing of the rubber particles has been much closer. As time proceeds the agglomerates become closer, a more ideal packing is obtained, with the result that there is a less ready disintegration. This is illustrated by the following microscopic observations:

Place on a microscope slide, about 0.6 cm. apart, one drop of freshly prepared cream and one drop of water. Carefully place a

cover glass over both drops in such a way that a sharp line is formed between the cream and the water. If the microscope is focused exactly onto this boundary line, the following may be observed:

Clusters of various sizes detach themselves, and these clusters diffuse into the water. The clusters themselves rapidly disintegrate into smaller aggregates and into individual rubber particles exhibiting a lively Brownian movement.

Now, it soon becomes apparent that in some cases disintegration is effected much more rapidly than in others, especially when the cream

Fig. 5-*a*.—Disintegration of "young" clusters, magnified 200 ×, transmitted light (latex = black).

Fig. 5-*b*.—Disintegration of "old" clusters, magnified 200 ×, transmitted light (latex = black).

is fresh; for instance, when the latex-konnyaku meal mixture has been left standing for only a few hours, disintegration is faster than when the mixture has stood one day or several days.

If a drop of latex is examined in the same manner shortly after mixing with the konnyaku meal solution, it even gives the impression that no agglomerates are present, since only individual particles from the cream layer diffuse into the water phase. Moreover, the cream/water interface becomes indistinct much more rapidly than when the cream is less fresh (Fig. 5-*a*, 5-*b*).

Microscopic examination of undiluted latex already mixed with konnyaku meal and pressed to a very thin layer between two slides

indicates, however, that the agglomerates must have formed immediately after mixing.

For the sake of completeness we may add that agglomeration can often be observed with the unaided eye or under a lens when a latex/konnyaku meal mixture is stirred in a beaker and when the liquid draining from the wall is examined.

IV. Factors Affecting the Creaming

In the foregoing paragraphs we have seen that the essential feature in the mechanism of creaming is the formation of a network of agglomerates and an upward migration thereof. Before, however, discussing the theoretical side of these phenomena we shall deal with the various factors affecting the creaming.

1. Time Factor

From what has been stated above it is evident that time constitutes an important factor. It will be remembered that after a creaming experiment has been initiated, it takes some time before the cream/serum interface begins to migrate upward (see Fig. 1). This lag, the so-called induction period, is to be explained by the fact that the cohering network of agglomerates cannot at once extrude the entrapped serum. Only after the serum vacuoles, by flowing together, have increased in size and channels have been formed can the serum find an outlet by which to leave the network and thus permit the latter to contract.

When the separated cream is redispersed through shaking and is then allowed to stand, creaming occurs again without, however, passing through the induction period (Vester, 22). Through shaking, the agglomerates are distributed over the total liquid phase, but no such perfectly coherent and homogeneous network can now be formed as at first.

2. Viscosity

It follows from Stokes' formula that the viscosity influences the rate of creaming. It is somewhat surprising that there should exist any relation between the viscosity of the latex used as a starting material and the ultimate outcome of the creaming, namely, the dry rubber content of the cream. Van Dalfsen (18), of our laboratory,

has investigated the viscosity and creaming capacity* of a large number of latices from various origins. The latices were classified into groups according to their viscosity, whereupon the average creaming capacity for each group was determined. The following graph (Fig. 6) depicts the results of these experiments.

Also, if the viscosity of a latex is artificially affected, this will manifest itself by a change in the creaming capacity. The factors affecting the viscosity of the latex will now be discussed.

3. *Mechanical Effects*

Latex is a system with pronounced thixotropic properties, which means that the viscosity can be temporarily lowered by mechanical agitation. The Naugatuck Chemical Company discloses a process by which enhanced and accelerated creaming is brought about by subjecting the latex to be creamed or the mixture of latex and creaming agent to vigorous agitation (13). Van Dalfsen (18) was able to verify this effect.

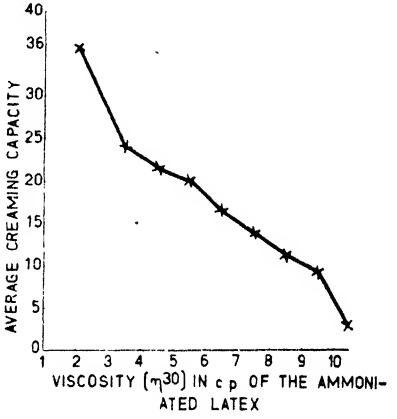

Fig. 6.—Relation between the viscosity (at 30° C.) and the creaming capacity of ammoniated latex.

Moreover, it is a well-known experience in creaming latex that when a mixture of latex and creaming agent has been thoroughly agitated for a while, the ensuing creaming proceeds more readily, the period of induction is shortened and a cream is obtained having a high dry rubber content.

An elegant method of applying mechanical agitation is by means of ultrasonic waves. Experiments carried out on a small scale in our laboratory proved the beneficial effects thereof on the creaming process. Bondy (4) has published analogous results.

The influence of alternating current (12) must probably be included in the same class of phenomena. The changing electrical field of

* Van Dalfsen defined the creaming capacity of a latex as the difference between the dry rubber content of the cream obtained and that of the latex.

force will cause the particles to move swiftly to and fro, more or less as they do when mechanically agitated.

By passing latex through a clarification centrifuge (5) an enhanced creaming capacity can be induced. Since this effect, in contradistinction to the one just discussed, is of a permanent nature, similar mechanical influences in this case are out of the question.

4. *Temperature*

At elevated temperatures the proteins present in the latex are coagulated, thus causing the latex to thicken or even to coagulate. Where the latex proteins have been largely eliminated or where they have been broken down to such a molecular weight that heating has no longer any flocculating effect, ammoniated latex can be heated to 100° C. with no destabilizing effects. In this case the increased temperature induces a lowering of the viscosity (15).

It can be readily understood, therefore, that heating accelerates creaming and causes a higher rubber concentration in the cream. In view of our theory of the creaming mechanism it is necessary to state that heating also causes more rubber to remain in the serum.

The following experiment will illustrate this point:

Our latex starting material was a diluted cream obtained by creaming once and having a dry rubber content of 26 per cent. With this material two creaming experiments were conducted, one at room temperature and another at 80° C. In both cases two concentrations of the creaming agent, konnyaku meal, were used.

Amount of konnyaku meal used	Creaming	
	at room temperature	at 80° C.
15 ml. 1% soln. per 100 ml. latex	DRC cream 55.4 % DRC serum 1.5 %	56.5 % 3.58%
20 ml. 1% soln. per 100 ml. latex	DRC cream 54.7 % DRC serum 0.88%	56.5 % 2.26%

5. *Pre-coagulation*

The Rubber Cultuur Maatschappij Amsterdam discloses a process whereby the application of pre-coagulation, either with formic acid or with calcium chloride, yields a latex with an enhanced creaming

capacity (16). Van Dalfsen (18) has shown that the latex obtained from pre-coagulation after stabilization with ammonia, has a lower viscosity than the original latex also stabilized with ammonia.

6. *Addition of Soap*

The addition of soap improves the creaming capacity of latex (14). Also, the viscosity of the latex is lowered when soap is added.

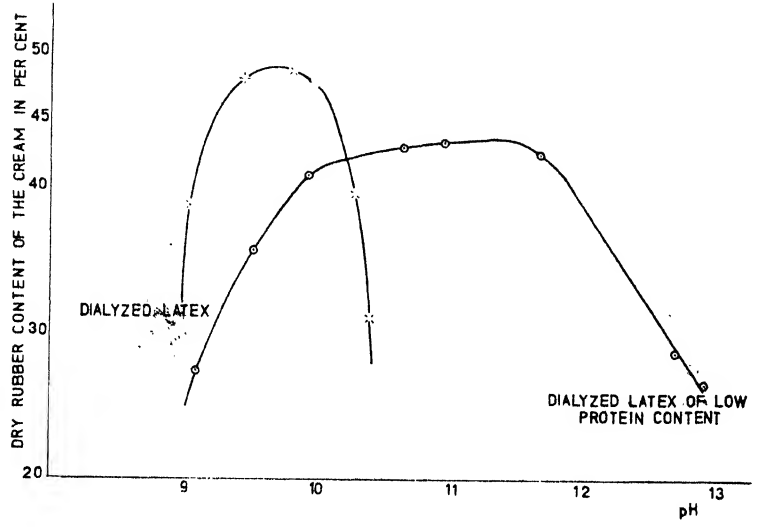

Fig. 7.—Effect of the *p*H on the creaming.

7. *Acidity (pH)*

Our experiments have shown (20) that the *p*H of the medium greatly influences the creaming. This influence can best be studied with dialyzed latex, especially dialyzed latex low in proteins. Where there are no electrolytes their influence is eliminated and the absence of buffer action makes it possible readily to attain the different *p*H's by adding varying amounts of ammonia or sodium hydroxide.

Figure 7 depicts the effect of the *p*H upon the concentration of rubber in the cream layer.

That the viscosity also has some influence is evident from the fact that it largely depends upon the *p*H. By adding ammonia to

fresh field latex the viscosity is greatly lowered, while at still higher *p*H's, which can only be attained with strong bases, such as the hydroxides of sodium and potassium, the viscosity increases.

8. Concentration of Electrolytes

We were also able to prove that electrolytes greatly affect the creaming in the sense that the rubber content in the cream obtained is lowered, whereas the clearness of the serum is improved. Figure 8

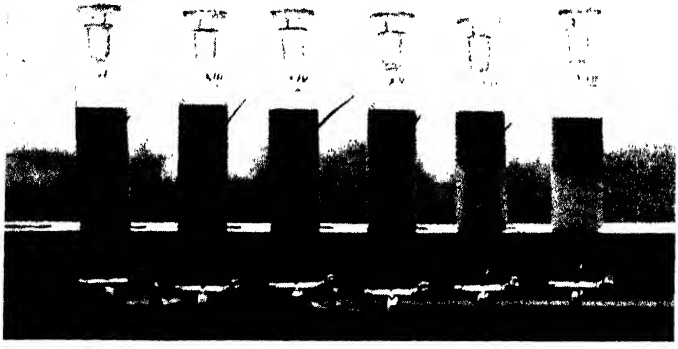

Fig. 8.—Creaming of dialyzed latex (of low protein content) with increasing amounts of $BaCl_2$. As the serum becomes clearer, the cream volume increases.

is an example of one of the many experiments conducted by us. These experiments also were carried out with dialyzed latex from which the proteins had been partly removed. The elimination of the proteins makes the latex more sensitive to electrolytes. Figures 9, 10 and 11 show the influence of various salts on the rubber content of the cream, while Fig. 12 shows the decrease in the rubber content of the serum when chlorides of potassium and aluminum are added.

These graphs indicate the following facts:

1. While electrolytes in general tend to lower the dry rubber content of the cream, they may in small concentrations produce a richer cream.

2. Bivalent ions already show their influence in much smaller concentrations than do monovalent ions. Trivalent ions do not show any greater influence than do bivalent ions.

3. The order of effectiveness for the monovalent ions is as follows:

$$Li > Na > K$$

4. The order of effectiveness for the bivalent ions is:

$$Ba = Ca > Sr$$

Here also the relation to the viscosity was evident, seeing that we were able to prove that the addition of electrolytes in all instances induced a lowered viscosity (Van Gils, 19, 20).

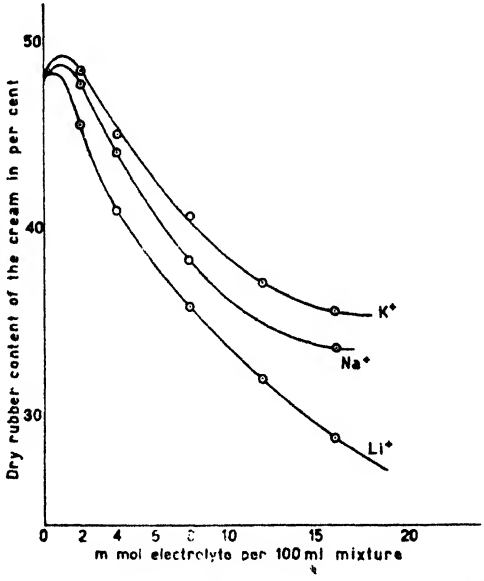

Fig. 9.—Effect of KCl, NaCl and LiCl on the creaming of dialyzed latex of low protein content.

9. *Concentration of the Creaming Agent*

The correct concentration of the creaming agent is of great importance for inducing satisfactory creaming. This concentration depends mainly upon the nature of the agent and, to a lesser extent, also upon the latex, that is to say, when one confines oneself to the use of normal ammoniated field latex.

When using very small quantities of the creaming agent the serum contains so much rubber that no separating line between the cream and the serum is noticeable. Upon increasing the quantity of creaming agent the serum becomes clearer and the boundary line more distinct. After passing a maximum the rubber content declines (20, 13). In actual practice one must compromise to obtain as rich a cream as possible with the lowest possible loss of rubber in the serum. The concentration of the creaming agent most favorable for creaming is called the optimum concentration. Figure 13 shows the relation between the concentration of the creaming agent and the dry rubber content of the cream and of the serum.

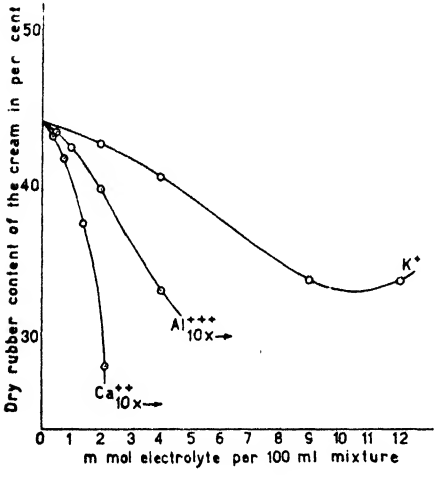

Fig. 10.—Effect of KCl, $CaCl_2$ and $AlCl_3$ on the creaming of dialyzed latex of low protein content.

To make the graph clearer, the concentrations pertaining to Ca^{++} and Al^{+++} have been multiplied by ten.

10. Rubber Content of the Latex

From Fig. 13 it will also be evident that the optimum concentrations of the creaming agent in three latices with a varying dry rubber content are different. To the extent that the latex is more dilute the optimum concentration of the creaming agent is increased while the rubber content of the cream is lowered. This has also been observed by Bondy (4). This investigator draws attention to the fact that "the structure of the primary agglomerates formed during the first stage of creaming determines the degree of packing in the cream ultimately obtained. The concentration of the dispersion at the start of aggregation appears to determine this structure."

When the cream obtained from a dilute latex is shaken vigorously and is then allowed to stand, another creaming occurs immediately and produces a much richer cream.

V. Discussion

When all the factors affecting the creaming are considered it will be seen that most of them can be reduced to changes in the viscosity. With this statement, however, the problem has not as yet been solved, because it is not clear why the viscosity should affect the ultimate outcome of the creaming.

The key to the problem is to be found in the observation discussed under Sections IV, 7 (pH) and IV, 8 (electrolyte concentration). It is a known fact that the colloidal behavior of the latex particles is controlled by the proteins adsorbed on the surface of the rubber particles, so that the electrical charge of the particles is greatly dependent upon the pH, as is the case with the proteins.

It is known, moreover, that the addition of electrolytes affects the electrokinetic potential of the colloid particles. As the electrokinetic potential in its turn depends upon the surface charge, we can reduce many of the phenomena here discussed to this potential.

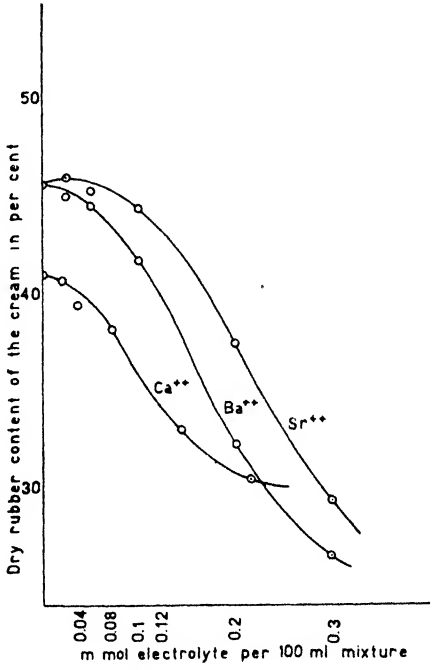

Fig. 11.—Effect of $CaCl_2$, $BaCl_2$ and $SrCl_2$ on the creaming of dialyzed latex of low protein content.

Before continuing the discussion of this point we must first draw attention to the following phenomenon.

When quartz particles are suspended in water and the suspension is allowed to stand, the quartz particles settle and have a certain volume, the so-called sedimentation volume. Now, Von Buzagh (23) has shown that when an electrolyte is added which lowers the electrokinetic potential of the particles, the sedimentation volume increases. If an electrolyte, such as aluminum chloride, is added which can reverse the charge of the quartz particles, surpassing a certain concentration will cause the sedimentation volume to decrease. See Fig. 14.

This phenomenon can be explained by the fact that the high electrokinetic potential of the particles causes them to repel each other strongly, so that they can slip easily past one another, effectively filling up the pores. Where the electrokinetic potential is lower the particles will cohere more readily, the slipping past each other being hindered.

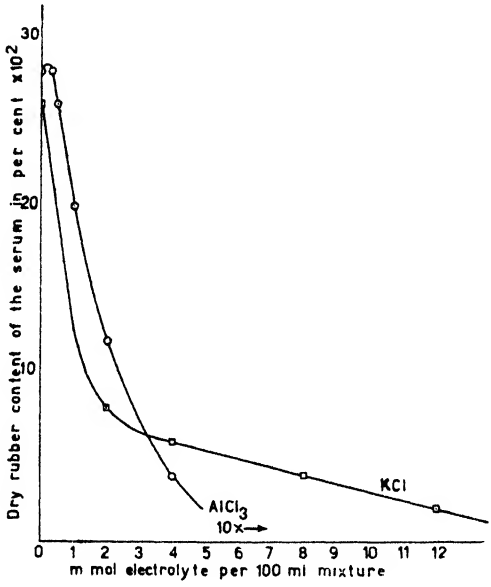

Fig. 12.—Effect of the electrolyte concentration on the dry rubber content of the serum.

1. Cluster Formation

We shall now proceed to give an explanation of the agglomeration, without which no creaming is possible. Freundlich (7) holds the opinion that we have to deal with a sensibilization ("sensitization"). This explanation, however, does not hold. In the first place, the creaming agent does not affect the stability of the latex (Baker, 2). In certain cases there is even an increase of the stability. Furthermore, Twiss and Carpenter (17) and also Bondy (4) have shown that the electrophoretic velocity of the latex particles is not affected when a creaming agent is added.

Bondy (4) and also Hauser and Dewey (10) assume that the creaming agent dehydrates the rubber particles. As a result of the decrease of the hydration forces, the particles attract one another in such manner that the resulting bond is wholly reversible. The following facts, however, oppose this view:

1. The creaming agent is strongly adsorbed to the rubber particles. This is doubted by Bondy and also by Hauser and Dewey but it is positively shown to be the case by Bächle (1) and also by Twiss and Carpenter (17).

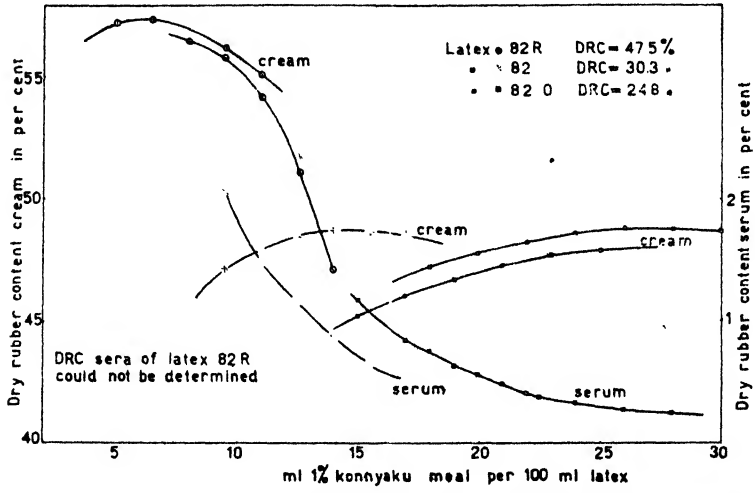

Fig. 13.—Dry rubber content of cream and serum as a function of the concentration of the creaming agent (konnyaku meal).

2. Dehydration increases with increase in temperature. We have observed that an increased temperature yields a more concentrated cream, but one also obtains a serum containing more rubber, which indicates that the agglomeration of the rubber particles is hampered.

3. When a creaming agent is added to latex, the viscosity is greatly increased, thus pointing to a coherence of the rubber particles induced by the molecules of the creaming agent.

4. The theory of Bondy cannot explain why enzymatic or thermal splitting of the creaming agent molecule causes the creaming power of the creaming agent to decline greatly.

Vester (22) also accepts dehydration as the cause of cluster formation. In contrast with the view of Bondy, however, he supposes that the creaming agent forms, together with the serum proteins, a viscous phase (coacervate) which surrounds the rubber particles and brings about their coherence. We were unable to confirm the microscopic observations of Vester concerning coacervate formation. Furthermore, it is contrary to Vester's view that latex poor in protein content and emulsions containing no proteins whatever can also be made to cream.

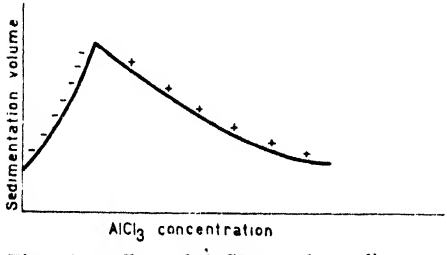

Fig. 14.—Effect of $AlCl_3$ on the sedimentation volume of quartz particles.

The explanation of Twiss and Carpenter is based on the view of McBain (11) that the high viscosity of hydrophilic colloids, to which the creaming agents also belong, is caused by the tendency of the particles to cohere, thus forming a network retaining the dispersing medium (water). This network resists deformations, which must occur when agitated or when flowing through a tube.

When a solution of a hydrophilic colloid is added to latex there is a linking up of the rubber particles with the molecules of the added colloid by adsorption at the boundary. If we keep in mind the fact that the particles of this colloid already are linked together, then we have here an explanation of the occurrence of the rubber particles in clusters.

We believe this view of Twiss and Carpenter to be very attractive. We also seek the solution of the cluster formation in the "anchoring effect," as it is called by the above-mentioned investigators. All creaming agents produce very viscous solutions which often gel easily and, in so far as is known, consist of long molecules.

2. *Explanation of the Creaming Phenomena*

We shall now proceed to investigate how the picture given here of the anchored rubber particles can provide an explanation for the various creaming phenomena.

Due to the anchoring of the rubber particles their Brownian move-

ment will be hindered, which enables the clusters to rise. This is the first phase of the creaming process and corresponds to the steep incline of the curve in Fig. 1. Then, and partly even simultaneously, a syneresis of the clustered mass occurs causing the particles to cohere more closely. This is the second phase of the process and corresponds to the part of the curve in Fig. 1 which runs almost horizontally. The phenomena described in Section III indicate that, as the packing becomes closer, a stronger bond is formed between the individual particles. To explain this we must go deeper into the forces of repulsion and attraction surrounding the rubber particle.

As is well known, latex and, even more so, latex cream are thixotropic systems. To explain the thixotropy Freundlich (8) and Hamaker (9) have submitted a theory in which they suppose that the London-van der Waals forces, which occur on the surface of a particle, take a course which causes such particles, at relatively large distances from the surfaces, to hold together reversibly. This reversible bond is the cause of the high viscosity. Through mechanical agitation the particles are torn loose from each other, with the result that the particles can move (slide) freely along one another, which manifests itself in the reduced viscosity.

The course of the above-mentioned forces of repulsion and attraction is depicted in Fig. 15. Instead of forces, we have plotted energies or potentials.

Curve A represents the course of the attraction energy. This energy is negative, but for the sake of clearness it has been drawn above the axis of abscissas. Curve R represents the repulsive energy. This energy is positive and has its source in the electrical and hydration forces which occur around the particle. The sum of A and R is represented by curve T.

When two particles approach each other they will be mutually attracted. In the energy minimum M_1 a certain state of equilibrium is produced. However, since this minimum is rather flat, the resulting bond is reversible. Where the particles collide with such force that the energy maximum T is exceeded, then a much stronger bond is suddenly formed resulting from the second energy minimum M_2 which is much lower. This bond is irreversible.

For the creaming phenomena discussed here the energy minimum M_1 is of some importance.

The London–van der Waals forces are determined by the substance of the particles and are not affected by the medium con-

taining the particles. The forces of repulsion, however, are largely dependent upon the adsorption layer (proteins) surrounding the particle, the *p*H and the electrolyte concentration of the medium.

As in the case of many colloids, it is quite probable that in latex also the charge is not distributed evenly over the surface of the

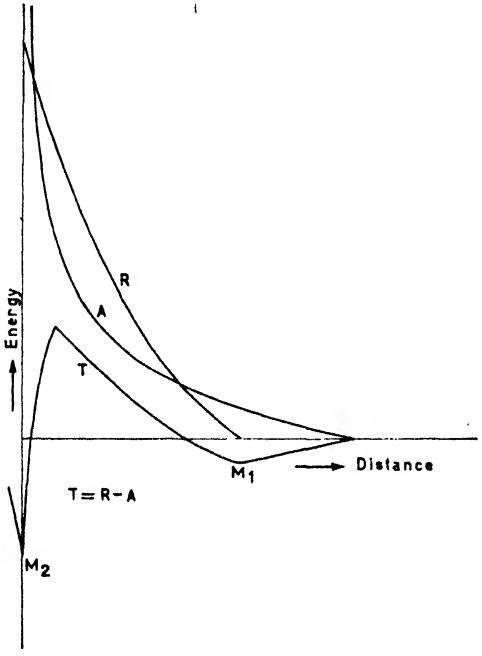

Fig. 15.—Forces of repulsion and attraction around the colloid particle.

particle. There are spots where the charge is large and where, therefore, the repulsive energies are great, whereas on other surface spots the charge is small. When the charge is sufficiently large, there will be no energy level M_1, and when the charge is small the energy level M_1 will attain a great depth. For the sake of briefness we shall, in the sequel, refer to repulsion spots and attraction spots.

In the freshly formed cream the particles will be disposed at random. However, since they have retained part of their Brownian movement, they will be able to dispose themselves gradually in such

manner as to take up a position in which the least number of their repulsion spots face each other. Therefore, the particles will vibrate and rotate until they have found the position producing the least energy. This is accompanied by a more compact structure, an enhanced mutual bond and an extrusion of serum.

It will now be clear why a higher temperature and mechanical agitation can induce a more compact structure (Section IV, 3 and 4). At the same time, at a higher temperature, it will be more difficult for the particles to be caught, thus allowing more rubber particles to enter the serum.

Also, when using too small an amount of creaming agent, the clusters will be incompletely formed. Many rubber particles are not "caught" and do not rise together with the clusters, so that they remain within the serum. Where we have used too much creaming agent the clusters become too stiff. The particles are no longer sufficiently mobile, and a more compact structure can be formed only with great difficulty (Section IV, 9).

The great influence exercised by the electrolyte concentration and by the *p*H must now also be clear. These factors control the course of the repulsion curve R, and therefore also the depth of the minimum M_1 (Fig. 15). The less pronounced these minima are and the fewer spots of attraction there are, the more easily the particles will slide along one another, and the more compact will be the ultimate structure (Section IV, 7 and 8).

The addition of soap results in a greater stability and also in a rise of the electrokinetic potential (Section IV, 6).

In addition, pre-coagulation results, as is well known, in a greater stability. Whether this goes side by side with a rise of the electrokinetic potential will still have to be investigated (Section IV, 5).

The manner in which the viscosity and the electrokinetic potential are interrelated requires no further elucidation.

It is clear now that the picture presented by Twiss and Carpenter can fully explain the creaming phenomena when it is extended in the manner we have indicated.

Bibliography

1. O. Bächle, *Kautschuk*, **12**, 232 (1936).
2. H. C. Baker, *Trans. Inst. Rubber Ind.*, **13**, 70 (1937).
3. R. O. Bishop and R. G. Fullerton, *Latex Preservation and Shipment*,

Planting Manual No. 4, Rubber Research Institute of Malaya, Kuala Lumpur, July, 1932.

4. C. Bondy, *Trans. Faraday Soc.*, **35,** 1093 (1939).

5. Centrale Proefstations Vereeniging, Netherlands Pat. 44,006.

6. J. E. De Groot, C. J. Van Hulssen and D. R. Koolhaas, *Chem. Weekblad*, **36,** 69 (1939).

7. H. Freundlich, *Kapillarchemie*, Vol. II, Akad. Verlagsgesellschaft, Leipzig, 1932, p. 471; *The Chemistry of Rubber*, Methuen, London, 1935, p. 11.

8. H. Freundlich, *Thixotropy*, Hermann, Paris, 1935, p. 19.

9. H. C. Hamaker, *Rec. trav. chim.*, **55,** 1015 (1936); **56,** 1, 727 (1937).

10. E. A. Hauser and Bradley Dewey, *Ind. Eng. Chem.*, **33,** 127 (1941).

11. J. W. McBain, *J. Phys. Chem.*, **30,** 239, 313 (1926).

12. Naugatuck Chemical Co., British Pat. 344,647, March 16, 1929.

13. Naugatuck Chemical Co., Netherlands Pat. Appl. 35,737, May 16, 1935.

14. Naugatuck Chemical Co., Netherlands Pat. Appl. 65,196.

15. E. Rhodes, *India Rubber J.*, **97,** 51 (1939).

16. Rubber Cultuur Maatschappij Amsterdam, Netherlands Pat. Appl. 70,520.

17. D. F. Twiss and A. S. Carpenter, *Proc. Rubber Techn. Conference*, London, 1938, p. 81.

18. J. W. Van Dalfsen, *Arch. Rubbercultuur*, **23,** 1 (1939).

19. G. E. Van Gils, *Ibid.*, **23,** 130 (1939); reprinted in *Rubber Chem. Tech.*, **13,** 422 (1940).

20. G. E. Van Gils, *Arch. Rubbercultuur*, **23,** 256 (1939); reprinted in *Rubber Chem. Tech.*, **13,** 761 (1940).

21. F. K. Th. Van Iterson, *Proc. Acad. Sci. Amsterdam*, **41,** 81 (Jan., 1938).

22. C. F. Vester, *Proc. Rubber Techn. Conference*, London, 1938, p. 126.

23. A. Von Buzagh, *Kolloidik*, T. Steinkopff, Dresden and Leipzig, 1936, p. 172; *Colloid Systems*, Tech. Press, London, 1937, p. 166; *Kolloidchem. Beih.*, **32,** 114 (1930).

STREAMING BIREFRINGENCE AND ITS RELATION TO PARTICLE SIZE AND SHAPE

JOHN T. EDSALL

Department of Physical Chemistry, Harvard Medical School, Boston, Mass.

CONTENTS

I. Introduction

It was observed by J. Clerk Maxwell (36) in 1870 that Canada balsam, although normally isotropic, becomes birefringent when subjected to shearing stress, the birefringence disappearing as soon as the stress is removed. Similar observations on liquids were made about the same time by Ernst Mach in Vienna, and the phenomenon was further studied by several investigators (30, 10, 69) in the following quarter century, who worked on various oils and resins, and on such systems as collodion. However, the relation between the observed phenomena and the shape of the molecules (or particles) in the liquids was not apprehended by these authors. It first became apparent through the studies of Freundlich, Zocher and their collaborators, beginning about 1916, that streaming double refraction in colloidal solutions was associated with the orientation of rod-shaped or disc-shaped particles. The effect appeared with particular intensity in sols of vanadium pentoxide, which were intensively studied by Freundlich, Stapelfeldt and Zocher (14). These sols were known on other grounds to consist of needle-shaped particles which gradually increased in length on standing. In 1930, the principal protein of striated muscle, the globulin, myosin, was shown by von Muralt and Edsall (39) to give intense double refraction of flow. Simultaneously with their report appeared the first communication by Signer (58), describing the same phenomenon in some of the synthetic polymers prepared by Staudinger and his school. The work of Vorländer and his collaborators (70, 71, 72) demonstrated the existence of similar, although far less intense, effects in pure organic liquids. Here again the magnitude of the double refraction was found to be greatest for elongated molecules, and practically zero for nearly spherical ones. During the last ten years a number of important studies, both experimental and theoretical, have greatly clarified our understanding of the phenomena involved, and have shown that the method is a powerful tool in the determination of molecular size and shape.

II. Position of the Optic Axis and Magnitude of Double Refraction in a Flowing Liquid

We shall now describe briefly the observed phenomena, before treating in detail the methods for producing and measuring them. The effect is most clearly seen when the liquid to be studied is placed in the annular space between two coaxial cylinders, one cylinder being

rotated while the other is held fixed. When observed between crossed nicol prisms or Polaroids, the liquid is isotropic and dark when at rest. On setting one cylinder into motion, the annular space becomes bright, except for a dark cross with four arms, each 90° from its neighbors. The position of this "cross of isocline" in various cases is represented in Fig. 1, the direction of the beam of light used for observation being perpendicular to the plane of the paper. The arms of the cross may coincide with the planes of vibration, *PP* and *AA*, of the light transmitted by the polarizer and analyzer, respectively (Fig. 1-*a*); they may be at 45° to these planes (Fig. 1-*b*); or they may lie in some intermediate position (Fig. 1-*c*). The larger

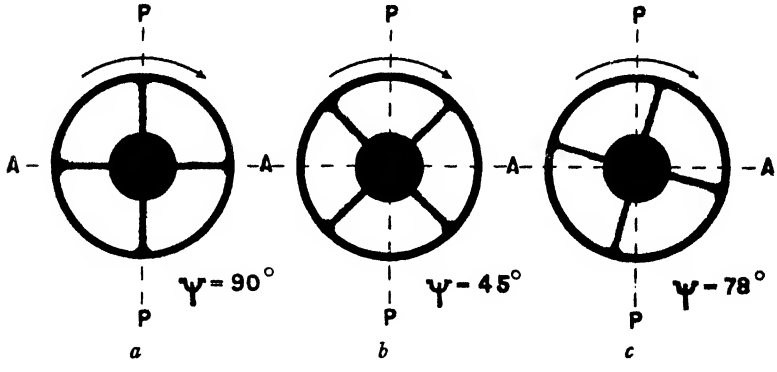

Fig. 1.—The cross of isocline, as it appears in a solution of ovoglobulin (*a*); of low molecular weight polystyrene (*b*); and of concentrated myosin (*c*).

of the two angles between the cross of isocline and the planes *PP* and *AA* is known as the "angle of isocline," Ψ (39).[1]

Consider now the motion of the liquid between the cylinders. If the outer cylinder rotates, as indicated in Fig. 1, with angular velocity Ω, the layer of liquid immediately adjacent to it moves with the same velocity. The layer of liquid immediately adjacent to the fixed inner cylinder remains at rest. If the flow of the liquid is laminar, not turbulent,[2] the intermediate layers of liquid move with different velocities, varying continuously from zero at the inner cylinder to Ω at the outer. The direction of the stream lines at any

[1] The corresponding German term is "Kreuzwinkel" (14).

[2] The conditions determining whether the flow is laminar are discussed below, under Experimental Methods.

point is normal to the radius vector drawn from the center of the inner cylinder to that point. The four arms of the cross of isocline appear in those regions in which the optic axis of the flowing liquid is parallel (or perpendicular) to PP or AA. The angle between the optic axis and the stream lines—known as the "extinction angle," χ—is always between 0° and 45°. Thus the extinction angle is the complement of the angle of isocline ($\Psi + \chi = 90°$), and either of these angles may be used to define the position of the optic axis. In the following discussion, we shall employ the extinction angle χ in describing the data.

The refractive index for light vibrating with the electric vector parallel to the optic axis may be denoted by the symbol n_e; for light vibrating perpendicular to this axis, by n_o. If $n_e > n_o$, the double refraction of the liquid is defined as optically positive; if $n_e < n_o$, as negative.[3]

The problem of the investigator in this field is to determine the extinction angle and the double refraction, $n_e - n_o$, as a function of velocity gradient, and to relate them to the properties of the particles or molecules in the liquid. Important parameters which must be known in order to interpret the results are temperature, viscosity and the concentration of the solute. In general it is necessary to work at low concentrations, where the solute molecules are far apart, if the results obtained are to be used in evaluating the size and shape of the particles.

III. Experimental Methods

1. Concentric Cylinder Apparatus: Conditions for Laminar Flow

The essential condition for the appearance of double refraction of flow is the production of a velocity gradient in the flowing liquid. The degree of orientation of the particles to be studied depends primarily upon the length of the particles, the viscosity of the medium and the magnitude of the velocity gradient. Small gradients suffice to produce a considerable degree of orientation of very long particles, such as old vanadium pentoxide sols, or myosin; in the study of

[3] Signer (58) has chosen for optically negative liquids, such as polystyrene solutions, to define the angle of isocline as lying between 135° and 180°; that is, as equal to $\Psi + 90°$, where Ψ is defined according to our convention. Signer's convention is chosen simply to define automatically the sign of the double refraction by the values reported for the isocline measurements.

shorter particles, very much higher gradients may be required. Well-defined velocity gradients are most readily produced, for experimental study, by the laminar flow of a liquid between two concentric cylinders; and this arrangement is also very suitable for making the necessary optical measurements on the system. The design and use of the concentric cylinder apparatus will therefore be described first; other techniques which have been found useful will be described more briefly at the end of this section.

In the concentric cylinder apparatus, one cylinder is held fixed, while the other rotates with a given angular velocity, Ω. Either the inner or the outer cylinder may be chosen as the rotor; both arrangements have been used in practice, by different investigators. If the velocity gradient is to be a clearly defined quantity, it is essential that the flow should be laminar, so that the stream lines are at every point perpendicular to the radius vector drawn to the point from the center of the inner cylinder. It is well known that many types of flow are laminar only below a certain critical velocity, which is dependent in general on the dimensions of the system, and on the kinematic viscosity[4] of the liquid (see for instance Hatschek (22)). Above this critical velocity turbulent flow sets in; and the optical properties of a birefringent liquid in turbulent flow are not at present amenable to any theoretical treatment. The stability of flow of a viscous liquid between concentric cylinders has been the subject of a very thorough theoretical and experimental study by G. I. Taylor (68). Both theory and experiment showed that if the inner cylinder rotates, while the outer one is fixed, the critical angular velocity Ω_c is given by the equation

$$\frac{\Omega_c^2}{(\eta/\rho)^2} = \frac{\pi^4}{2P} \frac{(R_1 + R_2)}{d^3 R_1^2} \tag{1}$$

Here η is the viscosity of the liquid, ρ its density, R_1 and R_2 are the radii of the inner and outer cylinders, respectively, and d is $R_2 - R_1$, the width of the gap between them. P is a numerical factor given by the equation:

$$P = 0.0571\,(1 - 0.652\,d/R_1) + \frac{0.00056}{1 - 0.652\,d/R_1} \tag{2}$$

This means in practice that if the gap between the cylinders is small ($d \ll R_1$), the critical angular velocity above which turbulent flow

[4] The kinematic viscosity of a liquid is the ratio of its viscosity coefficient to its density.

occurs is very nearly inversely proportional to the three-halves power of the gap. It is also directly proportional to the viscosity of the liquid. Concerning possible limitations of formula (1), see Buchheim, Stuart and Menz (7).

If, on the other hand, the outer cylinder rotates and the inner one is fixed, Taylor's theoretical analysis led to the conclusion that flow should be laminar at all speeds of rotation, and his experiments, at the highest speeds he then attained, were in harmony with this conclusion. In a later study, however, Taylor (68a) was able to produce turbulent flow with the outer cylinder rotating, but only at much higher speeds than when the inner cylinder was the rotor. The ratio of the critical speeds was a function of d/R_2; for $d/R_2 = 0.38$ the ratio was over 1000; for $d/R_2 = 0.1$ it was about 50; for $d/R_2 = 0.017$ it was 6. There is thus a great theoretical advantage, if turbulent flow is to be avoided, in making the outer cylinder the rotor, although this advantage becomes less marked as the gap between the cylinders is narrowed.

Actually, most investigators have made the inner cylinder the rotor. It is easier, with this arrangement, to hold the rotor in place with bearings fixed both above and below it, so that it rotates steadily about its axis even at high speeds. Also, it is important, since measurements should be made at constant temperatures, that water from a thermostat should be kept circulating around the outer cylinder. This is most easily achieved if the outer cylinder is fixed.

The velocity gradient in the flowing liquid, at the distance r from the center of the inner cylinder is (if the outer cylinder rotates with angular velocity Ω):

$$G = \frac{dV}{dr} = 2\Omega \frac{\frac{1}{r^2}}{\frac{1}{R_1^2} - \frac{1}{R_2^2}} \tag{3}$$

where R_1 and R_2 have the same meaning as in equations (1) and (2), and V is the velocity of the liquid at the point considered.

If the inner cylinder rotates with angular velocity Ω, the velocity gradient is:

$$G = \frac{dV}{dr} = \frac{\Omega R_1^2}{R_1^2 - R_2^2}\left(1 + \frac{R_2^2}{r^2}\right) \tag{4}$$

If $d \ll R_1$ ($d = R_2 - R_1$), these equations both approximate closely to the simple relation:

$$G \cong \frac{R_1\Omega}{d} \cong \frac{R_2\Omega}{d} \tag{5}$$

Under these conditions G is practically the same at all points in the liquid. For the derivation of (3) and (4), see for instance Page (46) or Hatschek (22). The dimensions of G are t^{-1}; it is commonly expressed in sec.$^{-1}$.

Corresponding to the critical angular velocity, Ω_c, defined by (1), there is thus a critical velocity gradient G_c, defined by (4) or (5). Above this gradient (in the apparatus with rotating inner cylinder), turbulent flow may be expected to set in.

TABLE I

DIMENSIONS OF CYLINDERS IN APPARATUS USED BY VARIOUS INVESTIGATORS, AND CRITICAL VELOCITY GRADIENTS

Authors	R_1	d	l	$G_c \times 10^{-4}$	$G_c\left(\frac{H_2O}{20°}\right)$
Vorländer and Walter (70)	1.05	0.10	4.6	1.42 ν	142
Signer and Gross (61)	2.470	0.0252	4.5	65 ν	6500
Nitschmann (42)	2.475	0.0427	4.44	17.5 ν	1750
Nitschmann and Guggisberg (43)	2.480	0.0209	4.65	103 ν	10300
Sadron (51) (52)	2.420	0.130	10	0.99 ν	99.4
Sadron (51) (52)	2.500	0.050	10	11.9 ν	1190
Sadron (51) (52)	2.528	0.022	10	91.4 ν	9140
von Muralt and Edsall (39)	0.91	1.09	9.9	(10 ν)	(1000)
von Muralt and Edsall (39)	1.30	0.70	9.9	(18 ν)	(1800)

All dimensions in centimeters.

R_1 = radius of inner cylinder; $d = R_2 - R_1$ = width of gap between cylinders; l = height of inner cylinder; G_c = critical velocity gradient for onset of turbulent flow; $G_c\left(\frac{H_2O}{20°}\right) = G_c$ for water at 20°C. ν = kinematic viscosity = viscosity coefficient ÷ density.

Rough values for the apparatus of von Muralt and Edsall are calculated from equations (1) and (2), and the studies of Taylor (68a, see especially Taylor's Fig. 11), on apparatus with rotating outer cylinder.

Vorländer and Kirchner (71) have used very long cylinders (up to 1 meter in length) but the values of R_1 and d employed by them were nearly the same as those employed by Vorländer and Walter.

In Table I, the dimensions of the inner and outer cylinders employed by various investigators are listed, with the corresponding values of the critical velocity gradients. These are significant, since several of these authors have reported measurements of double re-

fraction of flow at gradients considerably above these critical values. This is particularly true of a number of the measurements of Vorländer and his collaborators (70, 71) as Sadron (52) has pointed out. No quantitative significance can be ascribed to such measurements, although they are of the right order of magnitude. The effect of turbulent flow may be particularly deceptive, since measurements of the extinction angle and the double refraction may show no very sharp

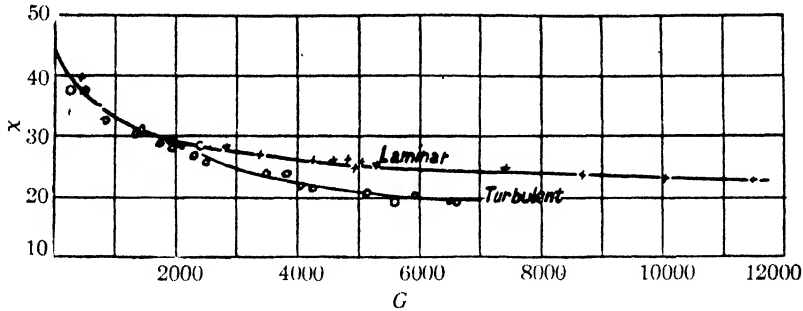

Fig. 2.—Extinction angle of nitrocellulose in cyclohexanone; effect of turbulent flow is seen in lower curve, for values of G above 2400 sec.$^{-1}$.

break between the regions of laminar and turbulent flow, although a break of some sort is always found. Fig. 2 shows the effect of turbulence on the position of the extinction angle in a solution of nitrocellulose dissolved in cyclohexanone (Sadron). Sadron has shown that turbulent flow may give either too high or too low values of the double refraction, according to circumstances.

The cylinders employed may be of various materials. Von Muralt and Edsall (39) used a glass outer cylinder, and an inner cylinder of chromium-plated brass (the chromium plating proved more inert toward proteins than any other metal tested). Signer (58) and Signer and Gross (61) employed cylinders made of very resistant plastics, which gave very good results; but for work of the highest precision, metal cylinders are practically necessary, as in the work of Sadron (51). Recently, Nitschmann and Guggisberg (43), in Signer's laboratory, have employed cylinders of stainless steel.

2. *The Optical Bench: Measurement of Extinction Angle*

The concentric cylinders form only one component of the apparatus for investigating double refraction of flow. The cylinders must be

carefully aligned on an optical bench which carries a light source, a polarizer and analyzer, condensing lenses and suitable devices for measuring the double refraction (see below).[5]

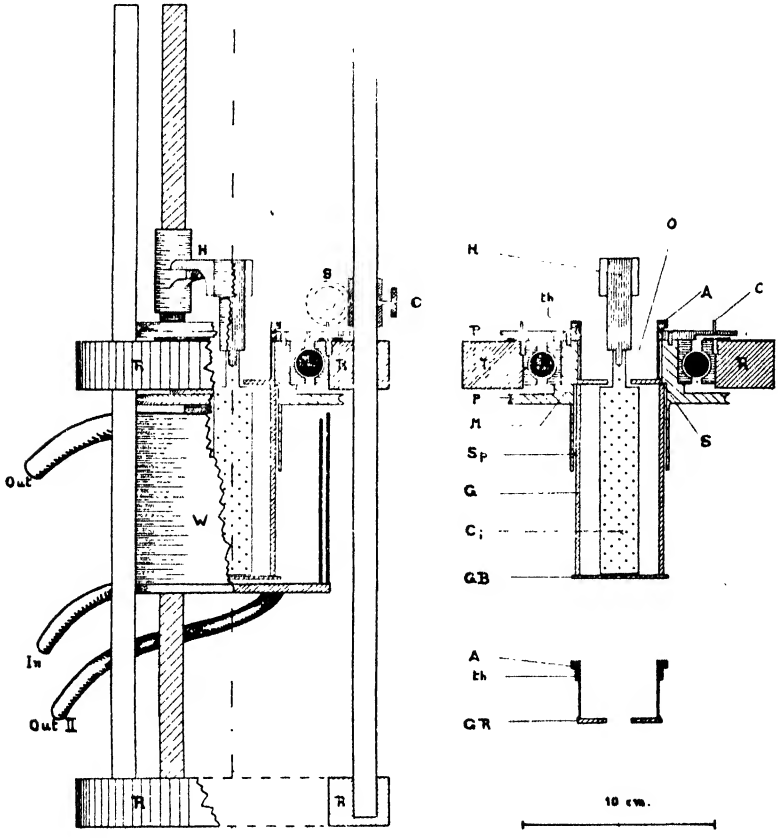

Fig. 3.—Details of concentric cylinder apparatus with rotating outer cylinder. *G*, glass outer cylinder; C_1, inner cylinder, chromium plated brass. *RR*, cast iron rings; outer cylinder rotates on ball bearings located within the upper ring. *W*, water jacket; *In* and *Out* denote inlet and outlet of water circulating system around outer cylinder. *H*, holder for inner cylinder. For further details see original paper.

Fig. 3 shows, as one representative of such systems, the concentric

[5] Signer (58) and Boehm (4, p. 4002) have developed very useful and compact types of apparatus, in which the concentric cylinder system is mounted on the stand of a polarizing microscope.

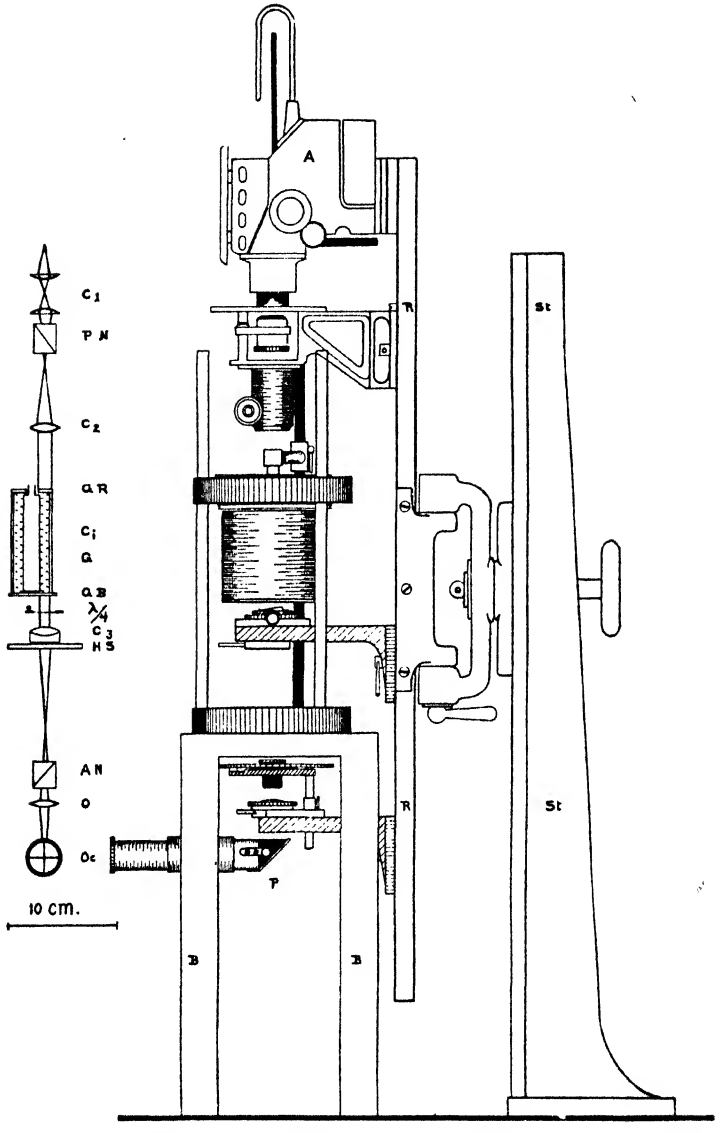

Fig. 4.—Optical bench used with cylinders shown in Fig. 3. *St*, cast-iron stand; *RR*, holder for movable riders. *BB*, separate bench supporting concentric cylinders. *A*, carbon arc lamp (later replaced by small high-pressure mercury arc). *P*, silvered reversing prism. C_1, C_2, C_3, condensing lenses; *PN*, polarizer; *AN*, analyzer; C_i, cylinders with liquid between; $\lambda/4$, quarter-wave plates; *HS*, half-shadow wedge; *O*, objective; *Oc*, ocular.

cylinder apparatus of von Muralt (39), and Fig. 4 shows the relations of the cylinders in the same apparatus to the entire optical system. All the optical parts are mounted separately in special riders on a large universal optical bench (manufactured by E. Leitz, Wetzlar) on which they can slide up and down on cast iron rails. The concentric cylinder apparatus rests on a separate stand; its position must be very carefully adjusted (for details see the original paper). For measurements of the extinction angle in the flowing liquid, the crossed polarizer and analyzer are rigidly coupled by a vertical rod with side arms attached to the nicol prisms (*AN* and *PN* in Fig. 4); thus the two nicols are rotated together until one arm of the cross of isocline is on the center of the cross hairs in the ocular *Oc.* The corresponding angle is then read on a circular scale attached to the analyzer. (During these measurements, the light beam passes directly from the space between the concentric cylinders to the analyzer *AN* in Fig. 4; the intervening components of the optical system shown in this figure are removed.) To determine the plane of vibration of the light transmitted by the nicols (*PP* and *AA*, Fig. 1) the rotation of the outer cylinder is stopped, and a quartz wedge is introduced at the position marked *HS* in Fig. 4. The optic axis of this wedge is parallel to its long axis, which is fixed parallel to the stream lines. The crossed nicols are now rotated until the field is again dark. The corresponding angle on the analyzer scale is read; the difference between this and the angle found for the cross of isocline is the extinction angle, χ (if it lies between 0° and 45°) or its complement, the angle of isocline, Ψ (if it lies between 45° and 90°).

3. *Measurement of Double Refraction,* $n_e - n_o$[6]

In all methods the first step is to set the crossed nicols at 45° to the position of the cross of isocline. The initially plane polarized light may then be considered as being resolved, during its passage through the liquid, into two plane polarized components of equal amplitude traveling with different speeds; one vibrating parallel to the optic axis (velocity c/n_e);[7] the other vibrating perpendicular to the optic axis (velocity c/n_o). These emerge from the liquid with a phase difference Δp, given by the relation

$$\Delta p = \frac{S}{\lambda_0}(n_e - n_o) \tag{6}$$

[6] Concerning double refraction and its measurement in general, see for instance Wood (76) and Hartshorne and Stuart (21).

[7] Here c is the velocity of light *in vacuo.*

Here λ_0 is the wavelength *in vacuo* of the incident light, and S is the length of the path traversed in the liquid, expressed in the same units as λ_0. Thus the emergent light is in general elliptically polarized because of this phase difference.

Δp, and hence $n_e - n_o$, may be determined by a compensator. The Senarmont compensator employed by von Muralt and Edsall (39), Sadron (51), Signer and Gross (61) and others consists of a birefringent plate ($\lambda/4$ in Fig. 4) with a phase difference of a quarter wavelength between the two components vibrating parallel and perpendicular to its optic axis. If this plate is set with its optic axis parallel (or perpendicular) to *PP* or *AA*, the elliptically polarized light emerging from the liquid is transformed into plane polarized light. Its plane of polarization has been rotated through an angle, Δ, given by the equation

$$\Delta = 180\Delta p = \frac{180S}{\lambda_0}(n_e - n_o) \tag{7}$$

Δ may be determined by rotating the analyzer (which now is set to turn freely without altering the position of the polarizer), until the light is again extinguished. The half-shadow wedge, *IIS*, in Fig. 4, is inserted to make the readings more accurate. This method is very good if the magnitude of Δ is between a few degrees and 180°. For larger, phase differences a Babinet compensator (see (21), (76) or (14)) should be used. The Brace compensator employed by Björnståhl and Snellman (64a) is valuable for the measurement of very small phase differences.

These methods involve the use of monochromatic light. Signer (58) and others have employed a technique utilizing plane polarized white light, which after traversing the liquid is passed through a birefringent plate with a full wavelength retardation (for instance, a gypsum first-order-red plate), and then through the analyzer. On resolving the emerging light in a spectroscope, a narrow dark band is seen in the spectrum. If the liquid is at rest, the center of the band is at the wavelength, λ, characteristic of the plate employed. When the liquid is set into motion, this band shifts to the wavelength $\lambda' = \lambda + \Delta\lambda$, where

$$\Delta\lambda = S(n_e - n_o) \tag{8}$$

Thus the shift of the band indicates the sign as well as the magnitude of the double refraction. This method is less sensitive than the

others, and requires an extremely intense light source; nevertheless it has been found very useful by several investigators.

When the gap between the cylinders is very narrow, as is necessary when very high velocity gradients must be attained for the orientation of small molecules, the optical measurements become much more difficult. The alignment of the apparatus must be extremely precise, and light reflected from the sides of the cylinders tends to distort the effects produced by the light transmitted through the liquid. Concerning some of the means employed to overcome these difficulties, see Frey-Wyssling and Weber (15). Björnståhl (2a) has explained in detail the optical systems most effective in giving maximum intensity of transmitted light, and eliminating reflected light.

A simpler type of concentric cylinder apparatus, useful for studies at low velocity gradients, has been designed by J. W. Mehl and the author, and constructed by Mr. David W. Mann. This apparatus has already been employed by Mehl (38) in studies on proteins of smooth muscle, and by H. O. Singher in unpublished studies on myosin in the writer's laboratory. The details of the apparatus will be reported later.

4. Observations of Flow in Tubes

The velocity gradients produced by flow of a liquid in a narrow tube can also be used in the production of streaming birefringence, polarized light passing through the liquid perpendicular to the direction of flow. Systems of this type were employed by Freundlich, Stapelfeldt and Zocher (14) in their study of vanadium pentoxide sol, the double refraction being determined with a Babinet compensator. Recently Lauffer and Stanley (32) employed a similar method in the study of tobacco mosaic and other viruses. They employed a photoelectric meter to determine the intensity of the elliptically polarized light. Other types of apparatus involving flow through tubes are described in considerable detail in the review by Boehm (4).

This type of apparatus is generally simpler to construct and operate than the concentric cylinder type. It has two serious disadvantages: (*1*) It is not adapted for the determination of the extinction angle, which is intimately related to molecular size and shape. (*2*) The velocity gradient is not constant throughout the region traversed by the light beam, as in the cylinder apparatus; instead the gradient

varies from zero at the center of the tube to a high value near the walls. Hence there is no uniquely defined value of the velocity gradient which can be correlated with a given double refraction measurement.

5. *Qualitative Methods of Observation*

If it is simply desired to detect double refraction of flow in a liquid which shows the effect strongly, or to detect gross changes in the magnitude of birefringence, the liquid may be placed in a small beaker, stirred with a glass rod and observed between crossed nicols or Polaroids. In solutions of substances such as myosin, tobacco mosaic virus or vanadium pentoxide sols, the liquid lights up brilliantly on stirring with a slow rotary motion, and the cross of isocline is clearly visible. The beaker used should be of glass which is nearly isotropic, and the glass rod used for stirring should be painted black. This method has been used by Edsall and Mehl (12) in studying the loss of birefringence in myosin produced by a great number of reagents, and by Greenstein and Jenrette (19) in a similar study of sodium thymonucleate.

Langmuir (34) has studied bentonite sols by sealing samples in glass tubes containing some air. The tubes were then tilted so that air bubbles passed slowly through the sol; the tubes were then placed in a rack and observed between crossed Polaroids. By this means Langmuir followed the decay of birefringence with time, and thus obtained evidence concerning relaxation times (see below) in these systems.

IV. Experimental Results and Their Theoretical Interpretation

1. *General Character of the Experimental Data*

From the many data now available, certain simple and definite relations emerge, which must be explained by any satisfactory theory.

In pure liquids, the extinction angle is always 45° (within the probable error of ±2°), and the double refraction is a linear function of the velocity gradient (70, 71, 72, 51, 52, 7, 64a). Table II gives some recent typical data of Buchheim, Stuart and Menz (7), as well as data by Sadron and by Vörlander. These are expressed in terms of the "Maxwell constant" or "dynamo-optic constant," M, defined by Sadron (51, 52) by the equation:

$$n_e - n_o = MG \qquad (9)$$

TABLE II

MAXWELL CONSTANTS FOR CERTAIN ORGANIC LIQUIDS†

Substance	Vorländer and Fischer (white light)			Sadron (λ = 546 mμ)			Buchheim, Stuart, Menz (λ = 546 mμ)		
	t° C.	η (recalcd.) poise	$M' \times 10^{12}$	t° C.	η poise	$M' \times 10^{12}$	t° C.	η poise	$M' \times 10^{12}$
Phenylethyl alcohol *prim.*			...	18		17.5	16	0.165	17.00
Nitrobenzene	17	0.0215	16.9	20	0.020	9.3			3.00
Aniline	16	0.0493	8.85	18	0.048	6.7			6.00
Heptyl alcohol *prim.*			...	20	0.070	4.5	16	0.0466	2.72
o-Dichlorobenzene	17	0.0142	5.82			..	15	0.0139	4.00
p-Xylene	16	0.007	2.65			..	16	0.0067	1.84
Chlorobenzene	15	0.009	2.14			..	16	0.0085	1.59
o-Xylene	16	0.0088	2.08			..	16	0.0078	1.43
m-Xylene	17	0.0065	1.62			..	16	0.0065	1.25
Toluene	17	0.0062	1.06			..	15	0.0062	0.97
Benzene	18	0.0065	0.57			..	15.5	0.0069	0.67

† From Buchheim, Stuart and Menz (7).

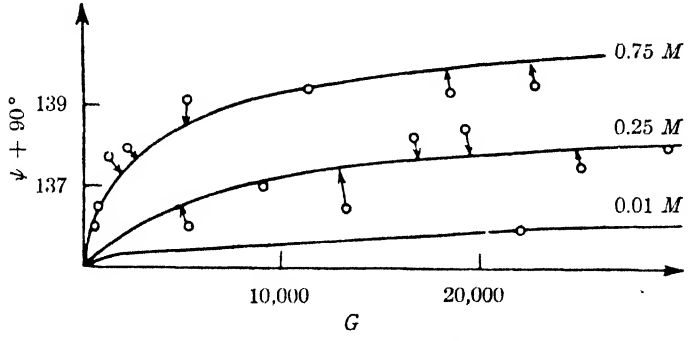

Fig. 5.—Angle of isocline as a function of velocity gradient in low molecular weight polystyrene, $0.1 m_o[\eta] = 5.6$.

In colloidal solutions, the extinction angle approaches 45° at low velocity gradients. As the gradient increases, however, χ decreases, and for long particles at very high gradients the optic axis may approach parallelism with the stream lines ($\chi = 0°$). Indeed,

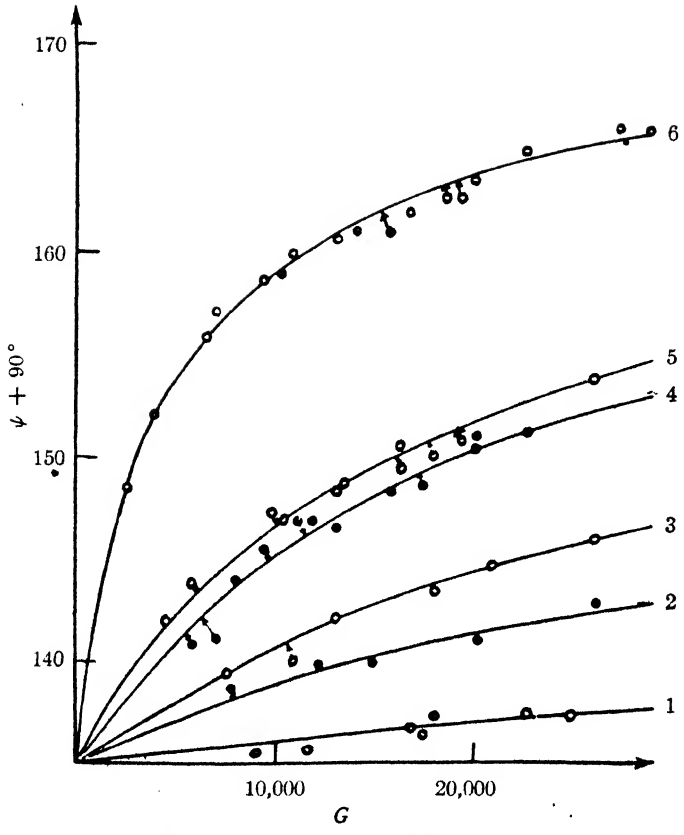

Fig. 6.—Angle of isocline of six nitrocellulose preparations of different molecular weights, as a function of velocity gradient, G. The six preparations are characterized as follows:

1. $0.1m_o[\eta] = 17$; conc. 0.035 mol.
2. $0.1m_o[\eta] = 33$; conc. 0.015 mol.
3. $0.1m_o[\eta] = 55$; conc. 0.010 mol.
4. $0.1m_o[\eta] = 100$; conc. 0.005 mol.
5. $0.1m_o[\eta] = 115$; conc. 0.005 mol.
6. $0.1m_o[\eta] = 245$; conc. 0 002 mol.

Boehm and Signer (5) found that ovoglobulin gives $\chi = 0°$ for all velocity gradients at which its double refraction is measurable.[8]

[8] The protein they studied may actually have been ovomucoid rather than ovoglobulin. See Needham and Robinson (40).

Typical measurements are shown in Figs. 5 and 6, taken from the work of Signer and Gross (61). The former figure shows that polystyrene of low molecular weight gives extinction angles differing only very slightly from 45°, even at very high velocity gradients. On the other hand, polystyrenes of high molecular weight (not shown in the figures) give extinction angles of 5° to 10° in the same range of velocity gradients. Fig. 6 shows the extinction angles of six nitrocellulose solutions of different molecular weight, dissolved in cyclohexanone. With increase of molecular weight, the extinction angle at a given velocity gradient progressively decreases; that is, the optic axis sets itself more nearly parallel to the stream lines. The relative molecular weights are approximately given by the ratio of specific viscosity to concentration, at high dilution. The specific viscosity is defined as

$$\eta_{sp} = \eta/\eta_0 - 1 \tag{10}$$

where η is the viscosity of the solution, and η_0 that of the pure solvent.

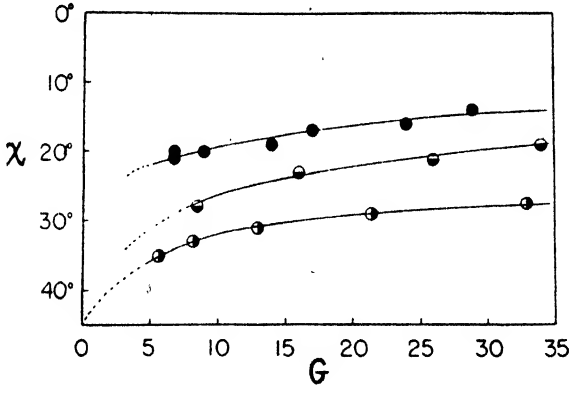

Fig. 7.—The extinction angle χ, as a function of the velocity gradient, G (sec.$^{-1}$). ●, snail myosin (at 25°), conc 5.3×10^{-4} g. N/cc.; ◑, octopus myosin (25°), 5.9×10^{-4} g. N/cc.; ◒, rabbit myosin (3°), 4.5×10^{-4} g. N/cc.

In Fig. 7, similar curves are shown for three different types of myosin, studied by Mehl (38) and by von Muralt and Edsall (39). The general character of the curves is similar to those for polystyrene and nitrocellulose, but here it is to be noted that the velocity gradients employed are of an altogether lower order of magnitude (5 to 35

sec.$^{-1}$ instead of 5000 to 30,000 sec.$^{-1}$). Since, as we shall see, the position of the extinction angle is an index of the degree of orienta-

TABLE III

POLYSTYRENES OF LOW MOLECULAR WEIGHT IN CYCLOHEXANONE

$0.1 m_0[\eta]$	c	$\eta_{abs.}$	η_{sp}	$\frac{n_e - n_0}{G} \times 10^{10}$	$\frac{n_e - n_0}{G\eta c} \times 10^{10}$
0.6	0.5	0.0298	0.33	0.0388	2.60
	0.75	0.0388	0.73	0.0736	2.53
	1.0	0.0475	1.12	0.121	2.55
1.0	0.4	0.0314	0.40	0.050	4.00
	0.75	0.0428	0.91	0.125	3.90
1.6	0.2	0.0298	0.33	0.0413	6.93
	0.4	0.0395	0.76	0.113	7.15
	0.5	0.051	1.01	0.165	7.31
	0.55	0.0484	1.16	0.190	7.13
	0.6	0.0518	1.31	0.230	7.40
	0.75	0.0627	1.80	0.302	6.43
2.2	0.125	0.0288	0.28	0.0378	10.7
	0.2	0.0330	0.48	0.0742	11.2
	0.25	0.0363	0.62	0.0990	10.9
	0.3	0.0403	0.80	0.137	11.3
	0.35	0.0438	0.96	0.163	10.6
	0.5	0.0567	1.53	0.268	9.45
	1.0	0.126	4.55	0.959	7.61
2.7	0.1	0.0284	0.27	0.0381	13.4
	0.2	0.0357	0.59	0.0886	12.4
	0.3	0.0440	0.96	0.165	12.5
5.6	0.03	0.0261	0.17	0.0182	23.3
	0.05	0.0287	0.28	0.0353	24.6
	0.075	0.0325	0.45	0.0582	23.9
	0.09	0.0348	0.55	0.0790	25.2
	0.1	0.0364	0.63	0.0910	25.0
	0.125	0.0408	0.82	0.123	24.4
	0.25	0.0668	1.98	0.312	18.7
	0.5	0.146	5.50	1.08	14.8
	0.75	0.279	11.4	2.34	11.2

m_0 here denotes the mol. wt. of the unit from which the polymer is built up (m_0 = 104 for polystyrene), and $[\eta]$ is the intrinsic viscosity, defined by Kraemer and Lansing (27a) as $[\eta] = \lim_{c \to 0} \left(\frac{\eta_{sp}}{c}\right)$. Here c = g. solute per 100 cc. solution.

Extinction angle χ was 45° in all solutions except the last five listed here. For the values of χ in these solutions see Fig. 5. (From Signer and Gross (61)).

tion of the particles in solution, the myosin particles (or molecules) must be much more elongated than those of polystyrene or nitrocellulose, and are therefore more readily oriented.

The double refraction of a low molecular weight polystyrene is shown in Fig. 8. At all concentrations, $n_e - n_o$ is a linear function of

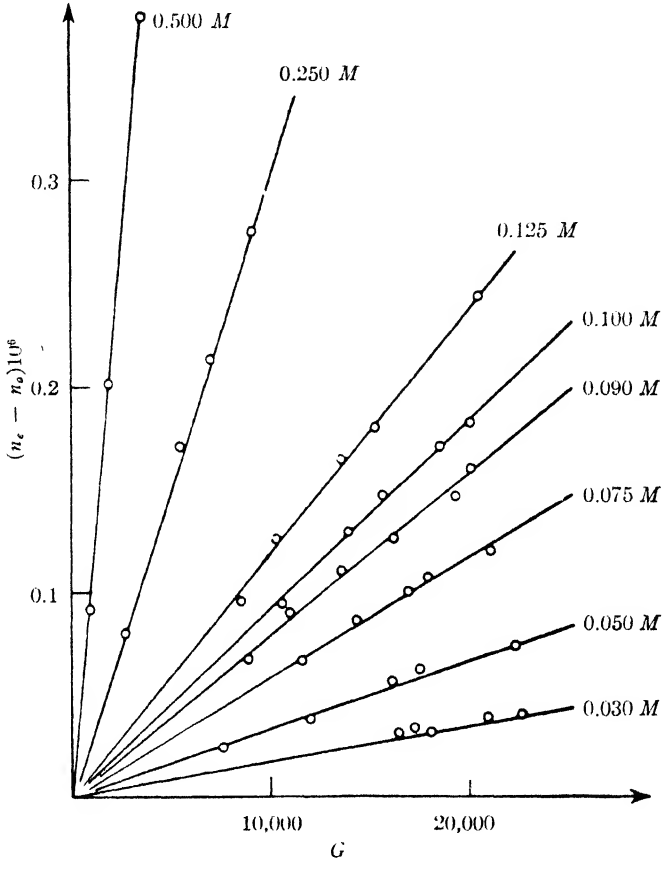

Fig. 8.—Double refraction of low molecular weight polystyrene, $0.1m_o[\eta] = 5.6$. Solvent: cyclohexanone.

velocity gradient, and at high dilutions it appears to be nearly proportional to concentration at a given gradient. Signer and Gross (61) concluded indeed that the expression $\frac{n_e - n_o}{G\eta c}$ is a constant for poly-

styrene of a given mean molecular weight (Table III), and the same rule appears to hold for many other substances.

For very elongated molecules, the double refraction is no longer a linear function of velocity gradient; the curves bend over toward the horizontal axis at high velocity gradients, with some suggestion that a saturation value is being approached. This is illustrated by Fig. 9, which gives data on rabbit myosin (39). Curves of a generally similar character have been found for vanadium pentoxide sols (14).

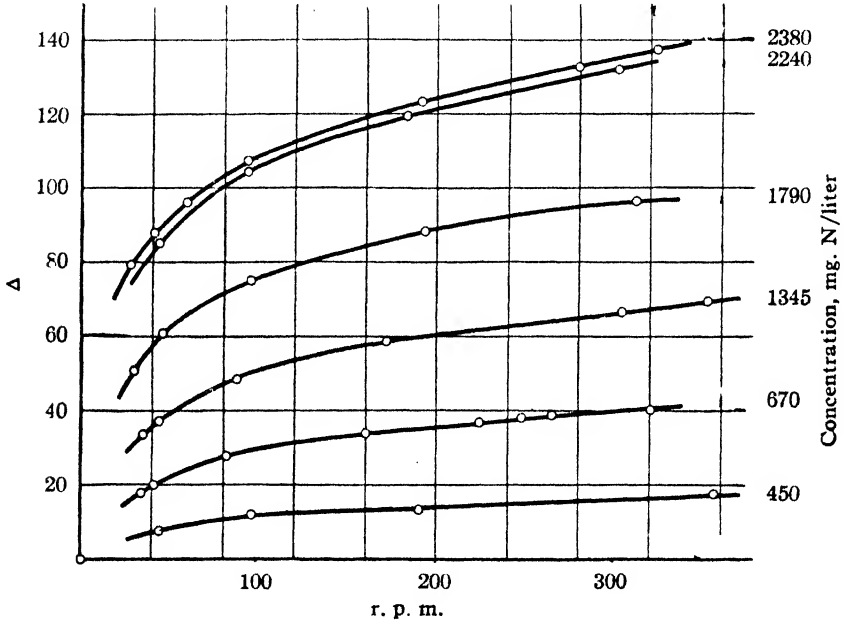

Fig. 9.—Double refraction of rabbit myosin at various concentrations (expressed in mg. protein nitrogen per liter). For definition of the angle Δ, see equation (7). $n_e - n_o = 30.8 \times 10^{-9}\ \Delta°$. The velocity gradient, G, is proportional to the speed of rotation of the outer cylinder (r. p. m.). For the apparatus used, $G = 21.1$ sec.$^{-1}$ for 100 r. p. m.

Colloidal solutions showing double refraction of flow are invariably much more viscous than solutions of spherical particles at the same concentration. Furthermore, solutions in which the extinction angle is distinctly less than 45° give non-Newtonian flow; they show what has been called "anomalous" or "structural" viscosity. The measured viscosity is a function of the velocity gradient, decreasing in

general as the gradient increases. The viscous properties of these liquids, as well as their birefringence during flow, are determined by the asymmetry of the solute particles. Concerning the theory of the viscous properties of such solutions, see Burgers (8), Huggins (23), Peterlin (48) and Simha (64).

2. *Rotary Motion of Ellipsoidal Particles Subjected to a Velocity Gradient*

We have now examined the main experimental facts which must be explained. A satisfactory theory must determine the orientation of rod-shaped or disc-shaped particles under the influence of a velocity gradient; the optical properties of the flowing liquid are then to be determined from the optical properties of its components and from the manner of their orientation. The orienting forces are opposed by the thermal motion of the molecules, which tends to make them assume a random distribution. In the absence of orienting forces, therefore, the liquid as a whole is isotropic, even though the solute particles are themselves highly anisotropic.[9] The actual degree of orientation in the flowing liquid depends on the ratio of the velocity gradient to the thermal kinetic energy of the particles.

First we may consider the case in which the particles are so large that their Brownian movement is negligible. To obtain a model useful for theoretical calculations, we shall assume in what follows that the particles are ellipsoids of revolution; the length of the semi-axis of revolution is denoted by a, that of the equatorial semi-axis by b. Such a model may be inadequate to represent the complexity of form of many large molecules and colloidal particles, but it appears to give results in good accord with other more direct methods of determining size and shape, where the latter are available.

The hydrodynamic problem of the motion of such ellipsoids in a field of flow was treated by Jeffery (24), in an extremely thorough and searching study, concerned primarily with the viscosity of such systems. The ellipsoids, of course, undergo both translation and rotation; the former is of no importance for our purposes, so that we may choose the origin of coordinates in the center of the ellipsoid. The X axis is chosen to coincide with the stream lines; the XY plane is

[9] We are not concerned here with liquid crystals, in which the interactions of the molecules lead to large-scale orientation, even in the absence of an external field of force. The relation of liquid-crystal formation to streaming birefringence is discussed briefly at the end of this chapter.

the plane of flow; and the Z axis indicates the direction of the light beam which traverses the liquid. The orientation of the liquid relative to the stream lines and the light beam is described by the angles ϕ and θ, which are defined in Fig. 10. For the components of rotation of the ellipsoid, under a velocity gradient G, Jeffery finds:

$$\frac{d\phi}{dt} = -\frac{G(a^2 \sin^2 \phi + b^2 \cos^2 \phi)}{a^2 + b^2} \qquad (11)^{10}$$

$$\frac{d\theta}{dt} = G\frac{(a^2 - b^2)}{(a^2 + b^2)} \sin \theta \cos \theta \sin \phi \cos \phi \qquad (12)$$

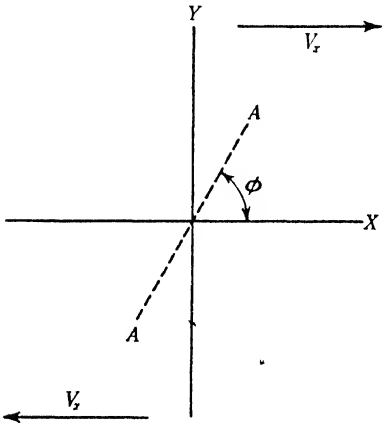

Fig. 10.—Orientation of an ellipsoidal molecule in a flowing liquid of constant velocity gradient. The positive Z axis points perpendicularly up from the plane of the paper. The projection of the axis of revolution of the ellipsoid on the XY plane is denoted by the line AA. The movement of the liquid is parallel to the X axis, and is described by the equation $V_x = GY$ (G = gradient), V_x = velocity of liquid. The meaning of the angle ϕ is shown in the figure ($\phi = 0°$ when an axis of ellipsoid lies in XZ plane). θ is the smaller of the two angles between the axis of the ellipsoid and the positive Z axis.

The effect of the velocity gradient is to cause a continued rotation of the ellipsoid. A prolate ellipsoid ($a > b$) rotates most rapidly when the a axis is perpendicular to the stream lines ($d\phi/dt$ maximum when $\phi = 90°$), most slowly when this axis is parallel to the stream lines. The converse relation holds for an oblate ellipsoid ($a < b$). In either case, the particle remains in continued rotation. Orientation by a velocity gradient is thus very different from the orientation of dipoles in an electric field, in which (in the absence of Brownian movement) true equilibrium, with the dipoles parallel to the field, is obtained. However, very elongated ellipsoids ($a \gg b$) spend nearly all their time with the a axis parallel to the stream lines, and extremely flattened ellipsoids ($a \ll b$) with the a axis perpendicular to the stream lines.

[10] Equation (11) corresponds to equation (47) in Jeffery's paper, but differs from it in form because we have chosen the axes differently for convenience in the later discussion of Boeder's theory.

3. *Influence of Brownian Movement: Motion of Thin Rods in Two Dimensions*

When Brownian movement is considered, in addition to the hydrodynamic forces, the problem becomes far more complex. We shall simplify the discussion, following Boeder (3), by considering the motion of very thin rods ($b = 0$), the motion of which is restricted to the XY plane in Fig. 10. Thus the orientation of one of the rods is uniquely defined by a single parameter, the angle ϕ, which may lie between 0° and 180° (a rotation of the rod through 180° in the XY plane leaves its orientation unaltered, since its ends are indistinguishable). Let Δn be the number of particles in the system, per unit volume, whose axes lie between the angles ϕ and $\phi + \Delta\phi$. Then we may characterize the average state of the particles by a distribution function $\rho(\phi)$, defined by the relation:

$$\rho(\phi) = \lim_{\Delta\phi \to 0} \frac{\Delta n}{\Delta\phi} \tag{13}$$

If the distribution is isotropic, ρ = constant. If preferred orientations are established by an external force, the tendency of the Brownian movement is to decrease the number of molecules in these preferred orientations. The net number of molecules, dn, whose orientation shifts in the time, dt, across the angle ϕ from lower to higher values, due to the Brownian movement, is

$$\left(\frac{dn}{dt}\right)_{\phi} = -\Theta \frac{\partial \rho}{\partial \phi} \tag{14}$$

Here Θ, the rotary diffusion constant, is a measure of the mobility of the particle in its rotation in the XY plane.

The net number of particles shifting their orientation in unit time, across the angle $\phi + d\phi$, from lower to higher values, is

$$\left(\frac{dn}{dt}\right)_{\phi + d\phi} = -\Theta \frac{\partial \rho}{\partial \phi} - \Theta \frac{\partial^2 \rho}{\partial \phi^2} d\phi \tag{15}$$

The difference between $\left(\frac{dn}{dt}\right)_{\phi}$ and $\left(\frac{dn}{dt}\right)_{\phi + d\phi}$, divided by the interval $d\phi$, gives the rate of change of the function $\rho(\phi)$ with time, in the region $d\phi$, due to the Brownian movement.

$$\left(\frac{\partial \rho}{\partial t}\right)_B = \Theta \left(\frac{\partial^2 \rho}{\partial \phi^2}\right) \tag{16}$$

Equations (14) and (16) are the exact analogues, for rotary diffusion, of Fick's two laws of translational diffusion. (See, for instance, Williams and Cady (75)). The dimensions of the rotary diffusion constant, however, are t^{-1}, while those of the translational diffusion constant are l^2t^{-1}.

Consider now the change in the function ρ due to the velocity gradient. This gradient causes the particles to rotate with an angular velocity $\omega = d\phi/dt$, given by (11) for the case when $b = 0$;

$$\omega = -G \sin^2 \phi \tag{11a}$$

Disregarding the Brownian movement, the number of particles moving through the orientation ϕ in unit time is $(\rho\omega)_\phi$. The number turning toward higher ϕ values from the angle $\phi + d\phi$ in unit time is $(\rho\omega)_{\phi + d\phi}$. Thus the net rate of change of the function ρ with time, due to the streaming, is

$$\left(\frac{\partial \rho}{\partial t}\right)_S = -\frac{\partial(\rho\omega)}{\partial \phi} \tag{17}$$

The total change of ρ with time is the sum of that due to the streaming and that due to the Brownian movement (equations (16) and (17)):

$$\frac{\partial \rho}{\partial t} = \Theta \frac{\partial^2 \rho}{\partial \phi^2} - \frac{\partial(\rho\omega)}{\partial \phi} \tag{18}$$

We are concerned with the steady state, achieved after the flow has proceeded for some time,[11] in which ρ does not alter with time. On setting (18) equal to zero, and integrating, we obtain

$$\Theta \frac{\partial \rho}{\partial \phi} - \rho\omega = C_1 \tag{19}$$

or, making use of (11a) and dividing by Θ:

$$\frac{\partial \rho}{\partial \phi} + \alpha\rho \sin^2 \phi = C \tag{19a}$$

in which $\alpha = G/\Theta$ is a measure of the relative intensity of the orienting and disorienting forces. (19a) is the fundamental equation of double refraction of flow, for the two dimensional case.

Boeder (3), who first formulated this equation, has also given its solution in detail. Fig. 11 shows the orientation distribution function ρ as a function of ϕ, for various values of α. When α is small, ρ is a maximum at 45° to the stream lines; as α increases, the height of the

[11] Concerning the time required to attain this steady state, see Peterlin (48).

maximum increases, and its position shifts over more and more toward parallelism with the stream lines. It is the position of this maximum which determines the position of the extinction angle χ, while the height of the maximum gives an indication of the magnitude of the double refraction. The details of the calculation of both these quantities have been given by Boeder; the results are shown in Fig. 12. The general form of the curves for χ and the double refrac-

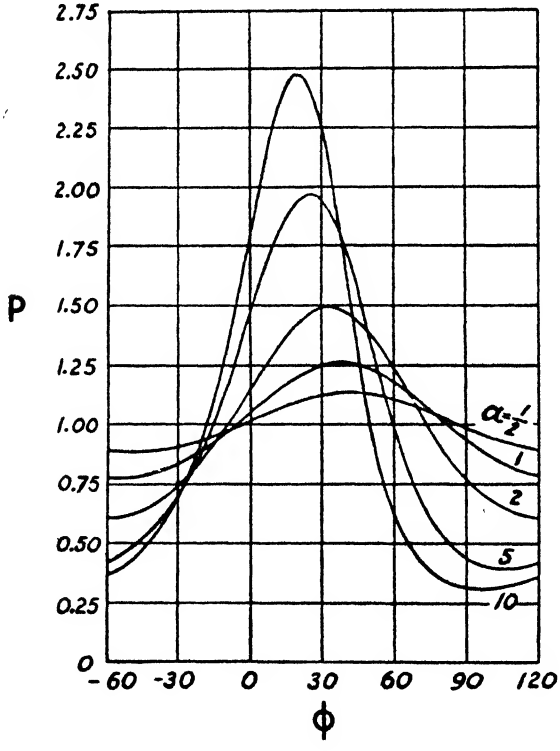

Fig. 11.—The orientation distribution function, ρ, as a function of ϕ (see Fig. 10) for various values of $\alpha = G/\Theta$.

tion as a function of velocity gradient is clearly similar to those found experimentally for many colloids (Figs. 5–9, incl.); and Boeder himself made measurements on sols of cotton yellow, which are in good agreement with these calculated curves.

The behavior of pure liquids is readily understood on Boeder's

theory. The Brownian movement of small molecules is so intense that their rotary diffusion constants are very high. Even at the highest velocity gradients attainable, the values of α are still much less than unity, and the extinction angle is therefore always 45°, within the experimental error.

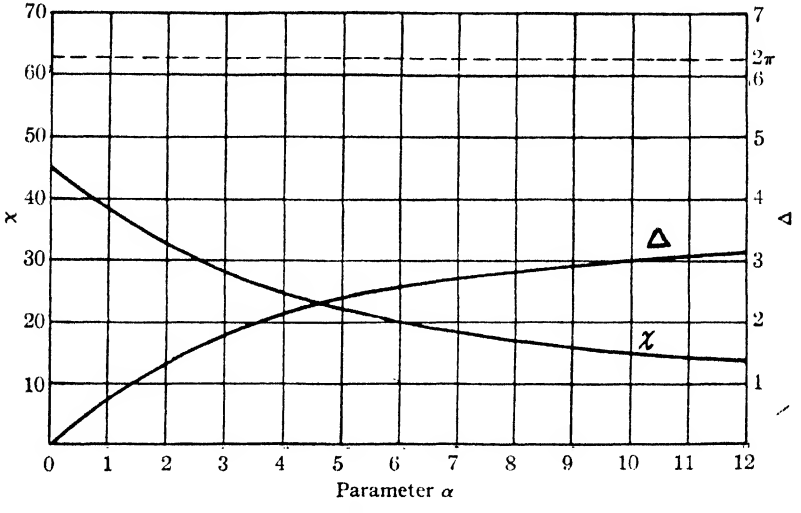

Fig. 12.—Extinction angle, χ, and double refraction, Δ, of a solution of thin rod-shaped particles. The limiting value of Δ, corresponding to complete orientation, is set equal to 2π. Abscissa: $\alpha = G/\Theta$. Ordinate: χ or Δ.

4. *The Three Dimensional Orientation Problem*

Boeder gave also a less complete treatment of the orientation of rod-shaped particles in three dimensions; for low values of α he derived the approximate formula for the extinction angle (χ in radians):

$$\chi = \frac{1}{2}\tan^{-1} 6/\alpha = \frac{\pi}{4} - \frac{\alpha}{12}\left(1 - \frac{\alpha^2}{108} + \cdots\right) \qquad (20)$$

Recently Peterlin (48) and Peterlin and Stuart (49) have considered the problem of the orientation of ellipsoids of revolution by a velocity gradient, and have developed a very complex mathematical expression for the orientation distribution function in three dimensions, as a function of α and of the axial ratio (a/b) of the ellipsoids. They obtain for χ at low values of α:

$$\chi = \frac{\pi}{4} - \frac{\alpha}{12}\left[1 - \frac{\alpha^2}{108}\left(1 + \frac{24}{35}\frac{a^2 - b^2}{a^2 + b^2} + \ldots.\right)\right] \qquad (21)$$

which for small α values is seen to be practically identical with (20).

For the magnitude of the streaming double refraction, Peterlin and Stuart obtain

$$\frac{n_e - n_o}{n} = \Phi \frac{2\pi}{n^2}(g_1 - g_2) \cdot f\left(\alpha, \frac{a}{b}\right) \qquad (22)$$

Here n denotes the refractive index of the liquid at rest, and Φ the volume fraction of the colloidal component which gives rise to the double refraction, the solvent being supposed to be isotropic at all velocity gradients. $(g_1 - g_2)$ is an optical factor further discussed below in connection with the influence of the solvent, and $f(\alpha, a/b)$ is an orientation function which is in general very complex. For small values of α, however, it reduces to

$$f\left(\alpha, \frac{a}{b}\right) = \frac{\alpha}{15}\left(\frac{a^2 - b^2}{a^2 + b^2}\right)\left[1 - \frac{\alpha^2}{72}\left(1 + \frac{6}{35}\frac{a^2 - b^2}{a^2 + b^2}\right) + \ldots.\right] \qquad (23)$$

Peterlin and Stuart (49) and Snellman and Björnståhl (64a) have shown that the flowing liquid is optically a biaxial, not a uniaxial, crystal. All experimental arrangements hitherto employed, however, can reveal only a single optic axis. The equations given here apply to the actual experimental conditions.

5. *Rotary Diffusion Constants and Relaxation Times: Their Relation to Molecular Size and Shape*

From the χ-α curves given in Fig. 12, or more accurately at low values of α from Equation (20) or (21), we may evaluate the rotary diffusion constant from measurements of the extinction angle. These curves or equations fix the value of α corresponding to a given value of χ. But $\alpha = G/\Theta$, and G, the velocity gradient, is known experimentally from the dimensions of the apparatus and the angular velocity of the rotating cylinder. Hence, given α, the rotary diffusion constant, Θ, is known. We must now consider the relation of Θ to the size and shape of the ellipsoidal molecule or particle.

Θ, like the translational diffusion constant, D, may be expressed in terms of the change in position of the molecules due to their Brownian movement. Imagine all the solute molecules oriented by an external force, so that their principal axes are parallel, and suppose this orienting force suddenly removed, so that the subsequent

motion of the molecules is due only to their Brownian movement. After the lapse of a short time, t, a given molecule will have shifted through an angle ϕ relatively to its original orientation. Then Θ is directly proportional to the mean square value of ϕ for all the molecules in the system.

$$\Theta = \frac{1}{2}\frac{\overline{\phi^2}}{t} \tag{24}$$

The derivation of equation (24) is exactly analogous to the derivation of the corresponding equations for translational diffusion (see, for instance, Williams and Cady (75)).

Θ, like D, is directly proportional to the thermal energy of the molecule; similarly, it is inversely proportional to a rotary frictional constant, ζ, which is a function of the size and shape of the molecule and the viscosity of the medium in which it is immersed; ζ is a measure of the torque which must be applied to cause the molecule to rotate with unit angular velocity (47).

$$\Theta = \frac{KT}{\zeta} \tag{25}$$

Here K is Boltzmann's constant, and T the absolute temperature. In the general case of an ellipsoid with three semi-axes, a, b and c, of different lengths, three different rotary frictional constants are required to characterize the resistance of the medium to rotation of the molecule about each of these axes. There are three corresponding rotary diffusion constants.

$$\Theta_a = \frac{KT}{\zeta_a};\ \Theta_b = \frac{KT}{\zeta_b};\ \Theta_c = \frac{KT}{\zeta_c} \tag{26}$$

We shall confine our subsequent discussion to ellipsoids of revolution, for which

$$\zeta_b = \zeta_c.$$

For many purposes, it is more convenient to characterize the rotary Brownian movement by another quantity, the relaxation time τ. We may imagine the molecules oriented by an external force so that their a axes are all parallel to the x axis (which is fixed in space). If this force is suddenly removed, the Brownian movement leads to their disorientation. The position of any molecule after an interval of time may be characterized by the cosine of the angle ϑ between its a axis and the x axis. (The molecule is now considered to be free to turn in any direction in space—its motion is not con-

fined to a single plane, but instead may have components about both the b and c axes.) When the mean value of cosine ϑ for the entire system of molecules has fallen to $1/e$ ($e = 2.718\ldots$ is the base of natural logarithms), the time that has elapsed is defined as the relaxation time τ_a, for motion of the a axis.[12] The relaxation time is greater, the greater the resistance of the medium to rotation of the molecule about this axis, and it is found that a simple reciprocal relation exists between the three relaxation times τ_a, τ_b, τ_c, for rotation of each of the axes, and the corresponding rotary diffusion constants defined in equation (26).

$$\tau_a = \frac{1}{\Theta_b + \Theta_c}; \tau_b = \frac{1}{\Theta_a + \Theta_c}; \tau_c = \frac{1}{\Theta_a + \Theta_b} \tag{27}$$

For an ellipsoid of revolution, these equations become:

$$\tau_a = \frac{1}{2\Theta_b}; \tau_b = \tau_c = \frac{1}{\Theta_a + \Theta_b} \tag{27a}$$

If the solute molecule is spherical, and is very large in comparison to the solvent molecules, the inner frictional constant ζ is given by a formula due to Stokes:

$$\zeta_{\text{sphere}} = 8\pi\eta r^3 \tag{28}$$

where r is the radius of the sphere and η is the viscosity of the solvent. The molecule is characterized by a single rotary diffusion constant Θ, and a single relaxation time:

$$\Theta = \frac{1}{2\tau} = \frac{KT}{8\pi\eta r^3} \tag{29}$$

This formula, due to Einstein, was experimentally verified by Jean Perrin (47a) by direct microscopic observation of spherical colloidal mastic particles (with radius 6.5×10^{-4} cm.), which contained small enclosures of impurities on the surface, thus permitting their rotary motion to be directly followed.

Generalizing the hydrodynamical equations derived by Stokes for spheres, Edwardes (13) calculated the coefficients ζ_1, ζ_2 and ζ_3 for ellipsoids as a function of their axial ratios. The general equations are complicated; but for ellipsoids of revolution, which may be characterized by only two values of ζ, they assume a simpler form, and have been employed by Gans (17) and F. Perrin (47) to evaluate the rotary diffusion constants of molecules which may be

[12] Concerning relaxation times, see Debye (9) and F. Perrin (47).

treated as ellipsoids of revolution. The formulas of Gans and of Perrin are not identical, but the numerical values of θ calculated from them are nearly so, so that the formulas of either author may be used in practice. In the following discussion we shall employ Perrin's equations.

The volume of the ellipsoid (of axial ratio a/b) is

$$V = \frac{4\pi}{3} ab^2 \tag{30}$$

The rotary diffusion constant θ_0 and relaxation time τ_0 of a sphere of the same volume would be given by the relations

$$\theta_0 = \frac{1}{2\tau_0} = \frac{KT}{8\pi a b^2 \eta} \tag{31}$$

Consider first the case of an elongated ellipsoid of revolution ($a > b$). Rotary Brownian movement of the a axis about the b axis is characterized by the relaxation time τ_a and the corresponding rotary diffusion constant $\theta_b = \frac{1}{2\tau_a}$ (see Equation (27a)). These constants are conveniently expressed by their values relative to those for a sphere of the same volume. Denoting by q the ratio b/a, Perrin's equation reads

$$\frac{\tau_a}{\tau_0} = \frac{\theta_0}{\theta_b} = \frac{2(1 - q^4)}{\frac{3q^2(2 - q^2)}{\sqrt{1 - q^2}} \ln \frac{1 + \sqrt{1 - q^2}}{q} - 3q^2} \tag{32}$$

τ_a/τ_0 is always greater than unity, and increases very rapidly as a/b increases. If $a \gg b$, (32) reduces approximately to the simpler formula:

$$\frac{\theta_b}{\theta_0} = \frac{\tau_0}{\tau_a} = \frac{3b^2}{2a^2}\left[-1 + 2 \ln \frac{2a}{b}\right] \tag{32a}$$

If $a > 5b$, the values of θ and τ, calculated from formula (32a), agree within 1% with those calculated from the exact formula (32). Hence θ_b, from (31) and (32a), equals approximately:

$$\theta_b = \frac{3KT}{16\pi\eta a^3}\left[-1 + 2 \ln \frac{2a}{b}\right] \tag{33}$$

Thus for a given value of a/b, the rotary diffusion constant of an elongated ellipsoid is inversely proportional to the cube of its length.

For the relaxation time τ_b of an elongated ellipsoid of revolution

involving rotation of the b axis, which may involve turning about both the a and the $c(= b)$ axis, Perrin finds

$$\frac{\tau_b}{\tau_0} = \frac{2\Theta_0}{\Theta_a + \Theta_b} = \frac{4(1 - q^4)}{\frac{3q^2(2q^2 - 1)}{\sqrt{1 - q^2}} \ln \frac{1 + \sqrt{1 - q^2}}{q} + 3} \tag{34}$$

If $a \gg b$, then $(q \to 0)$, and (34) reduces approximately to

$$\frac{\tau_b}{\tau_0} = \frac{2\Theta_0}{\Theta_a + \Theta_b} = \frac{4}{3\left(1 - \frac{b^2}{a^2} \ln \frac{2a}{b}\right)} \tag{34a}$$

Thus τ_b for an elongated ellipsoid is always greater than τ_0, but never becomes greater than $4\tau_0/3$, even when a/b becomes infinite.

For a flattened ellipsoid ($a < b$, and $q > 1$) a different set of equations holds. For rotation about the equatorial (b) axis

$$\frac{\tau_a}{\tau_0} = \frac{\Theta_0}{\Theta_b} = \frac{2(1 - q^4)}{\frac{3q^2(2 - q^2)}{\sqrt{q^2 - 1}} \tan^{-1} \sqrt{q^2 - 1} - 3q^2} \tag{35}$$

and for rotation about the a axis (axis of revolution)

$$\frac{\tau_b}{\tau_0} = \frac{2\Theta_0}{\Theta_a + \Theta_b} = \frac{4(1 - q^4)}{\frac{3q^2(2q^2 - 1)}{\sqrt{q^2 - 1}} \tan^{-1} \sqrt{q^2 - 1} + 3} \tag{36}$$

If $b \gg a$, both (35) and (36) reduce approximately to

$$\frac{\tau_a}{\tau_0} \cong \frac{\tau_b}{\tau_0} \cong \frac{2b}{a[3 \tan^{-1} b/a]} \cong \frac{4b}{3\pi a} \tag{36a}$$

and substituting the value of τ_0 from (31)

$$\tau_a \cong \tau_b \cong \frac{16\eta b^3}{3KT} \cong \frac{1}{2\Theta_b} \cong \frac{1}{2\Theta_a} \tag{36b}$$

Thus for a flattened ellipsoid, as b/a becomes infinite, both relaxation times becomes infinite, and the corresponding rotary diffusion constants approach zero. When b/a is very large, the relaxation times are proportional to the cube of the b semi-axis, and do not depend at all on the length of the a semi-axis.

6. *Influence of the Solvent on Sign and Magnitude of the Double Refraction*

Many years ago, Wiener (74) considered the anisotropy of what he called a "Stäbchenmischkörper"—a system composed of a large

number of ellipsoids, small compared with the wavelength of light, aligned with their a axes all parallel. Wiener showed that such a system is birefringent, even if the ellipsoids are optically isotropic, provided the refractive index of the ellipsoids is different from that of the medium in which they are immersed. If the ellipsoids are rod-shaped, the double refraction is positive (referred to the a axis of the ellipsoids as principal axis); if they are disc-shaped, it is negative. Such systems are actually found in many biological tissues, such as muscle, tendon, nerve and many others (57). Such structures, when soaked thoroughly in a medium of a given refractive index, n_s, show birefringence which is roughly a parabolic function of n_s. This is shown in Fig. 13 (upper curve), which represents the measurements of Weber (73) on an artificial myosin fiber in media of different refractive indices. Even at the minimum of the curve (which occurs near n_s = 1.58, approximately the mean refractive index of the protein) the double refraction is still large, showing that myosin is inherently optically anisotropic. A fiber made from gelatin gives a similar curve, but the double refraction is zero at the minimum, indicating no optical anisotropy. The form of these curves corresponds closely to that predicted by Wiener's theory. Similar considerations should apply to the oriented molecules in a flowing liquid, allowing for the fact that orientation is incomplete,

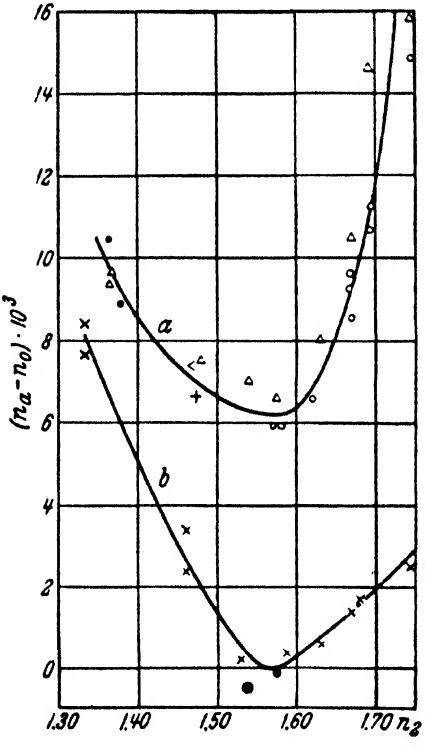

Fig. 13. Birefringence of myosin fiber (a) and gelatin fiber (b), as a function of refractive index (n_s) of medium in which fiber is immersed.

This problem was again taken up by Sadron (53) in 1937. He showed, on the basis of Signer's data and of his own, that the double refraction of polystyrene and of nitrocellulose in a series of different solvents is positive in solvents of low refractive index, passing through zero to negative values as the refractive index of the solvent increases. He also derived a theoretical equation to explain the character of the curves he found. This equation, however, appears incapable of explaining the minimum found in such curves as those of Fig. 13; and the later work of Peterlin and Stuart (49) gives a detailed treatment in terms of electro-magnetic theory, which may be regarded as a more generalized form of Wiener's analysis. Equation (37) gives the streaming birefringence as a product of an orientation factor, $f(\alpha, a/b)$, and of an optical anisotropy factor, $g_1 - g_2$. The latter, expressed in terms of the refractive index of the solvent, n_s, and of the principal refractive indices, n_1 and n_2, of the ellipsoidal molecule is

$$g_1 - g_2 = \frac{1}{4\pi} \frac{(n_1^2 - n_2^2) + e(n_1^2 - n_s^2)(n_2^2 - n_s^2)/n_s^2}{\left[\frac{n_1^2 + 2n_s^2}{3n_s^2} - \frac{2e}{3}\frac{n_1^2 - n_s^2}{n_s^2}\right]\left[\frac{n_2^2 + 2n_s^2}{3n_s^2} + \frac{e}{3}\frac{n_2^2 - n_s^2}{n_s^2}\right]} \tag{37}$$

Here e is a factor which is a complicated function of the axial ratio of the ellipsoids. For very long rods, $e = +0.5$; for spheres, $e = 0$; for flattened discs, $e = -1$.

The most significant point about this equation is that, of the two terms in the numerator, one depends only on the optical anisotropy of the molecule and is independent of its geometrical form; the second term is zero for spheres, but different from zero for either oblate or prolate ellipsoids even if the ellipsoids are optically isotropic (unless n_1 or $n_2 = n_s$). It is the presence of this second term which leads to approximately parabolic curves such as those shown in Fig. 13. The data of Sadron may probably be explained by the assumption that polystyrene and nitrocellulose are both inherently optically negative, $(n_1 - n_2) < 0$, the double refraction arising from the second term in the numerator being very large and positive for small n_s, and vanishing for $n_s = n_1$ or $n_s = n_2$. For $n_s > n_2$, however, this term should increase again; this has not been observed experimentally, and might not occur in any solvent experimentally available. It should be pointed out, also, that Peterlin and Stuart consider their theory as strictly applicable only to particles all of whose principal dimensions lie between 10 and 1000 Ångströms. The threadlike synthetic polymers are too small in cross section to meet this requirement, but the

theory applicable to thicker molecules probably applies also to them in semi-quantitative fashion.

Signer (58) studied the streaming birefringence of polystyrene in several different solvents, with results in fair accord with Wiener's theory. More lately, Lauffer (31, 33) made a similar study of tobacco mosaic virus in glycerol-aniline-water mixtures. The birefringence disappeared, within the limits of experimental error, when the refractive index of the solvent was near 1.57, and reappeared when the refractive index of the solvent was lowered. The infectivity of the virus was apparently not lost in these solvents (compare, however, Bawden and Pirie (1)). Lauffer concluded that the virus particles are optically isotropic ($n_1 = n_2$ in equation (37)). Bernal and Fankuchen (2) have found that the virus particles have an internal structure based on a hexagonal or pseudohexagonal lattice, built up from sub-units about 11 Å cube. Such a structure should not be completely isotropic, but it may well be very nearly so; so the findings of Lauffer and of Bernal and Fankuchen are mutually compatible.

7. *Depolarization of Scattered Light*

A number of authors have studied the depolarization of scattered light from colloidal solutions, and have drawn inferences concerning the anisotropy of the particles. Accurate observations on scattered light require extreme care in the arrangement and execution of the experiments. Furthermore, the underlying theory (16) shows that dielectric particles—a category which includes all the common colloids except metallic sols—depolarize scattered light to an extent determined by their optical anisotropy, not by their geometrical form. Actually it has been shown by Lotmar (35) that even solutions of such highly asymmetrical particles as myosin or nitrocellulose give a depolarization factor, for scattered light, of the same order of magnitude as that of low molecular organic gases and vapors, indicating a similar degree of optical anisotropy in both classes of materials. These papers by Lotmar may be recommended as giving an excellent critical survey of theory and experiment in this field.

8. *Influences of Polydispersity on Streaming Birefringence*

We have seen that many systems experimentally studied give results in general accord with Boeder's theory. Certain discrepancies

in the data, however, are apparent to critical examination. For instance, solutions of nitrocellulose in butyl acetate (Signer and Gross (61), Figs. 8 and 10 of their paper) give linear curves for $n_e - n_o$ plotted against velocity gradient, although the extinction angle differs decidedly from 45° at the higher gradients studied. Theoretically, the $n_e - n_o$ curves should deviate appreciably from linearity under these conditions. Another type of discrepancy is shown by myosin, in which a limiting value of $\chi = 12°$ ($\Psi = 78°$) is attained over a considerable range of velocity gradients, although from the simple theory, χ should approach 0° asymptotically as the gradient increases. Consideration of such discrepancies led Sadron (54) to consider the behavior of systems containing a number of different colloidal components, each with its own characteristic rotary diffusion constant. Depending on the relative rotary diffusion constants and the relative concentrations of the components, curves of extremely various character may be obtained. Let φ_i be the extinction angle, and δ_i the double refraction, produced by the ith component alone, dissolved in a given solvent, at a given velocity gradient. (δ_i may be either positive or negative.) Then Sadron concludes that in a solution containing all the colloidal components in an isotropic solvent at the same velocity gradient, the extinction angle χ and the double refraction Δ of the system as a whole are given by the equations:

$$\tan 2\chi = \frac{\sum^{i} \delta_i \sin 2\varphi_i}{\sum^{i} \delta_i \cos 2\varphi_i} \tag{38}$$

$$\Delta^2 = \left[\sum^{i} \delta_i \sin 2\varphi_i\right]^2 + \left[\sum^{i} \delta_i \cos 2\varphi_i\right]^2 \tag{39}$$

These equations are derived on the assumption that all the i components are present in low concentration, and that they do not interact (independent orientation).

Figs. 14*a* and 14*b* show the application of these equations to a system with two colloidal components, with δ of the same sign (55). Component No. 1: acetyl-cellulose of low molecular weight (1.082 g./100 cc. solvent); viscosity,[13] 0.0842 at 18.6°. Component No. 2: acetyl-cellulose of high molecular weight (0.0465 g./100 cc. solvent); viscosity, 0.0264 at 18.6°. Fig. 14*a* gives the φ and δ curves for each of these solutions; and Fig. 14*b* gives χ and Δ for a solution

[13] Sadron (55) writes here "kinematic viscosity," but the context suggests that he may mean the viscosity coefficient in poises.

(viscosity 0.0936) containing both together, each at the same volume concentration and in the same solvent (cyclohexanone) as in Fig. 14*a*. The observed curves for the mixture are very close to those calculated from equations (38) and (39).

Still more peculiar curves may be obtained if the two components give double refraction of opposite sign. Such a case is exemplified by Figs. 15*a* and 15*b*. Component No. 1 is methyl cellulose in dilute aqueous sodium chloride; concentration, 0.190 g./100 cc.; viscosity

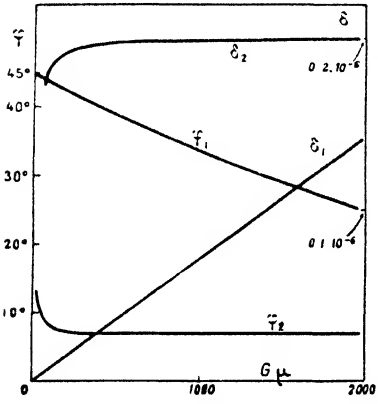

Fig. 14*a*.—Extinction angle (φ) and double refraction (δ) of low molecular weight acetyl-cellulose (component 1) and high molecular weight acetyl-cellulose (component 2). Abscissa: velocity gradient multiplied by viscosity of solution Solvent: cyclohexanone.

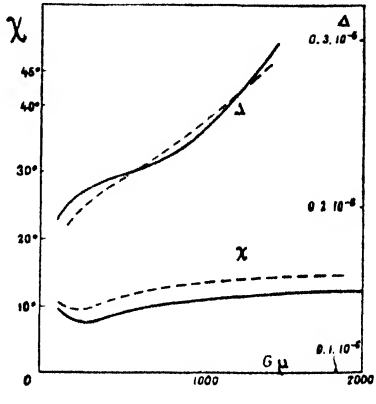

Fig. 14*b*.—Double refraction (Δ) and extinction angle (χ) of a solution containing both components, 1 and 2, each at the same concentration as in Fig. 14*a*. Full curves: experimental values. Dotted curves: calculated from Equations (38) and (39).

at 18.6°, 0.0171. Component No. 2 is sodium thymonucleate, in the same solvent; concentration, 0.0387 g./100 cc.; viscosity at 18.6°, 0.0102. The curve for the mixture of the two components shows the remarkable feature that χ, with increasing velocity gradient, shifts from positive values, across the stream lines, to negative values. Such a curve can be given only by a polydisperse system. The theoretical and experimental curves here do not agree as well as in Fig. 14, although their general character is alike; it is probable that the two components interact appreciably.

Sadron, Bonot and Mosimann (56) have shown that certain serum albumin fractions give χ curves similar to that of Fig. 15*b*; this is true for serum globulin dissolved in a glycerol-water mixture. After extraction of the globulin with ether and acetone at 0°, the anomaly disappears, and the system behaves like a single component. Presumably a lipoid, of negative birefringence, is removed by the extraction, leaving the positive protein component to exert its influence alone. Serum globulin in water also behaves like a single component;

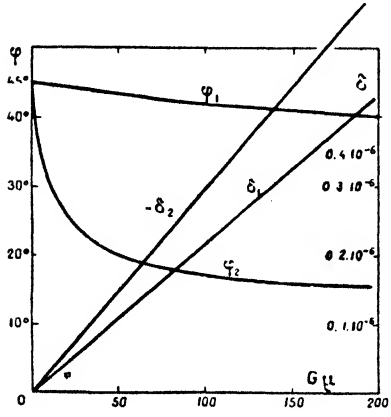

Fig. 15*a*.—φ and δ values for methylcellulose (component 1) and sodium thymonucleate (component 2). Abscissa: velocity gradient multiplied by viscosity of solution Solvent: dilute aqueous sodium chloride.

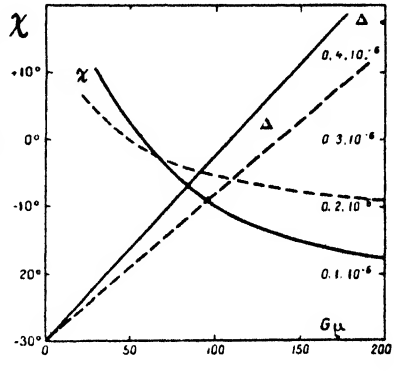

Fig. 15*b*.—χ and Δ values in a solution containing both components 1 and 2, each at the same concentration as in Fig. 15*a*. Full curves: experimental values. Dotted curves: calculated from Equations (38) and (39).

here presumably the protein and lipoid are firmly united. Addition of glycerol breaks up the combination.

These studies in polydispersity are fundamental in this field; they should always be borne in mind, in the interpretation of apparently anomalous experimental results.

9. *Theories of Double Refraction Due to Deformation*

Kuhn (28), after discussing streaming double refraction due to orientation, along the lines of Boeder's theory, proposed an alternative theory according to which the observed effects may be due to deformation and subsequent orientation of initially isotropic par-

ticles by the stresses and pressures in the flowing liquids. The form of the χ-velocity gradient curves, on this theory, as given by Kuhn, is entirely different from that given by Boeder's orientation theory (Fig. 12) and does not appear to fit the observed relations for either proteins or synthetic high polymers. (See the critical discussion by Signer and Gross (61).) An orientation-deformation theory of a somewhat similar sort has also been proposed by Haller (20). Without going into a detailed critical discussion here, we may conclude that double refraction due to deformation of elastic particles plays only a very subsidiary role as compared with orientation effects, in the colloids chiefly studied hitherto.[14]

10. Rotary Diffusion Constants and Lengths of Some Synthetic Polymers and Certain Proteins

Although the theory of double refraction of flow has now been developed on a solid basis, the experimental results available for calculating rotary diffusion constants are few. Practically all systems studied have been polydisperse (even the individual components shown in Figs. 14 and 15 are not monodisperse); the polystyrenes studied by Signer and Gross (61) were carefully fractionated by them, but not truly monodisperse; the nitrocelluloses which they used were even more polydisperse. Hence it is only a rough approximation to characterize the results obtained on such preparations by a single rotary diffusion constant. Generally the calculation of this constant is made from measurements at relatively low velocity gradients, at which χ does not differ from 45° by more than 10°. Under these conditions equation (20) or (21) may be applied as a good approximation. It is apparent from Sadron's analysis, however (see equations (38) and (39) and Figs. 14 and 15), that under such circumstances the extinction angle is determined primarily by the component of lowest rotary diffusion constant, which is oriented most readily at low velocity gradients. The apparent length of the particles, as calculated from the diffusion constant by equation (33) or (36b), for instance, is thus found to be greater than the true mean length of the particles.

[14] A theory of orientation birefringence due to hydrodynamic tension and pressure in the flowing liquid was put forward in 1928 by Raman and Krishnan (49a). Their theory would require that $\chi = 45°$ at all velocity gradients, and is therefore incompatible with the data on colloids. Even for pure liquids the theory gives rise to difficulties. For a critical discussion see Sadron (52).

Allowing for this tendency, we may consider some of the data of Signer and Gross (61), which are probably still the best available on a series of polymers of different mean molecular weights. The low molecular weight polystyrenes give always an extinction angle practically indistinguishable from 45°; hence Θ cannot be determined from the χ values. Consideration of Boeder's theory showed, however, that in a series of polymeric homologues, the *relative* Θ values should be proportional to the reciprocal of the function $\frac{n_e - n_o}{G\eta c}$. Relative values so calculated by Signer and Gross are shown in Table IV. It is a striking and rather unexpected fact that the Θ

TABLE IV

POLYSTYRENES OF LOW MOLECULAR WEIGHT

$0.1 m_o[\eta]$	$\frac{-(n_e - n_o)}{G\eta c}$	$\Theta_{rel.}$ from $n_e - n_o$	Mol. wt. from viscosity	$\Theta_{rel.} \times M \times 10^4$
0.6	2.5	9.8	2,600	2.6
1.0	3.9	6.3	5,500	3.5
1.6	7.2	3.4	9,200	3.1
2.2	10.9	2.2	12,500	2.8
2.7	12.8	1.9	15,000	2.9
5.6	24.4	1.0	31,000	3.1

For definition of m_o and $[\eta]$ in tables IV, V and VI, see table III.
(From Signer and Gross (61), p. 179.)

values so obtained are nearly inversely proportional to the molecular weight as determined from viscosity measurements by the equation of Staudinger (66, especially p. 56 ff.)

$$\frac{\eta_{sp}}{c} = K_m M \tag{40}$$

where K_m is a constant for a given type of polymer and M is the mean molecular weight. It is not possible here to discuss the numerous controversies which have arisen concerning the Staudinger equation; it may be accepted in this discussion as a rough measure of the mean molecular weight. The root mean square distance between the ends of the chain, in a thin long-chain molecule with rotation around adjacent bonds, should vary as the square root of the number of links in the chain; hence with $M^{1/2}$ (Kuhn (29)) the rotary diffusion constant of an elongated ellipsoid should vary

inversely as the cube of its length, except for a nearly constant factor which depends on the ratio a/b (Eq. (33)). Thus, if the ellipsoidal model is applicable, the rotary diffusion constant should be proportional to l^{-3} approximately, and hence to $M^{-3/2}$, rather than to M^{-1}, as in Table IV. However, because of polydispersity, the longest particles in each preparation probably make the chief contribution to the measured rotary diffusion constant; and the length of these longest particles probably does not increase as rapidly as the mean molecular weight.

In the nitrocellulose studies of Signer and Gross, rotary diffusion constants were calculated directly by Boeder's theory from the observed χ and G values. Their results are given in Tables V and VI. The estimated lengths, from equation (33), are also given.

TABLE V

ROTARY DIFFUSION CONSTANTS OF NITROCELLULOSES IN BUTYL ACETATE

$0.1m_0[\eta]$	θ from extinction angle	Mol. wt. from viscosity	Length ($2a$) from Eq. 33	$\theta_{rel.}$ from $n_e - n_o$
55	17,700	41,000	900 Å	17
270	2,750	220,000	2000 Å	2.5
380	1,160	450,000	2700 Å	1

Concerning the axial ratios (a/b) used in calculating the length, $2a$, see text. (From Signer and Gross (61), p. 179.)

TABLE VI

ROTARY DIFFUSION CONSTANTS OF NITROCELLULOSES FROM THE EXTINCTION ANGLE (TEMP. 20° C).

Gradient sec.$^{-1}$	Nitrocellulose $0.1m_0[\eta] = 55$		Nitrocellulose $0.1m_0[\eta] = 270$ or 245	
	In butyl acetate	In cyclohexanone	In butyl acetate	In cyclohexanone
5,000	18,200 sec^{-1}	13,300 sec^{-1}	2,800	1,400
10,000	17,500	12,500	2,800	1,900
15,000	17,400	13,600	2,500	2,300
20,000	17,800	14,800	2,600	2,500
25,000	18,000	15,700	2,800	2,700
Length ($2a$) from Eq. (33)	900 Å	700 Å	2000 Å	1700 Å

In applying equation (33), the axial ratio a/b has been assumed to be 10 for the nitrocellulose of smaller molecular weight, and 50 for the larger. The calculated value of $2a$ changes very little, even for large changes in the assumed value of a/b. (From Signer and Gross, (61) p. 180.)

Allowing for the fact that these lengths are probably those of the longer particles in each preparation, they are in very reasonable accord with the mean molecular weights as calculated from viscosity measurements.

Signer (59) has shown that polystyrene preparations, which from osmotic and viscometric measurements appeared to have extended branches projecting sideways from the main chain, give much less double refraction and χ values nearer 45° than do straight chain polymers of the same mean molecular weight. This is, of course, the expected result, since for a given molecular weight the length is greatest, and the rotary diffusion constant least, for a straight chain.

Signer and Sadron (62) have shown a curious effect in polystyrenes of high molecular weight. $n_e - n_o$ in dilute solutions is a linear function of velocity gradient up to G values of 10,000 to 18,000 sec.$^{-1}$, depending on the concentration. Above a critical value of G, the curves turn upward and a second linear portion of higher slope is obtained. The effects observed were not due to turbulence, since the conditions were carefully chosen to insure laminar flow. Signer and Sadron interpret their results as depending on a stretching of the molecule by the tensions in the flowing liquid, occurring suddenly above a critical velocity gradient. It would be interesting to know how rapidly or slowly the stretched molecules revert to the unstretched form; this, however, cannot be settled from the data given.

During the last few years, in Signer's laboratory, a number of very carefully fractionated, practically monodisperse, nitrocellulose preparations have been obtained. Nitschmann and Guggisberg (43, p. 579) refer to very recent work in Signer's laboratory on these preparations, showing that the size and shape of these molecules as deduced from streaming birefringence is in excellent agreement with values obtained from viscosity and from sedimentation and diffusion. They refer, in this connection, to the thesis of A. Wissler (Bern, 1940). These investigations promise to be of the highest importance for our understanding of this field; unfortunately the data are not available to me at the time when this report is written.

The careful work of de Rosset (10a) on methyl methacrylate polymers unfortunately appeared too late for discussion here.

The dimensions of certain proteins and of sodium thymonucleate, estimated from streaming birefringence, are given in Table VII. The value for fibrinogen is probably only a very rough estimate, and all the preparations must be regarded as probably polydisperse.

TABLE VII

ROTARY DIFFUSION CONSTANTS AND APPROXIMATE LENGTHS OF CERTAIN PROTEINS AND OF SODIUM THYMONUCLEATE

Substance	Ref.	Temp. ° C.	Θ(sec.$^{-1}$)	*Length, $2a$ (Eq. 33)
Myosin (rabbit)	(39)	3	7	11,600 Å
Myosin (snail)	(38)	25	ca. 1	ca. 28,000 Å
Myosin (octopus)	(38)	25	3.5	18,000 Å
Tobacco mosaic virus, *p*H 6.8	(37)	3	25	7,200 Å
Tobacco mosaic virus, *p*H 4.5	(37)	3	0.75	24 000 Å
Sodium caseinate (in 1.6 N Na_2SO_4)	(42) (43)	20	700	2,200 Å
Fibrinogen	(6)	20 (?)	ca. 1200	ca. 1,800 Å
Sodium thymonucleate	(63) (25)	20 (?)	180	4,500 Å

The lengths given here are not always those given in the original communications. Mehl (37, 38) and Nitschmann and Guggisberg (43) have used the equation of Werner Kuhn (28) for the length S:

$$\Theta = \frac{8KT}{\pi\eta S^3}$$

The results given here, however, are all still attended with some uncertainty. The value of a/b was taken as 100 for myosin, and for tobacco virus at *p*H 4.5, in applying Equation (33); it was taken as 50 for tobacco virus at *p*H 6.8 and as 5.8 for Na caseinate in 1.6 N Na_2SO_4, the latter being the value estimated (43) from viscosity measurements. The same value of a/b was arbitrarily chosen for fibrinogen and the value of 200 for sodium thymonucleate.

The sodium caseinate solution in 1.6 N Na_2SO_4 was certainly highly aggregated; many of the casein solutions studied by Nitschmann and Guggisberg (43) consisted of much smaller particles.

Tobacco mosaic virus has also been studied by Kausche, Guggisberg and Wissler (25) and by Robinson (50), with results in generally good agreement with those of Mehl (37).

For references to other proteins on which qualitative studies have been made, see Edsall (11).

The double refraction of all protein solutions yet studied is positive; that of sodium thymonucleate is negative.

Snellman and Björnståhl (64a) calculate a length of 890 to 960 Å for *Helix* Hemocyanin, and of 1280 Å for horse antibody globulin (mol. wt. 990,000); and lengths of 1560 Å and 3300 Å, respectively, for the anti-pneumococcus polysaccharides, SI and SIII, of Heidelberger. For various hydrolyzed or nitrated pectins, Snellman and Säverborn (64b) calculate lengths ranging from 2100 to 3800 Å. Unfortunately these important papers reached me too late for more detailed discussion.

Hence the estimated lengths again tend to be those of the longer molecules in the polydisperse preparations. It is interesting, however, to note that the estimated length of the myosin molecules is of the order of magnitude of that of the anisotropic bands in striated muscle fibers, which range from 1 to 5 μ (10,000 to 50,000 Å).

The studies on tobacco mosaic virus are of particular interest, since here direct determinations of particle length have been made by electron microscopy (26, 27, 65). These determine the length of the fundamental unit as 2800 to 3300 Å (diameter about 150 Å) and confirm earlier studies by more indirect methods in showing a very strong tendency to aggregation of these units, giving particles with lengths two or three times as great or even more. Side-by-side aggregation also occurs. Mehl's data (37) on tobacco virus at *p*H 6.8 give a length, from streaming birefringence, between two and three times as great as the 3000 Å found by electron microscopy. The preparation used by Mehl had been prepared (in Stanley's laboratory) by ammonium sulfate precipitation, and was probably more highly aggregated than the later preparations obtained by ultracentrifugation. Allowing for this, and for the fact that the rotary diffusion constant obtained at low velocity gradients depends primarily on the longer particles, if several different particle sizes are present, the two methods may be said to give results in very satisfactory agreement. It would be very desirable to make observations, by streaming birefringence and with the electron microscope, on the same virus preparation and at the same time.

The rotary diffusion constants hitherto determined by streaming birefringence lie between 1 and 20,000 sec.$^{-1}$, corresponding to relaxation times of 1 sec. to 2.5 $\times$ 10^{-5} sec. For proteins, which have very large electric moments and a fairly rigid structure, dielectric constant dispersion measurements have been used with great success, notably by Oncley (44), in determining relaxation times when these lie between about 10^{-5} and 10^{-8} sec. Small molecules, such as amino acids, have relaxation times of the order of 10^{-11} sec. in water at room temperature. The dielectric dispersion method and the streaming birefringence method, taken together, cover the entire range from 1 sec. (or more) to 10^{-11} sec.; but the technique of the streaming method is still insufficiently developed[15] to give thoroughly

[15] Except for the apparatus of Sadron (51), which appears to give excellent results at high velocity gradients. As yet, however, no detailed description of the apparatus has been published.

satisfactory results for relaxation times much below 10^{-8} sec. Consequently it is seldom possible to study the same molecule by both the streaming and the dielectric technique. An extension of both techniques into the region where they overlap should give results of great value.

An excellent critical discussion concerning the shapes of protein molecules as determined by sedimentation and diffusion, dielectric dispersion, viscosity and streaming birefringence, has been given by Oncley (45).

Since the rotary diffusion constant varies roughly as the inverse cube of the particle length, moderate changes in particle length may produce very great changes in double refraction of flow. For instance, the intense streaming birefringence produced by myosin solutions falls to extremely low values in a few minutes when the myosin is treated with any one of a large number of reagents at low concentrations (39, 12). These include guanidinium salts, chlorides of calcium, magnesium and barium, iodides and thiocyanates. The change is so striking that it may be followed with ease by stirring the solution in a beaker between crossed Polaroids (see Experimental Methods). Lithium and ammonium (or methylated ammonium) ions and urea produce the same effect at higher concentrations. At *p*H values alkaline to 10.3 or acid to 5, similar changes were found to proceed with very great rapidity. Some of the reagents producing these changes also altered the titratable sulfhydryl groups of myosin (18), but no systematic relation whatever was found between the two effects. The great diminution observed in streaming birefringence ran always parallel to a decrease in the viscosity of the solution. Both effects indicated a breaking up of the very elongated particles of native myosin into shorter and less asymmetrical particles.

These effects are similar to the dissociation reactions of proteins in acid or alkaline solutions, and under the action of various chemical reagents, as observed by the ultracentrifuge (67). The streaming method, when applicable, has the advantage of simplicity and rapidity of operation; the change of birefringence can be observed practically from moment to moment, and the kinetics of the process can thus be followed (compare Edsall and Mehl, Ref. 12, Fig. 1 and Mehl, Ref. 38, Fig. 3). However, the class of molecules to which this technique is applicable is naturally restricted.

Greenstein and Jenrette (19) have studied the change in birefringence in sodium thymonucleate, produced by various reagents,

in the same way. The diminution, often amounting to virtual disappearance of double refraction, was as marked as in myosin, and was produced by many of the same reagents. Notably guanidinium halides, especially the iodide, produced very powerful effects. Diminution of viscosity, as in myosin solutions, ran parallel with loss of birefringence. In sodium thymonucleate the effects observed were readily reversible, and the birefringence was restored practically to its original value when the added salt was removed. In myosin, however, Edsall and Mehl (12) failed to find conditions for restoring the double refraction after it had once disappeared.[16]

11. Intermolecular Action and Liquid Crystal Formation

We have discussed the relation between birefringence and particle size and shape for the case of dilute solutions, in which the different particles orient independently, and the system is anisotropic only in the presence of external orienting forces. At higher concentrations, however, the forces between the particles may be so great as to determine their orientation even in the absence of an external field, thus leading to liquid-crystal formation. The most striking case of this sort has been found in tobacco mosaic virus protein (Bernal and Fankuchen (2)). Solutions of virus, of medium strength, divide into two layers. The top layer, which is the more dilute, is an isotropic liquid showing marked birefringence on flow; the lower, more concentrated, layer is spontaneously birefringent, and consists of regions in which (as shown by x-ray analysis) the particles lie with their long axes parallel. In a plane at right angles to the long axis the particles are arranged in a regular hexagonal pattern; the inter-particle distance varies with the concentration, but the hexagonal pattern is the same for air-dried gels and for solutions down to 13%, and probably well below this concentration. On the other hand, there is no regularity in the arrangement of the particles in the direction parallel to their long axes.

The particles are held in this parallel configuration presumably by inter-ionic forces, the nature of which has been analyzed particularly by Levine ((34a) and unpublished work cited by Bernal and Fankuchen (2)) and by Langmuir (34). Langmuir has also given a very interesting discussion of double refraction in bentonite

[16] Recently Needham, Shen, Needham and Lawrence (41) have reported that the double refraction of myosin solutions is restored simply on standing a few hours at 37°. This surprising observation calls for further study.

sols which consist of disc-shaped particles; one of the sols studied by Langmuir gave permanent birefringence at a concentration of 1.16% (effective diameter of particles 300 Å). The relaxation time of more dilute sols was determined by observing the time taken for birefringence to disappear after stress was removed. This time varied enormously with the concentration, showing that the observed effects were due primarily to interaction between the particles, there being a very high energy barrier opposing the rotation of a particle, due to the field of force arising from its neighbors.

The summary here given of these investigations is inevitably very brief and merely outlines some of the most important findings. It appears certain, however, that the interaction of geometrically anisotropic particles to form oriented structures, even when the particles are widely separated by the solvent medium, is a phenomenon of the utmost importance in both colloid chemistry and biochemistry. This review has been concerned with the form of the individual particles, but this is only a preliminary step, leading to the study of the mode of their interaction in an organized system.

Bibliography

1. F. C. Bawden and N. W. Pirie, *Biochem. J.*, **34**, 1278 (1940).

2. J. D. Bernal and I. Fankuchen, *Nature*, **139**, 923 (1937); *J. Gen. Physiol.*, **25**, 111, 147 (1941).

2a. Y. Björnståhl, *J. Opt. Soc. Am.*, **29**, 201 (1939).

3. P. Boeder, *Z. Physik*, **75**, 258 (1932).

4. G. Boehm, Abderhalden's *Handb. Biol. Arbeitsmethoden*, Abt. II, Teil 3 (second half), p. 3939.

5. G. Boehm and R. Signer, *Helv. Chim. Acta*, **14**, 1370 (1931).

6. G. Boehm and R. Signer, *Klin. Wochschrift*, **11**, 599 (1932).

7. W. Buchheim, H. A. Stuart and H. Menz, *Z. Physik*, **112**, 407 (1939).

8. J. M. Burgers, *Second Report on Viscosity and Plasticity*, Chapter 3. Amsterdam Academy of Sciences, Amsterdam, Nordemann Publ. Co., New York, 1938.

9. P. Debye, *Polar Molecules*, McGraw-Hill Book Co., New York, 1929.

10. G. de Metz, *Ann. Physik*, **35**, 497 (1888).

10a. A. J. de Rosset, *J. Chem. Phys.*, **9**, 766 (1941).

11. J. T. Edsall in C. L. A. Schmidt, *Chemistry of the Amino Acids and Proteins*, C. C. Thomas, Springfield, 1938, p. 527.

12. J. T. Edsall and J. W. Mehl, *J. Biol. Chem.*, **133**, 409 (1940).

13. D. Edwardes, *Quart. J. Pure Applied Math.*, **26**, 70 (1893).

14. H. Freundlich, F. Stapelfeldt and H. Zocher, *Z. physik. Chem.*, **114**, 161, 190 (1924–25).

15. A. Frey-Wyssling and E. Weber, *Helv. Chim. Acta*, **24**, 278 (1941).

16. R. Gans, *Ann. Physik*, **62**, 331 (1920); **65**, 97 (1921).

17. R. Gans, *Ann. Physik*, **86**, 628 (1928).
18. J. P. Greenstein and J. T. Edsall, *J. Biol. Chem.*, **133**, 397 (1940).
19. J. P. Greenstein and W. V. Jenrette, *J. Natl. Cancer Inst.*, **1**, 77 (1940).
20. W. Haller, *Kolloid Z.*, **61**, 26 (1932).
21. N. H. Hartshorne and A. Stuart. *Crystals and the Polarizing Microscope*, E. Arnold & Co., London, 1934.
22. E. Hatschek, *The Viscosity of Liquids*. Van Nostrand Co., New York, 1928.
23. M. L. Huggins, *J. Phys. Chem.*, **42**, 911 (1938); **43**, 439 (1939).
24. G. B. Jeffery, *Proc. Roy. Soc.* (*London*), (A) **102**, 161 (1922–23).
25. G. A. Kausche, H. Guggisberg and A. Wissler, *Naturwissenschaften*, **27**, 303 (1939).
26. G. Kausche and H. Ruska, *Biochem. Z.*, **303**, 221 (1939–40).
27. G. Kausche, E. Pfankuch and H. Ruska, *Naturwissenschaften*, **27**, 292 (1939).
27a. E. O. Kraemer and W. D. Lansing, *J. Phys. Chem.*, **39**, 153 (1935).
28. W. Kuhn, *Z. physik. Chem.*, (A) **161**, 1, 427 (1932); *Kolloid Z.*, **62**, 269 (1933).
29. W. Kuhn, *Kolloid Z.*, **68**, 2 (1934); *Z. physik. Chem.*, (A) **175**, 1 (1935).
30. A. Kundt, *Ann. Physik*, **13**, 110 (1881).
31. M. A. Lauffer, *J. Phys. Chem.*, **42**, 935 (1938).
32. M. A. Lauffer and W. M. Stanley, *J. Biol. Chem.*, **123**, 507 (1938).
33. M. A. Lauffer and W. M. Stanley, *Chem. Rev.*, **24**, 303 (1939).
34. I. Langmuir, *J. Chem. Phys.*, **6**, 873 (1938).
34a. S. Levine, *Proc. Roy. Soc.* (*London*), (A) **170**, 145, 165 (1939).
35. W. Lotmar, *Helv. Chim. Acta*, **21**, 792, 953 (1938).
36. J. Clerk Maxwell, *Collected Papers*, Cambridge Univ. Press (1890), Vol. II, p. 379.
37. J. W. Mehl, *Cold Spring Harbor Symposia Quant. Biol.*, **VI**, 218 (1938).
38. J. W. Mehl, *Biol. Bull.*, **79**, 488 (1940).
39. A. L. v. Muralt and J. T. Edsall, *J. Biol. Chem.*, **89**, 315, 351 (1930); *Trans. Faraday Soc.*, **26**, 837 (1930).
40. J. Needham and J. R. Robinson, *Compt. rend. soc. biol.*, **126**, 163 (1937).
41. J. Needham, S.-C. Shen, D. M. Needham and A. S. C. Lawrence, *Nature*, **147**, 766 (1941).
42. H. Nitschmann, *Helv. Chim. Acta*, **21**, 315 (1938).
43. H. Nitschmann and H. Guggisberg, *Ibid.*, **24**, 434, 574 (1941).
44. J. L. Oncley, *J. Phys. Chem.*, **44**, 1103 (1940); J. L. Oncley, J. D. Ferry and J. Shack, *Ann. N. Y. Acad. Sci.*, **40**, 371 (1940).
45. J. L. Oncley, *Ibid.*, **41**, 121 (1941).
46. L. Page, *Introduction to Theoretical Physics*. Van Nostrand Co., New York, 1928, Chapter VI.
47. F. Perrin, *J. phys. radium*, (7) **5**, 497 (1934).
47a. J. Perrin, *Compt. rend.*, **149**, 549 (1909).
48. A. Peterlin, *Z. Physik.*, **111**, 232 (1938); *Kolloid Z.*, **86**, 230 (1939).
49. A. Peterlin and H. A. Stuart, *Z. Physik*, **112**, 1, 129 (1939).
49a. C. V. Raman and K. S. Krishnan, *Phil. Mag.*, **5**, 769 (1928).
50. J. R. Robinson, *Proc. Roy. Soc.* (*London*), (A) **170**, 519 (1939).

51. C. Sadron, *J. phys. radium*, (7) **7**, 263 (1936).
52. C. Sadron, *Schweizer Arch. angew. Wiss. Tech.*, **3**, 8 (1937).
53. C. Sadron, *J. phys. radium*, (7) **8**, 481 (1937).
54. C. Sadron, *Ibid.*, (7) **9**, 381 (1938).
55. C. Sadron and H. Mosimann, *Ibid.*, (7) **9**, 384 (1938).
56. C. Sadron, A. Bonot and H. Mosimann, *J. chim. phys.*, **36**, 78 (1939).
57. F. O. Schmitt, *Physiol. Rev.*, **19**, 270 (1939).
58. R. Signer, *Z. physik. Chem.*, (A) **150**, 257 (1930).
59. R. Signer, *Helv. Chim. Acta*, **19**, 897 (1936).
60. R. Signer, *Trans. Faraday Soc.*, **32**, 296 (1936).
61. R. Signer and H. Gross, *Z. physik. Chem.*, (A) **165**, 161 (1933).
62. R. Signer and C. Sadron, *Helv. Chim. Acta*, **19**, 1324 (1936).
63. R. Signer, T. Caspersson and E. Hammersten, *Nature*, **141**, 122 (1938).
64. R. Simha, *J. Phys. Chem.*, **44**, 25 (1940).
64a. O. Snellman and Y. Björnståhl, *Kolloid-Beihefte*, **52**, 403 (1941).
64b. O. Snellman and S. Säverborn, *Ibid.*, **52**, 467 (1941).
65. W. M. Stanley and T. F. Anderson, *J. Biol. Chem.*, **139**, 325 (1941).
66. H. Staudinger, *Die hochmolekularen organischen Verbindungen*. Julius Springer, Berlin, 1932.
67. T. Svedberg and K. O. Pedersen, *The Ultracentrifuge*. Clarendon Press, Oxford, 1940, Part IV A.
68. G. I. Taylor, *Phil. Trans. Roy. Soc.* (*London*), **A 223**, 289 (1923).
68a. G. I. Taylor, *Proc. Roy. Soc.* (*London*), (**A**), **157**, 546, 565 (1936).
69. K. Umlauf, *Ann. Physik*, **45**, 306 (1892).
70. D. Vorländer and R. Walter, *Z. physik. Chem.*, **A118**, 1 (1925).
71. D. Vorländer and U. Kirchner, *Z. physik. Chem.*, (**A**) **152**, 47 (1931).
72. D. Vorländer and J. Fischer, *Ber.*, **65**, 1756 (1932).
73. H. H. Weber, *Arch. ges. Physiol.*, **235**, 205 (1934).
74. O. Wiener, *Abhandl. Math-Phys. Kl. Sächs. Akad. Wiss.*, **32**, (1912).
75. J. W. Williams and L. C. Cady, *Chem. Rev.*, **14**, 171 (1934).
76. R. W. Wood, *Physical Optics*, 3rd edition. Macmillan, New York, 1934; the second edition (1905) contains useful material on circular and elliptical polarization, not given in the third edition.

Through the kindness of Prof. R. Signer, I have received a copy of the thesis of A. Wissler (Bern, 1940) (see p. 309). This reports, in detail, double refraction studies on carefully fractionated methylcelluloses and nitrocelluloses of various molecular weights, on gelatin, on sodium thymonucleate, and on tobacco mosaic and potato-X viruses. The dimensions of the cellulose derivatives agreed well with those from sedimentation and diffusion. Unfortunately it is not at present possible to discuss these important studies in more detail.

SYNTHETIC-RESIN ION EXCHANGERS

ROBERT J. MYERS

The Resinous Products and Chemical Company, Inc., Philadelphia, Pa.

CONTENTS

I. Discovery of Ion-Exchange Resins

Adams and Holmes (1) in 1935 reasoned that since the phenolic hydroxyl group is not involved in the condensation of phenols with formaldehyde to form insoluble resins of the "Bakelite" type, the hydroxyl group should be free to ionize in the usual manner and therefore be available for ion exchange. Experiments proved that phenol-formaldehyde resins, preferably those based on catechol, did possess base-exchange activity and permitted ion exchange when treated with solutions of inorganic salts. Amine-formaldehyde resins likewise adsorbed acid molecules from aqueous solution. This discovery has opened a new era in the chemistry of synthetic resins since the vast array of resins which have been prepared may now be reassessed on the basis of chemical properties rather than on the basis of physical properties, which have formed the criterion of their industrial utility. It focused attention to the fact that some synthetic resins are insoluble macromolecular electrolytes, capable, in spite of their insolubility, of metathetical reactions with ordinary electrolytes, and

as such, possessing special properties of practical value. In the field of base-exchange phenomena also, the work of Adams and Holmes led to a new viewpoint since for the first time ion-exchange phenomena could be studied on truly synthetic organic compounds whose composition and chemical properties could be varied at will.

Following this discovery the development of synthetic resins as ion exchangers has been rapid, though chiefly devoted to the preparation of materials of practical value in the purification of fluids, such as boiler-feed water and commercial products. Whereas the older exchangers were of a siliceous or humic character, and the more recently developed "carbonaceous zeolites" (principally derived from the sulfonation of coal, lignite, peat, etc.) were based upon natural organic substances of poorly defined chemical constitution, considerable interest was aroused when it was realized that synthetic-resin ion exchangers offered a non-siliceous character combined with "tailor-made" physical and chemical properties to any desired extent or degree within wide limits. As in the case of the siliceous exchangers, the industrial utility of these compounds has stimulated research on their practical aspects, and the patent literature has grown at a much more rapid rate than the literature devoted to scientific investigations of the ion-exchange process as it occurs in synthetic resins. However, several significant papers have appeared which presage interesting investigations in this field.

II. Types of Ion-Exchange Resins

Synthetic-resin ion exchangers have been prepared which are either acidic or basic in function and it is theoretically possible that synthetic resin ampholytes could be prepared. In fact, some synthetic-resin exchangers, primarily designed to perform as acid adsorbents, show some cation-exchange capacity as a consequence of phenolic nuclei in the molecule.

The synthetic resins with acidic function are to be recognized as insoluble macromolecular acids and form salts with the common bases; the synthetic resins with basic function are, similarly, insoluble macromolecular bases and form salts with common acids. In each instance it is usually possible to identify the chemical groups or radicles which are responsible, respectively, for the acidic and basic properties.

While wool, silk, horn and other protein-containing materials are not synthetic resins, they have long been known to contain acid- and

base-combining groups (*e. g.*, free amino and carboxyl groups) which permit their use as ion exchangers (*cf.* Austerweil (4)). The wool may be esterified to increase its anion-exchange capacity, or diazotised and coupled with di- or polyamines. Cotton may also be dyed with direct dyes which are diazotised on the fiber and coupled with developers having an amine function, to produce anion exchangers. Synthetic resins, such as glyptals and polystyrolenes, may be used by carrying out the condensation on nitro-products which are afterward reduced. Arylhydrazones or oxazones of oxycellulose or their reduced nitro derivatives, as well as derivatives of starch may also be used as anion exchangers (4). The base-exchange capacity of casein and formaldehyde-casein has been studied (14). The cation-exchange capacity of cellulose is partly due to the non-cellulosic constituents (lignin, etc.) and partly to carboxyl groups on the cellulose molecule (33a).

1. Synthetic Resins With Acid Properties

The original work of Adams and Holmes (1) indicated that polyhydric phenols, when condensed with formaldehyde, gave resins which exhibited exchange capacity. Monohydric phenols were not observed to give adsorption or exchange of cations, although Akeroyd and Broughton (2) as well as Bhatnagar, Kapur and Puri (5) later noted that monohydric as well as polyhydric phenols showed exchange capacity. The polyhydric phenolic nucleus of naturally occurring tannins offered a cheap source of raw material and Holmes' investigations dealt largely with tannins condensed with formaldehyde. Burrell (10) showed that only tannins of the catechol type produce resins which display calcium exchange. Kirkpatrick (22) also produced gels from tannins and formaldehyde which had base-exchange properties.

The exchange of calcium ions for hydrogen or sodium ions in simple phenolic resins may be considered to take place on the phenolic hydroxyl group. The exchanger, therefore, may be considered as an insoluble nucleus of the Bakelite or "C" stage type of resin, in which active or ionizable phenolic groups are bound to a non-diffusible "insoluble" structure. Later work by Holmes and the I. G. Farbenindustrie (37) showed that increased exchange capacity, particularly at low *p*H, is obtained by the incorporation of strongly acidic groups, such as alkyl or aryl sulfonic acids into the resin, which was effected by a condensation of the phenolic body with formaldehyde and sodium

sulfite (1, 37) whereby methylene sulfonic acid groups were introduced, or by a condensation of sulfonic acids of aromatic hydroxy compounds with formaldehyde (38). Increased exchange capacity may also be produced by the use of aldehyde-sulfonic acids (19) and the products may be hardened further by co-condensation with urea, thiourea and hydroxybenzenes (18).

2. *Synthetic Resins With Basic Properties*

Synthetic resins which exhibited anion exchange, or acid-adsorbent properties, were prepared by Holmes (1) by condensing aromatic amines, such as aniline or metaphenylene diamine, with formaldehyde. Aniline itself, as well as other aromatic amines, may be oxidized to insoluble dyes of the aniline black type, which may be used to adsorb acids from water (30, 12). The condensation of the amine with an aldehyde such as a monosaccharide (13, 16) yields an exchanger which may be regenerated with alkali. As in the case of the cation-exchanger, the anion-exchanger resin may be considered as an insoluble nucleus with "active spots" for acid adsorption. However, the condensation of aromatic amines with aldehydes proceeds both on the ring and through the amino-groups, so that low values for the adsorption of sulfuric acid and hydrochloric acid by a metaphenylene diamine resin, as found by Broughton and Lee (9) are to be expected. In order to fortify the adsorptive capacity of metaphenylene diamine resins, there may be incorporated into the resins during preparation alkyl groups to form quaternary ammonium bases, or the amine resin may be co-condensed with aliphatic polyamines or polyimines to give a more basic material (17). Treatment with cyanamide or dicyandiamide introduces the strongly basic guanidino group, while the aromatic amine may be eliminated altogether and resins prepared by the condensation of aliphatic polyamines with polyhalogen derivatives of a hydrocarbon (17). The hard, impervious resins formed by the condensation of metaphenylene diamine with aldehydes exhibits a pronounced effect of surface development on anion-adsorptive capacity (see below) and they may be improved by preparing the resin as a thin layer on a carrier body of coke or pumice (16).

Holmes noted no cation exchange in resins of the glyptal, vinyl and urea-formaldehyde types. Burrell (10) also found no sodium-calcium base exchange in resins of the rosin-maleic anhydride type. Whereas these investigations dealt with substances undoubtedly previously prepared for other industrial applications, it is probable that

suitable research would uncover resinous materials of other types which would undergo ion exchange, although the industrial utility of such materials may be doubtful. The more efficient resinous ion exchangers have the structure of homogeneous gels (26). As in silica gel, this combines a large inner surface, assuring high reactivity, with mechanical strength. The resins which have been prepared may be regarded as single examples in a scheme of the greatest variety. In principle, it should be possible to prepare a whole scale of resinous exchangers with any desired physical and chemical properties, provided that fundamental principles of resin chemistry and preparative technique are employed.

3. *Functional Groups of Synthetic-Resin Ion Exchangers*

The types of synthetic-resin ion exchangers which have been described in the literature may be classified on the basis of the functional group, as follows:

TYPES OF SYNTHETIC-RESIN ION EXCHANGERS

Functional group	Principal region of application
Acid Resins	
—SO_3H (nuclear)	Very low *p*H
—CH_2SO_3H	Low *p*H
—COOH	Neutral solutions
—OH (phenolic)	High *p*H
—CH_2OH —CH_2SH	Not yet investigated
Basic Resins	
—NH_2 (aromatic)	Acid solutions
—NH_2 (aliphatic)	Acid and neutral solutions
=NH (aromatic and aliphatic)	Not fully investigated
≡N (aromatic and aliphatic)	Not fully investigated

III. Nature of Exchange by Synthetic Resins

The ion-exchange and adsorption reactions of synthetic resins follow reactions similar to those of older exchange materials and identical in principle with metathetical reactions between ordinary electrolytes:

1. $NaR + Ca^{++} \rightleftarrows CaR + Na^{+}$
2. $HR + Na^{+} \rightleftarrows NaR + H^{+}$
3. $X + H_2SO_4 \rightleftarrows X.H_2SO_4$
4. $X.HCl + H_2SO_4 \rightleftarrows X.H_2SO_4 + HCl$
5. $X + H_2O + SO_4^{=} \rightleftarrows X.H_2SO_4 + OH^{-}$

The above equations are not balanced since the valence of the resin (R = cation exchange resin; X = acid-adsorbent resin) is unknown. The first two equations indicate that synthetic-resin exchangers undergo cation exchange in either a "sodium cycle" or a "hydrogen cycle." The extent of the reaction is, of course, governed by *p*H and the apparent dissociation constant of the cation-exchange resin.

The third equation is based upon what is known at present concerning the mechanism of the acid adsorption by basic resins. The reaction appears to be an adsorption of the acid as whole molecules. The fourth equation in similar fashion illustrates anion interchange on such a resin.

Some resins "split" neutral salts more or less effectively, depending upon the ease with which the salt is hydrolyzed. This type of reaction is expressed in Equation (5).

The reaction between the sodium derivative of phenol-ω-sulfonic acid type resin and calcium chloride has been shown to be a true base-exchange reaction (25). That is, an analysis of the effluent from an exchanger column showed that the anion concentration of influent and effluent were identical, the total cation concentrations of each were the same, while for a given amount of calcium adsorbed, there appeared in its place an equivalent amount of sodium ion. Likewise, the reaction between the hydrogen derivative of the same resin and calcium chloride or sodium chloride has been shown to be stoichiometric in character (25) and the titration with alkali of the effluent from a hydrogen-exchanger column is exactly equivalent to the salt concentration in the solution fed to the column. So exact is this behavior that it has been utilized in the laboratory in the analysis of solutions of calcium, sodium, ammonium and copper salts.

Schwartz, Edwards and Boudreaux (11) studied the variables involved in the adsorption of acids by a metaphenylene diamine-formaldehyde resin. The adsorption of hydrochloric acid and sulfuric acid was found to be influenced by the extent of developed surface, time of contact, initial concentration and the nature of the drying of

the resin. While Schwartz and co-workers did not record the fact, their adsorption data give isotherms of the Freundlich type. The adsorption of acid molecules by the "anion exchanger" appeared to be a reaction with whole molecules of the acid to form a hydrochloride or hydrosulfate of the amine resin (11, 15), as is generally true for ammonia and substituted amines. Very little "splitting" of neutral salts, such as sodium chloride, occurs when such a salt is treated with amine resins, although sodium sulfate solutions emerge from an anion adsorbent column distinctly alkaline. Easily hydrolyzed salts, such as ammonium chloride and aluminum salts, are readily converted to the corresponding hydroxides with removal of the acid, probably as whole molecules. This phenomenon has led to the somewhat misleading use of the term "hydroxyl-exchangers" in the description of the process.

The reactions are reversible, as indicated above, the equilibrium being determined by mass action factors. Thus, in the case of the inorganic exchangers, the cation-exchange resins may be regenerated with sodium chloride or hydrochloric or sulfuric acid, depending on whether the "sodium" or "hydrogen cycles" are used. The anion adsorbent is regenerated with sodium hydroxide or sodium carbonate or other alkaline solutions.

The mechanism of the exchange reactions on synthetic resins has received practically no attention. This is unfortunate since a full understanding of the process cannot be had until more complete information concerning equilibria in static systems is obtained, and the theories of exchange equilibria, which have been developed for siliceous exchangers, have been applied in this field.~ Thus a study of *p*H-neutralization curves would permit a test of the general mass action law relationship

$$\frac{[H^+]}{[Na^+]} = \frac{k_1}{k_2}\frac{[HA]}{[NaA]}$$

for the equilibria between a hydrogen exchanger HA and its alkali salt NaA. A similar relation should hold for the acid-adsorbent resin. While Schwartz, Edwards and Boudreaux did not record the fact, their data fit the Freundlich adsorption equation very well and a more complete review of the data might permit a test of the applicability of an equation similar to that derived by Jenny and Wiegner (20a)

$$\frac{[y_1]p_1}{[y_2]p_2} = K\frac{x_1}{x_2}$$

which is based upon two Freundlich adsorption isotherms of the type

$$\frac{y_1}{m} = k_1 x_1^{1/p_1}$$

where y_1 and y_2 are the moles of ions 1 and 2, respectively, bound per g. solid exchanger, x_1 and x_2 are the moles per liter of ions 1 and 2 in the external solution at equilibrium.

Griessbach (15) appears to be the only investigator to have formulated similar equations for the exchange equilibria of a hydrogen-exchange resin. His treatment is given in detail since the monograph in which it appeared is not readily available in this country.

If a hydrogen exchanger partially in the form of its salt is allowed to come to equilibrium with a solution of the monovalent salt wherein the ratio of concentrations of hydrogen ion and exchanging cation $[Na^+]$ is represented by x_1/x_2, then exchange will take place until the amount of either ion, z, reacted satifies equations (1) and (4):

$$\frac{[HA]}{[NaA]} \cdot \frac{k_1}{k_2} = \frac{[H^+]}{[Na^+]} \tag{1}$$

wherein $[HA]$ = concentration of hydrogen derivative in moles hydrogen per gram of resin.

$[NaA]$ = concentration of sodium derivative in moles sodium per gram of resin.

$[H^+]$, $[Na^+]$ = concentration of cations in moles per liter of solution, and k_1 and k_2 are the Freundlich adsorption isotherm constants for the two separate equilibria,

$$\frac{y_1}{m} = k_1 x^{1/p_1} \tag{2}$$

$$\frac{y_2}{m} = k_2 x^{1/p_2} \tag{3}$$

assumed to hold for the hydrogen and sodium ions, respectively. (Griessbach also assumes $p_1 = p_2 = 1$.)

As a result of the exchange the equilibrium conditions may be defined in terms of the quantities exchanged:

$$\frac{y_1 - z}{y_2 + z} \cdot \frac{k_1}{k_2} = \frac{x_1 + z}{x_2 - z} \tag{4}$$

where z is the number of equivalents exchanged.

If the hydrogen exchanger is gradually neutralized with an amount x of alkali, and if the neutralization occurs in an electrolyte solution containing from the outset a constant amount, c, of neutral salt, we have:

$$\frac{y_1 - z}{y_2 + z} \cdot \frac{k_1}{k_2} = \frac{z - x}{x + c - z} \tag{5}$$

Here the difference $z - x$ represents the amount of hydrogen ions in equilibrium with the solid phase when the ratio of salt to acid form is

$$\frac{y_1 - z}{y_2 + z} = \frac{y_1'}{y_2'} \tag{6}$$

and the neutral salt concentration is c.

For the case $z - x = \Delta h$ there follows

$$\frac{\Delta h}{c - \Delta h} = \frac{k_1 y_1'}{k_2 y_2'} \tag{7}$$

and

$$\frac{c}{\Delta h} = 1 + \frac{k_2 y_2'}{k_1 y_1'} \tag{8}$$

On rearranging and converting to logarithmic form, the expression becomes

$$p\mathrm{H} = \log \frac{1}{\Delta h} = \log \frac{1}{c} + \log \left(1 + \frac{k_2 y_2'}{k_1 y_1'}\right) \tag{9}$$

As above, c is the small amount of neutral salt added to the reaction solution at the start, and y_2/y_1 denotes the "loading ratio" of the ion exchanger at the instant of measurement. The quotient k_2/k_1 is to be interpreted as the ratio of the apparent dissociation constants of the ion-exchanger salt and the ion-exchanger acid.

If $p_1 \neq 1$, a corresponding expression may be derived, similar to the Wiegner equation:

$$p\mathrm{H} = \log \frac{1}{c} + \log \left[1 + \frac{k_2}{k_1} \left(\frac{y_2}{y_1}\right)^p\right] \tag{10}$$

and a still more complicated equation may be derived when $p_1 \neq p_2$.

The accuracy attainable in measuring hydrogen ion concentration makes it possible to put these functions to experimental test. Griessbach's data are shown in Figs. 1–5.

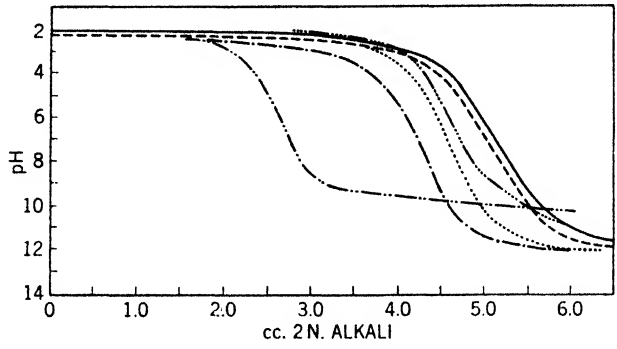

Fig. 1.—Specific influence of the replacing ion on the titration curves of K-Resin (5-g. sample).

-·-·-·- LiOH
····· NaOH
---------- KOH
-··-·-··- NH_4OH
———— RbOH
-·····-····· $Ba(OH)_2$

The difference in the buffering capacity of various ions is clearly shown in Fig. 1, which represents the neutralization of a nuclear sulfonic acid resin with alkalies. An explanation of the difference in the curves is to be sought in the differences in the activities of the cations, hydration effects and ionic size. Similar curves for a carbonaceous exchanger are shown in Fig. 2, where the specific effect of the cation is again apparent. Even though resinous exchangers possess quite an elastic structure, the various ions exert specific influences, as in the case of zeolite exchangers.

Figure 3 represents four families of theoretical curves calculated from Equation (10), with various exponents, for various ratios of k_2/k_1 and for various ratios of y_2/y. The slopes and positions of the theoretical pH-neutralization curves change as the constants k_1, k_2 and p are varied. The curves are based upon an arbitrary y, an arbitrary m and an arbitrary c. When $p = 1$, the Mass Action Law obtains. In Fig. 4 the pH-neutralization curves for various hydrogen exchangers are seen to fit certain of the theoretical curves. Thus it should be possible to characterize different types of exchangers by

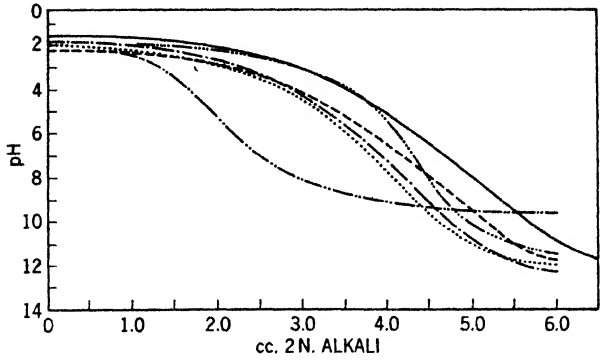

Fig. 2.—Titration curves for commercial carbonaceous exchanger A (7.1 per cent sulfur) (5-g. sample).

LiOH
NaOH
KOH
NH_4OH
RbOH
$Ba(OH)_2$

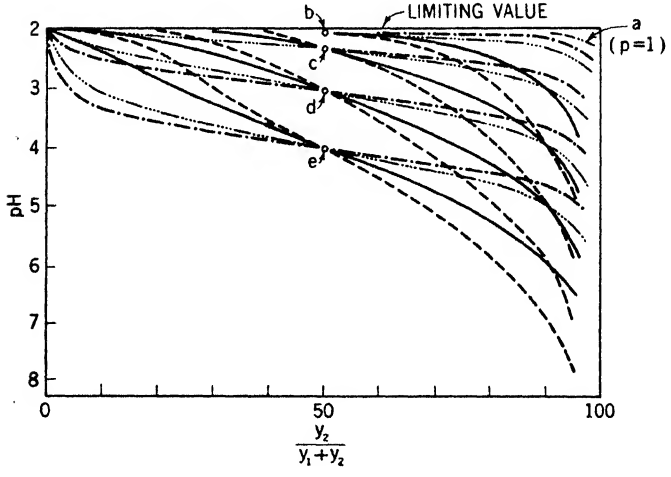

Fig. 3.—Theoretical curves for pH *vs.* loading ratio of the exchanger. The exponent p has the following values: (*a*) $k_2/k_1 = 0.01$, (*b*) $k_2/k_1 = 0.1$, (*c*) $k_2/k_1 = 1.0$, (*d*) $k_2/k_1 = 10$, (*e*) $k_2/k_1 = 100$.

$p = 0.67$
$p = 1.0$
$p = 2.0$
$p = 3.0$

means of well-defined constants, a definite step toward an understanding of base-exchange phenomena in resins. However, it may be noted that all of Griessbach's data were obtained at one concentration (0.01 *N*) of neutral salt. In view of the work of Steinhardt and Harris (34a) on the base-combining capacity of wool, it would be of interest to study the variations in the *p*H-neutralization curves as the ionic strength of the solution is changed, since the base-binding capacity of the resin should be a function of this variable.

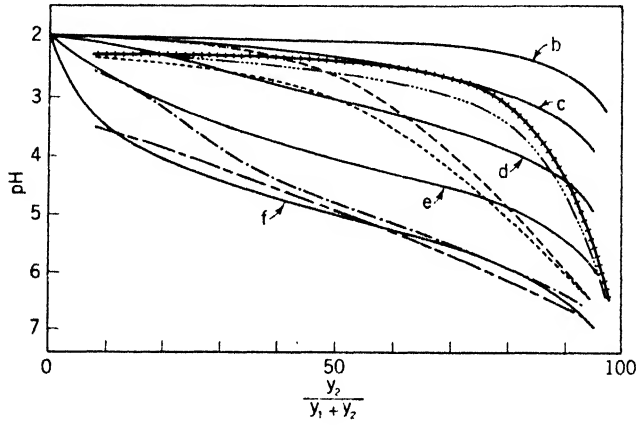

Fig. 4.—Comparison of observed and theoretical relations between *p*H and loading ratio. For the theoretical curves, the exponent p is taken as 1.5. The neutral salt concentration c is 0.01 *N*. Full lines are theoretical curves with the following k_2/k_1 values: (*b*) 0.1; (*c*) 1.0; (*d*) 10; (*e*) 100; (*f*) 1000.

—|—|—|—|—|— nuclear sulfonic acid resin
—·····—····· omega sulfonic acid resin
—·—·—·—·— carboxylic acid resin
— — — — — stabilized greensand
---------- commercial carbonaceous exchanger *A*
····· carbonaceous exchanger *O*

Figure 5 illustrates the effect of active acidic group on the character of the *p*H-neutralization curve. The increased base-combining capacity of the resin as strong acidic groups are introduced is obvious from the figure. Results such as this further illustrate the opportunities for research in base-exchange phenomena offered by synthetic resins. Variation of the chemical character of the exchanger is now

possible for the first time and significant contributions to an understanding of the reactions await the investigator.

Since results are presented graphically in Griessbach's paper, it is possible to draw qualitative conclusions only, as numerical constants cannot be calculated. However, as shown in Fig. 3, the mid-point of the titration curve is independent of the exponent p. Thus it should be possible to compare different exchangers by titration with the same base, and the numerical value of k_2/k_1 (which would serve as a

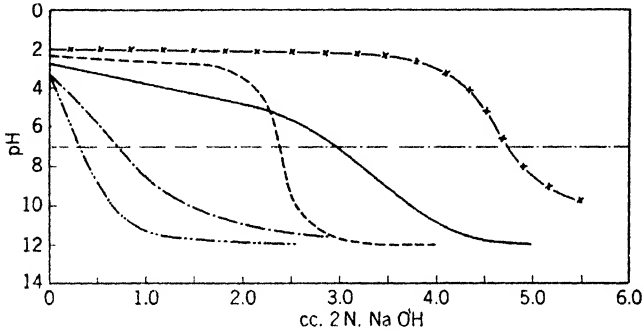

Fig. 5.—Titration curves for cation-exchangers. Five grams resin used unless otherwise stated.

	Designation	Active group
-X-X-X-	K-Resin	$-SO_3H$
----------	A-Resin	$-CH_2SO_3H$
————	C-Resin	—COOH
-·-·-·-·-	R-Resin	—OH
—·—·—·—	De-cationized greensand (20-g. sample)	

measure of the acid strength of the resin) could be deduced from the mid-point.

IV. Methods of Examination of Synthetic-Resin Ion Exchangers

The exchange or adsorption of ions by synthetic resins has been followed in both static and dynamic systems by the various investigators in this field. Simple adsorption experiments have been conducted by Akeroyd and Broughton (2), Broughton and Lee (9), Bhatnagar and co-workers (5), Schwartz and co-workers (11) and Myers, Eastes and Urquhart (27). These workers placed weighed

quantities of dried resin in contact with solutions of various concentrations and determined the extent of exchange or adsorption after equilibrium, or a pseudo-equilibrium, had been established. Dynamic exchange capacities in columns of synthetic resins have been determined by Holmes (1), Griessbach (15), Burrell (10) and Myers and Eastes (25). Industrial field studies have been reported by Seyb (33), Knodel (23), Griessbach (15) and Myers and Eastes (25).

In view of the industrial applications of synthetic resins, much attention has been devoted to the "usable" or break-through capacity of a resin in an exchange column, operated under conditions prevailing in commercial practice, rather than the total exchange capacity as determined by equilibrium conditions. Since variables such as diffusion, concentration and temperature are often included in determinations of break-through capacity, it is extremely difficult to characterize resins by this measurement alone, although the practical utility of the material is determined on this basis. Hence a scientific comparison of synthetic resins and their colloid-chemical characterization may be best started with a study of equilibrium conditions. Break-through capacities should be considered in the light of possible effects of diffusion and reaction velocities, as well as of equilibrium conditions in static systems.

V. Chemical Properties of Synthetic Resins in Static Systems

Akeroyd and Broughton (2) studied the adsorption of calcium from a solution of calcium hydroxide by a phenol-formaldehyde resin, condensed in an acid system. The adsorption was found to be extremely slow, and essentially complete only after 7 days' contact. There was a very slow adsorption after 300 hours' contact. Barium hydroxide, sodium hydroxide and trimethyl benzyl ammonium hydroxide were studied with phenol, resorcinol, quinol, catechol and phloroglucinol resins. The adsorption was calculated on the basis of a replacement of the hydroxyl hydrogens by the —CaOH group, so that a monohydroxylphenol should theoretically combine with 8.9 millimoles Ca per gram, a dihydroxylphenol should combine with 15.5 millimoles Ca per gram and a trihydroxylphenol, 20.8 millimoles per gram. Experimentally, the resins approached these values, which confirmed the predominantly chemical character of the adsorption. Viewed as a chemical reaction, it was concluded that the size of the ion was important due to steric hindrance, and that the total possible

adsorption would be dependent upon the degree of polymerization and the structure of the phenol. An ammonia-catalyzed resorcinol-formaldehyde resin showed lower adsorptive power for calcium hydroxide than did an acid-catalyzed resin. In catechol the ortho-

TABLE I

ADSORPTION OF ACID AND CONDITIONS OF PREPARATION OF RESINS

No.	Molar ratios in reaction mixtures		Initial mixing temp. °C.	Drying temp. °C.	Equilibrium adsorption from 0.0198 *N* H_2SO_4 m. moles/g.
	HCl / amine	HCHO / amine			
			Aniline Resins		
1	1.1	2.4	25	100	0.32
2	1.2	2.2	100	100	0.08
3	0.7	2.6	25	25	1.28
4	1.2	2.1	25	100	0.15
5	1.2	2.1	25	100	0.75
			Metaphenylene Diamine Resins		
6	2.4	4.0	25	100	1.40
7	2.2	4.0	25	100	1.55
8	2.2	4.0	25	100	1.50
9	2.2	4.0	0	25	1.48
10	2.2	4.0	0	25	1.50
11	2.2	4.0	100	100	1.55
12	2.2	1.2	25	100	2.47
13	2.2	1.2	25	25	2.75

0.2 Gram resin shaken at 25° with H_2SO_4. No. 4 resin dried before treatment with ammonia. Nos. 8, 12, 13 made with acid then treated with ammonia before drying.

hydroxyl groups were more readily accessible, and equilibrium was established in seven days with a resin based on catechol, while in resorcinol three months were required for equilibrium.

Broughton and Lee (9) found unexpectedly low values for the equilibrium adsorption of sulfuric and hydrochloric acids by aniline-formaldehyde and metaphenylene diamine resins, which was attributed to a condensation of the amine and aldehyde through the

amino groups as well as through the nucleus. Unlike the phenolic resins studied by Akeroyd and Broughton (2), adsorption by the amine-formaldehyde resins was usually rapid, equilibrium being frequently attained within 24 hours. Equilibrium values for the adsorption of sulfuric acid by the amine-formaldehyde resins were considerably smaller than those shown by the phenolic resins and were found to be sensitive to proportions of reactants, temperature of drying, etc. Table I, from the paper by Broughton and Lee, contains several points of significance.

If polymerization had occurred without involving the amino-groups, the aniline resin would have had a theoretical equilibrium adsorption of 9.0 millimoles per gram, the metaphenylene diamine resin an adsorption of 15.8 millimoles per gram. The low values found indicate that the amino groups were involved in the condensation. Protection of the amino-group during condensation does not, however, lead to a satisfactory resin.

The dipole moment of the solvent may be expected to exert some influence on the base-combining capacity of a synthetic resin. The only work of this character was done by Bhatnagar, Kapur and Puri (5), who studied the adsorption of salts, acids and bases by phenol-aldehyde and amine-aldehyde resins. The adsorption of benzoic acid by an acid-condensed phenol-formaldehyde resin from a series of solvents was in the decreasing order, water, carbon disulfide, carbon tetrachloride, acetone, ethyl alcohol, benzene and methyl alcohol. It was concluded that a solute is apt to be weakly adsorbed from solvents in which it is very soluble and from solvents possessing weak dipole moments, although the results do not actually justify such a general conclusion. Furthermore, the reaction was treated as a case of physical "adsorption" and benzoic acid was used whereas an organic base, such as benzyl trimethyl ammonium hydroxide, which is soluble in both aqueous and non-aqueous media, might have been better suited for use with a cation-exchange resin.

The usual increase in adsorption with ascension in a homologous series of organic acids has been noted by Bhatnagar, Kapur and Puri (5). This fact, coupled with the observation (5) that the adsorption of inorganic bases by a resorcinol-formaldehyde resin followed the Freundlich adsorption isotherm, lends weight to Griessbach's use of the Jenny-Wiegner equation (see above).

Inorganic bases are bound more readily by cation-exchange resins than are organic bases, such as aniline (5), in accord with the concept

that synthetic resins are macromolecules that exhibit base-combining capacities which are a function of the dissociation constants of the reacting base. It is to be expected that very strong organic bases of the quarternary ammonium type should behave in a similar manner as do strong inorganic bases.

The mechanism of the exchange phenomenon occurring in synthetic resins would appear to be more advantageously treated as a base- or acid-combining reaction of a typical colloid rather than as the surface adsorption reported in the Indian literature. Undoubtedly, synthetic resins of both the acid and the basic type will exhibit surface "adsorption" of acids, bases and neutral salts in much the same manner as any highly porous body, such as silica gel, exhibits such an adsorption. However, a fundamental approach to the mechanisms involved would appear to be most advantageously based upon the usual metathetical reactions which are to be expected with a particular resin. Thus, adsorption isotherms of the Freundlich type should be interpreted in the light of the equilibria which involve all the ions. An "adsorption isotherm" of a metallic salt solution in contact with a hydrogen exchanger should be studied in the light of *both* exchanging ions, as the adsorption isotherm may be expected to change with the concentration of either. Some work along this line has been done by Prof. C. C. Furnas of Yale University (13a), who has found that the exchange of copper for hydrogen on a carbonaceous exchanger is best interpreted as a function of *p*H.

Thus, in the "adsorption" of salts by synthetic resins it is necessary to analyze for all the constituents originally present as well as those which may be formed by ion-exchange, to determine whether the process is physical "adsorption" or an ion-exchange reaction. Since the chemical reactions, if they are of the ion-exchange character, occur at the surfaces of the resin particles, in the case of hard impervious resins the reaction may be considered as a species of adsorption. On the other hand, many resins are so porous that they show no appreciable effects of developed surface (27) and in this case the "adsorption" is most probably a chemical reaction throughout the mass of resin, obscured sometimes by diffusion effects.

Tsuruta (35) reported that an ammonia-condensed phenol-formaldehyde resin showed a decrease in the adsorption of fatty acids with an increase in molecular weight, whereas Bhatnagar, Kapur and Puri had found the reverse to be true with an acid-condensed phenol-formaldehyde resin. In view of this Bhatnagar, Kapur and Bhat-

nagar (7) investigated the adsorption of fatty acids by both acid and base-catalyzed resins, and concluded that the reverse order of adsorption with base-catalyzed resins was due to the very fine ultrapores of the base-catalyzed resins, which would therefore show a preferential adsorption of the smaller molecules. The adsorption of substituted acetic acids by a metaphenylene diamine resin was found to be increased by the introduction of acidic groups into the acid, while basic groups hindered the adsorption.

The nitrogen content of the ammonia-condensed resin prepared by Bhatnagar and associates appears to have been overlooked. Since simple amines are known to condense with phenol in the presence of formaldehyde, it is quite possible that the resin thus prepared may have contained basic groups, such as

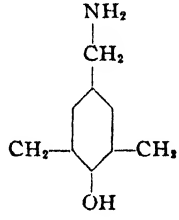

which would account to some extent for its different properties. Thus a resin so prepared may be considered a "basic resin" and no assumption of fine ultrapores as postulated by Bhatnagar would seem necessary to explain its similarity to resins based on metaphenylene diamine, or to soybean protein-formaldehyde condensates (8).

The adsorption of hydrochloric and sulfuric acid by a metaphenylene diamine resin was studied in detail by Schwartz, Edwards and Boudreaux (11). The adsorption was followed by a determination of both the total acid remaining and the anion introduced. The adsorption was found to be an adsorption of whole molecules of acid, in accordance with the fact that sodium chloride showed little or no adsorption of chloride in neutral and basic solutions. Sulfuric acid was adsorbed to a much greater extent than hydrochloric, and the adsorption was found to be a function of developed surface. The greater adsorption of sulfuric acid over hydrochloric acid has been noted by others (5, 27) and may be due to reaction as a monobasic acid, thus:

$$X + HCl \longleftrightarrow X \cdot HCl \qquad (11)$$

TABLE II

RATE OF REACTION BETWEEN BASIC RESINS AND ACID SOLUTIONS

Solution Volume: 120 cc. Room Temperature (ca. 25° C.)

Initial Concentrations { HCl—16.6 m. eq. per liter; H_2SO_4—16.6 m. eq. per liter

x = equilibrium concentration, in m. equiv./liter

y = adsorption, in m. moles/g. resin.

Metaphenylene Diamine-HCHO Resin

Time of contact, hrs.	Hydrochloric Acid				Sulfuric Acid			
	0.2 g. resin		0.75 g. resin		0.2 g. resin		0.75 g. resin	
	x	y	x	y	x	y	x	y
1	15.4	0.70	12.8	0.61	13.9	1.60	6.8	1.37
2	15.2	0.80	11.3	0.83	12.8	1.99	5.1	1.83
3	15.1	0.83	10.8	1.03	12.0	2.76	3.7	2.06
4	14.7	1.11	9.3	1.15	11.6	2.96	3.3	2.12
5	14.5	1.26	8.8	1.23	11.0	3.35	2.6	2.23
6	14.3	1.34	8.6	1.26	11.1	3.29	2.6	2.23
8	14.3	1.40	8.4	1.34	11.0	3.33	2.6	2.25

Alkylene Polyamine-HCHO Resin

Time of contact, hrs.	Hydrochloric Acid				Sulfuric Acid			
	0.1 g. resin		0.2 g. resin		0.1 g. resin		0.2 g. resin	
	x	y	x	y	x	y	x	y
1	14.2	2.78	11.2	3.24	11.6	5.96	8.3	5.02
2	13.4	3.80	9.7	4.13	10.4	7.35	5.2	6.86
3	12.9	4.36	9.2	4.47	10.2	7.60	5.2	6.78
4								
5	12.1	5.42	7.8	5.23	9.6	8.41	4.2	7.47
6	11.7	5.77	6.9	5.78	9.0	9.06	3.7	7.68
8	12.0	5.50	7.0	5.73	9.1	8.95	3.3	7.95

$$X + H_2SO_4 \longleftrightarrow X \cdot H_2SO_4 \qquad (12)$$

$$X + H_3PO_4 \longleftrightarrow X \cdot H_3PO_4 \qquad (13)$$

and *not*

$$2X + H_2SO_4 \longleftrightarrow X_2 \cdot H_2SO_4 \qquad (14)$$

However, Myers, Eastes and Urquhart (27) have found that the acid-binding capacity of an alkylene polyamine resin showed a variation which cannot be accounted for on this basis alone, as hydrochloric

acid was bound to the extent of 2.46 millimoles per gram, sulfuric acid was bound to 4.1 millimoles per gram and phosphoric acid was bound to 8.0 millimoles per gram. Probably other specific factors, such as hydration and molecular size of acid, also are operative.

While a great amount of general information may be gathered from the observations of Schwartz, Edwards and Boudreaux, and Bhatnagar and co-workers, it may be stated that a fundamental approach to the study of ion-exchange resins should start with a study of the combination of the resin with various acids and bases as a function of concentration and *p*H. Griessbach's work (mentioned above) represents a start in the study of cation-exchange resins, while the results of Myers, Eastes and Urquhart (27) represent likewise a preliminary approach to the study of acid-absorbent ("anion-exchange") resins.

For the study of the variables involved in the determination of adsorption isotherms, two typical resins were selected by Myers, Eastes and Urquhart. One was a low-capacity metaphenylene diamine resin prepared as disclosed in U. S. Patent No. 2,151,883 (1). The high-capacity anion-exchange resin was an alkylene polyamine-formaldehyde resin. The general technique consisted of placing a weighed quantity of the dried resin in contact with a definite volume of a solution of electrolyte and stirring at room temperature for a definite length of time. The solution was then filtered, and the filtrate analyzed for the characteristic ion. The anion exchangers were studied in detail since preliminary investigations had shown that the manner in which the adsorption isotherms were determined was of much greater importance in this case than with the cation exchangers. The resins were dry-screened to a minus 20-plus 40 mesh grading, "activated" by treatment over night with a 5% Na_2CO_3 solution (20 cc. per gram), washed free of alkali and air-dried. This product was used both in the adsorption isotherm determinations and in the column studies.

Table II indicates that a "practical" equilibrium adsorption value is attained in six hours' contact with both anion exchangers when in contact with either HCl or H_2SO_4. In view of these results, the adsorption isotherms were determined on 5–6 hour samples throughout the remainder of this work. A few experiments on long-time contact revealed that a slow but measurable adsorption continued beyond eight hours' contact time.

The data also indicate that (1) sulfuric acid is bound more readily by both resins, even to a greater amount than can be accounted for on the basis of single valencies, as mentioned above; (2) the metaphylene

diamine resin showed a binding capacity for hydrochloric acid which was relatively independent of residual concentration while the binding capacity of the same resin for sulfuric acid was a function of residual concentration, (3) the alkylene polyamine resin bound hydro-

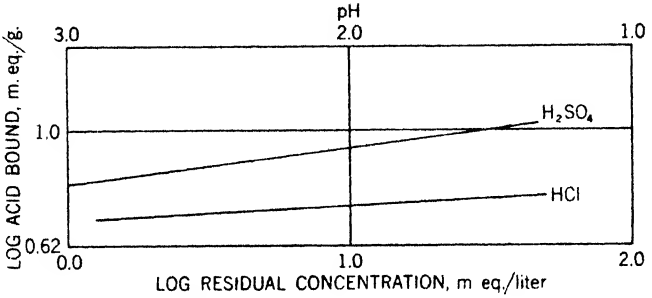

Fig. 6.—Acid bound by alkylene polyamine resin.

chloric and sulfuric acid to a definite amount, with little or no dependence upon concentration. The alkylene polyamine resin was definitely a porous gel while the metaphenylene diamine resin appeared to be an impervious solid.

The quantities of the acids bound by the two resins as a function of concentration were determined after 5–6 hours' contact and the results were found to accord with a Freundlich adsorption isotherm relationship, as shown in Figs. 6 and 7:

$$\log u = \log k + n \log c \tag{15}$$

where u is amount of acid bound in m.eq. per g resin; c is residual concentration in m.eq. per liter; and k and n are constants. From the data given in Figs. 7 and 8,

	HCl		H_2SO_4	
	k	n	k	n
Metaphenylene diamine resin	0.49	0.396	1.30	0.388
Alkylene polyamine resin	4.94	0.048	6.60	0.076

The acid bound by metaphenylene diamine resin becomes therefore:

$$\text{for HCl,} \quad u = 0.49c^{0.396} \tag{16}$$

$$\text{for } H_2SO_4, \quad u = 1.30c^{0.388} \tag{17}$$

which means that the binding capacity of this resin is in an intermediate range, since n is less than 1.0. If the binding capacity of the resin were very low, n should approach 1.0, and the amount of acid bound would be proportional to the concentration; in other words a

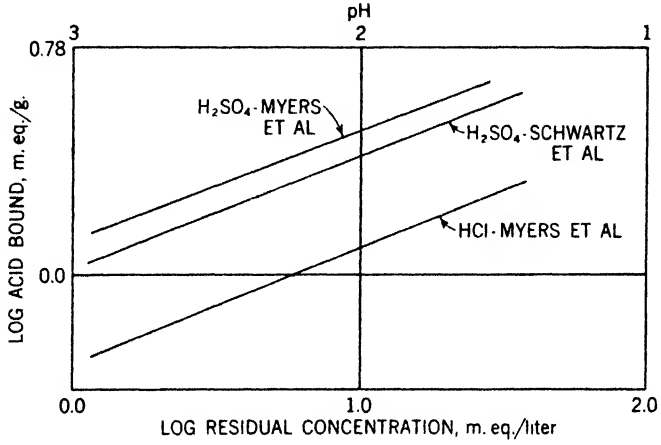

Fig. 7.—Acid bound by metaphenylene diamine resin.

typical Henry's law relationship would hold. The acid bound by the alkylene polyamine resin is likewise expressed by the equations,

$$\text{for HCl,} \quad u = 4.94c^{0.048} \tag{18}$$

$$\text{for } H_2SO_4, \quad u = 6.60c^{0.076} \tag{19}$$

These values indicate that most of the "active spots" which are responsible for acid binding are covered or reacted with the acid under the conditions of the experiments reported by Myers, Eastes and Urquhart. This is quite likely, as the pH range covered, from 1.0 to 3.0, probably represents the lower end of a pH-neutralization curve whose mid-point lies on the alkaline side of pH 7.0. It should be of interest to extend such studies on the acid-binding properties of basic resins well into alkaline regions.

The exchange capacity of synthetic resins in the "sodium cycle" is readily determined by saturation with a solution of the ion under investigation. Thus the total exchange capacity of a quebracho tannin-formaldehyde resin which contained ω-sulfonic acid groups was found by Myers, Eastes and Myers (26) to be 2.0–2.4 m.eq. calcium per

gram. The exchange capacity was also found to be independent of particle size, and equilibrium was established after only two hours' contact. These results may be taken as proof that the synthetic resin ion exchanger was of a very porous gel structure. The much higher capacity of synthetic resins, as compared to the siliceous exchangers, may be seen from the fact that the latter possess exchange capacities of the order of 1–3 milliequivalents per gram (20). Since the exchange capacity is imparted by hydrophilic groups, progressive "loading" of a resin molecule with additional exchangeable atoms soon leads to solubility, or such excessive swelling when the resin is placed in water that the volume-capacity (a most important quantity in industrial applications) decreases rather than increases. It is theoretically possible to design synthetic resins with two and even three exchangeable atoms per phenolic nucleus (whose exchange capacity would be tremendous) but experience teaches that such materials would probably disperse spontaneously in water and form colloidal solutions.

VI. Chemical Properties of Synthetic Resins in Dynamic Systems

The industrial application of exchange resins in water softening and in the desalting of waters to produce a pseudo-distilled water has focused attention on the behavior of such products in exchange columns, where the exchange occurs in a dynamic system.. Laboratory evaluation of synthetic resins is accordingly (26) carried out in columns of resin through which the solution to be treated flows at rates comparable to those occurring in industrial units. Furthermore, since the economic value of an exchanger is related to the quantities of regenerant required to produce a given exchange capacity, the columns are operated under conditions which do not regenerate the exchangers to full capacity. Likewise, the break-through capacity is determined rather than the full capacity, at a particular regenerant ratio; that is, the capacity is determined as that quantity of ion which is adsorbed completely up to the point where it first appears to a detectable or specified amount in the effluent.

Thus, a quebracho-ω-sulfonic acid-formaldehyde resin investigated by Myers, Eastes and Urquhart was found to possess a total exchange capacity for calcium (when replacing sodium) of 2.4 milliequivalents of calcium per gram dry resin, or 1360 milliequivalents calcium per liter of wet resin packed in the exchanger bed. However, a ratio of 16 equivalents of sodium chloride to one of calcium would be neces-

sary to regenerate nearly completely the exchanger column after exhaustion with calcium ion. Since this is unfeasible in commercial practice, an equivalent ratio of 3.0 is generally employed. Such a treatment partially regenerates the exchanger column and a "usable" capacity of 570 milliequivalents of calcium per liter of resin is obtained.

Moreover, due to a low reaction velocity and to diffusion effects (the resin particles must be discrete particles of such size that resistance to hydraulic flow is not excessive), the capacity up to the point when the exchanging ion first appears in the effluent is usually considerably less than the capacity up to the point of saturation with the solution employed (26). Thus, whereas Myers, Eastes and Urquhart (27) found that the equilibrium values of the adsorptive capacity of a series of anion exchangers closely approximated the break-through capacities of the same resins in exchanger columns, in general this is not true, since restricted conditions are employed with respect to the extent of regeneration and time of contact in the column.

The evaluation of commercial exchange adsorbents in the laboratory offers an opportunity for a judicious interpretation of fundamental physico-chemical characteristics of ion-exchange substances in the correlation of easily determined quantities with practical exchange capacities. The present method of small-scale studies in laboratory columns under conditions simulating those found in large-scale exchanger beds becomes laborious and costly when hundreds of new products must be examined under a variety of conditions, such as concentrations and types of exchanging ions, regenerants and regenerant ratios. While such studies in columns must eventually be made before practical application is undertaken, the development of simple testing techniques based upon fundamental principles should not only obviate much of the labor involved in the evaluation of exchange adsorbents, but serve as well to clarify the mechanism of ion exchange. Myers, Eastes and Urquhart (27) made an attempt to correlate adsorption isotherms with exchange capacity as determined in columns. The exchange phenomenon in a column of a synthetic-resin ion exchanger was considered as a species of chromatographic adsorption, in which a "band" of exchanged (or adsorbed) cation or anion moved progressively downward through the column. The "break-through" capacity, the point at which the exchanging ion first appeared in the column effluent was regarded as the adsorption

value for the resin in contact with a solution with an ion concentration equal to that of the original solution fed to the column. Such a picture of the adsorption was consistent with the observation that a hydrogen-exchange resin separated calcium from sodium when two ions were present in a solution fed to the column. While the jet-black color of most hydrogen exchangers prevented the visual observation of such phenomena, certain anion-exchange resins, originally of a light-orange color, formed a reddish orange band superimposed on a brown band when a mixture of hydrochloric and sulfuric acids was flowed through a column of the resin. Analysis of the bands revealed that the reddish orange band was the pure hydrosulfate, the brown band the pure hydrochloride form of the resin.

Wilson's theory (40, see also 34b) of chromatography was examined and suitably extended as follows to apply to the calculation of the probable exchange capacity of a resin from a knowledge of the adsorption isotherm for the ion in question. Wilson showed that insertion of the appropriate boundary conditions into the differential equation,

$$\left(\frac{\partial Q}{\partial v}\right)_x dv\, dx + \left(\frac{\partial c}{\partial x}\right)_v dv\, dx = 0 \tag{20}$$

(which describes the adsorption changes occurring at a point x centimeters from the top of a column of adsorbent containing M grams of adsorbent per centimeter length of column when a volume v of a solution of solute at an initial concentration c_0 is fed to the column, the adsorption isotherm for the given solute on the adsorbent being $q/m = f(c)$, or $Q = Mf(c)$, where Q is the number of millimoles adsorbed per centimeter length of column in equilibrium with a solution whose concentration is c) leads to the discontinuous solution,

$$\text{for } 0 \leqslant x < vc_0/Mf(c_0), \quad Q = Mf(c_0) \tag{21}$$

$$\text{and } x > vc_0/Mf(c_0), \quad Q = 0 \tag{22}$$

which accounts in a satisfactory manner for the sharpness and the occurrence of bands. Now when a sufficient volume of solution v has been fed to the column to extend $vc_0/Mf(c_0)$, the length of the band, to l, the length of the column, "break-through" occurs. Since break-through is customarily expressed in terms of grams adsorbate per gram of adsorbent, and since

$$\frac{vc_0}{lM} = f(c_0) = \frac{\text{grams adsorbate}}{\text{grams adsorbent}} = \text{capacity} \tag{23}$$

a knowledge of adsorption isotherms should permit a calculation of break-through capacity of columns of adsorbents when break-through occurs. In order to determine whether adsorption isotherms could be applied in this fashion to ion-exchange phenomena, the isotherms were determined for several anion- and cation-exchange resins, and

TABLE III

COMPARISON OF ADSORPTION ISOTHERM CAPACITIES (CALCULATED) AND EXCHANGE COLUMN CAPACITIES (OBSERVED)

Expt. No.	Resin type	Acid	Acid concn. mg./liter*	Dynamic capacity mg./g. obs.	Static capacity mg./g. calcd.
	Anion Exchangers: Good Agreement				
DU-222	Phenylene diamine (20/30)	HCl	490	34.3	37.0
DU-222A	Phenylene diamine (20/30)	H_2SO_4	529	94.0	92.0
DU-128	Alkylene polyamine resin	HCl	613	192.0	226.0
DU-128A	Alkylene polyamine	HCl	449	220.0	220.0
DU-159	Alkylene polyamine-A	H_2SO_4	566	393.0	420.0
DU-185	Alkylene polyamine-B	H_2SO_4	493	368.0	410.0
DU-207A	Modified phenolic-II	HCl	490	67.0	65.0
DU-207	Modified phenolic-III	HCl	490	33.0	22.8
DS-188	Modified phenolic-IV	HCl	490	74.2	82.0
DS-216	Modified phenolic-IV	H_2SO_4	529	204.0	211.0
	Anion Exchangers: Poor Agreement				
DU-217	Phenylene diamine	HCl	490	20.6	52.0
DU-217A	Phenylene diamine	H_2SO_4	529	116.6	178.0
DS-192	Modified phenolic-II	HCl	483	45.5	65.0
DS-190	Modified phenolic-I	HCl	483	45.0	22.7

* This is equivalent to parts per million in the particular aqueous systems employed since the densities of the solutions were essentially equal to 1.

the calculated values derived therefrom were compared with the values obtained by direct measurement in exchange columns.

The total exchange capacity was calculated from the Freundlich adsorption isotherms obtained on the various resins, at concentrations of solute corresponding to those employed in the column experiments. The results were then compared with the exchange capacities actually observed. Table III lists a comparison of observed and calculated values on anion-exchangers. The comparison was grouped into pairs

showing good agreement and poor agreement between the two values.

The number of cases in which very good agreement obtains between the calculated and observed capacities definitely out-numbers the instances of poor agreement. The results may be taken as evidence that the concept on which the calculations are based was fundamentally sound. The poor agreement is, with but one exception, due to a low column exchange value. These cases may be due to premature break-through, produced by channelling in the bed. On the other hand, Wilson's theory demands a non-diffuse front proceeding down the column, and this could not be assured in all cases. The capacities determined in the columns and calculated from the adsorption isotherms are total capacities, based upon the assumption that a single chromatogram is being produced as the solution passes progressively down through the column of fully regenerated adsorbent. In actual commercial practice, the "usable" capacity, or capacity obtained with a fixed quantity of regenerant (which is, however, insufficient to produce complete regeneration) is of importance. If the regeneration is considered as the superposition of one chromatogram on another, it is conceivable that a suitable mathematical analysis should permit the calculation of exchange capacity at any arbitrarily chosen regenerant ratio.

Griessbach has outlined (15) another method of approach to the dynamic systems. It is assumed that the contact time is sufficient to permit maintenance of static equilibrium at the surface of the resin particles at the front of the advancing column of liquid. It then follows from equation (4) above, that

$$\frac{(y_1 - z)k_1}{(y_2 + z)k_2} = \frac{dz/dt}{\frac{dx}{dt} - \frac{dz}{dt}} = \frac{dz}{dx - dz} \tag{24}$$

where dx is the amount of salt passing in time dt, and dz is the amount of hydrogen ion exchanged in the same interval. On rearrangement, we have:

$$dx = \left[1 + \frac{k_2(y_2 + z)}{k_1(y_1 - z)}\right]dz \tag{25}$$

Upon integration and inserting $y_1 + y_2 = s_0$ where s_0 = total capacity, and replacing y_1 by y_0, we have finally:

$$z = y_0\left[1 - \exp.\frac{-k_1x + (k_2 - k_1)z}{k_2 s_0}\right] \tag{26}$$

For the case where $k_1 = k_2$ (usually true when neutral ions of equal valence are exchanged), equation (26) simplifies to:

$$z = y_0 \left(1 - \text{exp.} \frac{-k_1 x}{k_2 s_0}\right) \tag{27}$$

In the exchange of hydrogen for other cations, the two k values are not in general equal and equation (26) must be used.

The more complicated case of two ionic constituents in the solution passing through the bed has also been considered by Griessbach, but the derivations do not appear to be fully above question. Unfortunately no experimental test of the formulas appears to have been made.

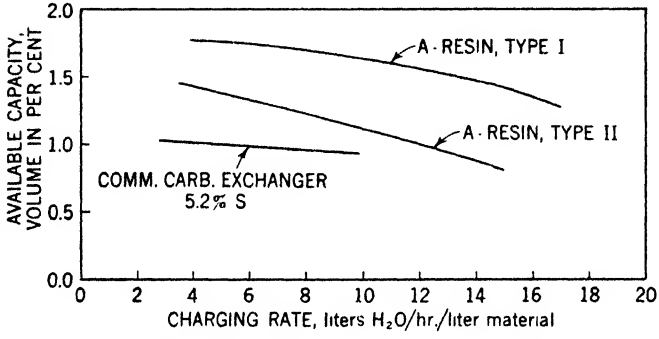

Fig. 8.—Dependence of available capacity on the specific charging rate.

Considerable empirical information can be gained from simple exchange column studies. Holmes in his original work on synthetic resin exchangers (1) employed columns and found that ion-exchange occurred between resins based upon tannins of oak, larch, gambier, mangrove, quebracho, cutch and wattle. A variety of inorganic ions were examined and found to be adsorbed to various degrees. Complete removal of ions such as calcium and magnesium was easily effected; this forms the basis of the industrial utility of resins of this type. Ammonia was removed from a gas stream, while amine-aldehyde resins adsorbed acids to effect total removal. Weak acids such as acetic and phenol were adsorbed. A preferential adsorption of certain metallic ions was reported.

The findings of Holmes immediately stimulated researches upon the adsorption of ions by synthetic resins in dynamic systems. The

laboratories of the I. G. Farbenindustrie, in developing the commercial aspects of the resins, studied the relative performance of synthetic resins and the older exchange adsorbents in commercial water-softening units. Griessbach (15) studied the exchange capacity and exchange velocity of resins and commercial exchangers in a large unit (7–15 cubic meters), operating at 40° C., to reduce the hardness of water from approximately 60 milligrams calcium carbonate per liter to below 1 milligram per liter. His data (see also Fig 8.) are indicative of the relative performance to be expected of ion-exchange resins:

Exchanger	1*	2	3	4	5	6	7
Greensand	85	11–12	10	0 30	350	7	28.6
Carbonaceous zeolite	100	7	50	0.86	450	15	22.2
Phenol-ω-sulfonic acid resin	200	20	27	1 30	500	10	20.0

* 1—water throughput, cu. meters/hour.
2—specific rate of charge, cu. meters water/cu. meter exchanger.
3—time of run, hours
4—available volume capacity, kg. CaO/100 liters exchanger.
5—salt required, per cent of theory
6—amount of exchanger used, cu. meters.
7—chemical efficiency

Thus, the synthetic resin exchanger, operating in the sodium cycle to replace calcium and magnesium by sodium ions, was sufficiently rapid in its exchange to permit much higher flow rates at essentially the same regenerant ratio (column 5), but with much higher capacity.

The exchange capacities of both cation and anion exchangers in laboratory columns and in a semi-commercial unit were studied by Myers and Eastes (25), and by Myers, Eastes and Myers (26). The exchange capacity of a phenol-ω- sulfonic acid resin was found to be affected by regenerant ratio, rate of flow of regenerant, direction of flow of solution and other variables. The original papers should be consulted for the many details of commercial importance; briefly, the following were found:

1. A phenol-ω-sulfonic acid resin in the sodium cycle exhibited a high rate of exchange in that a change in flow rate over a ten-fold range did not influence the break-through capacity of the bed for calcium ion. Such behavior is in general characteristic of synthetic resins with a porous gel structure.

2. The regeneration of the calcium form of the resin by sodium chloride was approximately 50% efficient in the first portions of regenerant to emerge from the column. The regenerant ratio markedly

affected the capacity of the resin for calcium ion and the relationship was expressed over a considerable range by the equation:

$$y = 1.86 \log x + 3.10 \text{ (for 4\% NaCl solution)}$$

where y = lbs. calcium carbonate exchanged per cubic foot of resin and x = lbs. sodium chloride used per cubic foot of resin. Downflow regeneration was more effective than upflow regeneration. The adsorptive capacity of the phenol-ω-sulfonic acid resin for calcium ion was such that a high concentration of sodium ions in the water being treated was tolerated without an appreciable effect on the capacity or efficiency of removal of calcium ions. The break-through capacity was found to be independent of calcium concentration, in accordance with the findings reported above that the adsorption capacity of the cation-exchange resin was independent of the residual concentration.

3. An alkylene polyamine-formaldehyde anion-exchange resin was examined and it was found that the regenerant (4% sodium carbonate) was exceedingly efficient provided that the rate of flow through the column was of the order of 1 gallon per square foot/minute (245 centimeters per hour linear velocity). The efficiency was essentially 100% on a stoichiometric basis up to some 80% of the capacity of the bed. Sulfuric acid was more readily adsorbed than hydrochloric acid. Sodium hydroxide solutions showed still higher efficiencies of regeneration, but the wash water requirements were excessive.

4. Whereas the above mentioned cation-exchange resin showed no effect of particle size (developed surface) on break-through capacity for calcium ion, the break-through capacity of a metaphenylene diamine resin for ionorganic acids was markedly a function of particle size. The diamine resin was examined microscopically and found to be a hard impervious resin as compared to the porous gel structure of the other resin.

5. The capacity of the anion-exchange resins for acids was a function of the concentration of the acids. Again, the aromatic diamine resin showed a considerable variation in exchange capacity with concentration, while the porous alkylene polyamine resin was much less effected.

6. Calcium was removed from a solution at *p*H 1.8 as well as from a solution of *p*H 9.0. The anion exchangers removed acids from solutions of *p*H 1.8 to give effluents of *p*H 6.8–7.0. The exchange of calcium for sodium or hydrogen ions was stoichiometric in character. The adsorption of the acid molecules by the anion-exchange resins

resulted in a "swelling" or "breathing" (15) of the resin and the sedimentation volume obtained after backwash and settling was as much as 28% greater than the resin in the regenerated, free amine form.

Myers, Eastes and Urquhart (27) found that the alkylene polyamine anion exchanger showed a high degree of preferential adsorption of sulfate over chloride. It was observed that when a light-yellow colored anion exchanger was treated with a mixture of hydrochloric and sulfuric acids (total concentration, 500 milligrams per liter, mole ratio, 1:2), an orange band appeared and proceeded down the column, preceded by a dark brown band, as the solution was continuously fed to the column. When the brown band reached the bottom of the column, chloride ion first appeared in the effluent. The column was divided into sections (ca. 2 inches long) and the resin in each section was analyzed for sulfur and chlorine. The results were as follows:

Section	% Sulfur	% Chlorine	Color
1	11.64	0.00	Orange
2	11.59	0.00	Orange
3	11.59	0.00	Orange
4	11.36	0.00	Orange
5		1.17	Orange
6	3.20	12.32	Bands overlap
7	0.00	18.31	Brown
8	0.00	13.00	Brown

Thus, the synthetic resins undergo preferential adsorption to produce chromatograms. Considerable interest and opportunities for research appear to be offered by this behavior. The phenol-ω-sulfonic acid resins also exhibit a certain degree of specificity in adsorption of metallic ions, such as copper and zinc, as shown by Griessbach (15) and Myers, Eastes and Urquhart (27).

The investigations of the exchange capacity of synthetic resins in dynamic systems have been largely devoted to studies on hardness-producing cations, in the case of the cation exchangers, and on hydrochloric or sulfuric acid, in the case of anion-exchanger resins. This is quite natural in view of the commercial applications of such products. Even for these ions, there is considerable room for research on the effects of rates of flow, *p*H, temperature, concentrations and type of adsorbate on the exchange of ions in exchanger columns, and the study of other types of ions is practically untouched.

The fundamental investigations on the colloid-chemical properties of synthetic resins have lagged far behind their commercial development. It is to be hoped that the unique possibilities for research in this field will attract investigators.

VII. Applications of Synthetic-Resin Ion Exchangers

While a discussion of the applications of ion-exchange resins is not properly a subject for inclusion in a review of their colloid-chemical properties, the many unique applications now possible for the first time may be briefly mentioned since the technical development of some may well involve fundamental investigations on the character of the exchange.

The potential uses for ion-exchange resins are almost as numerous as the resin types which are theoretically possible. As in the case of every new industrial tool, the base-exchange process has often been hailed as the key to the solution of innumerable problems. However, the application of synthetic ion-exchange resins to specific problems offers a higher degree of probable success than was achieved in earlier applications in view of the high exchange capacity, high exchange velocity and general stability, both mechanical and chemical, of the newer adsorbents (26).

Since the use of a hydrogen exchanger results in the replacement of all cations by hydrogen ions, and the use of an anion absorbent results in the complete removal of free acids (except carbonic), the passage of tap water through a double system of hydrogen and hydroxyl exchangers removes all dissolved salts and results in the production of water comparable to distilled water in quality. Carbonic acid may be removed by aeration, and traces of either acid or salt remaining may be removed by the use of a third, or "buffer-filter" (15), which consists of a hydrogen- or anion-exchanger half-converted to the exhausted form. Traces of acid are neutralized or absorbed, while traces of salt are converted to the acid. The effluent is truly neutral and of exceedingly low total solids content (31). The following example illustrates the possibilities in this connection:

	Elect. cond. $L \times 10^6$	Total solids Mg./liter
Before treatment	187	116
After combined resin treatment (range of values)	2.0–6.2	2.5
Laboratory distilled water	5.0	2.6

The softening of water by the use of the cation-exchange resin in the sodium cycle has been described above and may be considered feasible in the treatment of water for industrial and domestic use, where only the hardness of the water is objectionable. Similarly, the purification of water for industries, such as high-pressure steam generation, beverage manufacture, ice manufacture, textile processing, etc., where water of a very low total solids content is desired, should present a fertile field of application for resinous exchangers. The chemical industries, especially those engaged in the manufacture of drugs, C. P. chemicals, etc., should be able to obtain complete removal of salts by the resin exchanger process, or obtain very pure water for use in preparations, washing of precipitates, etc. By blending of "decationized" water from a hydrogen exchanger with raw water, or by blending with water which has been treated with a sodium exchanger, the reaction of the free mineral acids with the bicarbonates in the water effects a reduction in alkalinity and total solids, as well as in hardness (36).

By means of cation or anion exchangers, it is possible to prepare salts by the use of resin ion exchangers (21, 28). Double decomposition may be employed to prepare inorganic or organic salts, but the concentrations involved, and the large excesses required may make the operation economically unfeasible, save in special applications Thus, sodium nitrate has been prepared from sea water and calcium nitrate.

The use of ion-exchange resins for recovery of valuable electrolytes present in very dilute aqueous solutions offers methods of obtaining materials which could not be otherwise obtained. The recovery of copper from industrial effluents (15, 32) or from mine waters appears to be practical. Similarly, the removal of undesirable metal ions (iron from zinc chloride or ammonium sulfate) may conceivably be effected as a consequence of ion interchange, or chromatographic adsorption. The organic character of ion-exchange resins may well prove beneficial in that the adsorbed metal could be obtained by simple ashing of the adsorbent, a method which could not be used with zeolites.

In the removal of electrolytes from aqueous solutions of non-electrolytes, such as pharmaceutical preparations, enzyme extracts, dyestuffs and sugars (34) the ion-exchange resins should find advantageous uses for the removal of all salts or specific ions. Gelatin solutions may be freed of all dissolved salts by passage through first a hydrogen-

exchange resin and then an anion-exchange resin (26). An adsorption of gelatin occurs but this does not interfere with the action of the exchanger. The salts in crude sugar solutions may be removed altogether by such a treatment, with the conductivity of the effluent equal to that of distilled water.

The anion-exchange resin may be used to remove traces of acidity by simple adsorption, with no neutral salt being imparted to the solution. Such a method is obviously superior to mere neutralization. Similarly, the hydrogen-exchanger may be used to impart acidity by reaction with neutral salts already present. Waste acids and bases may be utilized by employing them to regenerate the cation and anion exchangers.

Other applications of resinous exchangers may be conceived on the basis of the physical and chemical properties already described in the literature. Specific applications will no doubt encourage further research on these new interesting products.

Bibliography

1. B. A. Adams and E. L. Holmes, *J. Soc. Chem. Ind.*, **54**, 1–6 T (1935); British Patents 450,308 and 450,309 (June 13, 1936) and 474,361 (November 25, 1937). French Patents 796,796 and 796,797 (April 15, 1936). U. S. Patents 2,104,501 (Jan. 4, 1938), 2,151,883 (March 28, 1938), 2,191,853 (February 27, 1940).

2. E. I. Akeroyd and G. Broughton, *J. Phys. Chem.*, **42**, 343 (1938).

3. G. Austerweil, *Bull. soc. chim.*, (5), **3**, 1782 (1936); *Ibid.*, **6**, 55 (1939).

4. G. V. Austerweil and L'Auxiliaire des chemins de fer et de l'industrie, French Patent 832,866 (October 4, 1938). British Patent 497,928 (December 23, 1938).

5. S. S. Bhatnagar, A. N. Kapur and M. L. Puri, *J. Indian Chem. Soc.*, **13**, 679 (1936).

6. S. S. Bhatnagar, A. N. Kapur and M. S. Bhatnagar, *Ibid.*, **16**, 249 (1939).

7. S. S. Bhatnagar, A. N. Kapur and M. S. Bhatnagar, *Ibid.*, **16**, 261 (1939).

8. S. S. Bhatnagar, A. N. Kapur and M. S. Bhatnagar, *Ibid.*, **17**, 361 (1940).

9. G. Broughton and Y. N. Lee, *J. Phys. Chem.*, **43**, 737 (1939).

10. H. Burrell, *Ind. Eng. Chem.*, **30**, 358 (1938).

11. W. R. Edwards, Jr., M. C. Schwartz and Grace Boudreaux, *Ind. Eng. Chem.*, **32**, 1462 (1940).

12. Établissements Phillips et Pain, French Patent 826,408 (March 31, 1938).

13. F. Fischer and W. Fuchs, *Brennstoff-Chem.*, **8**, 291–293 (1927).

13a. C. C. Furnas, private communication; C. C. Furnas and R. H. Beaton, *Ind. Eng. Chem.*, **33**, 1500 (1941).

14. E. Graf, *Kolloid-Beihefte*, **46**, 229–310 (1937).

15. R. Griessbach, *Ueber die Herstellung und Anwendung neuerer Austauschadsorbienten, inbesonders auf Harzbasis*, Verlag Chemie, Berlin, 1939.

16. E. L. Holmes, L. E. Holmes and W. G. Prescott, British Patent 506,291 (May 5, 1939).

17. I. G. Farbenindustrie, Akt.-Ges., French Patent 820,969 (November 24, 1937). British Patent 489,173 (July 20, 1938).

18. I. G. Farbenindustrie, Akt.-Ges., French Patent 838,332 (March 2, 1939).

19. I. G. Farbenindustrie, Akt.-Ges., French Patent 845,669 (April 5, 1939).

20. H. Jenny, *J. Phys. Chem.*, **36**, 2217 (1932).

20a. H. Jenny and G. Wiegner, *Kolloid-Z.*, **42**, 268 (1927).

21. H. Johnson (to Norsk Hydro-Elektrisch), Norwegian Patent 59,035 (Feb. 28, 1938).

22. W. H. Kirkpatrick, U. S. Patents 2,094,359 (Sept. 28, 1937) and 2,106,486 (Jan. 25, 1938).

23. H. Knodel, *Chem. Fabrik*, **1940**, 363.

24. D. A. MacLean and L. A. Wooten, *Ind. Eng. Chem.*, **31**, 1138 (1939).

25. R. J. Myers and J. W. Eastes, *Ibid.*, **33**, 1203, (1941).

26. R. J. Myers, J. W. Eastes and F. J. Myers, *Ibid.*, **33**, 697 (1941).

27. R. J. Myers, J. W. Eastes and D. Urquhart, *Ibid.*, **33**, 1270 (1941).

28. N. V. Octrooien Maatschappij, British Patent 474,978 (Nov. 2, 1937).

29. S. Odén and E. W. Langelius, *J. Phys. Chem.*, **25**, 311 (1921).

30. Permutit Company, British Patent, 490,799 (Aug. 22, 1938).

31. A. Richter, *Angew. Chem.*, **52**, 679 (1939); *Melliand-Textilber.*, **29**, 579 (1939).

32. A. Richter, W. Busch and M. O. Schürmann (to I. G. Farbenindustrie, A.-G.) U. S. Patent 2,141,763 (December 27, 1939).

33. E. Seyb, *Chem. Fabrik*, **1940**, 30.

33a. A. M. Sookne and M. Harris, *J. Res. Nat. Bur. Standards*, **25**, 47 (1940).

34. P. Smit, U. S. Patents 2,171,408 (Aug. 29, 1939), 2,191,063 (Feb. 20, 1940), 2,205,635 (June 25, 1940) and 2,198,393 (April 23, 1940); *Arch. Suikerind. Nederland in Ned. Indië*, **1**, 143 (1940).

34a. J. Steinhardt and M. Harris, *J. Res. Nat. Bur. Standards*, **24**, 335 (1940).

34b. A. Tiselius, this volume, p. 81.

35. S. Tsuruta, *J. Soc. Chem. Ind. Japan*, **41**, 129-B (1938).

36. W. Vaughn, U. S. Patent 2,190,853 (Feb. 20, 1940).

37. H. Wassenegger, R. Griessbach and W. Sutterlin, U. S. Patents 2,228,159 and 2,228,160 (January 7, 1941).

38. H. Wassenegger and K. Jaeger, U. S. Patent 2,204,539 (June 11, 1940).

39. L. C. Wheeting, *Soil Sci.*, **29**, 12 (1930).

40. J. N. Wilson, *J. Amer. Chem. Soc.*, **62**, 1583 (1940).

THE STUDY OF COLLOIDS WITH THE ELECTRON MICROSCOPE

THOMAS F. ANDERSON

RCA Fellow of the National Research Council,
RCA Manufacturing Co., Camden, N. J.

CONTENTS

I. Introduction

The fundamental limit of resolution of a microscope, *i. e.*, the smallest distance δ by which two particles may be separated and still be

resolved as *two* particles, is given by the formula

$$\delta = \frac{0.61\,\lambda}{N.A.} \tag{1}$$

where λ is the wave length of the radiation used and $N.A.$ is the limiting numerical aperture of the microscope. In the past fifty years the light microscope has been developed to the point of perfection; that is, the practical limit of 1.4 for $N.A.$ has been reached. With 4000 Å. as the wave length limit of human vision, we have δ = 1700 Å. as the limit of visual resolution. The only practical method to obtain higher resolving powers is to use shorter wave lengths. Thus, using ultraviolet light with λ = 2537 Å., Barnard (7, 8, 9) has succeeded in obtaining microphotographs showing a resolution of 750 Å. It should, of course, be pointed out that particles having even smaller diameters than this can be seen with the dark-field microscope, but no direct deductions regarding their sizes and shapes can be made. Unfortunately, the use of still shorter wave lengths of light is limited by the lack of suitable refracting media for the construction of lenses.

The use of high-velocity electrons in microscopy was made possible by the discovery of lenses for the formation of images by fast electrons. It has been shown (Busch (15)) that any cylindrically symmetrical magnetic or electric field has the property of bending an electron beam passing through it nearly parallel to the field axis, to form an image of the source of the electrons in a manner quite analogous to the image-forming action of a glass lens (which, incidentally, also possesses cylindrical symmetry) in changing the course of a beam of light. It may be readily appreciated that the use of electrons gives promise of almost undreamed-of resolutions, for the de Broglie wave length of an electron of mass m moving with a velocity v and energy eV (V measured in volts) is given by

$$\lambda_{(em.)} = \frac{h}{mv} = \frac{1.22 \times 10^{-7}}{\sqrt{V + 0.98 \times 10^{-6}\, V^2}}; \tag{2}$$

this gives 0.05 Å. as the wave length of an electron having an energy of 60,000 electron volts. Thus, even with lenses having apertures as low as 0.001, resolutions of 30 Å. could be attained!

In 1928 Rupp (36) published the description of a device for obtaining magnified images of objects with electrons. This was followed by an announcement by Knoll and Ruska (24) of an electron microscope using magnetic lenses; since then numerous workers (27, 10, 34, 3,

12, 41, 21, 33, 43) have constructed microscopes using magnetic and electrostatic lenses. One book (1) has been published on the construction and performance of electron microscopes. Since 1939 workers using both types of lens have been able to claim resolutions of 100 Å. or better. We thus have available* an instrument for the direct observation and determination of sizes and shapes of colloidal materials which are so small that only indirect methods, involving sedimentation velocities and equilibria, flow properties (viscosities and double refraction), light and x-ray scattering, to mention only a few, could be used formerly for their study.

In the following sections the application of the electron microscope to the determination of sizes and shapes of colloidal particles will be discussed. The electron microscope itself will first be described with particular reference to the nature of image formation and the various phenomena associated with it. The various techniques employed for mounting specimens will then be described, and the actual results of the few critical particle size and shape determinations which are available will be reviewed and compared with those determined by other methods.

II. The Electron Microscope

1. Construction

The arrangement of lenses, specimen, source of radiation, etc., in the compound electron microscope is quite analogous to that in the compound light microscope (Fig. 1). Electrons are emitted from a hot tungsten filament at a stable potential of from 30 to 250 kv. and are accelerated to ground through an anode shaped to converge the electrons toward the specimen. The concentration of the electron beam onto the object is further controlled by a condenser lens. An objective lens then focuses the electrons which pass through the object in such a manner that an electron image (magnification $\sim$200×) of the object is formed at the focal plane of the projection lens. A part of this image is further magnified by the projection lens to form an image (magnification from 2000 to 30,000×) on a fluorescent screen for visual observation, or on a photographic plate for permanent record. It should be borne in mind that since gas molecules would scatter electrons, besides causing discharges and destruction

* At least two concerns have electron microscopes on the market at the present time, RCA in this country and Siemens Halske in Germany.

of the cathode filament, the entire electron path must be kept in a high vacuum (10^{-4} to 10^{-5} mm. of mercury) maintained by high-speed pumps.

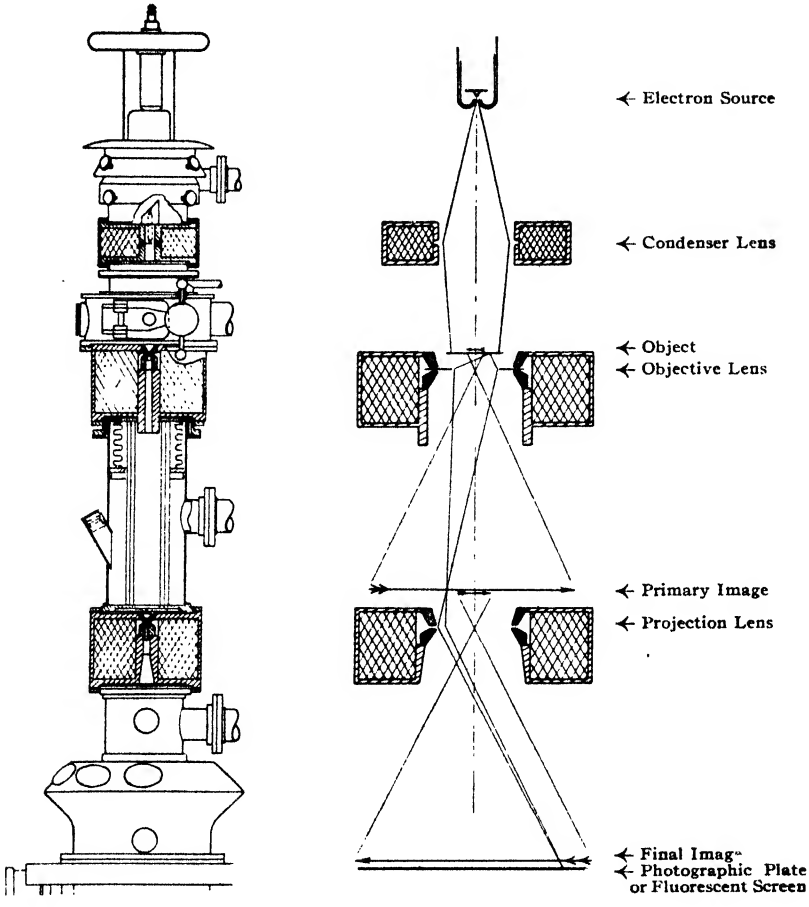

Fig. 1.—The electron microscope.

On the left is a scale drawing and on the right is a schematic diagram of the instrument showing the arrangement of lenses and the formation of images.

In addition to these fundamental elements, a number of devices should be incorporated in an electron microscope to facilitate operation. These include a fluorescent screen at the focal plane of the ob-

jective lens for observation of the object at low magnification; the mounting of the object on a stage which is movable for the selection of the interesting part of the specimen; and appropriate air locks for the introduction of specimens and photographic plates in order to avoid the necessity of pumping out the entire apparatus after each change of specimen or photographic plate. In addition it should be possible to take stereoscopic pictures with the microscope.

2. *Properties of Electron Lenses*

It will be readily appreciated that moving electrons are deflected either by magnetic or electrical fields. Electron lenses may accordingly be divided into two types: the magnetic type in which the electrons pass through coaxial pole pieces having cylindrical symmetry, and the electrostatic type in which the electrons pass along the axis of a series of coaxial cylindrical apertures charged to different potentials. In each case a real or virtual image of the source of electrons is formed by the lens, as in light optics, in accordance with the familiar equation:

$$\frac{1}{f} = \frac{1}{r_o} + \frac{1}{r_i}$$

Here f is the focal length of the lens, r_o is the distance from the lens to the object and r_i is the distance from the lens to the image. A real image is formed if $r_o > f$, a virtual image if $r_o < f$. Also, as in light optics, the magnification of the object by the lens is equal to the ratio r_i/r_o.

Now the performance and limitations of any microscope are largely determined by the image-forming characteristics of the lenses employed. It will be well, therefore, to review briefly the characteristics of electron lenses (Ramberg and Morton (35) and references given therein). The focal length, f, of a magnetic lens of small thickness is given by the equation:

$$\frac{1}{f} = \frac{0.022}{V} \int_{-\infty}^{\infty} [H(z)]^2 \, dz \qquad (3)$$

where z is the coordinate along the lens axis and H is the magnetic field strength on the axis. From this equation it is apparent that the greater the field strength along the lens axis, the shorter the focal length will be. Since in a magnetic lens the field strengths depend on the currents flowing in the electromagnets, focusing is easily accomplished by varying these currents and holding the object-objective

distance fixed. Once the proper focus is reached the currents must, of course, be kept constant during the taking of a picture.

The focal length of a thin electrostatic lens, in which electrons have the same velocity after passing through as before, is given by the formula

$$\frac{1}{f} = \frac{1}{8V^{1/2}} \int_{-\infty}^{\infty} \frac{1}{[\varphi(z)]^{3/2}} \left(\frac{\partial \varphi(z)}{\partial z}\right)^2 dz \qquad (4)$$

where $\varphi(z)$ is the electric potential on the axis referred to the point where the velocity of the electron is zero (*i. e.*, at the cathode from which the electrons originate).

From equations (3) and (4) it is seen that the focal length of a simple lens is dependent on the accelerating potential V, being inversely proportional to V for the magnetic type. Thus the magnetic type of lens requires that the accelerating potential does not vary by more than about 0.01% if defects arising from variations of focal length due to this cause are to be unimportant. Microscopes employing electrostatic lenses require no such high constancy of accelerating potentials, for here the device of supplying the lens and the cathode from a common voltage supply is employed. A variation in V thus amounts to multiplying V and each term in φ by a constant which cancels out of the expression on the right of equation (4). Thus in electrostatic and permanent magnet microscopes focusing is more easily accomplished by varying the object-objective distance, as in the light microscope. Each type of microscope thus has its advantages and limitations, although it would appear that most workers in the field have chosen the type employing electromagnets for initial construction.

3. *Possibility of Improvement of Lenses*

Electron lenses are subject to all the types of aberration which glass lenses possess. To overcome them only a small part of the lens is used, corresponding to extremely small numerical apertures ($\sim$0.001) and a resolution of 30 Å. for 0.05 Å. electrons. If larger apertures could be used, much finer resolution should be attainable, but to take advantage of the higher resolutions which larger apertures would afford, lenses with smaller aberrations would have to be employed. Now the problem of eliminating the present aberrations is a difficult one. Theoretically, glass lenses can be ground and polished to any desired configuration, but in electron lenses only the shapes of the

pole pieces can be altered and they merely determine the boundary conditions for Laplace's equation, which then determines the distribution of lines of force in the electron lens. The situation might be looked upon as being analogous to that which would exist in light optics if we were limited to the use of hanging transparent drops as lenses and could change only the hydrostatic pressure of the liquid and the shape of the tip which held the drop.

Also, in light optics, sets of positive and negative lenses may be matched to give a combination which is achromatic and practically free from aberration. Here we are indeed thwarted, for a magnetic electron lens having a negative focal length would have to have fields in which $[H(z)]^2$ is negative (equation (3)); H would then have to be imaginary. In spite of the few difficulties which have been mentioned it does seem probable that, as knowledge of electron optics advances, improvements of electron lenses will be made.

4. *Depth of Focus*

Von Borries and Ruska (11) give the following equation for the depth of focus T of the electron microscope:

$$T = \frac{1}{\sin \alpha_k} = \frac{\alpha'}{\delta} \tag{5}$$

where α_k is the aperture of the electron beam coming from the condenser lens, and α' is the distance a pair of particles separated by a distance δ can be moved relative to the objective (without change in the objective focal length) before the disks of confusion of the two particles coalesce. If this aperture is extremely small, $\sin \alpha_k = \alpha_k = 1/1000$, and $T = 1000$. Taking δ as 10 Å. we then have $\alpha' = 10{,}000$ Å. $= 1\ \mu$. This depth of focus is all the more astonishing when we compare it with an analogous calculation for the light microscope. Here the above-mentioned authors take $\sin \alpha_k = 0.95$* or $T = 1.05$. Then a value of $\delta = 0.2\ \mu$ gives $\alpha_1 = 0.2\ \mu$. The advantage of this tremendous depth of focus in the electron microscope is that the object appears sharp in the entire field of view and the figure obtained is actually a projection of the entire object on the image plane.

* Dr. E. G. Ramberg of the RCA Laboratories has suggested that $\tan \alpha_k$ rather than $\sin \alpha_k$ would be appropriate in this case. Making this substitution we would have $\tan \alpha_k = 3$, $T = 0.33$ and, if $\delta = 0.2\ \mu$, $\alpha' = 0.07\ \mu$ for the light microscope.

5. *Determination of the Shape of the Projected Image*

The projected shapes of particles can be accurately determined down to details whose dimensions approach the resolving power of

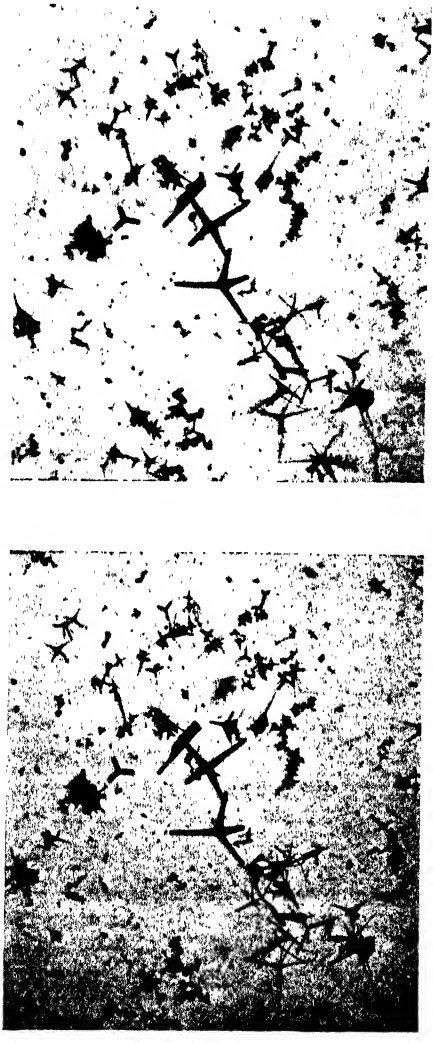

Fig. 2.—Stereoscopic picture of zinc oxide crystals collected on a collodion membrane. Magnification 4700×. (RCA Laboratories.)

the instrument. For particle sizes near this limit, just as in the light microscope, uncertainties in shapes of very small particles are introduced because sharp corners appear to be rounded off. B. von Borries

and G. A. Kausche (13) have considered this problem and point out that the rounding of the corners in the image of a polygon takes the approximate shape of a circle tangent to the straight edges, so that as the center of this circle approaches the center of the figure the particle cannot be distinguished from a circle. Arbitrarily taking the point at which the length of the chord of the rounded arc is equal to the length of the straight edge in the image as the point at which the figure can just be distinguished from a circle, and making certain other assumptions, they derived the expression

$$\frac{d}{\delta} = 2\left(1 + \cos\frac{\pi}{n}\right)\sqrt{\frac{n}{\pi}\cot\frac{\pi}{n}} \qquad (6)$$

for the ratio of the diameter d of a circle having the same area as the n-sided polygon to the resolution δ. Thus, an equilateral triangle could barely be recognized when this ratio is equal to 2, the regular hexagon is just distinguishable for a ratio of seven, and a regular dodecagon is recognizable when the ratio is about 15. It should be pointed out that these values of d/δ apply to particles of high density which produce images of high contrast. For particles of low density giving images of low contrast the appropriate values of d/δ are greater. This can be readily appreciated from the fact that particles giving rise to very low contrast could scarcely be detected at all no matter what the resolving power might be.

6. *Determination of Shapes in Three Dimensions*

Since the depth of focus is so great in the electron microscope, optical sections cannot be taken for the determination of shapes in three dimensions, as is done in light microscopy. However, shapes can be determined more easily by either of two other methods. If the specimen studied consists of a large number of similar particles on a collodion film the particles can often be viewed in profile where the film has broken and folded over on itself.

A more satisfactory method of determining three-dimensional shapes is to take stereoscopic pictures (2, 3, 6, 26, 30). Here, as in ordinary stereoscopy, two pictures of the object are taken with the object inclined at two different angles to the optical system. When the pictures are suitably mounted and viewed in a stereoscope the object appears to stand out in three dimensions. Also, the plates can be measured, and with a knowledge of the angles involved, the relative positions of any points in the object can be calculated. Fig-

ure 2 is such a stereoscopic pair of pictures of zinc oxide crystals taken with the electron microscope showing clearly the shapes of the individual particles and their relative positions.

It is to be noted that most specimens studied in the electron microscope are quite flat in relation to the focal length of the objective lens so that all parts of the object are imaged at very nearly the same magnification. The phenomenon of perspective thus plays a very minor role; small parts of stereoscopic pictures can thus be magnified and matched, the stereoscopic angle being very nearly constant for all parts of the specimen. As in ordinary stereoscopy the precision of the measurement of depth can be increased by increasing the stereoscopic angle. Eitel and Gotthardt (17*a*) have found certain clay particles to be as thin as 250 ± 50 Å. in this manner. Eventually, it should be possible to measure depths of particles to a precision approaching the resolving power of the microscope.

III. Interactions between Electrons and Matter

The performance and limitations of a microscope are also determined by the nature of the interaction between the radiation used and the specimen. Refraction, absorption and reflection of light all play a part in the performance of the light microscope, while scattering and reflection of electrons play analogous roles in the electron microscope. In the next few sections the nature of the interaction of the electron beam with the specimen will be considered in relation to image formation and contrast.

1. Image Formation

In the electron microscope a narrow beam of electrons is caused to pass through the specimen as illustrated in Fig. 3. In so doing the electrons are scattered in a manner identical to that obtained in electron diffraction experiments. Diffraction rings or spots are obtained for crystalline materials, rings on a diffuse background for amorphous materials. If the planes in a crystal be separated by distances d, the angles ϑ at which rings or spots occur will be given by the familiar relation

$$\sin\left(\frac{\vartheta}{2}\right) = \frac{n\lambda}{2d} \tag{7}$$

where λ is the electron wave length (equation (2)) and n is the order of

the reflection. The relation for amorphous materials is quite complex.

If the electron beam is directed so as to go through a narrow objective aperture (indicated by the central dotted circle in Fig. 3) those electrons which pass through the specimen without being scattered will contribute to the brightness of the image of the specimen. The thicker and more dense the specimen is, the more electrons it will scatter out of such an aperture and the darker it will appear in the final image. Also, even thin crystals oriented with respect to the beam so as to give an intense Bragg reflection will appear black in the image. Images of the transmission type, called "bright-field" images, are the most common in electron microscopy.

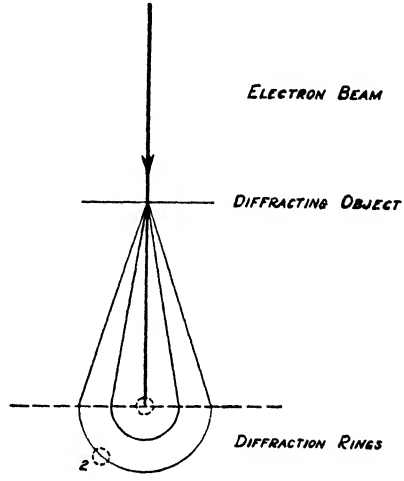

Fig. 3.—The scattering and diffraction of electrons by an object in the electron microscope.

A bright-field image is obtained when the objective aperture is placed to gather transmitted electrons; a dark-field image is obtained when this aperture is placed at "2" to gather electrons scattered by the object.

If, on the other hand, the electron beam is directed so as to miss the objective aperture, only electrons scattered by the specimen into the aperture will pass through it to form an image. The position of the aperture in this case is indicated by the dotted circle labeled "2" in Fig. 3, so placed that electrons in a diffraction ring pass through the aperture. Parts of the specimen oriented so as to contribute to the intensity of the ring at this point will appear bright in the image, as well as amorphous material which gives diffuse scattering into the aperture. This arrangement is the equivalent of dark-field illumination employed in light microscopy. Figure 4 is a dark-field electron micrograph of bacteria with a bright-field picture of the same field for comparison.

Large apertures may also be used which collect both the direct and parts of the scattered beams. The bright-field and dark-field images

will then appear very nearly superimposed in the final image at proper focus, a fact which makes it easier to focus without an aperture than with one.

2. *Contrast*

As previously mentioned, thicker and more dense specimens generally scatter more electrons and thus appear darker than thin specimens of low density in bright-field pictures. From this it would appear that quantitative determinations of the amount of transmission

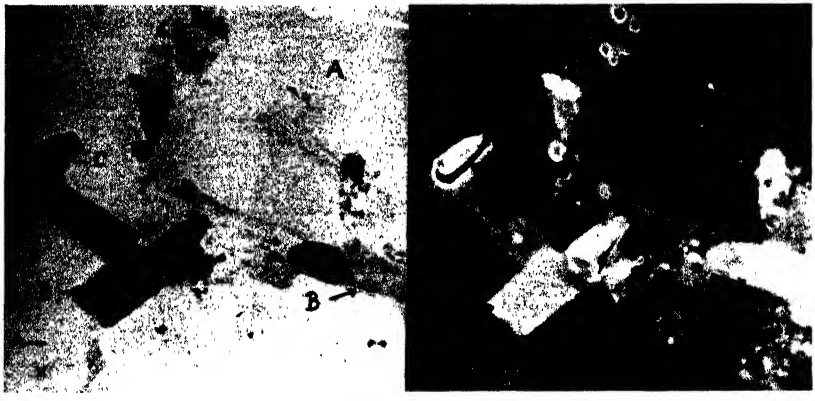

Fig. 4.—Bright-field and dark-field pictures of *Bacillus megatherium*. Thin areas *A* which appear bright in light-field and dark in dark-field, thicker areas *B* which are dark in light-field and bright in dark-field, and very thick areas *C* which appear dark in both bright- and dark-field. (RCA Laboratories.)

as a function of thickness and density might be made which would serve as a calibration for future determinations of thickness and density; even particle and molecular weights might be determined in this way. Marton and Schiff (30) have made calculations of atomic cross sections for fast electrons using the Born approximation and have made rough comparisons of the results with the observed transmissions of various materials. They estimate by this means that certain sodium laurate curd fibers are 115 Å. thick, that certain thin collodion films are from 58 to 110 Å. thick, and that certain antimony particles in an evaporated metal film are about 36 Å. thick (Fig. 3 of Marton and Schiff). Aside from the experimental difficulties, there still remain to be solved the questions as to how the structure, orientation and chemical composition affect transmission.

3. *Scattering of Electrons by Matter*

For a better understanding of the problems involved, let us consider electron scattering by an amorphous specimen—one in which Bragg reflections occur from no resolvable part. Theoretically the problem of scattering over relatively large angles (0.5°) has been solved for the purpose of structure determinations of molecules in the gaseous phase (14). Here the scattering is separated into three classes: elastic, inelastic and molecular. The elastic scattering I_E is caused by interaction of the electrons in the beam with the charges on the atomic nuclei in the specimen. It is plotted in Fig. 5 as a function of s where

$$s = \frac{4\pi \sin\left(\frac{\vartheta}{2}\right)}{\lambda} \qquad (8)$$

The term I_E is large relative to the other types of scattering for large angles of scattering where the moving electron has come close to the charged nucleus. However, the electrons which do not approach the nucleus so closely are scattered over smaller angles because of the inverse square law and because the nuclear charge is shielded by the atomic electrons. Eventually, for small angles of scattering, the moving electrons are more apt to be scattered by the atomic electrons than by interaction with the nuclear charge. This type of scattering is just the inelastic scattering I_I mentioned above. Here the interaction between electrons results either in the activation of the molecule to an excited electronic state or in the moving electrons knocking one or more electrons out of the molecule; the moving electron, of course, loses a corresponding amount of energy in the process. The term I_I is also plotted in Fig. 5. It is seen that the total atomic scattering I_T closely approximates I_I for small values of ϑ, and I_E for large values of ϑ. The third type of scattering, molecular scattering, arises from interference effects between scattering nuclei in the mole-

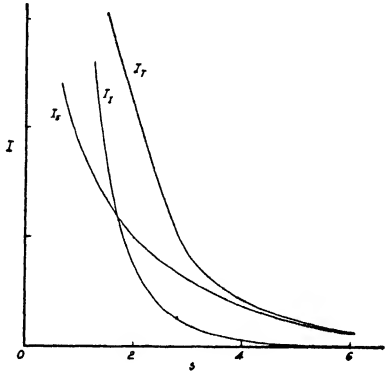

Fig. 5.—The scattering of electrons by an amorphous material as a function of s where $s = \frac{4\pi \sin \vartheta/2}{\lambda}$.

I_E is elastic scattering, I_I is the inelastic scattering and I_T is $I_E + I_I$.

cule. For large angles it imparts a series of little waves to I_T, the diffraction rings of Fig. 3, whose shape is characteristic of the scattering molecule.

The dependence of scattering on the electronic energy may be seen by combining equations (2) and (7) thus

$$\sin \vartheta/2 = \frac{\lambda s}{4\pi} = \frac{1.22 \times 10^{-7} s}{4\pi\sqrt{V}} \tag{9}$$

Scattering of a given kind—that is, with a given value of s—will be over an angle which decreases with decreasing λ or with increasing V.

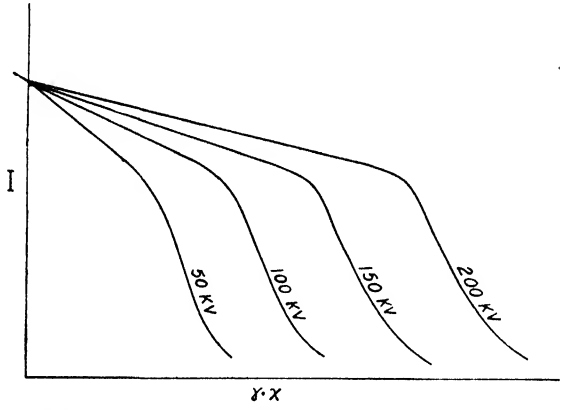

Fig. 6.—Schematic diagram of transmitted electron intensities for different voltages as a function of the product of γ, the density, and x, the thickness of the specimen.

For higher voltages, then, there will be more scattering over small angles corresponding to a greater degree of penetration. This effect is indicated graphically in Fig. 6 where a qualitative plot is shown of transmitted intensities at different voltages as a function of thickness x, and density γ of the specimen.

The curves are roughly linear with increasing thickness of specimen until in a critical range of values of γx multiple electron scattering occurs; here the curves rapidly fall off to very low values. This critical value of γx is, of course, larger for higher voltages, corresponding to greater penetration. Also, in regard to resolution in thick specimens we should note that the increased scattering in thick specimens is accompanied by velocity losses of the electrons which result

in the deterioration of the image. This effect is less pronounced when higher voltages are used, so that better resolution is obtained in thick specimens at higher voltages, as well as greater penetration. This is illustrated by Fig. 7, a series of micrographs of crystals of hydrated aluminum oxide taken at different voltages. It is to be noted that a line of reasoning analogous to the above indicates that thicker specimens can be studied in the dark-field to greater advantage at higher voltages than at low.

Fig. 7.—Electron micrographs of hydrated aluminum oxide ($Al_2O_3 \cdot H_2O$) taken at different voltages to illustrate the increase of transmission with increasing acceleration of electrons.

Note that the thin detail, *e. g.*, from the collodion membrane, disappears as the voltage is increased while thick detail such as that due to the overlapping of the crystals disappears as the voltage is decreased.

In this and in each of the succeeding electron micrographs, one micron is indicated by a bar, thus: |—|. (RCA Laboratories.)

Another effect should be mentioned in connection with the extent of electron scattering; namely, the depth of focus has been found to decrease as the thickness-density product of the specimen increases in relation to the electron voltage. This is probably due to the fact that the increased scattering in thick specimens increases the range of angles at which electrons leave the object. This increases the effective aperture over the condenser aperture α_k. Thus the edges of a thick specimen are observed to remain relatively sharp while detail within the specimen appears and disappears as the focus is changed. Of

course these considerations apply only if the effective aperture is limited by the condenser, *i. e.*, if the objective aperture is larger than the condenser aperture.

The resolution which can be obtained also depends on the thickness-density product of the specimen. This is due to three effects: First, multiple or diffuse scattering causes interior details of a thick particle to appear fuzzy, just as particles do when viewed through a ground glass, or when suspended in cloudy water. Second, owing to the chromatic aberration of electron lenses, a sharp image is not obtained if the velocities of the electrons are distributed over a wide range of values, as is the case for a thick specimen in which inelastic scattering is predominant. Third, even those electrons which are scattered elastically pass through the outer parts of the objective lens aperture; then because of the spherical aberration of the lens they strike the image at a different point than unscattered electrons which pass close to the lens axis. The latter effect also contributes to the bright halo along the edge of the image of a thick object (11).

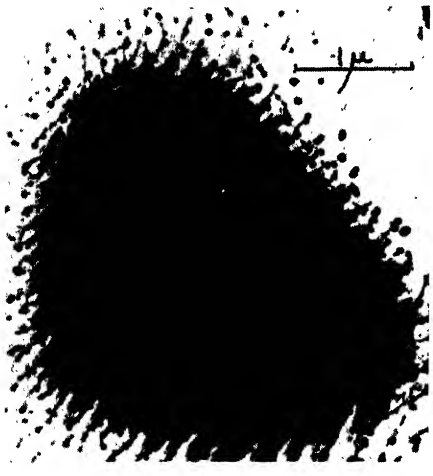

Fig. 8.—A large sulfur crystal which sublimed or exploded in the high vacuum of the electron microscope when struck with the electron beam. (By Barnes and Burton (9*a*).)

4. *Effect of Electron Beam on Specimen*

The energy lost by the electrons when they are scattered by the specimen is, of course, taken up by the specimen. The maximum energy density of electrons striking the specimen in the electron microscope has enormous values ranging from 1 to 10 kw./mm.^{2} For thin specimens only a minute fraction of this energy is absorbed, while for thick specimens a considerable part may be taken up and

converted into heat. Thus small organic particles such as bacteria may be browned slightly after continued bombardment, though their electron images remain unchanged. On the other hand, large inorganic crystals can often be observed (9*a*) to melt or evaporate in the beam, for example, the sulfur particle shown in Fig. 8. For taking pictures, intensities ranging from one one-hundredth to one one-thousandth the maximum value are used.

Electrons are also absorbed by the specimen. Parts of the object may thus become charged and large objects often gather sufficient charge such that in repelling one another they break the collodion membrane on which they are mounted. Neither heating effects nor charging effects are great enough to give trouble for most specimens which otherwise can be studied to advantage in the electron microscope. They only present difficulties for the study of thick specimens, which because of their opacity are, in general, unsuited for study anyway.

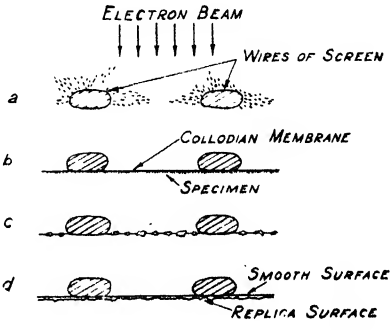

Fig. 9.—Specimens prepared in different ways for the electron microscope: (*a*) by collection directly on screen; (*b*) by collection on a thin membrane; (*c*) by inclusion of specimen in membrane; and (*d*) by the preparation of a membrane, one surface of which is a replica of the solid surface to be studied. Note that membranes are mounted below the screen so that the screen protects the membrane from electron bombardment as much as possible.

IV. Mounting Specimens for Study in the Electron Microscope

The ordinary methods of mounting specimens for microscopic study on conventional glass slides cannot be used in the electron microscope, for the electrons would not go through such thick glass. Instead, specimens are mounted over an aperture or on a thin membrane. For supporting the specimens on the thin membrane, a fine screen having about 200 holes to the inch is used. Following are described a few of the techniques which have been successfully used, but it must be remembered that each type of specimen requires its own technique, and the investigator may have to devise new ones to fit particular needs.

1. Collection Directly on Screen

For mounting materials in the form of long fibers no supporting membrane is needed. Such things as asbestos and soap fibers can be mounted simply by dipping the screen into a suspension (or solution)

Fig. 10.—Electron micrograph of cubic crystals of magnesium oxide smoke collected directly on screen from a burning strip of magnesium. (RCA Laboratories.)

of the material to be studied and allowing the adhering drop to evaporate. Smoke particles can be collected by holding the screen in a flame or over an arc; the smoke particles then adhere to the screen and to one another to form chains of particles which extend over the holes in the screen (Fig. 9*a*). Figure 10 is an electron micrograph of smoke particles (MgO) mounted in this way.

2. *Techniques Using Thin Membranes*

In the majority of cases specimens can be mounted on a collodion membrane about 100 Å. thick. Such membranes are made by allowing a drop of 2% collodion in amyl acetate to spread on a clean water surface. The membrane is then attached to the supporting wire screen by placing a piece of the screen on the membrane (still floating on the water surface) and picking up the screen with membrane attached from beneath with a tool which fits around the piece of screen. The drop of water adhering to the membrane can then be removed with a capillary tube. When properly prepared such membranes show no resolvable structure in the electron microscope, *i. e.*, down to about 25 Å.

A drop of a suspension of the material to be studied may then be placed on the membrane—on the side away from the screen—and allowed to evaporate forming a preparation of the type sketched in Fig. 9*b*. Many specimens, such as those shown in Figs. 4, 8 and 17, are prepared in this way. One should be careful that the salt concentration in the suspension is a minimum; otherwise, salt crystals will form when the specimen is dried and obscure the field of view.

If one desires to see individual particles in the microscope, the concentration of the suspension should be such that the particles will not crowd each other on drying—hence the smaller the particles are, the more dilute the suspension should be. Some protein solutions have been mounted at a concentration of 10^{-8} g./cc. to insure separation of the particles on drying. Some particles show a strong tendency to clump together on drying. Von Ardenne (4) has recently described an apparatus for vibrating the specimen during drying to reduce such effects.

Some specimens are, of course, damaged on drying. Freeze-drying seems to be a solution to this difficulty—that is, the wet mounted specimen is frozen rapidly before drying by plunging it into a liquid which has been cooled to liquid-air temperatures. The specimen is then placed in a high vacuum and the water pumped off from the still frozen specimen. This is the most gentle drying procedure known; since bacteria dried in this way are viable for years in the dry state, it may safely be assumed that the structure of ordinary colloids will be relatively unaffected by it. The freeze-drying technique is also applicable to the drying of threadlike specimens mounted directly on the wire mesh as previously described.

Smoke particles can also be collected on thin membranes by filling a container, *e. g.*, a bell jar or an inverted beaker, with the smoke and allowing the particles of smoke to settle upon it. Once they touch

Fig. 11.—Electron micrograph of a thin film of rubber cement spread on water. Note carbon particles imbedded in film. (RCA Laboratories.)

the membrane they adhere firmly to it. The zinc oxide crystals shown in Fig. 2 were collected in this manner.

Dry specimens, such as fine powders which are not easily dispersed in water, can often be dispersed in the collodion solution itself. When a membrane is prepared in the usual manner from such a suspension, the particles of interest will be found imbedded in the membrane and

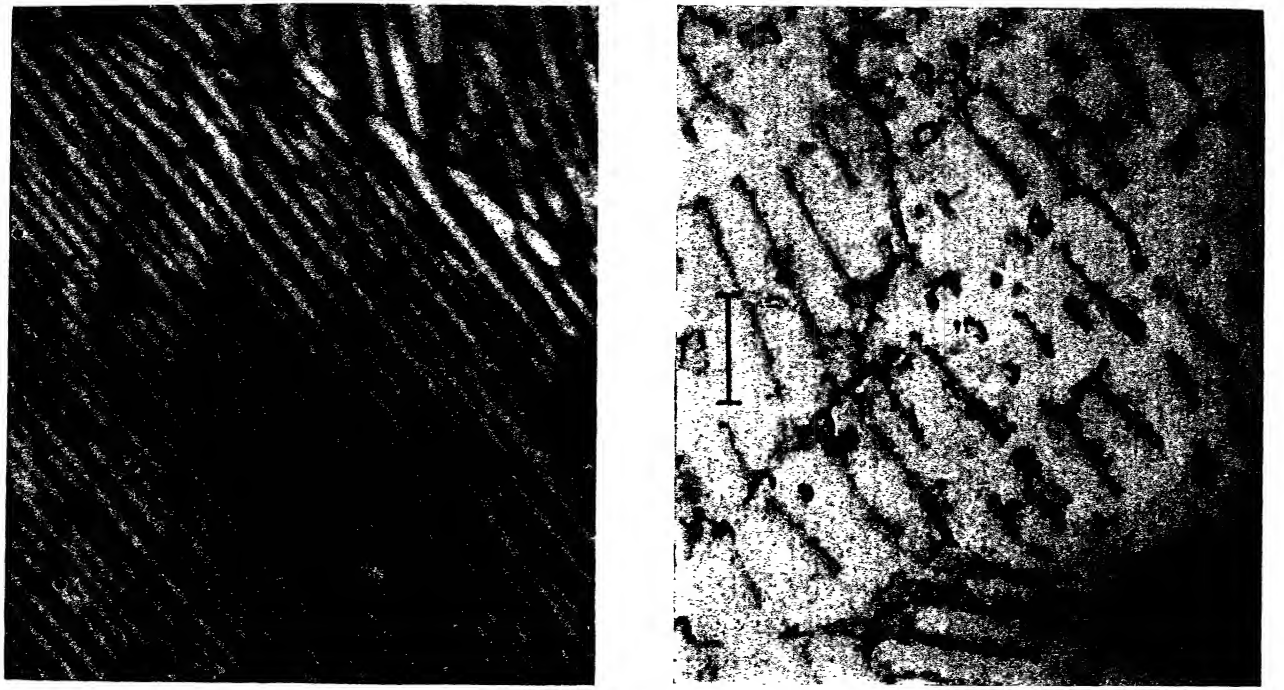

(*a*) (*b*)

Fig. 12.—Electron micrographs of replicas of polished and etched pearlite.

(*a*) A vinylite film prepared on the metal surface and then stripped off. This film was probably distorted in the process of stripping.

(*b*) A replica of pearlite prepared by the "double replica" technique, using silver and collodion. (RCA Laboratories.)

can be studied directly (Fig. 9*c*). Some substances themselves, such as rubber cement (Fig. 11), will spread on water to form a membrane which can be picked up on a screen and studied directly. It should be mentioned that, in order to be observable, particles imbedded in a film must either be thicker than the film, have a density greater or less than that of the film, or give crystalline reflections in the microscope.

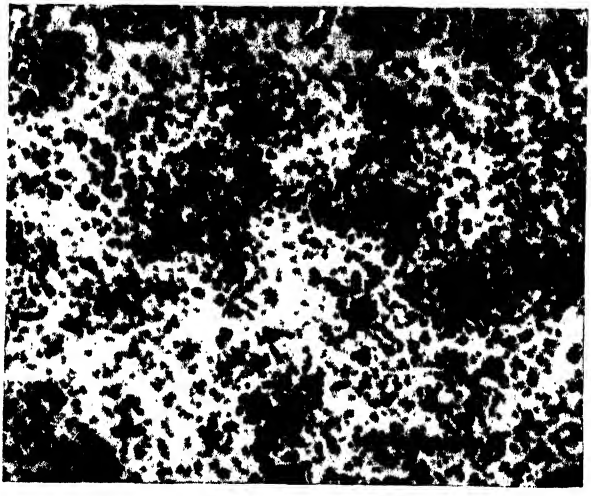

Fig. 13.—Colloidal (Micronex) carbon imbedded in a collodion membrane.
The size distribution of the particles is given in Fig. 14.
(By Prebus and Columbian Carbon Co. (16).)

3. *Replica Techniques*

The surfaces of solids can also be studied with the electron microscope (42). This is made possible by the fact that thin films of collodion and other substances can be prepared by spreading a thin layer of the dissolved substance on a solid surface. The surface tension of the solvent then causes the upper surface to be smooth after the solvent has evaporated, while the surface in contact with the solid follows the contour of the solid. Such a film can often be removed from the solid by ruling little squares on it with a razor blade and dipping it through a clean water surface. If the water wets the solid it will come between the solid and film and the film will float off onto the surface of the water. The film which is a negative replica of the solid surface (Fig. 9*d*) can then be picked up on a screen in the usual

manner and studied in the electron microscope. The picture obtained will then correspond to the contour of the surface on which the film was initially spread, as illustrated in Fig. 12*a*.

In cases in which the film cannot be removed from a solid in this manner, a double replica method can be employed. Silver, or some other metal, is evaporated onto the surface to be studied to form a relatively thick film, about 20 μ in thickness. This film can then be stripped from the solid, the surface which was adjacent to the solid having the contour of the solid. A thin collodion film can then be spread on this surface, as above, and freed after drying by simply dissolving the metal in dilute acid (nitric acid if silver is used). The thin collodion membrane, a positive replica of the original surface, can then be "fished out" of the acid with a piece of supporting screen, and washed in water to remove acid. Sharper detail in etched metal and glass surfaces is obtained when this "double replica" technique is used than by the single replica method (Fig. 12*b*).

V. The Determination of Sizes and Shapes of Colloidal Particles

The electron microscope permits the direct determination of the sizes and shapes of colloidal particles to an accuracy limited only by the 50 to 25 Å. resolving power. It is thus particularly useful in cases in which the indirect methods are relatively helpless or yield results which are ambiguous or intrinsically in error. In this section we shall review the already extensive literature on the determination of sizes and shapes of small particles in the electron microscope and, whenever possible, compare the results with those obtained by indirect methods of investigation of the same particles.

1. Colloidal Carbon—Spherical Particles

The Columbian Carbon Research Laboratories (16) have made a thorough study of sizes of carbon-black particles both by indirect methods and with the electron microscope of the University of Toronto. Space does not permit a complete description of the results obtained, but we can review the principal conclusions as outlined in Table I.

The average diameter of the primary particles, shown in Fig. 13, proved to be of the order of one-half that determined by indirect methods, in which the particle count was involved. Particle count methods were considered to be unreliable, since they give diameters

which are too large because (*1*) smaller particles cannot be seen in the light microscope, (*2*) groups of particles are easily mistaken for one large particle, and (*3*) the calculated mean diameter must be too large if there is a distribution of particle diameters. The last objection arises from the fact that the total mass $\left(\pi\rho\sum^{n} d_i^3\right)/6$, where ρ is the density and d_i is the diameter of the ith particle, is assumed to be divided equally between the n particles. The mean mass of the parti-

TABLE I

A COMPARISON OF THE PROPERTIES OF MICRONEX COLLOIDAL CARBON AS DETERMINED BY INDIRECT METHODS WITH THOSE DETERMINED WITH THE ELECTRON MICROSCOPE

Property	Indirect methods	Electron microscope
Mean particle diameter	Particle count method 50–60 mμ	30 mμ
Range in particle diameters	15–600 mμ	5–800 mμ
Particle shape	No evidence; various conjectures	Spherical with some evidence for plane surfaces
Particle surface	No evidence; burr or feather-like surfaces conjectured	Essentially smooth
Size of ultimate crystal unit	1–5 mμ (x-ray diffraction)	No evidence
Type of crystal habit	Graphitic	No evidence

cles being $(\pi\rho\sum d_i^3)/6n$, it is assumed that the average diameter is $\left(\frac{1}{n}\sum^{n} d_i^3\right)^{1/3}$ which is, of course, false because of the inequality

$$\frac{1}{n}\sum^{n} d_i \leq \left(\frac{1}{n}\sum^{n} d_i^3\right)^{1/3};$$

the two sides of this expression are equal only if all the d_i's are equal. The above report contains a detailed analysis of these considerations, in which calculations based on a distribution of particle size are made.

The range in particle diameters (Fig. 14) proved to be much larger than was previously supposed, accounting for the large discrepancy

between methods noted above. While earlier investigators postulated that the particles were flat disks or spheres with burr or feather-like surfaces to account for the large surface area, the electron microscope showed the particles to be spheres with smooth surfaces—the unexpected smallness of the particles accounting directly for the large surface area. While the electron microscope has so far not given any evidence regarding the type of crystal habit, it is interesting to note that x-ray diffraction studies have shown the spherical particles to be made up of graphitic crystals whose sizes range from 1 to 5 mμ, as estimated from the observed diffuseness of the scattering.

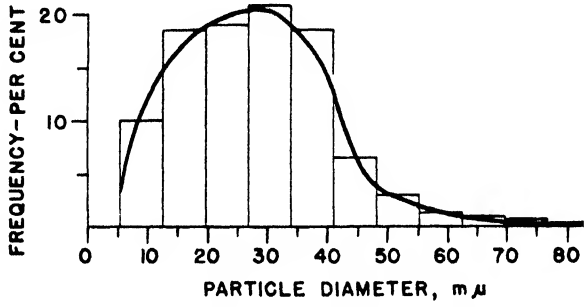

Fig. 14.—The frequency distribution of the diameters of the carbon particles shown in Fig. 13. (By Columbian Carbon Co. (16).)

2. *Colloidal Gold—Crystalline Particles*

B. von Borries and G. A. Kausche (13) have reported a rather extensive study of the size and shape of the particles in various suspensions of colloidal gold, in which sizes ranged from values which can be determined with the light microscope to sizes which could only be detected in the ultramicroscope.

They found the particles to be crystalline down to dimensions approaching the resolving power of the electron microscope, finding triangular, hexagonal, rhombic, tetragonal and an occasional octagonal crystal. From the frequency with which the different forms occurred, they concluded that the primary form is octahedral. It should be pointed out that no other method of investigation now available could have been able to distinguish the individual shapes of particles of these minute dimensions.

The diameters of thousands of particles in each of four suspensions

of different sizes were also measured in this work, and for each suspension the size distribution closely fitted a Gauss curve. Moreover, they found that the essential characteristics of the size-distribution curve for each suspension could be obtained from measurements on only 100 to 200 particles, which indicated to them that no selective grouping of particles with respect to size occurred in drying the suspension for study. When a suspension which later proved to be a mixture of two suspensions was studied (Fig. 15), two peaks in the size distribution curve were obtained, as shown in Fig. 16.

Fig. 15.—An electron micrograph of a mixture of two different sized gold particles. (By von Borries and Kausche (13).)

The average size obtained in the suspensions containing larger particles agreed well with the value determined by the manufacturer by an unspecified method. However, the average particle sizes in the remaining suspensions were found to be 2 to 3 times larger than those given by the manufacturer. The authors could not decide whether there actually existed a disagreement between the methods of measurement or whether the colloid, which was a year and a half old, had become aggregated. In the latter case, however, they would have expected to find not larger particles, but larger clumps of particles. It would be highly desirable that particle size determinations on the same gold sol be made by a number of indirect methods for comparison with electron microscope values. This colloid, however, has the disadvantage of not being homogeneous.

3. *Tobacco Mosaic Virus—Rod-Shaped Particles*

Ultracentrifugally purified tobacco mosaic virus is ideally suited for the desired comparison between methods of determining sizes of colloidal particles (40). Electron micrographs of such a preparation

are shown in Figs. 17 and 18. The particles are remarkably uniform in width and length. Being about 150 Å. wide, the outlines of some of the particles in Fig. 18 seem to be square on the ends. From this we can obtain an idea of the resolution in the figures if we assume that the same resolution is required to determine that the end of a

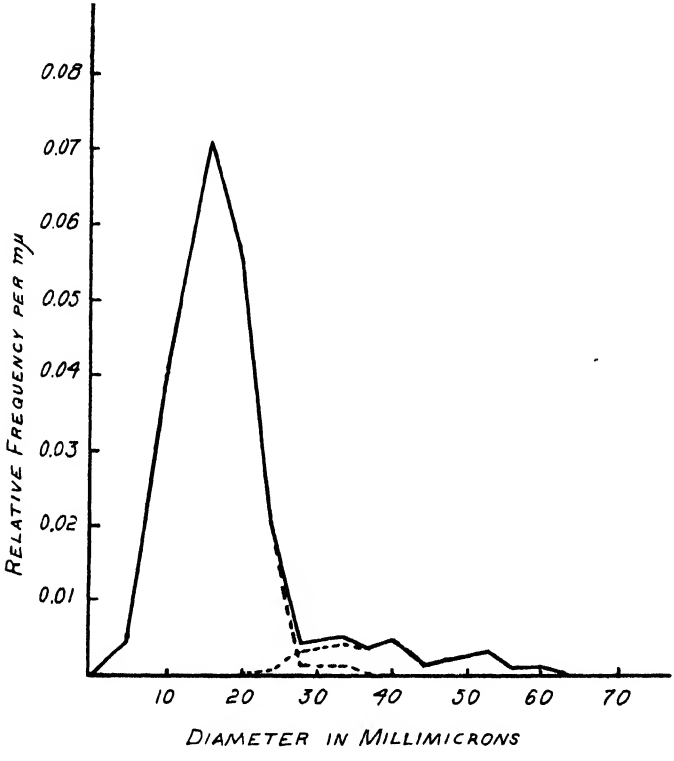

Fig. 16.—Frequency distribution of the diameters of gold particles in the mixture shown in Fig. 15. (By von Borries and Kausche (13).)

rectangle 150 Å. wide is square as is required to tell that a square 150 Å. on the side is square. Inserting the appropriate values in equation (6), we obtain:

$$\delta \leqq \frac{150 \text{ Å.}/\sqrt{\pi/4}}{2\left(1 + \cos\frac{\pi}{4}\right)\sqrt{\frac{4}{\pi}\cot\frac{\pi}{4}}} \leqq 56 \text{ Å.}$$

Actually, because of the low contrast obtained for tobacco mosaic virus, δ might be considerably smaller than 56 Å.

The lengths of a large number of particles were measured and the frequency distribution given in Fig. 19 was obtained. It is seen that a length of 280 mμ predominates. On a weight basis, over 50% of the material exists in the form of particles having a length of 280 mμ while over 70% is in the form having lengths within 7% of this value.

The value of 150 Å. obtained from x-ray measurements for the width and that of 2800 Å. obtained with the electron microscope

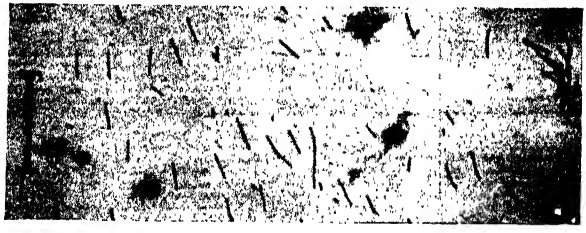

Fig. 17.—An electron micrograph of tobacco mosaic virus particles applied to a collodion film at a concentration of 0.01 mg. per ml. (RCA Laboratories.)

for the length seem to be the best estimates of the dimensions of this strain of tobacco mosaic virus. The density of tobacco mosaic virus has been found to be 1.33. Since

$$\text{Molecular weight} = \frac{\text{Particle weight}}{\text{Weight of the H atom}}$$

we have for a cylinder 150 Å. in diameter and 2800 Å. long, whose density is 1.33:

$$\text{Molecular weight} = \frac{6.57 \times 10^{-17}}{1.66 \times 10^{-24}} = 39.8 \times 10^{6}$$

The agreement between this value and that of 42.6×10^{6} estimated (25) by kinetic methods is unusually good and suggests that the indirect methods involving kinetic theory are essentially valid and capable of yielding results of considerable accuracy, even for asymmetrical particles, when correctly used.

It is not known whether the particles shorter than 2800 Å. observed in Fig. 17 and recorded in Fig. 19 occur regularly in solutions of tobacco mosaic virus or whether they are produced at the time the

specimen is mounted. It seems unlikely that they represent the image of particles of ordinary length not lying flat, for surface tension forces

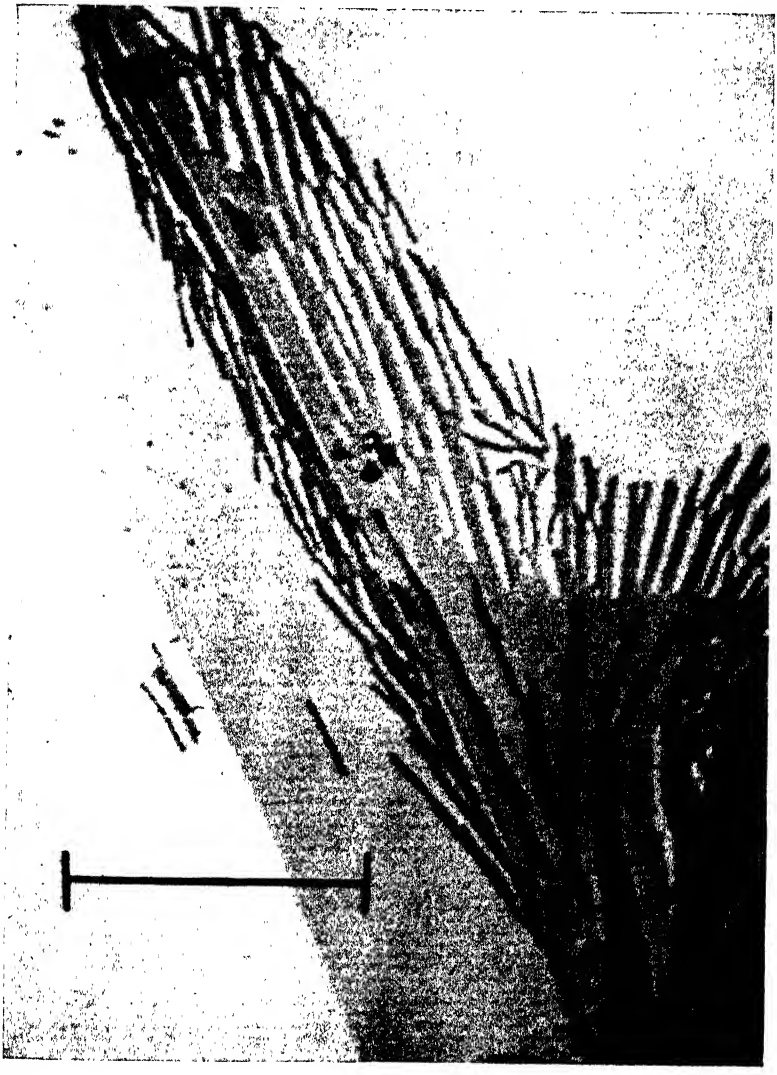

Fig. 18.—Tobacco mosaic virus applied to a collodion membrane at a concentration of 0.01 mg. per ml (RCA Laboratories.)

would tend to flatten all the molecules. In addition, the density of the images is the same for short and long particles, a condition which would not obtain if some were tilted at different angles to the beam

and electrons had to pass through different thicknesses. Shorter particles have not been detected either from activity measurements or in the analytical ultracentrifuge. They may, however, possess no virus activity or be present in too small numbers to be detected by indirect methods. If these particles actually exist in virus solutions they may be of special biological significance.

Kausche, Pfankuch and Ruska (23*a*) found predominant lengths of 300 and 150 mμ in another sample of tobacco mosaic virus, as well as multiples of these values, and were consequently unable to conclude

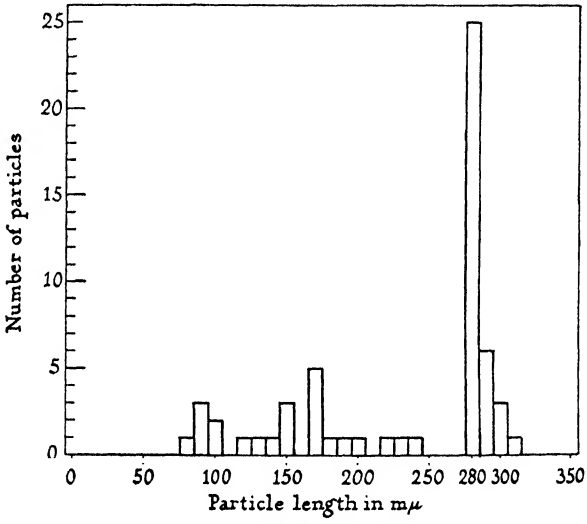

Fig. 19.—Distribution of lengths of particles in an ultracentrifugally prepared sample of tobacco mosaic virus. (By Stanley and Anderson (40).)

which was the fundamental length. On the other hand, Melchers and co-workers (31) have studied two other strains of tobacco mosaic virus and found their particle lengths to be 1400 Å. and 1900 Å. in the electron microscope. The correlation between particle length and sedimentation constant is shown by the fact that particles 1400 Å., 1900 Å. and 2800 Å. have sedimentation constants of 180, 183 and 187 $\times$ 10^{-13}, respectively, when corrected for concentration. If these sedimentation constants are not fortuitous, but represent reproducible values, the correlation is in accord with expectations. The above workers also found that the size distribution curve for a mixture of

the two strains exhibited two distinct peaks corresponding to the two lengths found for the original suspensions. This suggests that the relative abundance of particles in mixtures of different strains could be determined in this way.

4. Detection and Measurement of Extremely Small Particles

In order that a particle may be detected with any microscope, it must produce an area in the image which has a noticeably different contrast from the surrounding areas. The smallest detectable difference in density of a small area on a photographic plate is, in practice, of the order of 10%. This means that in order to be detected a single atom must scatter electrons in such a way that the circle of confusion in its image contains 10% less electrons than the surrounding area. Two opposing factors now enter into consideration: the angular distribution of scattered electrons as a function of atomic number; and the aperture of the objective lens which determines, first, how large a cone of scattered electrons fails to pass through the lens to contribute to the image density and, second, the area of the circle of confusion (related to resolving power) over which the contrast difference is spread. It turns out that for a perfect electron lens (no aberrations) there is an optimum numerical aperture of the order of 0.1 at which single atoms can be detected with electrons at a given voltage.

Hillier (22, 23) has estimated that the smallest single atom which can be detected in the bright-field with an electron microscope using 60-kv. electrons having perfect lenses would have an atomic number of 25. There appears to be no theoretical reason, however, why arbitrarily small single stationary atoms could not be detected in the dark-field. In both bright-field and dark-field, however, the single atom would have to be supported, and the practical problem of distinguishing scattering from the single atom as differentiated from that of the supporting substance would have to be met. Of course, present microscopes would only be able to detect atoms having many times an atomic number of 25 because the aberrations in the lenses make necessary the use of apertures smaller than the optimum for perfect lenses.

Von Ardenne (5) estimates the smallest metal particles which he has observed to be about 10 Å. in diameter, while the smallest organic particles, because of their lower contrast, must have diameters of at least 40 Å., corresponding to a molecular weight of 5×10^4, to be observed. He has estimated the diameters of haemocyanin, edestin and glycogen (see also a more detailed study of glycogen by E. Huse-

mann and H. Ruska, *J. prakt. Chem.*, **156**, 1–10 (1940)) to be about 220 Å., 80 Å. and 80 Å., respectively, giving molecular weights of 4×10^6 for haemocyanin and 3×10^5 for edestin and glycogen. Although these values are in good agreement with the values 6.7×10^6, 3.1×10^5 and 2.8×10^5, respectively, determined by indirect methods, the error involved in the electron microscope determina-

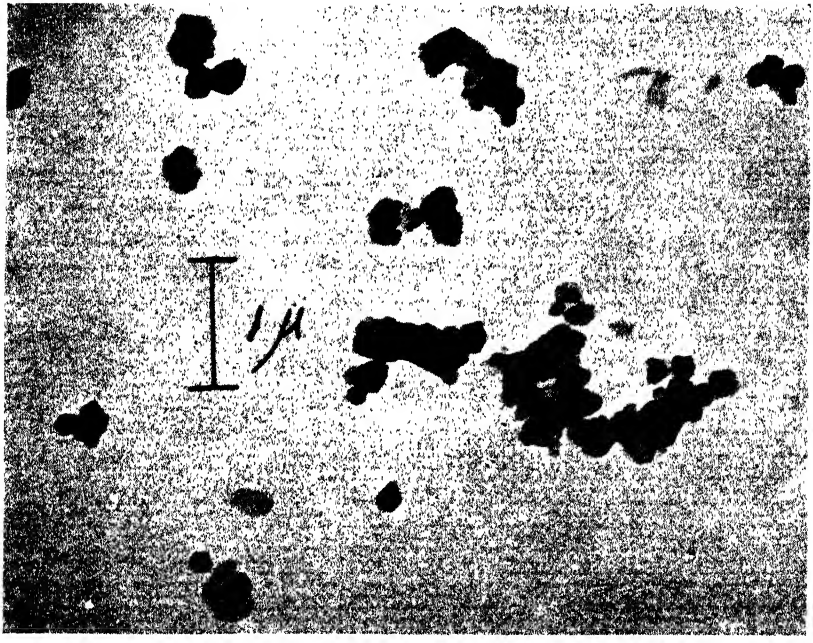

Fig. 20.—Kaolinite.
Sample supplied by Professor Truog, University of Wisconsin.
(RCA Laboratories.)

tions is necessarily rather large, especially for the latter two molecules. Von Ardenne points out that greater contrast and hence more precise values could be obtained if a method of surrounding organic molecules with metallic atoms were available.

5. Miscellaneous Qualitative Studies

A large number of qualitative determinations of sizes and shapes of sub-microscopic particles have been made (32), and in many cases qualitative correlations with other data have been obtained.

Schmieder (39) has measured the sizes of pigment particles which are below the resolution of the light microscope. He found that the covering power of the pigment decreased with decreasing particle size in this range; this is in agreement with the results obtained by indirect methods.

Eitel and others (17, 18, 19) have made a study of the distribution of sizes, shapes, surfaces and estimated thicknesses of certain clay minerals by means of the electron microscope. Figure 20 presents a picture of kaolinite. Ruska (37) and Ruska and Kretschmer (38) have studied the structure of cellulose fibers. Marton, McBain and Vold (29) have investigated the structure of a curd of sodium laureate and find (Fig. 21) that it consists of a mass of fibers in the form of thin ribbons. Some of the sodium laureate also appeared as granules 100–200 Å. in diameter irregularly spaced along the fibers. The fibers were found to branch to form a felt containing many capillary spaces capable of retaining water at very low humidity. The number of studies in which the minute structure of materials can be investigated is almost unlimited. One more might be mentioned, however; von Ardenne (1) has published pictures of catalysts—aluminum oxide gel, silica gel, palladium on asbestos (Fig. 22), vanadium pentoxide, etc.—revealing the sizes and distributions of active surfaces. Incidentally, von Ardenne (1) has also shown pictures of ultra-filters from which pore diameters can be accurately determined.

Besides the mere determination of sizes and shapes of colloidal particles, the electron microscope is also applicable to the study of chemical reactions in these minute dimensions. One such investigation has been made—the study of the photo-chemical reduction of silver in silver bromide and the subsequent developing and fixing processes involved in photography. When a silver bromide (or silver chloride) crystal is exposed to an intense electron beam in the electron microscope the crystal can be observed (1, 20) to decompose slowly into bromine (or chlorine), which vaporizes, and metallic silver, which remains behind in the form of small particles from 300 to 2000 Å. in diameter. Also, if silver bromide crystals are exposed to intense light and then fixed with sodium thiosulfate individual photolytic silver particles 800 Å. in diameter can be seen (20); they increase in size with increasing exposure to light, being formed by migration of silver particles to the latent image centers.

The action of developing solutions on exposed silver bromide is

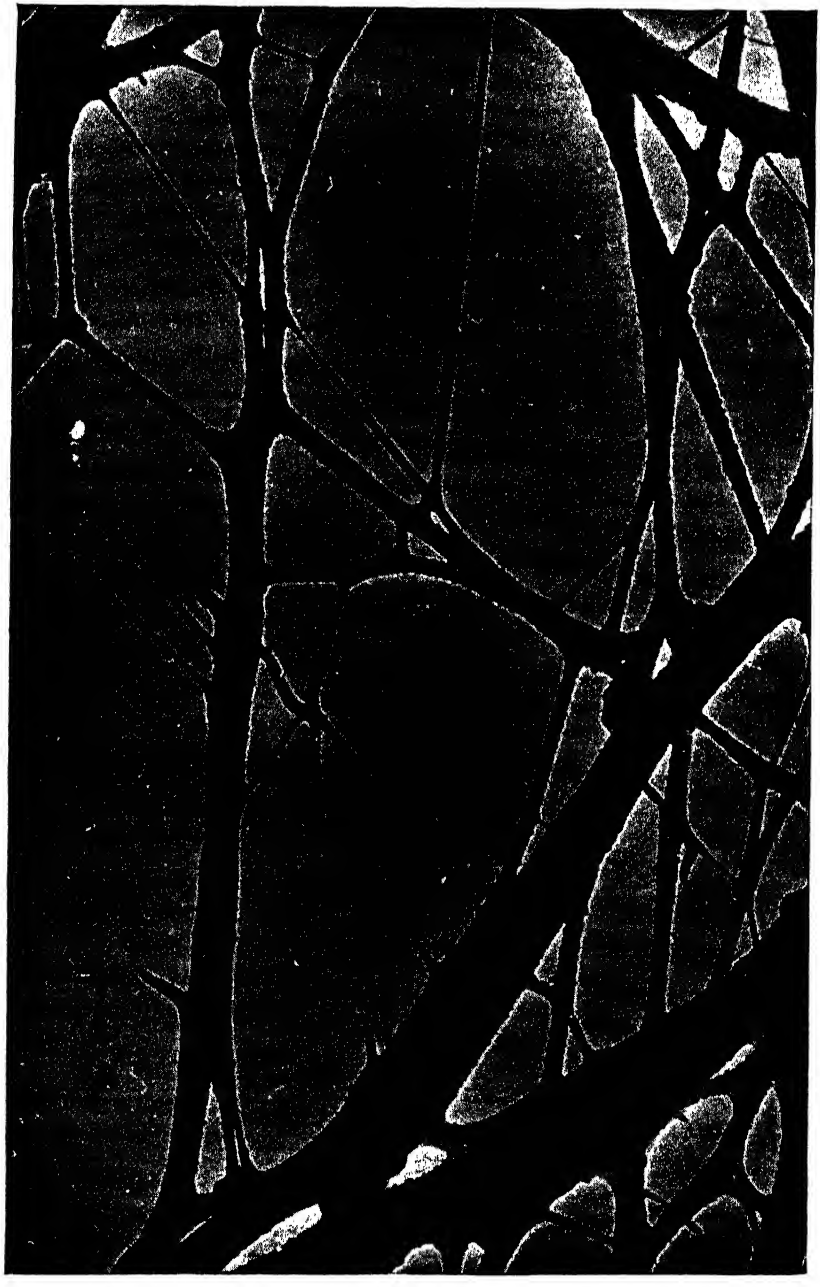

Fig. 21.—Fibers of sodium laurate curd showing presence of granules 100–200 Å. in diameter. (By Marton, McBain and Vold (29).)

particularly interesting (20). During the ordinary development processes, fine threads of silver grow out from exposed grains of silver

Fig. 22.—Fresh palladium catalyst mounted on asbestos fibers. (By von Ardenne (1).)

bromide, the thickness of the threads depending on the kind of developing solution which is used. After fixing has removed the unreduced silver bromide, bundles of such silver fibers are left behind to form the photographic image. Physical development (deposition of silver on latent image points) and paraphenylenediamine development produce clumps of silver particles rather than filamentous structures. When the extremely minute 300 Å. Lippmann crystals

are developed, each crystal forms a single ribbon about 100 Å. wide and 1500 Å. long, which is longer and thinner than the original crystal. The electron microscope has indeed given us new insight regarding the fundamental mechanisms involved in photographic processes, and should prove to solve many related theoretical and practical problems.

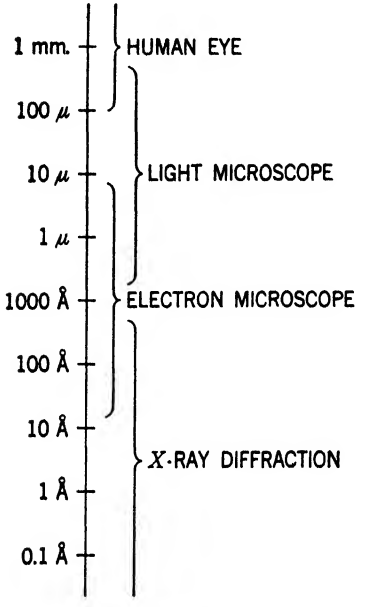

Fig. 23.—Comparison of various methods for the formation of magnified images and the determination of small distances.

Note that the range of the electron microscope lies between that of the light microscope on the one hand and that of x-ray diffraction techniques on the other.

VI. Conclusions

The range of usefulness of the electron microscope, 10 μ to 3 mμ, coincides almost exactly with the sizes of particles with which the science of colloids is concerned. It overlaps the ranges of two other direct methods of investigation: that employing the light microscope on the one hand, and the indirect but precise methods employing x-ray and electron diffraction techniques on the other (Fig. 23). This healthy state of affairs makes possible the direct check of the electron microscope results both for large particles, as has been done in the previously mentioned study of gold sols and for small, as in the studies of the width of tobacco mosaic virus particles. In the range not covered by the light microscope and diffraction methods, it is the only direct method of investigation at present and consequently will be particularly useful in this region; for it is here that colloid science has developed many valuable indirect methods of study for which no independent direct check has been available. The electron microscope will provide just such a check and serve as a criterion of the correct use of these methods. But it will do more than this. The indirect methods are rather helpless in the determination of shape, except in cases of homogeneous colloids where the deviation from the spherical is great. The electron micro-

scope permits the determination of shapes directly, within the limitations of resolving power, of course, but with no limitations imposed by lack of homogeneity of the material.

When we consider all that has been accomplished in the three years since high resolution electron microscopes were built, it seems safe to predict that the electron microscope will be the right-hand tool of the colloid science of the future. One cannot fail to admire the men who early saw the potentialities of the electron microscope and have struggled to make it the practical tool of research it is today.

The author wishes to acknowledge his indebtedness to Dr. V. K. Zworykin and members of the RCA Research Laboratory Staff, as well as to Dr. Stuart Mudd, Chairman of the Committee on Biological Applications of the Electron Microscope. He is grateful to Dr. James Hillier and Dr. E. G. Ramberg for numerous helpful discussions in connection with the preparation of this paper

Bibliography

1. M. von Ardenne, *Elektronen Übermikroskopie, Physik-Technik-Ergebnisse*, J. Springer, Berlin, 1940.
2. M. von Ardenne, *Naturwissenschaften*, **28**, 113–127 (1940).
3. M. von Ardenne, *Z. Physik*, **115**, 339–368 (1940).
4. M. von Ardenne, *Kolloid-Z.*, **93**, 158–163 (1940).
5. M. von Ardenne, *Z. physik. Chem.*, **(A)187**, 1–12 (1940).
6. M. von Ardenne, *Z. angew. Phot.*, **2**, 14 (1940).
7. J. E. Barnard, *J. Roy. Microscop. Soc.*, **1919**, 1.
8. J. E. Barnard, *Lancet*, **ii**, 117 (1925).
9. J. E. Barnard, *Med. Research Council Brit.*, **1**, 115 (1930).
9a. R. B. Barnes and C. J. Burton, *Ind. Eng. Chem., News Ed.*, **19**, 965–967 (1941).
10. B. von Borries and E. Ruska, *Wiss. Veröffent. Siemens-Werken*, **17**, 99–106 (1938).
11. B. von Borries and E. Ruska, *Naturwissenschaften*, **27**, 281–287 (1939).
12. B. von Borries, *et al.*, *Ibid.*, **28**, 350–351 (1940).
13. B. von Borries and G. A. Kausche, *Kolloid-Z.*, **90**, 132–141 (1940).
14. L. O. Brockway, *Rev. Modern Phys.*, **8**, 231–266 (1936).
15. H. Busch, *Arch. Elektrotech.*, **18**, 583 (1927).
16. Columbian Carbon Company, *The Particle Size and Shape of Colloidal Carbon as Revealed by the Electron Microscope*, Binney and Smith Co., distributors, New York, 1940.
17. W. Eitel, H. O. Müller and O. E. Radczewski, *Ber. deut. Botan. Ges.*, **20**, 165 (1939).
17a. W. Eitel and E. Gotthardt, *Naturwissenschaften*, **28**, 367 (1940).
18. W. Eitel and C. Schusterius, *Ibid.*, **28**, 300–303 (1940).
19. W. Eitel and O. E. Radczewski, *Ibid.*, **28**, 397–399 (1940).

20. C. E. Hall and A. L. Schoen, *J. Optical Soc. Am.*, **31**, 281–285 (1941).
21. J. Hillier and A. W. Vance, *Proc. Inst. Radio Eng.*, **29**, 167–176 (1941).
22. J. Hillier, *Thesis*, University of Toronto, 1941.
23. J. Hillier, *Phys. Rev.*, **60**, 743–745 (1941).
23*a*. G. A. Kausche, E. Pfankuch and H. Ruska, *Naturwissenschaften*, **27**, 292–299 (1939).
24. M. Knoll and E. Ruska, *Ann. Physik*, **12**, 607–640 (1932).
25. M. A. Lauffer and W. M. Stanley, *Chem. Rev.*, **24**, 303 (1939).
26. H. Mahl, *Kolloid-Z.*, **91**, 105–117 (1940).
27. L. Marton, *Bull. acad. roy. Belg., Class. sci.*, **21**, 606–617 (1935).
28. L. Marton, M. C. Banca and J. F. Bender, *RCA Rev.*, **5**, 232–243 (1940).
29. L. Marton, J. W. McBain and R. D. Vold, *J. Am. Chem. Soc.*, **63**, 1990–1993 (1941).
30. L. Marton and L. I. Schiff, *J. Applied Phys.*, **12**, 759–765 (1941).
31. G. Melchers, G. Schramm, H. Trurnit and H. Friedrich-Freska, *Biol. Zentr.*, **60**, 524 (1940).
32. G. A. Morton, *RCA Rev.*, **6**, 131 (1941).
33. H. O. Müller and E. Ruska, *Kolloid-Z.*, **95**, 21–25 (1941).
34. A. Prebus and J. Hillier, *Can. J. Res.*, (**A**)**17**, 44–63 (1939).
35. E. G. Ramberg and G. A. Morton, *J. Applied Phys.*, **10**, 465–478 (1939).
36. E. Rupp, *Z. Physik*, **52**, 8–15 (1928).
37. H. Ruska, *Kolloid-Z.*, **92**, 276–285 (1940).
38. H. Ruska and M. Kretschmer, *Ibid.*, **93**, 163–166 (1940).
39. F. Schmieder, *Ibid.*, **95**, 29–33 (1941).
40. W. M. Stanley and T. F. Anderson, *J. Biol. Chem.*, **139**, 325–338 (1941).
41. V. K. Zworykin, J. Hillier and A. W. Vance, *Elec. Eng.*, **60**, T 157–161 (1941).
42. V. K. Zworykin and E. G. Ramberg, *J. Applied Phys.*, **12**, 692–695 (1941).
43. V. K. Zworykin, J. Hillier and A. W. Vance, *Ibid.*, **12**, 738–742 (1941).

ANOMALIES IN SURFACE TENSIONS OF SOLUTIONS

ERNST A. HAUSER

Department of Chemical Engineering, Massachusetts Institute of Technology, Cambridge, Mass.

CONTENTS

I. Introduction

The fundamental property of a liquid surface is its tendency to contract until under the prevailing conditions the smallest possible area is attained. This tendency to contract can be explained by the attraction between the molecules, which limits their motion sufficiently to prevent many of them from moving into the vapor phase. Inside the liquid, however, both translatory and rotary motions take place with but little hindrance. In the bulk of a liquid each molecule is surrounded by identical neighbors; therefore, attraction occurs uniformly in all directions in the final analysis. Surface molecules, however, are in an entirely different situation. Here the attraction is not uniform in all directions because there are not enough molecules

outside of the surface to compensate for the attraction caused by the neighboring and underlying molecules. Therefore, a surface molecule will be subjected to a strong inward pull perpendicular to the surface. The phenomenon of surface contraction demonstrates the existence of free energy and it is this surface free energy which must be considered the fundamental property of surfaces. For the purpose of simplifying calculations, it has become customary to substitute for the surface free energy a tension acting parallel to the surface and in all directions. This hypothetical tension is termed "surface tension." It is expressed in dynes per centimeter and designated in the literature with γ or σ. In the following discussion the latter will be used.

From the above it becomes evident that a pure liquid, *i. e.*, a liquid containing only one type of molecule, will reduce its surface free energy by diminishing its total surface to a minimum. The free energy per unit area of such a system can be changed only in cases where the surface molecules possess ends with different fields of forces. If they can be so oriented that the ends with the largest fields of force point into the bulk (1), then the minimum possible reduction in surface free energy will be achieved.

II. Surface Adsorption in Solutions

If a liquid is composed of more than one substance and the fields of attracting forces resulting from equal surface areas of the different molecules are not of the same intensity, a decrease in the free surface energy of the solution must occur. This time such decrease results from the fact that the molecules exerting greater attracting forces have the tendency to migrate into the bulk of the solution, leaving those with the smaller force fields in the surface. Logically, therefore, the surface will show a higher concentration than the interior of that constituent which exerts lesser attraction. A change in concentration of a constituent of a fluid at the surface is generally termed adsorption. Positive adsorption denotes an increase of concentration of a constituent at the surface; negative adsorption is synonymous with a decrease.

The moment a solution composed of solute molecules with different intensities of attraction force is formed or whenever kept thoroughly mixed, its composition is uniform throughout. The molecules which happen to lie in the surface at any given time differential are immediately attracted to the interior. This is true for any type of molecule

located in the surface. The inward pull, however, will be stronger on those molecules which have the greatest attractive fields of force, and therefore they will move to the interior more rapidly than the others. At the same time the kinetic agitation of the molecules in the fluid will try to maintain equal concentration throughout the system. Thus, a state of equilibrium can be reached only when a balance has been attained between the tendency to equalize the concentration and the tendency for those surface forces to produce a surface composed entirely out of that constituent which has the least free surface energy.

This reasoning introduces the importance of a time factor which must be considered whenever accurate measurements of the surface tension of solutions are contemplated.

From the above reasoning the following further deductions can be made. If a solution exhibits a surface tension lower than that of the pure solvent, this can only be accounted for by assuming that the solute has been concentrated at the surface. If the surface tension of the solution is higher than that of the pure solvent, then the solute molecules have been pulled into the interior as far as possible.

If a solute has a very low surface tension a considerable decrease in surface tension of its solutions, as compared to those of the pure solvent, may be expected. A decrease in the surface tension of a solution should logically take place with increasing solute concentration until the surface layer is composed almost entirely of solute molecules. If the same reasoning is applied to solutions containing negatively adsorbed solutes, it is evident that a large increase in surface tension over that of the pure solvent cannot be expected. The surface layer will be composed of pure solvent contaminated only by a few molecules of the solute.

III. Gibbs' Adsorption Equation

The relation between adsorption (positive or negative) and the changes in surface tension resulting therefrom was first deduced thermodynamically by Gibbs. His fundamental contribution, which today still must be considered as the backbone of any development in the field of surface chemistry, can be expressed by the following considerably simplified equation:*

* For a detailed evaluation the reader is referred to Gibbs' original article (9), to the many excellent commentaries (26) of his work and to the various published simplified approximations of his equation to be found in the literature (1).

$$U = -\frac{c}{RT}\frac{d\sigma}{dc}$$

where U is the excess of substance in the surface layer; c is the concentration of substance in the bulk of the liquid; σ is the surface tension; R, the gas constant; and T, the absolute temperature.

IV. Experimental Confirmation of Gibbs' Equation

Until recently, two methods had been suggested for the purpose of experimentally verifying Gibbs' equation. The first one, suggested by Donnan (5), consisted of passing bubbles of gas through a column containing a solution of a solute which adsorbs positively. The bubbles are forced to unite after emerging from this column. The effective surface of the solution is increased by passing the gas bubbles through it, thus permitting a larger amount of solute to adsorb in the surface and to be carried away with the bubbles. Therefore, the solution obtained after the collapse of the united bubbles should have a higher concentration of solute than the original solution. By analyzing such increased concentration and estimating the total area of the bubbles, it is possible to calculate the surface tension of the solution by Gibbs' equation and compare it with results obtained from direct measurements by one or the other of the known methods. Although not all of the experiments using Donnan's method verified Gibbs' equation, the majority gave results which were in satisfactory agreement with those to be expected from a perusal of Gibbs' adsorption equation. So far, the discrepancies have always been explained by criticizing Donnan's method in one way or another (1).

The possibility that the methods used to determine the surface tension of the solutions themselves might not have conformed with the rigid demands imposed by a strict interpretation of Gibbs' deductions has seemingly been overlooked.

The second method was suggested by McBain (23, 25). It consisted, in principle, of removing a thin layer from the surface of a solution contained in a long trough by shooting an accurately ground microtome blade fixed on a carriage over the entire length of the trough. The concentration of solute carried off by the knife of this ingenious piece of equipment was then analyzed. Let a be the weight of the solution removed from area A, c' its concentration and c the original concentration in the bulk, expressed in grams per gram solvent; then the weight of solvent removed per unit area is

$$\frac{a_1}{A} = \frac{a}{(1 + c')A}$$

where a_1 is the weight of solvent removed from the area A. The amount of solute in this amount of solvent is, in the solution which has been removed, a_1c'/A, and in the original bulk, a_1c/A; the difference $(a_1/A)(c' - c)$ is then identical with U in Gibbs' equation.

A great number of determinations carried out with this method were within experimental error in excellent agreement with those obtained from Gibbs' equation.

If the area which a molecule of certain fatty acids covers in an adsorbed film is calculated by Gibbs' equation, it is found to be in excellent agreement with experimental data. All this seems to justify the statement that the verification of Gibbs' adsorption equation should be considered finally established.

V. Discrepancies Between Theory and Experiment

If this point of view is accepted, however, and there is good reason that it should be, then the question why certain solutions exhibit anomalous behavior in regard to surface tension deserves special attention. If the anomalies so far reported are the result of the method applied in obtaining the data, then it seems most important either to eliminate the fault or to apply a method which can avoid the occurrence of erroneous results. If the method is not to blame for such anomalous data, then it is up to the investigator to explain these anomalies without discarding the fundamental principles embodied in Gibbs' equation.

The most outstanding anomalies which have been reported so far are those mentioned by Gibby and Addison (10) on the adsorption of various dyestuffs; by Gilbert (11) on the adsorption of long-chain fatty acids; the statements of Jones and Ray (15) that the surface tension of very dilute inorganic salt solutions drops below the surface tension of the solvent; the distinct minima in the surface tension of soaps at low concentration of solute, as reported by McBain (24) and others; a similar effect in the latex of the Hevea rubber tree, as reported by Hauser and Scholz (14); and the finding of distinct maxima and minima in the surface tension-concentration curves of certain organic compounds in non-polar neutral solvents, recently reported by Hauser and Grossman (13).

VI. Measurement of Surface Tension

Out of a great number of methods or procedures which have been suggested for the determination of boundary tension, only a few are in common use. These depend upon observing: *1*, the behavior of a liquid in a capillary tube (15, 21, 28); *2*, the force required to pull a wire ring or staple out of the liquid surface (18, 22); *3*, the weight or volume of drops falling from a vertical tube of known size (12); or *4*, the maximum pressure required to form bubbles in a liquid from a tube of known size (29, 31). Each of these methods has serious limitations (1).

1. The Pendent-Drop Method

This condition suggested a re-survey of the field in the hope that a new method could be developed which would be free of the limitations or objections of those now in general use. A study of the procedure followed in the determination of surface tension measurements with the use of high-speed photography not only offered some explanation for discrepancies in the results previously obtained, but also demonstrated a number of outstanding advantages which a static method, based on the study of a pendent drop, would have.

Once the surface is formed, it is not subjected to any changes due to outside influence prior to or during the measurement. It is the only known method which permits an accurate study of changes in surface composition with time, a phenomenon of predominant importance in the study of various systems.

The method which was decided upon consists in suspending a small drop of the liquid to be tested from the end of a vertical tube which is mounted in a thermostat (2). The surface of the drop will be a surface of revolution whose shape and size can be determined by measurements made on a large photographic image obtained with a special camera built for the purpose, or by projection of the image onto a screen. Since the equations determining the equilibrium of the drop are known, the boundary tension of the liquid can be calculated from a few simple measurements made on a photograph of a hanging drop.

This method has been undeservedly in disrepute for a number of years because the first workers who attempted to employ it had no satisfactory pendent-drop camera and used methods of calculation which were tedious and of low precision.

Since the publication of the first results of surface tension determinations by the pendent-drop method, a number of changes in the equipment originally suggested have been made by various research workers (3, 20, 27). The principle, however, has remained unchanged. It consists essentially of producing a silhouette photograph or projection of a drop hanging from a vertical cylindrical tip, by the use of appropriate optical equipment (Fig. 1).

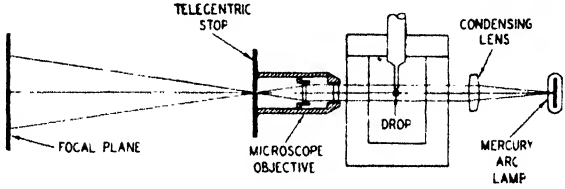

Fig. 1.—Pendent-drop apparatus (schematic).

Pendent-Drop Calculations. Two methods of calculation of the surface tension of the liquid proved most amenable for mathematical treatment (1), namely the method of the plane of inflection and the method of the selected plane. Before these had been decided upon the method of Ferguson (6), the method of Worthington (32, 33), the method of two planes (4) and the method of the plane of the equator (4) had been carefully scrutinized and discarded as not being satisfactory in combining best the qualities of speed, accuracy and precision. Therefore, only the first two methods mentioned will be discussed in greater detail.

Method of the Plane of Inflection. The mathematical treatment is based on two fundamental equations. The first of these states that the pressure caused by the curvature of the surface is equal to the product of the boundary tension and the mean curvature.* The second states that when the drop is in equilibrium the vertical forces acting across any horizontal plane are balanced.

$$p = \sigma(1/R + 1/R') \tag{1}$$

$$2\pi x\sigma \sin \phi = Veg + \pi x^2 p \tag{2}$$

where p is the pressure due to the curvature of the surface; σ is the boundary tension; R and R' are the two principal radii of curvature;

* This equation originated with Thomas Young (34) and Pierre Laplace (17). A simple derivation is given by N. K. Adam (1).

x is the horizontal distance to the axis of the drop; ϕ is the angle between the normal to the interface and the axis; V is the volume of fluid hanging from the plane; e is the difference in density between the two fluids; and g is the acceleration of gravity.

These equations may be combined and solved for σ in a number of ways. A satisfactory method is to pass a horizontal plane through the drop at the level where the profile curve passes through a point of inflection (Fig. 2).

The external radius of curvature, R', is infinite at the plane of inflection, and therefore equation (1) reduces to

$$p = \frac{\sigma}{R}$$

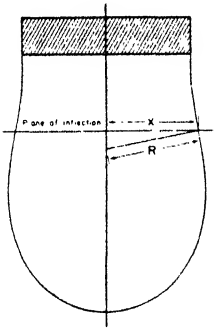

Fig. 2.—Method of the plane of inflection.

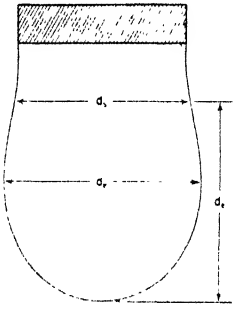

Fig. 3.—Method of the selected plane.

Substituting this value of p in equation (2), and solving for the boundary tension, σ, we obtain for this special case

$$\sigma = \frac{Veg}{2\pi x \sin \phi - \frac{\pi x^2}{R}}$$

and since

$$\sin \phi = \frac{x}{R}$$

$$\sigma = \frac{g}{\pi} \frac{VeR}{x^2} \qquad (3)$$

This equation is mathematically exact, but its use is subject to two severe limitations: *1*, It is necessary to locate the true plane of inflection. This is a difficult graphical problem. If a plane is used which is slightly above the true plane of inflection, the measured value of V will be too large and the measured value of x will be too small. If a plane is used which lies slightly below the true plane of inflection, the opposite will be true. In either case, a double error is introduced in the computed value of the boundary tension. *2*, It is necessary to compute the volume of the drop from its profile. This is a tedious process which must either be done by graphical integration or with a special, very costly, planimeter.

Method of a Selected Plane. A less direct method of attack leads to a more rapid and precise solution. It is first necessary to examine the differential equation of the surface of the drop.

If z is the vertical coordinate measured away from an origin placed at the point where the axis of rotation cuts the surface of the drop, and if b is the radius of curvature of the drop at the origin, the pressure due to the curvature is at any point equal to

$$p = \frac{2\sigma}{b} - gez \tag{4}$$

If equations (1) and (4) are combined, we obtain

$$\sigma(1/R' + 1/R) = \frac{2\sigma}{b} - gez$$

and the radii of curvature can be eliminated, since

$$R' = \frac{\left[1 + \left(\frac{dz}{dx}\right)^2\right]^{3/2}}{d^2z/dx^2}$$

and

$$R = \frac{x}{\sin \phi} = \frac{x\left[1 + \left(\frac{dz}{dx}\right)^2\right]^{1/2}}{\frac{dz}{dx}}$$

Then

$$\frac{\frac{d^2z}{dx^2}}{\left[1 + \left(\frac{dz}{dx}\right)^2\right]^{3/2}} + \frac{\frac{dz}{dx}}{x\left[1 + \left(\frac{dz}{dx}\right)^2\right]^{1/2}} = \frac{2}{b} - \frac{gez}{\sigma}$$

or

$$\frac{d^2z}{dx^2} + \frac{1}{x}\frac{dz}{dx}\left[1 + \left(\frac{dz}{dx}\right)^2\right] = \left[\frac{2}{b} - \frac{gez}{\sigma}\right]\left[1 + \left(\frac{dz}{dx}\right)^2\right]^{3/2}$$

This is a second-order, second-degree differential equation whose integrated form is unknown. It can be reduced to the dimensionless form,

$$Z'' + \frac{Z'}{X}[1 + (Z')^2] = [2 - \beta Z][1 + (Z')^2]^{3/2} \tag{5}$$

if we set

$$\beta = \frac{geb^2}{\sigma} \tag{6}$$

and let $X = x/b$, $Z = z/b$, $Z' = dZ/dX$ and $Z'' = d^2Z/dX^2$, which is equivalent to using b as the unit of length.

This derivation follows that of Bashforth and Adams (4) with the exception that the algebraic signs of e and of β are defined so as to be positive for pendent drops.

The differential equation (5) is seen to contain *two* parameters β and b, whose values identify the particular drop represented by the equation.

By rearranging equation (6), it is possible to express the boundary tension as a function of the two parameters β and b and of the effective specific weight (ge). No method is known by which either β or b can be determined precisely and quickly from a picture of a drop. We must therefore transform equation (6) to a form which uses parameters whose values can be measured easily and accurately.

The size of a drop is most conveniently gauged by measuring its diameter at the equator, and the shape can be described by giving the ratio of the diameters measured at two different horizontal planes. If one diameter is at the plane of the equator, and the other is taken at a distance from the end of the drop equal to the equatorial diameter (Fig. 3), the shape can be described by the ratio

$$S = \frac{d_s}{d_e} \tag{7}$$

where d_e is the diameter at the equator, and d_s is the diameter at the arbitrarily selected plane.

It has been shown that the quantities β and S are functions of the drop shape. A third quantity, which is a function of the drop shape, is the ratio of the diameter at the equator to the radius of curvature at the origin, d_e/b. Accordingly, we can define a new quantity

$$H = \beta \left(\frac{d_e}{b}\right)^2 \tag{8}$$

which will be a function of S.

Equation (6) can now be solved for σ, combined with equation (8), and used in conjunction with a table of values of H as a function of S (2) to determine the value of the boundary tension from a photograph of a pendent drop.

$$\sigma = \frac{geb^2}{\beta} = \frac{ge(d_e)^2}{\beta\left(\frac{d_e}{b}\right)^2} = \frac{ge(d_e)^2}{H} \tag{9}$$

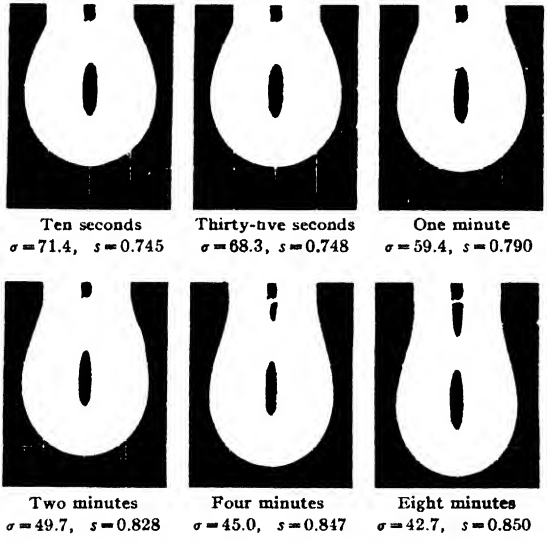

Fig. 4.—Change of drop shape and surface tension with age of 0.0025% aqueous sodium oleate.

Equation (9) is exact and convenient. Its precision depends upon the accuracy with which the linear measurements can be made and upon the labor which is expended in preparing the table of values of H as a function of S.

Not only does this method permit an accurate study of the changes the surface tension of solutions may undergo with time (Fig. 4), but also it is the only method in which the surface is at no time subjected to any influence from the outside. It seems, therefore, ideally suited for the study of the previously mentioned anomalies.

VII. Effect of Concentration on Surface Tension

1. Classification of Surface Tension vs. Concentration Curves

McBain and his collaborators (24) differentiate between three types of surface tension *vs.* concentration curves in water solutions (Fig. 5). The curve represented by type 1 corresponds to the case of positive adsorption of the solute and is in full agreement with Gibbs' theorem. Type 2 is specific for the case of negative adsorption and conforms also with Gibbs' theoretical postulate. In curves of type 3 the surface tension drops sharply in very dilute solutions, then passes through a minimum followed by a steady rise with concentration. But even during this rise the surface tension still remains far below that of the pure solvent. Such types of curves have been frequently reported in the study of surface tension of soaps and sulfonic acids.

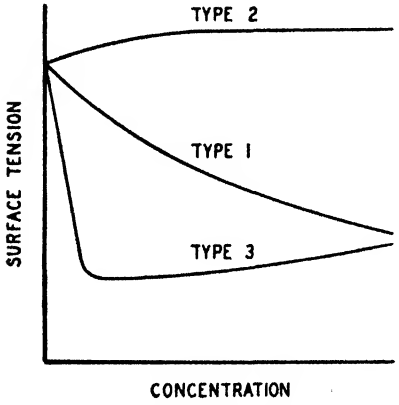

Fig. 5.—Different types of surface tension-concentration curves (according to McBain (24)).

2. McBain's Theory for Surface Tension Minima

McBain (24)* explains this type of curve in the following way: "A soap solution must for all the reasons stated be covered with soap, the oleic radicals being outwards. Under this must, according to the Gibbs theorem, be sandwiched the relative excess of water above that in the soap solution. However, Miss Laing showed (M. E. Laing, *Proc. Roy. Soc.* (*London*), **A109,** 28 (1925)) by analysis of soap foam that soap, not water, is positively adsorbed.

"Now such a soap solution has actually a surface tension as low as 23 dynes. This is far below the 32.5 dynes of pure oleic acid and still further below the 40 dynes of a complete coating of insoluble oleic acid on water. To account for this very great lowering to 23 dynes instead of 40, some other very important factor must have been overlooked in all previous discussions.

"The factor we suggest is a submerged electrical double layer due

* Original manuscript prior to translation into German by E. A. H.

to the electrolytic dissociation of the soap that is spread upon the surface. The diffused double layer therefore lies underneath at least one molecular length of oleic radical and probably extends far deeper. Any double layer must lower the surface tension in the manner familiar to every scientist from electrocapillary curves.

"Our measurements of the surface conductivity of a monomolecular film of oleic acid upon water* show that the oleic acid is about 10 per cent dissociated, and that therefore a submerged double layer corresponding to this amount actually exists. Similar evidence is obtainable from the familiar movement of bubbles and droplets in an electric field. However, the effect of this submerged double layer has always been ignored in discussing surface tension and, in particular, in calculating adsorption from and discussing the Gibbs theorem. It has also been completely forgotten in discussing oil films on water.

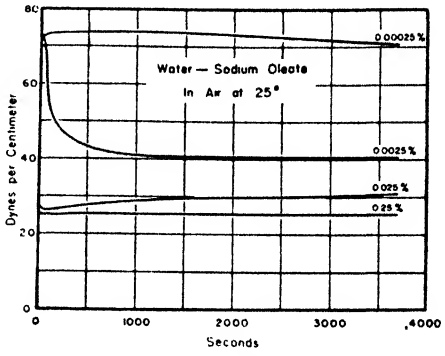

Fig. 6.—Surface tension of aqueous sodium oleate *versus* time (according to Andreas, Hauser and Tucker, (2)).

"Here at last we have the first explanation ever put forward to account for the rising portion of surface tension curves of type 3. The surface tension of these soap solutions, also far below that of water, rises with concentration, although the coating presumably remains constant because close packed. The rise is due to the well-known fact that soaps are not fully dissociated and that the dissociation decreases with concentration. Hence, the effect of the double layer diminishes and the surface tension rises towards its normal expected value."

The question whether this explanation can be generally accepted will be discussed later.

VIII. Effect of Time and Concentration on Surface Tension

Since the method of pendent drops seems particularly well adapted for the study of such phenomena, a series of experiments was carried

* McBain and Foster, *Colloid Symposium*, 1934, *J. Phys. Chem.*, **39**, 331 (1935) McBain and C. R. Peaker, *Proc. Roy. Soc.* (*London*), **A125**, 394 (1929)

out to determine the surface tension of sodium oleate and stearate against air, as well as the interfacial tension of a solution of sodium oleate in water against mineral oil (2).

1. Surface Tension of Soap Solutions

If the surface tension is evaluated from equally aged drops of solutions of sodium oleate varying in concentration from 0.00025 to 8.00 per cent, a curve of type 3 is obtained. This indicates that the sur-

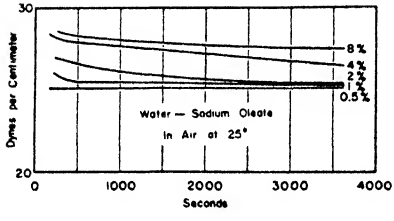

Fig. 7.—Surface tension of aqueous sodium oleate *versus* time (according to Andreas, Hauser and Tucker (2)).

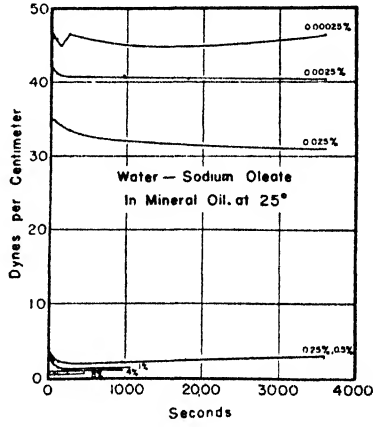

Fig. 8.—Interfacial tension of a water solution of sodium oleate against mineral oil with time (according to Andreas, Hauser and Tucker (2)).

face tension passes through a definite minimum with increasing concentration of solute. The pendent-drop method, however, also permits the study of any changes in surface tension with time, occurring in a solution of a given concentration. The results of a series of such experiments are shown in Figs. 6 and 7.

It will be noticed that extremely dilute solutions, 0.00025 or 0.0025 weight per cent, of this soap have an initial surface tension which is almost the same as that of pure water. During the first few seconds that the drop ages, the surface tension may increase. This is especially noticeable in the 0.00025 per cent curve, which rises rapidly, levels off and then slowly decreases. It remains at a value of slightly more than 72 dynes/cm. for the first 3000 sec. The second sample in

the series, containing 0.0025 per cent of sodium oleate, shows this same initial increase above the surface tension of pure water. However, in this case the rise is very rapid, and within the first 15 sec. the surface tension starts to fall, having approximately reached an asymptote after about 1500 sec. Still more concentrated solutions, 0.025 and 0.25 per cent, show a *decrease* during the first few seconds, which is followed by a slow recovery. The 0.025 per cent solution seems to be approaching the same asymptote as the 0.0025 per cent solution, but it is approaching it from the lower side.

A minimum surface tension is observed for a solution containing 0.5 per cent sodium oleate and the aging curve for this solution is a horizontal straight line. More concentrated solutions have slightly higher surface tensions and all of them decrease with time, approaching the asymptote defined by the curve for the 0.5 per cent solution.

Similar curves were obtained for sodium stearate against air and for the interfacial tension of sodium oleate against mineral oil (Fig. 8).

The most significant points in these observations are that the surface tension of solutions of higher concentration decreases with time, that of solutions of about 0.5% concentration remains constant, those of still lower concentrations show a tendency to rise with time and those of extreme dilution exhibit for the first six minutes a tension which is even greater than that of the solvent.

The phenomenon of a minimum in the surface tension of soap solutions *versus* concentration had previously been reported by Hauser and Scholz (14) in their work on the surface tension of fresh rubber latex. This semi-colloidal dispersion of rubber hydrocarbon in a watery medium also exhibits a curve of type 3. Although at that time no suggestion was made as to the cause of this phenomenon, it may now be assumed that small amounts of saponified resins are responsible for this result.

2. *Surface Tension of Amino-Acid Solutions*

Swearingen and Hauser (30) have investigated the changes in surface tension with time of different aliphatic amino acids. Whereas isoelectric solutions of both glycine and alanine show pronounced negative adsorption, α-amino-*n*-butyric acid exhibits no appreciable surface activity after a certain degree of surface stability has been reached with time. This seems to be due to the antagonistic effect between the large electric moment and the hydrophobic character of this dipolar ion. In the early stages of aging a tendency toward

negative adsorption of solute is noticeable, followed by a small positive adsorption and a corresponding reduction in surface tension. Solutions of α-amino-n-valeric acid show, in low concentrations, immediate positive adsorption followed by a slight increase in surface tension with time (Figs. 9 and 10).

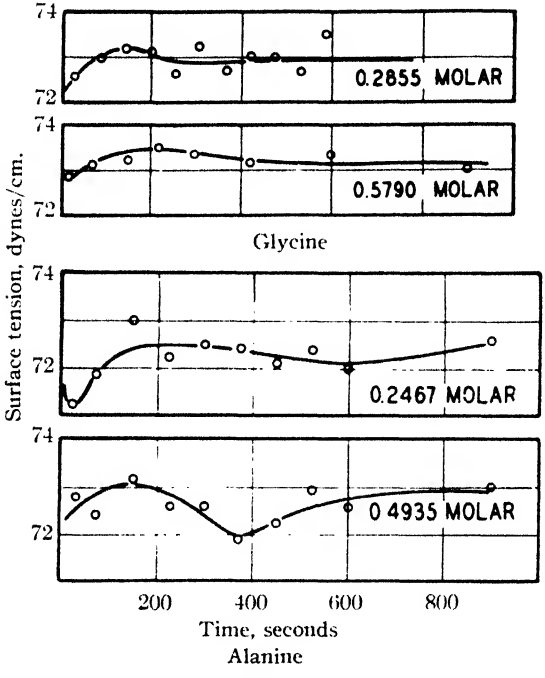

Fig. 9.—Surface tension *versus* time for isoelectric solutions of amino acids in water (according to Swearingen and Hauser (30)).

3. *Surface Tension of Electrolyte Solutions*

One of the most interesting and most debated anomalies so far reported is that observed by Jones and Ray (15) in their study of the surface tension of very dilute salt solutions. According to their observations solutions of KCl, K_2SO_4, $CsNO_3$ and other salts exhibit pronounced positive adsorption at concentrations below 0.006 normal. As explanation they offer the interaction between polarized water molecules and the ions of the electrolyte. In extreme dilutions this interaction tends to force ions into the surface layer whereas at higher

concentrations the interionic forces become predominant, resulting in negative adsorption.

4. *Surface Tension of Non-Ionic Solutions*

Recently Hauser and Grossman (13) studied the effect of solutes of similar chemical but of different polar and steric properties upon the

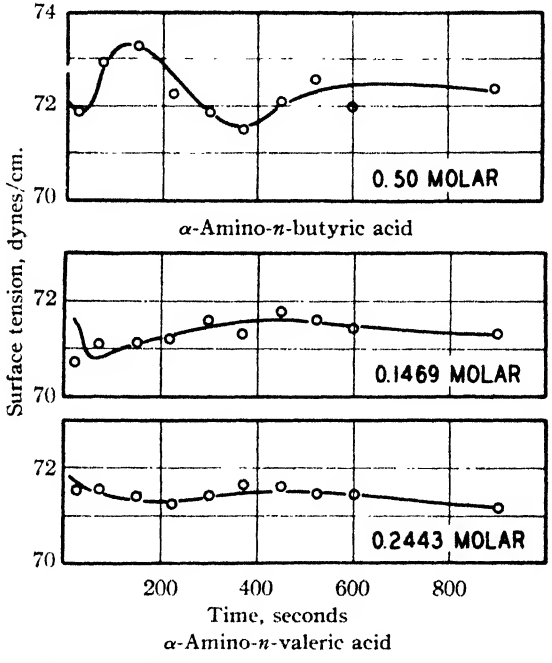

Fig. 10.—Surface tension *versus* time for isoelectric solutions of amino acids in water (according to Swearingen and Hauser (30)).

surface tension of non-polar neutral solvents by the pendent-drop method. To be specific, they studied the surface tension of such compounds as the isomers of dinitrobenzene, nitrobenzene, 1-nitronaphthalene, 1,8-dinitronaphthalene and 1,5-dinitronaphthalene in benzene. Preliminary tests showed that after aging the pendent drop for 30 sec. no changes of surface tension of the solutions with time occurred. Therefore, all measurements were carried out 2 and 3 min. after drop formation.

The surface tension of solutions of the meta and para isomers of

dinitrobenzene show first a sharp initial rise at low concentration, followed by a less pronounced but linear increase with higher concentration of solute. The benzene solutions of *o*-dinitrobenzene, nitrobenzene and 1-nitronaphthalene exhibit a maximum and a minimum in their surface tension concentration curves (Figs. 11 and 12).

These experiments are of special significance in so far as non-ionic solutions are used. In such solutions two types of forces have to be considered. One is the force acting between two electric dipoles, and the other is the attraction between two non-polar molecules. In the application of dipolar forces it should be recalled that a molecule may be non-polar, if non-polarity is judged by the lack of a dipole moment for the molecule, but may nevertheless bring dipolar forces into play. This is due to the nature of the dipole moment. A molecule is considered to be a dipole whenever the vector sum of its bond moments is larger than zero. The bond moments, however, result from the formation of a dipole consisting of two attached atoms of different electro-negativities. If such "atomic" dipoles are sufficiently separated to prevent nullification of their effects by their proximity as well as by their vector negation, they will act like a molecular dipole.

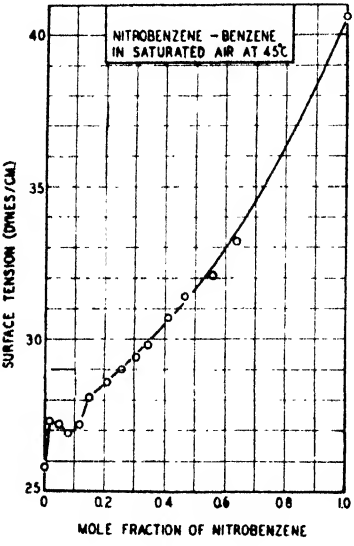

Fig. 11.—Surface tension *versus* concentration for nitrobenzene in benzene (according to Hauser and Grossman (13)).

The dipole moment of the solvent benzene is zero. It is a truly non-polar substance exerting only molecular attraction forces. The isomers of dinitrobenzene vary in their dipole moment in accordance with the steric moments of the molecule. This moment decreases in the sequence of ortho to meta to para position. Nitrobenzene and 1-nitronaphthalene should both exert about the same forces since they possess nearly the same dipole moments.

If one applies the properties of the components of the solutions just discussed to the fundamental causes for differences in surface

tension, it becomes evident that the presence of a solute exerting dipolar forces in a non-polar solvent must result in negative adsorption of the former. This again is in full accord with Gibbs' theorem. The surface tension of the solution will rise over that of the solvent. With increasing concentration of the solute the influence of its dipolar forces becomes noticeably more effective, and proportionally more solute molecules move into the interior. The surface tension continues to rise but at a slower rate.

In contrast to this behavior the surface tension-concentration curves for solutions of *o*-dinitrobenzene, nitrobenzene and 1-nitro-

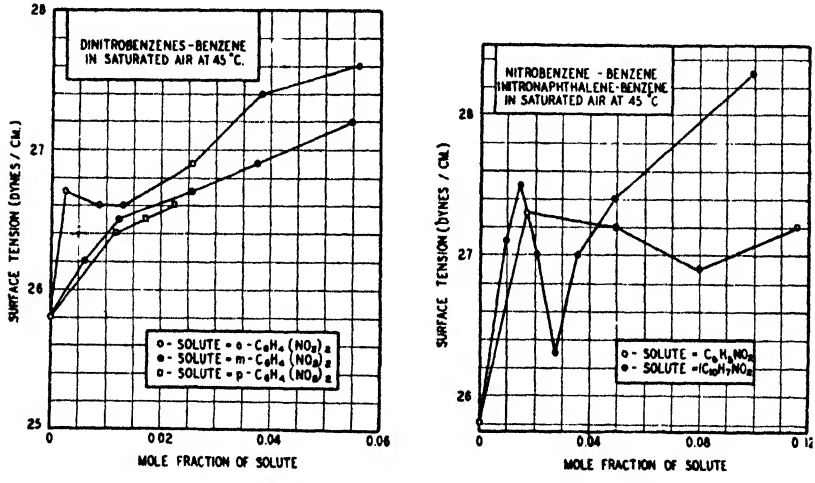

Fig. 12.—Surface tension *versus* concentration of dinitrobenzenes and 1 nitronaphthalene in benzene (according to Hauser and Grossman (13)).

naphthalene show a different behavior. The initial sharp rise is followed by a drop and a subsequent renewed increase at a somewhat lower rate. The greater dipolarity of these compounds—as compared to those previously discussed—offers a simple explanation for the more pronounced initial rise in surface tension as well as for the higher rate of surface tension increase with higher concentration of solute. These results are again in accord with Gibbs' theoretical postulates. The minimum occurring between the two rises still remains to be explained.

A comparison of the steric properties of the solutes investigated and the surface tension-concentration curves obtained seems to offer

an explanation. It is evident that only those solutes sterically unbalanced, *e. g.*, *o*-dinitrobenzene, show the peculiar minimum in their surface tension-concentration curves. The conclusion therefore seems to be justified that this minimum is connected with the steric property of the molecule.

In solutions of low concentrations containing capillary negative solutes, it is reasonable to assume that the layer of liquid molecules at the exact vapor-liquid interface contains a very high percentage of solvent molecules. The forces which sterically unbalanced molecules of solute can exert will vary with their orientation. The forces that are exerted in the case of *o*-dinitrobenzene will be less if the phenyl radicals of the molecules, which exert only van der Waals forces, are adjacent to the surface layer of solvent molecules than if the solute molecules are in random orientation. This limited orientation will, therefore, result in a lower surface tension than would be expected if the solute molecules would not orient themselves in such fashion. This effect, combined with the desorption previously mentioned, can well account for the minima which have been observed. With increasing concentration of solute molecules the effect of such orientation is more than compensated for by the increase in attraction forces, and the surface tension rises again although at a somewhat lower rate than at the outset. This hypothesis does not contradict Gibbs' theorem since in no instance is the surface tension of the solution reduced below that of the solvent. It must, however, be emphasized that Gibbs' theorem is a general postulate which cannot take into account such minor changes, and all the so-called paradoxes occurring in surface phenomena are but secondary to the general trend. Thus, an explanation for such phenomena will always have to consider Gibbs' basic postulate as well as all chemical or colloid-chemical factors involved. It therefore seems highly improbable that all the paradox phenomena can be explained by one and the same formula.

IX. Critical Considerations

Dyestuff Solutions. The results obtained by Gibby and Addison (10) on the adsorption of a number of dyestuffs at interfaces may be satisfactorily explained by applying a reasoning similar to that of Hauser and Grossman (13). It seems perfectly conceivable that by proper orientation of the dyestuff molecules which are known to have complex dipolar properties, a lowering of surface tension can occur without the necessity of positive adsorption. The authors them-

selves must have fully realized when they made the following statement that some further information will be necessary before their results can be brought into line with Gibbs' equation. "It seems clear, therefore, that the difference between the observed and the calculated values of U cannot be due to lack of data for activities of solutes. Hence no further useful purpose can be served by endeavoring to apply Gibbs' equation in the absence of further information as to the influence of the electrical and other factors expressly excluded in its derivation."

Fatty Acid Solutions. Gilbert's (11) results on the surface tension of fatty acids in aliphatic and aromatic hydrocarbons also seem to find a satisfactory answer by the hypothesis discussed above.

The results of Swearingen and Hauser (30) on the changes of surface tension with time of α-amino-n-fatty acids may be explained in the following way. The maxima and minima, occurring in the aging curves of some of the isoelectric amino-acid solutions, offer rather striking evidence of the difficulty with which equilibrium is reached between surface and bulk phases in systems which are capable of antagonistic action. These maxima and minima must involve dipolar action as well as interionic attraction, since interionic attraction alone cannot account for the changes from negative to positive solute adsorption. The dipolar molecules of the solvent and the dipolar ions of the solute tend to oppose each other in their attempt to stabilize the system. Lenard (19) and Frumkin (8) have shown the surface layer of an air-water interface to be negatively charged, with the positive charge at a lower depth within the liquid phase. This electrical double layer at the surface layer will operate to cause the negative part of the dipolar ion to orientate in the vicinity of the positive side of the electrical double layer, with the positive part of the dipolar ion directed into the bulk of the solution. In the initial stages of the aging process for the first three acids, water preferentially enters the surface layer, with the resultant increase in boundary tension. The migration of water from the bulk of the solution into the surface layer can be due to a combination of the "squeezing out effect" produced by the stronger electric field of the dipolar ions, and the smaller mobility of the dipolar ions in the vicinity of the surface layer, due to directed orientation of these dipolar ions by the surface electrical double layer.

After a short time interval, this resultant accumulation of water molecules in the surface layer and dipolar ions in the bulk phase be-

low the surface layer establishes a considerable concentration gradient between these two phases, with the result that some of the dipolar ions beneath the surface are forced to swing their positively charged hydrocarbon end up into the surface layer with an attendant drop in surface tension. This alternate, forced migration of water molecules and dipolar ions into the surface is thought to be responsible for the maxima and minima, where they occur in the aging curves of the isoelectric acid solutions for the first three acids of the series. With the α-amino-*n*-butyric acid, the lengthened hydrocarbon chain has increased the hydrophobic character of the dipolar ion to such a magnitude that this effect largely predominates over the dipole and interionic effects, so that there is an immediate positive solute adsorption, with only slight irregularities in the aging curves. These irregularities are even less pronounced in the case of α-amino-*n*-valeric acid.

McBain (24) has offered an explanation for the occurrence of very pronounced minima in the surface tension-concentration curves for soap solutions. His explanation has been previously cited. Apparently in soap solutions a curve of type 3 (Fig. 5) could also be explained by the well-known fact that soaps are concentration-variable colloids. Thus, in extreme dilutions the migration of the soap molecules into the surface will be considerably easier than at higher concentrations, where the micelle has attained an appreciable size. Since the "molecule" is capillary-active in both cases, a reduction in surface tension occurs in accordance with Gibbs' equation. The so-called paradox again proves to be a matter not of principle but of degree.

Jones-Ray Effect. Let us now consider the Jones and Ray (15) effect. The minute decrease in surface tension which was observed (less than 0.02%) may account for the fact that other research workers have not always been able to reproduce the effect. Although this phenomenon certainly does not affect the validity of Gibbs' theorem, since the trend of the surface tension-concentration relationship is not involved, it nevertheless deserves attention. Langmuir (16) has suggested an explanation of the phenomenon. He assumes that the capillary, if filled with pure water, carries an adsorbed film of water, thus decreasing its effective diameter. Therefore, the liquid will rise to a greater height than that which would correspond to the diameter of the capillary as measured. In the presence of electrolytes the potential of the capillary and, therefore, the film thickness decrease, increasing the effective diameter of the capillary. This in turn results

in an apparent decrease in surface tension. The rise in surface tension occurring at a higher concentration of electrolyte can then be explained in the customary way. As a possible check for this theory Langmuir suggests the addition of thorium nitrate in a concentration of 10^{-6} M as this should bring the ζ-potential of the glass to about zero.

The explanation offered by Langmuir is certainly worth very careful consideration. The fact that different glasses exhibit different ζ-potentials if placed in identical environments, *i. e.*, adsorb water films of different thickness, may explain some of the previously mentioned discrepancies. Further work is necessary, however, to settle definitely the question whether Langmuir's explanation is acceptable. It is known that the ζ-potential of glass in an electrolyte solution and its changes with concentration depend to a large extent on the type of ions present. In the case of uni-univalent electrolytes Freundlich and Ettisch (7) have shown an increase in the ζ-potential up to concentrations between 10^{-7} and 10^{-6} M, followed by a decrease. Therefore, there must be an increase in film thickness at first before the phenomenon on which Langmuir bases his reasoning can occur. Consequently, it can be expected that the surface tension of electrolyte solutions of lower molarity than those investigated by Jones and Ray should give apparently higher values than the particular concentrations of electrolyte investigated by them.

Two zero values for the ζ-potential must be considered in the case of thorium salts. The first one occurs approximately at 10^{-7} M, the second one at about 10^{-4} M. At a concentration of 10^{-6} M, a maximum possible ζ-potential occurs, according to the data of Freundlich and Ettisch (7). Langmuir's criticism of the Jones and Ray effect has demonstrated the importance which film thicknesses can attain in regard to surface tension measurements in narrow capillaries. As a consequence thereof it is necessary that the type of glass used or the changes of its ζ-potential *versus* concentration of electrolyte be defined. In the light of the above and in accordance with known colloid phenomena it certainly is not advisable to generalize.

Since the rise in surface tension occurring at higher electrolyte concentration is a linear function—according to the data of Jones and Ray (15)—it should be possible to extrapolate this curve to zero electrolyte concentration and to evaluate from it the theoretically correct surface tension of water. Also, using Langmuir's equation (16) as developed in his criticism of the Jones and Ray effect, the actual thick-

ness of the water film adsorbed on the capillary at zero concentration of electrolyte could be evaluated.

The Jones and Ray effect can also be explained on the following basis: It is known that a liquid will show the highest surface tension when its surface molecules are oriented in such a way that their strongest force fields are directed toward the bulk of the liquid (1). Upon the addition of small amounts of foreign ions the orientation of this surface layer is bound to be interrupted (independently of the presence of capillary active or inactive molecules). Theoretically this must result in a small reduction of the surface tension. With increasing concentration of capillary-inactive electrolyte this effect is increasingly overshadowed by the strong attraction forces producing an increase in surface tension in accordance with Gibbs' theorem.

The author has attempted to offer a critical survey of the much-debated "anomalies" of surface tension of solutions. He has referred only to some of the most outstanding cases and therefore does not claim this review to include all anomalies which so far have become known, nor does he claim the following bibliography to be complete. The contributions to the fundamentals of surface chemistry by men like Adam, Bartell, Harkins, Langmuir, McBain and many others have not been specifically referred to for the same reason.

Bibliography

1. N. K. Adam, *The Physics and Chemistry of Surfaces*, 2nd edition, Oxford Univ. Press, 1938.
2. J. M. Andreas, E. A. Hauser and W. B. Tucker, *J. Phys. Chem.*, **42**, 1001 (1938).
3. F. E. Bartell and J. K. Davis, *J. Phys. Chem.*, **45**, 1321.(1941).
4. F. Bashforth and J. C. Adams, *An Attempt to Test the Theories of Capillary Action*, Cambridge Univ. Press, 1883.
5. F. G. Donnan and I. T. Barker, *Proc. Roy. Soc.* (*London*), **A85**, 557 (1911).
6. A. Ferguson, *Phil. Mag.*, (6) **23**, 417 (1912).
7. H. Freundlich and E Ettisch, *Z. physik. Chem.*, **116**, 401 (1925).
8. A. Frumkin, *Ibid.*, **109**, 34 (1924); **111**, 190 (1924).
9. J. W. Gibbs, *Collected Works*, Longmans, Green & Co., New York, 1928.
10. C. W. Gibby and C. C. Addison, *J. Chem. Soc.*, **1936**, 119; **1936**, 1306.
11. E. C. Gilbert, *J. Phys. Chem.*, **31**, 543 (1927).
12. W. D. Harkins and F. E. Brown, *J. Am. Chem. Soc.*, **38**, 246 (1916); **41**, 499 (1919).
13. E. A. Hauser and A. J. Grossman, paper presented at the 50th Anniversary Symposia, Univ. of Chicago, Sept. 22, 1941.
14. E. A. Hauser and P. Scholz, *Kautschuk*, Nov., 1927, p. 332.

15. G. Jones and W. A. Ray, *J. Am. Chem. Soc.*, **57**, 957 (1935); **59**, 187 (1937).
16. I. Langmuir, *Science*, **88**, 430 (1938).
17. P. S. Laplace, *Mecanique celeste*, suppl. to Vol. X, Paris, 1806.
18. P. Lenard, *et al.*, *Ann. Physik*, **74**, 381 (1924).
19. P. Lenard, *Ibid.*, (4) **47**, 463 (1915).
20. J. L. Mack, J. K. Davis and F. E. Bartell, *J. Phys. Chem.*, **45**, 846 (1941).
21. J. L. Mack and F. E. Bartell, *J. Am. Chem. Soc.*, **54**, 936 (1932).
22. A. Macy, *J. Chem. Educ.*, **12**, 573 (1935).
23. J. W. McBain and C. W. Humphreys, *J. Phys. Chem.*, **36**, 300 (1932).
24. J. W. McBain, T. F. Ford and D. A. Wilson, *Kolloid-Z.*, **78**, 1 (1937).
25. J. W. McBain and R. C. Swain, *Proc. Roy. Soc. (London)*, **A154**, 608 (1936).
26. J. Rice, *Commentary on Gibbs' Work*, 1937.
27. G. W. Smith and L. V. Sorg, *J. Phys. Chem.*, **45**, 671 (1941).
28. S. Sugden, *J. Chem. Soc.*, **119**, 1483 (1921).
29. S. Sugden, *Ibid.*, **121**, 858 (1922).
30. L. E. Swearingen and E. A. Hauser, unpublished data pertaining to a study on the aging of surfaces of aqueous solutions of some aliphatic amino acids.
31. A. E. J. Vickers, *et al.*, *J. Soc. Glass Tech.*, **18**, 224 (1933).
32. A. M. Worthington, *Proc. Roy. Soc. (London)*, **32**, 362 (1881).
33. A. M. Worthington, *Phil. Mag.*, (5) **19**, 46 (1885).
34. T. Young, *Phil. Trans.*, **5**, 65 (1805).

AUTHOR INDEX*

*Italic numerals refer to the bibliographies of the different papers.

C

D

H

I

J

N

O

T

Y

Z

SUBJECT INDEX

T

U

V